



Some pages of this thesis may have been removed for copyright restrictions.

If you have discovered material in Aston Research Explorer which is unlawful e.g. breaches copyright, (either yours or that of a third party) or any other law, including but not limited to those relating to patent, trademark, confidentiality, data protection, obscenity, defamation, libel, then please read our [Takedown policy](#) and contact the service immediately (openaccess@aston.ac.uk)

Biodegradable Thermoplastic Polyurethanes

Amanda Goodby

Doctor of Philosophy

Aston University

November 2014

© Amanda Goodby, 2014 asserts her moral right to be identified as the author of this thesis

This copy of the thesis has been supplied on condition that anyone who consults it is understood to recognise that its copyright rests with its author and that no quotation from the thesis and no information derived from it may be published without appropriate permission or acknowledgement.

ASTON UNIVERSITY

Biodegradable Thermoplastic Polyurethanes

AMANDA GOODBY

DOCTOR OF PHILOSOPHY

SUMMARY

The overall aim of this work was to investigate the biodegradability of a number of polyurethane elastomers synthesised by different methods and targeted for a specific agricultural purpose in which the polyurethane was required to be degradable in soil after its useful life.

Polyurethanes were synthesised commercially using two different methods; a '**one-shot**' method where all of the reactants were added simultaneously, and a '**pre-polymer**' method, in which the isocyanate and polyol were reacted together before addition of the chain extender. The effect of the method of synthesis on the rate of degradation and biodegradation was investigated using accelerated alkaline hydrolysis, enzymatic hydrolysis and soil burial, where it was found that the polyurethane synthesised by the '**pre-polymer**' method hydrolysed faster under alkaline conditions (**21 days**) than that synthesised by the '**one-shot**' method (**56 days**). This was found to be due to differences in the polymer morphology, with an increase in microcrystalline domains occurring during the '**one-shot**' process.

The effect of the chemical constituents of the synthesised polyurethanes on the rate of degradation and biodegradation were also investigated. Comparison of polyurethanes synthesised with an aliphatic (**H₁₂MDI**) and an aromatic isocyanate (**MDI**) resulted in an increase in the rate of alkaline hydrolysis with the use of **H₁₂MDI**. This was found to be affected mainly by differences in the morphology, with an increase in microphase separation and a decrease in microcrystalline regions in the case of the use of **H₁₂MDI**

Polyurethanes were synthesised using different polyols; **PEA**, **PCL**, **PEG** and **PCL/PEG (50:50)** to investigate the effect of the polyol on the rate of biodegradation, where it was found that the polyurethane containing a combination of the two polyols, **PCL/PEG (50:50)**, degraded under both accelerated hydrolysis conditions and soil burial. This was thought to be due to the combination of both hydrophilic (**PEG**) and hydrophobic (**PCL**) characters of the polyols, which had contributed to increasing the diffusion of water into the polymer matrix (hydrophilic **PEG**), and also to inducing the microbial degradation by hydrophobic interactions (**PCL**).

The incorporation of the additives; **iron stearate**, **cellulose** and **Cloisite 30B** were examined as a means of increasing the degradation and biodegradation of the polyurethane polymers. Addition of **iron stearate** was found to decrease the thermal stability of the polyurethane, which resulted in an increase in polyurethane degradation under alkaline conditions at 45°C, and biodegradation under soil burial conditions at 50°C. The incorporation of **cellulose** into the polyurethane increased the rate of alkaline hydrolysis and biodegradation in soil. This polyurethane (**PU CE**) was also susceptible towards enzymatic degradation by **Aspergillus niger**. The incorporation of the organically-modified nanoclay **Cloisite 30B** has decreased the microcrystalline domain structure contained within the polyurethane, and this was found to decrease the rate of alkaline hydrolysis dramatically (degraded within **7 days**).

Keywords: biodegradation, hydrolysis, crystallinity, soil, nanocomposite

Dedication

I would like to dedicate this thesis to my parents, Susan Carr and Michael Carr who always made me believe that I could accomplish anything, and also to my three children, Amber Knight, Luke Knight and William Goodby who have always been with me through everything.

Acknowledgements

I would first and foremost like to acknowledge my supervisor Professor Sahar Al-Malaika, who has not only supported and guided me throughout this project, but also prior to that, as a mentor during my undergraduate studies, without whom I would never have completed. She is a person to whom I both admire and aspire to become in the future. I would also like to acknowledge my sponsor company Eurothane Ltd who kindly provided funding and synthesised the polyurethanes for this project, and EPSRC who also provided funding for this project.

I would like to kindly thank Dr. Husam Sheena, who has also provided guidance, technical advice and support during this project. I would also like to thank all of the members of the PPP group; Cezary Lewucha, Selma Riasat and Khalid Doudin, without whom would have made these last three years very dull indeed, with a personal thank you to my good friends Cezary Lewucha who helped me extensively with DSC and made me laugh many times, and Selma Riasat with whom I have had great times over the years

I would like to thank Richard Darwood; my boss, who has supported me during writing up my thesis and made me laugh for the last 12 months.

Last but not least I would like to personally thank Dr. Gareth Griffiths; who has not only provided emotional support during my studies and has enriched my life, but has supported me technically, especially regarding the biological aspects of this project.

Table of Contents

	<i>Page</i>	
<i>Thesis Title</i>	1	
<i>Summary</i>	2	
<i>Dedication</i>	3	
<i>Acknowledgements</i>	4	
<i>Table of Contents</i>	5	
<i>List of Figures</i>	12	
<i>List of Tables</i>	21	
<i>List of Abbreviations</i>	23	
<i>Chapter</i>	<i>Title</i>	<i>Page</i>
1	<i>Introduction</i>	24
1.1	<i>Biodegradable Polymers</i>	24
1.2	<i>Polyurethane Background</i>	24
1.3	<i>Polyurethane Elastomer Chemistry</i>	27
1.3.1	<i>Effect of Isocyanates on Polyurethane Properties</i>	27
1.3.2	<i>Effect of Polyols on Polyurethane Properties</i>	28
1.3.3	<i>Effect of Chain Extender on Polyurethane Properties</i>	29
1.3.4	<i>Polyurethane Morphology; Phase Separation and Hydrogen Bonding</i>	30
1.3.5	<i>Method of Synthesis of Polyurethanes</i>	31
1.4	<i>Process of Degradation and Biodegradation in Polyurethanes</i>	37
1.4.1	<i>Solubilisation and Hydrolysis of Polyurethanes</i>	37
1.4.2	<i>Enzymatic Degradation of Polyurethanes</i>	38
1.4.3	<i>Biodegradation and Degradation of Polyurethanes under Soil Burial and Composting Conditions</i>	40
1.5	<i>The use of Additives to Increase Degradation and Biodegradation</i>	41
1.6	<i>Test Methods Measuring Degradation and Biodegradation</i>	45
1.7	<i>Aims and Objectives of this Study</i>	50
2	<i>Experimental and Analytical Techniques</i>	52
2.1	<i>Materials</i>	52
2.1.1	<i>Polyurethanes</i>	52
2.1.2	<i>Preparation of Polyurethane Samples</i>	52
2.1.3	<i>Additives and Solvents</i>	52

Chapter	Title	Page
2.2	<i>Characterisation of Polyurethane Samples</i>	57
2.2.1	<i>Solubility</i>	57
2.2.2	<i>Water Absorption</i>	59
2.2.3	<i>Characterisation of Polyurethane Chemical Structure by Attenuated Total Reflection Spectroscopy (FTIR-ATR)</i>	59
2.2.4	<i>Chemical structure of Isocyanates, Polyols, Chain extenders and additives used in the synthesis of PU samples by FTIR</i>	59
2.2.5	<i>Thermal stability of PU samples by thermogravimetric analysis (TGA)</i>	59
2.2.6	<i>Crystallinity measurements by Dynamic Scanning Calorimetry (DSC)</i>	60
2.3	<i>Testing Methods for Degradation and Biodegradation of Polyurethanes</i>	67
2.3.1	<i>Accelerated Degradation of PU by Alkaline Hydrolysis</i>	67
2.3.2	<i>Degradation of PU by Enzymatic Hydrolysis</i>	67
2.3.3	<i>Biodegradation of PU under Soil Burial Conditions at RT</i>	68
2.3.4	<i>Soil Burial PU Biodegradation at 50°C</i>	70
2.4	<i>Characterisation of Soil from Rothamsted Institute and Castle Bromwich</i>	71
2.4.1	<i>Measurement of Soil Acidity</i>	71
2.4.2	<i>Soil Dry Matter Content (DM)</i>	71
2.4.3	<i>Soil Water Holding Capacity (WHC)</i>	72
2.5	<i>Assessment of Degradation and Biodegradation of Polyurethanes</i>	72
2.5.1	<i>Assessment of degradation and biodegradation by Spectroscopy</i>	73
2.5.2	<i>Assessment of morphology changes to PU during degradation and biodegradation by dynamic scanning calorimetry</i>	74
2.5.3	<i>Changes to thermal stability of PU samples by thermogravimetric analysis (TGA) after degradation and biodegradation.</i>	75
2.5.4	<i>Visual changes during degradation and biodegradation to PU samples assessed by microscopy and photography</i>	75
3	<i>Effect of Polyurethane Method of Synthesis on Degradation and Biodegradation</i>	77
3.1	<i>Objectives and methodology</i>	77
3.2	<i>Results</i>	78
3.2.1	<i>Characterisation of Synthesised Polyurethanes PU ADP, PU PR and PU 98 - Group 1 (Method of Synthesis)</i>	78

Chapter	Title	Page
3.2.2	<i>Effect of Method of Synthesis (PU ADP, PU PR and PU 98) on the Rate of Alkaline Hydrolysis</i>	80
3.2.2.1	<i>Structural changes in PU ADP, PU PR and PU 98 monitored by FTIR-ATR</i>	81
3.2.2.2	<i>Effect of Method of Synthesis on Crystallinity and Thermal Stability during Alkaline Hydrolysis (PU ADP, PU PR and PU 98)</i>	82
3.2.3	<i>Susceptibility to soil degradation of Polyurethane Samples PU ADP, PU PR and PU 98 (Effect of Method of Synthesis)</i>	84
3.2.3.1	<i>Structural changes during soil burial at 50°C in PU ADP, PU PR and PU 98 monitored by FTIR-ATR</i>	84
3.2.3.2	<i>Structural changes during soil burial at RT after 20 months in PU ADP, PU PR and PU 98 monitored by FTIR-ATR</i>	85
3.2.3.3	<i>Effect of Method of Synthesis on Crystallinity after 20 months soil burial (PU ADP, PU PR and PU 98)</i>	85
3.2.4	<i>Susceptibility of Polyurethane Samples PU ADP, PU PR and PU 98 (Effect of Method of Synthesis) towards enzymatic degradation</i>	87
3.2.4.1	<i>Structural changes during enzymatic degradation using lipases in PU ADP, PU PR and PU 98 monitored by FTIR-ATR</i>	87
3.2.4.2	<i>Structural changes during enzymatic degradation using proteases in PU ADP, PU PR and PU 98 monitored by FTIR-ATR</i>	88
3.3	<i>Discussion</i>	89
3.3.1	<i>Effect of Method of Synthesis (PU ADP, PU PR and PU 98) on the Rate of Alkaline Hydrolysis</i>	89
3.3.2	<i>Susceptibility to soil degradation of Polyurethane Samples PU ADP, PU PR and PU 98 (Effect of Method of Synthesis)</i>	93
3.3.3	<i>Susceptibility of Polyurethane Samples PU ADP, PU PR and PU 98 towards Enzymatic Degradation (Effect of Method of Synthesis)</i>	93
3.3.4	<i>Overall Summary of the effect of the Method of Synthesis on Polyurethane Degradation and Biodegradation</i>	95
4	<i>Effect of Polyurethane Structural Composition on Degradation and Biodegradation; Effect of Isocyanate</i>	130
4.1	<i>Objectives and methodology</i>	130
4.2	<i>Results</i>	131
4.2.1	<i>Characterisation of PUH ADP - Group 2 (Effect of Isocyanate)</i>	131

Chapter	Title	Page
4.2.2	<i>Effect of Isocyanate (PU ADP and PUH ADP) on the Rate of Alkaline Hydrolysis</i>	133
4.2.2.1	<i>Structural changes of PU ADP and PUH ADP during alkaline hydrolysis monitored by FTIR-ATR</i>	133
4.2.2.2	<i>Effect of isocyanate on crystallinity and thermal stability during alkaline hydrolysis (PU ADP and PUH ADP)</i>	134
4.2.3	<i>Susceptibility to soil degradation of Polyurethane Samples – Effect of Isocyanate PU ADP and PUH ADP</i>	135
4.2.3.1	<i>Structural changes during soil burial at 50°C in PU ADP and PUH ADP monitored by FTIR-ATR</i>	135
4.2.3.2	<i>Structural changes during soil burial at RT after 20 months in PU ADP and PUH ADP monitored by FTIR-ATR</i>	136
4.2.3.3	<i>Effect of Isocyanate on PU ADP and PUH ADP morphology after 20 months soil burial</i>	136
4.2.4	<i>Susceptibility of Polyurethane Samples PU ADP and PUH ADP (Effect of Isocyanate) towards enzymatic degradation</i>	137
4.2.4.1	<i>Structural changes during enzymatic degradation using lipases in PU ADP and PUH ADP monitored by FTIR-ATR</i>	137
4.2.4.2	<i>Structural changes during enzymatic degradation using proteases in PU ADP, and PUH ADP monitored by FTIR-ATR</i>	138
4.3	<i>Discussion</i>	139
4.3.1	<i>Effect of Isocyanate (PU ADP and PUH ADP) on the Rate of Alkaline Hydrolysis</i>	139
4.3.2	<i>Susceptibility to soil degradation of Polyurethane Samples PU ADP and PUH ADP (Effect of Isocyanate)</i>	142
4.3.3	<i>Susceptibility of Polyurethane Samples PU ADP and PUH ADP towards Enzymatic Degradation (Effect of Isocyanate)</i>	143
4.3.4	<i>Overall Summary of the effect of the Method of Synthesis on Polyurethane Degradation and Biodegradation</i>	144
5	<i>Effect of Polyurethane Structural Composition on Degradation and Biodegradation; Effect of Polyol</i>	167
5.1	<i>Objectives and methodology</i>	167
5.2	<i>Results</i>	168
5.2.1	<i>Characterisation of PU PCL, PU PEG and PU PGPC (Effect of Polyol)</i>	168
5.2.2	<i>Effect of Polyol (PU ADP, PU PCL, PU PEG and PU PGPC) on the Rate of Alkaline Hydrolytic Degradation</i>	170

Chapter	Title	Page
5.2.2.1	<i>Comparison of Polyurethanes with different ester soft segments, PU ADP containing polyethylene adipate polyol and PU PCL containing a polycaprolactone polyol</i>	170
5.2.2.2	<i>Comparison of Polyurethane PU ADP (ester polyol) and PU PEG (ether polyol)</i>	171
5.2.2.3	<i>Comparison of PU PGPC (containing a soft segment blend of PCL and PEG) to PU PCL and PU PEG</i>	171
5.2.2.4	<i>Structural changes of PU ADP and PU PCL during alkaline hydrolysis</i>	172
5.2.2.5	<i>Structural changes of PU ADP and PU PEG during alkaline hydrolysis</i>	173
5.2.2.6	<i>Structural changes of PU ADP and PU PGPC during alkaline hydrolysis</i>	174
5.2.2.7	<i>Effect of polyol on crystallinity and thermal stability during alkaline hydrolysis (PU ADP, PU PCL, PU PEG and PU PGPC)</i>	175
5.2.3	<i>Susceptibility to soil degradation of Polyurethane Samples in group 3 – Effect of Polyol, PU ADP, PU PCL, PU PEG & PU PGPC</i>	176
5.2.3.1	<i>Structural changes during soil burial at 50°C in PU ADP, PU PCL and PU PEG and PU PGPC monitored by FTIR-ATR</i>	177
5.2.3.2	<i>Structural changes during soil burial at RT after 20 months in PU ADP, PU PCL, PU PEG and PU PGPC monitored by FTIR-ATR</i>	178
5.2.3.3	<i>Effect of polyol on morphology after 20 months soil burial (PU ADP, PU PCL, PU PEG and PU PGPC)</i>	178
5.2.4	<i>Effect of polyol (PU ADP, PU PCL, PU PEG & PU PGPC) on enzymatic degradation by lipases Rhizopus sp. and Aspergillus niger</i>	179
5.2.4.1	<i>Structural changes during enzymatic degradation using proteases in PU PCL, PU PEG and PU PGPC monitored by FTIR-ATR</i>	180
5.3	<i>Discussion</i>	181
5.3.1	<i>Effect of an ester soft segment on degradation and biodegradation of polyurethanes, PU ADP and PU PCL</i>	182
5.3.2	<i>Comparison between ester and ether soft segment on chemical structure, crystallinity and thermal stability during alkaline hydrolysis, soil burial and enzymatic hydrolysis (PU ADP & PU PEG)</i>	186

Chapter	Title	Page
5.3.3	<i>Effect of blended soft segment containing PEG (polyether) and PCL (polyester) on chemical structure, crystallinity and thermal stability during alkaline hydrolysis, soil burial and enzymatic hydrolysis</i>	189
5.3.4	<i>Overall Summary of the effect of the Polyol (soft segment) on Polyurethane Degradation and Biodegradation</i>	192
6	<i>The Role of Additives on the Degradation and Biodegradation of Polyurethanes</i>	222
6.1	<i>Objectives and methodology</i>	222
6.2	<i>Results</i>	223
6.2.1	<i>Characterisation of PU CE and PUI (Effect of additives cellulose and iron stearate)</i>	223
6.2.2	<i>Characterisation of PU PR30, PU CE30 and PUI 30 (Effect of Cloisite 30b)</i>	224
6.2.3	<i>Effect of Additives (PU CE and PUI) on the Rate of Alkaline Hydrolysis</i>	226
6.2.3.1	<i>Structural changes of PU CE and PUI during alkaline hydrolysis</i>	227
6.2.4	<i>Effect of Modified Nanoclay (Cloisite 30b) on the Rate of Alkaline Hydrolysis, (PU PR30, PU CE30 and PUI 30)</i>	228
6.2.4.1	<i>Structural changes of PU PR30, PU CE30 and PUI 30 during alkaline hydrolysis</i>	228
6.2.4.2	<i>Effect of Additives on Crystallinity during Alkaline Hydrolysis (PU PR30, PUI 30 and PU CE30)</i>	229
6.2.5	<i>Susceptibility to soil degradation of Polyurethane Samples PUI and PU CE (Effect of Additives)</i>	229
6.2.5.1	<i>Structural changes during soil burial at 50°C in PUI and PU CE monitored by FTIR-ATR</i>	230
6.2.5.2	<i>Structural changes during soil burial at RT after 20 months in PUI and PU CE monitored by FTIR-ATR</i>	231
6.2.6	<i>Susceptibility to soil degradation of Polyurethane Samples PU PR30, PU CE30 and PUI 30 (Effect of Modified Nanoclay, Cloisite 30b)</i>	231
6.2.6.1	<i>Structural changes during soil burial at 50°C in PU PR30, PU CE30 and PUI 30 monitored by FTIR-ATR</i>	232
6.2.6.2	<i>Structural changes during soil burial at RT after 20 months in PUI and PU CE monitored by FTIR-ATR</i>	232
6.2.7	<i>Susceptibility of Polyurethane Samples PUI and PU CE (Effect of Additives) towards enzymatic degradation</i>	233

<i>Chapter</i>	<i>Title</i>	<i>Page</i>
6.2.8	<i>Susceptibility of Polyurethane Samples PU PR30, PU CE30 and PUI 30 (Effect of Modified Nanoclay Cloisite 30b) towards enzymatic degradation</i>	234
6.3	<i>Discussion</i>	234
6.3.1	<i>Effect of Cellulose and Iron Stearate as Additives on Polyurethane Degradation and Biodegradation</i>	234
6.3.2	<i>Effect of Cloisite 30b on Polyurethane Degradation and Biodegradation</i>	238
6.2.3	<i>Overall Summary of the effect of different additives on Polyurethane Degradation and Biodegradation</i>	241
7	<i>Conclusions and Further Work</i>	283
7.1	<i>Conclusions</i>	283
7.2	<i>Recommendations for Further Work</i>	288
	<i>References</i>	290

List of Figures

<i>Figure</i>	<i>Title</i>	<i>Page</i>
<i>Chapter 1 Introduction</i>		
1.1	<i>Polyurethane Market and Applications</i>	26
1.2	<i>Phase Separation in Polyurethanes</i>	34
1.3	<i>Hydrogen Bonding Interactions in Polyurethanes</i>	34
1.4	<i>Synthesis of Polyurethane</i>	35
1.5	<i>Side Reactions which may Occur During Polyurethane Synthesis</i>	36
1.6	<i>Mechanism of Alkaline Hydrolysis of Ester and Amide Bonds in Polyurethane</i>	38
1.7	<i>Process of Enzymatic Degradation of Polyurethanes</i>	39
1.8	<i>Chemical Structure of Cellulose</i>	43
1.9	<i>Structure of a Two Layered Silicate</i>	44
<i>Chapter 2 Experimental and Analytical Techniques</i>		
2.1	<i>PU plaque and pellet samples provided by Eurothane Ltd</i>	53
2.2	<i>FTIR spectra of reactants used in PU synthesis (A) butane diol NaCl plate, (B) 4,4, - Methylene diisocyanate CCl₄ (C) H₁₂MDI</i>	62
2.3	<i>FTIR spectra of Polyols for PU ADP and PU PCL (A) Polyethylene adipate (B) Polycaprolactone</i>	63
2.4	<i>FTIR spectra of additives used in PU synthesis (A) Iron stearate (B) Cellulose powder (C) Cloisite 30B</i>	64
2.5	<i>Quantification of thermal stability of PU samples using DTGA curve</i>	65
2.6	<i>Thermograms of PU samples at heating rates of 20°C/min and 100°C/min</i>	65
2.7	<i>Determination of hard segment and soft segment transitions in PU samples</i>	66
2.8	<i>Determination of ΔH for hard segment and soft segment transitions in PU samples</i>	66
2.9	<i>Photographic Images of soil type 1 Rothamsted Institute (A) and soil type 2 Castle Bromwich (B)</i>	69

Figure	Title	Page
2.10	<i>Soil burial experiment at RT (A) and 50°C (B)</i>	70
2.11	<i>Calculation of peak heights during degradation by FTIR-ATR</i>	73
2.12	<i>Worked example of peak height changes during degradation by FTIR-ATR</i>	74

Chapter 3 Effect of Polyurethane Method of Synthesis on Degradation and Biodegradation

3.1	<i>Hydrophilicity of PU samples determined by weight percentage increase of water uptake</i>	100
3.2	<i>Chemical structure characterisation of PU samples PU ADP (A), PU PR (B), PU 98 (C) by FTIR-ATR</i>	101
3.3	<i>TGA thermal analysis characterisation of PU, PU ADP (A), PU PR (B), PU 98 (C)</i>	102
3.4	<i>Morphological characterisation of PU ADP (A), PU PR (B), PU 98 (C) showing Tg and endotherms relating to hard and soft segments</i>	103
3.5	<i>Schematic representation of hard and soft segment domains in TPU</i>	104
3.6	<i>Effect of Method of Synthesis on the rate of hydrolytic degradation with 10% NaOH (aq) (A) (see table 2.1 & 2.2 pg. for acronyms). Visual surface cracking (B)</i>	105
3.7	<i>Optical microscopic images of PU ADP, PU PR & PU 98 during alkaline hydrolysis</i>	106
3.8	<i>Photographic Images of PU ADP, PU PR & PU98 during hydrolytic degradation with 10% NaOH (aq)</i>	107
3.9	<i>Structural changes of NH and CH₂ bonds during alkaline hydrolysis of PU ADP, PU PR & PU 98 by FTIR/ATR</i>	108
3.10	<i>Structural changes of C=O and C-O-C urethane and ester linkages during alkaline hydrolysis of PU ADP, PU PR & PU 98 by FTIR/ATR</i>	109
3.11	<i>Changes in crystallinity during alkaline hydrolysis of Group 1 PU samples</i>	110
3.12	<i>Changes in thermal stability after alkaline hydrolysis of Group 1 PU samples</i>	111
3.13	<i>Effect of Method of Synthesis on the rate of biodegradation under soil burial conditions, soil 1 50°C (A), soil 1 RT (B), soil 2 RT (C)</i>	112

Figure	Title	Page
3.14	<i>Photographic images of PU ADP, PU PR & PU 98 during soil burial</i>	113
3.15	<i>Optical microscopic images of PU ADP, PU PR & PU 98 during soil burial</i>	114
3.16	<i>Effect of method of synthesis on C=O and C-O-C ester/urethane linkages during soil burial at 50°C of PU ADP, PU PR & PU 98 by FTIR/ATR</i>	115
3.17	<i>Effect of method of synthesis on N-H and CH groups in PU during soil burial at 50°C of PU ADP, PU PR & PU 98 by FTIR/ATR</i>	116
3.18	<i>Effect of method of synthesis on C=O, C-O-C ester/urethane linkages and NH and CH₂ groups after 20 months soil burial at RT of PU ADP, PU PR & PU 98 by FTIR/ATR</i>	117
3.19	<i>Effect of method of synthesis on morphology changes during biodegradation in soil at RT and 50°C of PU ADP, PU PR & PU 98.</i>	118
3.20	<i>Effect of method of synthesis on enzymatic degradation by Lipase Aspergillus Niger PU ADP, PU PR & PU 98 by optical microscope images</i>	119
3.21	<i>Effect of method of synthesis on structural changes during enzymatic degradation by Lipase Aspergillus niger and Rhizopus sp. on PU ADP, PU PR & PU 98 determined by FTIR-ATR</i>	120
3.22	<i>Effect of method of synthesis on enzymatic degradation by Protease Rhizopus sp. of PU ADP, PU PR & PU 98 by optical microscope images</i>	121
3.23	<i>Effect of method of synthesis on structural changes during enzymatic degradation by protease Rhizopus sp. on PU ADP, PU PR & PU 98 determined by FTIR-ATR</i>	122
3.24	<i>Mechanism of hydrolytic degradation of ester bonds and amide bonds contained in PU structure</i>	123
3.25	<i>Showing the effect of the method of synthesis on PU crystallinity</i>	124
3.26	<i>Effect of hydrolytic degradation on the hard and soft PU segments quantified by FTIR-ATR</i>	125
3.27	<i>Showing changes in the hard and soft segment of PU during hydrolysis dependant on the method of synthesis.(A) changes in the hard segment crystallinity, (B) thermal stability, (C) changes in the Tg and ester peak at 1159cm⁻¹of the soft segment</i>	126
3.28	<i>Showing changes to the PU samples during soil burial. (A) thermal stability of PU at 50°C, (B) visible comparison of PU with PLA (a polymer known to be biodegradable), (C) changes in crystallintiy of PU samples during soil burial at RT.</i>	127

Figure	Title	Page
3.29	<i>Hydrolysis of ester and amide bonds during enzymatic degradation</i>	128
3.30	<i>Showing changes to PU group 1 samples during enzymatic degradation (A) lipase Rhizopus sp. and Aspergillus niger (B) protease Rhizopus sp.</i>	129
Chapter 4 Effect of Polyurethane Structural Composition on Degradation and Biodegradation; Effect of Isocyanate		
4.1	<i>Hydrophilicity of PU samples determined by weight percentage increase of water uptake</i>	148
4.2	<i>Characterisation of PU samples PU ADP, chemical structure by FTIR-ATR (A), thermal stability by TGA (B), morphology by DSC (C)</i>	149
4.3	<i>Characterisation of PUH ADP, chemical structure by FTIR-ATR (A), thermal stability by TGA (B), morphology DSC (C).</i>	150
4.4	<i>Effect of isocyanate on the rate of hydrolytic degradation (A) with 10% NaOH (aq) (see table 2.1 & 2.2 pg. for acronyms). Visual surface cracking (B)</i>	151
4.5	<i>Effect of isocyanate on Visual changes of PU during hydrolytic degradation with 10% NaOH (aq), determined by optical microscope and photographs</i>	152
4.6	<i>Effect of isocyanate on structural changes of NH and CH₂ bonds during alkaline hydrolysis of PU ADP and PUH ADP by FTIR/ATR</i>	153
4.7	<i>Effect of isocyanate on structural changes of C=O and C-O-C ester/urethane linkages during alkaline hydrolysis of PU ADP and PUH ADP by FTIR/ATR</i>	154
4.8	<i>Changes in crystallinity during alkaline hydrolysis of Group 2 PU samples</i>	155
4.9	<i>Changes in thermal stability after alkaline hydrolysis of Group 2 PU samples</i>	156
4.10	<i>Effect of Isocyanate on the rate of biodegradation under soil burial conditions, soil 1 50°C (A), soil 1 RT (B), soil 2 RT (C)</i>	157
4.11	<i>Photographic and microscopic images of PU ADP & PUH ADP during soil burial</i>	158
4.12	<i>Effect of isocyanate on C=O and C-O-C ester/urethane linkages during soil burial of PU ADP & PUH ADP by FTIR/ATR, (A-D 50°C) (E-H RT)</i>	159
4.13	<i>Effect of isocyanate on enzymatic degradation by Lipase Aspergillus niger and Rhizopus sp. PU ADP & PUH ADP by optical microscope images</i>	160

Figure	Title	Page
4.14	<i>Effect of isocyanate on structural changes during enzymatic degradation by Lipase Aspergillus niger and Rhizopus sp. on PU ADP & PUH ADP determined by FTIR-ATR</i>	161
4.15	<i>Effect of isocyanate on enzymatic degradation by Protease Rhizopus sp. of PU ADP & PUH ADP by optical microscope images</i>	162
4.16	<i>Effect of isocyanate on structural changes during enzymatic degradation by protease Rhizopus sp. on PU ADP & PUH ADP determined by FTIR-ATR</i>	163
4.17	<i>Showing the effect of the isocyanate on hydrogen bonding (A), hydrolysis (B), and soft segment degradation in PU ADP and PUH ADP (C)</i>	164
4.18	<i>Showing the effect of the isocyanate on the rate of biodegradation during soil burial at 50°C and RT, monitored by FTIR-ATR</i>	165
4.19	<i>Showing the effect of the isocyanate on the enzymatic degradation of PU. Enzymatic degradation with lipase from Aspergillus niger (A-B), enzymatic degradtion with protease Rhizopus sp. (C-D). Visible degradation after 24 days immersed in buffer solution containing protease Rhizopus sp. (E-F)</i>	166

Chapter 5 Effect of Polyurethane Structural Composition on Degradation and Biodegradation; Effect of Polyol

5.1	<i>Hydrophilicity of PU samples determined by weight percentage increase of water uptake</i>	197
5.2	<i>Chemical structure characterisation by FTIR-ATR of PU PCL (A), PU PEG (B), PU PGPC (C)</i>	198
5.3	<i>Thermal analysis of PU using TGA; PU PCL (A), PU PEG (B), PU PGPC (C)</i>	199
5.4	<i>Morphology of PU using DSC; PU PCL (A), PU PEG (B), PU PGPC (C)</i>	200
5.5	<i>Effect of polyol on the rate of hydrolytic degradation (A) with 10% NaOH (aq) (see table 5.1 pg. for acronyms). Visual surface cracking (B)</i>	201
5.6	<i>Visual changes of PU during hydrolytic degradation with 10% NaOH (aq), determined by optical microscope</i>	202
5.7	<i>Visual changes of PU during hydrolytic degradation with 10% NaOH (aq), determined by photographic images</i>	203
5.8	<i>Effect of polyol on NH and CH₂ groups during alkaline hydrolysis of PU PCL (A-B), PU PGPC (C-D) & PU PEG (E-F) by FTIR/ATR</i>	204

Figure	Title	Page
5.9	<i>Effect of polyol on C=O and C-O-C ester/urethane linkages during alkaline hydrolysis of PU PCL (A-B), PU PGPC (C-D) & PU PEG (E-F) by FTIR/ATR</i>	205
5.10	<i>Changes in crystallinity during alkaline hydrolysis of PU samples PU PCL (A), PU PEG (B) and PU PGPC (C)</i>	206
5.11	<i>Effect of Polyol on the rate of biodegradation under soil burial conditions, soil 1 50°C (A), soil 1 RT (B), soil 2 RT (C)</i>	207
5.12	<i>Photographic images of PU ADP, PU PCL, PU PEG & PU PGPC during soil burial</i>	208
5.13	<i>Optical microscopic images of PU PCL, PU PEG & PU PGPC during soil burial</i>	209
5.14	<i>Changes in C=O and C-O-C ester/urethane linkages during soil burial at 50°C of PU PCL, PU PEG & PU PGPC monitored by FTIR/ATR.</i>	210
5.15	<i>Changes in N-H and CH₂ ester/urethane linkages during soil burial at RT of PU PCL, PU PEG & PU PGPC monitored by FTIR/ATR.</i>	211
5.16	<i>Changes in C=O and C-O-C ester/urethane linkages during soil burial at RT of PU PCL, PU PEG & PU PGPC monitored by FTIR/ATR</i>	212
5.17	<i>Effect of polyol on morphology changes during biodegradation in soil at RT and 50°C of PU PCL, PU PEG & PUPGPC</i>	213
5.18	<i>Effect of polyol on enzymatic degradation by lipase Rhizopus sp. PU PCL, PU PEG & PU PGPC by optical microscope images</i>	214
5.19	<i>Effect of polyol on enzymatic degradation by lipase Aspergillus niger. PU PCL, PU PEG & PU PGPC by optical microscope images</i>	215
5.20	<i>Effect of polyol on structural changes during enzymatic degradation by Lipase Aspergillus niger and Rhizopus sp. on PU PCL, PU PEG & PU PGPC determined by FTIR-ATR</i>	216
5.21	<i>Effect of polyol on enzymatic degradation by protease Rhizopus sp. PU PCL, PU PEG & PU PGPC by optical microscope images</i>	217
5.22	<i>Effect of polyol on structural changes during enzymatic degradation by protease Rhizopus sp. on PU PCL, PU PEG & PU PGPC determined by FTIR-ATR</i>	218

Figure	Title	Page
5.23	<i>Showing the effect of altering the soft segment from ADP to PCL. (A-B) PU films after alkaline degradation, (C-D) FTIR-ATR peak heights at 1161cm⁻¹ (E-F) crystallinity of PU ADP and PU PCL, (G-H) PU films after 20 months soil burial at RT, (I-J) Changes in crystallinity and soft segment degradation after soil burial.</i>	219
5.24	<i>Showing the effect of altering the soft segment from ADP to PEG. (A-B) PU films after alkaline and soil burial degradation, (C-D) FTIR-ATR peak height changes and soft segment degradation, (E-F) crystallinity of PU ADP and PU PEG, (G) Oxidative degradation mechanism for polyethers, (H) enzymatic degradation</i>	220
5.25	<i>Effect of a PCL/PEG soft segment blend. (A-B) PU films after alkaline and soil burial degradation, (C-D) FTIR-ATR peak height changes at 1161cm⁻¹, (E) Effect of PCL/PEG blend on phase separation, (G) Effect of PCL/PEG blend on PU hydrophilicity, (H-I) Effect of PCL/PEG blend on enzymatic degradation</i>	221
Chapter 6 The Role of Additives on the Degradation and Biodegradation of Polyurethanes		
6.1	<i>Hydrophilicity of PU samples (A) chemical structure characterisation of PU samples PUI (B), PU CE (C), by FTIR-ATR</i>	245
6.2	<i>Microscopic images showing dispersal of cellulose in PU CE (A-B) and iron stearate in PUI (C) in comparison to the control sample PU ADP (D)</i>	246
6.3	<i>TGA thermal analysis characterisation of PU, PU ADP (A), PU CE (B), PUI (C)</i>	247
6.4	<i>Morphology of PU using DSC; PU ADP (A), PU CE (B), PUI (C)</i>	248
6.5	<i>Hydrophilicity of PU samples determined by weight percentage increase of water uptake</i>	249
6.6	<i>Chemical structure characterisation of PU samples PU CE30 (A), PU PR30 (B), PUI 30 (C) by FTIR-ATR</i>	250
6.7	<i>TEM images showing dispersal of Cloisite 30B in PU PR30 (A-B), PU CE30 (C-D) and PUI 30 (E-F)</i>	251
6.8	<i>TGA thermal analysis characterisation of PU, PU PR30 (A), PU CE30 (B), PUI 30(C)</i>	252
6.9	<i>Morphology of PU using DSC; PU PR30 (A), PU CE30 (B), PUI 30(C)</i>	253

Figure	Title	Page
6.10	<i>Effect of additives on the rate of hydrolytic degradation (A) with 10% NaOH (aq) (see table 2.1 & 2.2 pg. for acronyms). Visual surface cracking (B)</i>	254
6.11	<i>Photographic Images of PU ADP, PU CE & PUI during hydrolytic degradation with 10% NaOH (aq)</i>	255
6.12	<i>Optical microscopic images of PU ADP, PU CE & PUI during alkaline hydrolysis</i>	256
6.13	<i>Structural changes of NH and CH₂ bonds during alkaline hydrolysis of PU ADP, PU CE & PUI by FTIR/ATR</i>	257
6.14	<i>Structural changes of C=O and C-O-C urethane and ester linkages during alkaline hydrolysis of PU ADP, PU CE & PUI by FTIR/ATR</i>	258
6.15	<i>Effect of Cloisite 30B on the rate of hydrolytic degradation with 10% NaOH</i>	259
6.16	<i>Photographic and microscopic Images of PU PR30, PU CE30 & PUI 30 during hydrolytic degradation with 10% NaOH (aq)</i>	260
6.17	<i>Structural changes of C=O and C-O-C urethane and ester linkages during alkaline hydrolysis of PU PR30, PU CE30 & PUI 30 by FTIR/ATR</i>	261
6.18	<i>Structural changes of C=O and C-O-C urethane and ester linkages during alkaline hydrolysis of PU PR30, PU CE30 & PUI 30 by FTIR/ATR</i>	262
6.19	<i>Morphology changes after alkaline hydrolysis of PU PR30, PU CE30 & PUI 30 by DSC</i>	263
6.20	<i>Effect of additives, cellulose and iron stearate on the rate of biodegradation under soil burial conditions, soil 1 50°C (A), soil 1 RT (B), soil 2 RT (C)</i>	264
6.21	<i>Photographic images of PU ADP, PU CE & PUI during soil burial</i>	265
6.22	<i>Optical microscopic images of PU ADP, PU CE & PUI during soil burial</i>	266
6.23	<i>Effect of additives cellulose and iron stearate on C=O and C-O-C ester/urethane linkages during soil burial at 50°C of PU CE & PUI by FTIR/ATR</i>	267
6.24	<i>Structural changes of N-H, C=O and C-O-C urethane and ester linkages after soil burial at RT for 20 months of PU CE & PUI by FTIR/ATR</i>	268
6.25	<i>Effect of additive Cloisite 30B on the rate of biodegradation under soil burial conditions, soil 1 50°C (A), soil 1 RT (B), soil 2 RT (C)</i>	269
6.26	<i>Photographic images of PU PR30, PU CE30 & PUI 30 during soil burial</i>	270

Figure	Title	Page
6.27	<i>Optical microscopic images of PU PR30, PU CE30 & PUI 30 during soil burial</i>	271
6.28	<i>Structural changes of C=O and C-O-C urethane and ester linkages after soil burial at 50°C for 3 and 5 months of PU PR30, PU CE30 & PUI 30 by FTIR/ATR</i>	272
6.29	<i>Structural changes of C=O and C-O-C urethane and ester linkages after soil burial after 20 months at RT of PU PR30, PU CE30 & PUI 30 by FTIR/ATR</i>	273
6.30	<i>Effect of additives on enzymatic degradation by Lipase Aspergillus niger PU ADP, PU CE & PUI by optical microscope images</i>	274
6.31	<i>Effect of additives on enzymatic degradation by Lipase Rhizopus sp. PU ADP, PU CE & PUI by optical microscope images</i>	275
6.32	<i>Effect of additives cellulose and iron stearate on structural changes during enzymatic degradation by Lipase Aspergillus niger and Rhizopus sp. on PU ADP, PU CE & PUI determined by FTIR-ATR</i>	276
6.33	<i>Effect of Cloisite 30B on enzymatic degradation by Lipase Aspergillus niger PU PR30, PU CE30 & PUI 30 by optical microscope images</i>	277
6.34	<i>Effect of Cloisite 30B on enzymatic degradation by Lipase Rhizopus sp. PU PR30, PU CE30 & PUI 30 by optical microscope images</i>	278
6.35	<i>Effect of Cloisite 30B on structural changes during enzymatic degradation by lipase Aspergillus niger and Rhizopus sp. on PU CE30, PU PR30 & PUI 30 determined by FTIR-ATR</i>	279
6.36	<i>Effect of cellulose and iron stearate on hydrogen bonding in PUs</i>	280
6.37	<i>Effect of Cloisite 30B on hydrogen bonding in PUs</i>	281
6.38	<i>Effect of Cloisite 30B on hydrogen bonding in PUs</i>	282
6.39	<i>Effect of organoclays on the rate of enzymatic degradation</i>	282

List of Tables

<i>Table Title</i>	<i>Page</i>
<i>Chapter 1 Introduction</i>	
1.1 <i>Common Reactants used in TPU Synthesis</i>	33
1.2 <i>Fungi shown to degrade Polyurethane</i>	41
1.3 <i>Test Methods previously used for Assessing Degradation and Biodegradation of Polyurethane</i>	49
<i>Chapter 2 Experimental and Analytical Techniques</i>	
2.1a <i>Chemical composition of PU samples without additives used in this study</i>	54
2.1b <i>Chemical composition of PU samples with additives used in this study</i>	55
2.2 <i>Film Pressing Conditions for Polyurethane Samples</i>	56
2.3 <i>Chemical Structure of Solvents</i>	56
2.4 <i>Solubility of PU Samples at RT</i>	57
2.5 <i>Characterisation of PU chemical structure by FTIR-ATR</i>	61
2.6 <i>Buffer solution compositions for enzymatic hydrolysis</i>	68
2.7 <i>Arbitrary assessment of visible degradation during testing</i>	76
<i>Chapter 3 Effect of Polyurethane Method of Synthesis on Degradation and Biodegradation</i>	
3.1 <i>Effect of Method of synthesis on PU Degradation</i>	98
3.2 <i>Effect of method of synthesis on morphology of PU characterised by DSC</i>	98
3.3 <i>Effect of chemical hydrolysis on morphology of PU characterised by DSC</i>	99
3.4 <i>Effect of soil burial on morphology of PU characterised by DSC</i>	99
<i>Chapter 4 Effect of Polyurethane Structural Composition on Degradation and Biodegradation; Effect of Isocyanate</i>	
4.1 <i>Effect of Isocyanate on PU Degradation</i>	146
4.2 <i>Effect of isocyanate on morphology of PU characterised by DSC</i>	147

Table Title	Page
4.3 Effect of chemical hydrolysis on morphology of PU characterised by DSC	147
4.4 Effect of soil burial on morphology of PU characterised by DSC	147
Chapter 5 Effect of Polyurethane Structural Composition on Degradation and Biodegradation; Effect of Polyol	
5.1 Effect of Polyol on PU Degradation	195
5.2 Effect of polyol on morphology of PU characterised by DSC	195
5.3 Effect of chemical hydrolysis on morphology of PU characterised by DSC	196
5.4 Effect of soil burial on morphology of PU characterised by DSC	197
Chapter 6 The Role of Additives on the Degradation and Biodegradation of Polyurethanes	
6.1a Effect of Additive on PU Degradation	242
6.1b Effect of Additive Cloisite 30B on PU Degradation	243
6.2 Assignment of N-H and C=O bands, area % of deconvoluted peaks	244

Abbreviations

ADP	Polyethylene Adipate
ATR	Attenuated Total Reflectance
BD	Butane Diol
DSC	Differential Scanning Calorimetry
FTIR	Fourier Transform Infrared
HDI	Hexamethylene Diisocyanate
H₁₂MDI	Dicyclohexylmethane -4,4-diisocyanate
IPDI	Isophrone Diisocyanate
LDPE	Low Density Polyethylene
MDI	Methylene Diphenyl Diisocyanate
PE	Polyethylene
PCL	Polycaprolactone
PEG	Polyethylene Glycol
PLA	Polylactic Acid
PU	Polyurethane
TDI	Toluene Diisocyanate
TGA	Thermogravimetric Analysis
TPU	Thermoplastic Polyurethane

Chapter 1

Introduction

1.1 Biodegradable Polymers

The increased production of synthetic polymers, along with greater durability and stability of these materials, has resulted in an abundance of polymeric waste being deposited into the environment. With ecology concerns at the forefront of many industrial processes globally, the pursuit of these materials being environmentally friendly is an ever important area of research and development. The focus of many current areas of investigation to solve these problems is by modification of polymeric materials to include biodegradability, and ultimately to produce materials with controlled life spans.

Biodegradation can be defined as a natural process by which organic chemicals in the environment are converted to simpler compounds, mineralized and redistributed through elemental cycles such as the carbon, nitrogen and sulfur cycles [1]. The biodegradation of polymeric materials is a complex process in which various factors may contribute, and can include; polymer characteristics, type of organism, and nature of pre-treatment. The polymer characteristics such as its mobility, tacticity, crystallinity, molecular weight, the type of functional groups and substituents present in its structure, and plasticizers or additives added to the polymer all play an important role in its degradation [2]. Considerable research has been done on biodegradation of natural polymers such as starch and cellulose, and commercially large -scale produced synthetic polymers, such as, PE and polyesters such as PLA and PCL [3-11]. However, less attention has been given to some commercially smaller scale polymers, one of which is polyurethane.

1.2 Polyurethane Background

Polyurethanes are a unique class of polymers which can be defined as such by the presence of a urethane group on the macromolecular chain. They are produced by the polyaddition reaction of a diisocyanate, a macromolecular diol and a short chain diol, and therefore can

involve an almost unlimited number of structures. This in turn can produce materials suitable for numerous functions. The vast array of polyurethane applications continues to grow as industries require deliverables with highly specific requirements such as life span, flexibility, hardness, strength and elasticity. These industrial needs can be met by this exceptional polymer, which can be tailor made by altering the three molecular constituents accordingly. Polyurethanes can be synthesised under many guises **Fig. 1.1**, and it is the class of polyurethanes known as elastomers which will be investigated in this research. Thermoplastic polyurethane elastomers (TPU) are flexible, elastic materials which can provide numerous physical property combinations and can be adapted to many applications such as construction, automotive and footwear, **Fig 1.1** [12, 13].

Although PU is a specialised polymer, the market for this material is set to increase over the years. The global polyurethane market was estimated at 13.65 million tons in 2010 and revenue market estimated to be worth \$33 million, **Fig 1.1** [14]. These figures are expected to rise to 18 million tons, with a predicted revenue of \$55.5 million by 2016 [14]. Similar to the case of other polymers such as LDPE (Low Density Polyethylene), bio-based raw materials and biodegradable materials present significant opportunities for the polyurethane industry, as they present an option of exploring new applications, especially in highly regulated markets such as the U.S. and Europe [14]. Therefore bio-based or 'green' polyurethanes are expected to be a critical part of the industry in the coming years, and the work presented in this thesis will focus on TPU for a very specific agricultural application which requires biodegradability after its useful lifespan. This aim was achieved by a two stage strategy. First by examining each constituent of TPU formulations to determine the effect each component has on the degradation and biodegradation of the polymer, and the second strategy was to increase the rate of degradation and biodegradation by the use of additives. In order to achieve this, each of the components in the TPU polymer was examined in detail and then the effect of each of the constituents on the properties of the TPU was determined, in order to design the required material. Therefore the subsequent sections in this introduction will give an insight into the molecules which make up TPU, and the effect of altering each constituent on the biodegradation of TPU. This will then be followed by an overview of the mechanisms involved in biodegradation, and the test methods used to monitor and measure both degradation and biodegradation, highlighting some of the criteria and limitations when selecting these test methods.

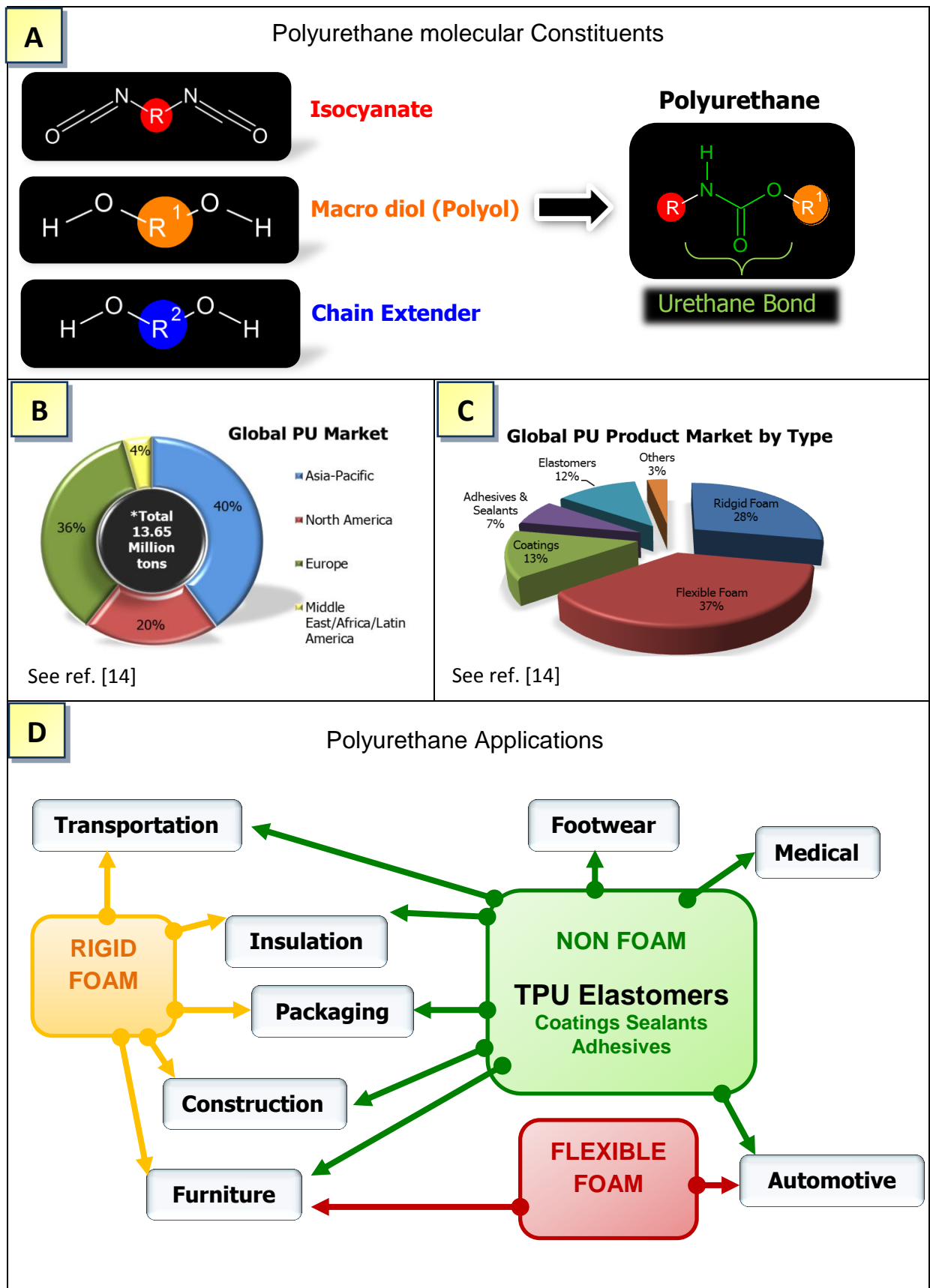


Figure 1.1 Polyurethane Market and Applications

1.3 Polyurethane Elastomer Chemistry

“The mere presence of others dramatically changes our behaviour” (anonymous)

Three essential components are required for the production of polyurethane elastomers, and the interactions between these components has a considerable effect on the properties of the final material, **Fig 1.1**. The choice of isocyanate, chain extender and polyol greatly influence the morphology and ultimately nature of the material. Therefore, each component will be discussed in relation to the hard and soft segment interactions, morphology and final material properties.

1.3.1 Effect of Isocyanates on Polyurethane Properties

Isocyanates are molecules which contain at least two isocyanate (NCO) groups, and are one of the components which make up what is known as the ‘hard segment’ in PUs, the other being the chain extender. A wide variety of isocyanates are available commercially, the most important being toluene diisocyanate (TDI), and methylene diisocyanate (MDI), see **Table 1.1**. Other commercially important isocyanates are; the aliphatic hexamethylene diisocyanate (HDI), isophrone diisocyanate (IPDI) and 4,4- dicyclohexyl diisocyanate (H_{12} MDI), see **Table 1.1**.

These compounds affect inter-chain interactions by hydrogen bonding, and consequently affect the mechanical properties of TPUs, for example aromatic diisocyanates give rise to rigidity and steric hindrance thus, increasing the mechanical properties such as modulus, tear and tensile strengths, however, their oxidative and ultraviolet stability is lower than aliphatic isocyanates [12, 13, 15]. The symmetry of isocyanates can also affect the final PU properties with bulky aromatic isocyanates, such as MDI with a symmetrical molecular structure, yielding final products with higher modulus and hardness, due to the formation of highly organised structures, however, asymmetrical isocyanates such as TDI yield elastomers with low modulus and hardness.

Some limited research has been performed on altering the isocyanate structure in TPU formulations in order to increase their biodegradability. An example of this was work undertaken by Hettrich and Becker [16], who synthesised isocyanates based on mono amino acids, these isocyanates contained ester linkages within the backbone, and were seen to hydrolytically degrade, however the degradation was slow, and the mechanical properties of synthesised PUs using these isocyanates were inferior to those containing MDI isocyanates [16]. However, in other work a PU was synthesised with an isocyanate based on L-lysine which was found to exhibit comparable mechanical properties to PUs synthesised with more

common isocyanates, and these PUs were considered to be biodegradable due to the combination of the PCL soft segment and the L-Lysine based isocyanate contained in the hard segment [17].

1.3.2 Effect of Polyols on Polyurethane Properties

The second component involved in TPU sysnthesis is the polyol or diol; a long chain molecule which can be bi-functional or of a greater functionality which contains either hydroxyl (OH) groups to produce urethane linkages or amine (NH₂) groups to produce urea linkages. These polyols form what is known as the ‘soft segment’ component of TPU.

Polyether and polyester diols are commonly employed in the synthesis of TPUs, and some of the most widespread are; poly(oxyethylene) diol poly(oxytetramethylene) diol, poly(ϵ -caprolactone) diol (PCL), poly(ethylene adipate) diol (PEA) and poly(butylene adipate) [18], with molecular weights usually between 1000 to 3000 [12, 18]. Choice of diol can affect the final properties of the PU greatly, and previous studies have shown polyester diols to confer higher tensile strength and hardness to PUs than those synthesised with polyether diols, due to the increased polarity of the ester carbonyl group which leads to stronger hydrogen bonds between the hard and soft segments [18]. However, polyester polyols are susceptible towards hydrolysis, whereas polyether polyols have generally been shown to be resistant towards hydrolysis [19].

It is not only the diols themselves which can affect the properties of PUs but also their molecular weight. A recent study in which PU was prepared using PCL and PEG polyols found that the molecular weight of the diols in the soft segment affected the water absorption properties of the PU; as the molecular weight of PEG increased, the water absorption of the polyurethane was enhanced dramatically [12]. Conversely, it was shown that an increase in molecular weight of PCL in the soft segment resulted in a decrease in water absorption ability [12]. Higher molecular weight polyols also result in PUs with increased elastic properties [20]. However, previous research has found that for some polyols, such as PEG and PEA an increase in molecular weight decreases hardness and tensile strength [20], therefore end use properties of the final product must be considered before choosing the type and molecular weight of a polyol to obtain the appropriate chemical, physical and mechanical properties, and designing a biodegradable PU is no different in this respect.

Numerous reports in the literature have shown PU to be somewhat susceptible towards degradation by fungi [21-24], and fungal biodegradation has been shown to be dependent on the soft segment structure of PU, with polyester diols being more susceptible towards degradation by fungi than PUs synthesised with polyether diols [25]. However, polyether

diols are known to be biodegradable, dependant on the polymer chain length, with molecular weights less than 1000 proving to be biodegradable [26]. However, the mechanisms by which polyethers degrade are different to that of polyesters. Polyether degradation occurs mainly by oxidative-mediated processes [27, 28], although some fungi and bacteria have been shown to degrade ether linkages by enzymatic means [29]. Also, many of the diols used in PU synthesis, such as PCL and PLA, are deemed to be ‘biodegradable’, and as such, have previously been incorporated into PU in an attempt to increase biodegradability [3, 6, 30-32]. Hydrophilicity has been shown to influence biodegradability of PUs and the addition of hydrophilic polyols such as PEG has been shown to increase the rate of degradation [33]. Therefore the choice of polyol is of paramount importance with respect to biodegradation.

1.3.3 Effect of Chain Extenders on Polyurethane Properties

The last of the three components used to synthesise TPU is the chain extender, and along with the diisocyanate forms the ‘hard segment’. The chain extender is usually a short chain molecule terminated with two hydroxyl groups (OH) known as a diol. The most common chain extender used commercially is butane-1,4- diol, although other diols such as hexane-1,6- diol, ethylene glycol and ethylene amine can be used, **Table 1.1**.

The structure and nature of the chain extender can result in alteration of the packing arrangement of the hard segment, which ultimately influences the crystallinity, thermal stability and mechanical properties of the polymer. For example, PUs with increased mechanical properties can be produced by the use of diamines due to the urea linkages formed which result in strong hydrogen bonding interactions [13, 34]. Specific mechanical properties can also be obtained by selection of the diol. For example, bulky diols produce elastomers with a high modulus. The number of methylene groups of the diol has also been shown to affect the modulus and tensile strength. Two to four methylene groups result in an increase in modulus and tensile strength, however, three and six methylene groups on the chain extender have been shown to decrease the modulus and tensile strength, **Table 1.1** [13, 34]

Modification of the hard segment by altering the isocyanate and chain extender to increase biodegradation has not been explored to the same extent as that of modification of the soft segment polyols, although some notable research has focused on the incorporation of amino acid-based chain extenders, and chain extenders containing phosphate ester groups in order to increase degradation and biodegradation of PUs [35, 36]. This research showed that both the amino acid chain extender and the chain extender containing phosphate ester groups conferred increased biodegradability to the PUs. However, the alteration of the chain

extender has also been shown to decrease bacterial adhesion to PU, when glycerophosphorlcholine was incorporated as a chain extender [37], thereby reducing degradation, and thus results from previous research have shown that it is not only the chemical components themselves which are important to obtain the properties required of a TPU, but also the interactions between the chemical constituents which produce the unique morphology of TPUs.

1.3.4 Polyurethane Morphology; Phase Separation and Hydrogen Bonding

The distinctive properties associated with polyurethanes are due to the complex morphology of the material. Polyurethanes are microphase separated materials consisting of a ‘hard segment’ (isocyanate and chain extender) and a ‘soft segment’ (polyol), and it is the interactions between these segments which produce PUs with very different properties. The ‘soft’ segment is said to confer elastomeric properties, while the ‘hard’ segment provides the physical strength and crosslinking, and therefore influences the tensile strength properties. Essentially, microphase separation occurs due to thermodynamic incompatibility between the polar high melting point hard segments, and the mainly non-polar low melting soft segments [12, 34]. The compatibility or incompatability between the hard and soft segments depends on many factors, and the extent of microphase separation is a parameter known as the degree of phase separation. A schematic representation of a phase separated and a phase mixed PU system is given in **Fig. 1.2**.

Polyol chemical composition and molecular weight have been shown to influence the degree of phase separation. For example, polyetherurethanes have been shown generally to be more phase separated than polyesterurethanes, due to stronger interactions between the ester and urethane groups than between the ether and urethane groups [38], and higher molecular weight polyols have also been found to decrease the phase separation [39]. Previous studies have also shown the phase separation to be influenced by the chemical constituents of the hard segment, and work by Kang and Stoffer showed that PUs synthesised with aliphatic isocyanates exhibited a lower degree of phase separation than PUs synthesised with aromatic isocyanates [40]. However, in contrast to this, PUs synthesised with HDI and MDI were compared, and the aliphatic HDI resulted in increased phase separation [41].

Another important factor which influences the degree of phase separation is that of hydrogen bonding. Hydrogen bonding in PUs occurs between the hydrogen atom on the N-H urethane group and the carbonyl oxygen of the C=O ester linkage (ester soft segment), or the alkyl ether oxygen atom (ether soft segment) or the carbonyl oxygen atom on the urethane group,

Fig. 1.3. FTIR has been used extensively to determine the degree and nature of hydrogen bonding in PUs [42-44]. The absorbance values for hydrogen bonds are denoted as ‘free’ (non-hydrogen bonded) and hydrogen bonded, the absorbances of which are given in **Fig 1.3.** [41, 43] If hydrogen bonding occurs in the hard segment domains only, then the degree of phase separation was found to increase, whereas, if hydrogen bonding occurs between the hard and soft segments, then the interphase hydrogen bonding increases the extent of phase mixing [12]. The extent and type of hydrogen bonding itself is dependent on material structure, composition and temperature, and numerous studies have examined the effect of isocyanates, chain extenders, polyols and the effect of annealing on hydrogen bonding [45-47]. For example, a study comparing the morphology and properties between two PUs each containing different isocyanates, found that the PU synthesised with the aliphatic HDI had more hydrogen bonding than the PU synthesised with MDI [46]. Another study compared PUs synthesised with a PEG soft segment and a polypropylene glycol soft segment (PPG), and concluded that the PPG soft segment reduced the amount of interphase hydrogen bonding due to the methyl side groups on the chain, in comparison to the PEG soft segment which enhanced interphase hydrogen bonding [47]

Each PU system is individual, and it is not only the chemical components which can affect the degree of phase separation and hydrogen bonding. Previous research has found that the method of synthesis of PU can also affect the morphological properties of PU [48, 49].

1.3.5 Method of Synthesis of Polyurethanes

The synthesis of polyurethane elastomers usually involves one of two processes, the one shot method and the prepolymer method, and each method bestows different morphological profiles on PUs.

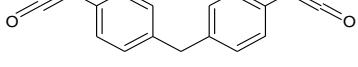
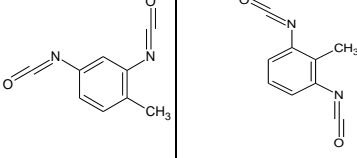
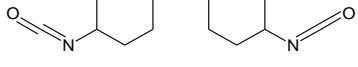
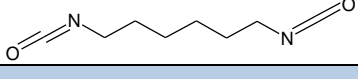
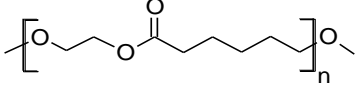
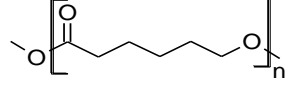
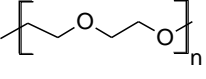
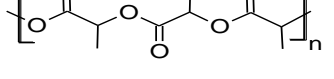
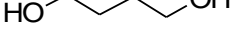
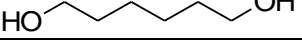
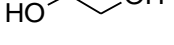
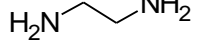
The one-shot method is a one step process and involves the addition of all reactants (polyol, diisocyanate and chain extender) simultaneously in the presence of a catalyst, where the mixture is directly allowed to polymerise, **Figure 1.4** [12, 38, 50]. The method of synthesis can alter the morphology of PUs, with the one shot method resulting in a PU with a higher degree of crystallinity than those synthesised by the pre-polymer method. Studies have shown that this is due to the chain build up during synthesis. During the one shot method a slightly favoured reaction between the chain extender and isocyanate results in the formation of crystalline ordered regions, which are obtained before extended polymer growth occurs with the addition of the polyol [12, 13]. However, as all of the reactants are added together, there is little control over the reaction, with the hard segment chain length being highly

disperse [48], which can result in PUs with inferior mechanical properties to those synthesised by the pre-polymer method. This has been attributed to a higher degree of mixing between the hard and soft segments arising from the greater molecular weight distribution of the hard segments [51]

The prepolymer method is a two step process in which a ‘pre-polymer’ is first formed by reacting the diisocyanate and the polyol to form an intermediate polymer of molecular weight 15,000 – 20,000. The pre-polymer is then converted into the final polyurethane by a further reaction with a diol or diamine chain extender **Fig. 1.4** [12, 38]. The pre-polymer or multi-step method is more controlled than the one shot process and produces fewer side reactions **Fig. 1.5**, and more regular block hard/soft sequence structures, thus imparting superior mechanical properties than those PUs synthesised by the one shot method [12, 52].

In order to design a biodegradable PU the method of synthesis and chemical constituents, and their effect on phase separation, hydrogen bonding and crystallinity needs to be examined as all of these factors affect not only the rate of degradation and biodegradation in PU but also the degradation mechanisms. However, in order to select appropriate chemical constituents, the process of degradation and biodegradation needs to be examined.

Table 1.1 Common Reactants used in TPU Synthesis

Isocyanates	Chemical Structure	PU properties bestowed
MDI		Increases mechanical properties such as modulus, tear and tensile strength Prone to light and UV oxidation
TDI		Lower modulus and hardness due to unsymmetrical nature of isocyanate Prone to light and UV Oxidation
H ₁₂ MDI		Light and UV stable
HDI		Light and UV stable
Polyols		
ADP		Prone to hydrolysis due to ester linkage Less hydrophilic than polyethers Higher tensile strength and hardness than polyethers
PCL		Prone to hydrolysis due to ester linkage Less hydrophilic than polyethers
PEG		Not prone to hydrolysis More hydrophilic than polyesters Higher tensile strength and hardness than polyethers
PLA		Prone to hydrolysis due to ester linkage Less hydrophilic than polyethers Higher tensile strength and hardness than polyethers
Chain Extenders		
1,4 Butane Diol		Increase in modulus and tensile strength
1,6 Hexane Diol		Decrease in modulus and tensile strength
Ethylene Glycol		Increase in hydrophilicity
Ethylene Amine		Increased mechanical properties due to formation of urea linkages

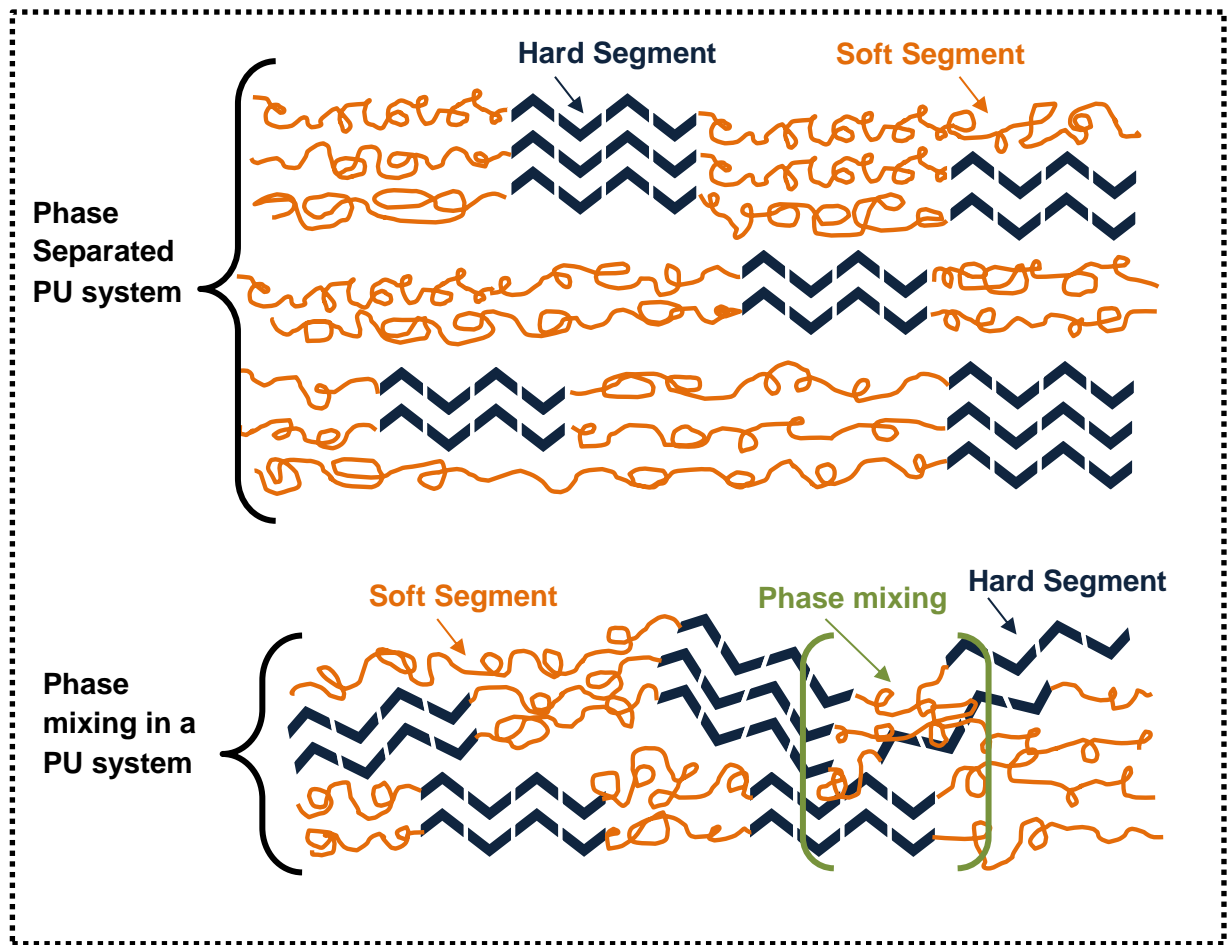


Figure 1.2 Phase separation in Polyurethanes

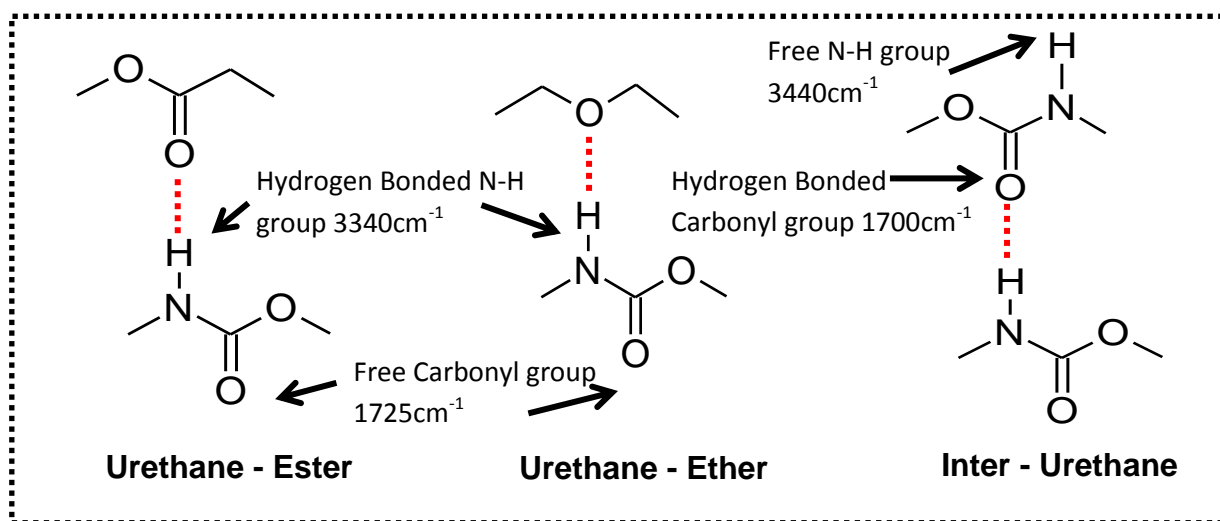


Figure 1.3 Hydrogen bonding interactions in PUs



Figure 1.4 Synthesis of Polyurethane

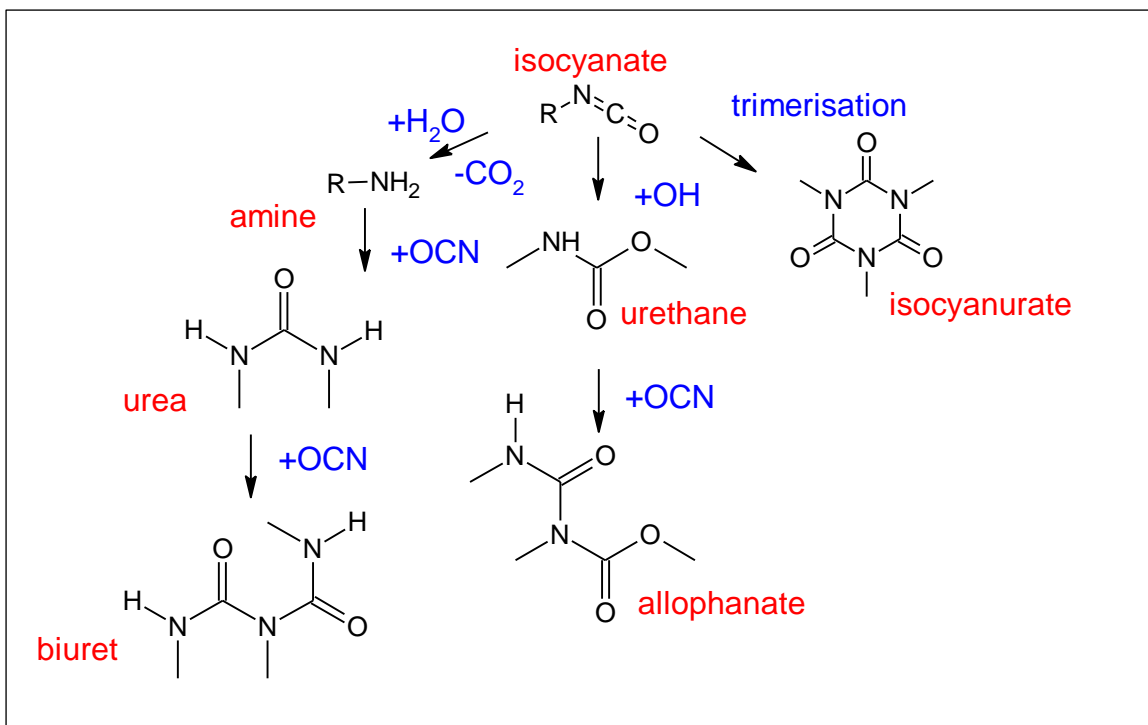


Figure 1.5 Side reactions which may occur during polyurethane synthesis

1.4 Degradation and Biodegradation Processes of Polyurethane

Degradation and biodegradation of polyurethanes can be induced by numerous factors which include, photo, thermal and biological influences, all of which result in changes to the material. These changes can include but are not limited to, mechanical, optical and physical properties, such as surface erosion, discolouration, cracking, phase separation and crystallinity changes [2]. These modifications ultimately result in chemical transformations, bond scission and the formation of a variety of degradation products dependent upon the chemical constituents of the PU. There are numerous mechanisms by which all polymers, including PU, undergo during biodegradation, and some of these processes include; solubilisation, hydrolysis and enzyme-catalysed hydrolysis [53]. The influence of each of these factors on the biodegradation of PU will be discussed below.

1.4.1 Solubilisation and Hydrolysis of Polyurethanes

Solubilisation refers to the hydration properties of a polymeric material and ultimately depends on the hydrophilic nature of the polymer [29]. Hydrophilicity has been shown to influence biodegradability of polyurethane, and the addition of hydrophilic polyols such as PEG has been shown to improve the hydrophilicity and degradation rate of polyurethanes. [26, 33]. Hydration or solubilisation results in the disruption of secondary PU structures such as hydrogen bonding, and this can result in changes to phase separation, and PU morphology, which in turn can result in conformational changes that give rise to an increase in polymer chain hydrolysis reactions [46, 54]. Hydophilicity of PU is dependent on each of the three constituents used, and the choice of initial reactants can either bestow or decrease hydrophilicity. A previous study investigating the surface wettability properties of a variety of PU elastomers, found that small molecular weight aliphatic isocyanates increase PU hydrophilicity, as opposed to aromatic isocyanates [55]. Generally though, it is the soft segment polyols which have been found to bestow hydrophilicity to PUs, and previous studies have shown that an increase in the hard segment content resulted in a reduction of water absorption capacity, a decrease in amorphous regions and hydrophilicity [56], all of which decrease the rate of hydrolysis of the PU.

Chemical hydrolysis in PU is essentially a scission of chemical bonds in the main polymer chains by a reaction with water, and is dependent on a variety of parameters such as, water activity, temperature, pH and time [57, 58]. In order for hydrolysis to take place, hydrolysable bonds must be present in the polymer, which in the case of PUs are usually the urethane groups in the hard segment and, the ester linkages contained in the soft segment (if the soft

segment contains a polyester backbone). Therefore, PUs containing ester diol soft segments are more prone to hydrolytic degradation than their polyether counterparts [25, 27]. A schematic representation of the hydrolysis of ester and urethane bonds under alkaline conditions is given in **Fig. 1.6**. The rate of hydrolytic degradation of PU has previously been shown to be dependent on many factors, however, one of the major influences on this has been shown to be that of PU crystallinity, with an increase in crystallinity resulting in a decrease in the rate of hydrolysis [25, 30, 59]. This is thought to be due to the limited diffusion of water molecules into the bulk, which results in inaccessibility of water molecules to the hydrolysable bonds. Chemical hydrolysis is not the only mechanism by which PUs undergo degradation. When exposed to microorganisms in the environment PUs can also be degraded enzymatically by fungal and some bacterial sources [19, 21, 22].

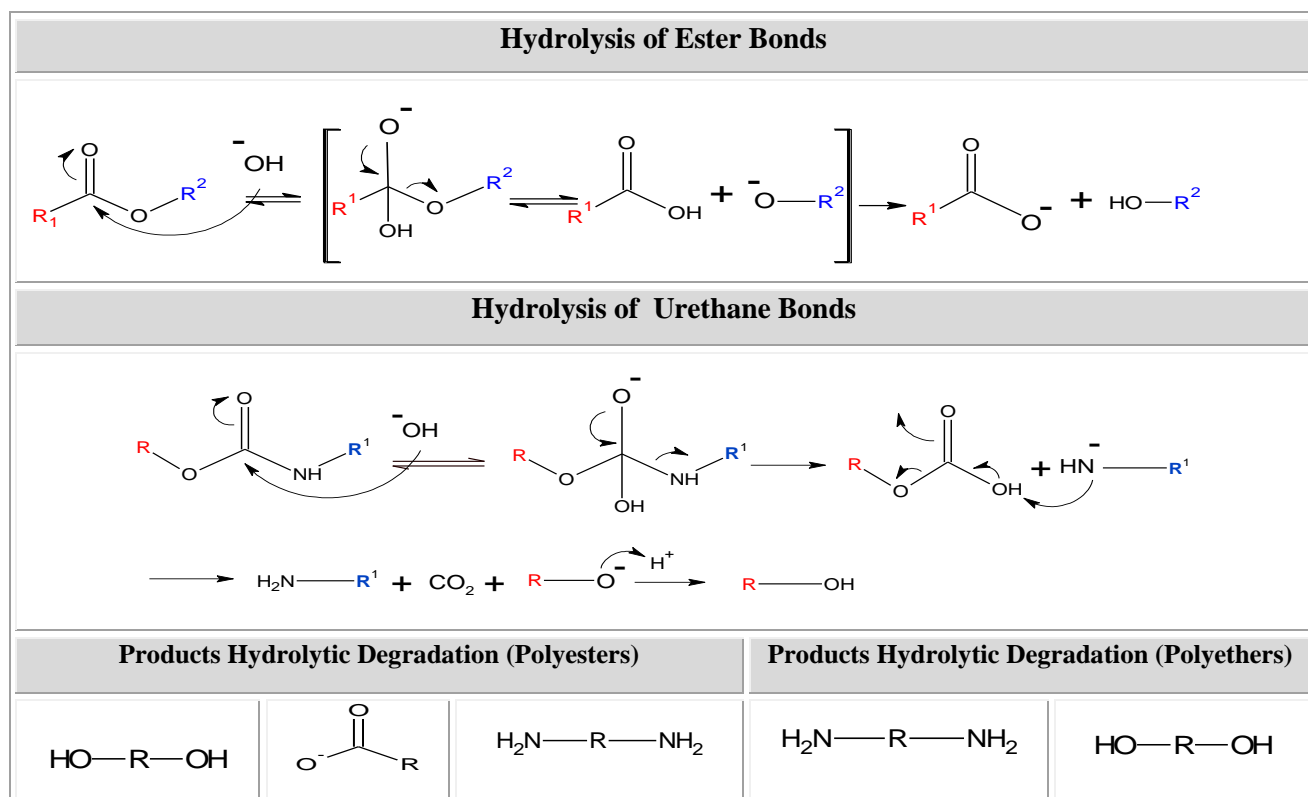


Figure 1.6 Mechanism of alkaline hydrolysis of ester and urethane bonds in PU

1.4.2 Enzymatic Degradation of Polyurethane

Fungi and bacteria degrade polymers and other substrates by enzymatic means. Enzymes are complex three-dimensional protein structures which serve as biological catalysts by lowering the activation energy of a reaction, thereby increasing the reaction rate in environments which would otherwise be unfavourable for chemical reactions [53]. The three-dimensional structure creates an active site where the interaction between the enzyme and

the substrate takes place. Enzymatic degradation is known to occur typically on the surface of polymeric materials, particularly amorphous surface regions, as high molecular weight enzymes cannot easily penetrate the solid bulk. Consequently polymer surface chemistry plays an important role on the rate of enzymatic degradation. Studies have also shown that large amounts of hard segment and crystalline regions results in a reduction in enzymatic activity as of that for chemical hydrolysis [60]. Generally several enzymes working synergistically are involved in polymer degradation, and degradation of PU has been associated with protease and esterase activities from fungi and bacteria along with polyurethanase activity detected in *Bacillus subtilis* strains [61].

The process of enzymatic degradation in PUs has been suggested by numerous authors, and it is generally accepted that degradation occurs in a two stage process by which a membrane-bound enzyme binds to the surface of the PU substrate, and then the urethane/ester bonds are cleaved enzymatically by hydrolysis. It is thought that 'free' enzymes are also released onto the medium, which although are not as efficient at binding to the surface, do contribute to degradation by abrading the surface of PU, thereby increasing contact surface area and roughness which in turn increases microbial adhesion. A mechanistic scheme providing an overview of this process has been given by Cregut et al. and is shown in **Fig.1.7.** [62]

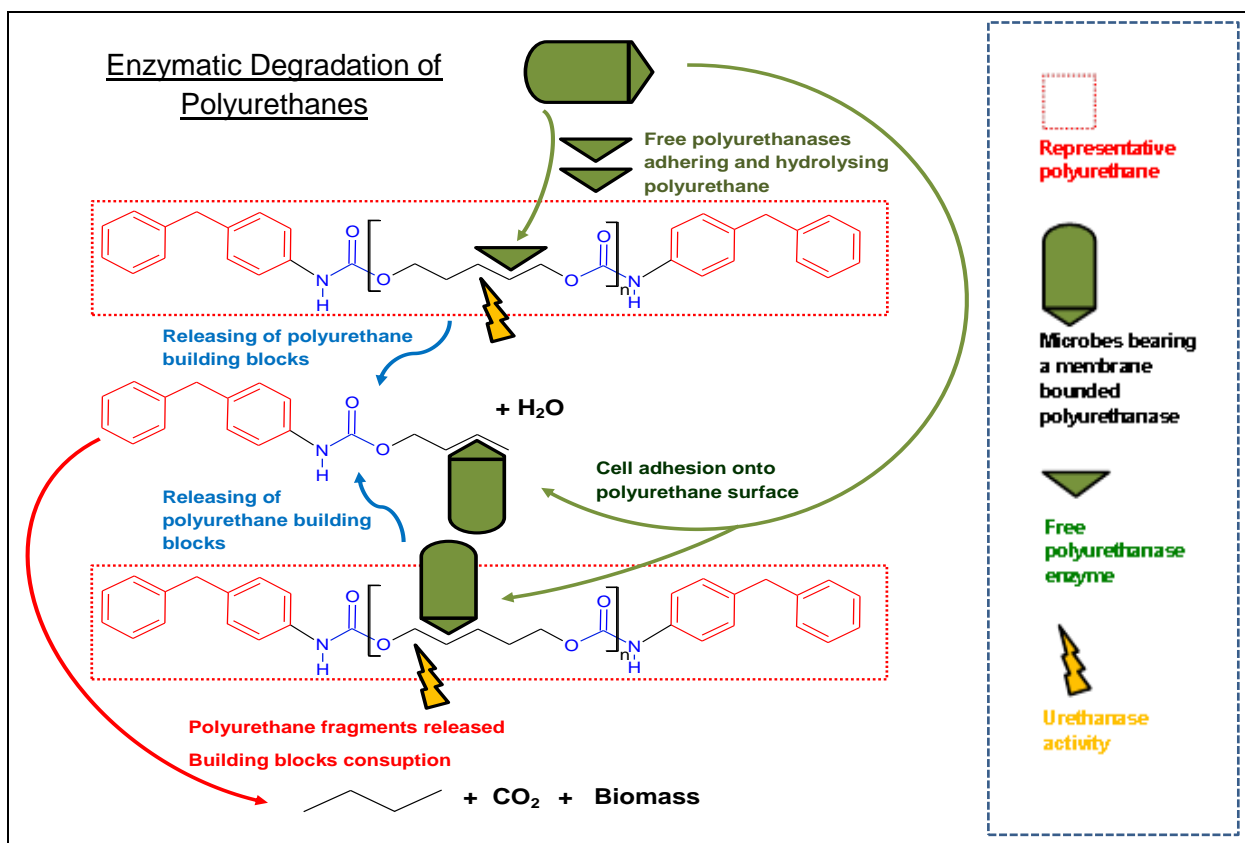


Figure 1.7 Process of enzymatic degradation of PUs

1.4.3 Biodegradation and Degradation of Polyurethane under Composting and Soil Burial Conditions

Composting can be defined as an accelerated natural degradation process that results from placing organic matter into piles or heaps to conserve metabolic heat. It is a controlled complex reaction which involves the oxidation of organic substances to produce a stable, humidified product (**equation 1**), and involves optimizing conditions for effective microbial activity such as oxygen availability, moisture content and temperature [63].



The natural degradation process in compost takes place in soil and can be considered to be synonymous with soil degradation with the exception that degradation rates are higher under composting conditions due to the higher temperatures involved, and as such is a rapid effective method in which to examine the biodegradability of polymers in the natural environment [64].

The degradation of PU under composting conditions and soil degradation are due primarily to enzymatic hydrolysis by microorganisms (**section 1.4.2**). The ester bonds contained within ester-based PU are susceptible to hydrolysis, and studies have shown that fungi have been reported as the main PU degraders, although some strains of bacteria have also been shown to degrade polyurethane, **Table 1.2**.

Attachment of a microorganism to a solid substrate is the first step in a series of events that occur during colonisation of a surface (**section 1.4.2**), and it has generally been found that substrate hydrophobicity is a defining factor on the adhesion of microorganisms onto the substrate [65]. This has also been found to be the case for PUs, and previous studies have shown that in the initial stages of composting/soil burial, microorganisms were shown to yield greater adhesion to polyurethanes with high surface hydrophobicity [57, 64].

The most favourable specifications for maximum degradation of PUs under composting conditions have been shown to be low hard segment content and low crystallinity [26, 64, 66]. There are many factors which can also contribute to the degradability of PU under composting/soil burial conditions, such as compost/soil matter, presence of specific types of microorganisms, their ability to adhere to the surface of the polymer, and raw materials used to synthesis the PU, all of which makes the degradation of PU under composting conditions a very complex process, and therefore many methods have been examined in order to increase biodegradation of polymers, one of which is the incorporation of additives.

Table 1.2 Fungi known to degrade polyurethane

Fungi	PUR	Ref	Fungi	PUR	Ref
<i>Alternaria</i> sp.	PUS	[22]	<i>Gliocladium roseum</i>	PS	[19]
<i>Aspergillus niger</i>	PS,PE	[19]	<i>Nectria</i> sp.	PUS	[22]
<i>A. flavus</i>	PS,PE	[19]	<i>Nectria gliocladiooides</i>	PS	[21]
<i>A. fumigatus</i>	PS	[19]	<i>Neonectria ramulariae</i>	PUS	[22]
<i>A. versicolor</i>	PS,PE	[19]	<i>Penicillium citrinum</i>	PS	[19]
<i>Aureobasidium pullulans</i>	PS,PE	[19]	<i>Penicillium inflatum</i>	PUS	[22]
<i>Chaetomium globosum</i>	PS	[19]	<i>Penicillium ochrochloron</i>	PS	[21]
<i>Cladosporium</i> sp.	PS,PE	[19]	<i>Penicillium venetum</i>	PUS	[22]
<i>Curvularia senegalensis</i>	PS	[19]	<i>Penicillium viridicatum</i>	PUS	[22]
<i>Cylindrocladiella parva</i>	PUS	[22]	<i>Plectosphaerella cucumerina</i>	PUS	[22]
<i>Fusarium solani</i>	PS	[19]	<i>P. funiculosam</i>	PS,PE	[19]
<i>Geomyces pannorum</i>	PUS	[22],[21]	<i>Trichoderma</i> sp.	PS,PE	[19]

PS- polyurethanes synthesised with polyesters, PE – polyurethanes synthesised with polyethers,
PUS – no specifications of soft segment.

1.5 The use of Additives to Increase Degradation and Biodegradation

Polymer additives encompass a vast range of chemical compounds that are added, during or after polymerisation and/or during processing, and are added for numerous reasons, and are dependant on many factors including; polymer type, processing conditions, life expectancy of the polymer and conditions to which the polymer is exposed to during its lifetime [67, 68]. The array of different types of additives is vast and includes but is not limited to; antioxidants, plasticizers, flame retardants, colourants, lubricants and fillers [67, 69]. Generally, additives are added to a polymer system to either enhance or alter the physical or mechanical properties of a polymer or to help prevent polymer degradation [69, 70] however, additives have also been used to increase polymer degradation and biodegradation [5, 71-73].

For example, previous studies incorporated iron stearate and other iron complexes as well as calcium stearate into polyethylene and polypropylene films [9, 10, 74-76]. The additives were seen to act as pro-oxidants and increased the rate of oxidative degradation of the polyethylene films.

Much research has also been undertaken where natural polymers have been used as additives in the hope of increasing biodegradation, and this approach includes many biopolymers such as chitin, cellulose and starch. Many of these biopolymers are large carbohydrate molecules known as polysaccharides, and are often one of the main structural elements of plants (cellulose) and animal exoskeletons (chitin), or play a major role in plant energy storage (starch). Previous research has examined the incorporation of biopolymers into polymer systems for a variety of reasons including improvement of mechanical and physical properties [77, 78]. However, the study reported in this thesis is concerned with the investigation of the use of different additives into PUs in order to potentially increase its degradation/biodegradability. Many of the biopolymers mentioned above have also been investigated as a means to increase biodegradation [4, 5]. For example, in a recent study starch was incorporated into a waterborne PU, where it was found that the addition of the starch had altered the morphology of the PU, increasing the amorphous domains within the PU and thereby increasing its degradation [79]. Chitin has also been previously examined for the purpose of increasing degradation of PUs, where it was incorporated into a PU backbone synthesised with PCL and MDI [78]. It was found that the addition of chitin not only increased the thermal stability of the PU, but also increased the rate of its degradation [78], however one of the more investigated polysaccharide biopolymers for use as an additive in polymers is cellulose [72, 80-82].

Cellulose is a linear macromolecule which consists of D-glucose units linked by $\beta(1\text{-}4)$ glycosidic bonds, **Fig.1.8**. Cellulose is seen as one of the most abundant organic substances in nature with it being the most abundant component of plant biomass [83]. Cellulose is crystalline in nature, forming intra and inter hydrogen bonding between the three hydroxyl groups situated on each glucose unit. Many microorganisms have been shown to degrade cellulose, utilizing a multitude of enzymes all working together synergistically [84], and numerous fungal and bacterial species have been shown to degrade cellulose and cellulosic material [84, 85]. In light of the biodegradability of this material, previous studies have shown that the addition of cellulose into polymer systems can increase the rate of degradation [81, 82]. However, many factors can affect degradation, and an investigation into the addition of cellulose fibres into polyethylene films concluded that the addition of 5-15% cellulose had limited effect on the rate of biodegradation of the films, but when the concentration was increased to 30%, significant signs of degradation occurred under composting conditions

after just 14 days [82]. Modification of celluloses has also been examined with respect to increasing biodegradability and previous work on this resulted in an increased rate of biodegradation of PCL when cellulose acetate was incorporated as an additive, however it was found that cellulose acetate itself was not susceptible towards biodegradation [81].

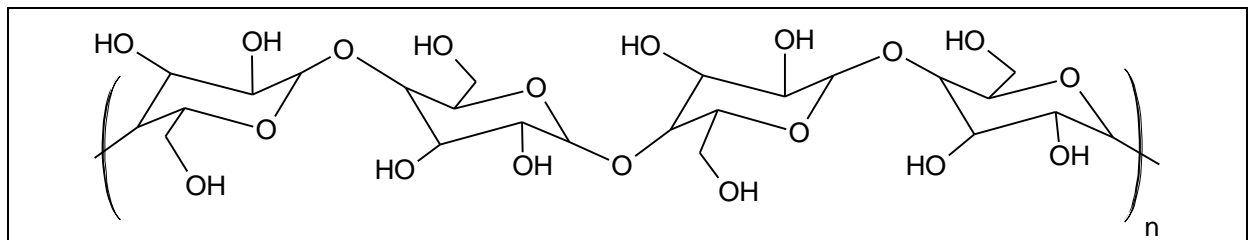


Figure 1.8 Chemical structure of cellulose

In recent years the incorporation of layered silicates has attracted a great deal of attention in all chemical disciplines, and this includes the area of polymers. It has generally been found that the incorporation of organoclays such as montmorillonite and its derivatives have resulted in improved mechanical, thermal and barrier properties of polyesters such as PCL and PLA [72, 86]. Recent investigations have also shown that the addition of these organoclays can have a significant impact on the microphase morphological structure of block co-polymers, and hence much research has been undertaken concerning the addition of these fillers into PUs, in order to improve mechanical and thermal properties [87-90].

Essentially organoclays are organically-modified phyllosilicates, and montmorillonite is a commonly used organoclay as a polymer additive. Montmorillonite is a phyllosilicate in which the trivalent Al-cation in the octahedral layer is partially substituted by a Mg-cation, **Fig.1.9**. A feature of this structure is that these ions do not fit into the tetrahedral layer therefore the layers are held together by relatively weak forces, which expand when water and other polar materials enter between the layers [91].

Although the incorporation of organoclays into polymers has primarily been used to improve mechanical and physical properties, some research has examined these compounds in respect of increasing biodegradation. However, results from these studies have produced conflicting opinions. For example, Wu et al. found that the addition of unmodified montmorillonite delayed the biodegradation of PCL under composting conditions [92], and similar findings were also obtained by Fukushima et al. where Cloisite 30B clays were incorporated into PCL and it was found that this decreased the rate of degradation, which was thought to be due to hindered access to the ester groups with the addition of the clay [73].

Opposite findings were obtained by Dutta et al. who found that the addition of bentonite accelerated the biodegradation of an epoxy-modified PU in a broth culture [93], and Singh et al. who added Closite 30B to PCL and found that the addition of this modified clay increased enzymatic, composting and fungal degradation [94]. Therefore, it can be noted that much conflicting evidence regarding increasing biodegradation by addition of modified clays has been published, and the rate of degradation is dependent on many factors such as; the polymer system, biodegradation conditions and type and concentration of the organoclay. Therefore each polymer system needs to be examined individually and the choice of the organoclay, its concentration and method used to test the process of degradation and biodegradation needs to be chosen carefully.

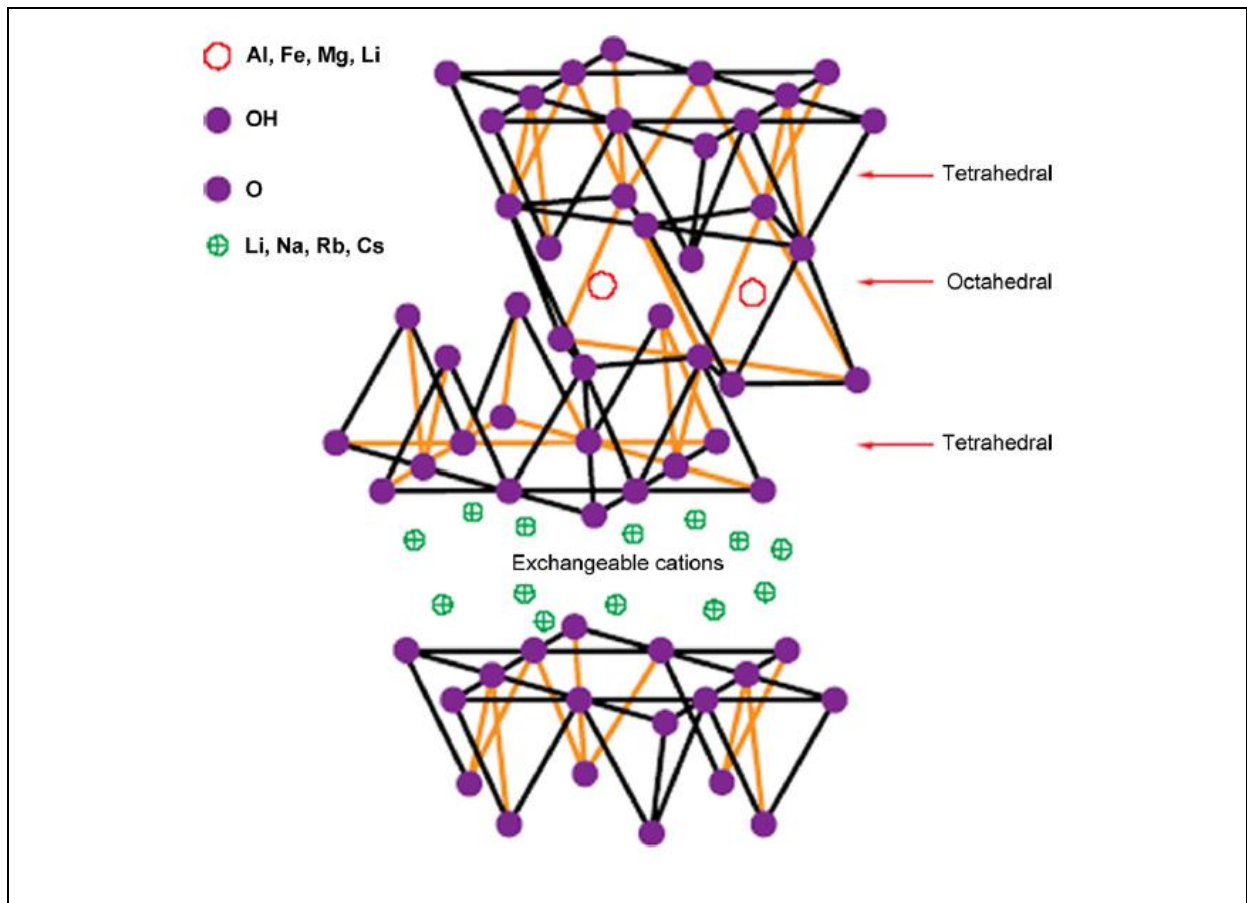


Figure 1.9 Structure of a two layered silicate

1.6 Test Methods Measuring Degradation and Biodegradation

The process of biodegradation of polymers is a highly complex process involving a multitude of degradative mechanisms, often working together synergistically [11, 57, 95]. Therefore, the test methods used to measure degradation and biodegradation of polymers can also be varied and complex. There are numerous standard accepted test methods to monitor degradation and biodegradation, and the most common are the ASTM (American Society for Testing and Materials) test methods [96, 97]. However, many of these methods are limited in their use with respect to polymer biodegradation, as many of these tests were not designed to measure biodegradation of polymers. Many factors need to be taken into account when choosing the appropriate test methods to monitor degradation and biodegradation, including; the type of polymer, properties of the polymer (solubility, molecular structure etc), environmental conditions to which the polymer is exposed to, and types of microorganisms which may come into contact with the polymer during its biodegradation and degradation [96, 97]. In light of this many of the standard test methods typically need to be modified, taking into consideration all of the parameters mentioned above. A further problem which is frequently encountered in the testing of polymer biodegradability, is the time span in which these experiments can sometimes take. Many of the standard test methods are developed for a period of between 28-100 days, however, degradation and biodegradation experiments involving polymers can often take many months or even years [96, 98, 99].

Polyurethane is a particularly difficult polymer in which to assign standard test methods regarding its degradation and biodegradation due, not only to the complex morphology of the polymer, but also to the wide variety of the constituents which can be used to synthesise this material. For example, one of the main degradation and biodegradation products of PU during degradation and biodegradation has been shown to be amines, therefore previous researches have used a ninhydrin assay test to determine the presence and quantification of amines as a means of determining the extent of PU biodegradation [100]. This assay is generally used in protein chemistry, in which the ninhydrin reacts with an alpha amino acid to form a coloured complex which is then measured spectrophotometrically [101]. However, this test method cannot be used for all PUs, as ninhydrin does not react with tertiary or aromatic amines [101], therefore cannot be used with PUs synthesised with aromatic isocyanates, which give rise to aromatic amines during degradation.

In general, testing can be grouped depending on the individual degradation/biodegradation mechanism being investigated. Test methods can generally include some form of chemical oxidative degradation or hydrolytic degradation; which is usually performed in a standard

buffer solution (this test method can also be altered to examine the effect of pH) [56], accelerated chemical hydrolysis; either alkaline (NaOH) [102] or acid (HCl) [79], enzymatic hydrolysis; in which specific enzymes are added to a buffer solution [64], microbial growth on PU [26], soil burial [21], and composting [64]. Generally a combination of some or all of these methods are used to give an indication of degradability/biodegradability of the PU, and **Table 1.3**, lists some of the common test methods that have been previously used to test degradation and biodegradation of PUs.

Determination of the extent of degradation/biodegradation during this testing, again has previously been shown to vary widely, dependant on the property of the PU which is to be investigated, and can involve properties such as changes in chemical structure, changes in morphology, thermal properties and visual degradation both macromolecular and micromolecular.

One of the most common methods used to measure degradation and biodegradation of PUs is that of weight loss. This method is used extensively, due to the simplicity and ease with which to monitor the rate of degradation. Samples are removed from the relevant medium and dried at 50°C for 24h and then weighed. Weight loss is generally given as a % weight loss from the weight of the initial sample. This method has been shown to be effective at measuring the rate of degradation, however a major disadvantage of this method is that initial stages of minor degradation are difficult to monitor, as weight loss is generally not observed until substantial degradation has occurred. Therefore, many previous studies have relied upon monitoring changes in the molecular weight of PUs by means of gel permeation chromatography (GPC). This technique is seen to be more sensitive in measuring initial stages of degradation, with decreases in molecular weight being observed even with the absence of weight loss [103].

Visual images can also be used to examine degradation, and these can be at a macroscopic and/or microscopic level. The usual methods used to examine degradation visually are photographic images, optical microscopy and scanning electron microscopy. The majority of degradation and biodegradation investigations usually employ at least one of these methods, with the initial sample providing a visual reference control. These methods can show visually whether some physical degradation has occurred, and microscopic images can be used as a good indication of initial stages of degradation. However, a disadvantage of this method is that it is generally only of a qualitative nature (not quantitative), and is therefore normally used in conjunction with other analytical techniques.

Changes to chemical structure both during and after degradation/biodegradation is often used during degradation experiments in order to elucidate possible degradation mechanisms and also to quantify the extent of degradation/biodegradation, and an array of techniques are available to do this dependant on the properties of the PU (solubility, elasticity and the sometimes fragile nature of the films after degradation). One of the most common methods employed is that of fourier transform infrared analysis (FTIR). This technique is a relatively fast and easy method in which to detect changes to chemical groups in PUs. Urethane, ester and ether groups can all be monitored using this method, along with amine and alcohol degradation products of PUs. Morphological properties such as hydrogen bonding can also be quantified using FTIR, and many previous studies have used this method to determine the extent of hydrogen bonding in PUs [43, 46, 87, 104]. Quantification of chemical degradation can be obtained using FTIR by numerous methods, and previous research has quantified the extent of degradation by measuring peak height/area and then dividing this by a specified reference peak. For complex peak areas and the extent of hydrogen bonding, deconvolution methods have previously been successful [43, 87, 104].

An advantage of this method is that the sample is not destroyed during analysis therefore time course studies can be performed on the same sample thereby obtaining a more accurate analysis. Also quantitative as well as qualitative information can be obtained. However, a disadvantage of this method is that changes to chemical structure are not specific, and exact structures of degradation products cannot be obtained without the use of other analytical techniques. Another problem encountered with this technique is accurate sample preparation in order to obtain spectral reproducibility, for example, film thickness will affect the absorbance values obtained, therefore in order to compare different samples, film thickness must be the same. Also, one of the major problems in using this technique is that sample films need to be very thin, in the range of 10 μ m, in order to obtain usable information. This is very difficult to achieve for many TPUs, due to the elastic nature of these polymers thin films make the polymer very difficult to handle, and the nature of degradation/biodegradation experiments can result in very fragile films quickly, which can make FTIR impossible for many PUs when performing degradation/biodegradation experiments. However, there are numerous methods to overcome this problem, and one method which has been used is the use of cryomicrotomy [105]. This has the advantage of being able to microtome sections of the polymer accurately at temperatures as low as -150°C to obtain films as thin as 10 μ m. FTIR can then be performed on these thin samples. This sectioning of the PU film would also provide information about chemical changes in the bulk of the sample. Another method used to overcome some of the problems with FTIR is by the use of attenuated total reflectance (ATR) [98, 106]. This method has the advantage of

minimal sample preparation, however, it should be noted that only the surface of the polymer can be measured to a depths of about $3\mu\text{m}$, therefore changes in the bulk of the samples cannot be measured using this method.

For PU, morphology is of paramount importance, and changes to morphology can indicate not only degradation but changes specifically relating to the individual hard and soft segment domains contained within the PU, thereby providing information on the rate of degradation of the hard and soft segments individually, and how each domain affects degradation. There are numerous methods used to elucidate morphological properties in PUs, and one of the most common is that of differential scanning calorimetry (DSC). This technique measures the energy required to produce a zero temperature difference between the sample and a reference sample. Much information can be obtained from this technique including glass transition, crystallinity and melting temperatures [107-109]. For PUs with complex morphological profiles, thermographs obtained by DSC usually contain numerous endotherms relating to the hard and soft segments dependant on the chemical constituents and extent of crystallinity, and previous studies have used this technique to examine changes to the hard and soft segment domains during degradation, crystallinity and phase separation, all of which have been shown to affect the rate of degradation in PUs [107-109].

Table 1.3 Test Methods previously used for Assessing Degradation and Biodegradation of Polyurethane

Test Method	Parameters	Analysis of the Extent of Degradation	Ref.
Hydrolysis Alkaline	<ul style="list-style-type: none"> • 3% & 10% solution at 37°C • 10% NaOH at 37°C • 3% NaOH at 37°C • 0.1 M NaOH at 37°C • 0.1 M KOH at 37°C 	<ul style="list-style-type: none"> Weight loss, SEM Weight loss Weight loss, SEM FTIR, DSC, GPC, SEM Weight loss, FTIR 	<ul style="list-style-type: none"> [102] [64] [110] [111] [79]
Hydrolysis Acid	<ul style="list-style-type: none"> • 0.1 M HCl at 37°C 	<ul style="list-style-type: none"> Weight loss, FTIR 	[79]
Hydrolysis PBS	<ul style="list-style-type: none"> • pH 7.4 at 37°C • pH 4.0, 6.8, 7.4 at 37°C • pH 7.4 at 37°C • pH 7.4 at 37°C • pH 7.0 at 37°C and 55°C • pH 6, 7, 7.4 at 52.5°C • PBS at 37°C 	<ul style="list-style-type: none"> Weight loss, ninhydrin assay, DSC, change in pH. GPC, DSC Weight loss Weight loss Weight loss, GPC Weight loss, SEM, NMR, GPC FTIR, DSC, GPC, SEM 	<ul style="list-style-type: none"> [100] [56] [78] [112] [103] [113] [111]
Hydrolysis 75% humidity	<ul style="list-style-type: none"> • Saturated NaCl solution at 70°C 	FTIR	[114]
Enzymatic Degradation phosphate buffer	<ul style="list-style-type: none"> • pH 7.2, <i>R. delemar</i> lipase • <i>Candida cylindracea</i> lipase pH 7.0 at 37°C 	<ul style="list-style-type: none"> Weight loss, SEM, DSC Weight loss 	<ul style="list-style-type: none"> [102] [64]
Enzymatic degradation Chymotrypsin	<ul style="list-style-type: none"> • pH 8 at 37°C 	SEM, GPC	[36]
Enzymatic degradation papain	<ul style="list-style-type: none"> • pH 6.2 at 37°C 	<ul style="list-style-type: none"> Weight loss, FTIR-ATR, optical microscopy, AFM 	[106]
Soil Burial	<ul style="list-style-type: none"> • 30°C humidity chamber, soil taken from garden • John Innes compost 2 at 20°C • Soil taken from natural environment, temp 25-32°C 	<ul style="list-style-type: none"> Weight loss, SEM, DSC, FTIR SEM Weight loss, SEM, FTIR 	<ul style="list-style-type: none"> [21] [26]
Composting	<ul style="list-style-type: none"> • Bioreactor, 58°C 4 days, 50°C until 27 days, 35°C until 45 days • Natural weathering conditions 24 months • Commercial composting site 	<ul style="list-style-type: none"> Weight loss, CO₂, SEM Weight loss, photographs, Optical microscopy, DSC DSC, Tensile testing 	<ul style="list-style-type: none"> [64] [99] [115]
Fungal Resistance	<ul style="list-style-type: none"> • Agar, <i>G. globosum</i> at 28°C for 130 days 	<ul style="list-style-type: none"> Weight loss, FTIR-ATR, SEM Weight loss, SEM 	<ul style="list-style-type: none"> [98] [116]
Bacterial/Fungal Inoculation	<ul style="list-style-type: none"> • Incubator at 37°C with <i>Pseudomonas aeruginosa</i> 	Weight loss	[26]

1.7 Aims and Objectives of this Study

This research involved working in conjunction with a polyurethane manufacturer (the sponsor company; Eurothane Ltd), with the main aim of developing TPU polymers that show increased biodegradation compared to the company's current TPUs, for use in a specific end product application. The product requires a six month usage targeted for an agricultural application, followed by degradation of the polymer in the soil.

From the literature review it was found that the morphology of TPUs has a profound effect on their properties, and this is in turn dependent on the chemical constituents and method of synthesis of the polymers. Therefore, three TPUs were synthesised at Eurothane Ltd, each with a different method of synthesis, one of which was the current TPU synthesised by the company and deemed as 'non-biodegradable'. This sample was used as a control with which to compare all other newly synthesised samples with respect to their biodegradation.

A further four samples were synthesised at Eurothane Ltd, each containing either a different polyol or diisocyanate, and were compared to the control sample, in order to examine the effect of the polyol and diisocyanate structures on degradation and biodegradation of the TPUs. Results from this work were then used to examine the effect of various additives on degradation and biodegradation of these TPU samples.

The objectives of this research were:

1. To examine known methods typically used to evaluate the degradation and biodegradation of polymers in order to develop and apply the appropriate test methods and analytical techniques, for monitoring the rate of degradation and biodegradation where the end use of the product required to be degradable in soil.
2. To analyse the control TPU polymer synthesised at Eurothane Ltd, with respect to its morphology, biodegradation and degradability, and to use this information as a baseline to compare with all the other samples synthesised having varying formulations and prepared by different methods.
3. To compare TPUs synthesised by the 'one shot' method and the 'pre-polymer' method in order to examine if the method of synthesis affects the rate of degradation and biodegradation of the prepared TPUs.

4. To examine the effect of altering the structures of the 'soft segment' polyol components and the diisocyanate of the 'hard segment', on degradation and biodegradation, by monitoring the changes in the chemical and physical properties of the TPUs before, during and after the degradation process.
5. To possibly increase the rate of degradation and biodegradation by the incorporation of additives which have been shown in the literature to either increase biodegradation in other polymeric materials, or which may alter the morphological profiles of TPUs, and to investigate the effect of each additive on the rate of degradation and biodegradation of the TPUs.

Chapter 2

Experimental and Analytical Techniques

2.1 Materials

2.1.1 Polyurethanes

Polyurethane (PU) samples, both as pellets and plaques (2mm thick), were provided by the sponsor company Eurothane Ltd. **Fig. 2.1. PU ADP** is the standard polyurethane that was synthesised by the company and used as a control sample throughout this work. The method of synthesis and the hard and soft segment composition of the polyurethanes, were varied to determine the effect of each component on the degradation of the polymer. The various polyurethane samples were grouped according to their structure and/or additives used; see **Table 2.1a & b** for the chemical compositions and acronyms of all PUs used. The samples received were prepared into films before further use.

2.1.2 Preparation of PU Film Samples

All characterisation and degradation experiments were performed on polyurethane films of a thickness between 100-120 µm. Films were prepared by melt pressing using a Turton and Bradley compression moulding machine which was preheated to the required temperature (between 180 °C and 220 °C depending on the composition of the sample) **Table 2.1a & b**. The pellets were placed between two heated platens each lined with a Teflon sheet and allowed to heat for a set amount of time under no pressure. A pressure of 1 MPa was then applied for the required time, see **Table 2.2** and then cooled under the same pressure for 15-20 mins until the temperature dropped down to 40-50 °C before removing from the press

2.1.3 Additives and solvents

All other chemicals used were of reagent grade and were used without further purification. Solvents employed were laboratory reagent grade supplied from Fisher chemicals, see **Table 2.3.**

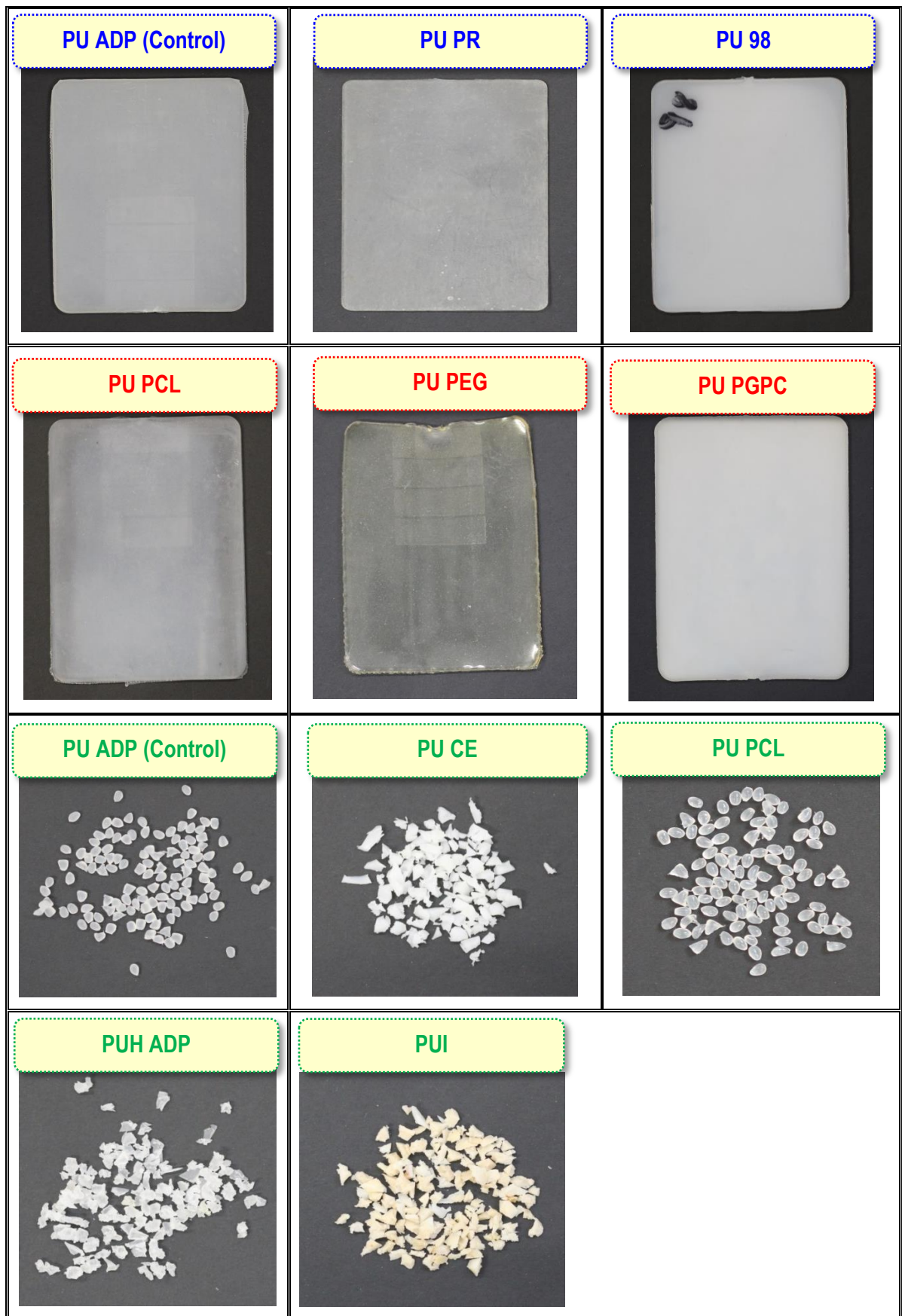


Figure 2.1 PU plaques and pellets samples provided by Eurothane Ltd.

Table 2.1a Chemical composition of PU samples without additives used in this study

PU	Composition	*HS-(Hard Segment), *SS (Soft Segment).	Structure	Mass (Kg)	MM	Ratio of reactants (Weight)
Acronym- PU ADP, PU PR & PU 98*						
HS	4,4 – Methylene bisphenyl diisocyanate (MDI)			5.6 *5.5	250	MDI:BD:PEA 3:2:1
HS	1,4 – Butane diol (BD)			1.5	90	
SS	Poly(ethylene adipate) (PEA)			10	2000	
Acronym- PUH ADP						
HS	Methylene dicyclohexyl diisocyanate ($H_{12}MDI$)				262	H ₁₂ MDI:BD: PEA 3:2:1
HS	1,4 – Butane diol (BD)	See PU ADP			90	
SS	Poly(ethylene adipate) (PEA)	See PU ADP			2000	
Acronym- PU PCL						
HS	(MDI)	See PU ADP			250	MDI:BD:PCL 3:2:1
HS	(BD)	See PU ADP			90	
SS	Polycaprolactone (PCL)				2000	
Acronym- PU PEG						
HS	(MDI)	See PU ADP			250	MDI:BD:PEG 3:2:1
HS	(BD)	See PU ADP			90	
SS	Poly(ethylene glycol) (PEG)				1000	
Acronym- PU PGPC				PEG	PCL	
HS	(MDI)	See PU ADP			250	MDI:BD: PCL:PEG 3:2:0.5:0.5
HS	(BD)	See PU ADP			90	
SS	50% (PCL) & 50% (PEG)	See PU ADP				

Figure 2.1b Chemical composition of PU samples with additives used in this study

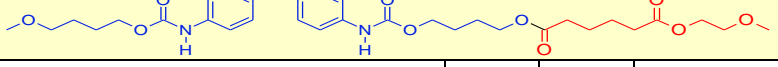
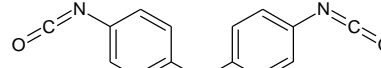
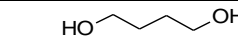
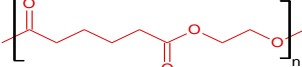
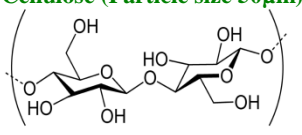
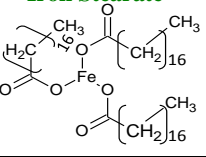
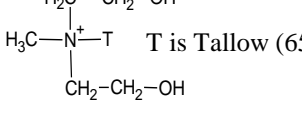
PU Composition *HS- Hard Segment, *SS Soft Segment.	Structure	Mass (kg)	MM	Ratio of reactants/ additives(wt %)
Acronym- PU CE, PUI				MDI:BD:PEA 3:2:1
HS 4,4 – Methylene bisphenyl diisocyanate (MDI)		5.6	250	
HS 1,4 – Butane diol (BD)		1.5	90	
SS Poly(ethylene adipate) (PEA)		10	2000	
Additives	Cellulose (Particle size 50µm) 	Iron Stearate 	0.5%	
Acronym- PU PR30	See PU PR (table 2.1a)			
HS (MDI)	See PU PR (table 2.1a)		250	MDI:BD: PEA 3:2:1
HS 1,4 – Butane diol (BD)	See PU PR (table 2.1a)		90	
SS Poly(ethylene adipate) (PEA)	See PU PR (table 2.1a)		2000	
Additives	H ₂ C—CH ₂ —OH H ₃ C—N ⁺ —T T is Tallow (65%,C ₁₈ ; ~30%,C ₁₆ ; ~5%,C ₁₄) 	Nano Clay - Cloisite 30B	12%	
Acronym- PU PCL30	See PU PCL (table 2.1a)			
HS (MDI)	See PU PCL (table 2.1a)		250	MDI:BD:PCL 3:2:1
HS (BD)	See PU PCL (table 2.1a)		90	
SS Polycaprolactone (PCL)	See PU PCL (table 2.1a)		2000	
Additives	Cloisite 30B (see PU PR30)		12%	
Acronym- PU PEG30	See PU PEG (table 2.1a)			
HS (MDI)	See PU PEG (table 2.1a)		250	MDI:BD:PEG 3:2:1
HS (BD)	See PU PEG (table 2.1a)		90	
SS Poly(ethylene glycol) (PEG)	See PU PEG (table 2.1a)		1000	
Additives	Cloisite 30B (see PU PR30)		12%	
Acronym- PU CE30	See PU CE			
HS (MDI)	See PU CE		250	MDI:BD: PEA 3:2:1
HS (BD)	See PU CE		90	
SS Poly(ethylene adipate) (PEA)	See PU CE		2000	
Additives	Cloisite 30B (see PU PR30)		12%	
Acronym- PUI 30	See PUI			
HS (MDI)	See PUI		250	MDI:BD:PEA 3:2:1
HS (BD)	See PUI		90	
SS Poly(ethylene adipate) (PEA)	See PUI		2000	
Additives	Cloisite 30B (see PU PR30)		12%	

Table 2.2 Film Pressing Conditions for Polyurethane Samples

PU Sample Code	Temperature (°C)	Pre heat (mins)	Time under full pressure of 1 MPa (mins)
PU ADP	180	3	2
PU PR	180	3	1.5
PU 98	200	2	1.5
PUH ADP	160	1.5	1.5
PU PEG	160	1.5	1.5
PU PGPC	160	2	1.5
PU PCL	180	3	2
PU CE	200	2	1.5
PUI	200	1.5	1.5

Table 2.3 Chemical Structure of Solvents

Chemical Name	Structure	B.P.(°C)	Purity	Supplier
Ethanol		78.3	Laboratory Grade	Fisher Scientific
N,N-dimethylformamide		153	Laboratory Grade	Fisher Scientific
Tetrahydrofuran		66	Laboratory Grade	Fisher Scientific
Acetone		56.2	Laboratory Grade	Fisher Scientific
Acetonitrile		82	Laboratory Grade	Fisher Scientific
Dimethylsulfoxide		189	Laboratory Grade	Fisher Scientific
n-Hexane		68	Laboratory Grade	Fisher Scientific

2.2 Characterisation of Polyurethane Samples

The PU samples were characterized by different methods, an overview of which is given in, **Scheme 2.1**

2.2.1 Solubility

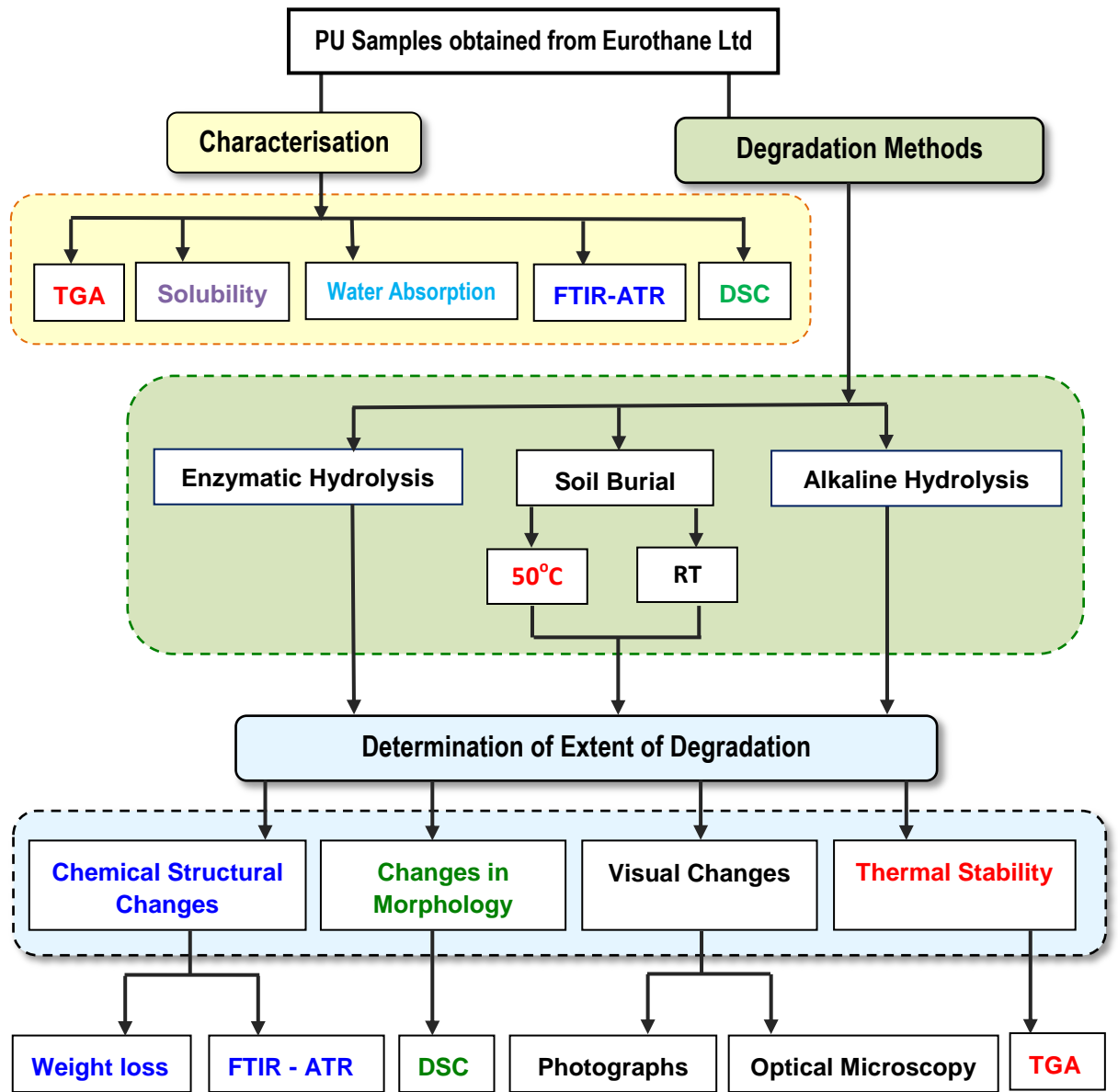
Solvent casting of the samples was required for some of the experimental work (synthesis of PU with nano clay), therefore the solubility of each PU sample was initially examined in different solvents (water, ethanol, acetone, acetonitrile, dimethyl sulfoxide, tetrahydrofuran, dimethylformamide and hexane) **Table 2.4**, to obtain the best solvent for casting the polymers. A cut film of each PU (1cm x 1cm of a thickness between 100-120 µm) was placed in a 50 ml conical flask containing 50 ml of the solvent and stirred on a hot plate stirrer (using a magnetic stirring bar) at RT for 24 hours to examine the solubility (in triplicate).

Table 2.4 Solubility of PU Samples at RT

Sample Code #	Solubility of PU Samples at RT							
	Water	Ethanol	Acetone	Acetonitrile	DMSO	THF	DMF	Hexane
PU ADP	N	N	N	N	Partial	Y	Y	N
PU PR	N	N	N	N	Partial	Y	Y	N
PU 98	N	N	N	N	Partial	Y	Y	N
PU PCL	N	N	N	N	Partial	Y	Y	N
PU PEG	N	N	N	N	Partial	Y	Y	N
PU PGPC	N	N	N	N	Partial	Y	Y	N
PUH ADP	N	N	N	N	Partial	Y	Y	N
PUQ	N	N	N	N	Partial	Y	Y	N

Y = Soluble, N = Insoluble

see Table 2.1a for polyurethane structures



Scheme 2.1 Experimental Methods used for the Characterisation and Degradation of PU Samples

2.2.2 Water Absorption

Bulk hydrophilicity is an important factor influencing the rate of hydrolytic degradation of PU, therefore, the hydrophilicity of each sample was quantified using the water absorption method. This was carried out by measuring the amount of water absorbed at room temperature. Each film (1 cm x 1 cm x 100-120 µm) was weighed and then placed in a 50 ml flask containing 50 ml of distilled water, and maintained at room temperature (in triplicate). Samples were removed at regular intervals, wiped with filter paper to remove excess water and reweighed. This process continued until the weight of the PU sample reached equilibrium. The water absorption was measured by the weight change of the sample, and was calculated using **equation 1**.

Equation 1

$$\text{Water Absorption (\%)} = \frac{m_w - m_d}{m_d} \times 100$$

m_w and m_d are the weights of the wet and dry samples, respectively

2.2.3 Characterisation of PU Chemical Structure by Attenuated Total Reflection Spectroscopy (FTIR-ATR)

Polyurethane samples were characterised by attenuated total reflection spectroscopy using a Perkin Elmer Spectrum one FT-IR Spectrometer, fitted with a Specac Golden Gate single reflection monolithic diamond ATR accessory. Samples were analysed as 100-120 µm thick films over the range 4000 cm⁻¹ to 500 cm⁻¹ for 16 scans, and the infrared assignments for each PU sample are given in **Table 2.5**.

2.2.4 Chemical Structure of Isocyanates, Polyols, Chain Extenders and Additives used in the Synthesis of PU Samples by FTIR

Reactants and additives used during PU synthesis were characterised by Fourier transform infrared spectroscopy on a Perkin Elmer Spectrum one FT-IR Spectrometer using NaCl plates (reactants) and KBr discs (additives). Reactants and additives were analysed over the range 4000 cm⁻¹ to 500 cm⁻¹ for 16 scans, and the infrared spectra are given in **Figs. 2.2 – 2.4**.

2.2.5 Thermal Stability of PU Samples by Thermogravimetric Analysis (TGA)

Thermal stability of each polyurethane sample was assessed prior to degradation experiments using a Perkin Elmer Pyris 1 thermogravimetric analyser (TGA) in order to determine thermal property changes after hydrolysis and soil burial. TGA analysis was performed on 0.5-1 mg samples under a nitrogen purge and a flow rate of 60 cm³/min. The

samples were heated to 650 °C at a rate of 10 °C min. Thermal stability was quantified by differential weight loss curve (DTGA); an example is given in **Fig. 2.5**.

2.2.6 Crystallinity measurements by Differential Scanning Calorimetry (DSC)

Characterisation of PU morphology for each sample was obtained prior to experiments by using differential scanning calorimetry (DSC). DSC measurements were performed on 5-8 mg circular samples under a helium purge at 40cm³/min using a Perkin Elmer Diamond DSC at a rate of 100°C a minute. All thermograms were baseline corrected and calibrated using indium. The samples were first heated to 200°C and held at this temperature for 3 min to remove thermal history, then cooled to -80°C, held for 3 min before heating to 220°C. Samples were heated at a high heating rate of 100°C/min to obtain greater sensitivity **Fig. 2.6**. Determination of the hard and soft segment transitions were ascertained as the midpoint temperature of each endotherm, using the peak find tool in the Pyris software program, **Fig. 2.7**. The glass transition for each sample was located by using the midpoint temperature between extrapolation of the onset temperature T_o , and extrapolation of the endset temperature T_e , **Fig. 2.7**. Quantification of morphological changes during degradation was required; therefore the crystallinity was obtained by measuring the area under each endotherm of the initial sample, (ΔH value) **Fig. 2.8**. This, was assumed to be theoretically 100%, and degraded samples were compared relative to this.

Table 2.5 Characterisation of PU chemical structure by FTIR-ATR

Assigned Group	Expected Region cm ⁻¹	Observed IR Frequency cm ⁻¹						
		PU ADP	PU PR	PU 98	PUH ADP	PU PGPC	PU PEG	PU PCL
NH stretch - free	3440	3329	3329			3315	-	3342
NH Stretch – Hydrogen Bonded	3520-3400	3297	3302	3302	3332	3298	3301	3302
CH ₂ – Asymmetrical Stretch	3000-2840	2955	2955	2955	-	2952	2952	2953
CH ₂ – Symmetrical Stretch	3000-2840	2920	2918		2926	2918	2910	2919
CH ₂ stretch	3000-2840	2875	2874	2874		2869	2870	2870
		2851	2852	2850	2855			2852
C=O stretch free (amide I)	1700-1750	1728	1727	1728	1730	1725	1723	1727
C=O stretch (amide I (H bonded))	1650 - 1700	1702	1703	1702	1706	1702	1702	1702
C=C aromatic	1400-1600	1597	1597	1597	-	1598	1598	1597
C-N Stretch + NH-Bend(amide II)	1650-1515	1529	1528	1529	1524	1530	1531	1528
CH ₂ Deformation	~1460	1472 1459	1477 1457	1457	1462 1450	1472	1468	1466
	~1400	1414	1414	1413	1414	1413	1413	1413
Aliphatic CH ₂ Wagging		1380	1380	1382	1380	1351	1350	1361
	1310	1309	1310	1310	1318			
Amide V (C-N stretch + N-H bend)	1220-1230	1220	1219	1220	1227	1220	1222	1220
(C=O)-OC ester soft segment	1210-1160	1159, 1136	1159, 1138	1159, 1138	1159, 1137	1145	-	1161
-C-O-C- antisymmetrical stretch ether	1300-1000	1074	1066	1077	1082	1069	1069	1064
In plane C-H bend (phenyl ring)	Ref. [11]	1018	1018	1019	-	1018	1018	1018
Out of plane C-H bend (phenyl ring)	810-840	815	816	816	-	816	817	815
Out of plane -(C=O)-O bend	Ref. [11]	769	769	769	779	770	769	770

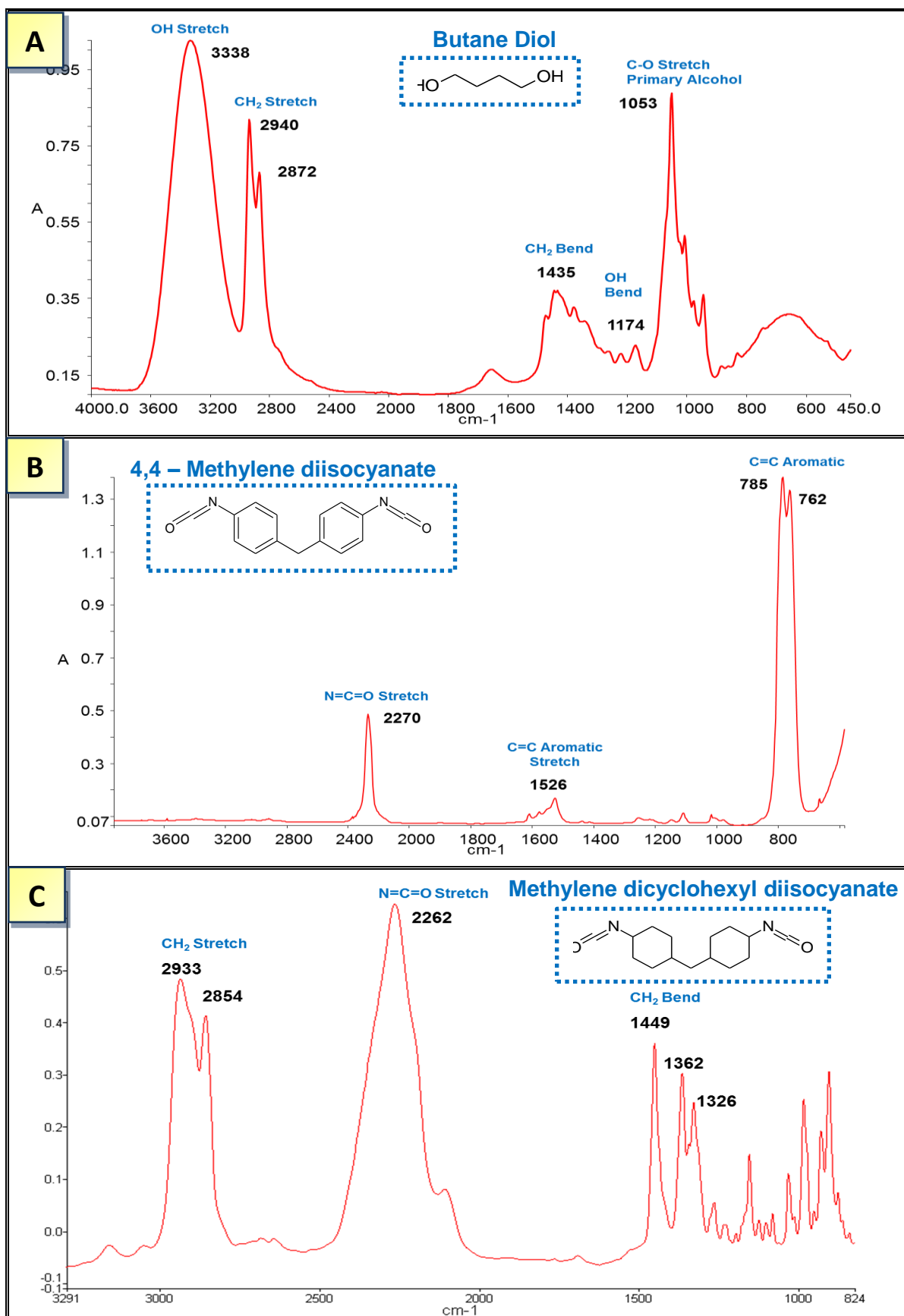


Figure 2.2 FTIR spectra of reactants used in PU synthesis (A) butane diol NaCl plate, (B) 4,4, - Methylene diisocyanate CCl₄ (C) H₁₂MDI

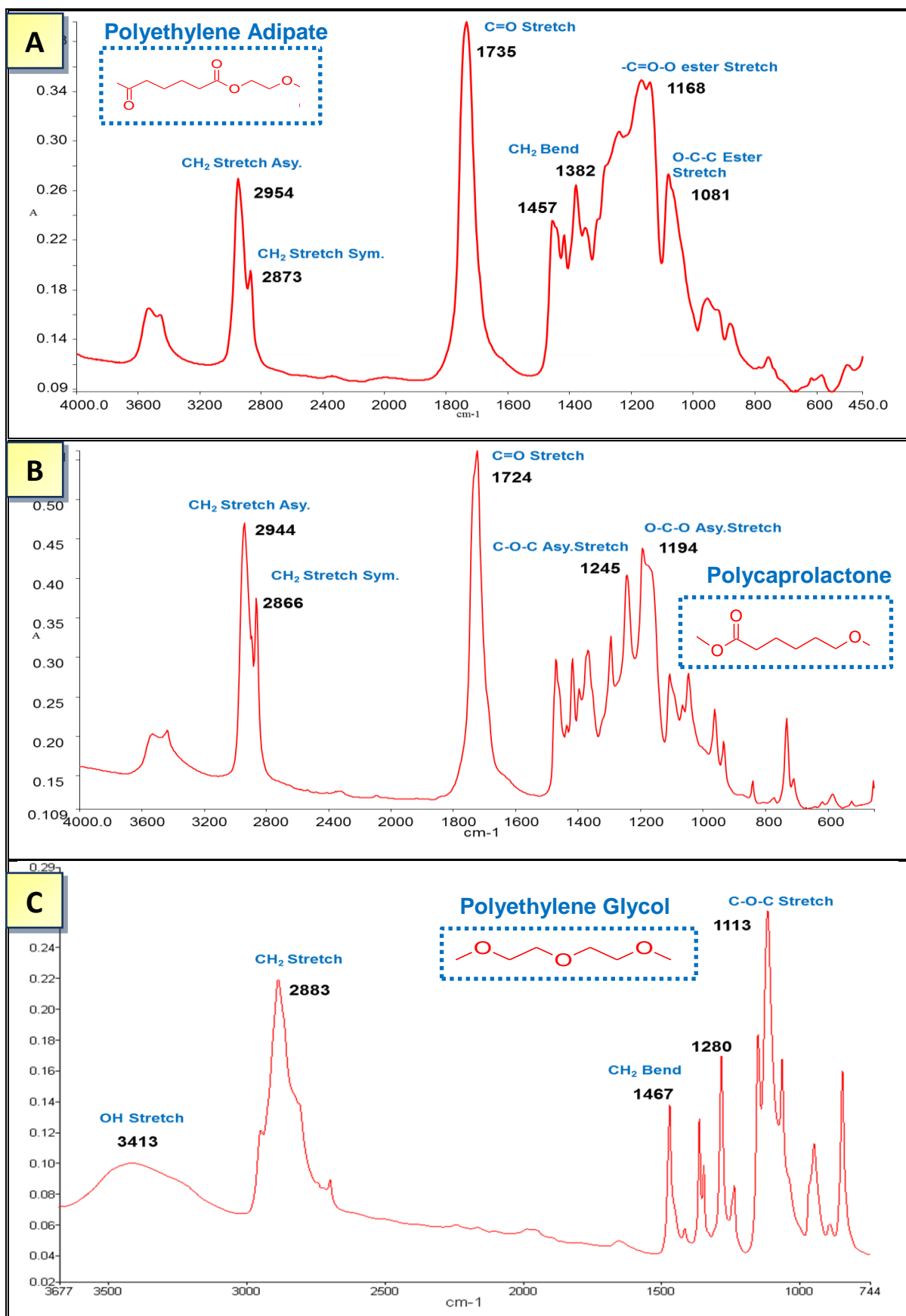


Figure 2.3 FTIR spectra of Polyols for PU ADP and PU PCL **(A)** Polyethylene adipate **(B)** Polycaprolactone

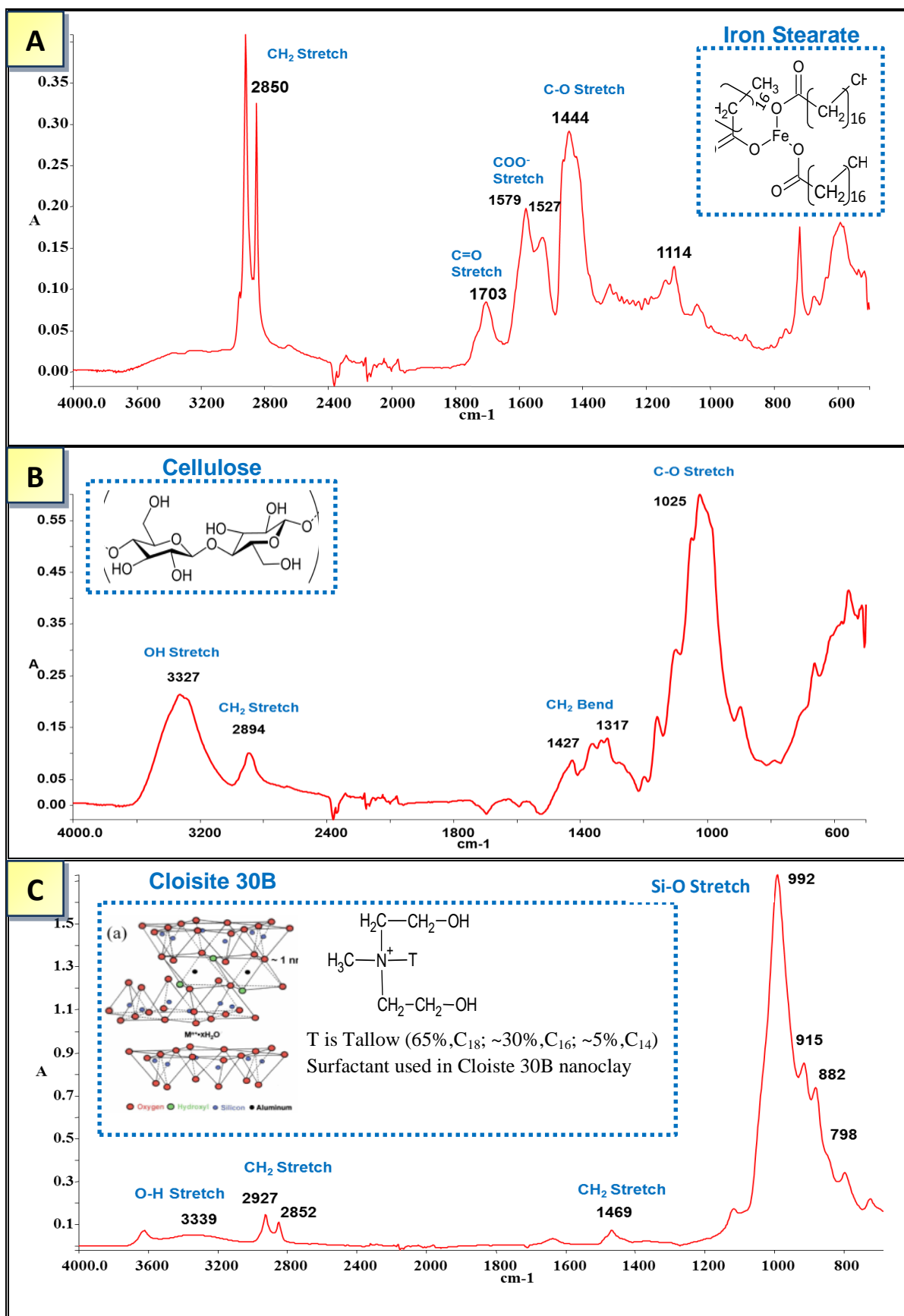


Figure 2.4 FTIR spectra of additives used in PU synthesis **(A)** Iron stearate **(B)** Cellulose powder **(C)** Cloisite 30B

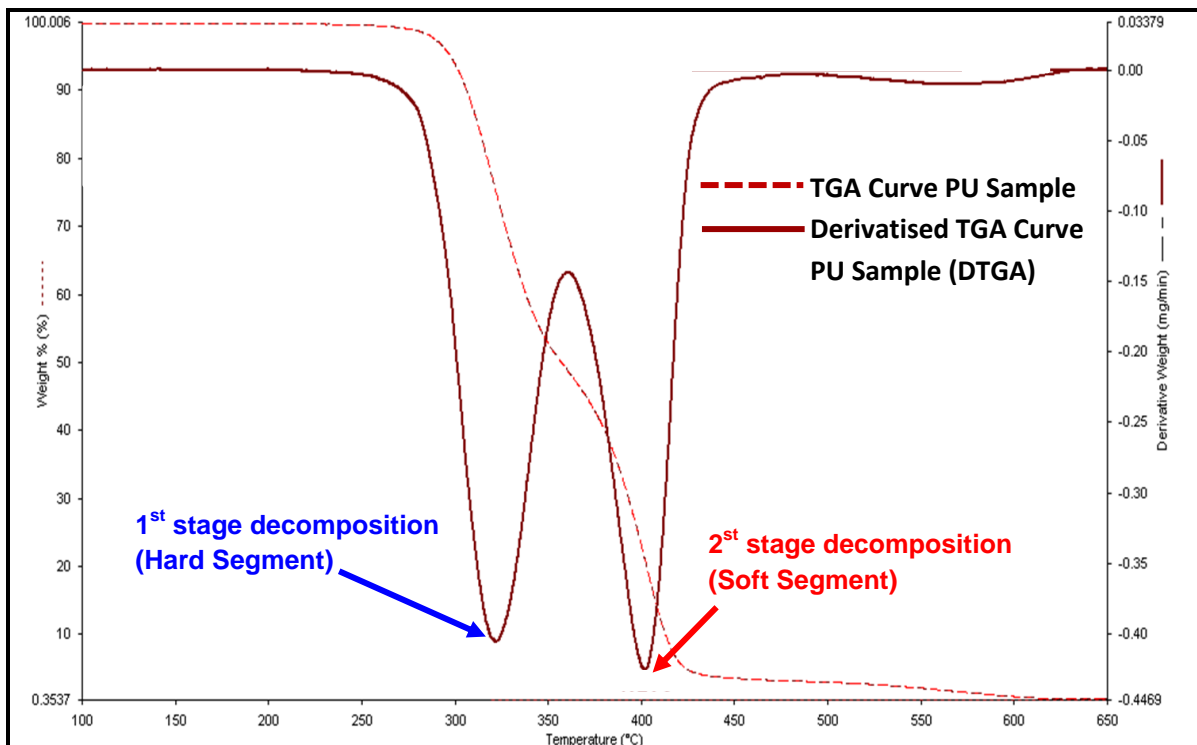


Figure 2.5 Quantification of thermal stability of PU samples using DTGA curve

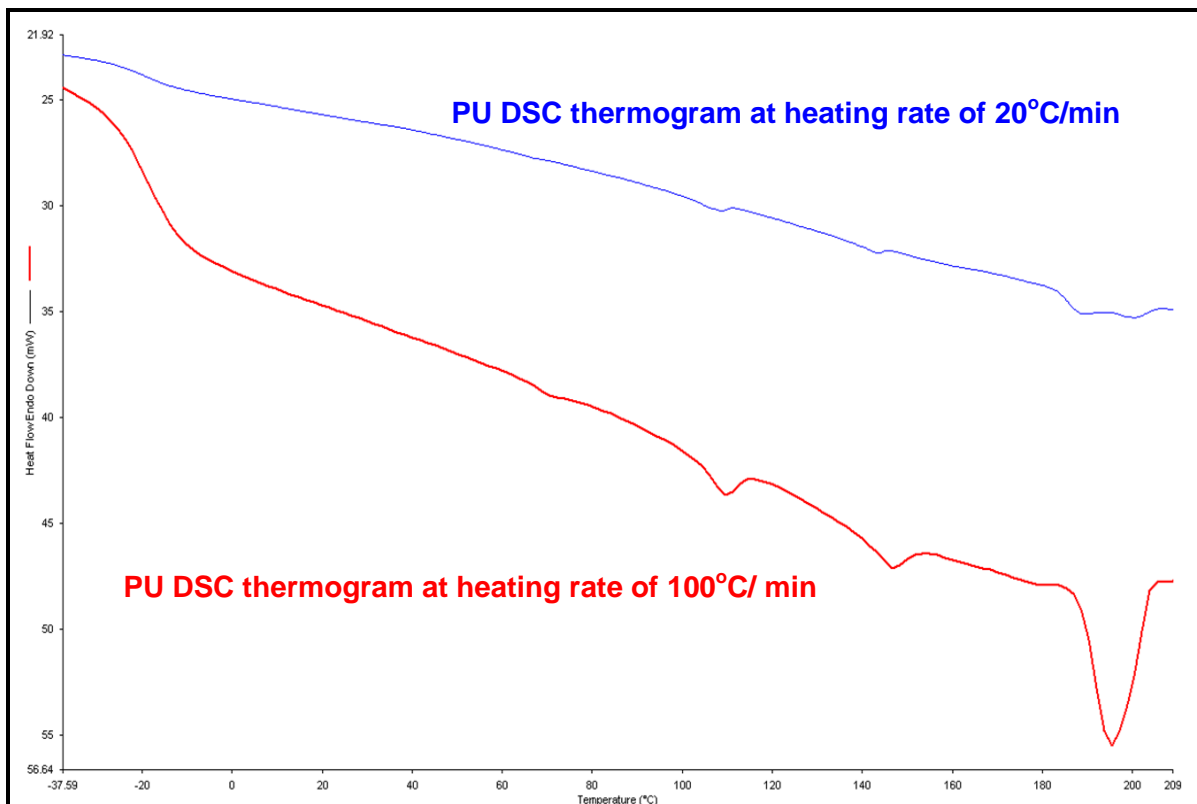


Figure 2.6 Thermograms of PU samples at heating rates of 20°C/min and 100°C/min

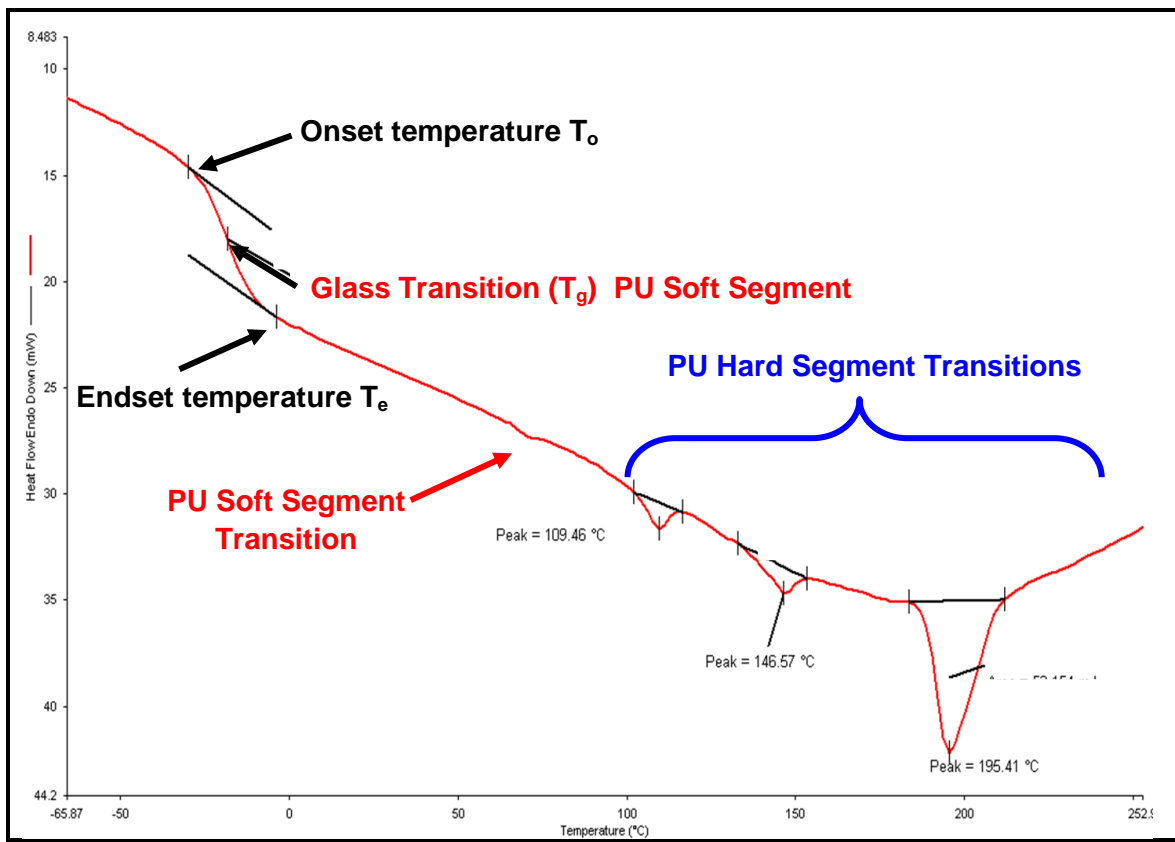


Figure 2.7 Determination of hard segment and soft segment transitions in PU samples from a DSC curve

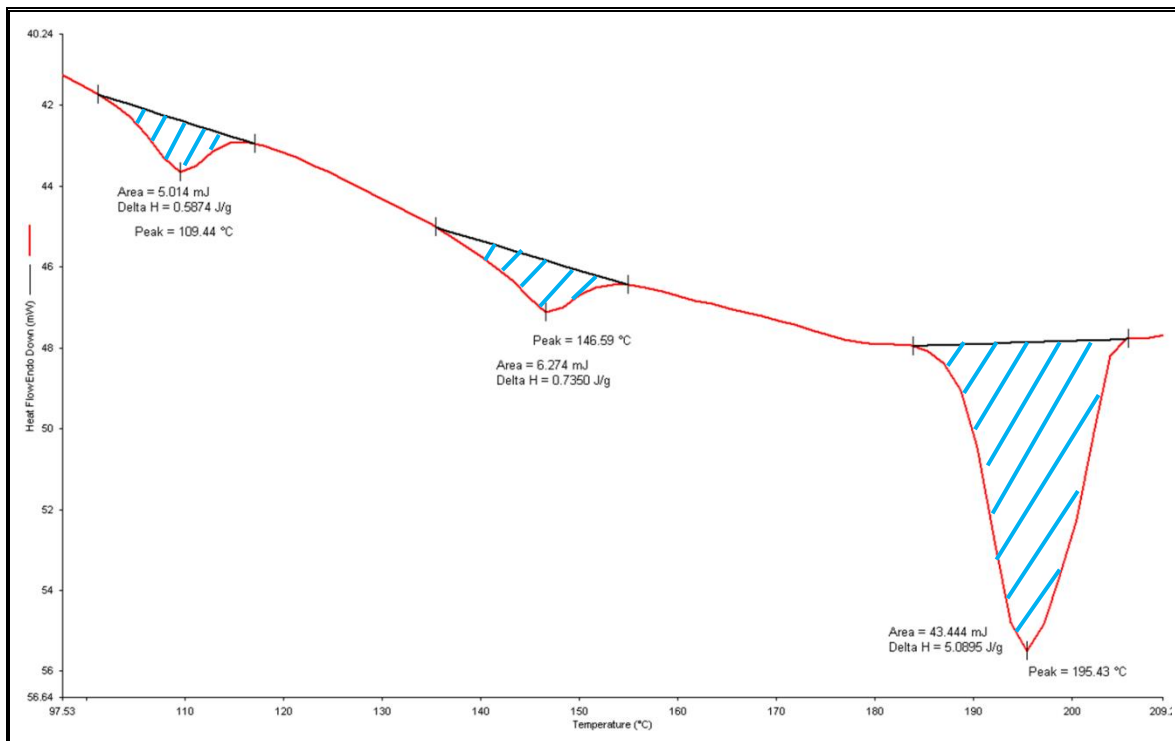


Figure 2.8 Determination of ΔH for hard segment and soft segment transitions in PU samples from a DSC curve

2.3 Testing Methods for Degradation and Biodegradation of PU

The susceptibility of degradation and biodegradation of PU samples were measured using different methods, see **Scheme 2.1**

2.3.1 Accelerated Degradation of PU by Alkaline Hydrolysis

Hydrolysis of the PU samples was performed on films ($1\text{ cm} \times 1\text{ cm} \times \approx 120\text{ }\mu\text{m}$) prepared from pellet and plaque samples **Fig. 2.1**. The films were dried under vacuum at $50\text{ }^{\circ}\text{C}$ prior to hydrolysis. Each film was weighed and submersed in a 15 ml aqueous solution of 10% NaOH, which was placed in a water bath at a temperature of $45\text{ }^{\circ}\text{C}$. The weight of each film was taken at regular intervals to determine % weight loss (**equation 2**). Before each measurement the films were washed with ethanol and distilled water, and dried under vacuum at $50\text{ }^{\circ}\text{C}$ until constant weight.

The percentage weight loss of the hydrolyzed films was calculated from the weights of the dried film samples before and after hydrolysis using **equation 2**.

Equation 2

$$W_{\text{loss}} (\%) = \frac{(W_{\text{before}} - W_{\text{after}}) \times 100}{W_{\text{before}}}$$

$W_{\text{loss}}(\%)$ is the percentage weight loss of hydrolyzed film, W_{before} is the dried weight of the film before hydrolysis, W_{after} is the weight of the dried weight of the film after hydrolysis.

2.3.2 Degradation of PU by Enzymatic Hydrolysis

Enzymatic hydrolysis of PU was performed on film samples ($1\text{ cm} \times 1\text{ cm} \times \approx 120\text{ }\mu\text{m}$) prepared from pellet and plaque PU provided by Eurothane Ltd, **Fig. 2.1**. The films were dried under vacuum at $50\text{ }^{\circ}\text{C}$ prior to hydrolysis. Each film was weighed and submersed in a 15 ml buffer solution, pH 5.8 and pH 2.8 dependent on the enzyme used (0.3 mg/ml), **Table 2.6**. The solutions were then placed in a water bath at a temperature of $37\text{ }^{\circ}\text{C}$. The enzyme activity was maintained by the addition of 2 ml enzyme/buffer solution (3mg/ml every 2 hours). The weight of each film was taken at regular intervals to determine % weight loss (**equation 3**). Before each measurement the films were washed with ethanol then distilled water and dried under vacuum at $50\text{ }^{\circ}\text{C}$ until constant weight.

The percentage weight loss of the hydrolyzed films was calculated from the weights of the dried film samples before and after hydrolysis (**see equation 2**).

Table 2.6 Buffer solution compositions for enzymatic hydrolysis

Enzyme	Activity	Buffer Solution Composition	pH
Lipase <i>Aspergillus niger</i>	200 U/g	K ₂ HPO ₄ – KH ₂ PO ₄	5.8
Lipase <i>Rhizopus sp.</i>	150 U/g	K ₂ HPO ₄ – KH ₂ PO ₄	5.8
Protease <i>Aspergillus saitoi</i>	60 U/g	Glycine – HCl	2.8-3.0
Protease <i>Rhizopus sp.</i>	20 U/g	Glycine – HCl	2.8-3.0

2.3.3 Biodegradation of PU under Soil Burial Conditions at RT

Polyurethane samples were buried in two different types of soil in order to ascertain susceptibility to microbial biodegradation in soil. Samples were washed with distilled water and ethanol, and then dried at 50°C prior to burial. The first soil used, named as soil type no. 1, **Fig. 2.9a** was from the Rothamsted Research Institute in Hertfordshire. The second soil used, soil type no. 2 was from a garden in Castle Bromwich, Birmingham **Fig. 2.9b**. The pH, water holding capacity and total solids were determined prior to the experiment, **Section 2.4**. Three (1 cm x 1 cm x \approx 120 μ m) PU film samples were placed in a glass beaker (800 ml) containing 300 g of soil, **Fig. 2.10A**. An appropriate amount of distilled water was then added to each beaker dependent on the water holding capacity. The beakers were then covered with a clear polyethylene bag pierced with 4 holes, and secured at the top with an elastic band. The beakers were then placed in a dark cool cupboard. Samples were removed at regular intervals washed with distilled water and ethanol and then dried at 50 °C under vacuum until constant weight.

The percentage weight loss of the films was calculated from the weights of the dried film samples before and after soil burial as of that for alkaline hydrolysis (see equation 2).

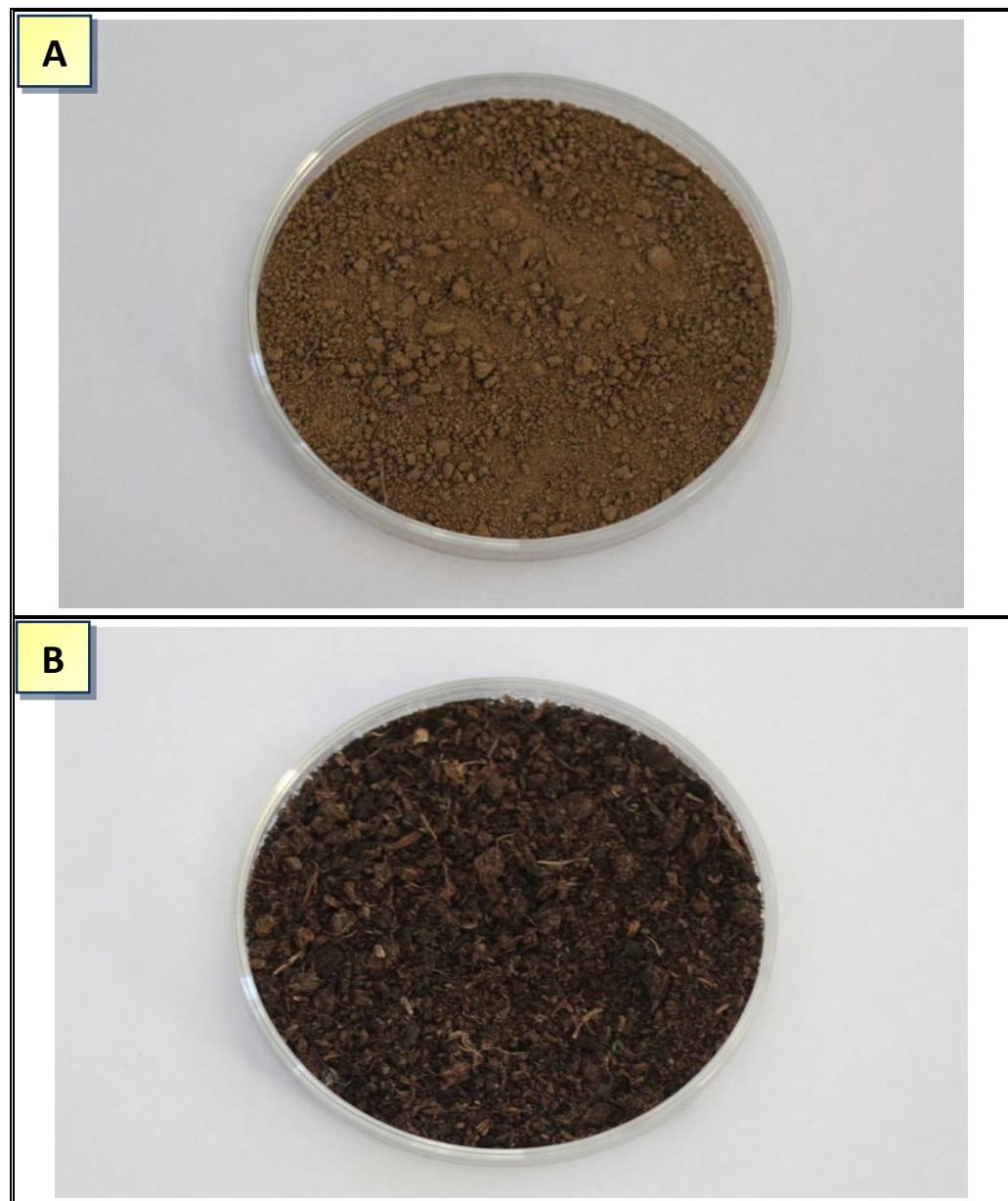


Figure 2.9 Photographic Images of soil type 1 Rothamsted Institute (A) and soil type 2 Castle Bromwich (B)

2.3.4 Soil Burial PU Biodegradation at 50°C

Due to the lengthy process of soil burial experiments at RT, a soil burial experiment was also performed at 50°C. Small air tight containers were used during this experiment in order to retain moisture at the higher temperature, **Fig 2.10B**. Samples were washed with distilled water and ethanol and then dried at 50°C prior to burial. Each (1 cm x 1 cm x \approx 120 μ m) PU film sample was placed in a separate container comprising 100g of soil type no.1 (Rothamsted Research Institute). An appropriate amount of distilled water was then added to each container dependent on the water holding capacity. The containers were then placed in an oven at 50 °C. Samples were removed at regular intervals washed with distilled water and ethanol and then dried at 50 °C under vacuum until constant weight.

The percentage weight loss of the films was calculated from the weights of the dried film samples before and after soil burial as of that for alkaline hydrolysis (see equation 2)

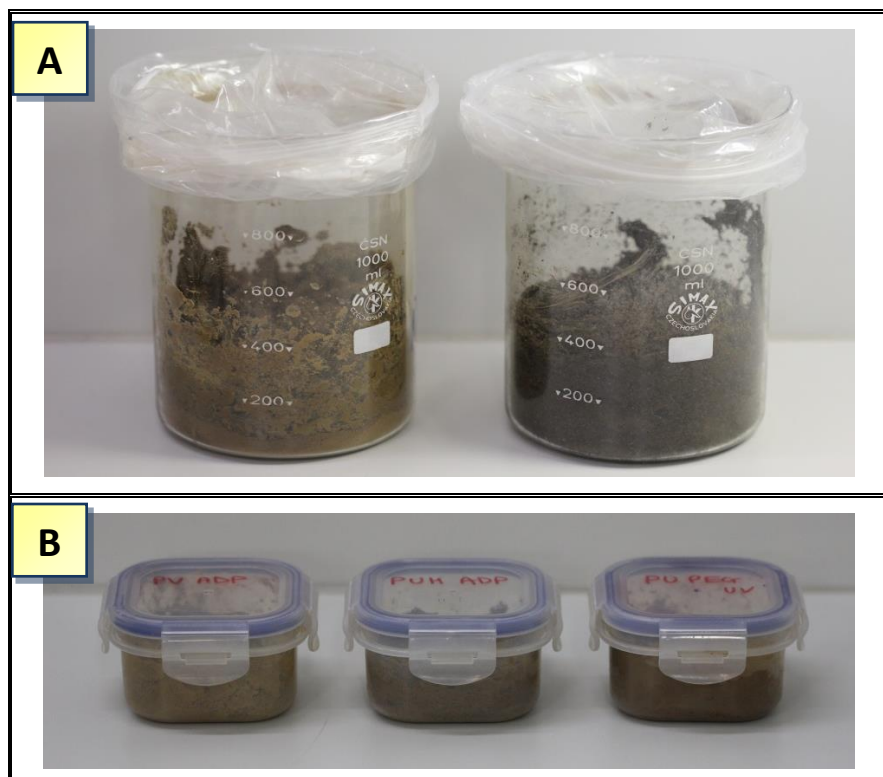


Figure 2.10 Soil burial experiment at RT (A) and 50°C (B)

2.4 Characterisation of Soil from Rothamsted Institute and Castle Bromwich

Prior to biodegradation of PU during soil burial, characterisation of the two types of soil used was undertaken.

2.4.1 Measurement of Soil Acidity

Soil acidity of each soil type was determined by measuring the pH of the soil. Each air dried soil sample (10g) was placed in a 50 ml glass beaker and 25 ml of distilled water added. The solution was then stirred continuously for 10 mins. The soil suspension was then left to stand for 1 hour to allow particulates to settle. The pH of the soil suspension was measured using a Fisher 300 pH meter with glass electrode. Prior to pH measurements of the soil samples, the pH meter was calibrated using standard buffer solutions of pH 7 and pH 4 at room temperature. pH measurements were then taken by inserting the electrode into the supernatant. The pH was recorded when the pH meter had a stabilized reading. Each experiment was performed in triplicate, and the pH for each soil sample was given as a mean of the three pH values obtained.

2.4.2 Soil Dry Matter Content (DM)

In order to obtain the water holding capacity of each soil type, the soil dry matter content needed to be ascertained. For each soil type three crucibles were weighed, and to each crucible was added 10 g of sieved soil (2 mm sieve). Each crucible was then re-weighed and placed in a preheated oven at 105 °C for 24 h. Crucibles were removed from the oven and placed in a desiccator containing silica gel until cool. The weight of the crucible with soil sample was recorded. The dry matter content (DM) was calculated from **equation 3**.

Equation 3

$$\text{DM\%} = (\text{Dry weight of soil} / \text{Fresh weight of soil}) \times 100$$

$$\text{Fresh weight of soil} = (\text{weight of crucible} + \text{weight of fresh soil}) - \text{weight of crucible}$$

$$\text{Dry weight of soil} = (\text{weight of crucible} + \text{weight of dry soil}) - \text{weight of crucible}$$

2.4.3 Soil Water Holding Capacity (WHC)

The soil water holding capacity of each soil type was determined volumetrically. Five 100 ml glass funnels containing ~0.3 g of glass wool inserted in the top of each funnel stem were placed onto a clamp stand. A short length of rubber tubing (8 cm) was attached to the mouth of each stem, and the end of the tubing was clamped with a clip. A 50 g moist soil sample was added into each of the three funnels. A 50 ml measuring cylinder was then placed under each of the five funnels (three sample funnels and two blank funnels). The two blank funnels contained glass wool only. 50 ml of distilled water was then added to each of the five funnels and left to saturate the soil (glass wool for blank) for 30 mins. After 30 mins the clips at the base of the rubber tubing were opened and the water that drained from each funnel was collected for 30 mins. The final volume of water collected after the 30 mins was then noted. The water retained by the soil was calculated using **equation 4**. The water holding capacity (WHC) was calculated according to **equation 5**.

Equation 4

$$A \text{ (ml)} = 50 - (\text{volume of water retained by glass wool} + \text{volume of water collected})$$

$$\text{Volume of water retained by glass wool} = 50\text{ml} - \text{volume of water collected from blanks}$$

$$\text{Volume of water collected from blanks} = \text{Blank 1} + \text{Blank 2} / 2$$

Equation 5

$$\begin{aligned} &\text{Soil Water Holding Capacity (WHC)} \\ &(\text{ml water held at 100% WHC per } 100\text{g oven dried soil}) \end{aligned}$$

$$2A + MC\% = \text{WHC (ml } 100\text{g}^{-1} \text{ fresh soil)}$$

$$MC\% \text{ (Moisture Content)} = 100 - DM \text{ (equation 3)}$$

2.5 Assessment of Degradation and Biodegradation of PU

The rate of degradation and biodegradation of PU samples was quantified using different methods, see **Scheme 2.1**

2.5.1 Assessment of Degradation and Biodegradation by Spectroscopy

FTIR-ATR analysis of the PU samples was performed at regular intervals during accelerated alkaline hydrolysis, enzymatic hydrolysis and soil burial. FTIR-ATR was used to determine changes in the chemical structure and hence the extent of degradation. This was achieved by measuring the difference in absorbance peak heights before, during, and after hydrolysis, **Fig. 2.11**. Although the area under the peak provides a more accurate quantification method, this could not be used for PU, as peak overlap occurs for many group absorbance values. Before each measurement, the films were washed with distilled water and dried under vacuum at 50 °C until constant weight. Spectral analysis was undertaken on a Perkin Elmer Spectrum one FT-IR Spectrometer fitted with a Specac Golden Gate single reflection monolithic diamond ATR accessory. Samples were analysed as 100-120 µm thick films over the range over 4000 cm⁻¹ to 500 cm⁻¹ for 16 scans. Normalisation of peak heights with degradation time were measured using a standard reference peak at 1600cm⁻¹ (aromatic isocyanate PU) and 1318cm⁻¹ (aliphatic isocyanate PU) [105, 117]. **equation 6**.

Changes in molecular structure during degradation were calculated by peak height % change. This was achieved by assuming the initial peak height (obtained from the PU characterization FTIR ATR, spectra **Section 2.2.3**) was 100%, and peak height changes during degradation were calculated as a % increase or decrease of this initial value according to **equation 7**. A worked example is given in **Fig. 2.12**.

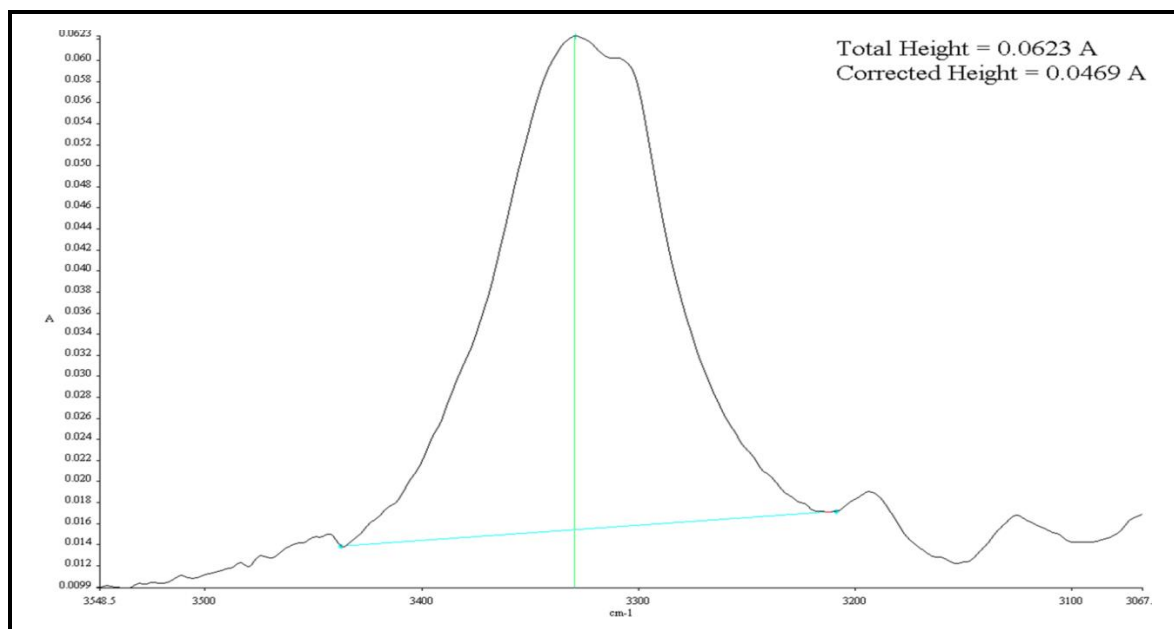


Figure 2.11 Calculation of peak heights during degradation by FTIR-ATR

Equation 6

Aromatic Isocyanate = (Height of abs. peak / Height of ref. peak at 1600cm^{-1}) x 100

Aliphatic Isocyanate = (Height of abs. peak / Height of ref. peak at 1318cm^{-1}) x 100

Equation 7

$$\left(\frac{(H_{ip}/H_{ir}) - (H_{dp}/H_{dr})}{(H_{ip}/H_{ir})} \right) \times 100$$

H_{dp} peak height after degradation,
 H_d , reference peak height after degradation
 H_{ip} initial peak height before degradation
 H_{ir} intial reference peak height before degradation

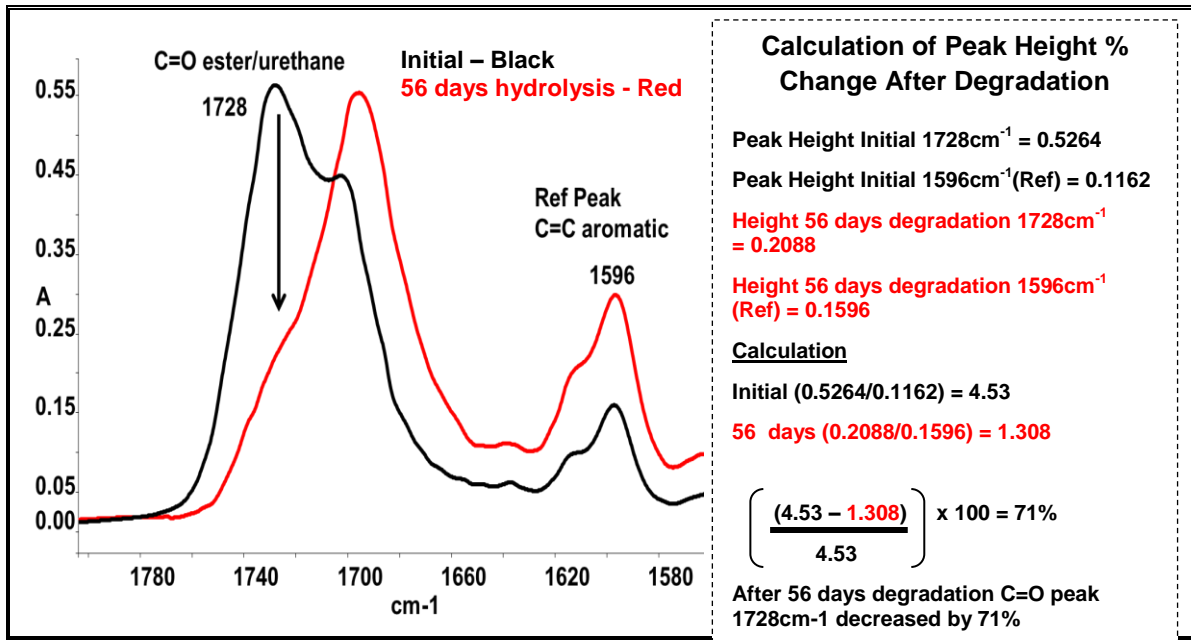


Figure 2.12 Worked example of peak height changes during degradation by FTIR-ATR

2.5.2 Assessment of Morphology Changes to PU during Degradation and Biodegradation by Differential Scanning Calorimetry

Changes in morphology/crystallinity of PU during accelerated alkaline hydrolysis, soil burial and enzymatic hydrolysis were monitored by DSC. Measurements were performed on 5-8 mg circular samples under a helium purge at 40 ml/min using a Perkin Elmer Diamond DSC at a rate of $100^\circ\text{C}/\text{min}$. All thermograms were baseline corrected and calibrated using indium. The samples were first heated to 200°C and held for 3 min to remove thermal history, then cooled to -80°C , held for 3 min before heating to 220°C . Samples were heated at a high heating rate of $100^\circ\text{C}/\text{min}$ to obtain greater sensitivity, Fig. 2.6. Determination of the hard and soft segment transitions were ascertained as the midpoint temperature of each endotherm using the peak find tool in the Pyris software program, Fig. 2.7. The glass

transition for each sample was located by using the midpoint temperature between the extrapolation onset temperature T_o , and the extrapolation endset temperature T_e , **Fig. 2.7**

Quantification of changes in crystallinity during degradation was obtained by relative changes from the initial PU sample **section 2.2.6** according to **equation 8**.

Equation 8

$$\left(\frac{(\Delta H_{\text{endotherm initial sample}} - \Delta H_{\text{endotherm degraded sample}})}{\Delta H_{\text{endotherm initial sample}}} \right) \times 100$$

2.5.3 Changes to thermal stability of PU samples by thermogravimetric analysis (TGA) after degradation and biodegradation.

Changes in the thermal stability of each sample during alkaline hydrolysis, soil burial and enzymatic hydrolysis were quantified by TGA using a Perkin Elmer Pyris 1 thermogravimetric analyser. TGA analysis was performed on 0.5-1 mg samples under a nitrogen purge of a flow rate 60 ml/min. The samples were heated to 650°C at a rate of 10°C/min. Thermal stability was quantified by differential weight loss curve (DTGA) obtained by differentiation of the thermogram of each sample; an example is given in **Fig. 2.5**.

2.5.4 Visual changes during degradation and biodegradation to PU samples assessed by microscopy and photography

Visual changes during alkaline hydrolysis, enzymatic hydrolysis and soil burial were monitored by transmission optical microscopy at a magnification of 20 x 0.4 µm. Each film was removed at regular intervals washed with distilled water and dried at 50 °C under vacuum. Each sample was then placed under the microscope and examined for signs of cracking and deformation of the PU sample. Photographs of each PU sample were also taken at regular intervals in order to record visual signs of degradation to the PU films.. The samples were then given a numbered rating dependent on the extent of visible degradation from the photographs taken, **Table 2.8**

Table 2.8 Arbitrary assessment of visible degradation during testing

No.	Arbitrary Scale of Degradation Stage
0	no signs of cracking deformation
1	slight signs of limited surface degradation
2	deformation of sample (curling) and discolouration
3	visible cracks showing
4	Small pieces of samples broken away from film
5	complete breaking of sample small pieces

Chapter 3

Effect of Polyurethane Method of Synthesis on Degradation and Biodegradation

3.1 Objectives and methodology

Polyurethanes are an important versatile class of polymers that have found a niche in an array of applications, including, medical, automotive, coatings, construction materials and furniture. Generally polyurethanes are chosen for their resistance towards degradation and hydrolysis, however with the increase in public awareness towards pollution and the environment, there has been an increased interest in degradable polyurethanes. It is well documented that the physical and chemical properties of polyurethanes are dependent on the chemical constituents of the polymer [38, 118, 119]. Thermoplastic polyurethanes consist of three components; a diisocyanate, a polyol and a chain extender, and it is the interactions between these constituents; such as hydrogen bonding and microphase separation, that bestow specific properties on the polyurethane (**Chapter 1, Section 1.3.4**). Thermoplastic polyurethanes can be synthesised in numerous ways [38], and the most common methods used are; the one shot method (in which all of the reactants are added at the same time), and the pre-polymer method (in which the isocyanate and polyol are mixed to form a pre-polymer then the chain extender is added to form the final polyurethane), see Chapter 1, **Fig.1.3 and Scheme 3.1**. The work described in this chapter was to determine the effect of the method of synthesis on the physical and chemical properties of the polymer. These results will give an indication of the susceptibility of each different polyurethane sample towards degradation and biodegradation. Three polyurethane samples (synthesised for this work by the sponsor company Eurothane Ltd.) having the same chemical composition but synthesised differently, were tested and reported here to determine the effect of the method of synthesis on the degradation and biodegradation of the samples. These polyurethane samples, which for the purpose of this study were labelled as **Group 1 PUs**, consist of; **PU ADP** (control sample synthesised by the one shot method, with excess isocyanate), **PU PR** (synthesised by the pre-polymer method, with excess isocyanate) and **PU 98** (no excess isocyanate was added, one shot method, **Table 3.1**).

Different factors can contribute to the overall rate of abiotic degradation such as weathering, UV light and burying conditions [25, 27, 120]. During this process, the polyurethane materials can undergo transformations which provoke degradation, and one of the most important parameters involved is that of chemical degradation and biodegradation by hydrolysis [57]. To obtain a broad indication of susceptibility of polyurethane to degradation, each sample was subjected to accelerated alkaline hydrolysis, enzymatic hydrolysis and biodegradation by soil burial. The rate of degradation was determined by weight loss, and structural changes monitored by FTIR-ATR, before, during and after degradation. Changes in morphology were determined by TGA and DSC, before and after degradation.

3.2 Results

3.2.1 Characterisation of Synthesised Polyurethanes PU ADP, PU PR and PU 98 - Group 1 (Method of Synthesis)

In order to examine and fully understand the chemical, physical and morphological changes in the polyurethane samples used in this study during degradation, full characterisation of each sample was undertaken prior to all experiments. This was achieved using a variety of analytical techniques including; FTIR-ATR (chemical structure), TGA (thermal stability) and DSC (morphology)

Samples were provided by Eurothane Ltd in plaque and pellet forms, therefore, prior to characterisation, samples were pressed into films of thickness of between 100-120 μm , see **Table 2.3**.

The solubility of all samples in this group (PU ADP, PU PR, PU 98) were found to be very low (insoluble) in acetone, acetonitrile, ethanol, water and hexane, see **Table 2.4**. The samples were partially soluble in dimethyl sulfoxide and fully soluble in tetrahydrofuran and dimethylformamide, although to fully dissolve a sample constant agitation was required for 24h, see **section 2.2.1**. Hydrophilicity has been shown to influence the biodegradability of polyurethane, and the addition of hydrophilic polyols such as PEG has been proven to improve the hydrophilicity and degradation rate of polyurethanes [33, 56, 121]. Therefore the hydrophilicity of each sample was measured by water absorption prior to the experimental work, see **section 2.2.2**. From the results shown in **Fig.3.1**, it can be noted that there was very little difference in the extent of water absorption between the different samples in this group (**PU ADP 4.5%, PU 98 4.5%, PU PR 3.6%**). Therefore it can be concluded that the method of synthesis did not significantly affect the bulk hydrophilicity.

Chemical structure was determined by FTIR-ATR, **Fig 3.2**. As polyurethanes are essentially microphase separated systems (see **section 1.3**), and consist of a hard segment (isocyanate and chain extender), and a soft segment (polyol), the FTIR-ATR spectra of each sample was examined with respect to specific absorptions for each of these segments. All of the samples in this group had similar spectra and therefore will be discussed together. The hard segment structure can be characterised by typical bands at 3329cm^{-1} (**PU ADP**) and around 3300cm^{-1} (**PU PR** and **PU 98**) corresponding to the stretching vibration of the N-H group [105, 114, 122] **Fig.3.2**. This can be coupled with the absorbances at around 1529cm^{-1} and 1220cm^{-1} relating to the N-H bending vibration with C-N stretching vibration (amide II band) [114, 122, 123] **Fig.3.2**. The absorbance at 1597cm^{-1} was used as the reference peak to normalise all spectra, and denotes the C=C vibration of the aromatic ring [123, 124]. This can be coupled with the absorbance at 815cm^{-1} characteristic to the C-H out of plane bending vibration of a 1,4-disubstituted aromatic ring [123, 124]. Numerous peaks in the spectra are representative of both the hard and soft segment structures and therefore cannot be defined as groups specific to either the hard or soft segment. The hard/soft segment structure can be characterised by the absorbance at about 1728cm^{-1} and 1701cm^{-1} corresponding to the urethane and ester stretching vibrations of the free and hydrogen bonded C=O groups, respectively [59, 105, 114] **Fig.3.2**. The absorbances at 1074cm^{-1} and 1060cm^{-1} show a typical C-O-C stretching vibration relating to the urethane bond in the hard segment and the O-C-C stretch of the ester bond in the soft segment [105, 125] **Fig.3.2**. Only the absorbance peaks at 1137cm^{-1} and 1158cm^{-1} are characteristic of the soft segment exclusively and relate to the C-(C=O)-O ester groups, **Fig.3.2** [124, 125].

The thermal stability of each sample was evaluated by TGA prior to degradation experiments in order to observe any effect of the method of synthesis on the thermal properties of the samples. Samples were heated at a constant rate under a nitrogen atmosphere. The onset decomposition temperature of the hard and soft segments were evaluated by derivative weight loss curve, see **section 2.3.4**. The thermal degradation of polyurethane under a nitrogen atmosphere occurs in a two stage process, and it is well documented that thermal decomposition of the polyurethane hard segment occurs prior to that of the soft segment [34, 102, 126, 127]. The reason for this is that thermal stability has been shown to be dependent on the weakest linkage in the structure, which in the case of polyurethanes has been shown to be the urethane bond (C-NH 98kJ/mol) [34, 102]. The thermographs for each sample are given in **Fig.3.3**. It can be observed that decomposition of the hard segment occurs in the descending order of **PU ADP (333°C)>PU 98 (325°C)** **PU PR (318°C)**. These results show that the hard segment thermal decomposition under an inert atmosphere occurs at a lower

temperature for the polyurethane sample synthesised by the pre polymer method (**PU PR**) than that of the one shot method (**PU ADP**).

DSC studies were undertaken to characterise the initial morphology before degradation. Samples were subjected to a heating temperature of 100°C per min under a helium atmosphere to 180°C to remove previous thermal history, then the temperature reduced to -100°C and heated again to 220°C. An indication of phase separation between the hard and soft segments in polyurethane can be obtained by the T_g value of the soft segment, and it has been shown previously that increased phase separation between the hard and soft segments decreases the T_g value [107, 109]. The DSC thermograms of group 1 PU samples **PU ADP**, **PU PR** and **PU 98** are shown in **Fig.3.4**. The T_g was found to be similar for **PU ADP (-18°C)** and **PU PR (-16°C)**. This indicates that altering the method of synthesis did not affect the dispersal of the hard segment within the soft segment, and therefore does not provide an explanation for the increased thermal stability of **PU ADP Fig.3.3**. However, there were notable differences between the endotherms relating to the hard segments of the PU samples. It is generally accepted that segmented elastomers can display up to three endotherms, relating to the hard segment domain [107, 109, 128]. For **PU ADP** all three endotherms relating to the hard segment were observed **Fig.3.4a**. The endotherm at **109°C** relates to the short range ordering of non-crystalline hard segment domains **Fig.3.4 & 3.5** [22-24]. The endotherm at **147°C** relates to long range ordering of non-crystalline hard segment domains **Fig.3.4 & 3.5** [22-24], and the third endotherm relating to the microcrystalline regions within the hard segment was observed at **195°C Figures 3.4 & 3.5** [22-24]. The ΔH values for each endotherm were calculated and are given in **Table 3.2**. From these results it can be seen that **PU ADP** exhibited the greatest microcrystalline region at **195°C, ΔH (6.08 J/g)** indicating that the hard segment domains in **PU ADP** were principally highly ordered microcrystalline regions. This is in contrast to **PU PR** in which the microcrystalline region was shown to be significantly lower at **ΔH (1.08 J/g), Fig. 3.4b & Table 3.2**. These morphological differences induced by the method of synthesis may have an effect on the degradation and biodegradation of TPU and will be assessed in **section 3.2.2**.

3.2.2 Effect of Method of Synthesis (PU ADP, PU PR and PU 98) on the Rate of Alkaline Hydrolysis

The three polyurethane samples with the same composition but synthesised differently (**Group 1: PU ADP, PU PR, PU 98, Table 3.1**, were immersed in 10% NaOH solution and

removed at weekly intervals to monitor their degradation, see Section 2.3.1. The chemical compositions of **PU ADP** (one shot method) and **PU PR** (pre-polymer method) were kept constant in order to evaluate any difference in the method of synthesis, **Table 3.1a**. There were significant differences both by weight loss, **Fig.3.6a** and visually, **Fig.3.6a & Figs.3.7 & 3.8**. After 21 days, **PU PR** exhibited the greatest weight loss, and had completely degraded after the 28 day period, **Fig.3.6a** and **Figs.3.7 & 3.8**. These differences may be due to morphology changes caused by the method of synthesis.

3.2.2.1 Structural changes in PU ADP, PU PR and PU 98 monitored by FTIR-ATR

During alkaline hydrolysis, FTIR-ATR was performed on the PU samples in order to determine structural changes during degradation. An initial spectrum of each sample was taken before hydrolysis, and group absorbances were assigned accordingly, **Section 3.2.1.1 & Fig.3.2**. Analysis of the spectra during hydrolysis was quantified by changes in peak height, and then relative peak height changes were calculated in comparison to the virgin polymer films prior to hydrolysis see **Section 2.5.1, Fig 2.11**. These calculations were then used to show changes in both the hard and soft segments during hydrolysis. Peak height % was used due to peak overlap within the spectra.

i) Spectral changes Hard Segment structure PU ADP, PU PR and PU 98

The hard segment structure was previously characterised by FTIR-ATR (see **section 3.2.1.**). The N-H bond of the urethane linkage in the hard segment showed dramatic changes during alkaline hydrolysis. **Fig.3.9a** shows that the peak at 3329cm^{-1} (**PU ADP**) increased during the 42 days (**+17%**) with the peak shifting to 3301cm^{-1} after 14 days. The same was also observed for **PU PR** with an increase in the peak at 3301 cm^{-1} (**2%**) after 21 days (**Fig.3.9c**) and in the case of **PU 98**, a decrease in this peak was observed after 42 days (**Fig.3.9e**). A decrease in the peak at 1529cm^{-1} (**-14% PU ADP, -16% PU PR after 21 days, -20% PU 98**) was observed, relating to the N-H bending vibration with C-N stretching vibration (amide II band), **Fig.3.9 b, d & f**. This peak also shifted to around 1518cm^{-1} after hydrolysis. These results indicate partial degradation of the hard segment; the increase in the N-H peak is characteristic of the formation of primary amine groups during hydrolysis. This suggestion can be further supported by the appearance of a shoulder at 3398cm^{-1} , **Fig 3.9 a & d** which is characteristic of the bending vibration of the N-H peak of aromatic amines [6,9,10].

ii) Spectral changes Hard/Soft Segment Structure PU ADP, PU PR and PU 98

Due to the structure of polyurethane, many peaks observed in the FTIR-ATR spectra cannot be assigned to solely the hard or soft segment structure, but may relate to specific groups in both segments, and these peak assignments will be discussed in this section.

Changes relating to the CH_2 moiety in the soft/hard segment structure were observed from the peak at 1477cm^{-1} , which increased during alkaline hydrolysis for all samples, and a decrease in the peak at 1459cm^{-1} relating to the urethane C-N linkage, **Fig.3.9 b, d, f.**. This may be due to an increase of the hard segment on the surface of the polyurethane film as the soft segment degrades. The peak at 1381cm^{-1} relating to the $\alpha\text{-CH}_2$ group was also seen to decrease and eventually disappeared after 21 days (PU PR), and 42 days (PU ADP, PU 98) **Fig.3.9**. A significant change was noted in relation to hard/soft segment groups, with the free C=O peak at 1727cm^{-1} decreasing by **81%** after 42 days of hydrolysis (**PU ADP**), **Figure 3.10a**, **87%** after 21 days (**PU PR**) and **82%** after 42 days (**PU 98**) **Figure 3.10 c & e**. The hydrogen bonded C=O peak at 1701cm^{-1} also decreased by **35%** (PU ADP), **33%** (PU PR) and **36%** (PU 98) which also shifted to 1695cm^{-1} after hydrolysis, **Figure 3.10 a, c & e**. A decrease in the peak at 1074cm^{-1} (**-40% PU ADP, -35% PU PR, -38% PU 98**) and 1060cm^{-1} (**-16% PU ADP, -19% PU PR, -14% PU 98**) denoting the C-O-C urethane bond and O-C-C ester bond was also observed, **Figure 3.10 b, d & f**.

iii) Spectral changes PU ADP Soft Segment structure

The soft segment structure of the polyurethane samples were characterised by the peaks at 1137cm^{-1} and 1159cm^{-1} denoting the (C-(C=O)-O ester) group, and **Figs.3.10b, d & f** display spectral changes during alkaline hydrolysis of these peaks, which decreased dramatically for all samples, and had completely disappeared after 42 days (**PU ADP, PU 98**). For **PU PR**, these peaks disappeared after 21 days, indicating that the ester linkages in the polyethylene adipate soft segment hydrolysed at a faster rate for the polyurethane synthesised by the prepolymer method.

3.2.2.2 Effect of Method of Synthesis on Crystallinity and Thermal Stability during Alkaline Hydrolysis (PU ADP, PU PR and PU 98)

DSC was performed on each of the PU samples in group 1 (method of synthesis) at regular intervals during alkaline hydrolysis in order to elucidate morphological changes to the hard and soft segment structure. From the results shown in **Fig 3.11a & b**, it can be seen that **PU ADP** (one shot method) and **PU PR** (pre-polymer method) exhibited different transitions during degradation. Prior to hydrolysis, **PU ADP** synthesised by the one shot method,

showed three endotherms relating to the MDI/BD hard segment and one endotherm relating to the polyethylene adipate soft segment, **Fig.3.11a**. It can be seen that, during alkaline hydrolysis, all of these peaks were seen to reduce and eventually disappear after 28 days. In contrast to this, **Fig.11b**, **PU PR** synthesised by the pre-polymer method, exhibited two endotherms at 148°C and 195°C relating the MDI/BD hard segment, which were seen to increase during hydrolysis, with the endotherm at 195°C denoting melting of the microcrystalline region increasing dramatically, **Fig. 11b**.

TGA was performed on each of these samples prior to hydrolysis, (see **section 3.2.1.1**), and after 21 days of alkaline hydrolysis (**PU PR** completely degraded after this time), in order to determine changes to the hard and soft segments. These results produced interesting findings. From **Fig. 3.12**. it can be seen that **PU ADP** (one shot) displayed two DTGA peaks at 309°C and 432°C after 21 days of hydrolysis relating to the hard and soft segments respectively [18-21]. The mass loss curves indicated that a large proportion of the soft segment had degraded (initial value 67%, after hydrolysis 25%), however most of the hard segment still remained, **Fig. 3.12**. These observations are in accordance with FTIR-ATR results (see section 3.2.2.2). The TGA results for **PU PR** (pre-polymer) after 21 days of hydrolysis exhibited a completely different thermogram to that of **PU ADP**, **Fig. 3.12** in that DTGA peaks were observed at 204°C, 260°C, 302°C and 406°C. The peaks at 302°C and 406°C related to the hard and soft segment thermal decomposition temperatures respectively [18-21]. However, the two peaks at 204°C and 260°C, which possibly relate to degradation products during hydrolysis of the soft segment, as these peaks were not observed in the intital thermogram of the sample, **Fig. 3.12**.

3.2.3. Susceptibility to soil degradation of Polyurethane Samples PU ADP, PU PR and PU 98 (Effect of Method of Synthesis).

PU samples were subjected to two different types of soil burial in order to assess their susceptibility towards microbial degradation in soil. The first type of soil burial involved placement of samples in 800ml glass beakers containing 300g of soil. The beakers were then covered and stored in a dark cupboard at room temperature (RT) (see **Section 2.3.3 & Figs.2.9 & 2.10**). The samples were removed at regular intervals to assess degradation. In the second soil burial experiment, samples were placed into small containers containing 100g soil and placed in an oven at 50°C in order to simulate a composting environment and removed at regular intervals to assess degradation (**see section 2.3.4 & Figs. 2.9 & 2.10**). Both experiments can be considered synonymous with each other, with the exception of faster degradation rates from the composting simulation experiment due to the higher temperature involved (~50°C), and as such is a rapid effective method in which to examine the biodegradability of PU in the natural environment [64].

After 20 months of soil burial at RT there was little weight loss observed for PU samples in either soil types, with the greatest weight loss occurring for **PU 98 at 7% soil type 1, 9% soil type 2, Fig.3.13b & c.** The PU film samples in this group (**PU ADP, PU PR, PU 98**) were still intact and did not show any visible signs of cracking, **Fig. 3.14.** However, some visible signs of degradation were observed microscopically for **PU ADP** (soil 1) and **PU PR** (soil 2) implying that some biodegradation of these films had occurred **Fig.3.15.**

PU samples subjected to soil burial at 50°C for 5 months displayed a greater weight loss than those at RT **Fig.3.13a**, with the greatest weight loss of **68%** for **PU 98**, although weight losses were also noted for **PU PR** at **32%** and **PU ADP, 21%**. From **Fig 3.14** it can be noted that the samples were not intact after 5 months. The films were broken and fragile when removed from the soil. In order to ascertain any structural changes taking place during soil burial FTIR-ATR was performed on each sample at regular intervals during the experiment.

3.2.3.1 Structural changes during soil burial at 50°C in PU ADP, PU PR and PU 98 monitored by FTIR-ATR.

The main spectral changes during soil burial involved the ester/urethane linkages in the samples, therefore these will be examined in detail. **Fig. 3.16 a, c & e** displays peaks relating to the free urethane/ester carbonyl group at 1727cm^{-1} , which decreased for all groups during soil burial, even after 3 months. However, there still remained a significant peak after 5

months despite the fact that the films had completely broken up **Fig. 3.14**. This suggests that not all of the adipate ester contained in the samples had degraded. This can be further supported, by the FTIR-ATR peaks at 1158cm^{-1} and 1137cm^{-1} denoting the O-C-C ester bond **Figs.3.16 b, d & f**, which again although decreased somewhat, still remained after 5 months.

A new peak at 1038cm^{-1} was observed for all samples after 3 and 5 months which may suggest the formation of alcohol/amine degradation products **Fig.3.16 b, d & f**. This can further be verified by **Fig. 3.16 a,c & e** which clearly displays the appearance of a significant peak at 1659cm^{-1} , and also by the increase in the N-H peak at 3330cm^{-1} denoting the formation of amine groups **Fig. 3.17a-c**.

3.2.3.2 Structural changes during soil burial at RT after 20 months in PU ADP, PU PR and PU 98 monitored by FTIR-ATR

Spectral changes during soil burial at RT after 20 months were similar to those as at 50°C (see above). The peaks at 1727cm^{-1} and 1701cm^{-1} relating to the free and hydrogen bonded urethane/ester carbonyl group respectively were seen to decrease after 20 months soil burial. A slight decrease in this peak was observed for **PU ADP** for both soil samples **Fig. 3.18a**, however the opposite was true of **PU PR**, with this PU being more susceptible to degradation in the garden soil type 2 **Fig. 3.18c**. The carbonyl peaks at 1727cm^{-1} and 1701cm^{-1} for **PU 98** was seen to decrease for both soil types **Fig. 3.18e**. These findings suggests that, although some degradation of each sample had occurred it was not substantial, and this observation can be supported by the peaks at 1158cm^{-1} and 1137cm^{-1} as shown in **Fig. 3.18b,d & f**, denoting the O-C-C ester bond which again, although decreased slightly, still remained after 20 months. The rate of biodegradation under soil burial conditions was deemed to be **PU98 > PU PR > PU ADP** for both soil types, however none of these samples were observed to be particularly degradable in soil at RT, as all samples remained intact throughout the experiment.

3.2.2.3 Effect of Method of Synthesis on Crystallinity after 20 months soil burial (PU ADP, PU PR and PU 98)

PU samples subjected to soil burial at RT were removed from the soil, and morphological changes during biodegradation were ascertained by DSC (morphological changes in samples buried in soil at 50°C could not be performed due to the fragile nature of the films).

From the results shown in **Fig. 3.19a**, it can be seen that after soil burial of **PU ADP** (one shot method), minor changes were observed in the DSC thermograms, with the most significant finding being, the disappearance of the peak at 109°C relating to the short range ordered MDI/BD hard segment. However, the endotherms at 147°C and 195°C relating the long range ordered and microcrystalline MDI/BD regions remained relatively unchanged. This indicates that although some minor degradation had occurred it was not significant. More noticeable changes were observed in the DSC thermograms after soil burial for 20 months for **PU PR** (prepolymer method), **Fig. 3.19b** with an increase in the endotherm at 195°C denoting the microcrystalline MDI/BD region. As of that for **PU ADP**, a slight difference in degradation of **PU PR** was noted in relation to soil type, with a greater increase in the endotherm at 195°C for soil type 2 (ΔH 8.5J/g). These findings can be supported by similar results for FTIR-ATR which indicated greater biodegradation in soil type 2 for **PU PR section 3.2.3.2.**

3.2.4. Susceptibility of Polyurethane Samples PU ADP, PU PR and PU 98 (Effect of Method of Synthesis) towards enzymatic degradation.

In order to ascertain susceptibility of the PU samples towards biodegradation and degradation, samples were placed in buffer solutions (37°C), each solution containing a fungal enzyme. Previously, studies have shown that PU is susceptible towards enzymatic degradation by esterases/lipases and proteases [21, 23, 24, 129]. As this PU was for agricultural purposes to degrade in soil after end use, fungal esterases/lipases and proteases were used. Two different lipases and two different proteases were used to examine the susceptibility of the PU samples to enzymatic degradation. Degradation was monitored by weight loss, visual changes using optical microscopy and chemical structural changes by FTIR-ATR.

Fungal lipases from *Rhizopus* sp. and *Aspergillus niger* and proteases from *Aspergillus saitoi* and *Rhizopus* sp. were used for enzymatic degradation of the PU samples. *Rhizopus* sp., is a common fungi associated with plants and vegetables and commonly found in soil [130-132], and many species of *Aspergillus* are also abundant in soils [23, 133-136], *Aspergillus niger* has also been previously shown to degrade some types of PU [24].

Samples were removed from enzyme/buffer solutions every 12 days for a period of 24 days (see section 2.3.2). For the protease degradation, the pH of the buffer was 2.8 therefore, samples were also placed the buffer solution only to determine whether any degradation occurred due to enzyme activity or the acidic buffer solution.

3.2.4.1 Structural changes during enzymatic degradation using lipases in PU ADP, PU PR and PU 98 monitored by FTIR-ATR.

There was little weight loss (not shown) observed after 24 days for all of the PU samples in this group for both lipases *Rhizopus* sp. and *Aspergillus niger*, which was both unexpected and disappointing. However, optical images did display some signs of surface degradation for *Aspergillus niger* after 24 days **Fig.3.20**, and therefore FTIR-ATR was performed to determine the extent of degradation.

Spectral changes after 24 days of enzymatic degradation of PU samples for both *Rhizopus* sp. and *Aspergillus niger* are given in **Fig.3.21**. It can be noted that there was relatively little change in the spectra for PU ADP for *Rhizopus* sp., **Fig 3.21a & b**. However, samples immersed in the buffer solution containing *Aspergillus niger*, did display a small decrease in

the peaks at 1725cm^{-1} and 1701cm^{-1} denoting the ester/urethane linkage, and at 1158cm^{-1} and 1137cm^{-1} which corresponds to the ester bond in the PEA soft segment. **Fig. 3.21b**, also displays a small decrease at 1073cm^{-1} which corresponds to the ester/urethane C-O-C bond. For **PU PR**, a small decrease in the peaks at 1725cm^{-1} and 1701cm^{-1} was observed after 24 days in enzymatic solution for both lipases **Fig.3.21c & d**. The same was observed for the peaks at 1158cm^{-1} , 1137cm^{-1} and 1073cm^{-1} . From these results it was noted that the method of synthesis did not significantly alter the rate of enzymatic degradation by the two lipases used for this experiment.

3.2.4.2 Structural changes during enzymatic degradation using proteases in PU ADP, PU PR and PU 98 monitored by FTIR-ATR.

Degradation by proteases was also disappointing in that little weight loss (not shown) was observed for *Aspergillus saitoi* and *Rhizopus* sp. However, fungal growth and visible cracking from microscope images of the PU samples were observed with *Rhizopus* sp. **Fig. 3.22**.

The FTIR-ATR spectra of the PU samples did highlight small differences regarding degradation of the urethane linkages contained within the hard segment and hard/soft segment interfaces. **PU ADP** displayed a reduction in the ester/urethane peaks at 1727cm^{-1} and 1701cm^{-1} , and also the N-H & C-N peak at 1527cm^{-1} relating to the hard segment, **Fig. 3.23**. this is in accordance with the microscopic images, which clearly displays cracks in the **PU ADP** film, **Fig.3.22**. A decrease was also observed at 1077cm^{-1} denoting the C-O-C urethane stretch, **Fig.3.23**. However, for **PU PR** and **PU 98**, an increase in the peak at 1727cm^{-1} was observed, denoting the ester/urethane linkage. This is more than likely due to fungal growth on the surface of the PU samples which can be seen for **PU 98**, **Fig. 3.22**. Although some signs of initial degradation were observed, there was no significant difference between the samples to support the supposition that the method of synthesis affected the rate of enzymatic degradation for the lipases/proteases used in this experiment.

3.3 Discussion

3.3.1 Effect of Method of Synthesis (PU ADP, PU PR and PU 98) on the Rate of Alkaline Hydrolysis

Hydrolysis is essentially a chemical reaction by which chemical bonds are broken in the main chain by a reaction with water, and is dependent on a variety of parameters such as, temperature, pH and time. Hydrolysis is also dependent on the structural characteristics of the polymer, the degree of its crystallinity, molecular weight and molecular weight distribution [57]. For example, structured molecular frameworks (crystalline domains) prevent the diffusion of H₂O, thereby reducing hydrolytic degradation of the polymer, and conversely a more disorganised molecular structure (amorphous regions) results in the polymer having a greater susceptibility to hydrolytic degradation [7]. For PU, hydrolysis can result in numerous degradation products such as carboxylic acids and amines, **Fig.3.24**, as both ester and urethane linkages contained within the PU structure are susceptible to hydrolysis. In order to design materials with a controlled life span, optimization of hydrophilic characteristics are essential. Therefore polyurethane samples were subjected to alkaline hydrolysis in order to monitor rate of degradation and the effect of the method of synthesis on degradation.

Prior to hydrolysis, PU films were characterised in order to ascertain changes during hydrolytic/biodegradation. Thermal stability of each PU sample was assessed by TGA. The results from the initial thermograms highlighted a difference in the thermal stability between **PU ADP** synthesised by the one shot method and **PU PR** synthesised by the prepolymer method, in that **PU ADP** was observed to be more thermally stable than that of **PU PR** **Fig.3.3**. As thermal decomposition in polyurethane commences with the hard segment [18-21], the distribution of the hard segment within the polymer matrix plays an important role in the thermal stability of the polyurethane, and aggregation of the hard segment could be a factor which influences the difference in the thermal stability between these samples. It has been shown in previous studies that dispersal of amorphous regions inside the hard segment weakens the structure [107-109]. Therefore greater phase separation between the hard and soft segments may confer higher thermal stability on the polyurethane. For this reason DSC characterisation was performed on each of these samples in order to ascertain morphological information of the polyurethanes.

DSC analysis was performed on each sample prior to hydrolysis and produced interesting findings. It was speculated that there may have been a difference in microphase separation,

dependent on the method of synthesis due to the increased thermal stability of **PU ADP** (see above). However, the T_g values were similar for **PU ADP** (-18°C) and **PU PR** (-17°C) were observed indicating little difference in phase separation between the samples. Nevertheless, a dramatic difference in crystallinity was observed from the thermograms of **PU ADP** and **PU PR**, as the microcrystalline region for **PU PR** was shown to be significantly less ΔH (1.8 J/g), **Fig. 3.25**. Interestingly **PU 98** synthesised by the one shot process with no excess isocyanate, also contained a greater proportion of microcrystalline hard segment regions ΔH (2.2 J/g) than **PU PR**, but it was not as crystalline as the control sample **PU ADP**. The 2% excess of isocyanate added to **PU ADP** produces extra crosslinking by the formation of allophante and buiret groups, therefore, the exclusion of this excess for **PU 98**, would result in less crosslinking and hence would be expected to increase the rate of degradation.

The morphological differences between **PU ADP** and **PU PR** can be explained by the method of synthesis. During the one shot process (**PU ADP**), all of the reactants are added at the same time with a lightly favoured reaction between BD and MDI [12, 137], **Fig.3.25**. It has been demonstrated that this method of synthesis results in highly crystalline mobile chain structures acting as crosslinks [38, 137]. Conversely, **PU PR** synthesised by the pre polymer method is more controlled and involves the rapid build-up of the molecular weight of the prepolymer by the chain extender (BD). It has been suggested that this then alters the morphology as the molecules become entangled and immobilized before order can be established, and therefore produces elastomeric polyurethanes with less crystalline regions [12]. This was indeed found to be the case for these particular PU samples with **PU ADP** (one shot) containing a greater proportion of microcrystalline regions than that of **PU PR** (pre-polymer), and thus can also explain the increased thermal stability of **PU ADP** under an inert atmosphere. It was surmised that these morphological differences induced by the method of synthesis would affect the rate of degradation and biodegradation of TPU, and FTIR-ATR, TGA and DSC were performed during hydrolysis to determine whether this was the case.

Weight loss results during alkaline hydrolysis indicated that the highest rate of hydrolytic degradation occurred for **PU PR**; synthesised by the pre-polymer method, with the film becoming fragile and eventually breaking up after 21 days. Conversely, the film synthesised by the one shot process; **PU ADP**, remained intact after 42 days, **Fig. 3.8**. These findings were supported by FTIR-ATR analysis during hydrolysis experiments. Changes in relative % peak heights revealed a substantial decrease of the peak at 1159cm⁻¹, **Fig 3.26**, denoting the

soft segment PU component; polyethylene adipate, for all samples in this group, even after 7 days **Fig.3.26a**. However a more substantial decrease was observed for **PU PR** after 7 days (70%) indicating that the PEA soft segment had hydrolysed at a faster rate. With only a relatively small amount of PEA remaining within the film after just 7 days it would be expected to observe a substantial amount of visual degradation, however this was not found to be the case **Fig.3.26a**. Therefore it can be surmised that the hard segment of the PU plays a major role in the rate of degradation. This hypothesis can be supported by FTIR-ATR, and from **Fig.3.26b** it can be noted that only a small decrease in the peak at 1520cm^{-1} denoting the NH coupled with the CN urethane linkage was observed. However, also noteworthy was the increase of the NH stretch at 3330cm^{-1} for **PU ADP** and **PU PR** as hydrolysis progressed, which could be due to the formation of aromatic amines, a degradation product during PU hydrolysis **Fig.3.26c**. However, the increase at 3330cm^{-1} could also be due to a conformational change on the surface of the PU, as the soft segment degrades, the surface of the PU is more likely to contain hard segment domains which would explain the increase of this peak.

From the results obtained by FTIR-ATR it can be concluded that the ADP soft segments on the surface of the PU films in all of the samples in this group of TPU's were hydrolysed after 28 days. However, the rate of hydrolytic degradation of the soft segments was in the order of **PU PR >PU 98 >PU ADP**, which indicates that degradation of the soft segment during hydrolysis is not only dependent on the constituents of PU but also on the method of its synthesis. However, hydrolysis of the soft segment alone did not result in the breakup of the PU films. Hydrolysis of the hard segments of all the TPU samples examined in this group occurred to a somewhat lesser extent, with the possible formation of degradation products such as primary aromatic amines. Therefore it can be surmised that the hard segment may be the limiting factor on the rate of hydrolytic degradation of PU, and hence the method of synthesis would be influential on the rate of hydrolytic degradation. In order to examine this theory more closely, thermal and morphological properties were examined.

DSC thermograms of the PU samples during alkaline hydrolysis showed that the hard segment of **PU PR** synthesised by the pre-polymer method showed highly ordered crystalline regions during alkaline hydrolysis, which increased with hydrolysis time, **Fig.3.27b**. This was deemed to be due to degradation of the soft segment during hydrolysis, which resulted in the highly crystalline hard segment blocks remaining. This is in accordance with results from FTIR-ATR which showed complete degradation of the soft segment, **Fig. 3.27c** Conversely, the thermogram for **PU ADP** synthesised by the one shot method, revealed that the hard segment microcrystalline endotherm at 195°C disappeared after 21 days **Fig.3.27a**. The

explanation for this could be due to two reasons; the first reason is that complete degradation of the hard segment had occurred, therefore no endotherms would be observed, or secondly, the ordered structure of the hard segment was lost to produce less ordered amorphous domains. The second explanation seems more likely due to the fact that the film still remained intact after 28 days of hydrolysis. This can be substantiated by results from FTIR-ATR which indicated that the soft segment had degraded by 95%, (C-C=O-O-C ester peak 1159cm^{-1}) **Fig. 3.27 a & b**, whereas a large proportion of the hard segment still remained.

Results from TGA, showed 4 mass loss peaks for PU PR after hydrolysis ($204^\circ\text{C}, 260^\circ\text{C}, 302^\circ\text{C}, 406^\circ\text{C}$) as opposed to 2 peaks initially ($318^\circ\text{C}, 390^\circ\text{C}$), **Fig. 3.27**. and it was speculated that the thermogram mass losses at 204°C , 260°C and 406°C may not relate to the original adipate soft segment, but may relate to a degradation product of the PU. This seems likely to be the case, as the DSC thermogram for **PU PR** displayed a substantial decrease in the ΔCp at T_g relating to the soft segment, with hydrolysis time **Fig 3.27f**. This decrease in ΔCp indicates a decrease in amorphous regions within the polymer structure and hence a substantial degradation of the ADP soft segment.

From the DSC and TGA results, it can be concluded that after alkaline degradation, the hard segment morphology of **PU ADP** (one shot method) had changed, from a large proportion of highly ordered crystalline regions into a completely amorphous domain. However, the hard segment domain, although amorphous, still kept the film intact, as the results from FTIR-ATR, and TGA showed substantial degradation of the soft segment, **Fig. 3.27c**. The PU sample synthesised by the pre-polymer method; **PU PR** highlighted a completely different morphological profile during hydrolytic degradation, in that the polyester adipate soft segment at the surface of the sample had completely degraded after 21 days, **Fig.3.10d**. The hard segment morphology changed with an increase in crystallinity indicating a highly crystalline structure. The increased rate of degradation of **PU PR** can be explained by the method of synthesis, in which MDI is linked to the ester soft segment by forming a pre-polymer, then extended with the BD chain extender, thereby resulting in a final PU with less crystalline domains within the hard segment than **PU ADP** (one shot).

3.3.2. Susceptibility to soil degradation of Polyurethane Samples PU ADP, PU PR and PU 98 (Effect of Method of Synthesis).

There was very little difference between the samples in this group with respect to the soil burial experiments both at RT and at 50°C. The increase in temperature did increase the rate of biodegradation in comparison to soil burial at RT. Although the soil burial at 50°C was to be considered synonymous to composting conditions [64], it would be more difficult to attribute the degradation specifically to either thermal degradation, biodegradation by microorganisms or a combination of both. However, results from TGA, see **Fig.3.28.** showed that the PU samples in this group were thermally stable at 50°C so it is unlikely that thermal degradation played a major role in soil degradation at this temperature. Results from soil burial at RT were very disappointing in that none of the PU films in this group exhibited any major visual signs of degradation for either soil type1 or soil type 2, when in comparison to PLA, a polymer known to be biodegradable [1, 6, 57, 138], **Fig.3.28.** There were some relatively minor changes observed from the FTIR-ATR spectra for all samples, **Fig.3.18.** DSC also showed similar results in that some morphological changes had occurred to the short and long range crystalline regions, but only to a small extent **Fig 3.28.** **PU PR** did exhibit a similar DSC thermograph after degradation in soil 1 for 20 months, similar to the alkaline hydrolysis thermograph after degradation, in that an increase in crystallinity was observed, **Fig 3.28.** This indicates that some limited degradation had occurred. However, in general these results were disappointing and unexpected, as a major difference was noted between **PU ADP** and **PU PR** during alkaline hydrolysis, and similar findings were predicted in respect of soil burial. However, biodegradation in soil is a complex process and is dependent on many factors such as water holding capacity, humidity, microorganisms etc. [21, 102, 115], and therefore one can only conclude that the chemical constituents of these samples were not conducive towards microbial degradation in these soil types at RT, therefore the method of synthesis did not significantly alter the rate of biodegradation.

3.3.3. Susceptibility of Polyurethane Samples PU ADP, PU PR and PU 98 towards Enzymatic Degradation (Effect of Method of Synthesis).

PU samples in group 1 (method of synthesis) subjected to enzymatic degradation with two different lipases; *Aspergillus niger* and *Rhizopus* sp. did display some limited degradation visually, and some minor differences were also noted in the FTIR-ATR spectra taken during the experiment.

Enzymes are essentially biological catalysts. By lowering the activation energy of a reaction they can induce an increase in reaction rate in an environment otherwise unfavourable for

chemical reactions. A generalised mechanistic scheme for enzymatic degradation of ester and amide linkages is given in **Fig.3.29**, The enzyme binds to the polymer substrate then subsequently catalyzes a hydrolytic cleavage. The reaction mechanism is common to hydrolases and generally involves three amino acid residues: aspartate, histidine and serine. This reaction leads to the formation of an alcohol end group and an acyl-enzyme complex which then reacts with water to produce a carboxyl end group and the free enzyme [57]. During enzymatic degradation with lipases a decrease in ester groups would be expected [129], and this was observed in the FTIR-ATR spectra for **PU ADP** and **PU PR** when subjected to degradation by *Aspergillus niger*. The spectra given in **Fig. 3.30**, displays a small decrease in the peaks at 1727cm^{-1} and 1701cm^{-1} relating to the ester/urethane bond for both **PU ADP** and **PU PR**. A small decrease was also observed for the peaks at 1137cm^{-1} and 1073cm^{-1} relating to the ester and C-O-C linkages in the PU, respectively. Although this decrease was noted, it was only found to be minimal and indicates that only a limited amount of degradation of the ester linkages had occurred after 24 days. Enzymatic degradation is known to proceed typically on the surface of polymeric materials, particularly the amorphous surface regions, as high molecular weight enzymes cannot easily penetrate the solid bulk, and studies have shown that large amounts of hard segment and crystalline regions results in a reduction in enzymatic activity [120, 129], therefore it would be expected that the method of synthesis would affect the rate of enzymatic degradation and therefore **PU PR** would be more susceptible than that of **PU ADP**, due to the highly crystalline profile of **PU ADP**, **Fig 3.30**. However, this was not deemed to be the case, with minimal degradation occurring in both **PU ADP** and **PU PR**, and therefore one can surmise that the chemical constituents of the PU were either not conducive towards enzymatic degradation by lipases or else the enzymes could not penetrate the polymer matrix in order to hydrolyse the components.

The PU samples were also subjected to enzymatic degradation by proteases from *Aspergillus saitoi* (not shown) and *Rhizopus* sp. However, only degradation with *Rhizopus* sp. displayed any changes in the PU samples. The FTIR-ATR spectra of the PU samples showed some small differences relating to degradation of the urethane linkages contained within the hard segment and hard/soft segment interfaces. **PU ADP** displayed a reduction in the ester/urethane peaks at 1727cm^{-1} and 1701cm^{-1} , and also the N-H & C-N peak at 1527cm^{-1} relating to the hard segment, **Fig. 3.30**. A decrease was also observed at 1077cm^{-1} denoting the C-O-C urethane stretch, **Fig.3.30**. The FTIR-ATR spectra for **PU PR** and **PU 98** displayed an increase in the peak at 1727cm^{-1} denoting the ester/urethane linkage was observed. This is more than likely due to fungal growth on the surface of the PU samples which can clearly be seen for **PU 98**, **Fig. 3.30**. Fungal growth on the sample may suggest that this PU would be degradable by this enzyme, however, only a limited degradation was

observed after the 24 days. Over a longer period substantial degradation may have occurred, but unfortunately, this was not possible due to the pH of the buffer of 2.8, which would have degraded the PU sample after long periods, and therefore it would have been difficult to determine whether degradation occurred as a result of the enzyme or the buffer solution. Overall, a slight difference was noted between the one shot method (**PU ADP**) and the prepolymer method (**PU PR**) regarding degradation by protease from *Rhizopus* sp. and more specifically the hard segment of these samples, in that a greater proportion of the amide bonds in **PU ADP** had degraded **Fig. 3.30**. However, this degradation was still deemed as minimal with all of the films remaining intact after the 24 days, and can conclude that the chemical constituents, and the interactions between these components contained in the PUs in this group; namely ADP, MDI and BD were not conducive towards enzymatic degradation by the enzymes used in this experiment.

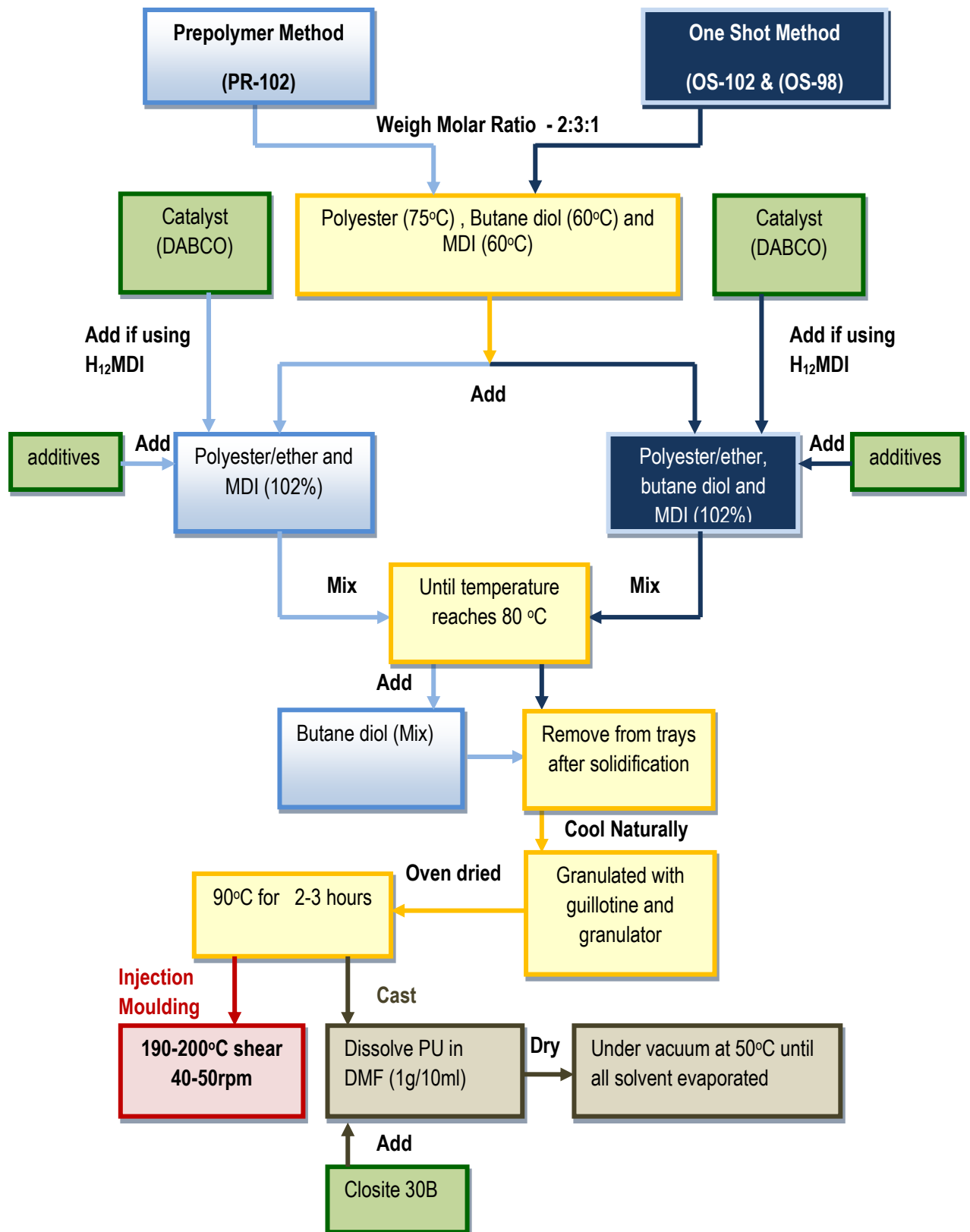
3.3.4 Overall Summary of the effect of the Method of Synthesis on Polyurethane Degradation and Biodegradation.

The work described in this chapter focused on the effect of the method of synthesis on the rate of degradation and biodegradation of PU. Degradation and biodegradation of PU is a complex process, and can be influenced by numerous factors, therefore alkaline hydrolysis, enzymatic hydrolysis and soil burial experiments were performed to provide a wide range of chemical/biological degradation processes which may occur during real time degradation/biodegradation of PUs. Changes during degradation were monitored by FTIR-ATR, DSC, TGA and microscopy to provide information regarding structural, morphological, thermal and visual changes to the samples respectively. From the results obtained it was found that the method of synthesis affected PU morphology, with the PU synthesised by the one shot method (**PU ADP**) being more crystalline and less susceptible to hydrolysis compared to **PU PR** (synthesised by the pre-polymer method).

The PU samples were not found to be particularly conducive towards enzymatic degradation by the fungal enzymes *Aspergillus niger*, *Aspergillus satoi* and *Rhizopus* sp. even though previous studies have shown some PUs to be susceptible to degradation by *Aspergillus niger* [19, 24]. Limited degradation occurred which was not considered to be significant. Altering the method of synthesis did not increase the rate of degradation by these enzymes, and this was an unexpected finding. The first step in enzymatic degradation/biodegradation is adherence of the enzyme to the surface of the substrate. Therefore, altering the method of synthesis would affect the morphology of the PU, and hence should affect the surface binding sites available for the enzyme. Indeed, results from DSC did highlight a change in the

morphology of the PU samples with **PU ADP**, (synthesised by the one shot method) exhibiting a more crystalline structure than **PU PR** (synthesised by the pre-polymer method), **Fig.3.4**. Therefore, it can only be concluded that with respect to enzymatic degradation in this group (group 1), the chemical components contained within the PU, have a greater influence than the method of synthesis, and the chemical components (ADP, MDI and BD), and the interactions between these components were not favourable substrates for the enzymes used in this study. This can also be supported by the soil burial results which displayed little difference between the PU samples synthesised by the one shot method; **PU ADP** and **PU PR** synthesised by the pre-polymer method, **Figs. 3.14 & 3.15**.

In summary, the method of synthesis did not affect the rate of enzymatic degradation and biodegradation by soil burial, however, degradation by chemical/alkaline hydrolysis did highlight a major difference between the PU sample synthesised by the one shot method (PU ADP), and the pre-polymer method (PU PR), **Fig 3.25**, and is more than likely due to the highly crystalline nature of the **PU ADP**. The PU synthesised by the pre-polymer method was found to be less thermally stable, less crystalline, and more susceptible to hydrolysis than the PU synthesised by the one shot method, **Figs. 3.25 & 3.6**. Therefore, in order to obtain PU's with limited shorter lifespans the pre-polymer method should be used, with a further possibility of increased biodegradation using alternative chemical constituents, and the effect of altering these constituents and their effect on degradation and biodegradation will be explored in chapter 4.



Scheme 3.1 Method of synthesis of PU one shot method and pre polymer method

Table 3.1 Effect of Method of synthesis on PU Degradation – Group 1

PU Code	Method of Synthesis	
	Synthesis Code	Description
PU-ADP	OS-102	One shot process with 2% excess MDI (102%) ; all reactants added simultaneously (MDI,PEA,BD), Injection Moulded
PU-PR	PR-102	Pre polymer process with 2% excess MDI (102%) ; MDI and PEA added simultaneously allowed to react for 30mins, then BD added, Injection Moulded
PU-98	OS-98	One shot process with no excess MDI (98%); all reactants added simultaneously, (MDI,PEA,BD), Injection Moulded
PU Code	Chemical Structure	
PU-ADP PU-PR PU-98	<p style="text-align: center;">Isocyanate; MDI</p> <p style="text-align: center;">M.w.t. Ratio: PEA:MDI:BD - 1:3:2</p> <p style="text-align: center;">Hard Segment</p> <p style="text-align: center;">Soft Segment</p> <p style="text-align: center;">Chain Extender; BD</p> <p style="text-align: center;">Polyol; PEA</p>	

Table 3.2 Effect of method of synthesis on morphology of PU characterised by DSC

Sample Code	Method of synthesis	Soft Segment			Hard Segment					
		Tg (oC)	Tm (oC)	ΔH (J/g)	Tm(oC) (I)	ΔH(J/g) (I)	Tm(oC) (II)	ΔH(J/g) (II)	Tm(oC) (III)	ΔH(J/g) (III)
PU ADP	OS-102	-18	71	0.1	109	0.5	147	0.8	195	6.1
PU PR	PR-102	-16	71	0.1	-	-	148	0.3	173, 195	0.87, 1.8
PU 98	OS-98	-12	72	0.1	-	-	150	0.2	197	2.2

Table 3.3 Effect of chemical hydrolysis on morphology of PU characterised by DSC

Sample Code	Hydrolysis time	Soft Segment			Hard Segment					
		Tg (°C)	Tm (°C)	ΔH (J/g)	Tm (°C) (I)	ΔH(J/g) (I)	Tm(oC) (II)	ΔH(J/g) (II)	Tm(oC) (III)	ΔH(J/g) (III)
PU ADP	time 0	-18	71	0.1	109	0.5	147	0.8	195	6.1
PU PR	time 0	-16	71	0.1	-	-	148	0.3	173, 195	0.87, 1.8
PU 98	time 0	-12	72	0.1	-	-	150	0.2	197	2.2
PU ADP	14 days	-18	-	-	109	0.47	148	0.74	198	5.11
PU PR	14 days	-16	-	-	121	0.11	148	2.05	194, 210	0.84 0.24
PU 98	14days	-14	-	-	-	-	148	0.47	175, 199	0.79 1.89
PU ADP	21 days	-30	-	-	-	-	-	-	-	-
PU PR	21 days	-20	72	0.1	-	-	148	0.96	205	26.9
PU 98	21 days	-15	-	-	-	-	148	0.56	209	10.96
PU ADP	28 days	-31	-	-	-	-	-	-	-	-
PU 98	28 days	-15	-	-	-	-	148	0.51	209	11.16

Table 3.4 Effect of soil burial on morphology of PU characterised by DSC

Sample Code	Soil burial 20 months RT	Soft Segment			Hard Segment					
		Tg (°C)	Tm (°C)	ΔH (J/g)	Tm (°C) (I)	ΔH(J/g) (I)	Tm(oC) (II)	ΔH(J/g) (II)	Tm(oC) (III)	ΔH(J/g) (III)
PU ADP	time 0	-18	71	0.1	109	0.5	147	0.8	195	6.1
PU ADP	Soil 1	-15	-	-	-	0	147	0.1	200	4.9
PU ADP	Soil 2	-17	-	-	-	-	147	0.34	199	5.26
PU PR	time 0	-16	71	0.1	-	-	148	0.3	173, 195	0.87, 1.8
PU PR	Soil 1	-16	-	-	-	-	148	0.2	199	8.5
PU PR	Soil 2	-16	-	-	-	-	148	0.1	197	2.0
PU 98	time 0	-12	72	0.1	-	-	150	1.2	197	2.9
PU 98	Soil 1	-20	-	-	-	-	148	1.3	192	0.7
PU 98	Soil 2	-21	-	-	-	-	148	0.9	192	0.5

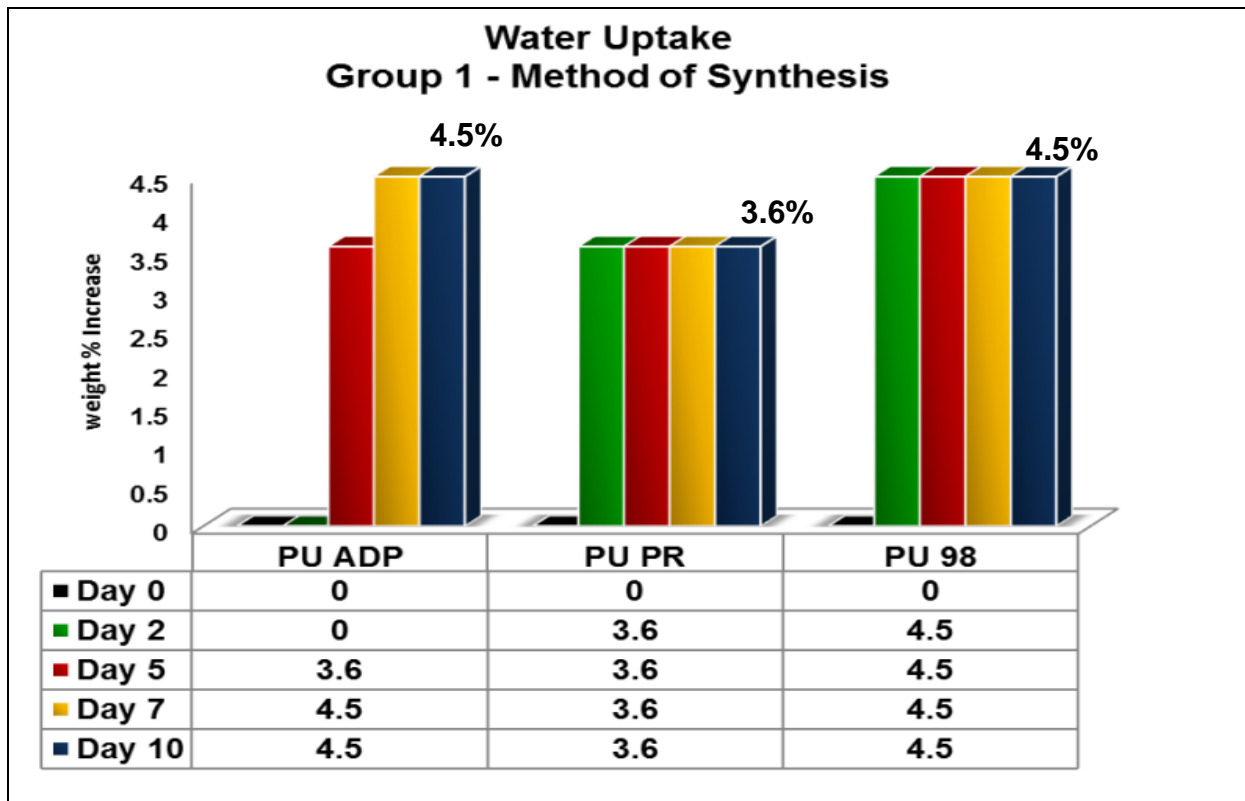


Figure 3.1 Hydrophilicity of PU samples determined by weight percentage increase of water uptake

PU ADP, PU PR, PU 98 – Hard Segment MDI/BD: Soft Segment PEA

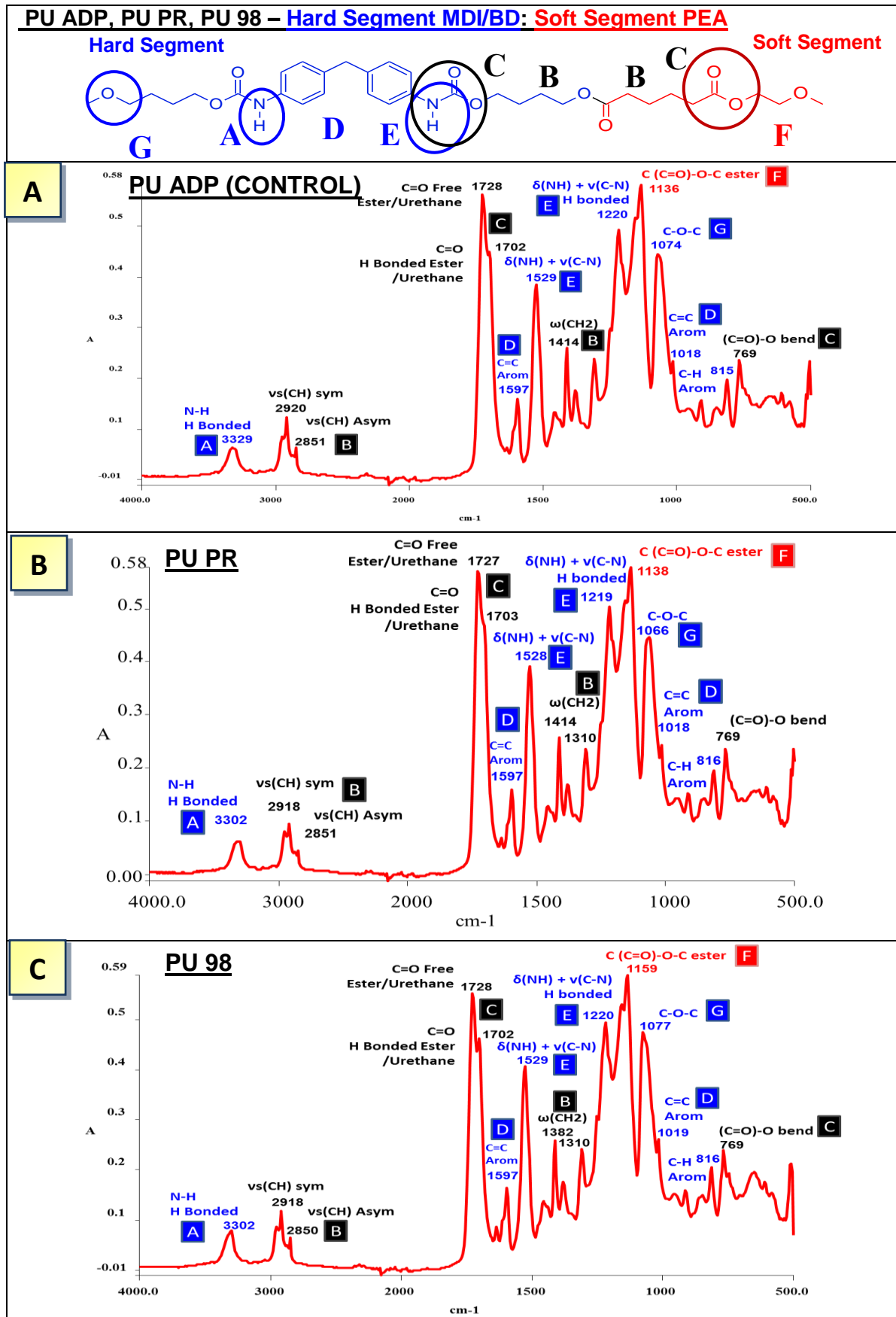


Figure 3.2 Chemical structure characterisation of PU samples PU ADP (**A**), PU PR (**B**), PU 98 (**C**) by FTIR-ATR

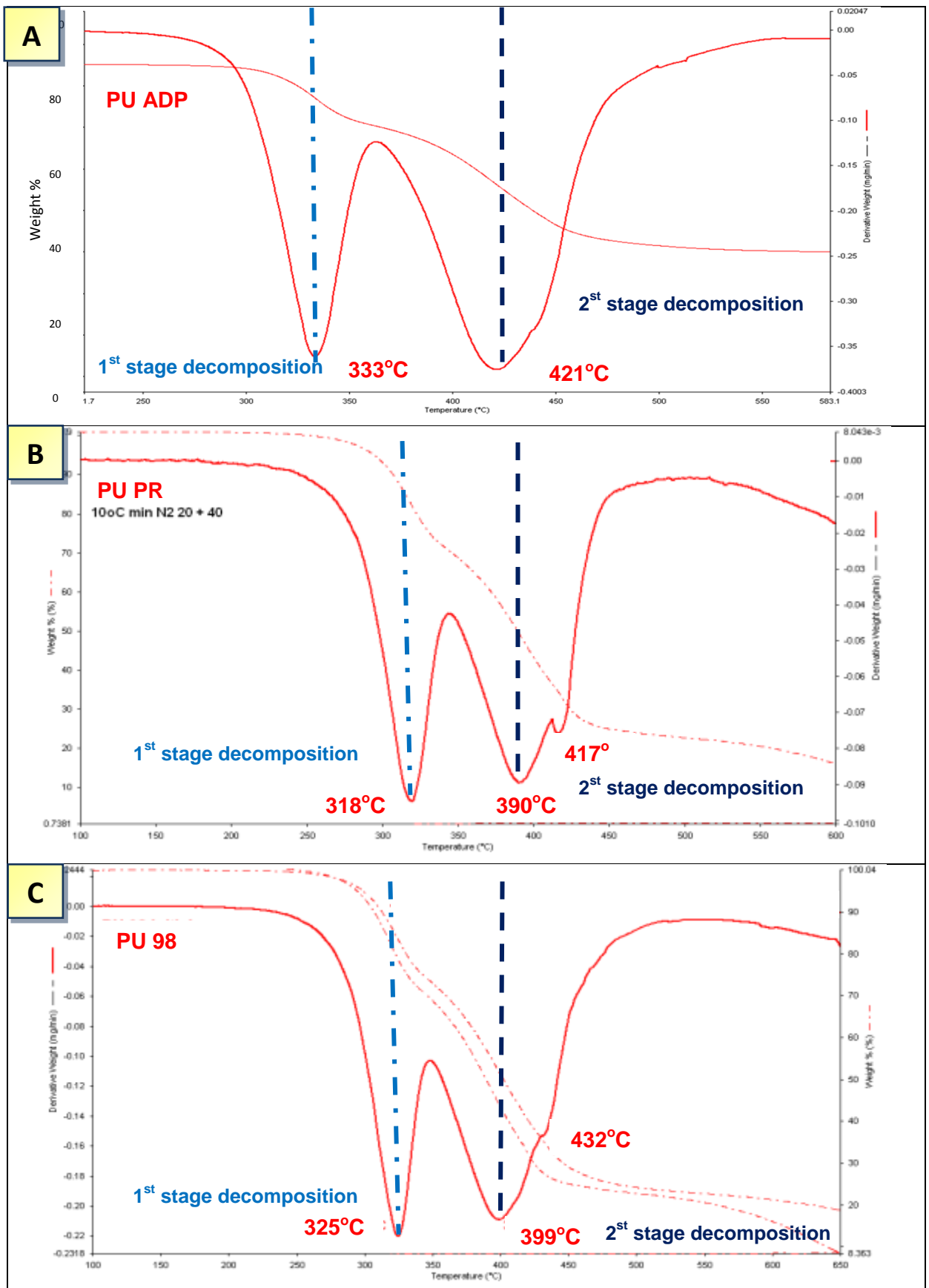


Figure 3.3 TGA thermal analysis characterisation of PU, PU ADP (A), PU PR (B), PU 98 (C)

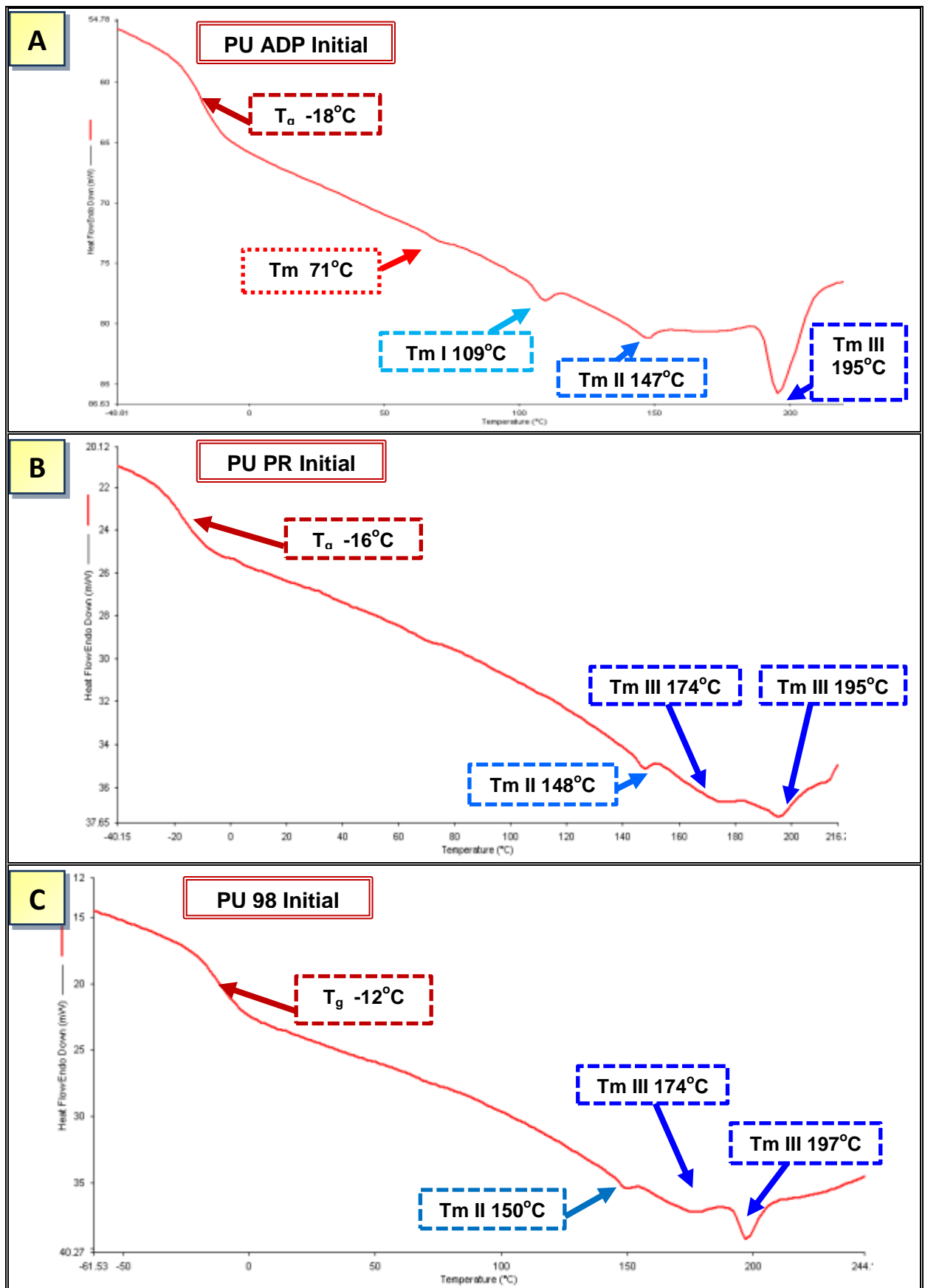
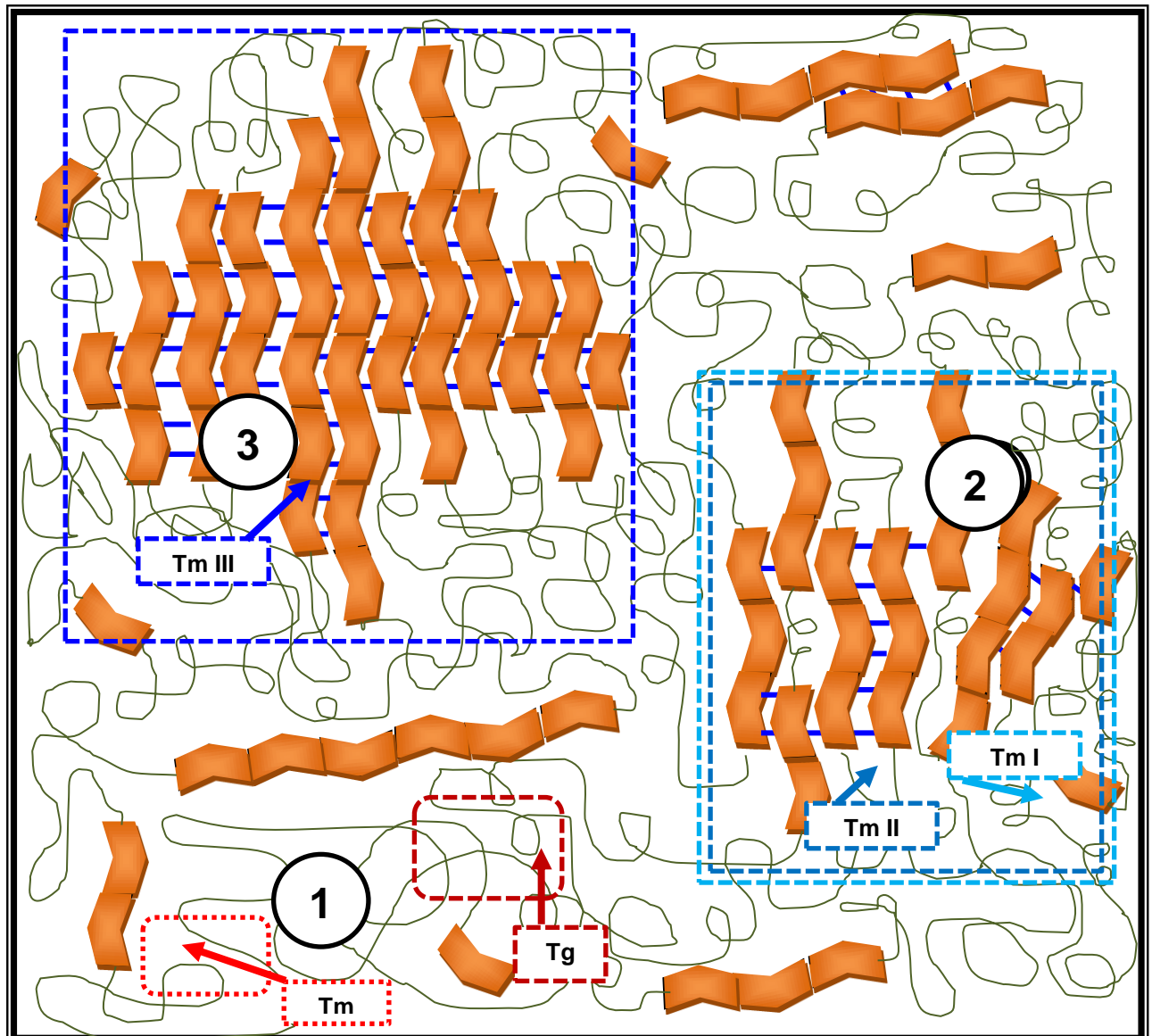
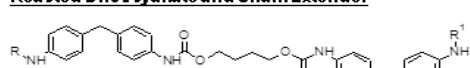


Figure 3.4 Morphological characterisation of PU ADP (**A**), PU PR (**B**), PU 98 (**C**) showing T_g and endotherms relating to hard and soft segments



Reacted Diisocyanate and Chain Extender



Soft Segment



Polyol soft segment-Ester Polyol soft segment-Ether



Ordered non-crystalline Hard Segments



Hydrogen Bonding in hard segment

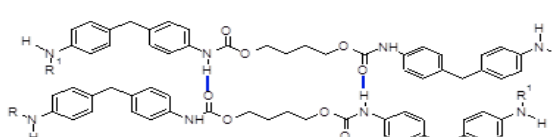
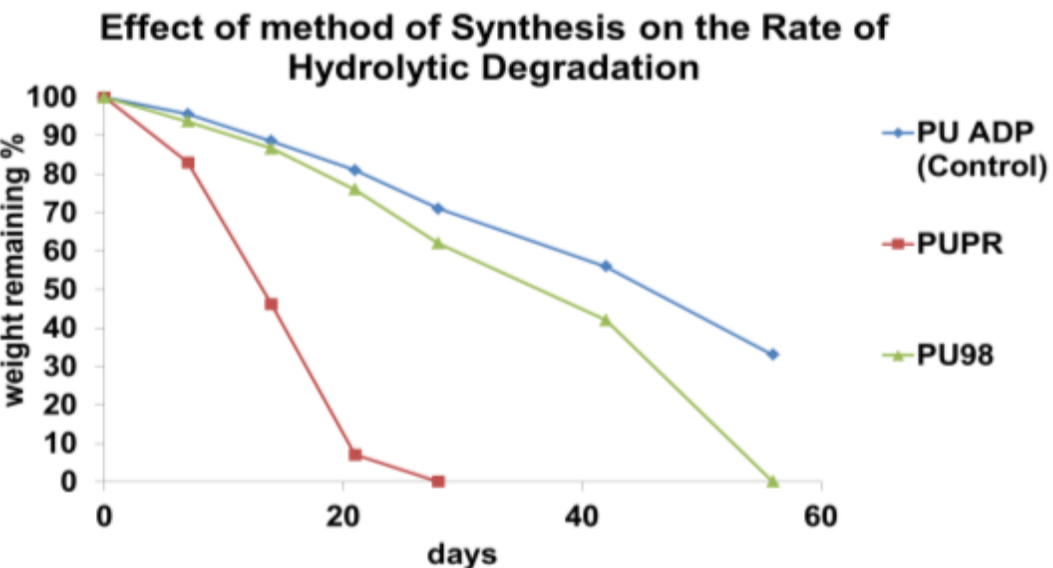


Figure 3.5 Schematic representation of hard and soft segment domains in TPU

A

Sample Code	Method of Synthesis	Weight Remaining %					
		0 days	7 days	14 days	21 days	28 days	42 days
PU ADP	One Shot/102% Isocyanate	100	96	89	81	71	56
PU PR	Prepolymer/102% Isocyanate	100	83	46	7	0	0
PU 98	One Shot/98% Isocyanate	100	94	87	76	62	42

B

Visual degradation during alkaline hydrolysis

■ PU ADP (control) ■ PU 98 ■ PUPR

Arbitrary scale of degradation stage

- min 0 no signs of cracking deformation
- 1 slight signs of limited surface degradation
- 2 deformation of sample (curling) & discolouration
- 3 visible cracks showing
- 4 Small pieces of sample broken away from film
- max 5 complete breaking of sample small pieces

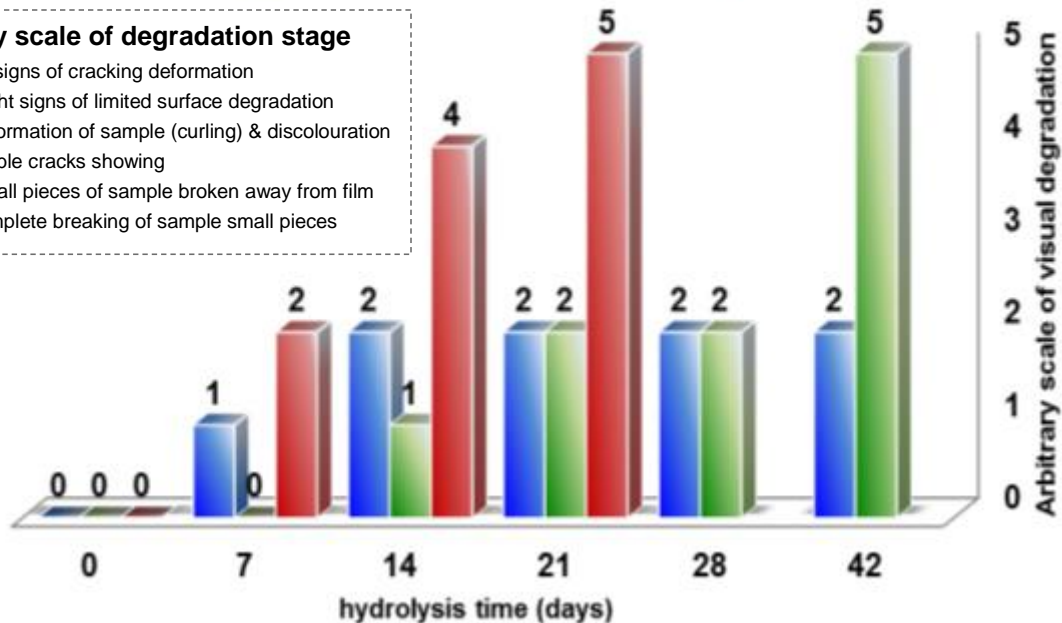


Figure 3.6 Effect of Method of Synthesis on the rate of hydrolytic degradation with 10% NaOH (aq) (A) (see table 2.1 & 2.2 pg. for acronyms). Visual surface cracking (B)

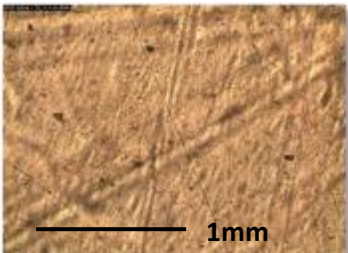
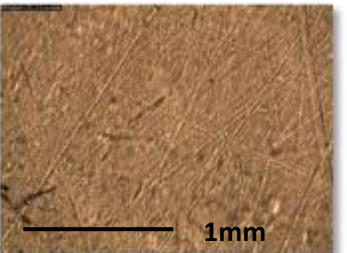
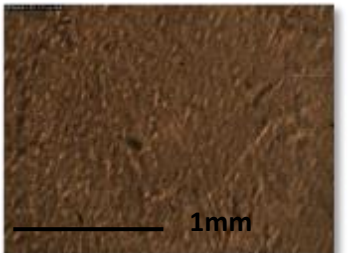
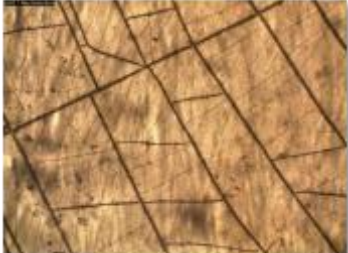
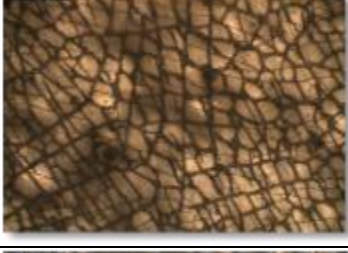
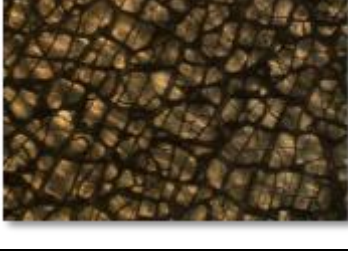
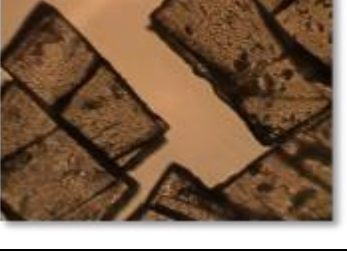
	PU ADP (one shot excess isocyanate)	PU PR (Prepolymer excess isocyanate)	PU 98 (one shot no excess isocyanate)
Initial			
7 days			
14 days			
21 days			
28 days		No Image PU PR fully degraded	
42 days		No Image PU PR fully degraded	

Figure 3.7 Optical microscopic images of PU ADP, PU PR & PU 98 during alkaline hydrolysis

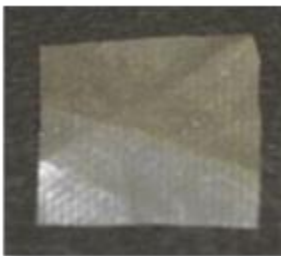
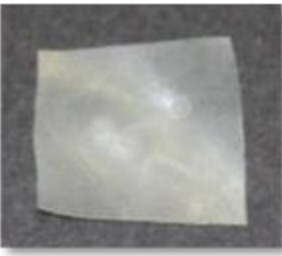
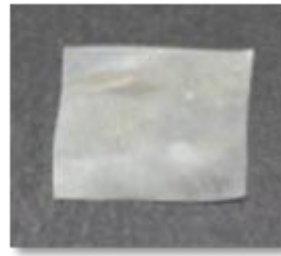
	PU ADP	PU PR	PU 98
Initial			
7 days			
14 days			
21 days			
28 days		No Image PU PR degraded	
42 days		No Image PU PR degraded	

Figure 3.8 Photographic Images of PU ADP, PU PR & PU98 during hydrolytic degradation with 10% NaOH (aq)

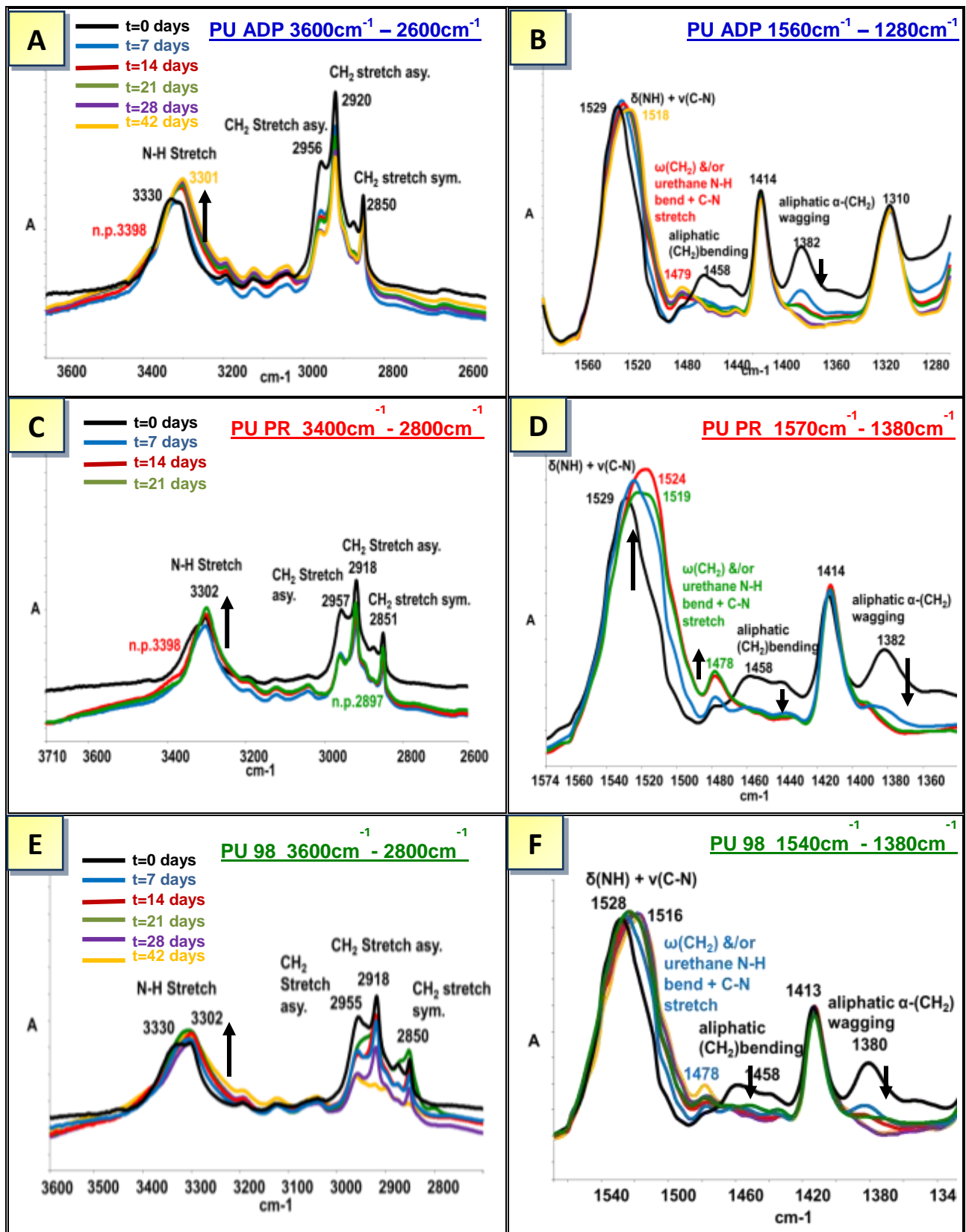


Figure 3.9 Structural changes of NH and CH₂ bonds during alkaline hydrolysis of PU ADP, PU PR & PU 98 by FTIR/ATR

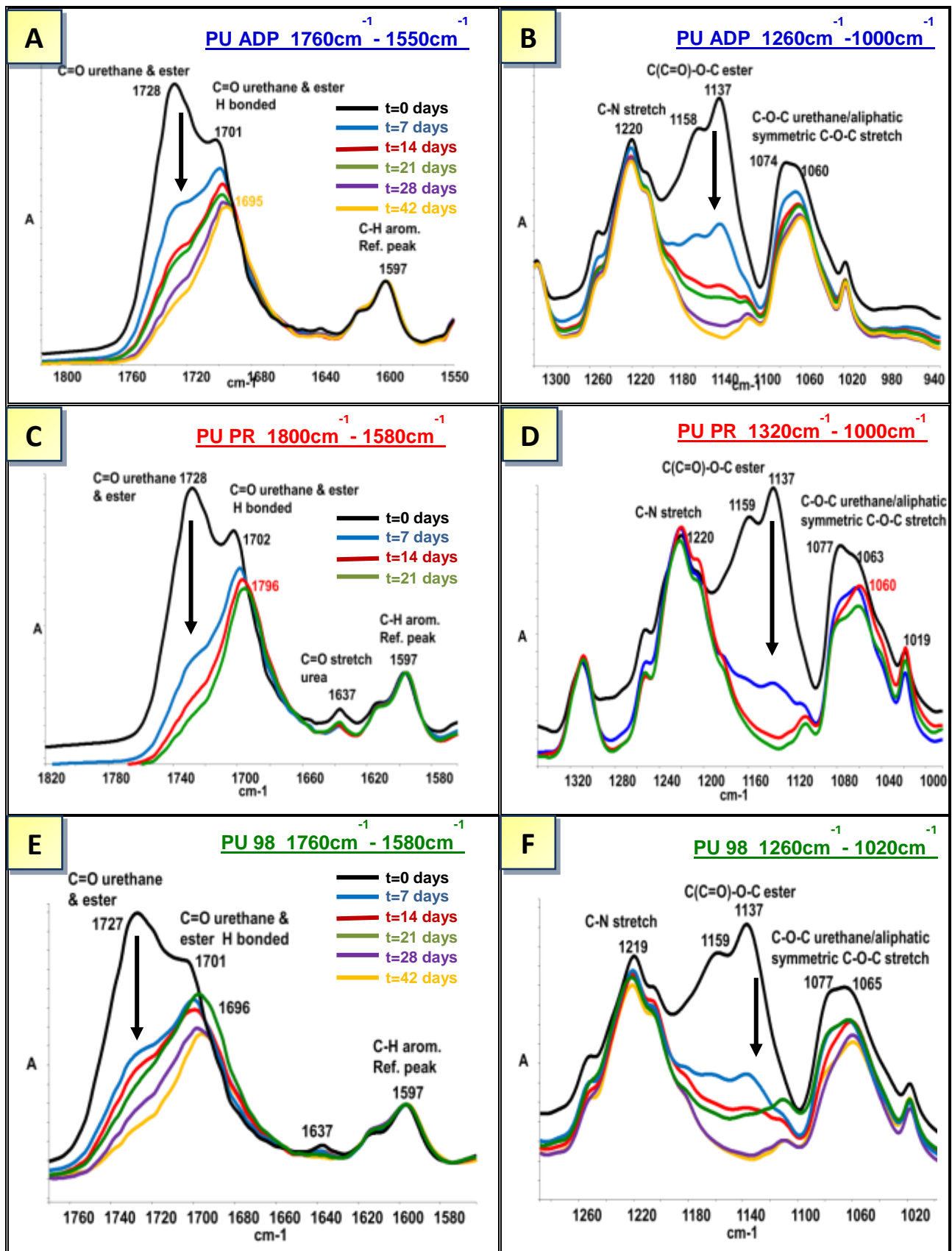


Figure 3.10 Structural changes of C=O and C-O-C urethane and ester linkages during alkaline hydrolysis of PU ADP, PU PR & PU 98 by FTIR/ATR

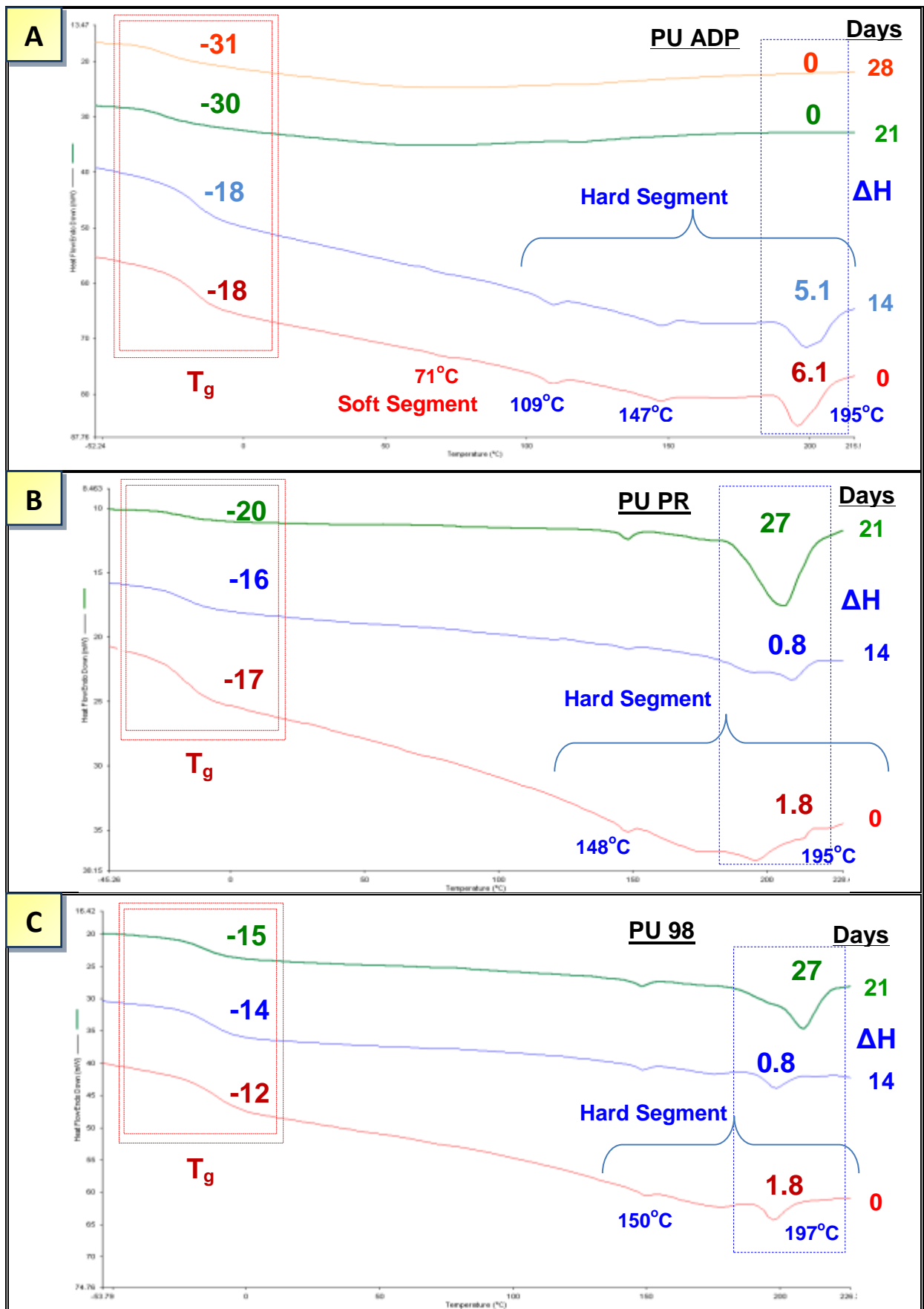


Figure 3.11 Changes in crystallinity during alkaline hydrolysis of Group 1 PU samples

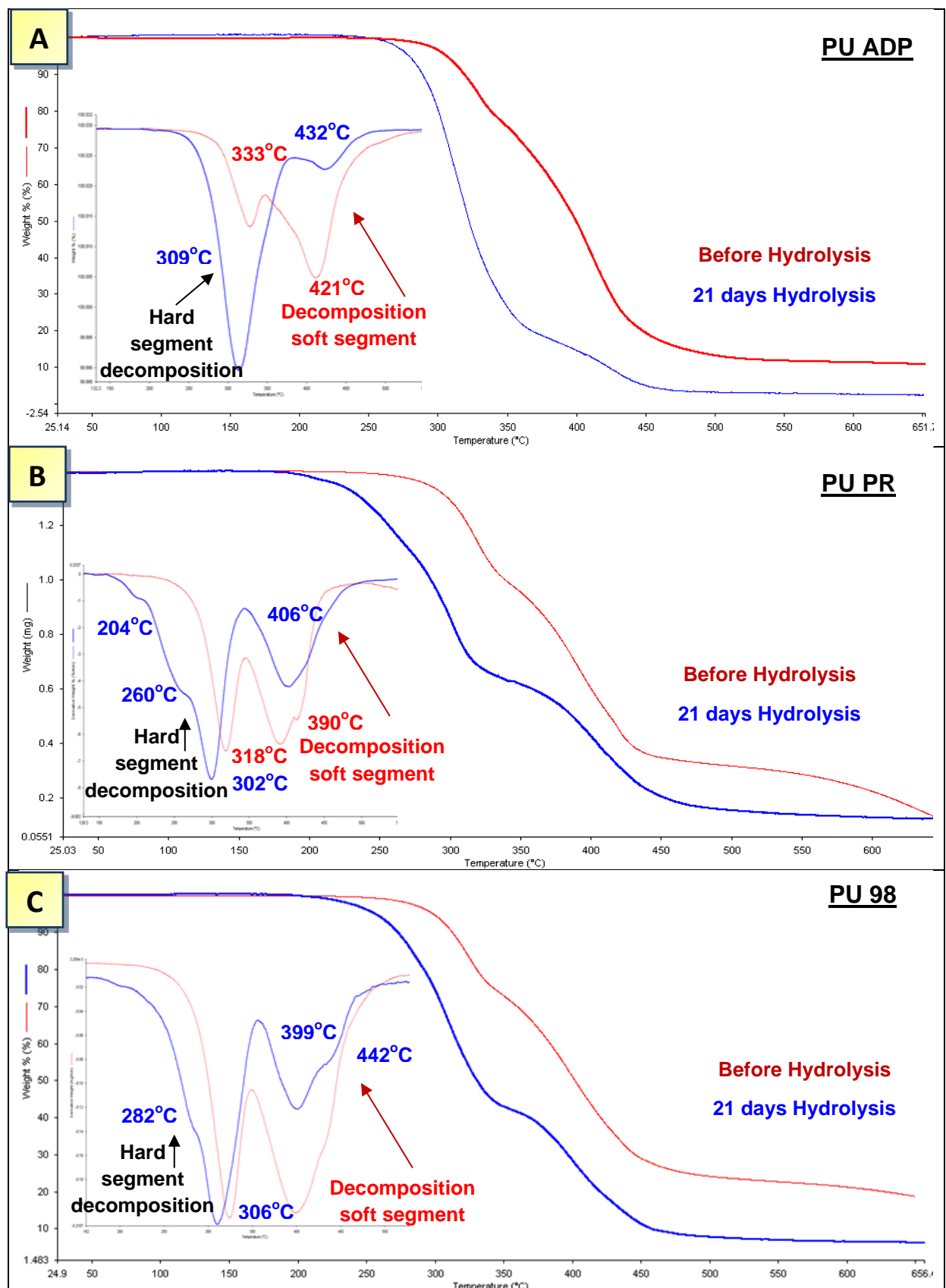


Figure 3.12 Changes in thermal stability after alkaline hydrolysis of Group 1 PU samples

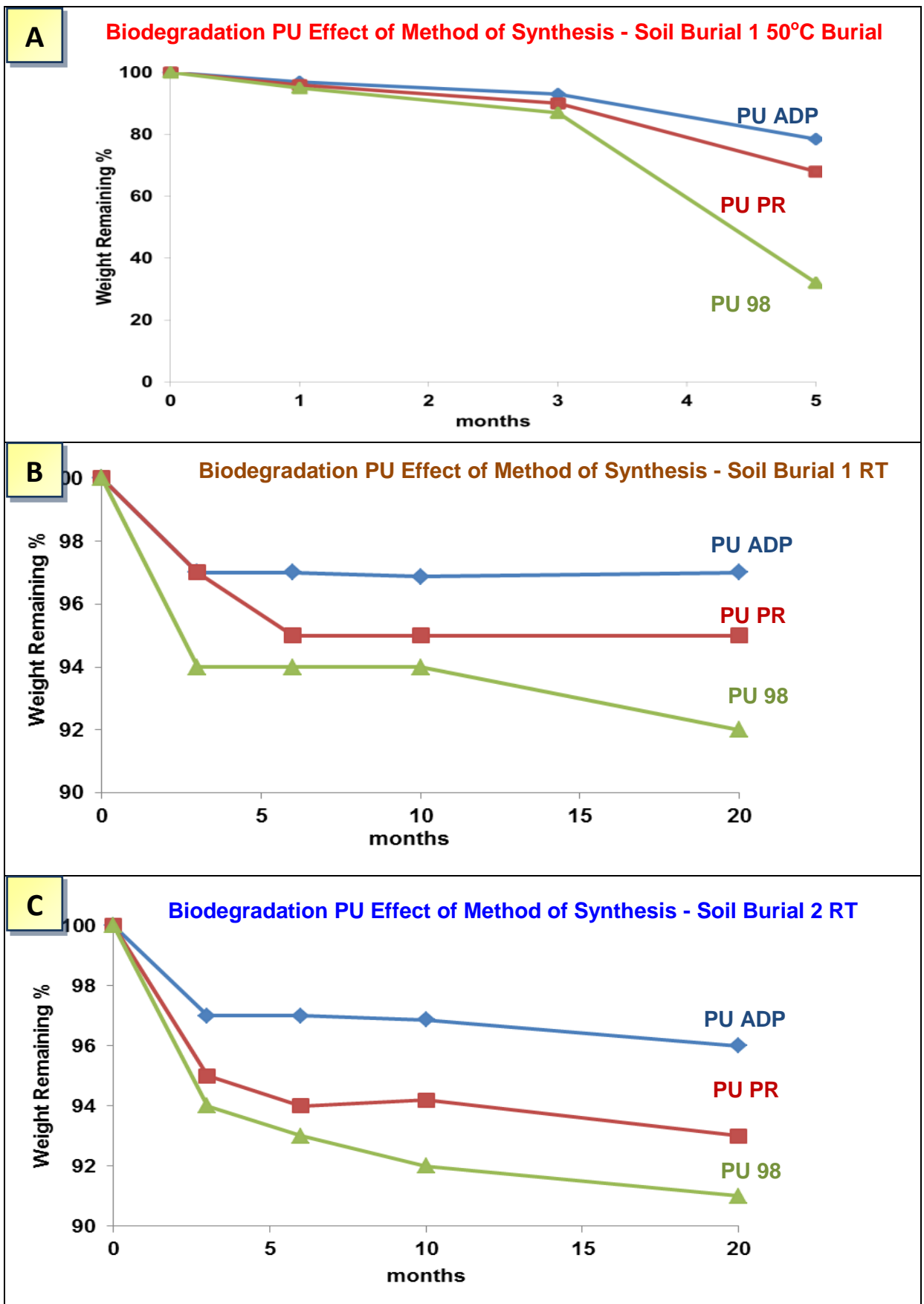


Figure 3.13 Effect of Method of Synthesis on the rate of biodegradation under soil burial conditions, soil 1 50°C (A), soil 1 RT (B), soil 2 RT (C)

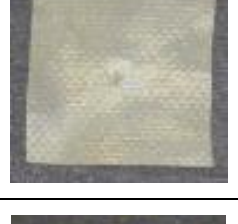
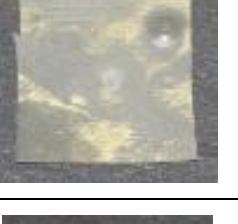
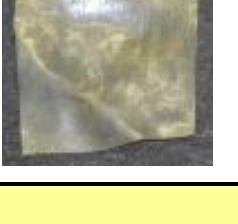
	PU ADP	PU PR	PU 98
Initial			
3 months			
Soil 1 RT			
Soil 2 RT			
Soil 1 50°C			
5 months			
Soil 1 50°C			
20 months			
Soil 1 RT			
Soil 2 RT			

Figure 3.14 Photographic images of PU ADP, PU PR & PU 98 during soil burial

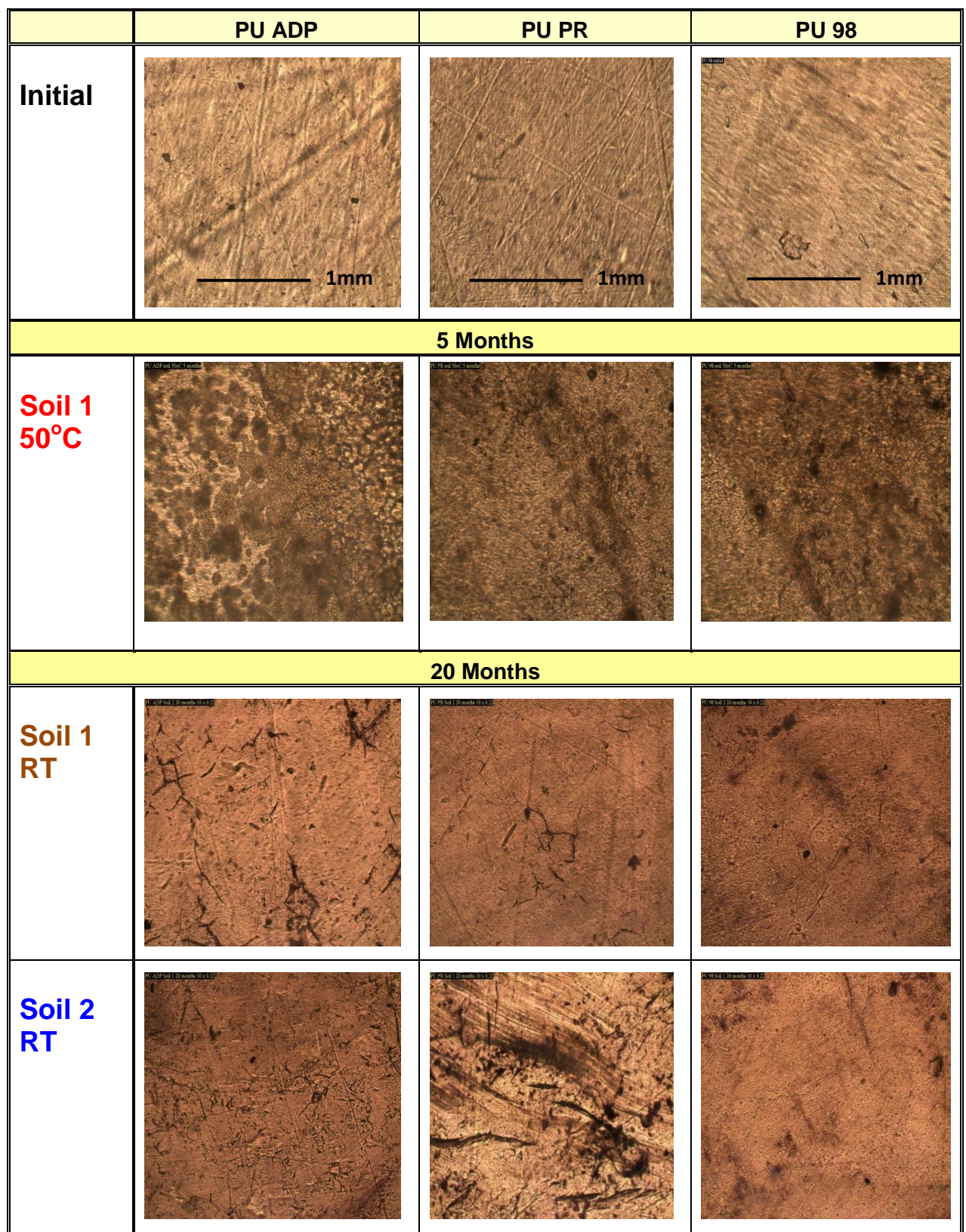


Figure 3.15 Optical microscopic images of PU ADP, PU PR & PU 98 during soil burial

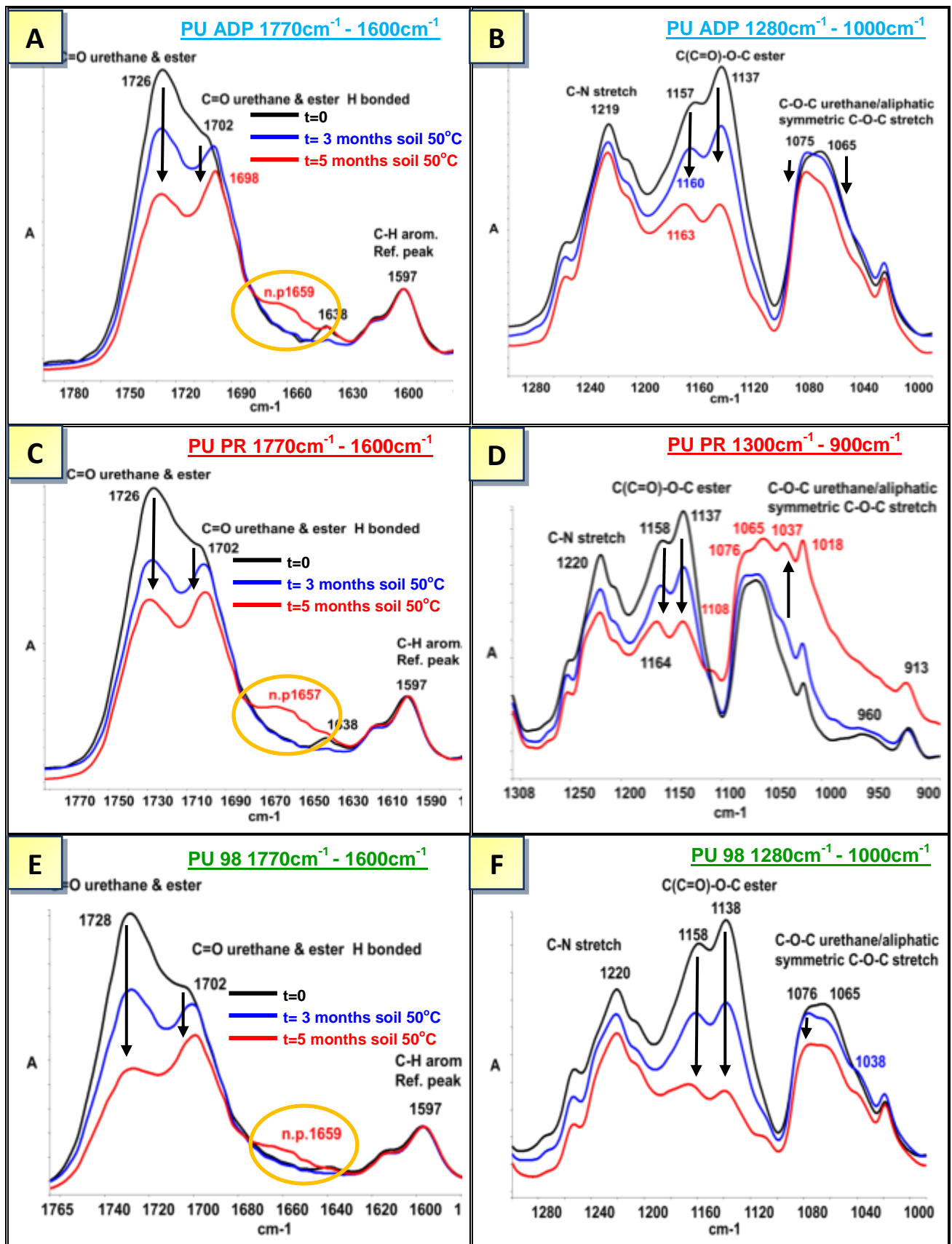


Figure 3.16 Effect of method of synthesis on C=O and C-O-C ester/urethane linkages during soil burial at 50°C of PU ADP, PU PR & PU 98 by FTIR/ATR

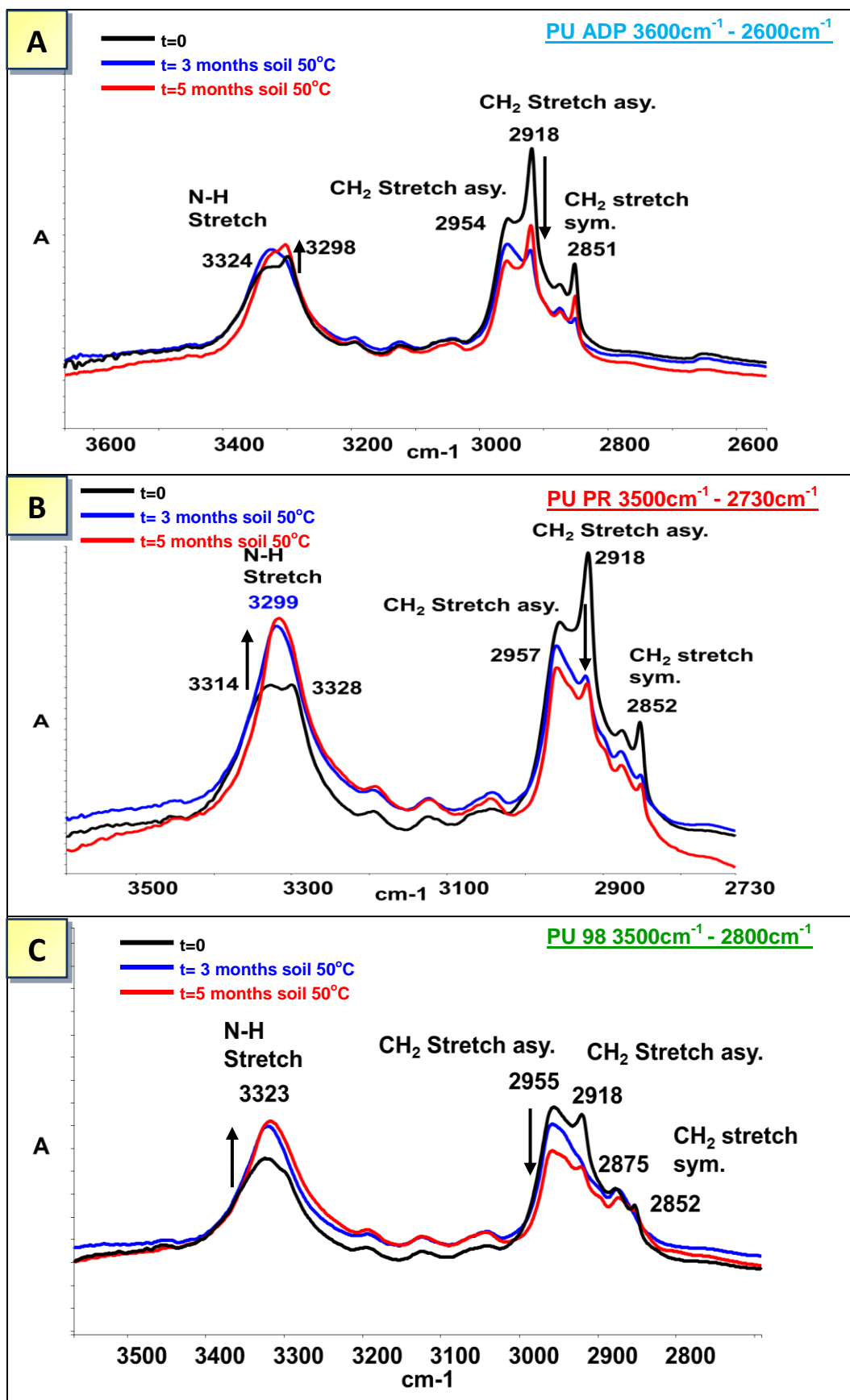


Figure 3.17 Effect of method of synthesis on N-H and CH groups in PU during soil burial at 50°C of PU ADP, PU PR & PU 98 by FTIR/ATR

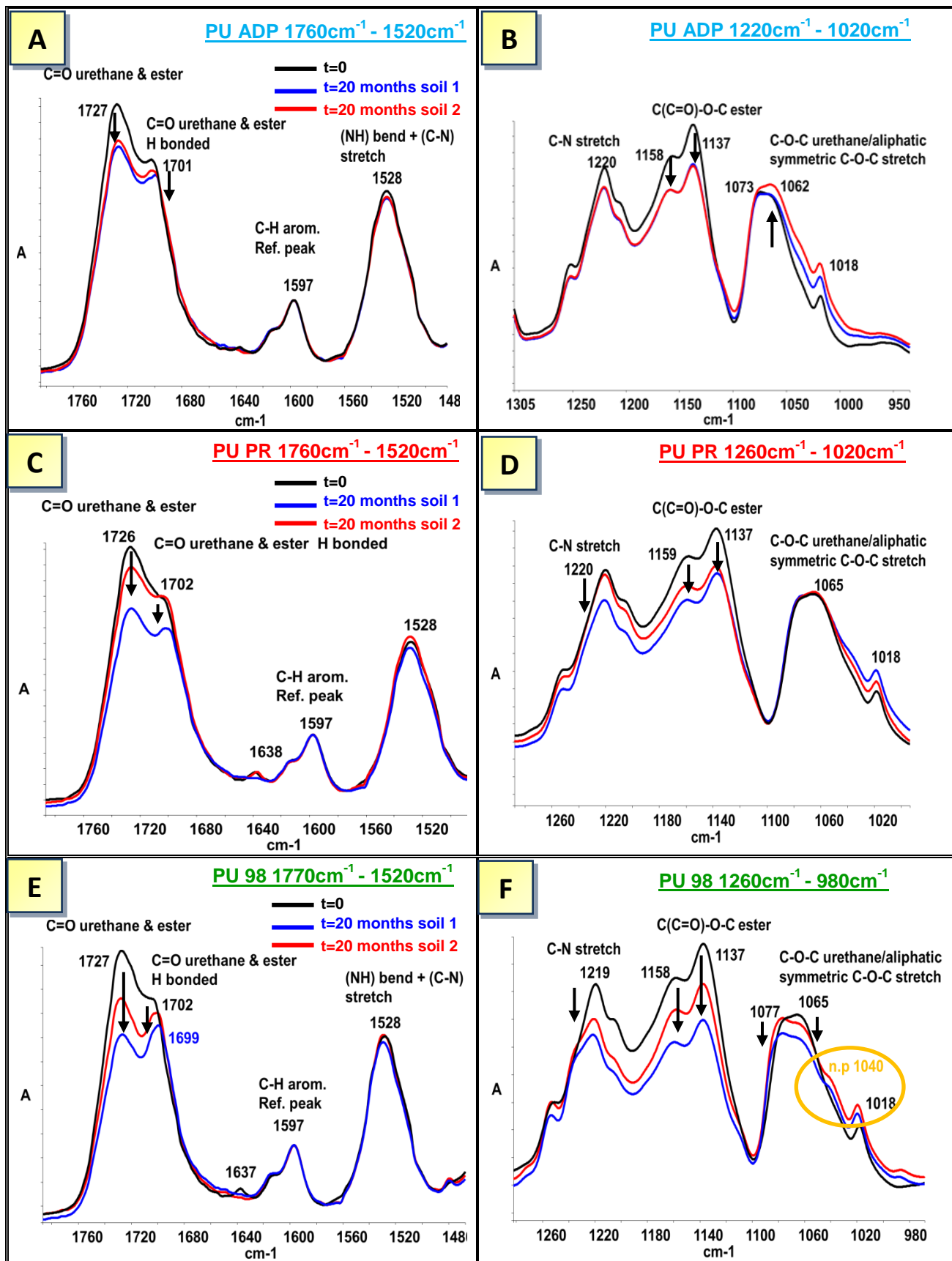


Figure 3.18 Effect of method of synthesis on C=O, C-O-C ester/urethane linkages and NH and CH₂ groups after 20 months soil burial at RT of PU ADP, PU PR & PU 98 by FTIR/ATR

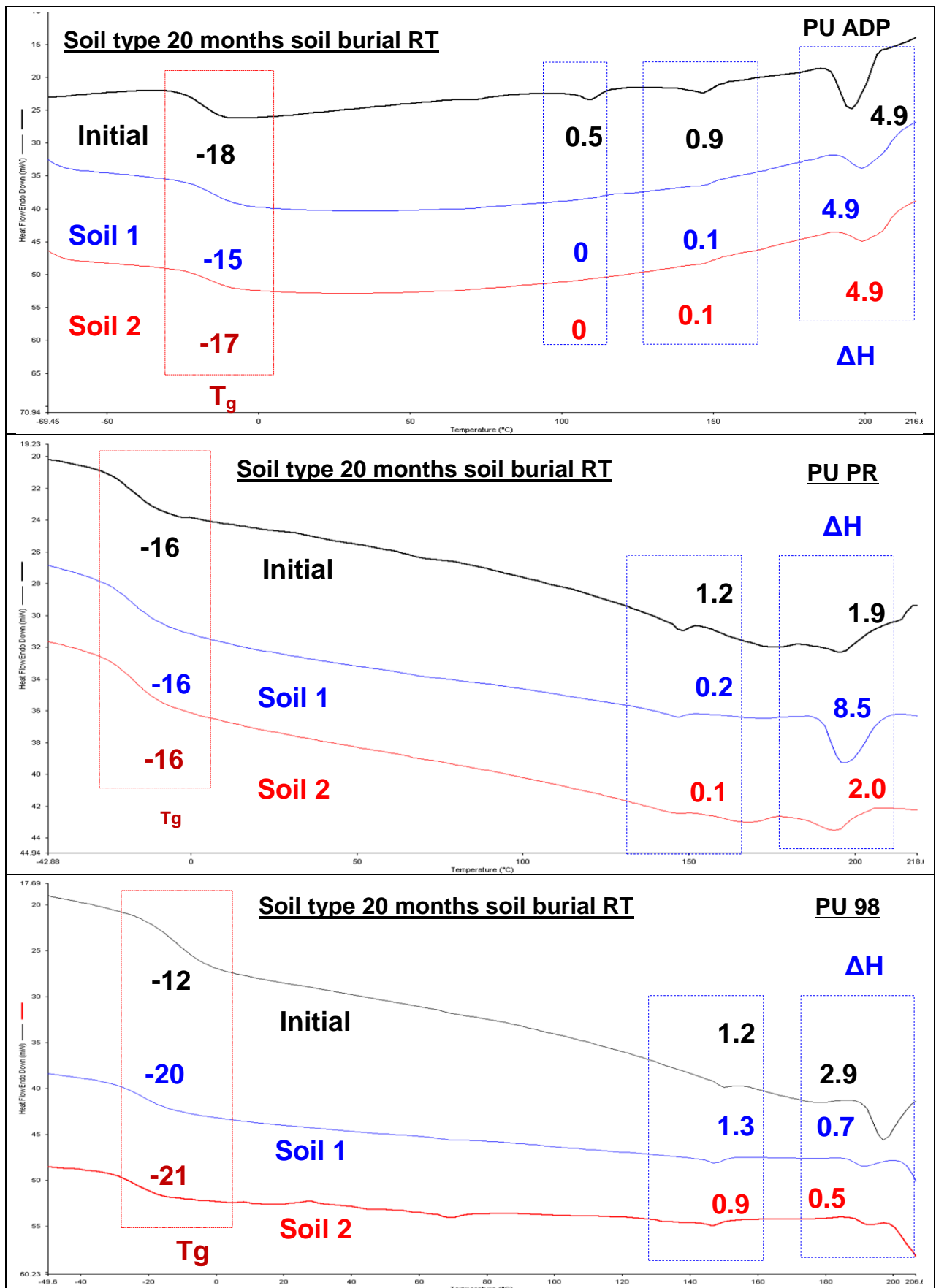


Figure 3.19 Effect of method of synthesis on morphology changes during biodegradation in soil at RT and 50°C of PU ADP, PU PR & PU 98.

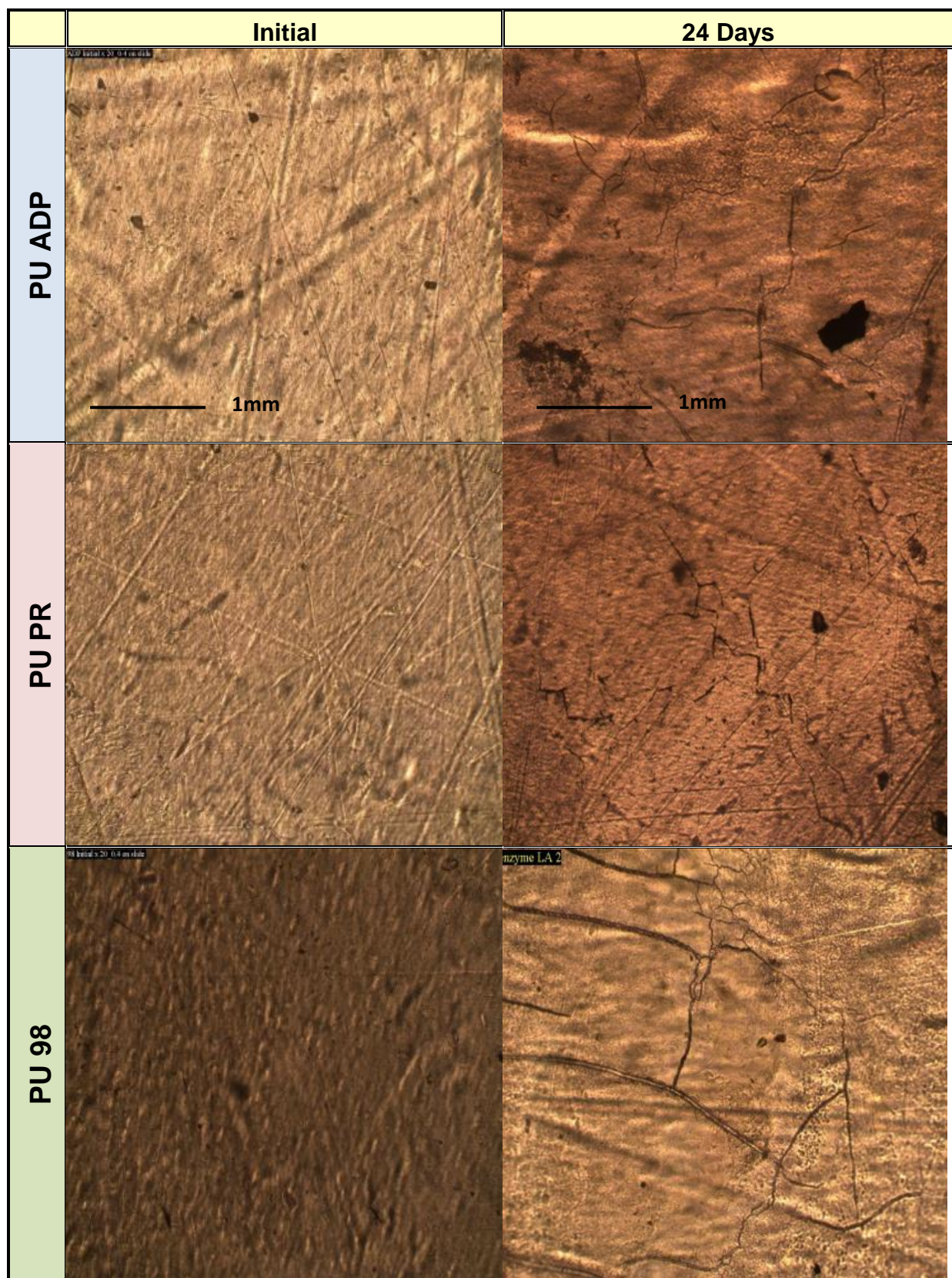


Figure 3.20 Effect of method of synthesis on enzymatic degradation by Lipase *Aspergillus Niger* PU ADP, PU PR & PU 98 by optical microscope images

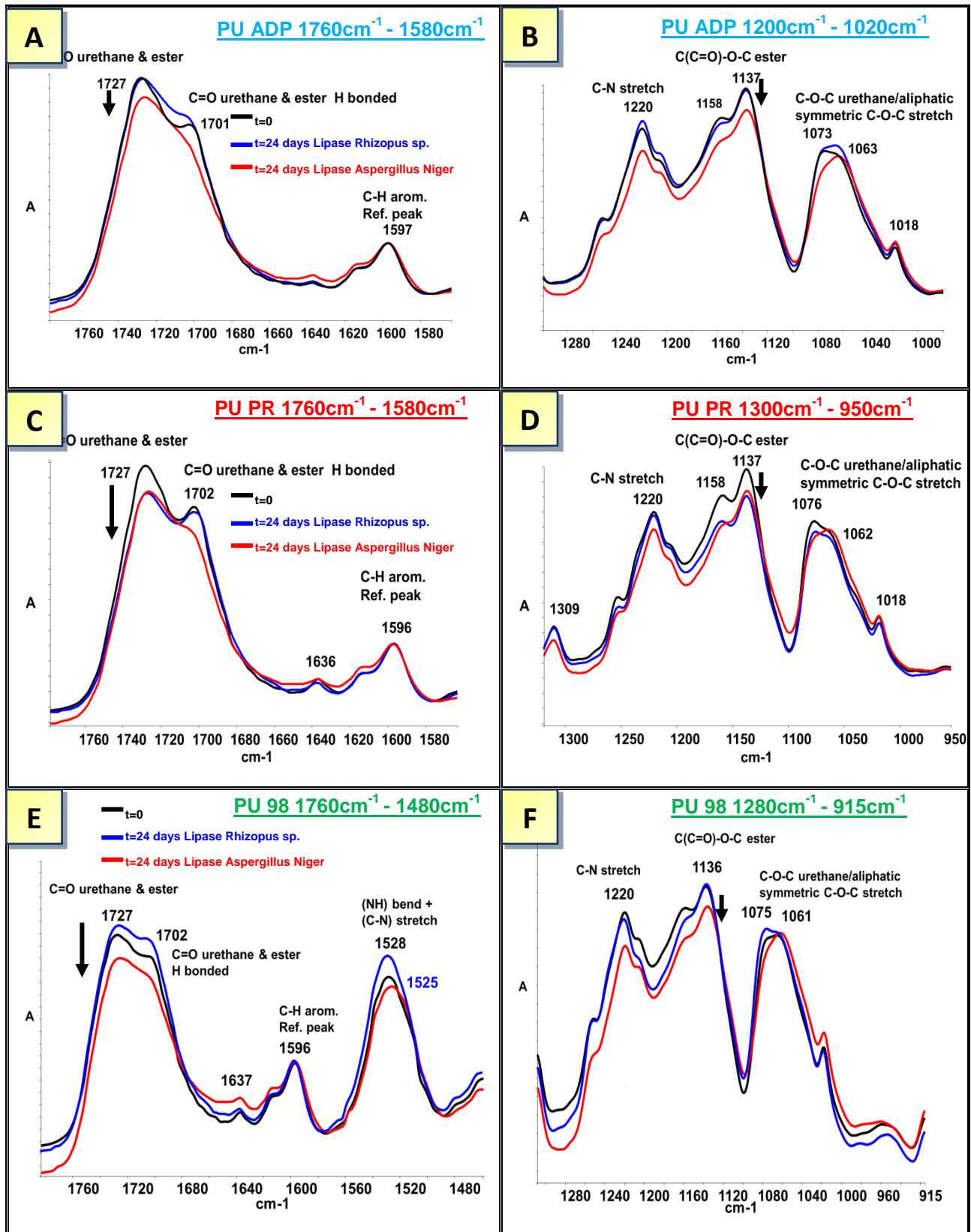


Figure 3.21 Effect of method of synthesis on structural changes during enzymatic degradation by Lipase *Aspergillus niger* and *Rhizopus* sp. on PU ADP, PU PR & PU 98 determined by FTIR-ATR

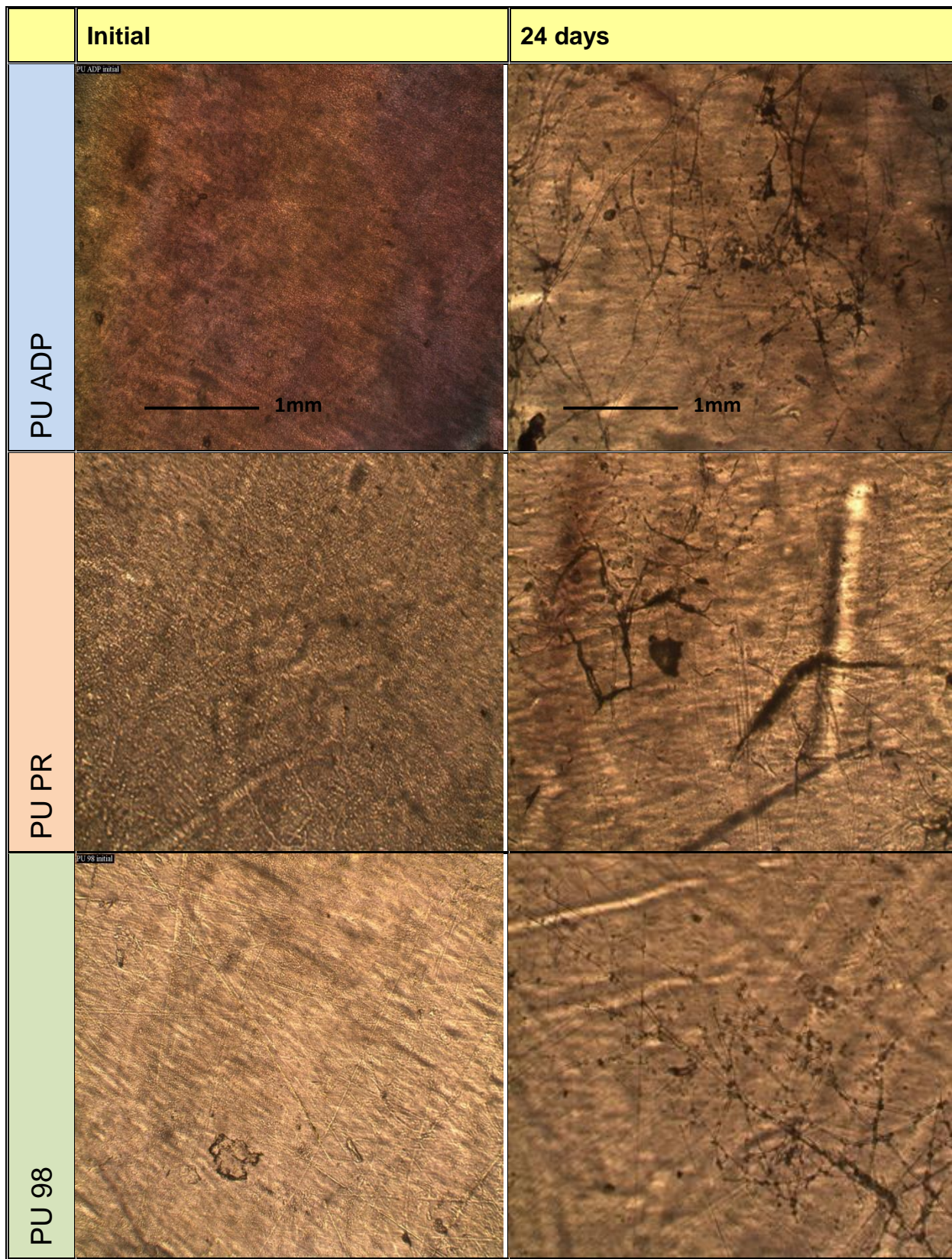


Figure 3.22 Effect of method of synthesis on enzymatic degradation by Protease *Rhizopus* sp. of PU ADP, PU PR & PU 98 by optical microscope images

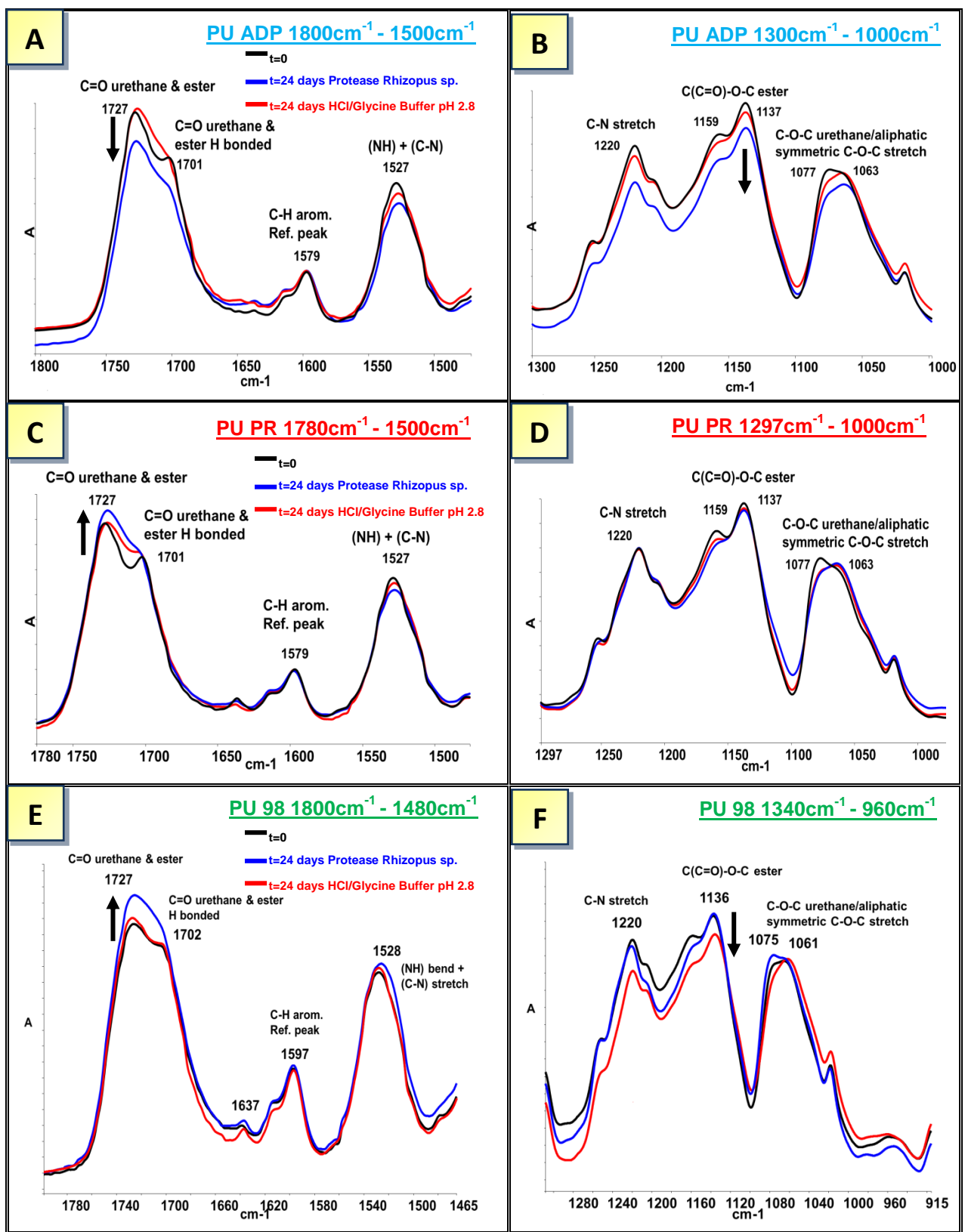


Figure 3.23 Effect of method of synthesis on structural changes during enzymatic degradation by protease *Rhizopus* sp. on PU ADP, PU PR & PU 98 determined by FTIR-ATR

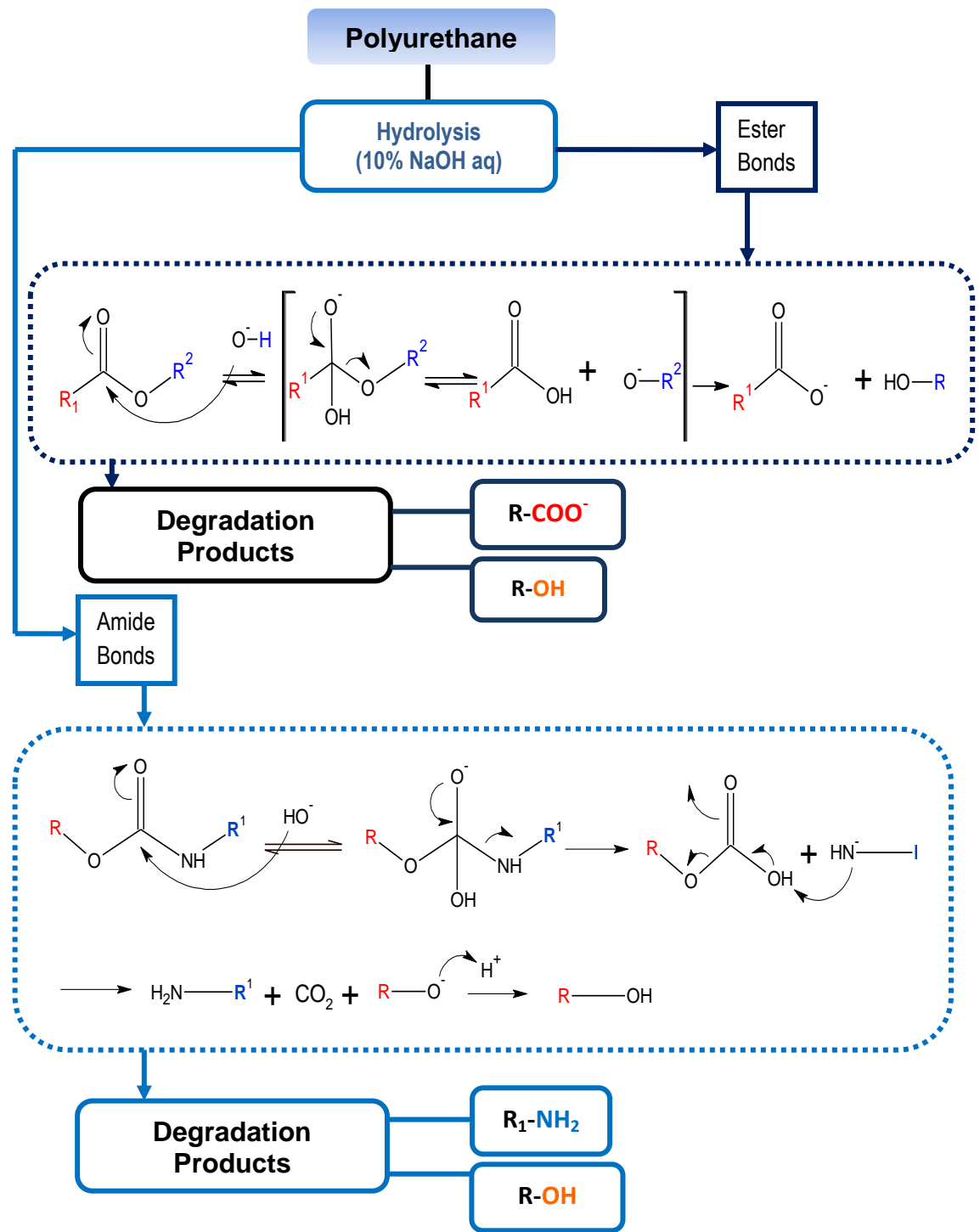


Figure 3.24 Mechanism of hydrolytic degradation of ester bonds and amide bonds contained in PU structure

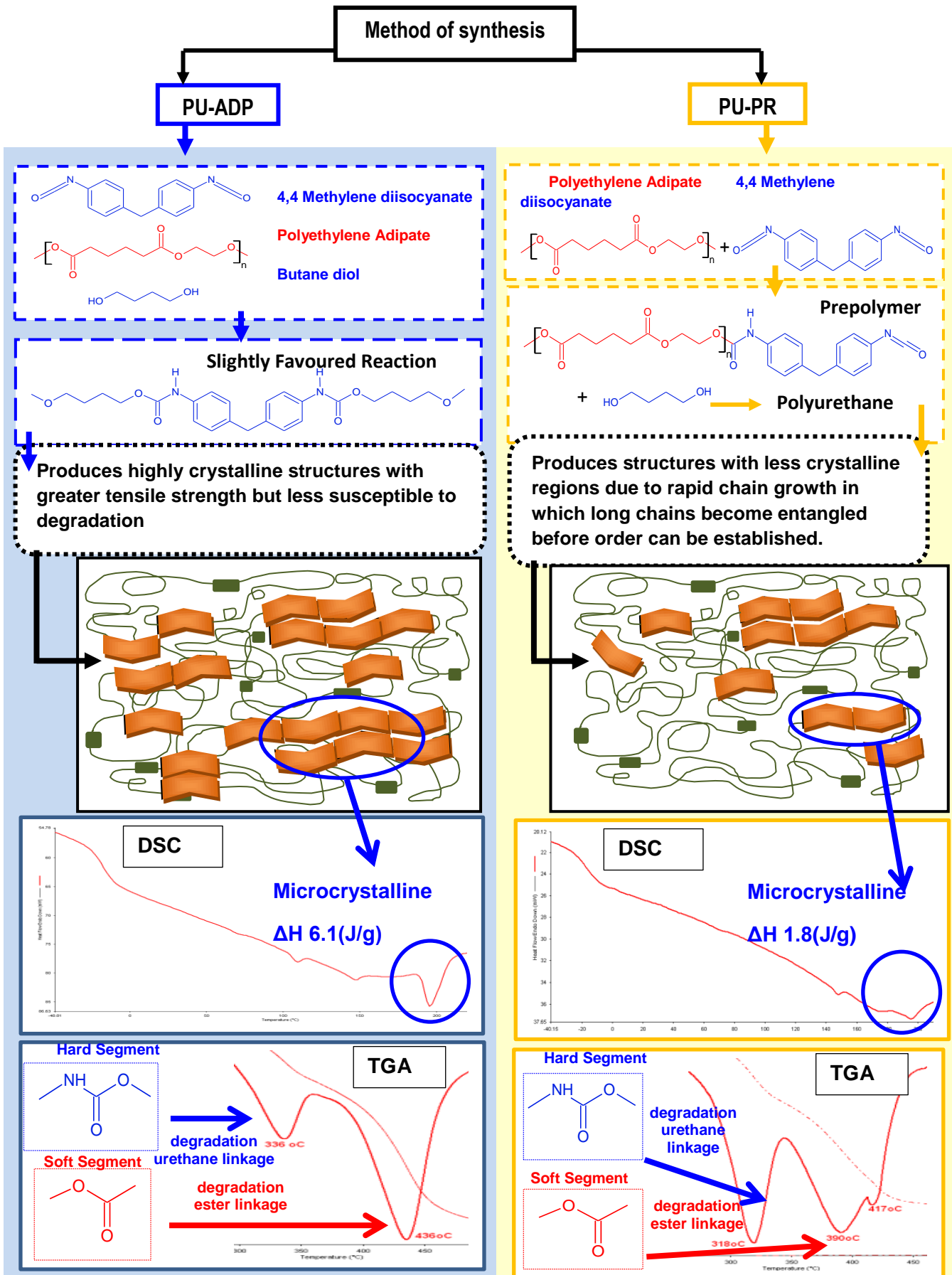


Figure 3.25 Showing the effect of the method of synthesis on PU crystallinity

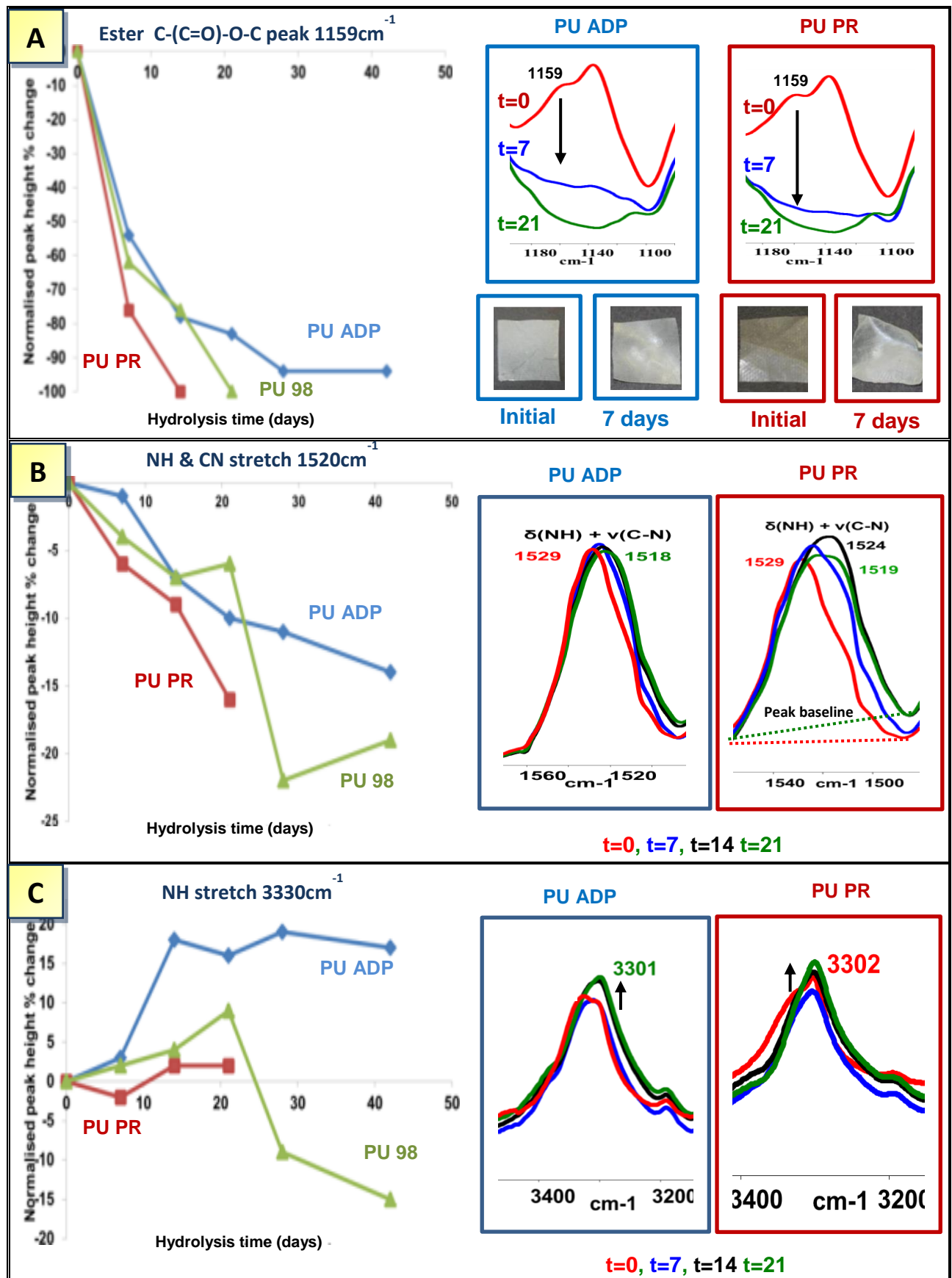


Figure 3.26 Effect of hydrolytic degradation on the hard and soft PU segments quantified by FTIR-ATR

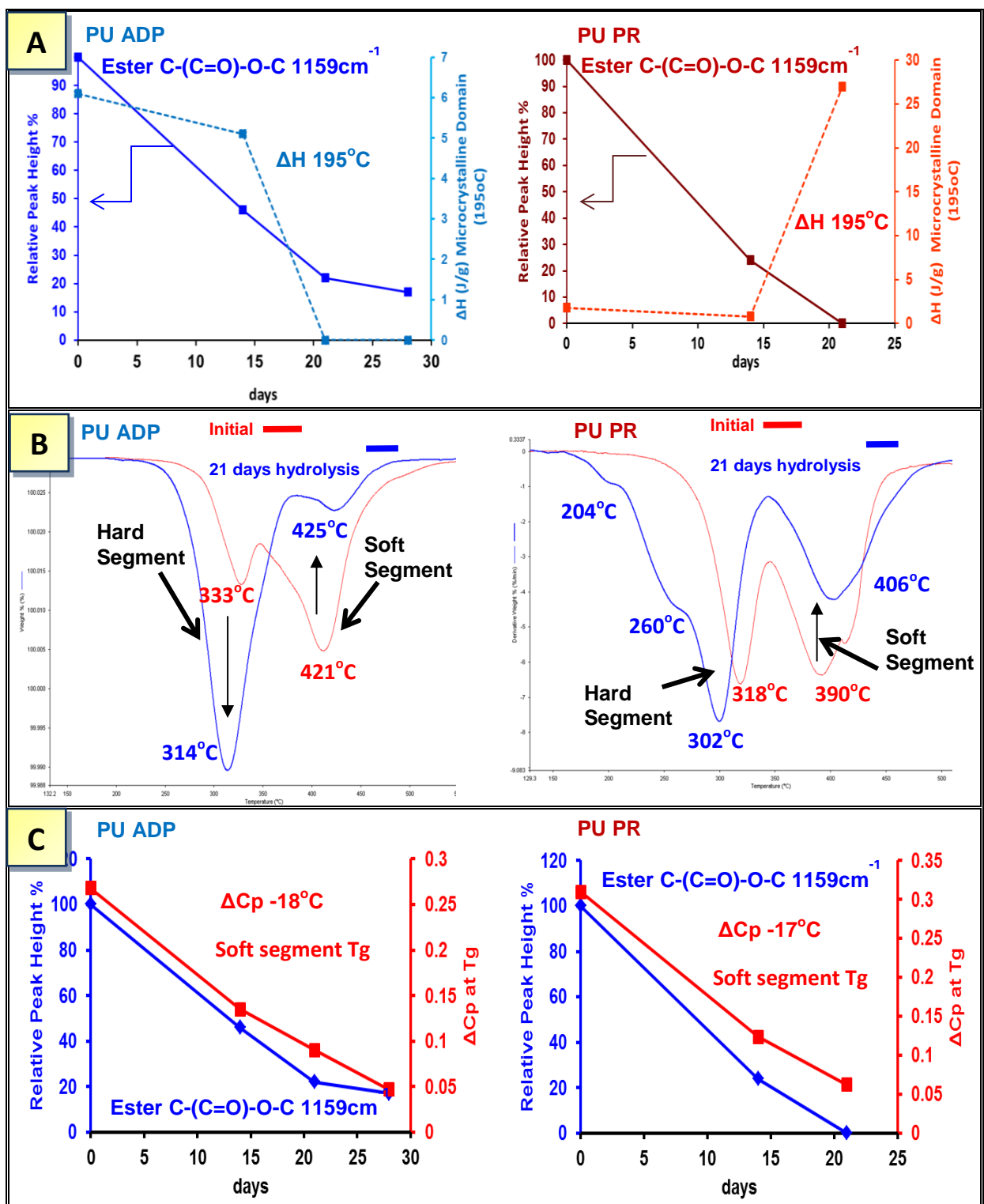


Figure 3.27 Changes in the hard and soft segment of PU during hydrolysis dependant on the method of synthesis. **(A)** changes in the hard segment crystallinity, **(B)** thermal stability from TGA, **(C)** changes in the Tg and ester peak at 1159cm⁻¹ of the soft segment from DSC.

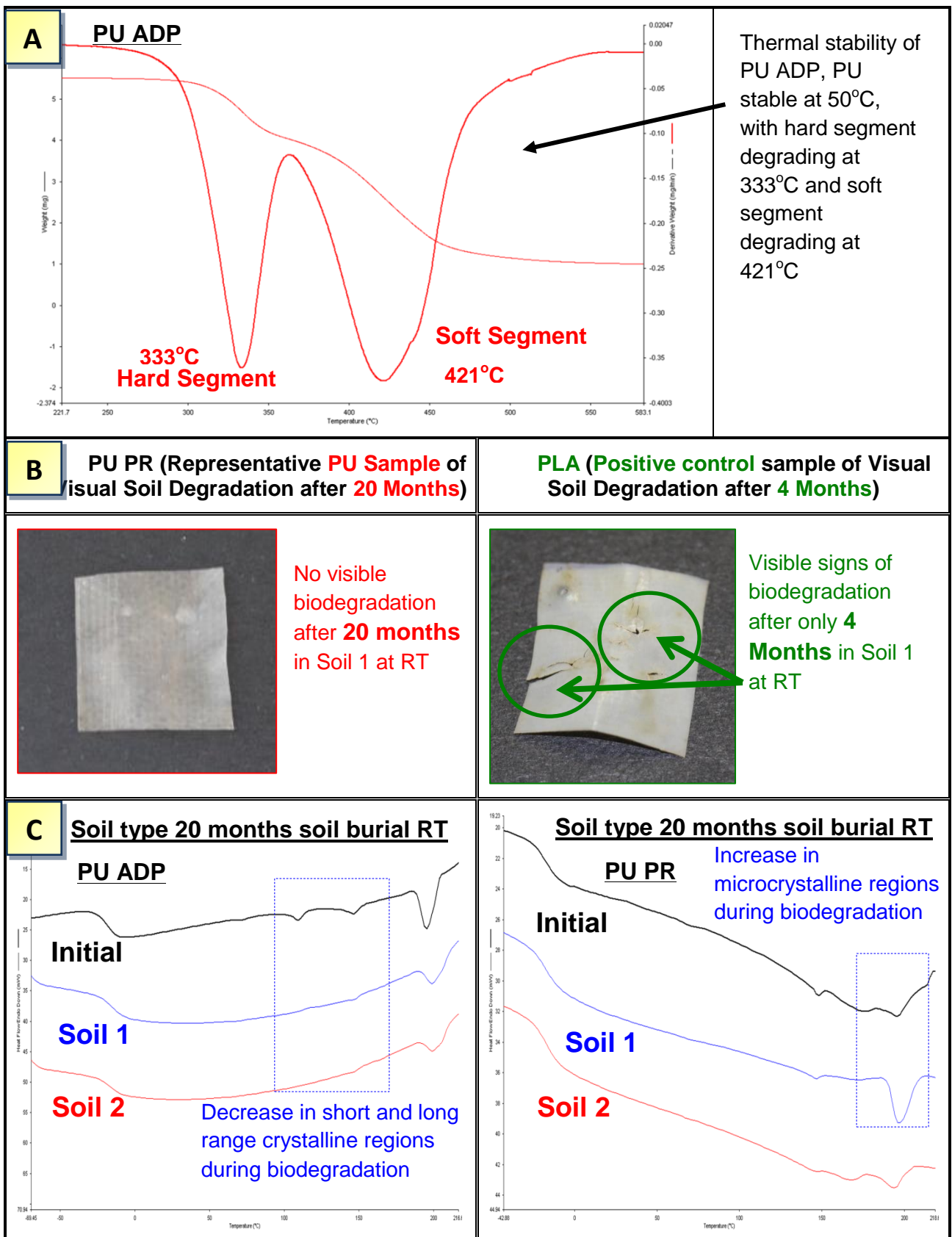


Figure 3.28 Showing changes to the PU samples during soil burial. **(A)** thermal stability of PU at 50°C, **(B)** visible comparison of PU with PLA (a polymer known to be biodegradable), **(C)** changes in crystallinity of PU samples during soil burial at RT.

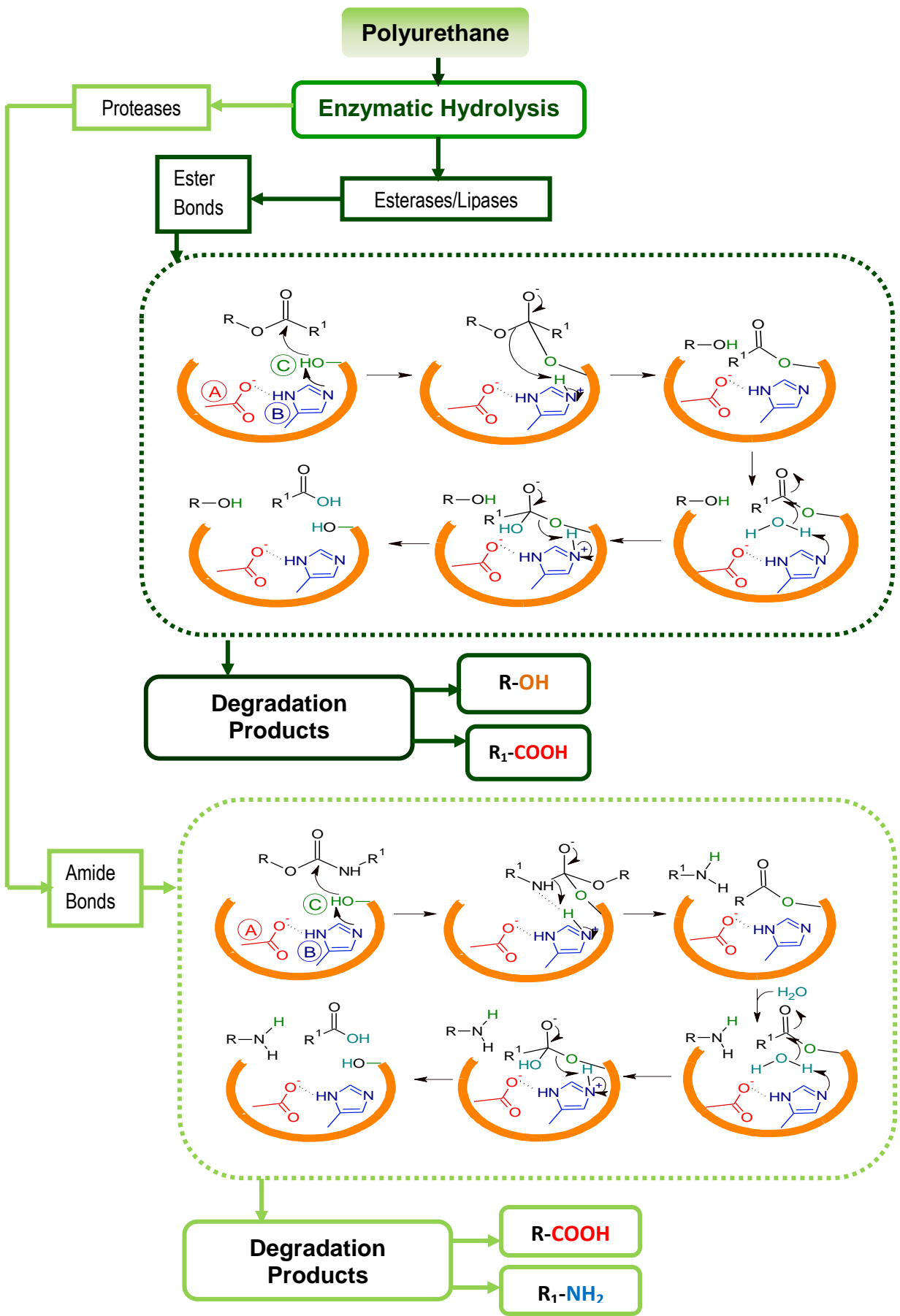


Figure 3.29 Hydrolysis of ester and amide bonds during enzymatic degradation

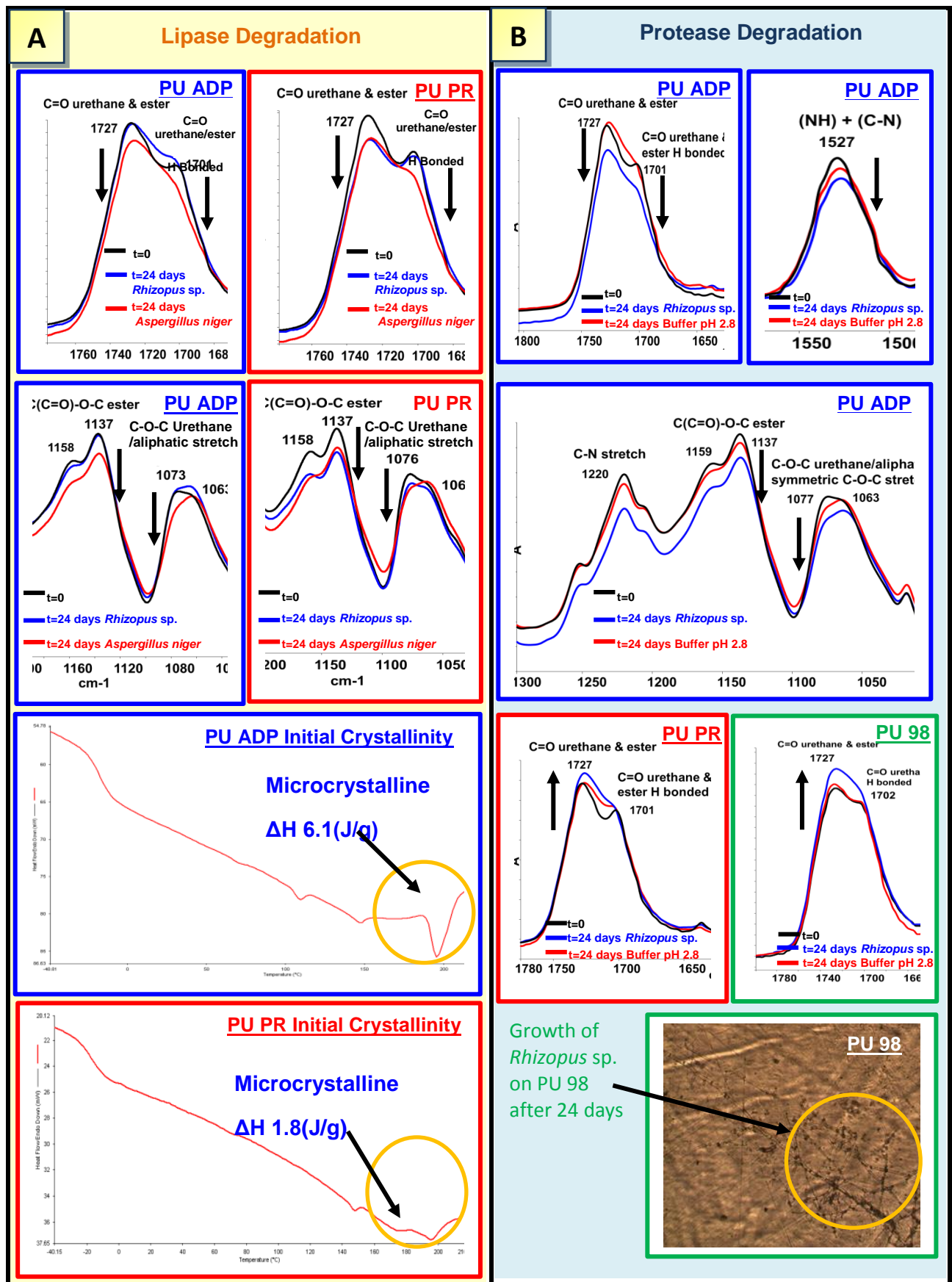


Figure 3.30 Showing changes to PU group 1 samples during enzymatic degradation (**A**) lipase *Rhizopus* sp. and *Aspergillus niger* (**B**) protease *Rhizopus* sp.

Chapter 4

Effect of Polyurethane Structural Composition on Degradation and Biodegradation; Effect of Isocyanate

4.1 Objectives and methodology

PU films containing an ADP soft segment and a BD/MDI hard segment, see **Table 4.1**, were synthesised by the two major synthesis methods for PU, that being; the one shot method and the pre-polymer method. In chapter 3, the hypothesis that the method of synthesis can affect the rate of degradation of PU was tested. For alkaline hydrolysis this was shown to be the case, where the **PU PR** sample (pre-polymer method) was found to be more susceptible to hydrolysis. However, soil burial and enzymatic degradation experiments did not induce any major degradation to any of the PU samples in this group, implying that the chemical constituents of the PUs were not conducive towards degradation by biological media. Therefore, the work described in this chapter examines the effect of altering the starting materials on the chemical and morphological profiles of the PUs, and ultimately how altering each component may influence the rate of degradation and biodegradation of the PU samples.

PUs are complex microphase separated polymers, the soft segment consists of a long chain polyol, and the hard segment consists of a short chain molecule functioning as a chain extender, and a bi-functional molecule called an isocyanate. Altering the isocyanate can affect many properties of the PU. Various studies have shown that altering the isocyanate from aromatic to aliphatic increases the stability towards UV- induced degradation [139, 140]. Previous research has also suggested that PUs synthesised with aliphatic isocyanates bestow increased resistance towards hydrolysis and thermal degradation [34, 46]. However, many factors can affect the rate of degradation, and the rate of hydrolysis of PUs. Ultimately degradation can be affected by microphase separation, the extent of hydrogen bonding and

crystallinity of PU, and all of which could in turn be affected by altering the isocyanate [44, 46, 126].

In consideration of this, this chapter examines two PUs (**Group 2**) with different isocyanates; **PU ADP** containing an aromatic isocyanate (MDI), and **PUH ADP** containing an aliphatic isocyanate ($H_{12}MDI$), **Table 4.1**. These samples were synthesised by Eurothane Ltd using their specific one shot method of synthesis, see **Scheme 3.1**. The same experimental procedures were employed for the PUs in this group with the PUs described in chapter 3, examining the susceptibility of each of the samples towards alkaline hydrolysis, enzymatic hydrolysis and soil burial. The results from these experiments will give an indication of the effect of the isocyanate on PU degradation and the influence of the isocyanate on phase separation, hydrogen bonding and morphology, and how each of these factors affect the polymer degradation and biodegradation.

4.2 Results

4.2.1 Characterisation of PUH ADP - Group 2 (Effect of Isocyanate)

Characterisation of each sample was undertaken prior to the hydrolysis experiments. This group consisted of **PU ADP** and **PUH ADP**, see **Table 4.1**. Characterisation of **PU ADP** was previously discussed in **Section 3.2.1**. therefore characterisation of **PUH ADP** only, will be discussed in this section. **PUH ADP** was found to be soluble in (THF) and (DMFA), therefore alteration of the isocyanate did not affect the solubility of the sample. Results obtained from water absorption experiments revealed that altering the isocyanate from aromatic to aliphatic decreased the water absorption of the PU film (**PU ADP 4.5%, PUH ADP 2%**) **Fig. 4.1**.

The chemical structure of **PUH ADP** was determined using FTIR-ATR, and examination of the initial spectrum revealed many similarities with the spectrum of **PU ADP** (**Section 3.2.1**). However, several notable differences were also observed, as would be expected due to the aliphatic isocyanate contained within the hard segment. As the hard segment of **PUH ADP** was not aromatic in nature, no peak was observed at 1597cm^{-1} as of that for **PU ADP**, **Fig. 4.2a & 4.3a**. Two peaks were also observed that were not present in **PU ADP**; at 1378cm^{-1} and 779cm^{-1} , which relate to the CH bend of the cyclohexane ring contained within the hard segment, **Fig. 4.3a**. The hard/soft segment structure of **PU ADP** (containing the aromatic isocyanate) was characterised by the absorbances at about 1728cm^{-1} and 1701cm^{-1} corresponding to the urethane and ester stretching vibrations of the free and hydrogen bonded C=O groups respectively [6,7,8]. However, three peaks in this region were observed for **PUH ADP** at 1730cm^{-1} , 1713cm^{-1} and 1691cm^{-1} , **Fig. 4.3a**. These peaks were designated

as C=O non-hydrogen bonded urethane/ester, C=O ester hydrogen bonded and C=O urethane hydrogen bonded, respectively [125, 140]

The thermal stability of each sample was determined using TGA under a nitrogen atmosphere similar to samples in group 1. The thermographs given in **Figs. 4.2b & 4.3b** highlight distinct differences between **PU ADP** (aromatic MDI) and **PUH ADP** (aliphatic H₁₂MDI). Degradation of the hard segment for **PU ADP** was found to occur at 336°C, whereas for **PUH ADP** this occurred at the lower temperature of 321°C. The thermal degradation of the soft segment was also varied depending on the choice of isocyanate, with the soft segment degrading at 436°C for **PU ADP** (aromatic isocyanate), and again at a lower temperature for **PUH ADP** was observed at 402°C. The difference in the thermal stability between these two samples was thought to arise from a change in morphology with isocyanate selection. Previous studies have shown that aromatic isocyanates are more reactive than their aliphatic counterparts [12, 34], and therefore this would affect the chain build up and ultimately morphology of the sample which in turn could affect the thermal stability of the PU sample. In order to assess this suggestion, DSC analysis was performed on each sample to ascertain the morphological profiles.

DSC analysis was performed on the virgin samples prior to degradation experiments. Samples were subjected to a heating temperature of 100 °C per min under a helium atmosphere to 180°C to remove previous thermal history, then, the temperature was reduced to -100°C and heated again to 220°C. From the results obtained, it can be seen in **Figs. 4.2c & 4.3c & Table 4.2** that a discernible difference was observed between **PU ADP** (aromatic isocyanate) and **PUH ADP** (aliphatic isocyanate), with a large endotherm observed at 195°C (ΔH 6.08) for **PU ADP** indicating that a significant proportion of the hard segment contained within the PU was of a microcrystalline nature. The same was not observed for **PUH ADP**, with no endotherm visible at this temperature, however, a small peak was observed at 120°C (ΔH 0.12) denoting short range non-crystalline regions within the hard segment [107]. These results indicate that the morphology of **PUH ADP** was predominately of an amorphous nature. A dramatic difference was also observed with respect to the Tg value of **PU ADP** and **PUH ADP**, with the Tg value for **PUH ADP** being 10°C lower than that of **PU ADP** (**PUH ADP** -28°C, **PU ADP** -18°C). An indication of phase separation between the hard and soft segments in polyurethane can be obtained by the Tg value of the soft segment, and it has been previously shown that increased phase separation between the hard and soft segments decreases the Tg value [107, 109]. Therefore it can be surmised that greater phase

separation occurred using the aliphatic isocyanate (**PUH ADP**). It was reasoned that these major differences in the morphology of the PU samples could affect the rate of degradation.

4.2.2 Effect of Isocyanate (PU ADP and PUH ADP) on the Rate of Alkaline Hydrolysis

PU ADP and **PUH ADP** were subjected to alkaline hydrolysis in order to determine the effect of the isocyanate on the rate of degradation. The samples were immersed in 10% NaOH solution and removed at weekly intervals to monitor their degradation. Both samples lost weight steadily during hydrolysis for the first 21 days, **Fig. 4.4a**. **PUH ADP** then exhibited a greater weight loss than **PU ADP** during the final 3 weeks (**PU ADP** 56% weight remaining and **PUH ADP** 35% weight remaining). Both samples showed similar visible signs of degradation after 28 days, **Fig. 4.4b & Fig. 4.5**, however, after 42 days **PUH ADP** had completely broken up, whereas, **PU ADP** still remained intact. These results indicate that PU synthesised with aliphatic isocyanates increases the rate of hydrolysis. In order to determine the structural changes taking place during degradation both samples were subjected to FTIR-ATR during alkaline hydrolysis.

4.2.1.1 Structural changes of PU ADP and PUH ADP during alkaline hydrolysis monitored by FTIR-ATR

An initial spectrum of each sample was taken before hydrolysis, and group absorbances were assigned accordingly **Figs 4.2a & 4.3a**. Analysis of the spectra during hydrolysis displayed distinct changes in both the hard and soft segments.

i) Spectral changes Hard Segment structure PU ADP and PUH ADP

The hard segment structure was previously characterised by FTIR-ATR. The N-H bond of the urethane linkage in the hard segment showed notable changes during alkaline hydrolysis. The peak at 3329cm^{-1} (**PU ADP**) and 3322 cm^{-1} (**PUH ADP**) increased during the 42 days (+17% **PU ADP**, +48% **PUH ADP**), **Fig. 4.6a & c**. The peak at 1529cm^{-1} relating to the N-H bending vibration with C-N stretching vibration (amide II band) was seen to decrease for **PU ADP** (-14%) which shifted to 1518cm^{-1} during the hydrolysis experiment **Fig.4.6b**, however for **PUH ADP** this peak increased during alkaline hydrolysis **Fig.4.6c**, which suggests partial degradation of the hard segment.

ii) Spectral changes Hard/Soft Segment Structure PU ADP and PUH ADP

The hard/soft segment groups for both samples showed significant changes during alkaline hydrolysis. Characterisation of the PEA soft segment carbonyl group and urethane linkages

was performed using FTIR-ATR, by examining the peaks between 1650cm^{-1} and 1750cm^{-1} . The spectrum of each sample was examined, and revealed differences between the two samples. **PU ADP** exhibited two peaks in this region **Fig. 4.7a**; at 1728cm^{-1} and 1701cm^{-1} (C=O urethane/ester free and hydrogen bonded, respectively), both decreasing during hydrolysis (see section 3.1.1). Conversely **PUH ADP** displayed 3 peaks in this region **Fig. 4.7c**. The C=O peak at 1730cm^{-1} denoting the free C=O ester and urethane moieties significantly decreased by 81% after 42 days of hydrolysis. The peak at 1713cm^{-1} signifying the hydrogen bonded ester C=O group also decreased but to a lesser extent (50%) **Fig. 4.7c**. This figure also shows the hydrogen bonded urethane C=O peak at 1691cm^{-1} which decreased after 42 days of hydrolysis (10%). A small peak was also observed at 1660cm^{-1} which may be due to a urea linkage obtained as a side reaction during polymerisation [52]. This peak increased significantly after 42 days which could indicate the formation of amine groups as a hard segment degradation product during hydrolysis [105]. A decrease was observed for the peak at 1074cm^{-1} (-40% **PU ADP**) and 1082cm^{-1} (-40% **PUH ADP**) denoting C-O-C aliphatic and urethane bond, **Fig. 4.7b & d**, also indicating degradation of the hard segment. Changes relating to the CH_2 moiety in the soft/hard segment structure were also noted by the peak at 1381cm^{-1} relating to the $\alpha\text{-CH}_2$ group **Fig. 4.6b & d**, which decreased with hydrolysis time and almost completely disappeared after 42 days.

iii) Spectral changes PU ADP Soft Segment structure

During alkaline hydrolysis the peaks at 1137cm^{-1} and 1158cm^{-1} (C-(C=O)-O ester) decreased dramatically for both samples **Fig. 4.7b & d**. This peak had completely disappeared after 42 days for **PU ADP**, indicating that the ester linkages in the polyethylene adipate soft segment had been hydrolysed. However, a small peak still remained after 42 days for **PUH ADP** although the sample had completely broken up which may suggest that a small proportion of the soft segment still remained.

4.2.1.2 Effect of isocyanate on crystallinity and thermal stability during alkaline hydrolysis (PU ADP and PUH ADP).

Changes in crystallinity and thermal stability of the PU samples during alkaline hydrolysis were monitored by DSC and TGA. From the results obtained **Figs 4.8 & 4.9**, it can be seen that the two samples show a dramatic difference after hydrolysis. The thermograph for **PU ADP** synthesised with an aromatic isocyanate (MDI) **Table 4.2** displayed three endotherms relating to the MDI/BD hard segment. During hydrolysis, all of these peaks were seen to reduce and eventually disappear after 28 days **Fig. 4.8a & Table 4.3**. In contrast to this, the thermograph for **PUH ADP** synthesised with an aliphatic isocyanate (H_{12}MDI) exhibited only

one endotherm at 120°C denoting short range ordering of the MDI/BD hard segment, **Table 4.2**. After 28 days this peak remained relatively unchanged with the ΔH value increasing slightly from 0.1 J/g to 0.25 J/g **Fig. 4.8b & Table 4.3**.

TGA thermograms for both PU samples in this group displayed substantial degradation of the soft segment, **Fig. 4.9**. However, two endotherms were observed relating to the soft segment for **PUH ADP** after 28 days of alkaline hydrolysis, as opposed to **PU ADP**, which displayed only one peak. Both samples also displayed a large DTGA peak at around 302°C indicating that a large proportion of the hard segment still remained.

4.2.3 Susceptibility to soil degradation of Polyurethane Samples – Effect of Isocyanate PU ADP and PUH ADP

In order to ascertain the effect of the isocyanate on the rate of biodegradation of PU, the samples were subjected to two different types of soil burial (**see Chapter 3, Section 3.2.3**).

After 20 months of soil burial at RT there was little weight loss observed for PU samples in either soil types, with only 3% weight loss occurring for **PU ADP** and **PUH ADP**, **Fig. 4.10b & c**. The film samples were still intact and did not show any visible signs of cracking, **Fig. 4.11**. However, some visible signs of degradation were observed microscopically for both samples with small cracks visible, implying that some limited biodegradation of these films had occurred **Fig. 4.11**.

PU samples subjected to soil burial at 50°C for 5 months displayed a greater weight loss than those at RT **Fig. 4.10a**, with the greatest weight loss of 32% for **PUH ADP**. A weight loss was also noted for **PU ADP**, 21%. From **Fig 4.11** it can be observed that the samples were not intact after 5 months. The films were broken up when removed from the soil, however little difference was discerned between the two samples in the extent of degradation.

In order to ascertain any structural changes taking place during soil burial both at RT and at 50°C, FTIR-ATR was performed on each sample at regular intervals during the experiment.

4.2.3.1 Structural changes during soil burial at 50°C in PU ADP and PUH ADP monitored by FTIR-ATR.

The main spectral changes during soil burial involved the ester/urethane linkages in the samples, therefore these will be examined in detail. **Fig. 4.12 a & b** display peaks relating to the free urethane/ester carbonyl group at 1727cm⁻¹, which decreased for both samples

during soil burial, even after 3 months. However, there still remained a significant peak after 5 months despite the fact that the films had broken up in the soil. This suggests that not all of the adipate ester contained in the samples had degraded. This can be further supported, by the peaks at 1158cm^{-1} and 1137cm^{-1} denoting the O-C-C ester bond **Fig. 4.12 c & d**, which again although decreased somewhat, still remained after 5 months for both samples. The appearance of a significant peak at 1659cm^{-1} was noted for both **PUH ADP** and **PU ADP**. This peak was also observed after 3 months for **PUH ADP** and may relate to the formation of amine groups as a result of hydrolytic degradation.

4.2.3.2 Structural changes during soil burial at RT after 20 months in PU ADP and PUH ADP monitored by FTIR-ATR

Some minor spectral changes were noted during soil burial at RT after 20 months. The peaks at 1727cm^{-1} and 1701cm^{-1} relating to the free and hydrogen bonded urethane/ester carbonyl group respectively were seen to decrease after 20 months soil burial **Fig. 4.12 e & f**. Little difference was noted with respect to soil type. A decrease in the peaks at 1158cm^{-1} and 1137cm^{-1} was also perceived, see **Fig. 3.12 g & h**, denoting the O-C-C ester bond, it was found that these peaks had decreased to a greater extent for **PU ADP** than **PUH ADP**, implying that a greater proportion of the soft segment had degraded, however, also noteworthy was a significant increase in the peak at 1045cm^{-1} for **PUH ADP**. This peak denotes the urethane/aliphatic ester peak, and the increase in this peak may be due to a conformational change at the surface, with more of the hard segment being exposed as the soft segment degrades.

4.2.2.3 Effect of Isocyanate on PU ADP and PUH ADP morphology after 20 months soil burial

PU samples subjected to soil burial at RT were removed from the soil, and morphological changes during biodegradation were ascertained by DSC. From the results shown in **Table 4.4**, it can be seen that after soil burial of **PU ADP** (aromatic), minor changes were observed in the DSC thermograms (not shown), with the most significant finding being, the disappearance of the peak at 109°C relating to the short range ordered MDI/BD hard segment. However, the endotherms at 147°C and 195°C relating the long range ordered and microcrystalline MDI/BD regions remained relatively unchanged. This indicates that although some minor degradation had occurred it was not significant. Altering the isocyanate did not increase the rate of biodegradation in soil with **PUH ADP** displaying no significant changes in the DSC thermograms (**Table 4.4**). No change was observed in either the Tg value at -28°C

or the short range ordered hard segment regions at 120°C. These findings imply that for **PUH ADP**, the hard segment remained the same even after soil burial, and altering the isocyanate from an aromatic to aliphatic did not affect the rate of biodegradation in soil at RT.

4.2.4. Susceptibility of Polyurethane Samples PU ADP and PUH ADP (Effect of Isocyanate) towards enzymatic degradation.

In order to ascertain susceptibility of the PU samples towards biodegradation and degradation, samples were placed in buffer solutions (37°C), each solution containing a fungal enzyme as of that for PU samples in group 1 (**see Chapter 3, Section 3.2.4**).

Samples were removed from enzyme/buffer solutions every 12 days for a period of 24 days (**see section 2.3.2**). For the protease degradation, the pH of the buffer was 2.8 therefore, samples were also placed in the buffer solution only to determine whether any degradation occurred due to enzyme activity or simply the acidic buffer solution.

4.2.4.1 Structural changes during enzymatic degradation using lipases in PU ADP and PUH ADP monitored by FTIR-ATR.

There was little weight loss (not shown) observed after 24 days for all of the PU samples in this group for both lipases *Rhizopus* sp. and *Aspergillus niger*. However, optical images did display distinct differences between the samples dependant on the isocyanate used **Fig. 4.13**. Some signs of surface degradation were observed for **PU ADP** when immersed in the buffer solution containing *Aspergillus niger* after 24 days, however the same was not observed for **PUH ADP**, and therefore FTIR-ATR was performed to determine any structural changes between the two samples.

Spectral changes after 24 days of enzymatic degradation of PU samples for both *Rhizopus* sp. and *Aspergillus niger* are given in **Fig. 4.14**. It can be noted that there was relatively little change in the spectra for **PU ADP** for *Rhizopus* sp., **Fig. 4.14a & b**. However, samples immersed in the buffer solution containing *Aspergillus niger*, did display a small decrease in the peaks at 1701cm⁻¹ denoting the hydrogen bonded ester/urethane linkages, and at 1158cm⁻¹ and 1137cm⁻¹ which corresponds to the ester bond in the PEA soft segment. **Fig. 4.14 b**, also displays a small decrease at 1073cm⁻¹ which corresponds to the ester/urethane C-O-C bond. For **PUH ADP**, the peaks at 1725cm⁻¹ and 1701cm⁻¹ were found to increase after 24 days in enzymatic solution for *Aspergillus niger*, however, relatively little change was observed in the peaks for *Rhizopus* sp. **Fig. 4.14 c & d**. The same was observed for the

peaks at 1158cm^{-1} , 1137cm^{-1} and 1073cm^{-1} . From these results it was noted that although altering the isocyanate from aromatic to aliphatic did induce some minor changes to the PU sample, it did not significantly increase susceptibility towards enzymatic degradation.

4.2.4.2 Structural changes during enzymatic degradation using proteases in PU ADP, and PUH ADP monitored by FTIR-ATR.

Degradation by proteases was also disappointing in that little weight loss (not shown) was observed for *Aspergillus saitoi* and *Rhizopus* sp. However, visible cracking from microscope images of the PU samples were observed with *Rhizopus* sp. **Fig. 4.15**.

The FTIR-ATR spectra of the PU samples did highlight small differences regarding degradation of the urethane linkages contained within the hard segment and hard/soft segment interfaces. **PU ADP** displayed a reduction in the ester/urethane peaks at 1727cm^{-1} and 1701cm^{-1} , and also the N-H & C-N peak at 1527cm^{-1} relating to the hard segment, **Fig. 4.16 a**. This is in accordance with the microscopic images, which clearly displays cracks in the **PU ADP** film. A decrease was also observed at 1077cm^{-1} denoting the C-O-C urethane stretch, **Fig. 4.16 b**. However, **Fig. 4.16c** displays changes in the **PUH ADP** film, in which an increase in the peaks at 1730cm^{-1} , 1712cm^{-1} and 1690cm^{-1} was observed, denoting the free ester/urethane, hydrogen bonded ester and hydrogen bonded urethane linkages respectively. Although no weight losses were observed for either **PU ADP** or **PUH ADP** during enzymatic degradation, a distinct difference was noted both in the microscopic images and FTIR-ATR spectra, with **PU ADP** containing the aromatic isocyanate being more susceptible towards enzymatic degradation by *Rhizopus* sp.

4.3 Discussion

Polyurethane elastomers have been shown to exhibit a two-phase morphology consisting of a soft segment which generally consists of either a polyether and/or a polyester chain, and a hard segment which consists of the interaction of the isocyanate and the chain extender. Previous studies have shown that the rate of degradation and biodegradation of PU is dependent on the morphology of the PU, with the crystalline nature of the hard segment influencing this greatly [60, 141, 142]. PUs containing a highly crystalline structure have been shown to reduce the rate of hydrolysis and biodegradation [25, 120]. Many factors can contribute to the overall rate of degradation and biodegradation of PU, and altering the chemical components of the PU can either increase or decrease the rate of degradation. The molecular make up of these constituents can alter a variety of PU properties such as; surface chemistry in respect of availability of enzyme binding sites, hydrophilicity of the PU, intermolecular hydrogen bonding, phase separation between the hard and soft segments and crystallinity [12, 38, 137]. The focus of this chapter is to examine the effect of the isocyanate on some of these properties, when exposed to experiments simulating degradation by chemical hydrolysis and biodegradability studies. These investigations produced some interesting findings.

4.3.1 Effect of Isocyanate (PU ADP and PUH ADP) on the Rate of Alkaline Hydrolysis

When subjected to alkaline hydrolysis **PUH ADP** was found to degrade faster than **PU ADP**. Results from FTIR-ATR were similar for both samples, with the exception of the increase in the peak at 1660cm^{-1} and an increase in the peak at 1524cm^{-1} for **PUH ADP**, **Fig. 4.7**. The increase in these two peaks is more than likely to be due to some degradation of the hard segment resulting in amine degradation products [105], see peak at 3322cm^{-1} in, **Fig. 4.6**. Peaks pertaining to the soft segment for these samples were similar in that a decrease in the C=O non-bonded peak at $\sim 1728\text{cm}^{-1}$ (**Fig. 4.7**), and also a decrease in the peak at around 1380cm^{-1} which relates to the CH_2 α -carbon, **Fig. 4.6b & d**. This would be expected as during hydrolysis the number of CH_2 α -carbon atoms would decrease, and **Fig. 4.17b** shows the possible degradation mechanism of the hard and soft segments, again indicating degradation of the soft segment and possibly some degradation of the hard segment.

Previous studies have stated that microphase morphology and intermolecular hydrogen bonding in polyurethane elastomers are two major factors which can influence the rate of

degradation [59, 60, 141]. FTIR analysis has been widely used in previous studies to determine the extent of hydrogen bonding in polyurethanes [46, 143]. Therefore, deconvolution of the FTIR-ATR peaks in the region of 3200 cm^{-1} - 3400cm^{-1} was undertaken **Fig. 4.17a**. These peaks relate specifically to the N-H groups contained within the PU and provides a good indication of hydrogen bonding between the N-H and C=O groups [43]. Peaks were deconvoluted using the Lorenzian distribution, and **Fig. 4.17a** clearly displays a distinct difference between **PU ADP** (aromatic isocyanate) and **PUH ADP** (aliphatic isocyanate). For **PU ADP**, the amount of free N-H groups and hydrogen bonded groups were almost identical whereas, **PUH ADP** contained considerably more hydrogen bonded N-H groups than free N-H groups, **Fig. 4.17a**. The rate of hydrolysis for **PUH ADP** was greater than **PU ADP**, **Fig. 4.4a**, and this was unexpected, as previous studies have stated that hydrolysis of PU chemical constituents are dependent on hydrogen bonding as follows; non bonded ester > non bonded urethane > hydrogen bonded ester > hydrogen bonded urethane [46]. Therefore, DSC analysis was performed to elucidate any differences in their microphase morphology.

PU ADP synthesised with an aromatic isocyanate (MDI) showed three endotherms relating to the MDI/BD hard segment with a large endotherm at **195°C**, **Fig. 4.2**, relating to the microcrystalline regions within the hard segment indicating that the hard segment domains in **PU ADP** were principally highly ordered. Conversely, **PUH ADP** synthesised with an aliphatic isocyanate (H_{12}MDI) exhibited only one endotherm at **120°C**, **Fig 4.3**, denoting short range ordering of the MDI/BD hard segment. These thermograms clearly show that the morphology of **PU ADP** was more crystalline than **PUH ADP**, and this must be a major factor that would influence the rate of its degradation.

In order to elucidate the phase separation of the samples, the Tg of each sample was examined, and was found to be distinctly different too, (dependent on the isocyanate used), and this is also a key factor in explaining the increased rate of hydrolysis of **PUH ADP** (aliphatic isocyanate). The Tg of **PU ADP** (aromatic) was found to be -18°C prior to hydrolysis, **Fig. 4.2c**). This value decreased with hydrolysis time to -31°C with a decrease in the ΔH value as the soft segment degraded **Fig. 4.8a**. Conversely, the Tg for **PUH ADP** prior to hydrolysis was -28°C and remained the same throughout the hydrolysis experiment, **Fig. 4.8b**, however a decrease in the ΔH value was also observed with the decrease of the soft segment **Fig. 4.8a**. These results indicate that **PU ADP** (aromatic) exhibited greater phase mixing than that of **PUH ADP** (aliphatic). An increase in phase mixing increases the formation of more ordered microcrystalline structures within the hard segment [107, 108], and this was clearly evident from the DSC thermograms for **PU ADP** and **PUH ADP** (**Figs.**

4.2c & 4.3c). This difference in phase separation can also explain the increased hydrogen bonding in the **PUH ADP**, **Fig 4.17a**. This is supported by literature in which studies have shown that an increase in phase separation increases the amount of hydrogen bonding in PU [121]. Carbonyls groups hydrogen bonded to N-H groups are generally located within the hard segment [121]. Free carbonyl groups occur when the hard segment is dispersed within the soft segment (ie greater phase mixing), therefore, greater phase separation results in less mixing between these domains, less dispersal of the hard segment within the soft segment, and hence a greater proportion of carbonyl groups are hydrogen bonded [121], which was found to be the case for **PUH ADP**.

TGA thermographs for both PU samples in this group indicated substantial degradation of the soft segment after 28 days of alkaline hydrolysis, **Fig. 4.9**. A slight difference between the two samples was noted, as two weight loss peaks were observed relating to the soft segment for **PUH ADP** which was not present in **PU ADP**, **Fig. 4.9 a & b**. This may be due to scission of the ester linkages resulting in lower molecular weight degradation products from the soft segment in the case of **PUH ADP** [59]. A large proportion of the hard segment still remained in both samples (TGA peaks @ 321°C & 333°C), **Fig. 4.9**, therefore substitution of the aromatic isocyanate (MDI) for the aliphatic isocyanate ($H_{12}MDI$) had minimal effect on degradation of the hard segment itself.

The results from both DSC and FTIR-ATR analysis suggest that although the extent of hydrogen bonding and crystallinity of PU have been previously shown to affect the rate of hydrolysis, the effect of highly ordered crystalline domains in **PU ADP**, and the synergistic effect of greater phase separation and higher degree of amorphous regions in **PUH ADP** resulted in an increase in the rate of hydrolysis for **PUH ADP**. The greater extent of hydrolysis of **PUH ADP** is therefore most likely due to a greater ability of water molecules to diffuse into the amorphous regions of **PUH ADP**. This supports the findings above that altering the isocyanate from aromatic to aliphatic did not significantly increase the rate of degradation of the hard segment specifically, but did alter the morphology of the PU, and subsequently this is likely to be the reason for the increased rate of hydrolytic degradation of **PUH ADP**.

4.3.2. Susceptibility to soil degradation of Polyurethane Samples PU ADP and PUH ADP (Effect of Isocyanate).

Previous studies have indicated that PUs synthesised with aromatic isocyanates produce toxic amine products as a result of biodegradation [46, 121]. Therefore it was considered beneficial to examine a PU containing an aliphatic isocyanate with respect to its biodegradation by soil burial. Results from alkaline hydrolysis experiments revealed that altering the isocyanate from aromatic to aliphatic increased the rate of hydrolytic degradation, and it was surmised that a difference would be observed in relation to soil burial experiments. However, this was not found to be the case, with similar findings observed for both **PU ADP** (aromatic) and **PUH ADP** (aliphatic). FTIR-ATR spectra for soil burial at 50°C was found to be comparable for both samples, with a substantial decrease of the C=O free urethane/ester peak (**PU ADP** 1725cm⁻¹, **PUH ADP** 1730cm⁻¹) and decrease in the C-(C=O)-O-C ester peak at 1137cm⁻¹, **Fig. 4.18a & b**. After 5 months a peak was also observed at ~1659cm⁻¹ for both samples, and this is more than likely associated with aromatic amine groups which are degradation products of the hard segment [105].

Soil burial at RT did produce a slight difference between **PU ADP** and **PUH ADP**, with some minimal degradation observed microscopically for both samples, **Fig. 4.11**. Results from FTIR-ATR spectra also supported this. **Fig. 4.18c & d**. display relative peak changes during soil burial at RT, and it can clearly be seen that although the C(C=O)-O-C ester bond (1137cm⁻¹) in the PU soft segment decreased, this was minimal, with a % peak reduction at 18% for **PU ADP** and 7% **PUH ADP** in soil 1, and 19% for **PU ADP** and 9% for **PUH ADP** for soil 2, **Fig. 4.18d**, indicating that more of the soft segment of **PU ADP** had been hydrolysed. Interestingly though, the C-O peak at 1045cm⁻¹ for **PUH ADP** was seen to increase dramatically after 20 months soil burial, **Fig. 4.18 f**. This peak increase may be due to the formation of alcohol degradation products [105] or a conformational change on the surface of the PU, exposing more of the hard segment structure during degradation of the soft segment [ref]. Results from DSC analysis supported this finding in that there was little change to the thermographs after 20 months soil burial (not shown). **PUH ADP** displayed an endotherm at 120°C denoting short range ordering of the MDI/BD hard segment, indicating that little change to this domain had occurred after soil burial.

It can be concluded from these results that although some degradation of the soft segment had occurred, altering the isocyanate from aromatic to aliphatic did not increase the rate of biodegradation significantly.

4.3.3 Susceptibility of Polyurethane Samples PU ADP and PUH ADP towards Enzymatic Degradation (Effect of Isocyanate).

PU samples in group 2 (effect of isocyanate) were subjected to enzymatic degradation with two different lipases; *Aspergillus niger* and *Rhizopus* sp. and the samples were shown to display some limited degradation visually, and some minor differences were also noted in the FTIR-ATR spectra taken during the experiment, **Fig. 4.19**.

During enzymatic degradation with lipases a decrease in ester groups would be expected [129], and this was observed in the FTIR-ATR spectra for **PU ADP** when subjected to degradation by *Aspergillus niger*. The spectra given in **Fig. 4.19a**, displays a small decrease in the peaks at 1727cm^{-1} and 1701cm^{-1} relating to the ester/urethane bond for **PU ADP**. A small decrease was also observed for the peaks at 1137cm^{-1} and 1081cm^{-1} relating to the ester and C-O-C linkages in the PU, respectively, **Fig. 4.19b**. Although this decrease was noted, it was only found to be minimal and indicates that only a limited amount of degradation of the ester linkages had occurred. In contrast to this, **PUH ADP** displayed an increase in the peaks at 1730cm^{-1} relating to the ester/urethane bond and 1137cm^{-1} denoting the C=O bond in the ester soft segment, **Fig. 4.19a & b**. This may have been due to adherence of the enzyme to the surface of the PU sample. Enzymatic degradation occurs in a two-step process in that, first the enzyme binds to the polymer substrate through a hydrophobic domain, and then the enzyme catalyses hydrolysis of the ester bonds [2, 62]. Due to the increase in these peaks it was difficult to determine whether **PUH ADP** had degraded more than **PU ADP**. However, examination of the microscopic images did not detect any noticeable changes between the two samples, **Fig. 4.19 e & f**, and therefore can surmise that altering the isocyanate from aromatic to aliphatic may have altered the surface of **PUH ADP**, to favour enzymatic adherence to the PU, but hydrolysis of the PU components was limited during the time period of the experiment of 24 days.

The PU samples were also subjected to enzymatic degradation by proteases from *Aspergillus saitoi* (not shown) and *Rhizopus* sp. However, only degradation with *Rhizopus* sp. displayed any changes in the PU samples. **PU ADP** displayed a reduction in the ester/urethane peaks at 1727cm^{-1} and 1701cm^{-1} , **Fig. 4.19c**, and also the N-H & C-N peak at 1527cm^{-1} relating to the hard segment. A decrease was also observed at 1077cm^{-1} denoting the C-O-C urethane stretch, **Fig. 4.19d**. The FTIR-ATR spectra for **PUH ADP** displayed an increase in the peak at 1730cm^{-1} denoting the ester/urethane linkage. This is more than likely due to adherence on the surface of the PU as of that for lipase *Aspergillus niger* (see above). However, microscopic images did reveal a slight difference between these samples in that

substantial cracking was observed for PU ADP **Fig 4.19e**. However, this degradation was still deemed to be only minimal, as little weight loss was observed for either sample (not shown). Both films did display some visible signs of deformation but still remained intact after the 24 days, **Fig. 4.19e & f**, and so it can be concluded that altering the isocyanate did not significantly increase the rate of enzymatic degradation by the enzymes used in these experiments.

4.3.4 Overall Summary of the effect of the Isocyanate on Polyurethane Degradation and Biodegradation.

The work described in this chapter focused on the effect of the isocyanate structure on the rate of degradation and biodegradation of PU. Altering the isocyanate was shown to have a profound effect on the phase separation, crystallinity and hydrogen bonding within the PU samples, with the aliphatic isocyanate resulting in a PU with increased phase separation (from DSC **Figs. 4.2 & 4.3**), and increased hydrogen bonding (**Fig. 4.17a**), but was found to decrease the amount of highly ordered crystalline structured regions. This change in morphology was shown to have a significant effect on degradation of the PU during alkaline hydrolysis, with the increased phase separation, and the reduction of crystalline regions in **PUH ADP** resulting in a faster rate of degradation. Although previous studies have shown that the amount of hydrogen bonding in PU can reduce the rate of degradation [46], this was not found to be the case for the samples examined in this study, and one can conclude that although this would invariably affect the rate of degradation, the presence of the highly crystalline regions in **PU ADP** hindered the rate of degradation to a greater extent.

The PU samples were not observed to be particularly susceptible towards enzymatic degradation by the fungal enzymes *Aspergillus niger*, *Aspergillus satoi* and *Rhizopus* sp. or soil burial experiments at RT, although **PUH ADP**, containing the aliphatic isocyanate did seem to confer a higher degree of enzymatic binding to the surface of the PU, **Fig. 4.18**, which may have resulted in degradation after a greater length of time. Soil burial at 50°C did not reveal any significant differences between the two samples, and both samples had degraded substantially after 5 months, **Fig. 4.11**, and these results indicate that these samples may degrade under composting conditions. Altering the isocyanate did not influence the rate of biodegradation significantly, but due to the possible toxic degradation/biodegradation products produced from PUs synthesised with an aromatic isocyanates [46, 121], it may be more environmentally friendly to use PUs with aliphatic isocyanates for biodegradable PUs.

In summary, altering the isocyanate did not affect the rate of enzymatic degradation and biodegradation by soil burial significantly, however, degradation by chemical/alkaline hydrolysis did highlight a major difference between the PU sample synthesised with the aromatic isocyanate (**PU ADP**), and the aliphatic isocyanate (**PUH ADP**), and is more than likely due to the highly crystalline nature of the **PU ADP**. The PU synthesised with the aliphatic isocyanate (**PUH ADP**) was found to be less crystalline and more phase separated, and consequently more susceptible to hydrolysis than the PU synthesised with the aromatic isocyanate (**PU ADP**). Therefore, in order to obtain environmentally friendly PU's with limited shorter lifespans, an aliphatic isocyanate should be used, with a further possibility of increased biodegradation using alternative soft segment chemical constituents, and the effect of altering these constituents and their effect on degradation and biodegradation will be explored further in chapter 5.

Table 4.1 Effect of Isocyanate on PU Degradation

PU Code	Composition			M.w.t Ratio polyol: isocyanate: chain extender	Method of synthesis (Table 3.1)		
	Soft segment- polyol	Hard segment					
		Isocyanate	Chain Extender				
PU-ADP	Polyethylene adipate (PEA)	Methylene diisocyanate (MDI)	Butane diol (BD)	1:3:2	OS-102		
PUH-ADP	Polyethylene adipate (PEA)	Methylenedicyclohexyl diisocyanate (H ₁₂ MDI)	Butane diol (BD)	1:3:2	OS-102		
PU Code	Chemical Structure						
PU-ADP							
PUH-ADP							

Table 4.2 Effect of isocyanate on morphology of PU characterised by DSC

Sample Code	Isocyanate	Soft Segment			Hard Segment					
		Tg (°C)	Tm (°C)	ΔH (J/g)	Tm(°C) (I)	ΔH(J/g) (I)	Tm(°C) (II)	ΔH(J/g) (II)	Tm(°C) (III)	ΔH(J/g) (III)
PU ADP	Aromatic (MDI)	-18	71	0.1	109	0.5	147	0.8	195	6.1
PUH ADP	Aliphatic (H ₁₂ MDI)	-28	-	-	120	0.12	-	-	-	-

Table 4.3 Effect of chemical hydrolysis on morphology of PU characterised by DSC

Sample Code	Hydrolysis time	Soft Segment			Hard Segment					
		Tg (°C)	Tm (°C)	ΔH (J/g)	Tm (°C) (I)	ΔH(J/g) (I)	Tm(°C) (II)	ΔH(J/g) (II)	Tm(°C) (III)	ΔH(J/g) (III)
PU ADP	time 0	-18	71	0.1	109	0.5	147	0.8	195	6.1
PUH ADP	time 0	-28	-	-	120	0.12	-	-	-	-
PU ADP	14 days	-18	-	-	109	0.47	148	0.74	198	5.11
PUH ADP	14 days	-29	-	-	120	0.2	-	-	-	-
PU ADP	28 days	-31	-	-	-	-	-	-	-	-
PUH ADP	28 days	-30	-	-	120	0.25	-	-	-	-

Table 4.4 Effect of soil burial on morphology of PU characterised by DSC

Sample Code	Soil burial 20 months RT	Soft Segment			Hard Segment					
		Tg (°C)	Tm (°C)	ΔH (J/g)	Tm (°C) (I)	ΔH(J/g) (I)	Tm(°C) (II)	ΔH(J/g) (II)	Tm(°C) (III)	ΔH(J/g) (III)
PU ADP	time 0	-18	71	0.1	109	0.5	147	0.8	195	6.1
PU ADP	Soil 1	-15	-	-	-	-	147	0.1	200	4.9
PU ADP	Soil 2	-17	-	-	-	-	147	0.34	199	5.26
PUH ADP	time 0	-28	-	-	120	0.12	-	-	-	-
PUH ADP	Soil 1	-27	-	-	118	0.1	-	-	-	-
PUH ADP	Soil 2	-27	-	-	119	0.1	-	-	-	-

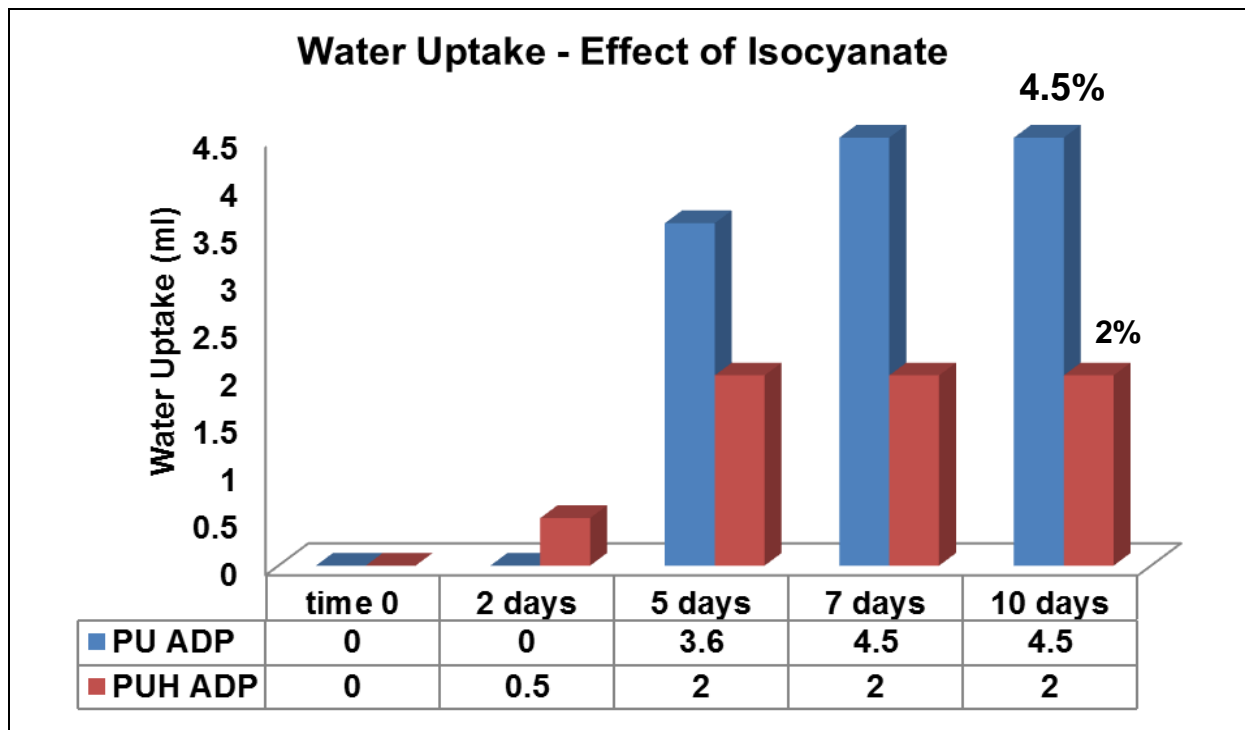


Figure 4.1 Hydrophilicity of PU samples determined by weight percentage increase of water uptake

PU ADP – Hard Segment MDI/BD: Soft Segment PEA

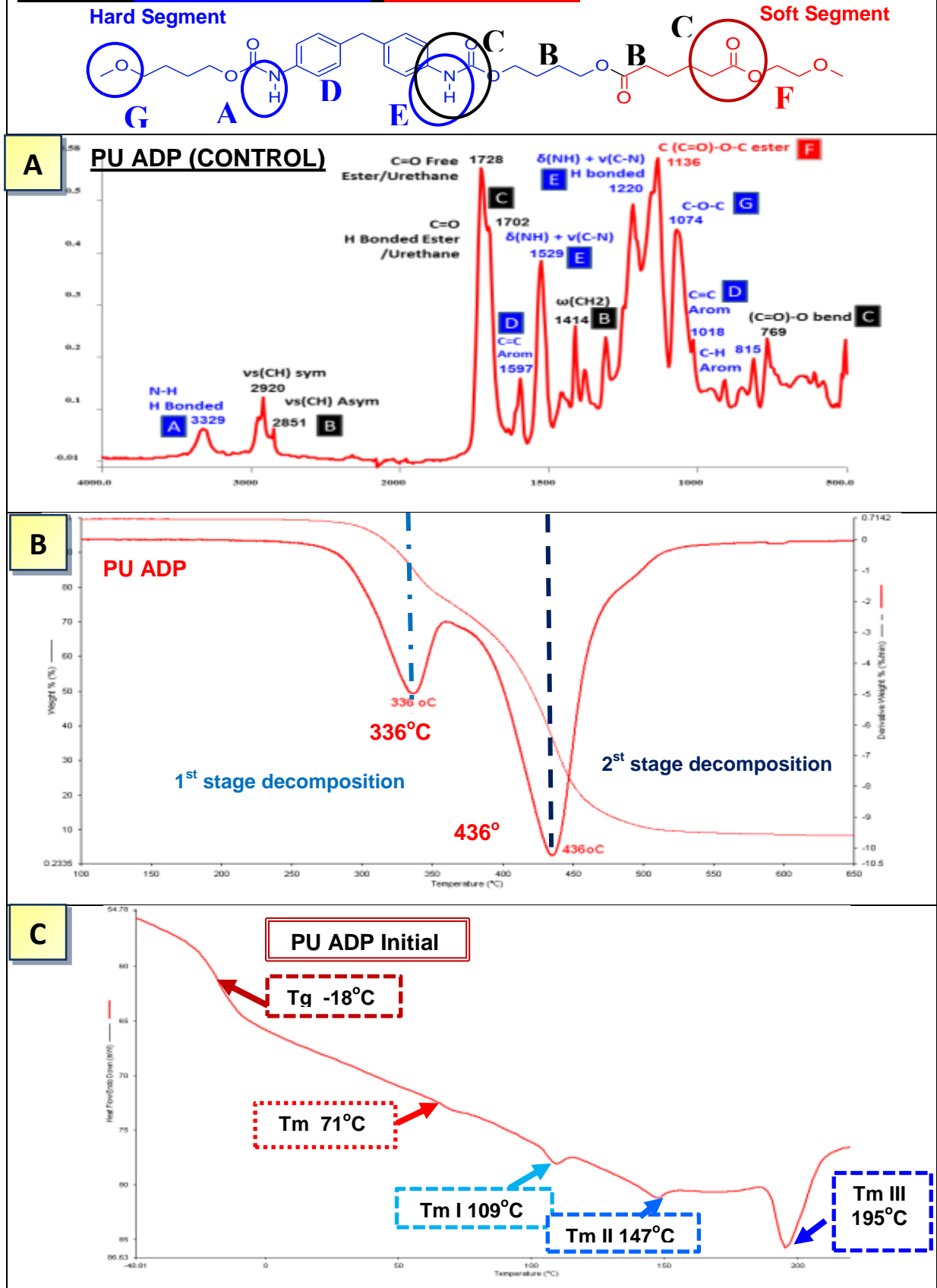


Figure 4.2 Characterisation of PU samples PU ADP, chemical structure by FTIR-ATR (A), thermal stability by TGA (B), morphology by DSC (C)

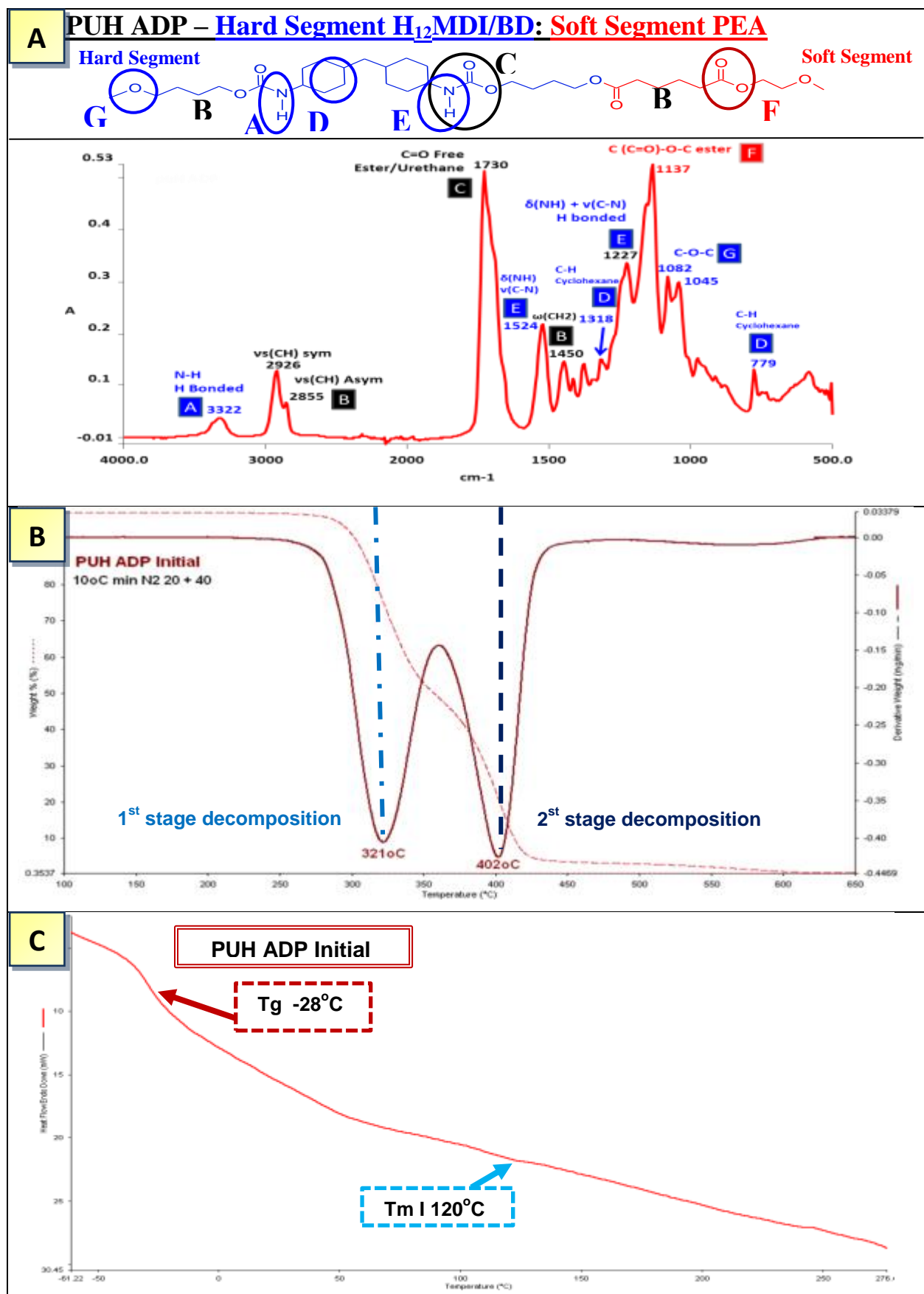
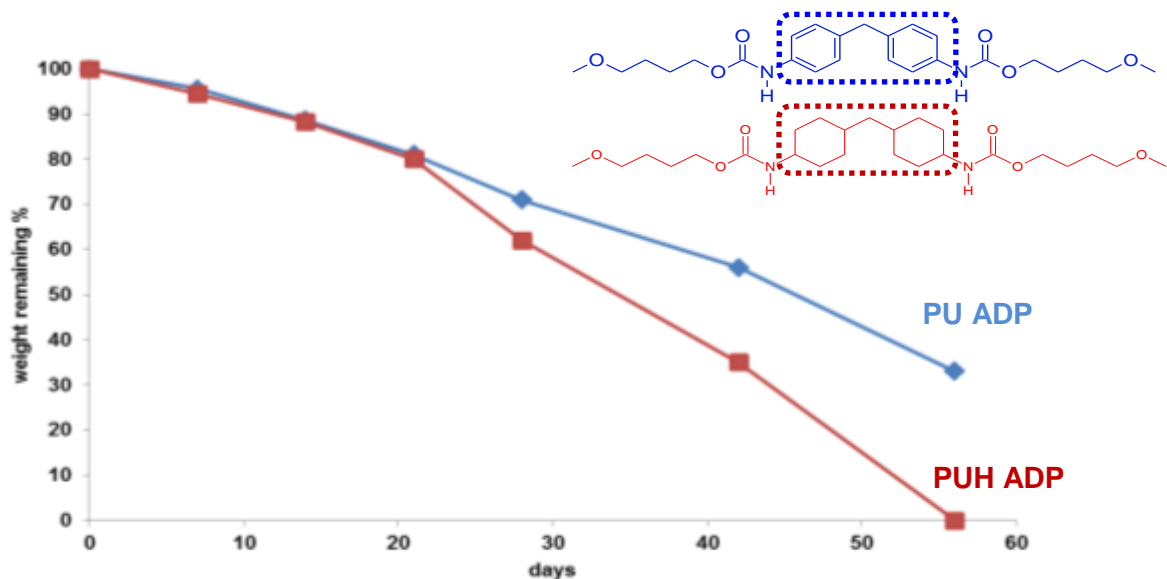


Figure 4.3 Characterisation of PUH ADP, chemical structure by FTIR-ATR (A), thermal stability by TGA (B), morphology DSC (C).

A

Effect of isocyanate on the rate of Hydrolytic Degradation



Sample Code

Isocyanate

Weight Remaining %

	0 days	7 days	14 days	21 days	28 days	42 days	56 days
--	--------	--------	---------	---------	---------	---------	---------

PU ADP	4,4 Methylene diisocyanate	100	96	89	81	71	56	33
--------	----------------------------	-----	----	----	----	----	----	----

PUH ADP	Hexamethylene Isocyanate	100	94	88	80	62	35	0
---------	--------------------------	-----	----	----	----	----	----	---

B

Visual degradation during alkaline hydrolysis

■ PU ADP (control) ■ PUH ADP

Arbitrary scale of degradation stage

- min 0 no signs of cracking deformation
- 1 slight signs of limited surface degradation
- 2 deformation of sample (curling) & discolouration
- 3 visible cracks showing
- 4 Small pieces of samples broken away from film
- max 5 complete breaking of sample small pieces

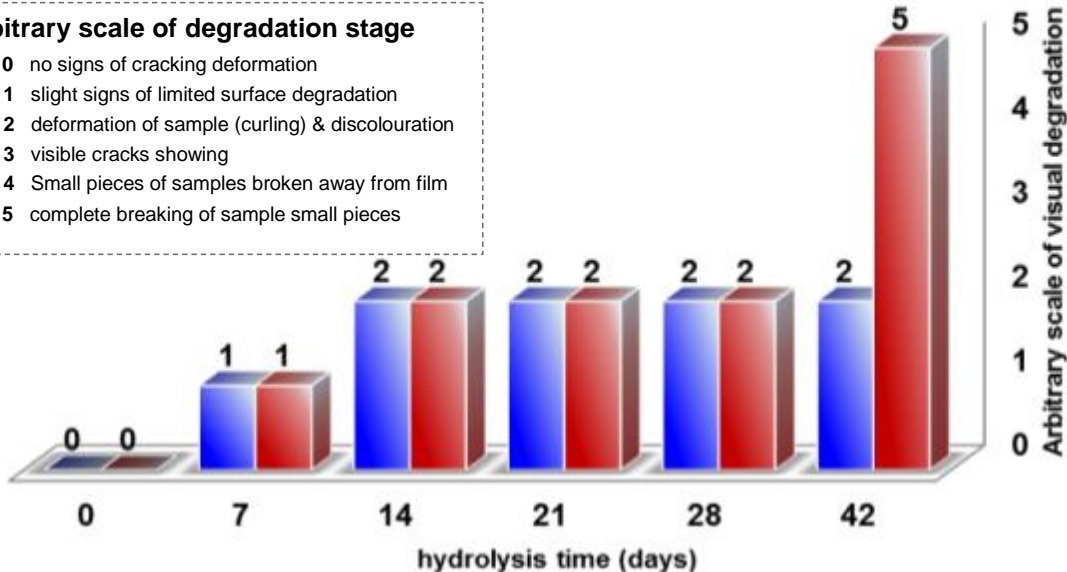


Figure 4.4 Effect of isocyanate on the rate of hydrolytic degradation (**A**) with 10% NaOH (aq) (see table 2.1 & 2.2 pg. for acronyms). Visual surface cracking (**B**)

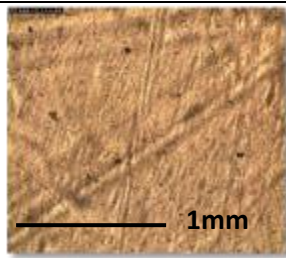
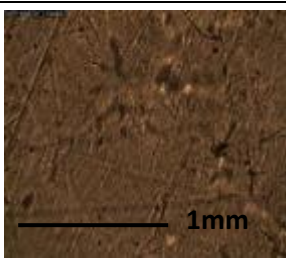
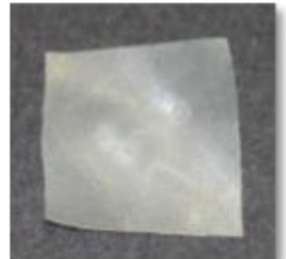
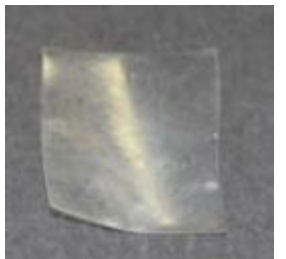
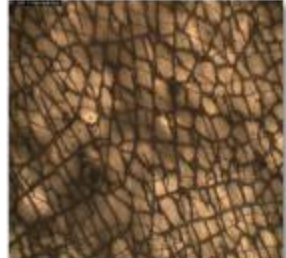
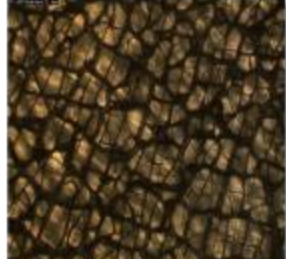
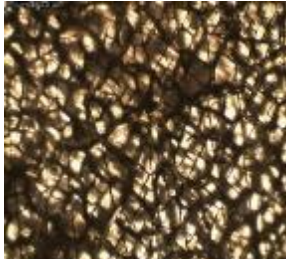
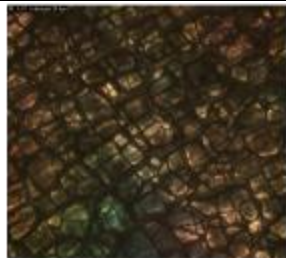
	PU ADP	PUH ADP	PU ADP	PUH ADP
Initial				
7 days				
14 days				
21 days				
28 days				
42 days				

Figure 4.5 Effect of isocyanate on Visual changes of PU during hydrolytic degradation with 10% NaOH (aq), determined by optical microscope and photographs

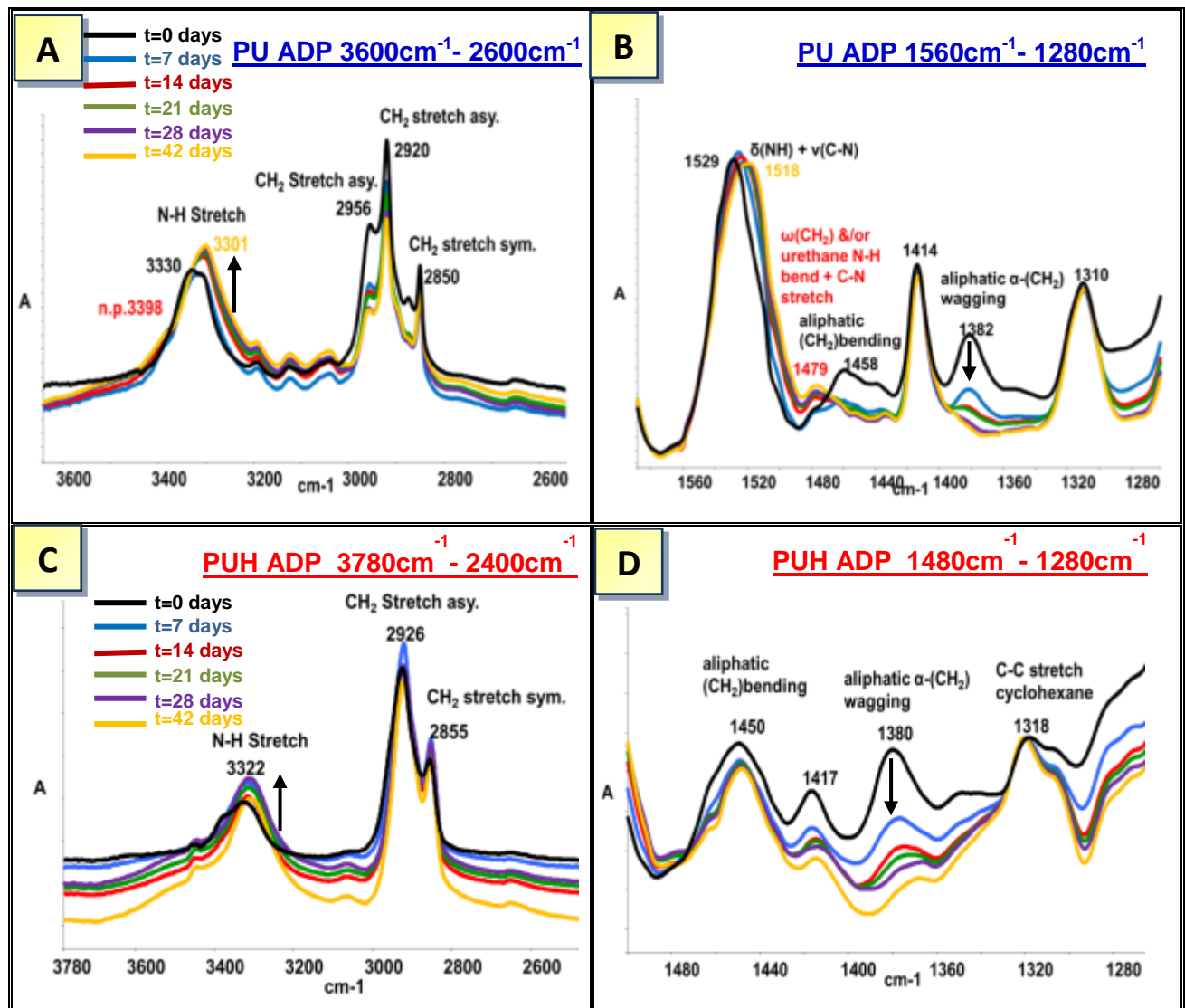


Figure 4.6 Effect of isocyanate on structural changes of NH and CH₂ bonds during alkaline hydrolysis of PU ADP and PUH ADP by FTIR/ATR

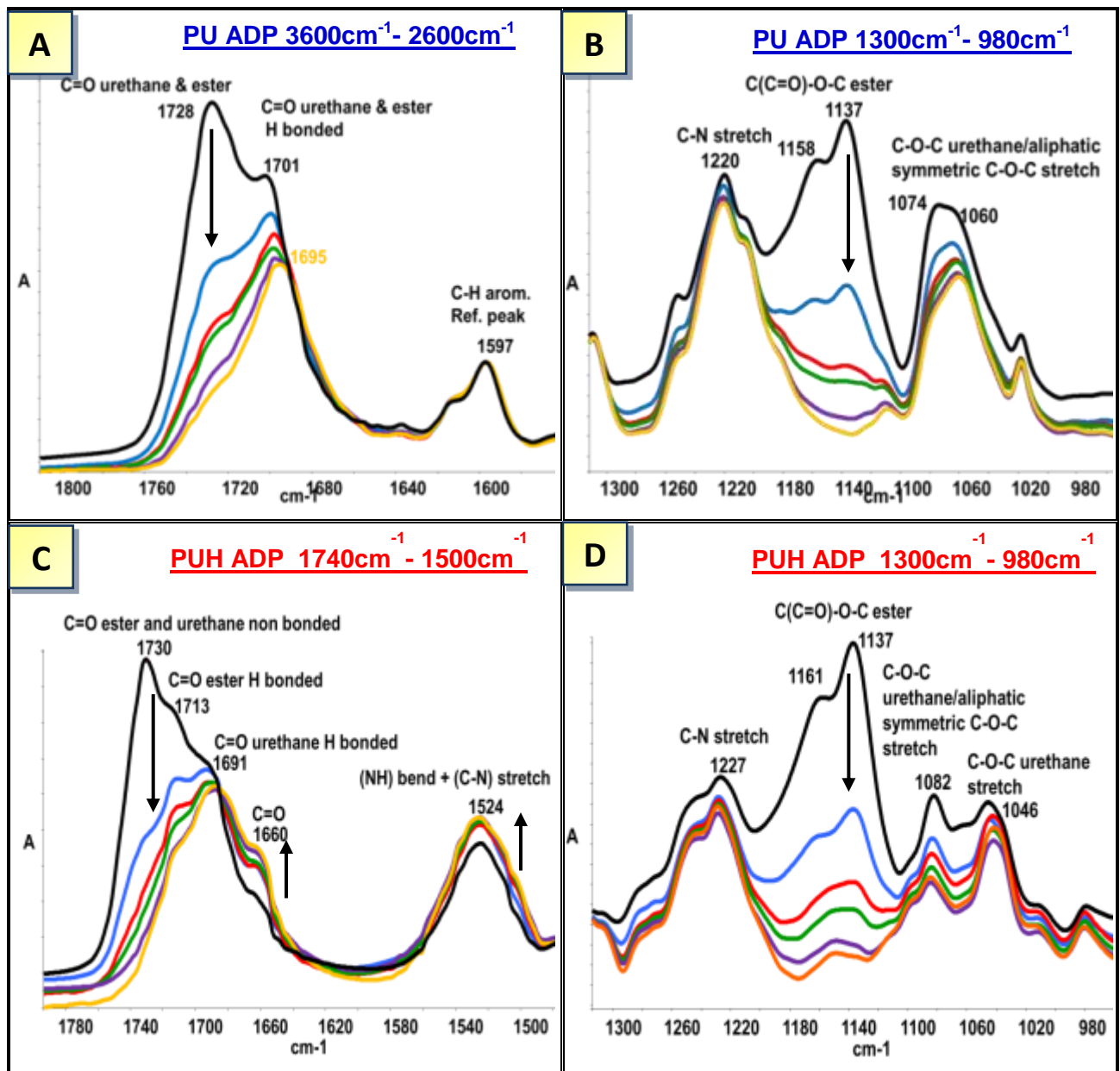


Figure 4.7 Effect of isocyanate on structural changes of C=O and C-O-C ester/urethane linkages during alkaline hydrolysis of PU ADP and PUH ADP by FTIR/ATR

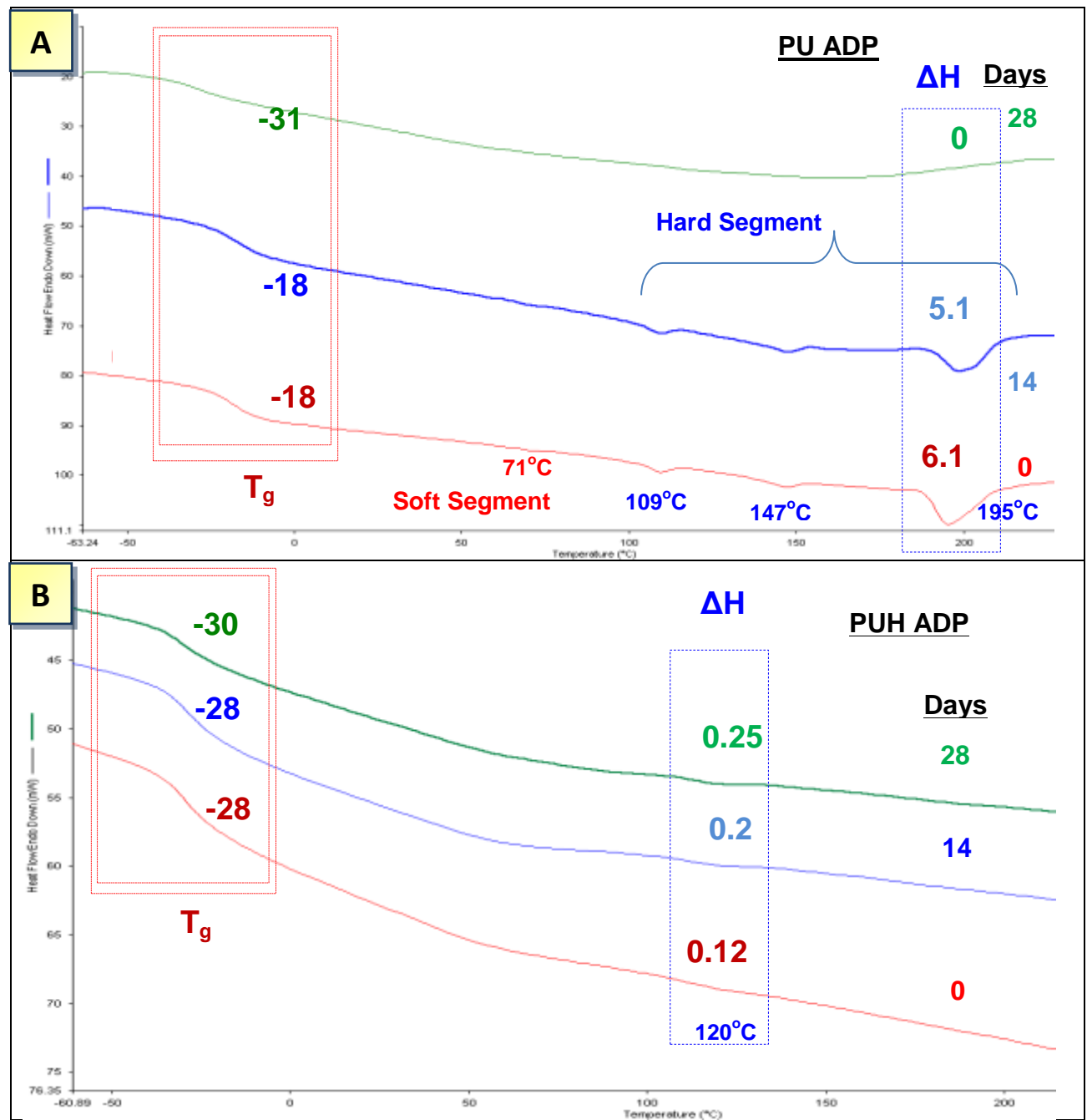


Figure 4.8 Changes in crystallinity during alkaline hydrolysis of Group 2 PU samples

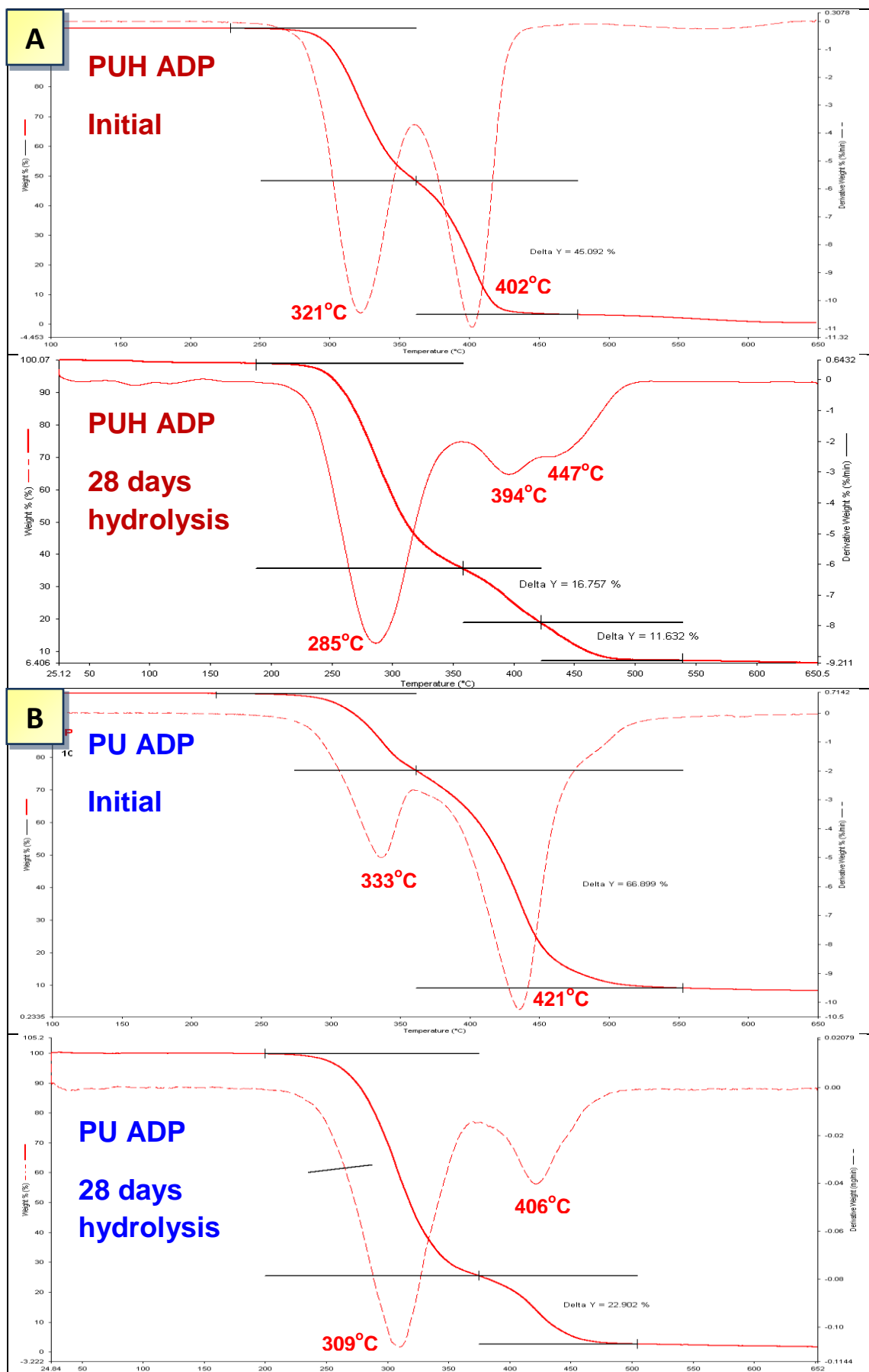


Figure 4.9 Changes in thermal stability after alkaline hydrolysis of Group 2 PU samples

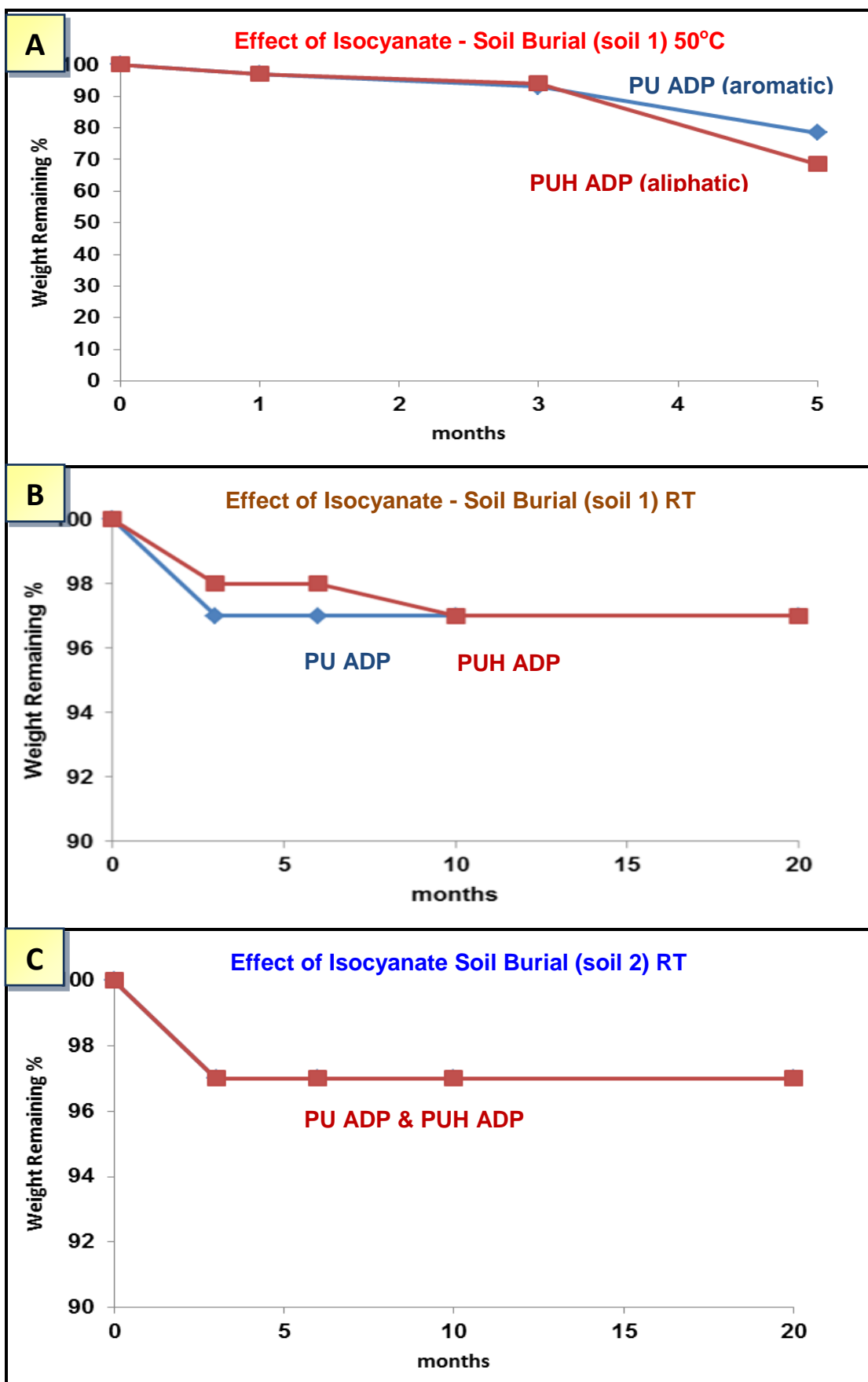


Figure 4.10 Effect of Isocyanate on the rate of biodegradation under soil burial conditions, soil 1 50°C (A), soil 1 RT (B), soil 2 RT (C)

	PU ADP	PUH ADP	PU ADP	PUH ADP
Initial				
5 Months				
Soil 1 50°C				
20 Months				
Soil 1 RT				
Soil 2 RT				

Figure 4.11 Photographic and microscopic images of PU ADP & PUH ADP during soil burial

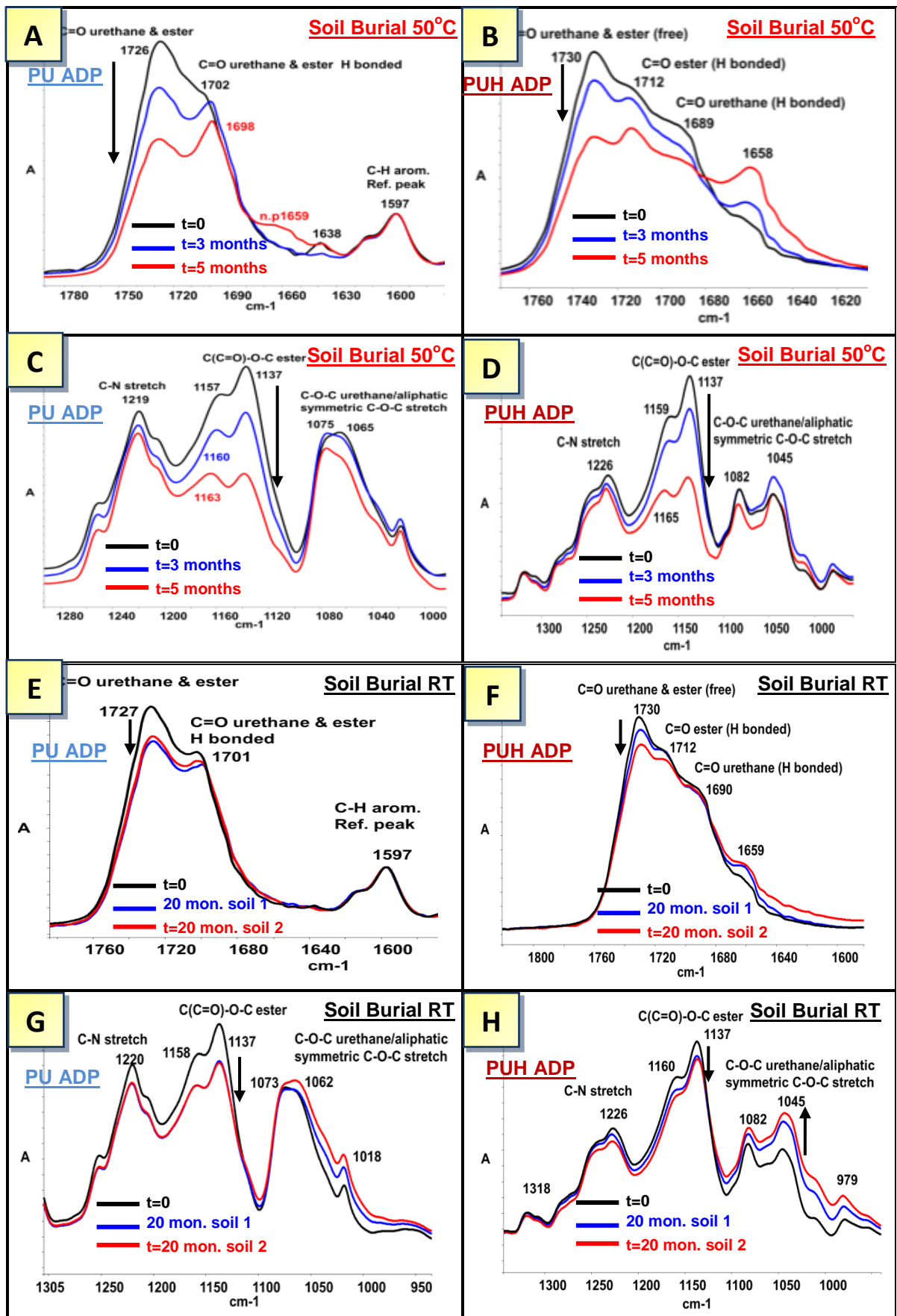


Figure 4.12 Effect of isocyanate on C=O and C-O-C ester/urethane linkages during soil burial of PU ADP & PUH ADP by FTIR/ATR, (A-D 50°C) (E-H RT)

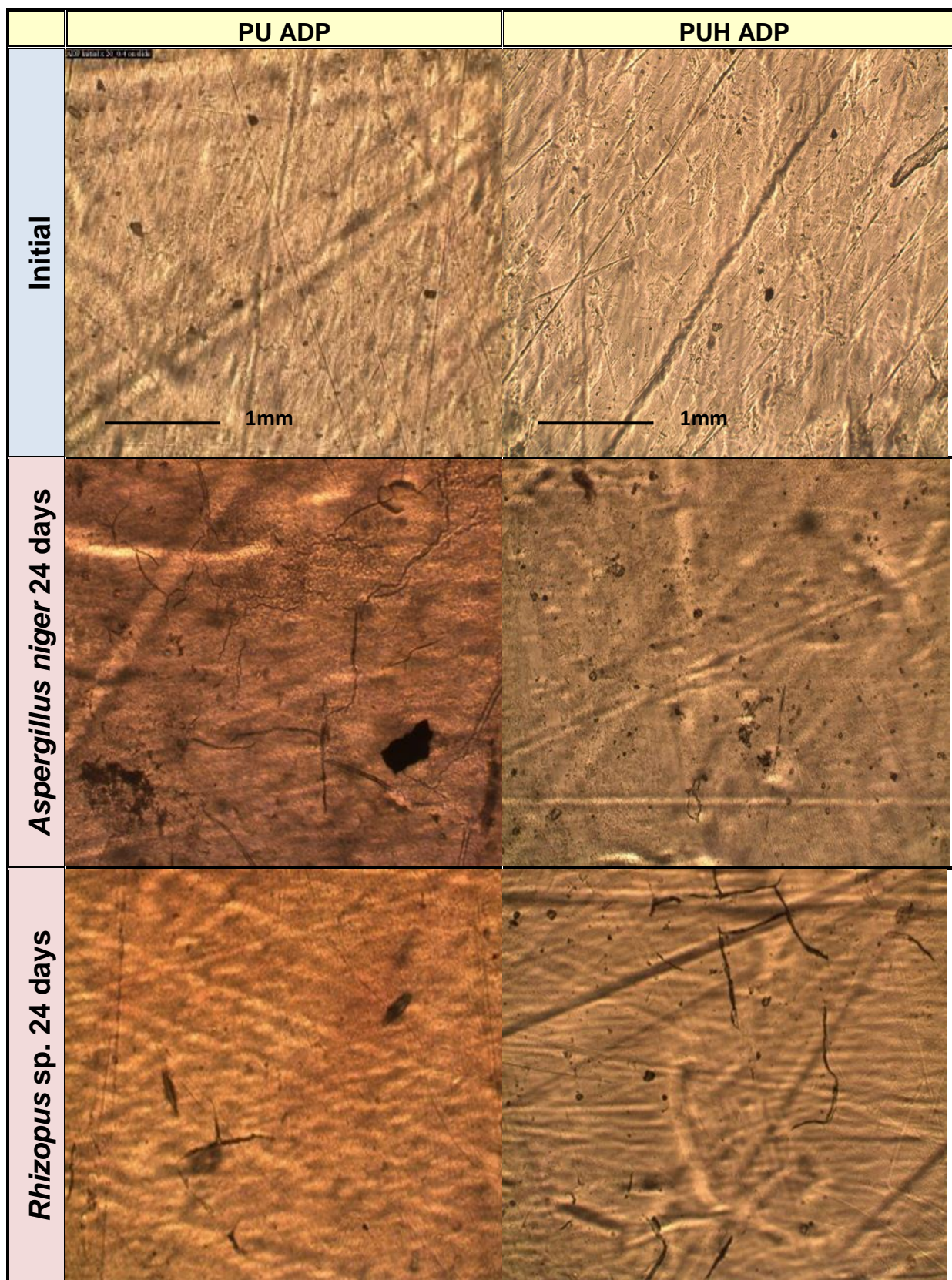


Figure 4.13 Effect of isocyanate on enzymatic degradation by Lipase *Aspergillus niger* and *Rhizopus* sp. PU ADP & PUH ADP by optical microscope images

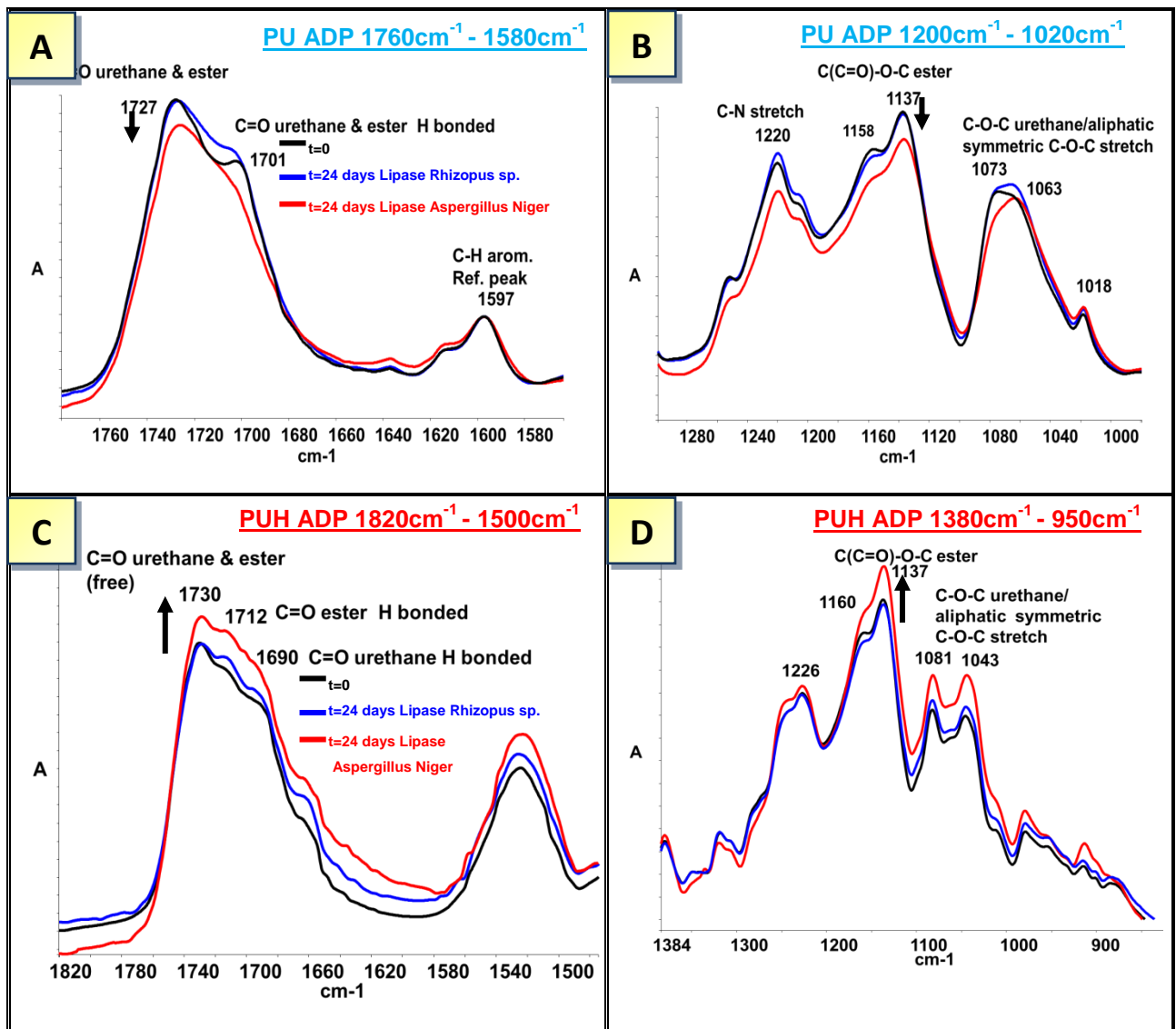


Figure 4.14 Effect of isocyanate on structural changes during enzymatic degradation by Lipase *Aspergillus niger* and *Rhizopus* sp. on PU ADP & PUH ADP determined by FTIR-ATR

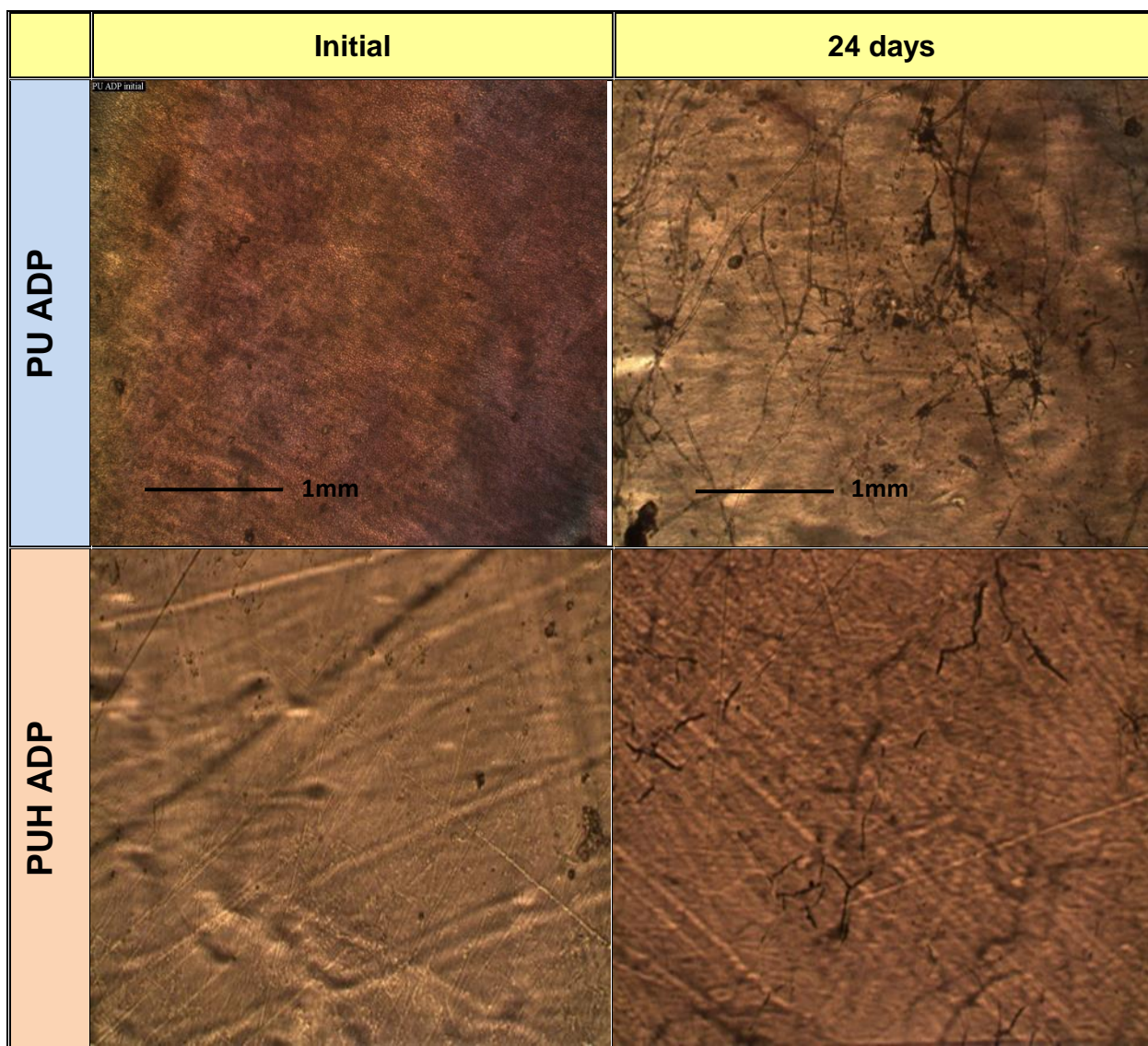


Figure 4.15 Effect of isocyanate on enzymatic degradation by Protease *Rhizopus* sp. of PU ADP & PUH ADP by optical microscope images

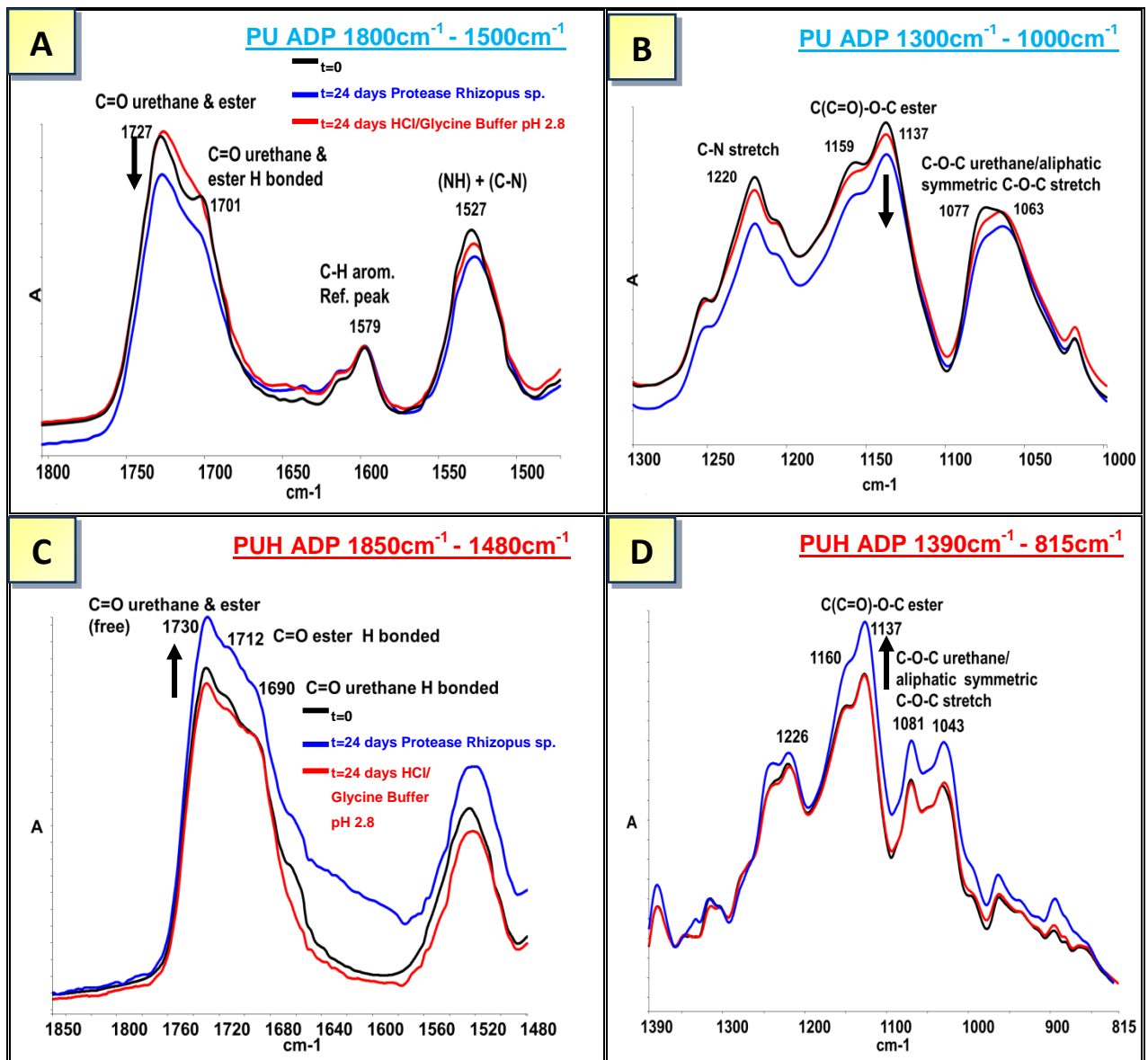


Figure 4.16 Effect of isocyanate on structural changes during enzymatic degradation by protease *Rhizopus* sp. on PU ADP & PUH ADP determined by FTIR-ATR

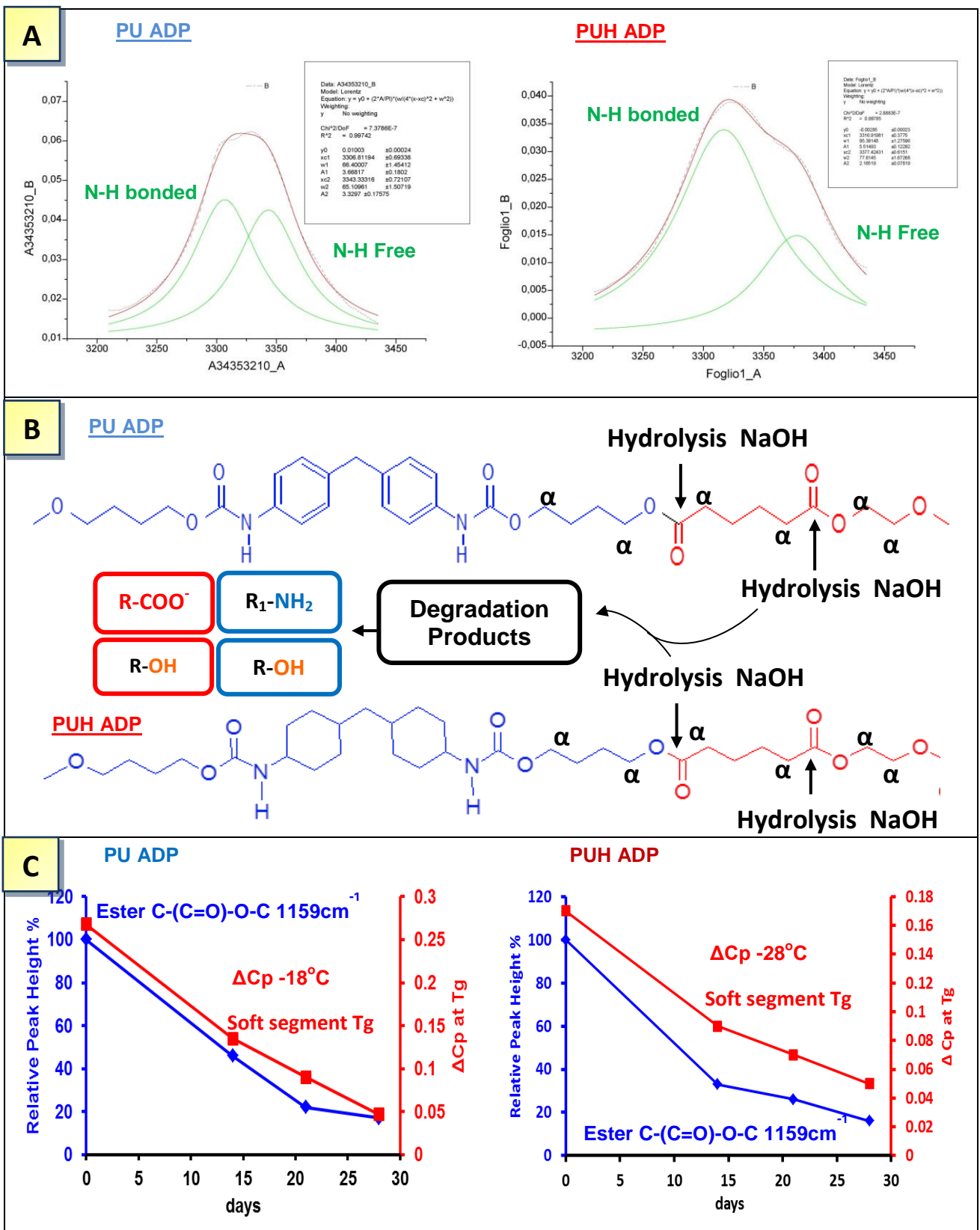


Figure 4.17 Showing the effect of the isocyanate on hydrogen bonding (A), hydrolysis (B), and soft segment degradation in PU ADP and PUH ADP (C)

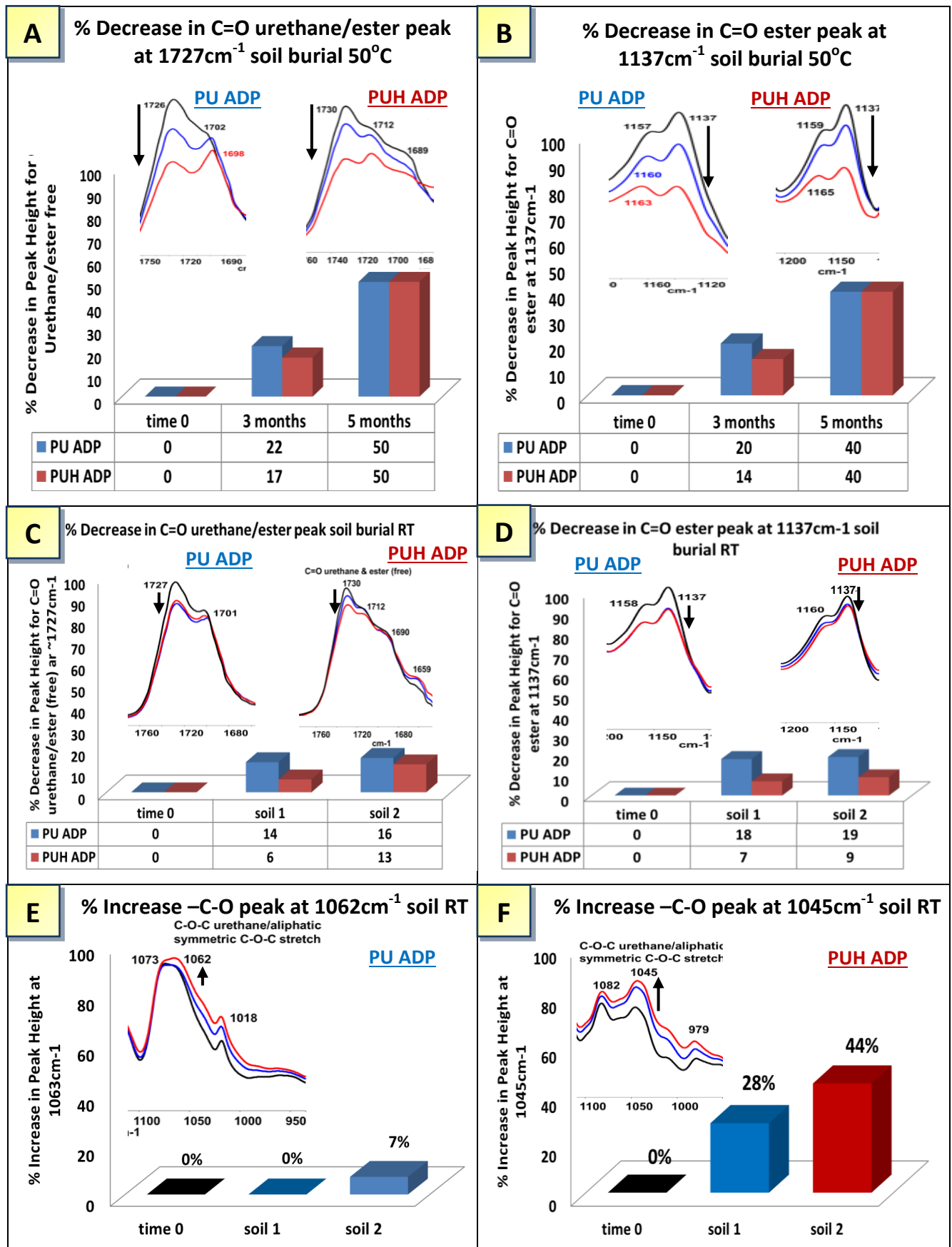


Figure 4.18 Showing the effect of the isocyanate on the rate of biodegradation during soil burial at 50°C and RT, monitored by FTIR-ATR

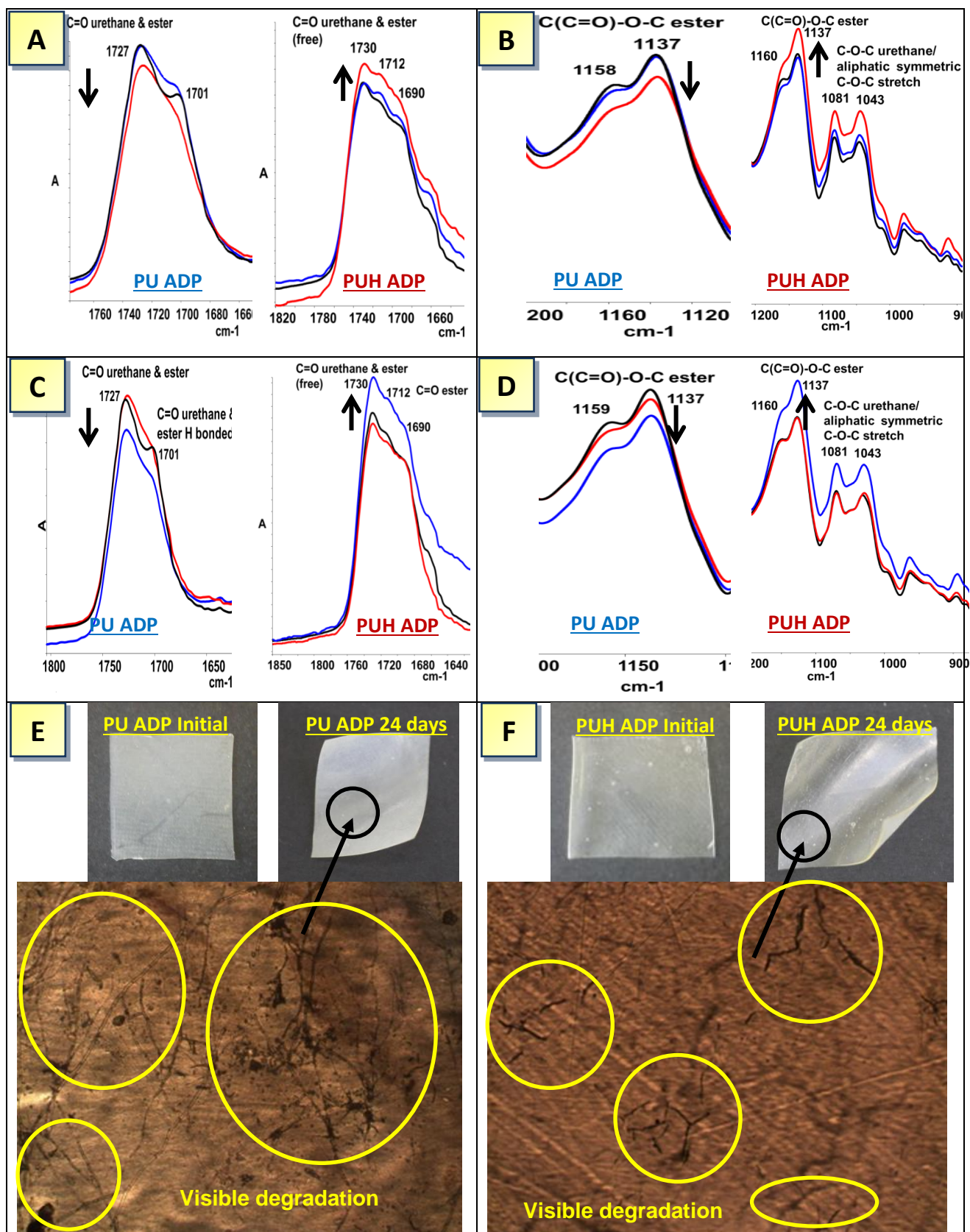


Figure 4.19 showing the effect of the isocyanate on the enzymatic degradation of PU. Enzymatic degradation with lipase from *Aspergillus niger* (A-B), enzymatic degradation with protease *Rhizopus* sp. (C-D). Visible degradation after 24 days immersed in buffer solution containing protease *Rhizopus* sp. (E-F)

Chapter 5

Effect of Polyurethane Structural Composition on Degradation and Biodegradation; effect of polyol

5.1 Objectives and methodology

Polyurethanes are complex polymers, and altering the initial reactants can have a dramatic effect on the final physical and chemical properties of the polymer. The effect of altering the isocyanate was examined in Chapter 4, and although differences in phase separation, hydrogen bonding and crystallinity were found, which in turn were dependant on the isocyanate used, soil burial experiments revealed that altering the isocyanate had minimal effect on biodegradability. Polyols or macr diols as they are sometimes known are long chain diols, usually polyesters or polyethers with a molecular weight between 500 and 5,000, however, molecular weights of 1,000 and 2,000 are typically used in PU synthesis [12, 20, 69]. These long chains form the ‘soft segment’ in PUs, and previous studies, have shown that the composition of the soft segment can have an influence on both the physical and chemical properties on the final material [47, 144, 145]. Hence, in this chapter the effect of altering the polyol in PU with respect to degradation and biodegradation will be examined, using a variety of PUs with different polyols synthesised by the sponsor company, Eurothane Ltd. Degradability and biodegradation were determined using alkaline hydrolysis with 10% NaOH solution at 45°C, enzymatic degradation by fungal lipases and proteases, and soil burial as was used for the PUs described in the previous chapters. Chemical compositional changes during degradation and biodegradation were monitored by FTIR-ATR, and in order to elucidate morphological properties such as phase separation and crystallinity, DSC analysis was performed. Four samples were analysed in this group; two PUs containing a polyester soft segment (polycaprolactone, [**PU PCL**] and poly(ethylene adipate) [**PU ADP** control sample]) **Table 5.1**, and one PU contained a polyether soft segment poly(ethylene glycol) (PEG), (**PU PEG**), **Table 5.1**. The last PU sample in this group contained a soft

segment which consisted of a 50:50 polyester and polyether blend, (**PU PGPC** polycaprolactone and polyethylene glycol).

5.2 Results

5.2.1 Characterisation of PU PCL, PU PEG and PU PGPC (Effect of Polyol)

Characterisation of each sample, **PU ADP**, **PU PCL**, **PU PEG** and **PU PGPC** was undertaken prior to hydrolysis experiments. Characterisation of **PU ADP** has previously been discussed in **Section 3.2.1.** and therefore will not be discussed here. Solubility was investigated, and all PU samples were found to be soluble in THF and DMF, therefore alteration of the polyol did not affect the solubility of the sample. Results obtained from water absorption experiments revealed that altering the polyol did affect the water uptake and was dependant on the polyol used. **Fig. 5.1**, shows the variation in water uptake, and it can be seen that the two PUs containing an polyester polyol (**PU ADP & PU PCL**) were relatively hydrophobic with minimal water uptake (**PU ADP 4.5%, PU PCL 2%**) compared to that of **PU PEG (56%)**, which contained a polyether polyol. **PU PGPC** contained a 50:50 mixture of polyethylene glycol and polycaprolactone, and the water uptake for this sample reflected this, with a 30% increase in weight after immersion in water for 10 days.

The chemical structure of **PU PCL** containing a PCL ester polyol, was determined using FTIR-ATR, and examination of the initial spectrum revealed many similarities with the spectrum of **PU ADP**, **Section 3.2.1.** The structure of the hard segment for **PU PCL** was characterised by the absorbances at 3302cm^{-1} and 1528cm^{-1} denoting the N-H stretch, and the combination of the C-N stretch and N-H bend respectively, **Fig. 5.2a** [124]. The hard/soft segment structure of **PU PCL** was similar to **PU ADP** (containing PEA polyol) and was characterised by the absorbances at 1728cm^{-1} and 1701cm^{-1} corresponding to the urethane and ester stretching vibrations of the free and hydrogen bonded C=O groups, respectively [6,7,8], and the peak at 1064cm^{-1} relating to the C-O-C group. However, a slight shift was noted in relation to the soft segment, as the C-O-C=O ester peak for **PU PCL** was observed at 1161cm^{-1} , **Fig. 5.2a** [146], whereas, for **PU ADP** the C-O-C=O ester peak was noted at 1137cm^{-1} .

PU PEG, which contained a PEG polyether soft segment, displayed similar peaks in relation to the hard segment structure as of that for **PU PCL** and **PU ADP**, with the peak at 3301cm^{-1} denoting the N-H stretch and the peak at 1531cm^{-1} corresponding to the combination of the N-H bend and C-N stretch, **Fig. 5.2b** [26, 147, 148]. However, due to the absence of ester groups contained within **PU PEG**, the hard segment can also be characterised by the peaks at 1722cm^{-1} and 1703cm^{-1} denoting the free and hydrogen bonded C=O urethane groups of

the hard segment respectively, **Fig. 5.2b** [26, 147, 148]. The C-O-C group pertaining to both the hard and soft segment is denoted by the peak at 1069cm^{-1} . Characterisation of the soft segment only could not be obtained using FTIR-ATR for **PU PEG** as the ether soft segment group C-O-C is also present in the hard segment at the hard/soft segment interface, **Table 5.1 & Fig. 5.2b**.

The final PU sample examined in this chapter; **PU PGPC** contained both PEG and PCL polyols (50:50 ratio), and the FTIR-ATR spectra regarding the chemical structure of **PU PGPC** confirmed this. The hard segment was characterised by the N-H stretch at 3315cm^{-1} and the C-N stretch/N-H bend at 1530cm^{-1} , **Fig. 5.2c** [105]. The hard/soft segment structure was similar to that of **PU ADP** and **PU PCL**, with peaks at 1725cm^{-1} and 1702cm^{-1} corresponding to the urethane and ester stretching vibrations of the free and hydrogen bonded C=O groups ,respectively. The peak at 1069cm^{-1} related to the C-O-C stretching vibration of the ether soft segment and the urethane hard segment. The PCL soft segment contained in **PU PGPC** was denoted by the peak at 1145cm^{-1} , **Fig 5.2 c** [105].

The thermal stability of each sample was examined using TGA under a nitrogen atmosphere as of that for samples in group 1. It was found that altering the polyol soft segment did not affect the thermal stability of the hard segment of the PU samples in this group. Greatest mass loss of the hard segment for **PU ADP** was found to occur at 336°C , and the thermographs for the other samples in this group are given in **Fig. 5.3**, and display similar temperatures, (**PU PCL 332°C, PU PEG 327°C, PU PGPC 330°C**). The thermal degradation of the soft segment was seen to alter depending on the choice of polyol. The greatest mass loss of the soft segment of **PU ADP** (PEA polyol) was found to be 436°C . All of the remaining PU samples in this group displayed lower soft segment thermal stability, (greatest mass loss temperatures; **PU PCL 396°C, PU PEG 384°C, PU PGPC 390°C**), **Fig. 5.3**.

DSC analysis was performed on the virgin samples prior to degradation experiments. Samples were subjected to a heating temperature of 100°C per min under a helium atmosphere to 180°C to remove previous thermal history, then, the temperature was reduced to -100°C and heated again to 220°C . From the results obtained it was found that each PU sample had its own unique morphological profile, and altering the polyol had a dramatic influence on the morphology of the PU, **Fig 5.4**. The thermogram for **PU ADP** (given in chapter 3 & Table 5.2) displayed a large endotherm observed at 195°C ($\Delta H 6.08$) indicating that a significant proportion of the hard segment contained within the PU was of a microcrystalline nature [107, 108]. The same was also observed for **PU PCL** (PCL polyol), with an endotherm at 197°C ($\Delta H 4.2$) indicating that **PU PCL** also consisted predominately of microcrystalline regions, **Table 5.2 & Fig. 5.4a**. In contrast to this, **PU PEG** (PEG polyol) did

not display any endotherms relating to the hard segment, and this suggests that this sample was completely amorphous [149], **Fig. 5.4b.** PU PGPC did exhibit one endotherm relating to the hard segment at 160°C (ΔH 4.9), **Table 5.2 & Fig. 5.4c**, and this indicates that a proportion of the hard segment was of an ordered nature [107, 108].

A dramatic difference was also observed with respect to the T_g value of the PUs in this group. The T_g value is an important parameter for PUs, as the T_g value has been shown to be a marker denoting the extent of phase separation [107]. Increased phase separation between the hard and soft segments decreases the T_g value [107, 109] and **PU ADP** and **PU PCL** exhibited T_g values which were very different, with **PU PCL** (T_g -28°C) demonstrating greater phase separation than **PU ADP**, (T_g -18°C) **Table 5.2**. Analysis of **PU PEG** revealed a T_g at -1°C, and this implies that the hard and soft segments were well dispersed within each other. Most noteworthy however, was the behaviour of **PU PGPC** with, **Fig. 5.4c & Table 5.2**. showing two T_g values at -48°C and -10°C and was thought to relate to the PCL and PEG soft segment chains respectively [66, 150]. It is interesting to note that the blend of PCL and PEG resulted in greater phase separation between the PCL and PEG soft segment chains and the hard segment, than in the case of the unblended soft segment, as in the individual PUs (**PU PCL** and **PU PEG**). Morphological analysis from PUs given in Chapters 3 and 4 highlighted that differences in morphology of PU is one of the major factors that affect the rate of their degradation.

5.2.2 Effect of Polyol (PU ADP, PU PCL, PU PEG and PU PGPC) on the Rate of Alkaline Hydrolytic Degradation.

5.2.2.1 Comparison of Polyurethanes with different ester soft segments, PU ADP containing polyethylene adipate polyol, and PU PCL containing a polycaprolactone polyol.

Changes during hydrolysis were initially noted visually using photographic and microscopic images, and by weight loss, **Figs. 5.5 - 5.7**. A dramatic difference was observed between the PU samples in this group. The two PU samples containing polyester soft segments (**PU ADP control with PEA and PU PCL with PCL**) exhibited quite different weight loss and visual profiles during hydrolysis. Microscopic and photographic images of the **PU ADP** (control sample) film during hydrolysis displayed discolouration and cracking of the sample. Conversely, **PU PCL** did not display any visual signs of degradation, **Figs. 5.5 – 5.7**. These findings can be supported by weight loss measurements taken during hydrolysis. After 42 days, **PU ADP** had a weight loss of 44%, (measured 56% weight remaining), however, **PU**

PCL did not lose weight during the 42 days (measured 100% weight remaining), **Fig. 5.5A**. This was unexpected as both PU samples contained polyester soft segments, and therefore should both be susceptible towards hydrolysis [103, 151-154]. This singularity was examined in detail and is discussed later in **section 5.3.1**

5.2.2.2 Comparison of Polyurethane PU ADP (ester polyol) and PU PEG (ether polyol)

The control sample **PU ADP** (polyester soft segment; PEA) was then compared to the PU sample **PU PEG** (polyether soft segment; PEG). Weight losses and visual degradation was observed for both of these samples; **PU PEG** weight remaining 68% **Fig. 5.5a**, **PU ADP** weight remaining 56%. Although the weight loss measurements implied that degradation had progressed further for **PU ADP**, photographs of each sample taken during hydrolysis did not confirm this. The **PU PEG** film had completely broken up after 42 days, whereas the **PU ADP** film, although discoloured, still remained intact **Fig. 5.7**. These conflicting results are probably due to the hydrophilic nature of **PU PEG**. Prior to hydrolysis, water uptake of each sample was measured, by immersing each film in a specific volume of water, and then measuring the % weight increase of the sample after 10 days, see **Section 2.2.2**. The water uptake for **PU ADP** was found to be 4.5%, whereas **PU PEG** was 56% **Fig 5.1**. Although each sample was dried under vacuum before each weighing, it is likely that some residual moisture still remained in the film bulk, therefore accounting for the weight loss and visual discrepancy of **PU PEG**.

5.2.2.3 Comparison of PU PGPC (containing a soft segment blend of PCL and PEG) to PU PCL and PU PEG

The final PU sample in this group **PU PGPC**, contained a 50:50 soft segment blend (PCL:PEG), and this sample was compared to all other samples in the group. **PU PGPC** exhibited a 25% weight loss after 42 days of alkaline hydrolysis (measured 75% weight remaining), **Fig. 5.5a**. Photographic images of the film sample did reveal signs of degradation after this time, **Figs. 5.6 & 5.7**, and it can be concluded that, **PU PGPC** (containing a blend of polyester/polyether soft segments) was not as susceptible to alkaline hydrolysis compared to **PU ADP** (PEA soft segment) or **PU PEG** (PEG soft segment), but was more susceptible than **PU PCL**, containing a PCL soft segment only. However, it is difficult to determine the extent of degradation merely from weight loss, and chemical

changes to all of the film samples during hydrolysis were ascertained by FTIR-ATR, and will be discussed in the next section.

5.2.2.4 Structural changes of PU ADP and PU PCL during alkaline hydrolysis

An initial spectrum of each sample was taken before hydrolysis, and group absorbances were assigned accordingly, **Fig. 5.2**. Analysis of the spectra during hydrolysis highlighted changes in both the hard and soft segments.

The hard segment structure of **PU ADP** and **PU PCL** were characterised, and similar peaks observed for both samples, **Chapter 3 Fig 3.2a (PU ADP) & Fig 5.2a (PU PCL)**. During hydrolysis similar changes were identified for both of these samples. The N-H peak at 3301cm^{-1} (N-H stretch) relating to the hard segment, increased with hydrolysis time, **Fig 5.8a (PU PCL) & Fig 3.9a (PU ADP)**, while the peak at 1219cm^{-1} (C-N + N-H) (1220cm^{-1} **PU ADP**) decreased with time, **Fig 5.9b (PU PCL) & Fig. 3.10b (PU ADP)** indicating partial degradation of the urethane linkages. The increased N-H peak at 3301cm^{-1} suggests the formation of amines; a degradation product of the urethane linkages in the hard segment [46, 105]. However, it should be noted, that these peak changes were relatively minimal for both **PU ADP** and **PU PCL**, therefore although some degradation had occurred, the majority of the hard segment still remained intact.

PU ADP and **PU PCL**, both containing ester soft segments, are more difficult to analyse in relation to the hard segment than PUs synthesised with polyether soft segments (see **PU PEG** above), as the groups at around 1728cm^{-1} and 1701cm^{-1} denoting the free and hydrogen bonded C=O urethane/ester groups indicate structural changes relating to both the hard and soft segments, and therefore must be interpreted collectively [114, 123]. There was a dramatic difference in these peaks during hydrolysis. For **PU ADP**, the peak at 1728cm^{-1} decreased by 78% after 42 days **Chapter 3, Fig 3.10a**. However, for **PU PCL**, this peak (1726cm^{-1}) increased during the first 21 days (+15%), and then decreased after 42 days (-10%), **Fig 5.9a**. Similar findings were also observed for the hydrogen bonded peak at 1701cm^{-1} **Fig. 5.9a**. There was also a notable difference between **PU ADP** and **PU PCL** in relation to the peak at around 1060cm^{-1} denoting C-O-C urethane/ester stretch **Figs 3.10b & 5.9b**. This peak decreased dramatically for **PU ADP**, and after 42 days had decreased by 40%. The opposite was observed for **PU PCL** with this peak increasing by 10%, which may be indicative of the formation of degradation products such as alcohols. Changes relating to the CH₂ moiety in the soft/hard segment structure were also observed for **PU ADP** by the peak at 1479cm^{-1} , which increased with hydrolysis time, **Fig. 3.9**, and the peak at 1458cm^{-1}

which decreased dramatically, **Fig. 3.9b**. The peak at 1382cm^{-1} relating to the $\alpha\text{-CH}_2$ group decreased and eventually disappeared after 42 days, **Fig. 3.9b**. However, these changes were not observed for **PU PCL**, with only a minor decrease of the CH_2 peaks occurring during hydrolysis. **Fig. 5.8b**.

The peaks at 1137cm^{-1} (**PU ADP**) and 1161cm^{-1} (**PU PCL**), relate to the soft segment polyester moiety with the peak at 1137cm^{-1} decreasing significantly for **PU ADP**. However, this was not the case for **PU PCL**, with the peak at 1161cm^{-1} exhibiting only a minimal decrease in comparison to that of **PU ADP**, **Figs 3.10b & 5.9b**. This indicates greater degradation of the PEA soft segment for **PU ADP** than the PCL soft segment in **PU PCL**.

5.2.2.5 Structural changes of PU ADP and PU PEG during alkaline hydrolysis

The hard segment structure of **PU ADP** (control, ester S.S.) and **PU PEG** (ether S.S.) were compared. As of that for **PU PCL** (see above) the peaks at 3301cm^{-1} and 1220cm^{-1} relating to the hard segment were similar for both **PU ADP** (see above) and **PU PEG**, **Figs. 5.8e & 5.9 f**. There were significant spectral differences observed between **PU ADP** and **PU PEG** during hydrolysis. The peaks relating to the hard segment for **PU ADP** indicated some degradation of the hard segment (see above). Conversely, only negligible changes in the peaks at 3301cm^{-1} (N-H stretch), 1221cm^{-1} (C-N stretch) and 1069cm^{-1} (C-O-C urethane stretch) were observed for **PU PEG**. This was unexpected, due to the weight loss exhibited during hydrolysis **Section 5.2.2.2.**, therefore the peaks relating to the C=O urethane linkages were examined. Although there were no significant decreases in the C=O peaks at 1722cm^{-1} and 1703cm^{-1} collectively, a minimal decrease was observed for the free C=O peak at 1722cm^{-1} (-15%), **Fig. 5.9e**. This indicates that some of the C=O groups pertaining to the free urethane groups had been hydrolysed, but the hydrogen bonded urethane groups remained intact. Overall, results from FTIR-ATR indicated that minimal degradation of the hard segment had occurred for **PU PEG**, with degradation progressing further for **PU ADP**.

Analysis of spectra regarding both the hard and soft segment domains for **PU PEG**, involved the CH_2 group absorbance peaks at 2869cm^{-1} , 2905cm^{-1} , 1458cm^{-1} and 1348cm^{-1} . A small decrease in the peak at 2869cm^{-1} was noted, however very little change was observed regarding the remaining CH_2 peaks, **Figs. 5.8e & f** which suggests that minimal degradation had occurred. This does not support findings from weight loss results or visual observations.

The peak relating to the soft segment for **PU PEG**, at 1100cm^{-1} denoting C-O-C ether linkages, was examined **Fig. 5.9f**. However, this group also pertains to the C-O-C groups at the hard/soft segment interfaces; therefore it was difficult to determine the extent of degradation of the soft segment by FTIR-ATR. A minimal decrease was perceived after 42 days, indicating that little degradation had occurred. These findings were not supported by previous weight loss or visual results.

5.2.2.6 Structural changes of PU ADP and PU PGPC during alkaline hydrolysis

Characterisation of the hard segment for **PU PGPC** was performed prior to hydrolysis, and analysis of the spectra highlighted similar peaks to that of **PU ADP** (see above) and **section 5.2.1**. The spectra for **PU PGPC** displayed numerous changes during degradation. The peak at 3315cm^{-1} (N-H stretch) increased slightly, **Fig. 5.8c**, and this coupled with the decrease at 1221cm^{-1} (C-N & N-H), **Fig. 5.9d**, suggest degradation of the urethane linkages within the hard segment to form amines; a degradation product of the hard segment, as of that for **PU ADP** (see above). The increase at 3298cm^{-1} was not as pronounced for **PU PGPC** as that for **PU ADP**.

The peaks at 1725cm^{-1} and 1702cm^{-1} denoting the free and hydrogen bonded C=O urethane/ester groups indicated structural changes relating to both the hard and soft segments during hydrolysis, with a significant decrease in the peak at 1725cm^{-1} , and a slight decrease at 1702cm^{-1} , **Fig. 5.9c**. A slight decrease was also observed at 1068cm^{-1} denoting urethane/ester linkages, **Fig. 5.9d**. The absorbance peaks at 2868cm^{-1} , 2917cm^{-1} , 1478cm^{-1} and 1350cm^{-1} denoting the CH_2 linkages all decreased during the 42 days. **Figs. 5.8c & d**.

PU PGPC contained two peaks relating to the soft segment which pertained to the PCL and PEG chains contained within the soft segment. The peak at 1161cm^{-1} relating to the C-(C=O)-O ester (PCL) soft segment displayed a significant reduction during hydrolysis, which indicated that hydrolysis of the ester groups (PCL) had occurred, **Fig. 5.9d**. A decrease was also observed for the peak at 1102cm^{-1} pertaining to the PEG, C-O-C stretch in the soft segment.

5.2.2.7 Effect of polyol on crystallinity and thermal stability during alkaline hydrolysis (PU ADP, PU PCL, PU PEG and PU PGPC).

Initial characterisation by DSC was performed on all samples in this group (group 3), and discussion of these thermograms are given in **Section 5.2.1**. During hydrolysis there was a noted difference between all of the PU samples.

Prior to hydrolysis both **PU PCL** and **PU ADP** exhibited similar hard segment endotherms, which indicated that both PU samples contained a large proportion of highly crystalline structured regions, **see Section 5.2.1**. During alkaline hydrolysis, **PU PCL** did not display any significant changes in crystallinity, with both the microcrystalline endotherm at 197°C, and the ordered endotherm at 128°C remaining unchanged even after 56 days, **Fig. 5.10a**. However, changes in crystallinity were observed for **PU ADP**, with the endotherm at 197°C denoting melting of microcrystalline hard segment domains, disappearing after 14 days, **Chapter 3, Fig. 3.11A**.

PU PEG did not exhibit any endotherms relating to either the hard or soft segment prior to alkaline hydrolysis, indicating that the material was amorphous in character **Section 5.2.1**. However, after 28 days of hydrolysis, an endotherm was observed for this PU sample at 152°C denoting structured regions within the hard segment. After 56 days of alkaline hydrolysis this endotherm disappeared, and an endotherm appeared at 167°C signifying highly crystalline regions, **Fig. 5.10b** [107].

Prior to hydrolysis, the DSC thermogram for **PU PGPC** (containing a blend of PEG and PCL soft segments), revealed an ordered hard segment arrangement, with an endotherm observed at 160°C, **Section 5.2.1**. During hydrolysis, a change in crystallinity was noted, with the appearance of two endotherms at 172°C and 128°C, resulting from highly ordered and ordered domains within the hard segment respectively, **Fig. 5.10c** [107, 109]. After 56 days, an increase in the ordered domains was observed with an endotherm noted at 137°C. This increase in the ordered domains was in conjunction with the disappearance of the crystalline regions denoted by the endotherm at 172°C.

The T_g value of each PU was also examined, as a change in T_g value can indicate phase separation, and a decrease in the $T_g \Delta Cp$ value relating to the soft segment, indicates degradation of the soft segment [59]. The T_g value of **PU PCL** (polycaprolactone S.S) remained unchanged, **Table 5.3**, and implied that limited degradation had occurred after 56 days. Conversely, **PU ADP** (polyethylene adipate S.S.) displayed a dramatic change in T_g with hydrolysis time, from -18°C to -31°C, **Table 5.3**. **PU PEG** also exhibited a change in T_g value during hydrolysis, decreasing from -1°C to -10°C after 56 days **Table 5.3**. A distinct

difference in T_g was also noted for **PU PGPC**. Initially, two T_g slopes were clearly visible at -48°C and -10°C, **Fig. 5.4**. After 56 days of alkaline hydrolysis, the T_g at -10°C remained the same. The T_g at -48°C was seen to increase with hydrolysis time to -38°C after 14 days, **Fig. 5.10**. However, the initial ΔCp value (T_g at -48°C) of 0.07 J/g also decreased with hydrolysis time, and after 56 days this T_g had disappeared **Table 5.3**. This suggests that the PCL soft segment contained within the polymer had degraded, but that the PEG segment still remained.

Results from alkaline hydrolysis highlighted significant changes associated with altering the polyol, and it was surmised that the same would apply when samples were subjected to soil burial. The results of this investigation are given in the next section.

5.2.3 Susceptibility to soil degradation of Polyurethane Samples in group 3 – Effect of Polyol, PU ADP, PU PCL, PU PEG & PU PGPC

In order to assess the effect of the polyol on the rate of biodegradation, the PU samples in this group were subjected to two different types of soil burial as of that in chapters 3 & 4

Soil burial at 50°C, produced unexpected findings in that **PU ADP** was found to degrade faster than all of the other PU samples in this group. The **PU ADP** film had broken up after 5 months, whereas **PU PCL**, **PU PEG** and **PU PGPC** were still intact and did not show any signs of biodegradation after 5 months, but all were found to degrade after 10 months **Fig. 5.11a & Fig 5.12**. The weight losses for each film also supported these findings; however, substantial weight still remained for **PU ADP** (79%) even after the film had broken up.

After 20 months of soil burial at RT there was little weight loss observed for **PU ADP**, **PU PCL** and **PU PEG** for both soil types, **Figs. 5.11 b & c**. However, **PU PGPC** did exhibit weight losses when buried in both soil 1 and soil 2, with a weight loss of 27% (soil 1) and 13% (soil 2) **Figs. 5.11 b & c**. After examination of the PU films, it was clearly seen both by eye and by microscopic images that substantial degradation had occurred for **PU PGPC** and **PU PCL**, with cracks and discolouration of the two films appearing, **Figs. 5.12 & 5.13**. **PU PEG** also exhibited some visible signs of degradation with small cracks observed on the film, **Fig. 5.12**. These results imply that altering the polyol has a great influence on the rate of biodegradation in soil. To examine the extent of biodegradation further, structural changes were monitored by FTIR-ATR.

5.2.3.1 Structural changes during soil burial at 50°C in PU ADP, PU PCL and PU PEG and PU PGPC monitored by FTIR-ATR.

The main spectral changes during soil burial involved the ester/urethane linkages in the samples therefore these will be examined in detail [102]. The peaks at 1726cm^{-1} and 1703cm^{-1} relating to the free and hydrogen bonded urethane/ester group respectively, decreased for **PU PCL** during soil burial **Fig. 5.14a**. The peak at 1161cm^{-1} denoting the C-O-C=O ester peak was also seen to decrease during soil burial. A significant peak at 1036cm^{-1} was observed after 11 months soil burial, and could be associated to the C-O linkage of alcohol degradation products, **Fig. 5.14b** [105]. After 5 months, a peak was also observed at 1661cm^{-1} which disappeared after 9 months indicating the formation of amine groups, a degradation product of the hard segment

PU PEG also displayed some notable changes during soil burial, with a significant decrease in the peaks at 1722cm^{-1} and 1702cm^{-1} denoting the C=O free and hydrogen bonded urethane linkages in the hard segment respectively, **Fig 5.14c**. Also noteworthy was a substantial decrease in the peak at 1221cm^{-1} corresponding to the C-N group. A decrease in the peak at 1069cm^{-1} (C-O-C) along with an increase in the peak at 1035cm^{-1} (C-O) signifies degradation of the hard/soft segments, and the subsequent formation of alcohol degradation products. As of that for **PU PCL** (see above), a new peak was observed at 1654cm^{-1} after 5 months which then shifted to 1642cm^{-1} after 11 months, and is more than likely indicative of amine groups, a degradation product of the hard segment, **Fig 5.14c**.

The FTIR-ATR spectra for **PU PGPC** given in **Fig. 5.14d & e**, did not seem to display changes in peak absorbances denoting extensive degradation as of that for **PU PCL** and **PU PEG**. Although a decrease at 1725cm^{-1} and 1702cm^{-1} was observed for **PU PGPC**, **Fig 5.14e** as of that for **PU PCL** and **PU PEG**, **Fig. 5.14a & c**, the decrease was not as substantial. A decrease in the peak at 1162cm^{-1} indicated that the PCL soft segment chain in **PU PGPC** had degraded, **Fig. 5.14f**, however, little change in the peak at 1068cm^{-1} was observed, and this implies that a large proportion of the PEG segment still remained, even after 11 months. A new peak was observed at 1658cm^{-1} as of that for **PU PCL** and **PU PEG** which suggests hard segment amine degradation products [105, 155].

5.2.3.2 Structural changes during soil burial at RT after 20 months in PU ADP, PU PCL, PU PEG and PU PGPC monitored by FTIR-ATR

Changes in **PU ADP** structure during soil burial at RT have previously been discussed, **see section 3.2.3.2**. There were some small changes to the FTIR-ATR spectra for **PU PCL** after soil burial, however these were minimal, and this was surprising as the **PU PCL** films displayed distinct cracking after removal from the soil, **Fig 5.12**. Small decreases were observed at 3301cm^{-1} and 1528cm^{-1} denoting the N-H and C-N urethane linkages, **Fig. 5.15a & b**. Small changes were also noted for the peaks at 1726cm^{-1} and 1702cm^{-1} denoting the free and hydrogen bonded ester and urethane C=O linkages respectively, **Fig. 5.16a**. A small decrease was also observed for the peak at 1161cm^{-1} denoting the ester linkages of the PCL soft segment, **Fig. 5.16b**.

Minor changes were also observed for **PU PEG** as of that for **PU PCL**, with small decreases noted for the peaks relating to the N-H and C-N urethane linkages at 3301cm^{-1} and 1531cm^{-1} , **Fig. 5.15c &d**. Other small changes relating to the hard segment were also noted by the peaks at 1722cm^{-1} and 1702cm^{-1} denoting the free and hydrogen bonded C=O urethane linkages respectively, **Fig 5.16c**. Small decreases were also observed at 1099cm^{-1} and 1069cm^{-1} which suggests some minor degradation to the C-O-C linkages in the PU.

The most noticeable changes in the FTIR-ATR spectra after soil burial was of that for **PU PGPC**, with a substantial decrease in the peak at 1725cm^{-1} for soil type 1 denoting the free C=O ester/urethane bonds, **Fig 5.16e**. The same was also observed for soil type 2 but to a lesser degree. Decreases were also noted at 3315cm^{-1} and 1530cm^{-1} denoting the N-H and C-H urethane linkages. Also observed was a small decrease in the peaks at 1350cm^{-1} and 1466cm^{-1} relating to the CH₂ groups in the PU, **Fig. 5.15f**. This was not seen for any of the other PU samples in this group. The peak at 1163cm^{-1} denoting the C-O stretching of the ester linkage was also seen to decrease after soil burial in both soil type 1 and 2, **Fig. 5.16f**.

5.2.3.3 Effect of polyol on morphology after 20 months soil burial (PU ADP, PU PCL, PU PEG and PU PGPC)

PU samples subjected to soil burial at RT were removed from the soil, and morphological changes during biodegradation were ascertained by DSC. **Fig. 5.17** displays the thermograms for **PU PCL**, **PU PEG** and **PU PGPC** both before soil burial and after 20 months of soil burial. **PU ADP** has previously been discussed, **see section 3.2.2.3**. For **PU PCL** some changes were observed relating to the hard segment, with the reduction of the

endotherm at 197°C (**ΔH 4.2 before soil burial, ΔH 2.5 soil 1, ΔH 2.4 soil 2**) relating to the highly ordered microcrystalline domains. The endotherms at 126°C relating the short range ordered hard segment were seen to increase after soil burial for both soil type 1 and 2, **Fig 5.17a & Table 5.4.** Phase separation between the hard and soft segments can be characterised by the T_g value, and for **PU PCL** the degree of phase separation was seen to decrease after soil burial, **Fig 5.17a & Table 5.4,** (initial T_g value at -28°C, soil type 1 T_g value -24°C , soil type 2 T_g value -23°C).

No changes were observed to the hard segment morphology of **PU PEG** with the absence of any endotherms either before or after soil burial. This implies that the hard segment was completely amorphous and remained so even after soil burial. Phase separation between the hard and soft segments were seen to decrease after soil burial, with the T_g value decreasing from -1 initially to -5 for soil type 1 and -6 for soil type 2 , **Fig 5.17b & Table 5.4.**

Prior to soil burial an endotherm at 160°C was observed for **PU PGPC**, which relates to long range ordered domains. This endotherm disappeared after 20 months of soil burial for both soil types, suggesting an amorphous hard segment, **Fig 5.17c.** There was also a noticeable difference in the T_g values for **PU PGPC**. Prior to soil burial two T_g s were observed at -48°C and -10°C and related to the soft segment chains PCL and PEG respectively. After soil burial the T_g at -10°C was seen to decrease slightly, **Fig 5.17c & Table 5.4,** (T_g value soil 1 -14°C, T_g value for soil 2 -11°C), thereby indicating an increase in phase separation. The T_g value at -48°C was seen to disappear after soil burial for both soil types, **Fig 5.17c**, and this indicates that the PCL chain in the soft segment had degraded.

5.2.4. Effect of polyol (PU ADP, PU PCL, PU PEG & PU PGPC) on enzymatic degradation by lipases *Rhizopus* sp. and *Aspergillus niger*.

Little weight loss (not shown) was observed after 24 days for all of the PU samples in this group for both lipases *Rhizopus* sp. and *Aspergillus niger*. However, optical images did highlight changes in the PU film during enzymatic degradation, **Figs. 5.18 & 5.19.** Both **PU PEG** and **PU PGPC** displayed visible cracking when examined microscopically after exposure to *Rhizopus* sp. lipase, **Fig. 5.18.** However, **PU ADP** and **PU PCL** did not exhibit any signs of degradation. Some indications of surface degradation for all samples were observed when immersed in the buffer solution containing *Aspergillus niger* after 24 days, **Fig. 5.19.** **PU PEG** seemed to be more susceptible towards lipase degradation by *Aspergillus niger* than the other PU films in this group, with pronounced cracking observed

microscopically. FTIR-ATR was performed to determine any structural changes in the samples.

Spectral changes after 24 days of enzymatic degradation of PU samples for both *Rhizopus* sp. and *Aspergillus niger* are given in **Fig. 5.20**, **PU ADP** has previously been discussed, **see section 3.2.4.1**. Surprisingly, it was noted that although there were some changes in the spectral peaks during enzymatic degradation, they were relatively minor, **Fig 5.20**. For **PU PCL**, the peaks at 1726cm^{-1} and 1702cm^{-1} decreased after exposure to *Aspergillus niger*, however, after contact with *Rhizopus* sp. these peaks were seen to increase. The peak at 1161cm^{-1} also decreased after 24 days after immersion of the **PU PCL** film in the *Aspergillus niger* buffer solution. These findings indicate that although some minor degradation had occurred when **PU PCL** was exposed to *Aspergillus niger*, the lipase, *Rhizopus* sp. had not degraded **PU PCL**.

After exposure to *Aspergillus niger*, microscopic images of **PU PEG** revealed that some degradation had occurred, however results from the FTIR-ATR spectrum did not correspond to these findings with only minor changes in the peaks at 1722cm^{-1} and 1702cm^{-1} occurring, **Fig. 5.20c**. In fact the peak at 1722cm^{-1} was seen to increase.

PU PGPC displayed some minor changes in the FTIR-ATR spectra, after exposure to the lipase from *Aspergillus niger*, however, very little change had occurred in relation to the lipase from *Rhizopus* sp. **Figs. 5.20e & f.** Images obtained using optical microscopy showed some cracks in the film after being exposed to *Rhizopus* sp, so to see such small changes in the spectra was surprising.

5.2.4.1 Structural changes during enzymatic degradation using proteases in PU PCL, PU PEG and PU PGPC monitored by FTIR-ATR.

Degradation by proteases was also disappointing in that little weight loss (not shown) was observed for *Rhizopus* sp. However, visible cracking from microscope images of the PU samples were observed, with **PU PCL** and **PU PGPC** showing the greatest signs of degradation **Fig. 5.21**.

The FTIR-ATR spectra of the PU samples given in **Fig. 5.22** did highlight some spectral peak changes after enzymatic degradation. The **PU PCL** spectra displayed an increase in the ester/urethane peaks at 1726cm^{-1} and 1703cm^{-1} , which was surprising, **Fig 5.22a**. These peaks were also seen to increase in the 2.8 pH buffer only, indicating that degradation of this sample had occurred due to the acidic buffer and not due to the activity of the enzyme.

Fig. 5.22b displays the peak at 1161cm^{-1} denoting the C-(C=O)-O-C ester linkages contained within the PCL soft segment and it can be noted that this peak had not decreased suggesting that little degradation of the soft segment had occurred. For **PU PEG**, the peaks at 1722cm^{-1} and 1702cm^{-1} were seen to decrease, and thereby indicated degradation of the C=O groups contained within the urethane linkages **Fig. 5.22c**. FTIR-ATR spectra for **PU PGPC** highlighted that the peaks at 1726cm^{-1} and 1703cm^{-1} had decreased. However, also noted was the decrease in the peak at 1161cm^{-1} , which was observed in the buffer solution without the enzyme, **Fig. 5.22e & f**. Therefore, the degradation observed in the **PU PGPC** film was most likely due to hydrolysis induced by the acidic buffer solution and not due to enzymatic degradation.

5.3 Discussion

Extensive studies into the influence of PU structure on functionality have shown that a wide variety of PUs can be tailor-made for specific purposes by altering the initial reactants, and increasing biodegradability of PU is no different in this respect. The importance of the polyol with regards to increasing biodegradability cannot be understated, and each polyol brings its own advantages and disadvantages in respect of biodegradability. For example, many studies have shown that polyesters tend to be more easily hydrolysable than polyethers, due to the C-O-C=O ester group contained with the chain [3, 4, 80, 96]. However, some polyesters can also be of a hydrophobic nature which may affect the rate of hydrolysis of these chains [71, 156, 157]. Polyethers on the other hand are generally more hydrophilic than polyesters, and polyethers like PEG can enhance water permeability, which has been shown to be a factor on the degradation rate of PU [33, 98]. However, one of the disadvantages of using polyethers like PEG in respect of hydrolytic degradation is that polyether chains do not contain a hydrolysable bond, and therefore are less prone to hydrolysis than their polyester counterparts [19].

Altering the polyol soft segment can also affect the PU morphology, and results from chapters 3 and 4 have highlighted PU morphology to be a major factor on the rate of degradation of PU. Therefore, three PUs with different polyols (PCL, PEG and a PCL/PEG blend) containing the same hard segment (MDI/BD) and synthesised by the one shot method were compared to **PU ADP** (hard segment MDI/BD, one shot synthesis), the current PU synthesised by Eurothane Ltd. **PU ADP** was denoted as the control sample, and the effect of each polyol on PU morphology, thermal stability, water permeability, rate of alkaline

hydrolysis and biodegradability were compared to the control sample (**PU ADP**) and produced interesting findings.

5.3.1 Effect of an ester soft segment on degradation and biodegradation of polyurethanes, PU ADP and PU PCL.

PU PCL which contained a PCL soft segment was compared to the control sample **PU ADP** which contained an ADP soft segment, in order to determine the effect of using different polyesters in PUs on the rate of hydrolytic degradation. It was found that although both of the soft segments of the PUs were esters, the rate of degradation and biodegradation differed. During accelerated alkaline hydrolysis degradation monitored by weight loss for the four PU samples in this group were found to be in the order of **PU ADP > PU PEG > PU PGPC > PU PCL**, with **PU PCL** not exhibiting any weight loss at all during the 56 days, **Fig. 5.5a** which implied that this PU had not been hydrolysed. Conversely, **PU ADP** was seen to degrade by this method after 56 days with a weight loss of 44% after 42 days. **Fig. 5.5a**.

These findings were also supported by microscopic images which clearly displayed extensive cracks in the **PU ADP** film after 42 days with none visible for **PU PCL**, **Fig. 5.23a & b**. This discovery was unexpected in that the PCL ester soft segment contained in **PU PCL** has previously been reported to be degradable in soil and compost [152, 156], and hence it would be expected that this soft segment chain would hydrolyse under accelerated alkaline conditions. In light of this, changes in chemical structure and morphology were examined using FTIR-ATR and DSC.

Similar peaks relating to the hard segment structure of **PU ADP** and **PU PCL** were observed, **Fig. 5.2a & Fig. 3.2a (Chapter 3)** which would be expected, as both contained the same hard segment composition (MDI/BD). The same was also observed with respect to the soft segment structure, which was characterised by only one peak at 1137cm^{-1} (**PU ADP**) and 1161cm^{-1} (**PU PCL**), relating specifically to the ester soft segment, **Table 2.5 (Chapter 2)**. All other peaks in the spectra of the PUs related to both the hard and soft segment structure and therefore could not be assigned as specifically relating to either domain. The main structural changes during degradation were noted for the peaks at around 1728cm^{-1} and 1701cm^{-1} denoting the free and hydrogen bonded C=O urethane/ester groups for **PU ADP**, with a decrease in the peak at 1728cm^{-1} by 78% after 42 days, **Fig. 5.23c**. However, for **PU PCL**, this peak (1726cm^{-1}) increased during the first 21 days (+15%), and then decreased after 42 days (-10%), **Fig. 5.23c**. Most noteworthy was the decrease of the peak at 1137cm^{-1} for **PU ADP**, denoting degradation of the ester linkages in the soft segment, **Fig. 3.10a (Chapter 3)**. This was not observed for **PU PCL**, with the peak at 1161cm^{-1} exhibiting only a minimal decrease in comparison to that of **PU ADP**, **Fig. 5.23d**, supporting the weight loss findings

that **PU PCL** had not degraded substantially. Although results from FTIR-ATR supported both weight loss, **Fig. 5.5a** and visual findings, **Fig. 5.7**, it did not elucidate an explanation into why the rate of degradation of **PU ADP** and **PU PCL** differed to such an extent, therefore morphology of the PU samples were examined by DSC during accelerated hydrolysis.

As the rate of degradation of PU has been previously shown to be influenced by the extent of crystallinity it was thought that this may have been the reason for the difference in the rate of degradation between **PU ADP** and **PU PCL**, however, this was not found to be the case. Prior to hydrolysis, DSC analysis revealed that both **PU PCL** and **PU ADP** exhibited similar hard segment endotherms, which indicated that both PU samples contained a large proportion of highly crystalline structured regions, **Fig. 5.23 e & f**. During alkaline hydrolysis, **PU PCL** did not display any significant changes in crystallinity, with both the microcrystalline endotherm at 197°C, and the ordered endotherm at 128°C remaining relatively unchanged even after 56 days, **Fig. 5.10a**. However, changes in crystallinity were observed for **PU ADP**, with the endotherm at 197°C disappearing after 21 days, indicating an increase in less ordered domains as the PU degraded, **Fig. 3.11a (Chapter 3)**.

Although these results supported the weight loss and the FTIR-ATR findings, it did not explain why the ADP ester had hydrolysed, as opposed to the PCL ester which had not. Therefore, the T_g value of the samples was examined to determine the extent of phase separation. Previous studies, [54, 66] have shown that the soft segment molecular weight can affect the T_g value, with lower molecular weight polymers increasing the T_g value due to the restricted mobility of the shorter soft segment molecular chains [54, 66]. However, this would not influence results obtained in this instance as both the soft segments contained in **PU PCL** (PCL) and **PU ADP** (ADP) had a molecular weight of 2000. T_g values of -28°C for **PU ADP** and -18°C for **PU PCL** were found, and it was surmised that this difference in T_g values was due to microphase separation between the hard and soft segments, however, previous studies have shown that the T_g for PEA (molecular weight 2000) was found to be -53°C and -59°C for PCL (2000 molecular weight) [64], therefore the difference seen between PU ADP and PU PCL is probably due to the different polyols used, so although difference between the samples was found, it did not provide an explanation for the increased rate of hydrolysis of **PU ADP** in comparison to **PU PCL**.

The hydrophobicity of the polymer chains also needs to be taken into consideration regarding the rate of alkaline hydrolysis, and numerous studies on PCL have reported on the hydrophobic nature, and hence dramatic reduction on the rate of degradation and hydrolysis of PCL [154, 158], in comparison to other more hydrophilic polymers. Results from water absorption experiments supported these findings, and revealed that altering the polyol

affected the diffusion of water into the PU. Although **PU ADP** was seen to be relatively hydrophobic (4.5% weight increase) in comparison to the polyether containing PUs (**PU PEG** and **PU PGPC**), **PU PCL** was found to be more hydrophobic than **PU ADP** with a weight % increase of only 2%, and can therefore be concluded that this hydrophobicity of the PCL segment is most likely to be the reason for the slower rate of hydrolysis of **PU PCL**.

Accelerated alkaline hydrolysis was performed on these samples to give an indication of rate of degradation which was performed over a short length of time. Soil burial experiments were also performed to provide a ‘real time’ study to examine the effect of the polyol on the rate of degradation and biodegradation on PU. Results from these experiments were interesting in that **PU PCL** was observed to degrade faster than **PU ADP** when subjected to soil burial at RT, which was in contrast to that of the accelerated hydrolysis. **PU ADP** or **PU PCL** did not display significant weight losses during soil burial, however upon removal of the PU films from the soil, **PU PCL** displayed distinct and visible cracking by eye and microscopic images highlighted the differences between these samples further, **Fig. 5.23 g & h**, indicating that **PU PCL** had degraded to a greater extent than **PU ADP**. Surprisingly, results obtained from FTIR-ATR did not display significant changes, with small decreases observed at 1161cm^{-1} (**PU PCL**), 1137cm^{-1} (**PU ADP**), **Fig. 5.16b & 3.18b (Chapter 3)** indicating degradation of the ester groups, and 3301 cm^{-1} and 1528cm^{-1} (**PU PCL** and **PU ADP**) denoting N-H degradation of the hard segment. In order to observe changes in morphology during soil burial, thermograms from DSC analysis were examined and revealed distinct differences between **PU ADP** and **PU PCL**.

The most notable difference observed between the thermograms for **PU ADP** and **PU PCL** was the change in microcrystalline regions given at 197°C , **Fig. 5.23 i & j**. This endotherm remained relatively unchanged for **PU ADP** after 20 months soil burial (**Initial ΔH 4.9 J/g, soil 1 burial ΔH 4.9 J/g**). In contrast to this, the endotherm at 197°C was seen to decrease significantly for **PU PCL** (**Initial ΔH 4.2 J/g, soil 1 burial ΔH 2.5 J/g**) **suggesting a decrease in crystallinity of the sample**. Also noteworthy was the decrease in the $T_g \Delta Cp$ value relating to the soft segment (**Initial ΔCp 0.25, soil 1 burial ΔCp 0.19 J/g**) **suggesting that a smaller proportion of the soft segment remained**. These results indicate that partial degradation of the PCL soft segment had taken place, which in turn then altered the morphology of the hard segment resulting in a reduction of highly ordered microcrystalline regions. The same was not observed for **PU ADP** with the $T_g \Delta Cp$ value remaining unchanged after soil burial (**Initial ΔCp 0.19, soil 1 burial ΔCp 0.19 J/g**), indicating that **PU ADP** had not degraded during soil burial, **Fig. 5.23 i & j**. These results were in contrast to accelerated hydrolysis, however the mechanism of biodegradation in soil is complex, and involves a multitude of physical, chemical and biological reaction

mechanisms all of which contribute to the breakdown of the polymer into oligomers and monomers [2, 57], and numerous studies have shown PCL to be degradable in soil and compost [5, 152]. One of the principal mechanisms of polymer biodegradation is that from hydrolysis by microorganisms, and in the case of PUs fungi have been shown to be the predominant organism responsible [21, 22]. Results reported in the literature have shown that the rate of biodegradation by microorganisms is influenced by the ability of microorganisms to adhere to the surface of the polymeric material [57]. The mechanism by which microorganisms adhere to the surface of polymeric materials is by hydrophobic interactions, and studies have shown that many microorganisms exhibit a preference for hydrophobic surfaces [29, 57], therefore it is reasonable to assume that one of the reasons for the increased rate of biodegradation of **PU PCL** in comparison to **PU ADP** is due in part to the hydrophobic nature of the PCL soft segment chain, **Fig. 5.1**. This hydrophobicity also explains the resistance towards accelerated alkaline hydrolysis, and therefore provides an explanation for the difference in degradability of **PU PCL** found between the two degradation test methods.

Enzymatic degradation was also monitored and used as an indication of degradation, however the results from these experiments were disappointing in that **PU PCL** and **PU ADP** did not exhibit any weight losses during the experiment and microscopic images did not reveal any major degradation of the films, **Figs. 5.18-5.19 & Figs. 3.20-3.22 (Chapter 3)**. This may be due to the relatively short length of time to which the PU films were exposed to enzymatic degradation, or that the PU samples **PU ADP** and **PU PCL** were not suitable substrates for the enzymes used in the experiment namely, lipases from *Aspergillus niger* and *Rhizopus* sp. **PU PCL** and **PU ADP** were also subjected to enzymatic hydrolysis by a fungal protease by *Rhizopus* sp. in which microscopic images from **PU PCL** highlighted extensive cracking after 24 days, **Fig. 5.21**, however, this may have been due in part to the acidic buffer which was required for optimisation of enzyme activity of the protease therefore it is difficult to attribute degradation to enzymatic degradation.

5.3.2 Comparison between ester and ether soft segment on chemical structure, crystallinity and thermal stability during alkaline hydrolysis (PU ADP & PU PEG).

Degradation of polyethers has been studied extensively, and it has been found that the molecular weight of polyethers affects degradability, with polyethers having a molecular weight of up to 1000 being degradable [26]. Therefore, a PU was synthesised containing a 1000 molecular weight PEG soft segment and compared to the control sample **PU ADP** which contained a PEA soft segment with a molecular weight of 2000. Prior to degradation, hydrophobicity was monitored and revealed a dramatic difference, **Fig 5.1**. Altering the polyol to a PEG (polyether) soft segment was found to enhance water permeability dramatically, with **PU PEG** increasing in weight after immersion in water by 56%, (**PU ADP** 4.5%), **Fig 5.1**. Accelerated hydrolytic degradation also revealed distinct differences between these two samples. Although **PU ADP** displayed the greatest weight loss during exposure to the 10% NaOH solution, examination of the films visually showed quite clearly that **PU PEG** had in fact broken up, whereas, although the **PU ADP** film was brittle, it still remained intact **Fig. 5.24a**. From these results, it can be stated that weight loss measurements were not an accurate indication of the rate of degradation, especially when examining hydrophilic polymers such as PEG, which can take up a large amount of water. Microscopic images during hydrolysis also produced some interesting differences, in that visible structured cracks were observed for **PU ADP**, which, increased proportionally to hydrolysis time, **Fig. 5.6**. However, the same was not observed for **PU PEG**, and possibly indicates some hydrolysis of the ester bonds occurring in **PU ADP** which are not present in **PU PEG**. In order to investigate this further, structural changes were examined by FTIR-ATR.

PU PEG displayed similar hard segment spectral peaks as of that for **PU ADP**. However, changes in peak height for **PU PEG** were negligible, with minimal change observed for the peak at 1100cm^{-1} denoting the C-O-C ether linkages, **Fig. 5.24C**. This indicates that minimal degradation of the soft segment had occurred. The same was observed for the peak at 1703cm^{-1} which related to the hydrogen bonded urethane linkages in the PU, however a decrease in the peak at 1722cm^{-1} , **Fig. 5.24C**, denoting free urethane linkages was observed, and therefore it can be surmised that a proportion of the free urethane linkages had degraded. These observations were unexpected in that weight loss and visual observations indicated that substantial degradation of the PU had occurred. As FTIR-ATR is an infrared spectroscopic technique which only penetrates the sample at a depth of around $2\mu\text{m}$, only changes on the surface of the sample can be observed, therefore degradation of **PU PEG** is more than likely to have occurred in the bulk. To investigate this further, morphological properties of the PUs were examined by DSC.

Initial thermograms of **PU ADP** and **PU PEG** revealed that the morphology of these two PUs were distinctly different. **PU ADP** displayed three endotherms relating to highly crystalline hard segment domains, **Fig. 5.24 e & f**, whereas **PU PEG** did not exhibit any endotherms, indicating that **PU PEG** was of an amorphous nature. A difference in the T_g value of the two PUs were also noted, with **PU ADP** having a T_g value of -18°C and **PU PEG** having a T_g value of -1°C . This may be due to two reasons. Firstly, the difference in T_g values can be partially attributed to the different molecular weights of the soft segments in **PU ADP (PEA 2000)** and **PU PEG (PEG 1000)**, and previous studies have shown that molecular weight influences the T_g value, with higher molecular weight polymers producing lower T_g s due to the greater mobility of the longer chains [66]. The second reason is concerning the microphase separation between the hard and soft segments in the PU samples, with greater phase separation inferred with lower T_g values [107, 109]. Therefore, the increased T_g value of **PU PEG** can also be attributed to a reduction in phase separation between the hard and soft segments. It would be reasoned that the reduced phase separation and amorphous nature of **PU PEG** would be favourable towards degradation in comparison to **PU ADP**, which was highly crystalline in nature and this supposition supports visual results from accelerated alkaline degradation. However, as the PEG soft segment in **PU PEG** does not contain any hydrolysable bonds, the $T_g \Delta Cp$ value denoting the soft segment was examined, as results from previous chapters and literature have found this value to be a good indication of degradation [59]. The results are given in **Fig. 5.24d** and clearly show that the majority of the PEG soft segment remained after 56 days, therefore degradation of this PU was not due to the break-up of the soft segment chains. It is more likely that degradation of **PU PEG** was due to hydrolysis of the urethane linkages contained in the hard segment. Although results from previous chapters have shown that hydrolysis of the PU hard segment is minimal, the nature of the PEG soft segment which does not contain hydrolysable bonds and the hydrophilicity of this polymer attests that this is the most plausible explanation. It is thought that the high water absorption capacity results in a swelling of the PU matrix which then facilitates degradation by creating more free volume within the matrix allowing more diffusion of water and consequently access to the urethane linkages which in turn increases hydrolysis of the PU.

PU PEG was subjected to ‘real time’ soil burial experiments as of that for **PU ADP** and **PU PCL**. Visual examination of the **PU PEG** films after removal from the soil did not reveal significant degradation. Some minor cracks were observed, however microscopic images also confirmed that limited degradation had occurred as of that for **PU ADP**, **Fig. 5.13**. FTIR-ATR analysis did highlight some changes to the hard and soft segments, with a decrease in the peaks at 1722cm^{-1} , 1702cm^{-1} and 1531cm^{-1} denoting the urethane linkages in **PU PEG**,

and a small decrease was also noted for the C-O-C ether peak at 1099cm^{-1} , **Fig. 5.16d**, indicating that partial degradation of the soft segment had occurred during soil burial. This was confirmed by results from DSC which revealed a decrease in the soft segment Tg Δ Cp value from 0.35 J/g (initial) to 0.18J /g (soil 1) and 0.20 J/g (soil 2), **Table 5.4**. These results were in contrast to results obtained from accelerated hydrolysis in which the soft segment had not degraded, which is likely due to be due the mode of the experiment and mechanistic degradation of the PEG soft segment. Under soil burial conditions many factors play a role in the degradation of polyethers, and it is generally thought to be a combination of oxidative degradation followed by microbial degradation facilitated by esterases and /or lipases [159]. A degradation mechanism of polyether urethanes has been proposed by Anderson et al

[160] and is given in **Fig. 5.24 g**. Degradation proceeds by the attack of a hydro-peroxy radical, after initiation by an activating factor. This causes a dehydration reaction resulting in an ester linkage within the ether backbone. This ester linkage is then hydrolysed by microorganisms within the soil substrate, to produce oligomers and monomers. Therefore it is proposed that the partial degradation of the PEG soft segment occurred through a combination of oxidative and microbial action during soil burial. However, although some limited degradation occurred during soil burial, neither **PU ADP** nor **PU PEG** displayed extensive biodegradation after soil burial for 20 months.

Degradation by lipases *Aspergillus niger* and *Rhizopus* sp. did highlight differences between **PU PEG** and **PU ADP**, with **PU PEG** being more susceptible towards both of these fungal enzymes than **PU ADP**. **Fig. 5.24h** displays microscopic images from **PU PEG** after exposure to *Aspergillus niger* and *Rhizopus* sp. lipases for 24 days, in which **PU PEG** clearly shows visible signs of degradation. Analysis of the FTIR-ATR spectra revealed that after being subjected to *Rhizopus* sp. the peaks at 1722cm^{-1} and 1702cm^{-1} relating to the urethane linkages in the PU film had decreased to a large extent, **Fig.5.24h**. However, after exposure to *Aspergillus niger*, the peak at 1722cm^{-1} was seen to increase, which is thought to be due to the formation of degradation products of **PU PEG**. The spectra also highlighted some degradation of the PEG soft segment, with the peak at 1097cm^{-1} decreasing. The degradation of both the hard and soft segments during exposure to *Rhizopus* sp. is thought to be due to a combination of hydrolysis from the buffer solution, which probably resulted in degradation of the hard segment and partial soft segment hydrolysis by an oxidative/enzymatic degradation mechanism as of that for soil burial.

5.3.3 Effect of blended soft segment containing PEG (polyether) and PCL (polyester) on chemical structure, crystallinity and thermal stability during alkaline hydrolysis

Results from degradation experiments of **PU PCL** and **PU PEG** samples highlighted major differences between PUs synthesised with a polyether and a polyester, in terms of crystallinity, phase separation and hydrophilicity, which ultimately affected the rate of degradation and biodegradation of the PU films, therefore a PU was synthesised (**PU PGPC**) which incorporated a blend of PCL and PEG (50:50). In order to examine the effect of a soft segment blend containing these two polymers on degradation, accelerated hydrolysis, soil burial and enzymatic hydrolysis was performed and examined in detail. Microscopic images of **PU PGPC** after 42 days of hydrolysis did not reveal any signs of degradation, however, visual photographs showed that the film was deformed and flaky, indicating that some degradation had occurred, **Fig. 5.25a**. This was also confirmed by FTIR-ATR spectra.

The peaks pertaining to both the hard and soft segments for **PU PGPC** exhibited significant changes during hydrolysis. The peaks at 1725cm^{-1} and 1702cm^{-1} , denoting the free and hydrogen bonded C=O urethane/ester groups indicated structural changes relating to both the hard and soft segments during hydrolysis, with a significant decrease in the peak at 1725cm^{-1} , and a slight decrease at 1702cm^{-1} , **Fig. 5.9c**. The CH_2 group absorbance peaks at 2868cm^{-1} , 2917cm^{-1} , 1478cm^{-1} and 1350cm^{-1} all decreased during the 42 days, although the decrease was minimal and not as extensive as that of **PU ADP**, **Fig 5.8d & Fig. 3.9b (Chapter 3)**. It is difficult to predict with certainty whether degradation had occurred within the hard segment, soft segment, or both, however from the interpretation of the peaks associated with the hard segment only (in which minimal changes had occurred), it is more than likely that the majority of these peak changes related to degradation of the soft segment. As **PU PGPC** contained a blend of PEG and PCL soft segments, two peaks were observed in the initial spectra which characterise the soft segment. The peak at 1161cm^{-1} relating to the C-(C=O)-O ester (PCL) soft segment displayed a significant reduction during hydrolysis, which indicated that hydrolysis of the ester groups (PCL) had occurred, **Fig. 5.25c**. This can further be supported by a reduction in the free C=O peak at 1724cm^{-1} . A decrease was also observed for the peak at 1102cm^{-1} pertaining to the PEG, C-O-C stretch in the soft segment but this was minimal. These findings indicate that complete degradation of the PCL ester segments within the soft segment had occurred, and that minimal degradation of the PEG segments had taken place. This would concur with results from **PU PEG** which indicated that the PEG ether soft segment was not conducive to alkaline hydrolysis. However, what is interesting to note, is that degradation of the PCL soft segment occurred in **PU PGPC**, which was not observed in **PU PCL**, with the PCL segment remaining

relatively unchanged after accelerated hydrolysis, **Fig.5.25 c & d**, see **Section 5.3.1**, therefore DSC, thermograms were examined to confirm this finding.

The initial thermogram prior to hydrolysis revealed two T_g values at -48°C and -10°C for **PU PGPC**, which would be expected due the blend of PCL and PEG contained in the soft segment, and from DSC thermograms from **PU PCL** and **PU PEG** it was reasoned that the T_g at -48°C denoted the PCL chains and the T_g at -10°C denoting the PEG chains **Fig. 5.25 e**. It was interesting to note that blending these polymers resulted in lower T_g values than the individual PCL and PEG segments contained in **PU PCL** and **PU PEG**. Therefore, it can be surmised that the soft segment was more phase separated when containing a blend of PCL and PEG than when these polymers were used alone. Results from previous chapters have revealed that an increase in phase separation may increase the rate of hydrolytic degradation. The hard and soft segments in **PU PGPC** were more phase separated than in **PU PCL**, and **PU PGPC** hydrolysed faster than **PU PCL**, **Figs. 5.10 & 5.5**, therefore this theory holds for these two PUs. However, **PU PEG** hydrolysed faster than **PU PGPC** but was found to be less phase separated, therefore it can be speculated that phase separation is not a major factor on the rate of degradation for **PU PGPC**. During accelerated alkaline hydrolysis, the $T_g \Delta Cp$ values was examined, and further confirmed results from FTIR-ATR regarding degradation of the PCL chains in the soft segment. The $T_g \Delta Cp$ was seen to decrease from -48°C to zero after 56 days. The $T_g \Delta Cp$ at -10°C denoting the PEG soft segment chains remained relatively unchanged during the experiment, **Fig 5.25 f**, again confirming results from FTIR-ATR that the PEG chains in **PU PGPC** had not degraded. Crystallinity of the PU was examined and **PU PGPC** was found to be relatively amorphous in character, which was completely different from **PU PCL** which contained a 100% PCL soft segment, therefore it can be surmised that the 50% addition of PEG into the soft segment disrupted the morphology of the hard segment chains and altered the morphology of the PU dramatically.

It is thought that both the increase in phase separation and decrease in crystallinity of **PU PGPC** did affect the rate of hydrolysis after exposure to alkaline degradation, however these were not considered to be major factors, as if this were the case, then logically **PU PGPC** should have degraded faster than both **PU PCL** and **PU PEG**, however, this was not observed, with **PU PEG** degrading faster than **PU PGPC**, **Fig. 5.7**. Therefore, it is suggested that the major factor on the rate of degradation of this PU is the hydrophilicity of **PU PGPC**. Results from water absorption experiments confirmed this, as **PU PGPC** was seen to increase in weight by 30% after immersion in water for 10 days, **Fig. 5.1**. This was compared to **PU PCL** which was deemed as hydrophobic with a 2% weight increase, **Fig. 5.25 g**. This would also explain the rate of hydrolytic degradation for the PUs in this group, which was

found to be in the order of **PU PCL**< **PU PGPC** < **PU PEG**, corresponding to the order of hydrophilicity of the samples at; **2% (PU PCL) < 30% (PU PGPC) < 56% (PU PEG)**.

Soil burial experiments revealed interesting findings in that degradation of **PU PGPC** was observed even after 3 months, with microbial attachment to the surface of the film visible by eye, **Fig. 5.25 b**. After 20 months the sample had not broken up, but cracking was observed on the surface and the film itself was fragile. Examination of the FTIR-ATR spectra confirmed visual results, as a substantial decrease in the free C=O ester/urethane peak at 1722cm^{-1} was perceived, and the peak at 1137cm^{-1} denoting the C=O ester bond contained in the PCL soft segment chains had also disappeared, indicating degradation of this polymer. Also changes in the CH₂ groups were also noted, with a decrease in the peaks at 2952cm^{-1} for soil type 1, **Fig. 5.15 f**. For soil type 2 relatively little change was observed for the peak at 1061cm^{-1} relating to the PEG C-O-C bond which was surprising, however this peak was seen to decrease for soil type 1, which indicated that some degradation of the PEG chains in the soft segment had degraded. DSC analysis supported these findings in that again, as of that for accelerated alkaline hydrolysis the T_g at -48°C was seen to disappear after removal from the soil after 20 months, **Fig.5.17c**, indicating that the PCL chains in the soft segment had degraded.

From these results it can be concluded that **PU PGPC** was more susceptible towards biodegradation than **PU PCL** or **PU PEG**. Soil burial results for **PU PCL** which contained a PCL soft segment highlighted that this PU was more prone to biodegradation than **PU ADP** or **PU PEG**, however, results for **PU PGPC** indicated that the addition of PEG into a PCL soft segment increased biodegradation, probably due to combination of a decrease in crystallinity of the polymer (in comparison to **PU PCL**), an increase in hydrophilicity from the PEG chains to enable hydrolysis (in comparison to **PU PCL**), and at the same time also retaining some hydrophobic domains from the PCL chains in order to facilitate hydrophobic interactions between the PU film and microflora contained in the soil, thereby inducing enzymatic degradation.

The final method used to analyse the degradability of **PU PGPC** was that of enzymatic degradation. The results given in **Fig. 5.25 h**, show that this PU was relatively resistant towards enzymatic degradation from the *Rhizopus* sp. lipase, however, some degradation of the PU film was observed microscopically after exposure to *Aspergillus niger* lipase. Results from FTIR-ATR also substantiated this in that little change in the spectra was observed after exposure to *Rhizopus* sp., however, a decrease in the peaks at 1702cm^{-1} and 1722cm^{-1} was observed after immersion for 24 days in the buffer solution containing *Aspergillus niger* lipase, **Fig. 5.20e**, indicating degradation of the C=O ester/urethane

linkages. The peak at 1137cm^{-1} was also seen to decrease with exposure to *Aspergillus niger* lipase, and this indicated that the PCL chains in the soft segment of **PU PGPC** had been hydrolysed. Analysis of **PU PGPC** after exposure to protease *Rhizopus* sp. was found to be problematic, in that the optimum pH for the protease activity was 2.8, at this acidic pH level **PU PGPC** was seen to degrade in the buffer solution alone, without the addition of the protease, **Fig.5.25 i**. In light of this, susceptibility of **PU PGPC** to this protease could not be determined, however, it can be stated that **PU PGPC** is susceptible towards acidic hydrolysis as well as alkaline hydrolysis.

5.3.4 Overall Summary of the effect of the Polyol (soft segment) on Polyurethane Degradation and Biodegradation.

The work described in this chapter focused on the effect of the polyol (soft segment) on the rate of degradation and biodegradation of PU. It was found that soft segments containing different esters affected the rate of degradation and biodegradation of PU. Accelerated alkaline hydrolysis of the PU samples resulted in degradation of **PU ADP** which contained an ADP soft segment, **Fig 5.5**. Alteration of the soft segment to a different ester (PCL) resulted in a dramatic reduction in the rate of hydrolytic degradation; with **PU PCL** remaining intact even after 56 days with limited signs of degradation of the PU film, **Fig. 5.5 & 5.7**. Soil burial conditions produced results that contrast those obtained from accelerated alkaline hydrolysis, as the **PU ADP** film was not seen to degrade after soil burial for 20 months, however, **PU PCL** was found to be more biodegradable with visible cracks in the film noted, **Fig. 5.12 & 5.13**. Previous studies, and results from chapters 3 and 4 indicated that the extent of crystallinity affect the rate of degradation in PU, however this was not deemed to be the case in this instance, as the extent of crystallinity for **PU ADP** and **PU PCL** was found to be similar, **Fig. 5.23 e & f**. Results from water absorption indicated that **PU PCL** was more hydrophobic than **PU ADP**, which supported previous literature in that the PCL ester soft segment in **PU PCL** is hydrophobic in nature, and this was believed to be the reason for both the resistance towards accelerated alkaline hydrolysis, as water was not able to penetrate into the PCL soft segment. The increased rate of biodegradation under soil burial conditions for **PU PCL** was thought to be due to increased adhesion of microorganisms onto the surface of the PU which occurred through hydrophobic interactions between the microorganisms and the hydrophobic soft segment.

Altering the polyol from a polyester (ADP) to a polyether (PEG) did influence the rate of degradation and biodegradation of the PU samples. Results from photographic and microscopic images after accelerated hydrolysis, enzymatic hydrolysis and soil burial

revealed that the PU containing a polyether polyol (**PU PEG**) was found to degrade faster than **PU ADP**, which contained a polyester soft segment. The main reason for these findings is thought to be due to a combination of the amorphous nature of **PU PEG**, and also the increased hydrophilicity of **PU PEG**, which then resulted in an increase in the diffusion of water into the PU matrix and thereby accelerated its hydrolysis. The mechanism of degradation for **PU PEG** is expected to depend on the experimental conditions, with accelerated hydrolysis resulting in degradation of the hard segment by the hydrolysis of the urethane bonds, while the soft segment remained relatively unchanged, **Fig.5.24 c & d**. Exposure of **PU PEG** films to soil burial and enzymatic hydrolysis resulted in partial limited degradation of both the hard and soft segments resulting from a combination of oxidative and microbial degradation mechanisms, **Fig. 5.24**.

The soft segment containing a combination of PCL and PEG (**PU PGPC**) resulted in a PU that degraded under both accelerated alkaline hydrolysis conditions and soil burial. The morphological profile of **PU PGPC** was found to be relatively amorphous in nature, and showed a greater degree of phase separation than its **PU PCL** and **PU PEG** counterparts, **Fig. 5.25e**. These two factors were considered to play a role in the rate of degradation and biodegradation of **PU PGPC**, however, the major factor regarding the rate of degradation of all of the samples in this group was deemed to be hydrophilicity of the PU sample, with a positive correlation observed between the rate of accelerated hydrolysis and hydrophilicity, **Fig. 5.25g**. The combination of a PEG and PCL soft segment resulted in a PU which contained hydrophilic domains from the PEG chains thereby enabling the diffusion of water into the PU, and also hydrophobic domains from the PCL chains conferring hydrophobic binding sites for degradation by microorganisms in the soil.

In summary, accelerated alkaline hydrolysis measured by weight loss revealed that the rate of hydrolysis was in the order of **PU ADP > PU PEG > PU PGPC > PU PCL**, **Fig 5.5**. However, examination of the films visually revealed that the extent of degradation was in the order of **PU PEG > PU PGPC > PU ADP > PU PCL**, **Fig 5.7**, which was also the order of the hydrophilic nature of the PUs. This difference between weight losses and visual images was mainly thought to be due to the hydrophilicity of **PU PEG** and **PU PGPC** which were thought to retain water in the bulk, even after drying, therefore distorting the weight loss measurements. Alteration of the soft segment from a PCL and ADP ester to a PEG ether resulted in a PU with increased hydrophilicity and reduced crystallinity, **Figs. 5.1 & 5.24e & f**, and these were thought to be the major factors involved in the rate of degradation. Results from soil burial indicated that **PU PCL** and **PU PGPC** was deemed to be the most biodegradable under these conditions, **Figs. 5.11 - 5.13**, and this was thought to be due to the hydrophobic PCL soft segment contained in both of the PUs, which would then result in

greater enzymatic hydrolysis from microorganisms by hydrophobic interactions. Overall, **PU PGPC** containing a 50:50 soft segment composition of PEG and PCL was thought to be the most biodegradable, and this PU also exhibited substantial degradation during accelerated alkaline hydrolysis.

Examination of the effect of the polyol on the rate of degradation and biodegradation revealed that the hydrophilicity/hydrophobicity of the soft segment was one of the main factors involved in the rate of degradation and biodegradation of PU. This chapter and the previous chapters examined the method of synthesis and the effect of the chemical constituents on the PU degradation, and as a result of this work, the next chapter will look at how different additives affect PU properties such as crystallinity, hydrophilicity and phase separation, and how these additives effect the rate of degradation and biodegradation.

Table 5.1 Effect of Polyol on PU Degradation

PU Code	Composition				M.w.t Ratio polyol: isocyanate: chain extender	Method of synthesis (Table 3.1a)		
	Soft segment polyol		Hard segment					
		Isocyanate	Chain Extender					
PU-ADP	Polyethylene adipate (PEA)		Methylene diisocyanate (MDI)	Butane diol (BD)	1:3:2	OS-102		
PU-PCL	Polycaprolactone (PCL)		Methylene diisocyanate (MDI)	Butane diol (BD)	1:3:2	OS-102		
PU -PEG	Polyethylene Glycol (PEG)		Methylene diisocyanate (MDI)	Butane diol (BD)	1:3:2	OS-102		
PU-PGPC	PCL:PEG (50:50)		Methylene diisocyanate (MDI)	Butane diol (BD)	1:3:2	OS-102		
PU Code	Chemical Structure							
PU-ADP	<p>The chemical structure shows a hard segment consisting of two isocyanate groups (NCO) linked by a methylene group (-CH2-), each attached to a 4,4'-diphenylmethane diisocyanate (MDI) molecule. This is followed by a soft segment consisting of a PEA (polyethylene adipate) chain, which is a poly(ether ester) formed by the reaction of adipic acid and ethylene glycol.</p>							
PU-PCL	<p>The chemical structure shows a hard segment consisting of two isocyanate groups (NCO) linked by a methylene group (-CH2-), each attached to a 4,4'-diphenylmethane diisocyanate (MDI) molecule. This is followed by a soft segment consisting of a PCL (polycaprolactone) chain, which is a poly(ether ester) formed by the reaction of caprolactone and ethylene glycol.</p>							
PU-PEG	<p>The chemical structure shows a hard segment consisting of two isocyanate groups (NCO) linked by a methylene group (-CH2-), each attached to a 4,4'-diphenylmethane diisocyanate (MDI) molecule. This is followed by a soft segment consisting of a PEG (polyethylene glycol) chain, which is a poly(ether ether) formed by the reaction of ethylene glycol and propylene glycol.</p>							
PU-PGPC	<p>The chemical structure shows a hard segment consisting of two isocyanate groups (NCO) linked by a methylene group (-CH2-), each attached to a 4,4'-diphenylmethane diisocyanate (MDI) molecule. This is followed by a soft segment consisting of a PEG:PCL block copolymer chain, where the PEG and PCL segments are alternately linked.</p>							

Table 5.2 Effect of polyol on morphology of PU characterised by DSC

Sample Code	Polyol	Soft Segment				Hard Segment					
		Tg (oC)	ΔCp (J/g)	Tm (oC)	ΔH (J/g)	Tm (°C) (I)	ΔH(J/g) (I)	Tm(oC) (II)	ΔH(J/g) (II)	Tm(oC) (III)	ΔH (J/g) (III)
PU ADP	Ester (PEA)	-18	0.27	71	0.1	109	0.5	147	0.8	195	6.1
PU PCL	Ester (PCL)	-28	0.25	66	0.4	126	0.7	-	-	197	4.2
PU PEG	Ether (PEG)	-1	0.35	-	-	-	-	-	-	-	-
PU PGPC	(PEG/PCL)	-48 -10	0.07 0.17	-	-	-	-	160	4.9	-	-

Table 5.3 Effect of chemical hydrolysis on morphology of PU characterised by DSC

Sample Code	Hydrolysis time	Soft Segment				Hard Segment					
		Tg (°C)	ΔCp (J/g)	Tm (°C)	ΔH (J/g)	Tm (°C) (I)	ΔH (J/g) (I)	Tm (°C) (II)	ΔH(J/g) (II)	Tm(oC) (III)	ΔH (J/g) (III)
PU ADP	time 0	-18	0.27	71	0.1	109	0.5	147	0.8	195	6.1
PU PCL	time 0	-28	0.25	66	0.1	126	0.7	-	-	197	4.2
PU PEG	time 0	-1	0.35	-	-	-	-	-	-	-	-
PU PGPC	time 0	-48 -10	0.07 0.17	-	-	-	-	160	4.9	-	-
PU ADP	14 days	-18	0.19	-	-	109	0.47	148	0.74	198	5.11
PU PEG	14 days	-4	0.35	-	-	-	-	152	0.2	-	-
PU PGPC	14 days	-38 -9	0.06 0.15	-	-	128	0.5	170	1.7	-	-
PU ADP	28 days	-31	0.11	-	-	-	-	-	-	-	-
PU PCL	28 days	-28	0.24	66	0.1	128	0.6	-	-	198	3.7
PU PEG	28 days	-6	0.32	-	-	-	-	150	1.2	-	-
PU PGPC	28 days	-40 -11	0.05 0.16	-	-	128	0.3	176	1.7	-	-
PU ADP	56 days	-31	0.05	-	-	-	-	-	-	-	-
PU PCL	56 days	-28	0.21	66	0.1	128	0.7	-	-	197	4.7
PU PEG	56 days	-10	0.30	-	-	-	-	167	4.4	-	-
PU PGPC	56 days	-	0 0.17	-	-	-	-	137	0.6	-	-

Table 5.4 Effect of soil burial on morphology of PU characterised by DSC

Sample Code	Soil burial 20 months RT	Soft Segment				Hard Segment					
		Tg (°C)	ΔCp (J/g)	Tm (°C)	ΔH (J/g)	Tm (°C) (I)	ΔH (J/g) (I)	Tm (°C) (II)	ΔH(J/g) (II)	Tm(oC) (III)	ΔH (J/g) (III)
PU ADP	time 0	-18	0.27	71	0.1	10 9	0.5	147	0.8	195	6.1
PU ADP	Soil 1	-15	0.20	-	-		0	147	0.1	200	4.9
PU ADP	Soil 2	-17	0.19	-	-	-	-	147	0.34	199	5.26
PU PCL	time 0	-28	0.25	66	0.1	12 6	0.7	-	-	197	4.2
PU PCL	Soil 1	-24	0.19	67	0.5	12 6	1.3	-	-	198	2.5
PU PCL	Soil 2	-23	0.21	67	0.7	12 6	1.2	-	-	198	2.4
PU PEG	time 0	-1	0.35	-	-	-	-	-	-	-	-
PU PEG	Soil 1	-5	0.18	-	-	-	-	-	-	-	-
PU PEG	Soil 2	-4	0.20	-	-	-	-	-	-	-	-
PU PGPC	time 0	-48 -10	0.07 0.17	-	-	-	-	160	4.9	-	-
PU PGPC	Soil 1	0 -14	0 0.15	-	-	-	-	-	-	-	-
PU PGPC	Soil 2	0 -11	0 0.17	-	-	-	-	-	-	-	-

Water Uptake - Effect of Polyol

Time	PU ADP (Control)	PU PCL	PU PEG	PU PGPC
time 0	0	0	0	0
2 days	0	1.2	52	30
5 days	3.6	2	52	30
7 days	4.5	2	56	30
10 days	4.5	2	56	30

Figure 5.1 Hydrophilicity of PU samples determined by weight percentage increase of water uptake

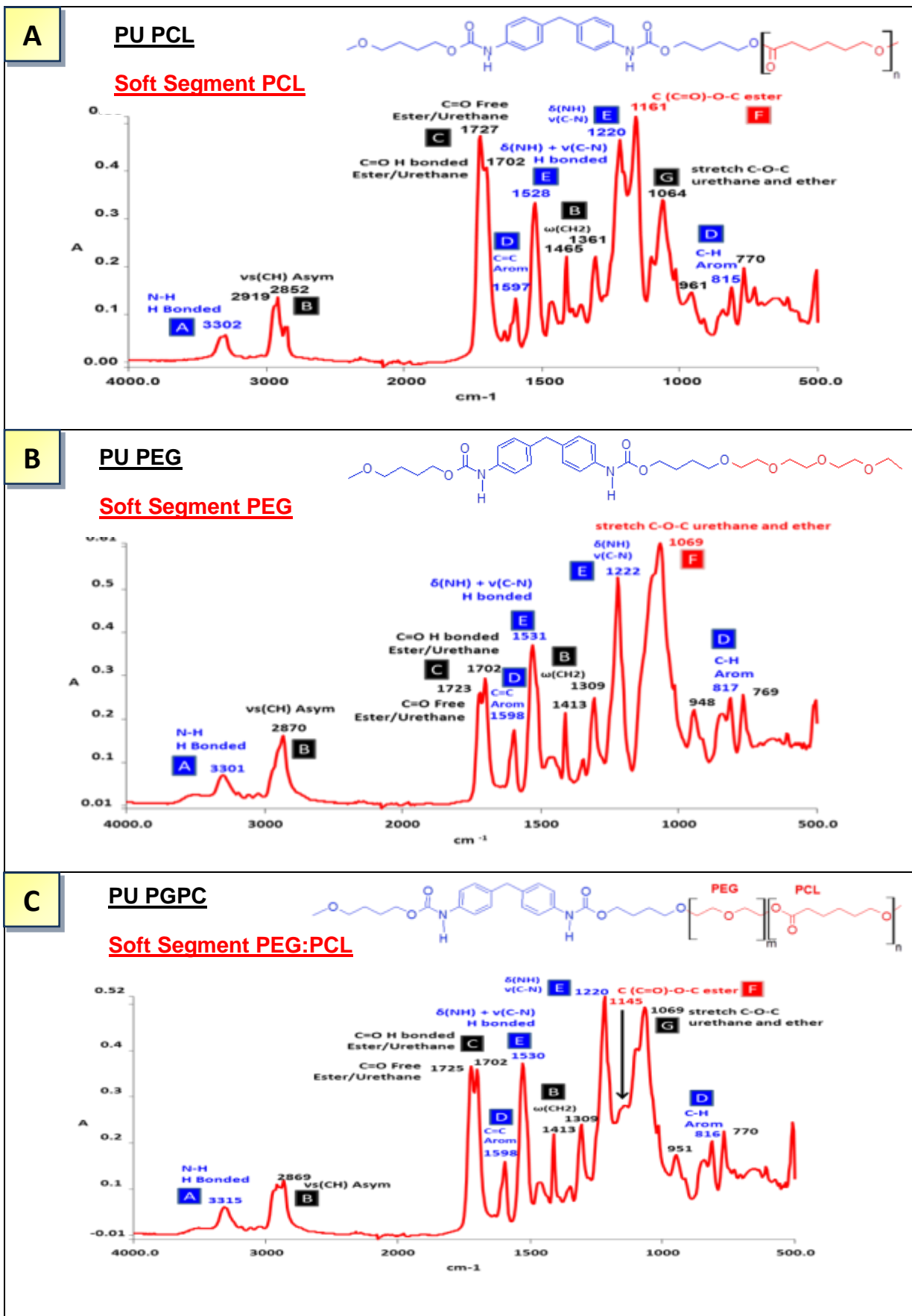


Figure 5.2 Chemical structure characterisation by FTIR-ATR of PU PCL (A), PU PEG (B), PU PGPC (C)

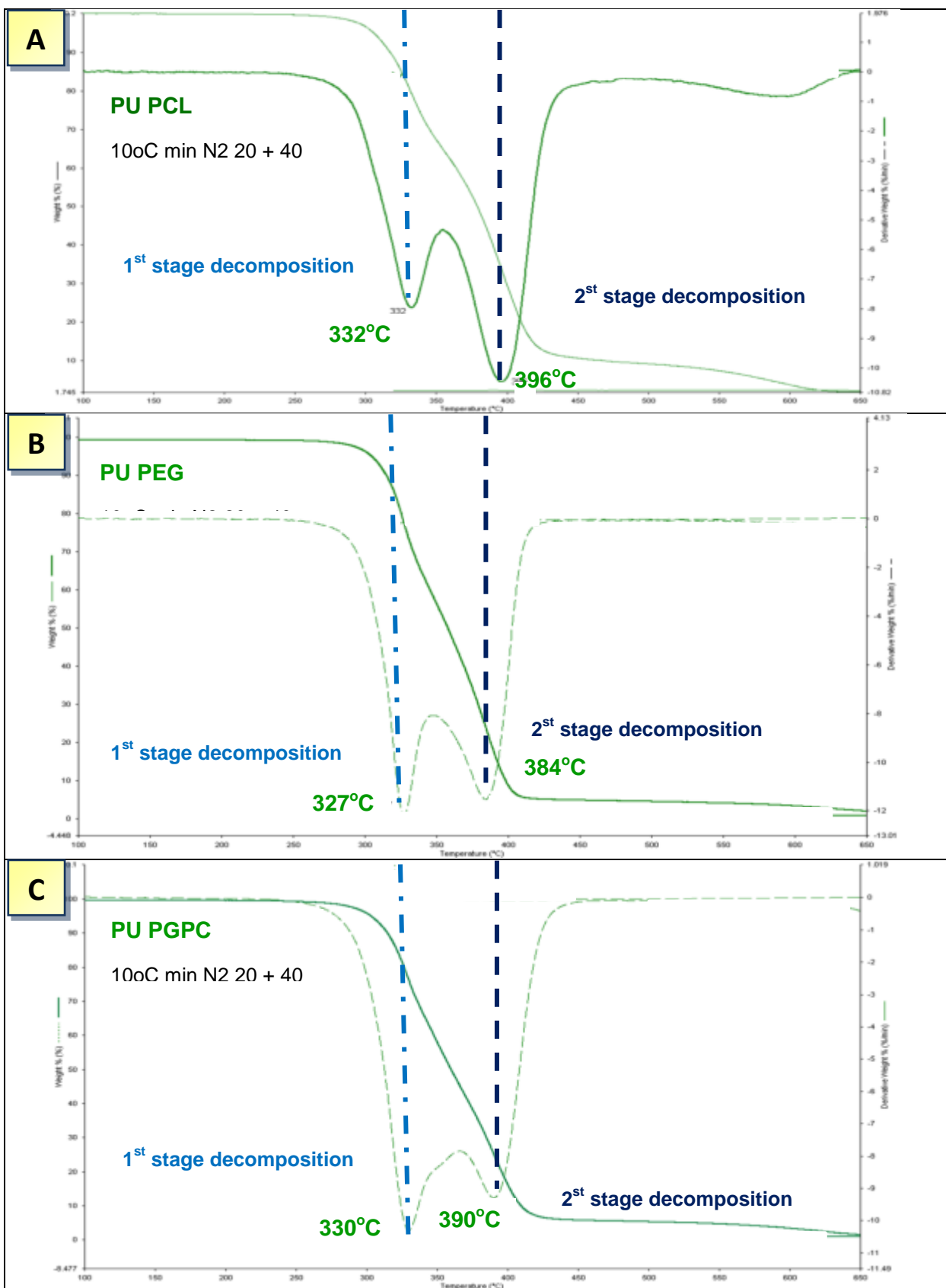


Figure 5.3 TGA of PU; PU PCL (A), PU PEG (B), PU PGPC (C)

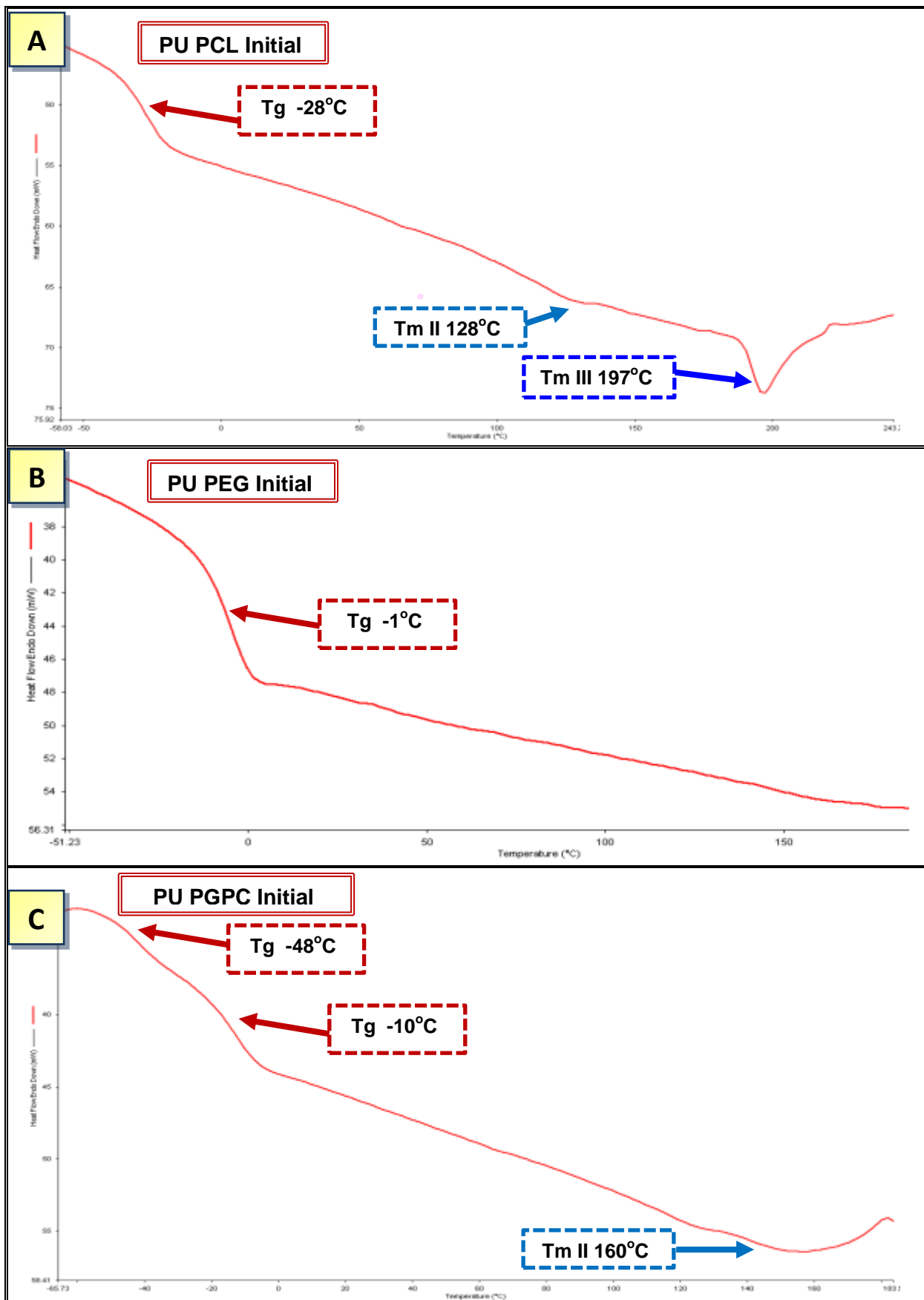


Figure 5.4 Morphology of PU using DSC; PU PCL (**A**), PU PEG (**B**), PU PGPC (**C**)

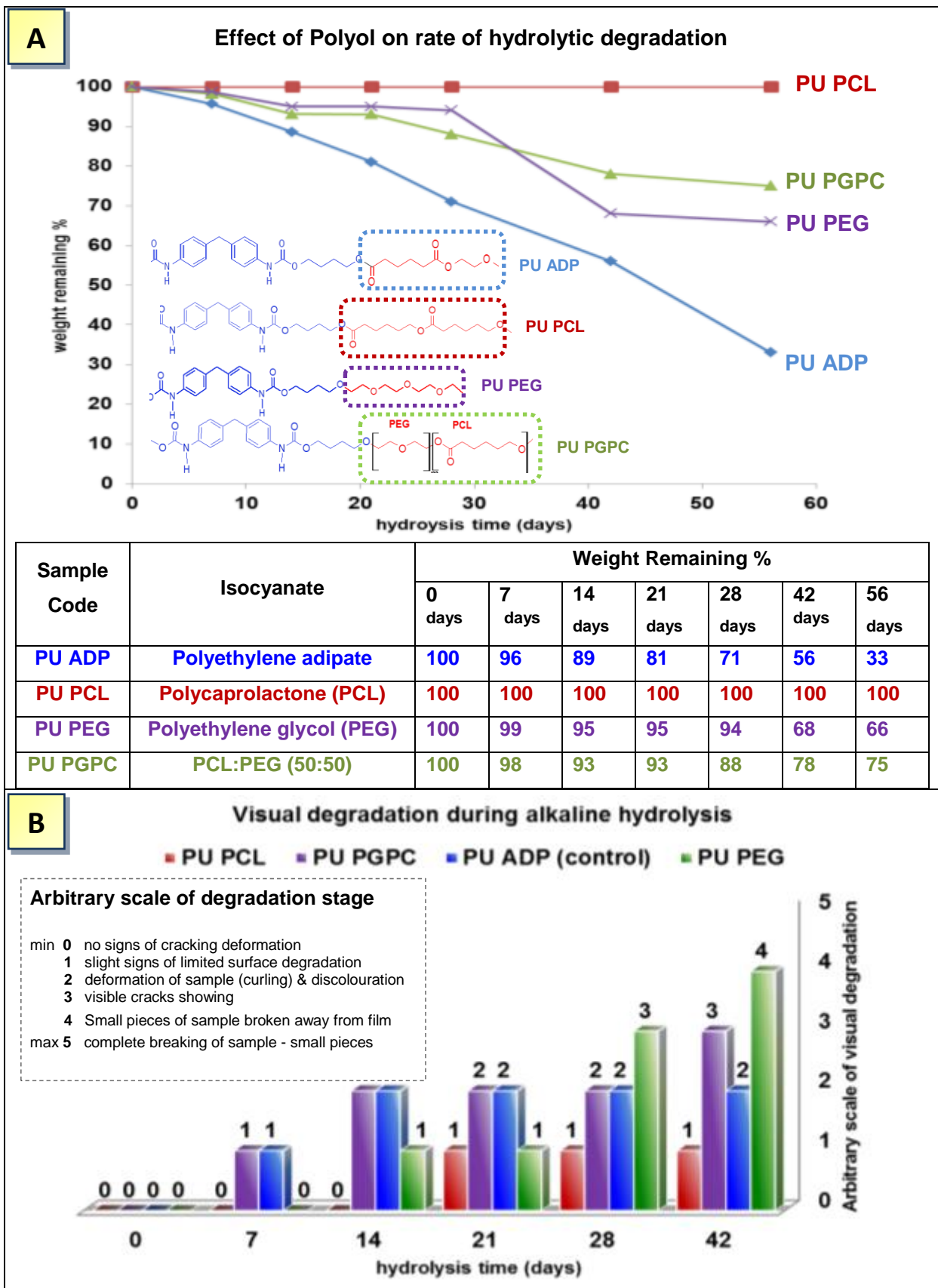


Figure 5.5 Effect of polyol on the rate of hydrolytic degradation (A) with 10% NaOH (aq) (see table 5.1 pg. for acronyms). Visual surface cracking (B)

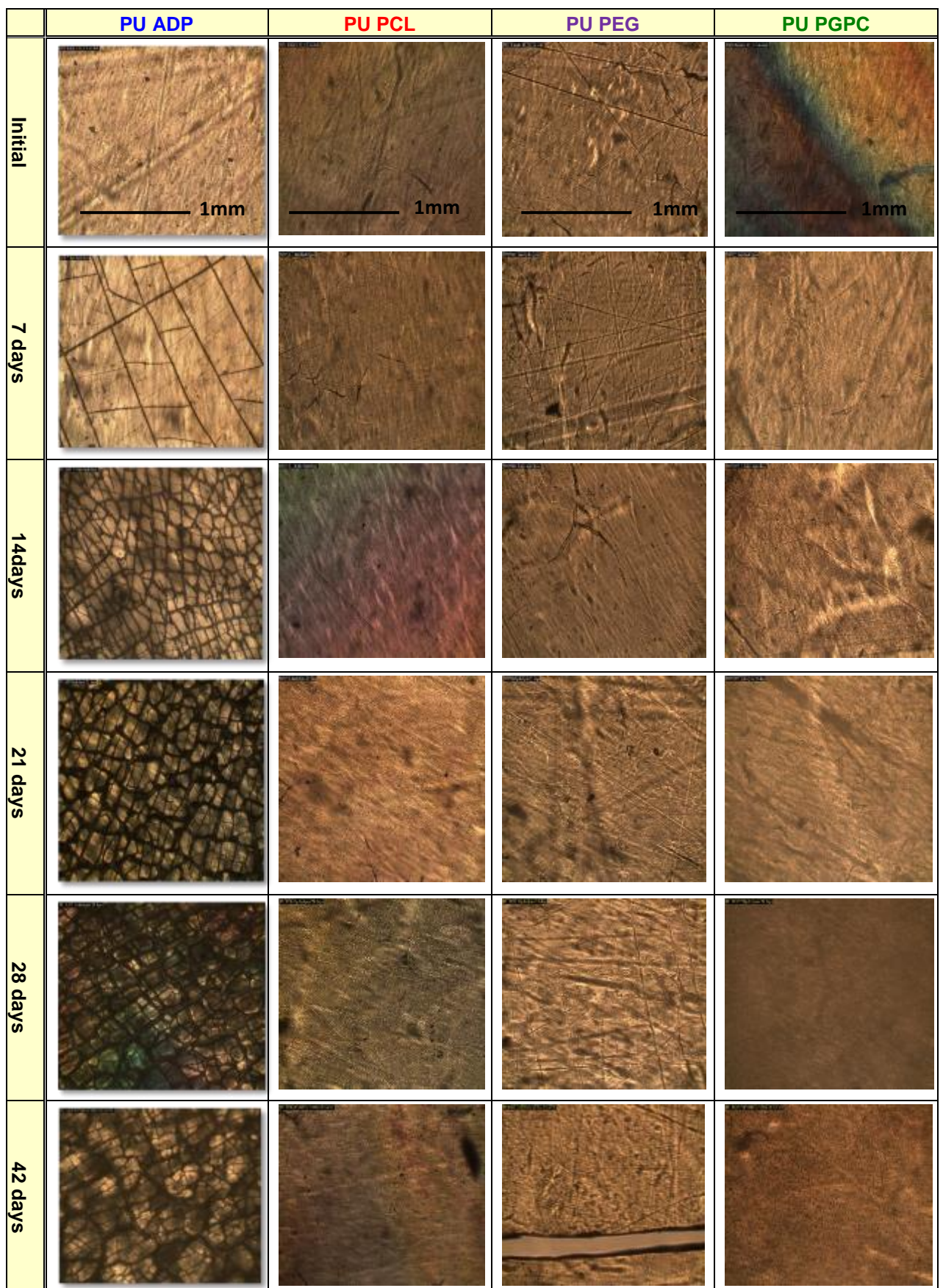


Figure 5.6 Visual changes of PU during hydrolytic degradation with 10% NaOH (aq), determined by optical microscope

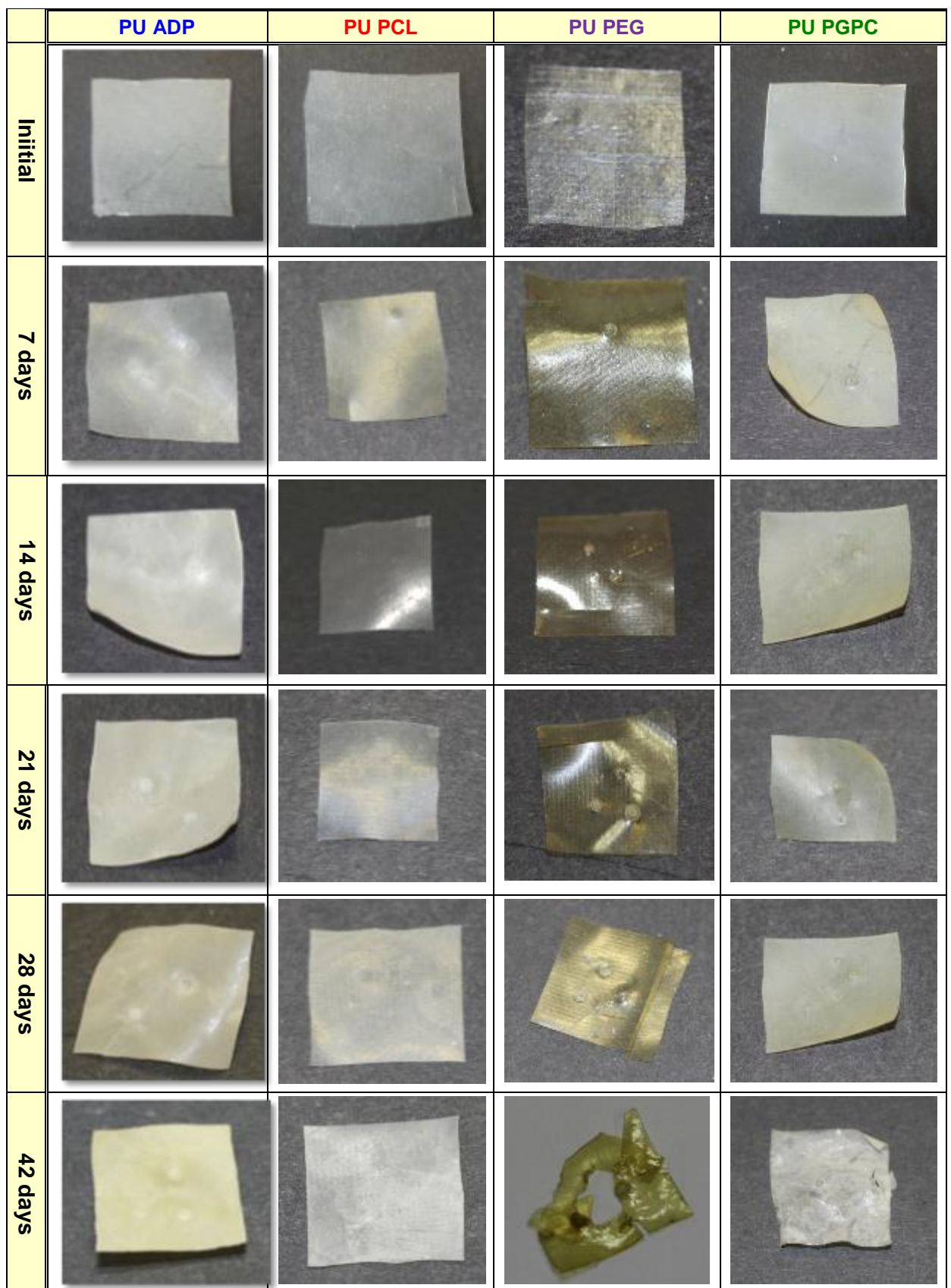


Figure 5.7 Visual changes of PU during hydrolytic degradation with 10% NaOH (aq), determined by photographic images

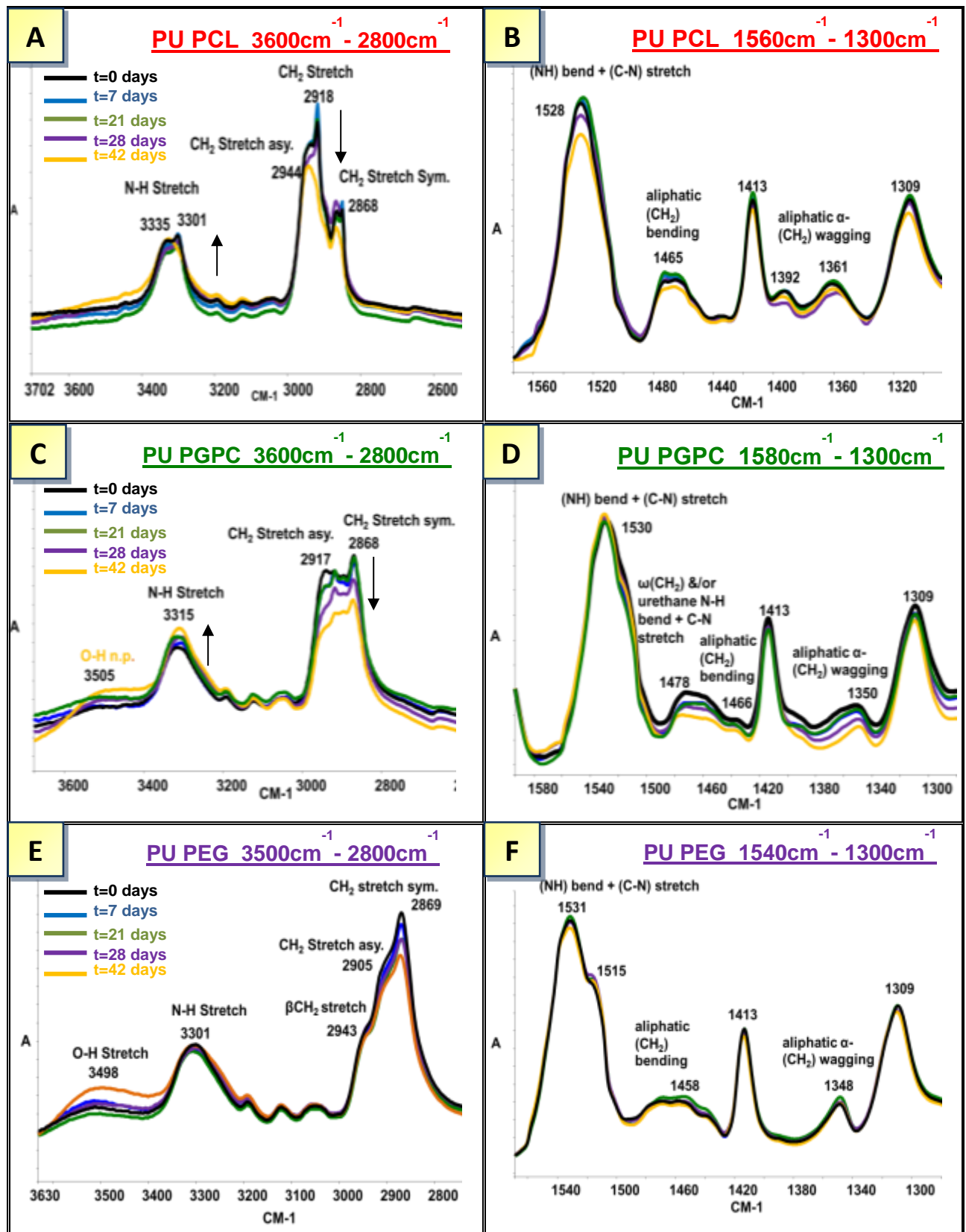


Figure 5.8 Effect of polyol on NH and CH₂ groups during alkaline hydrolysis of PU PCL (A-B), PU PGPC (C-D) & PU PEG (E-F) by FTIR/ATR

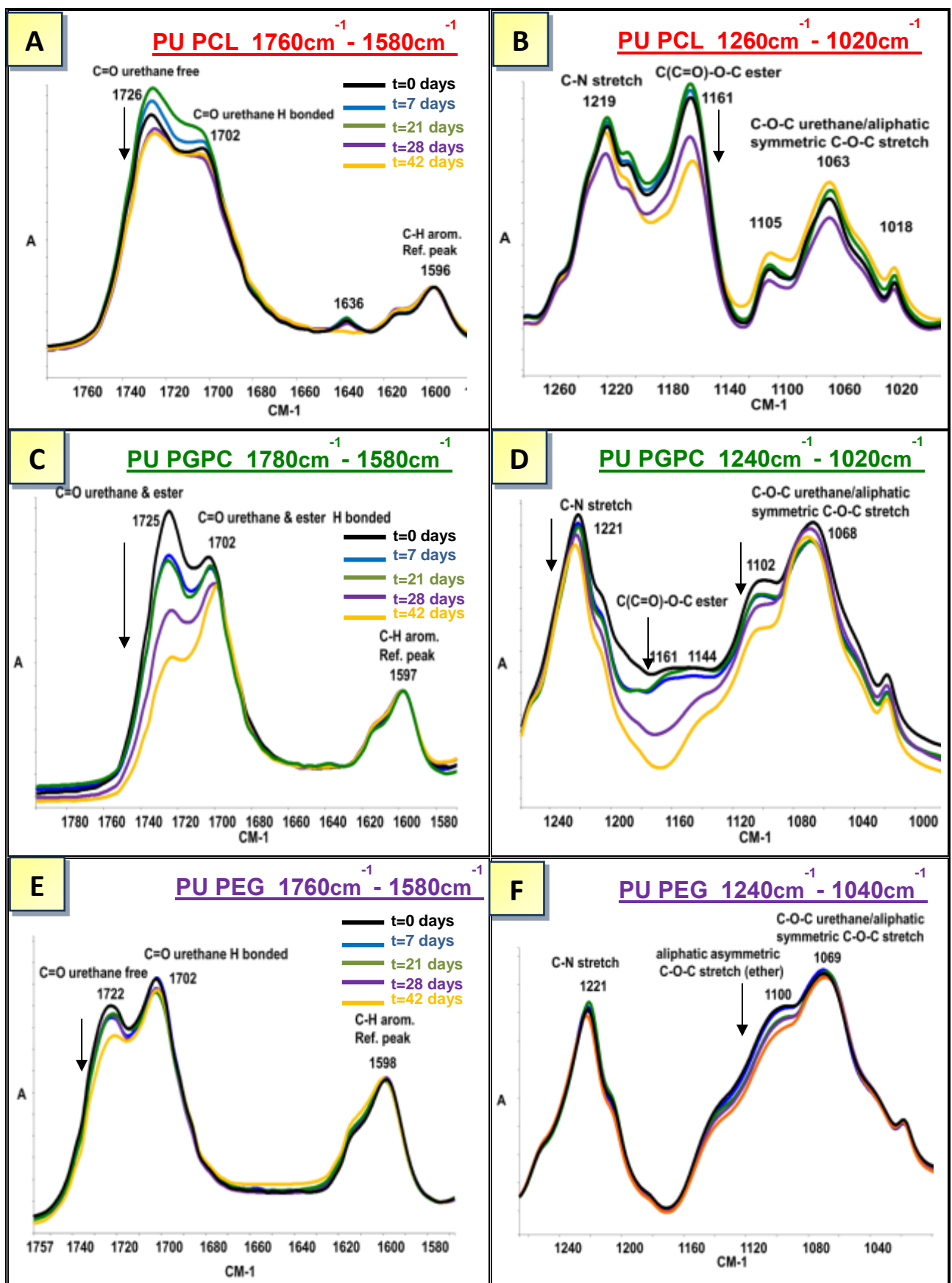


Figure 5.9 Effect of polyol on C=O and C-O-C ester/urethane linkages during alkaline hydrolysis of PU PCL (**A-B**), PU PGPC (**C-D**) & PU PEG (**E-F**) by FTIR/ATR

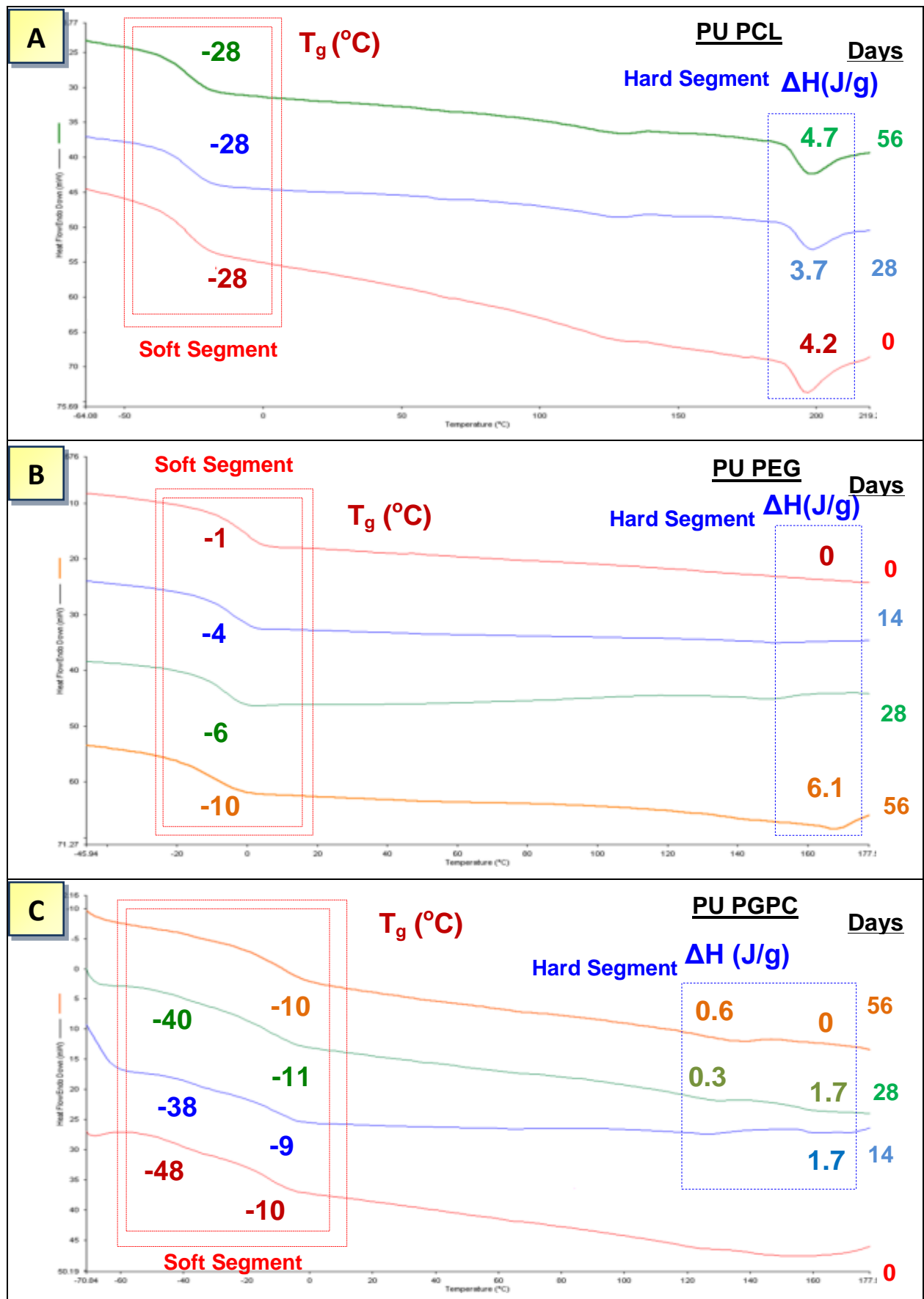


Figure 5.10 Changes in crystallinity during alkaline hydrolysis of PU samples PU PCL (A), PU PEG (B) and PU PGPC (C)

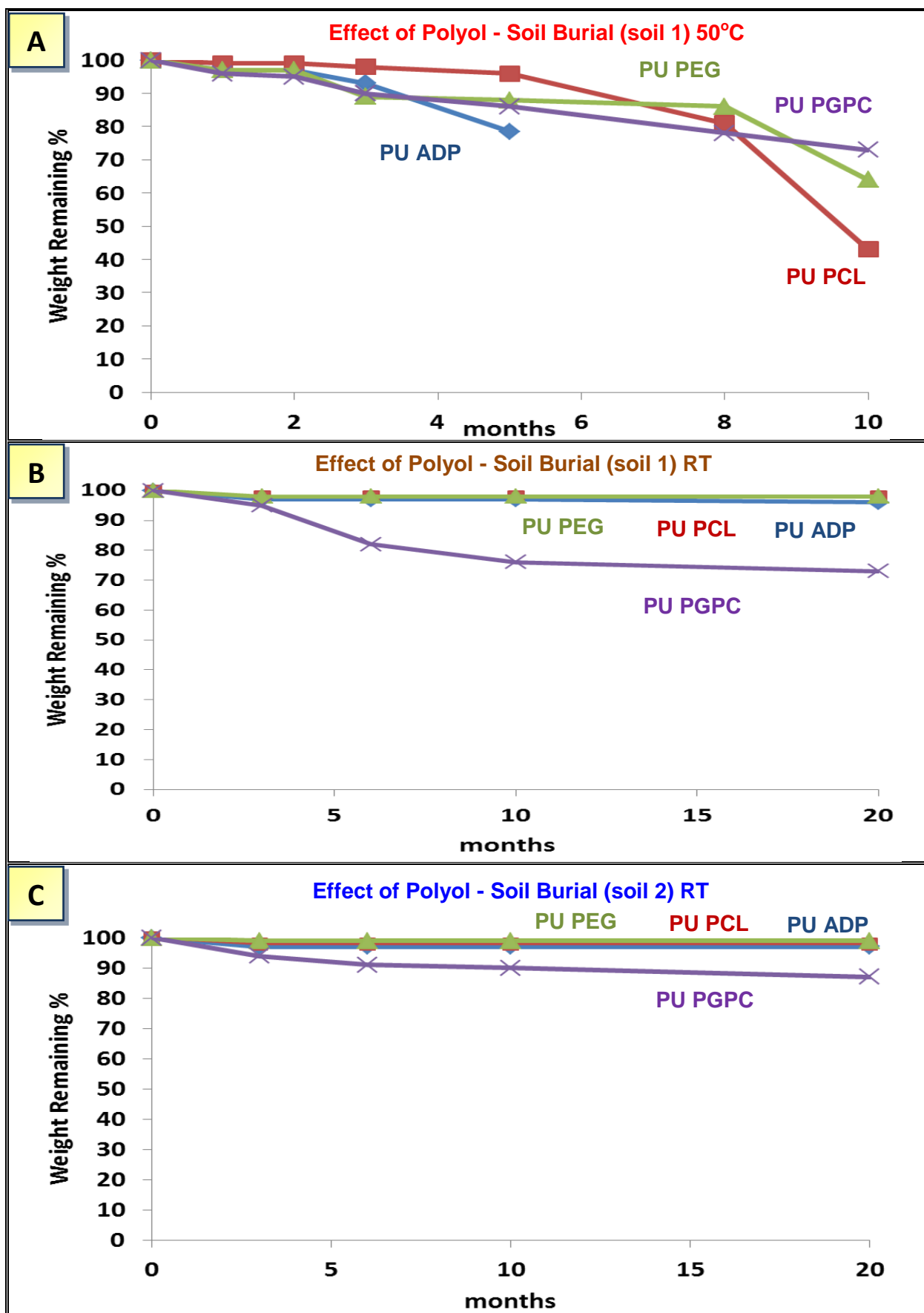


Figure 5.11 Effect of Polyol on the rate of biodegradation under soil burial conditions, soil 1 50°C (**A**), soil 1 RT (**B**), soil 2 RT (**C**)

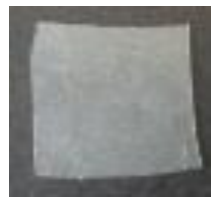
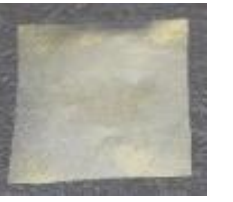
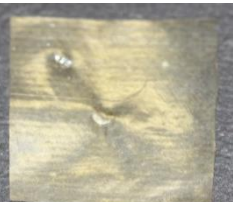
	PU PCL	PU PEG	PU PGPC	PU ADP (Control)
Initial				
3 Months				
Soil 1 RT				
Soil 2 RT				
Soil 1 50°C				
5 Months				
Soil 1 50°C				
20 months				
Soil 1 RT				
Soil 2 RT				

Figure 5.12 Photographic images of PU ADP, PU PCL, PU PEG & PU PGPC during soil burial

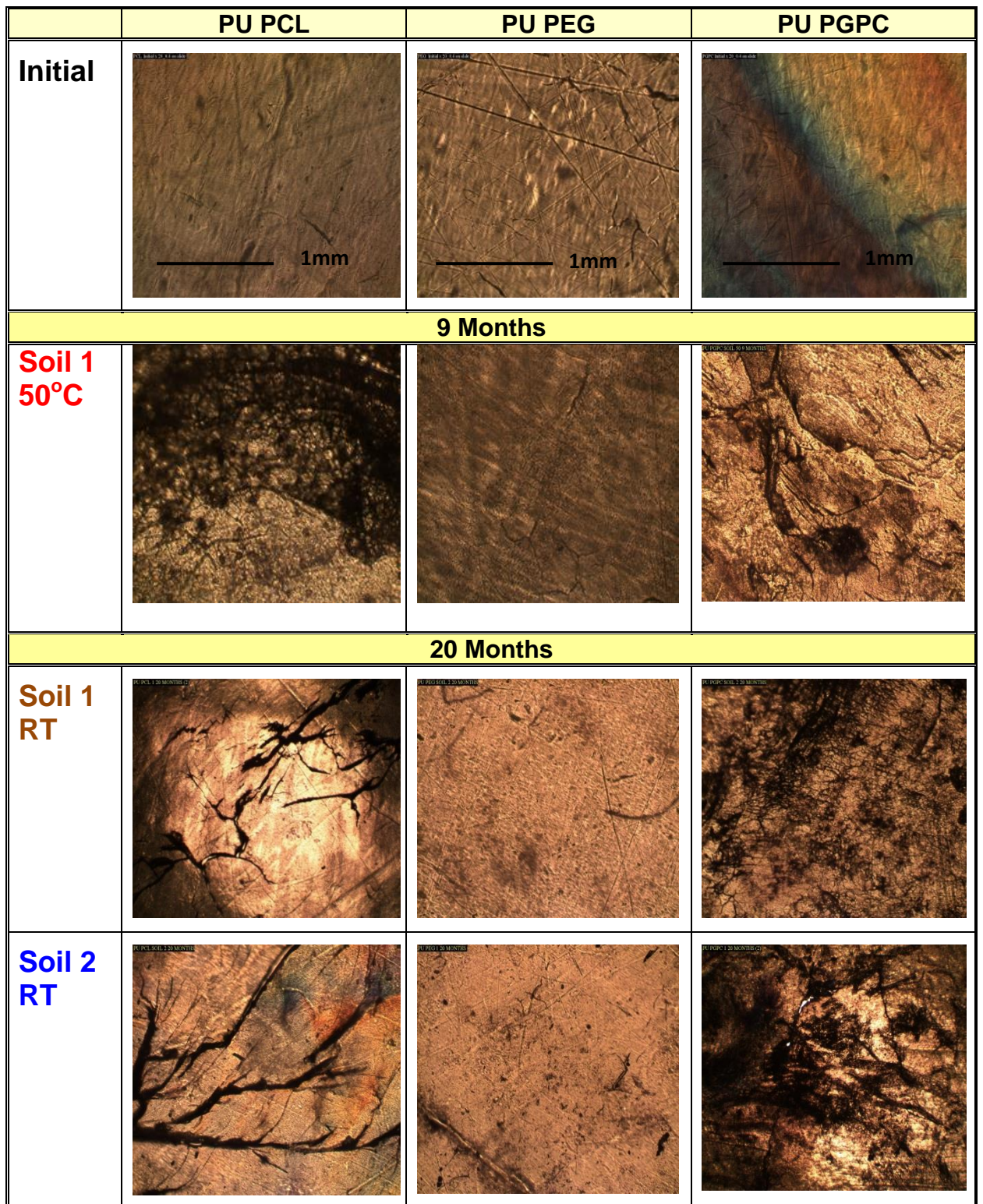


Figure 5.13 Optical microscopic images of PU PCL, PU PEG & PU PGPC during soil burial

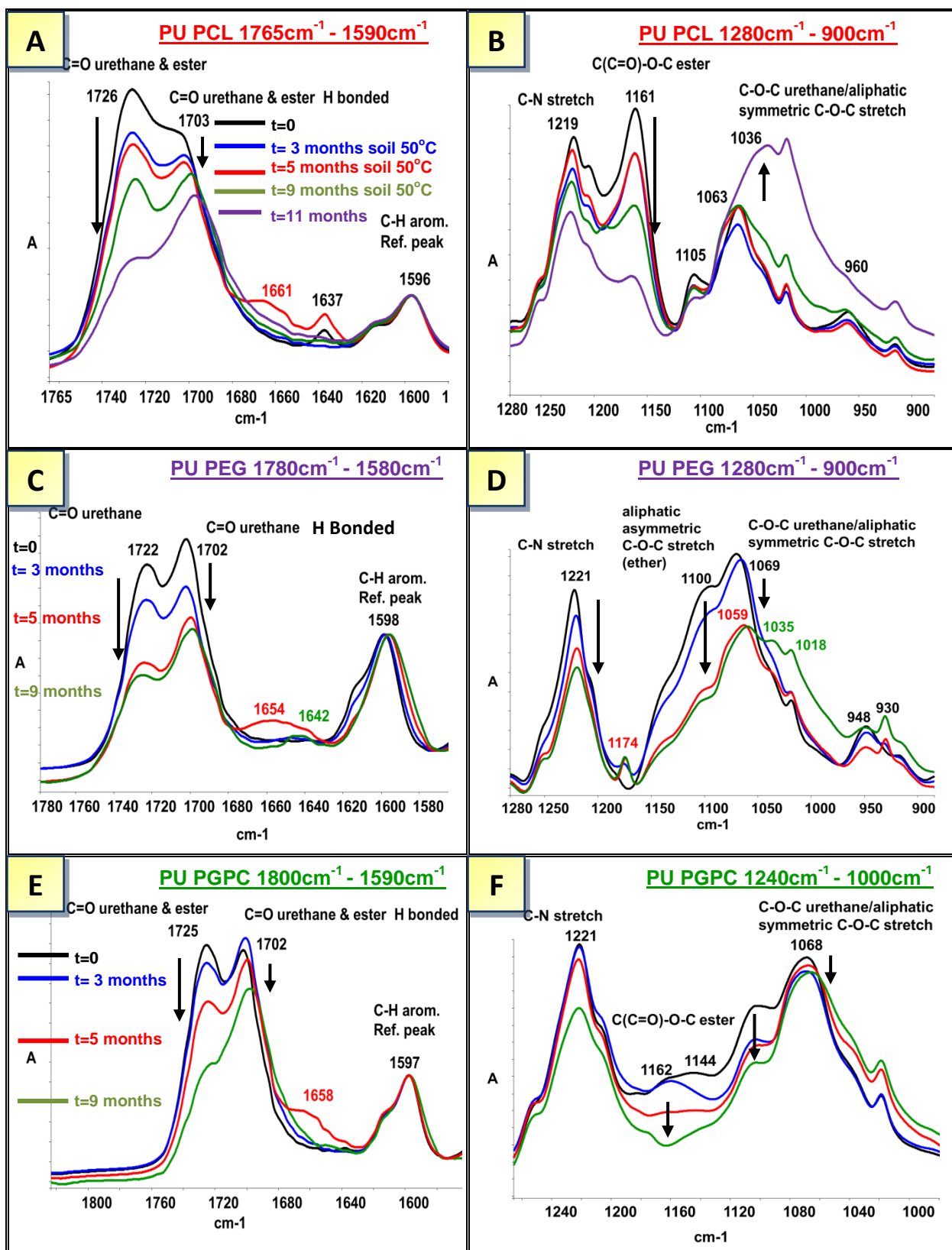


Figure 5.14 Changes in C=O and C-O-C ester/urethane linkages during soil burial at 50°C of PU PCL, PU PEG & PU PGPC monitored by FTIR/ATR.

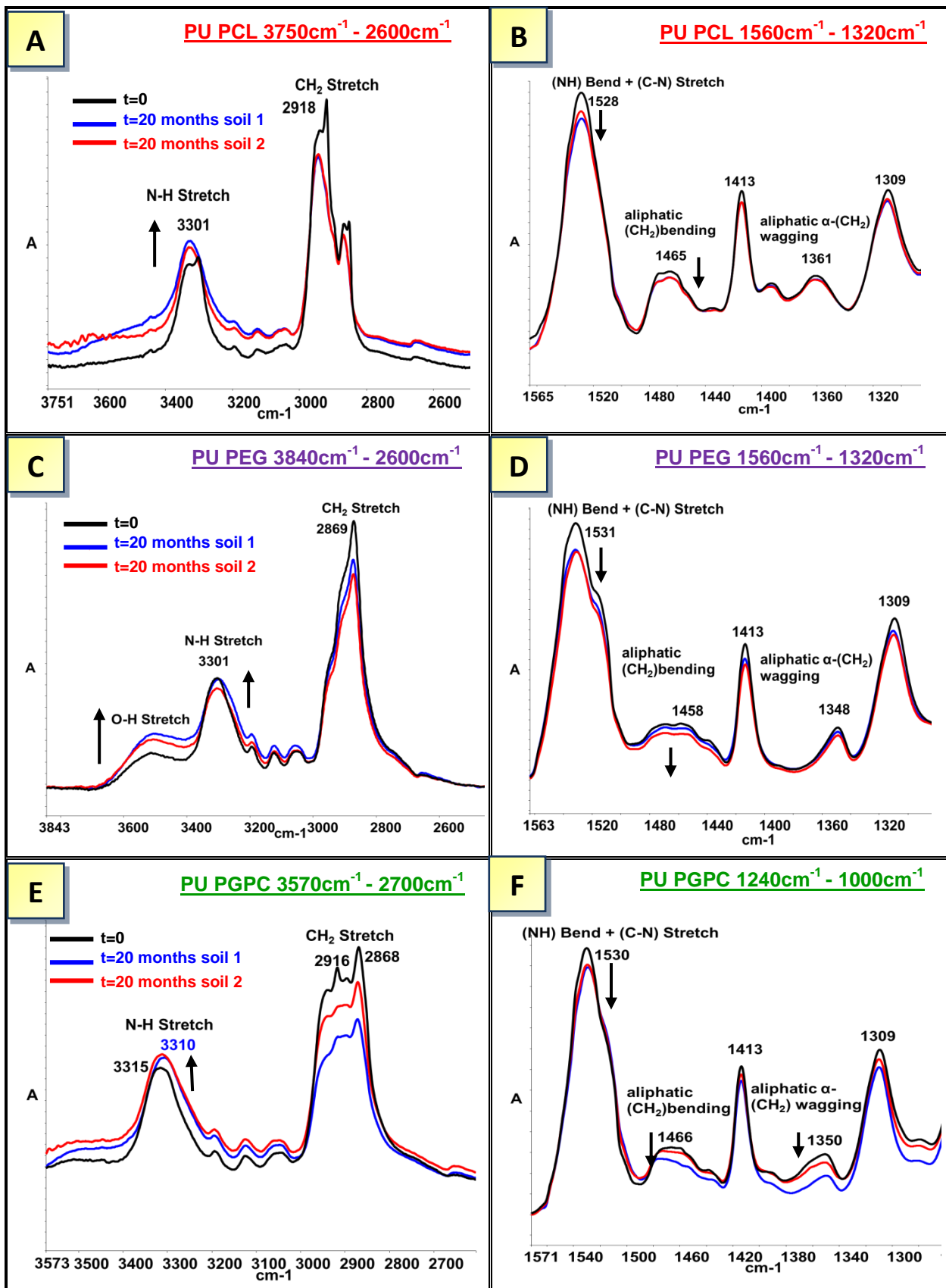


Figure 5.15 Changes in N-H and CH₂ ester/urethane linkages during soil burial at RT of PU PCL, PU PEG & PU PGPC monitored by FTIR/ATR.

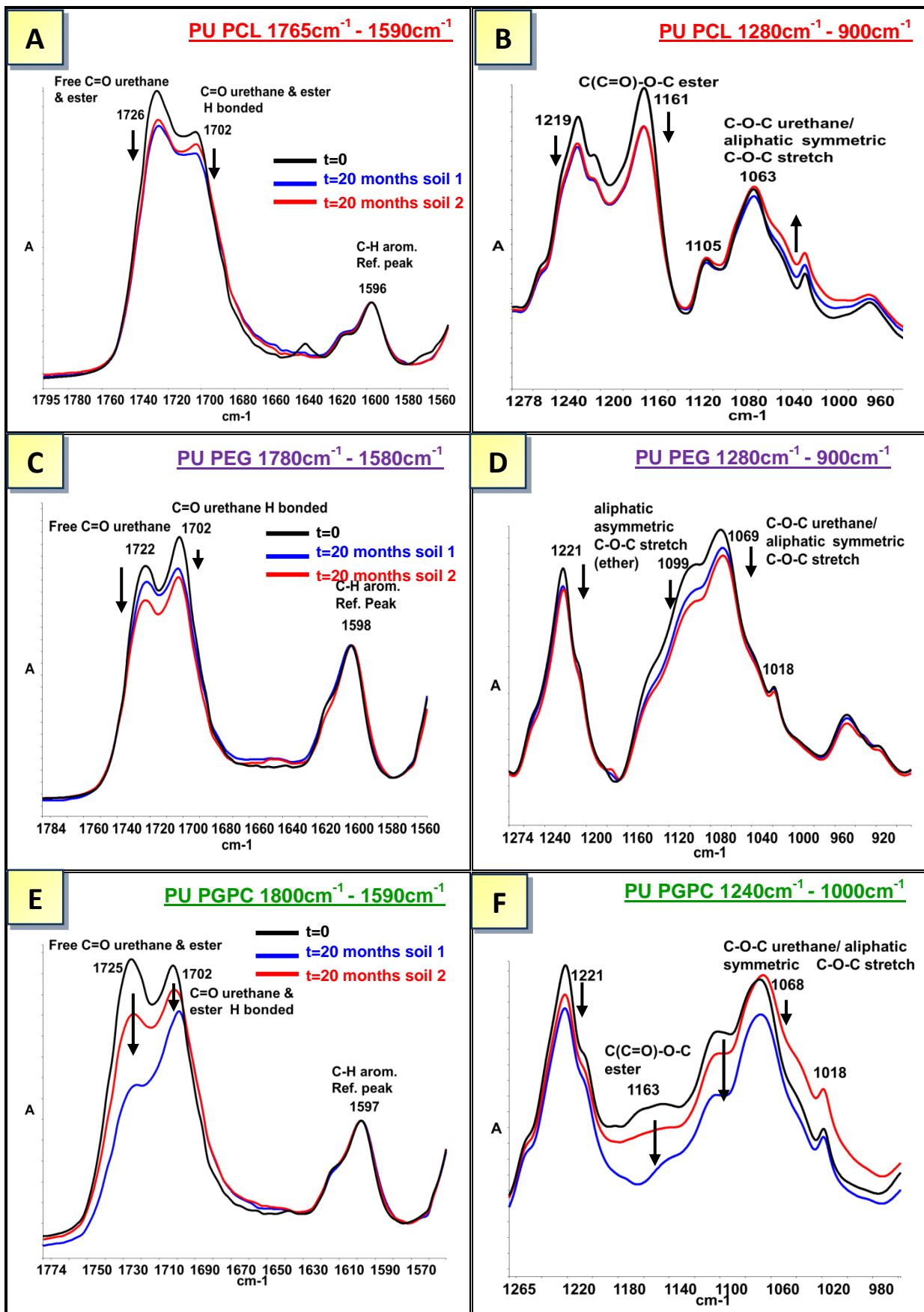


Figure 5.16 Changes in C=O and C-O-C ester/urethane linkages during soil burial at RT of PU PCL, PU PEG & PU PGPC monitored by FTIR/ATR.

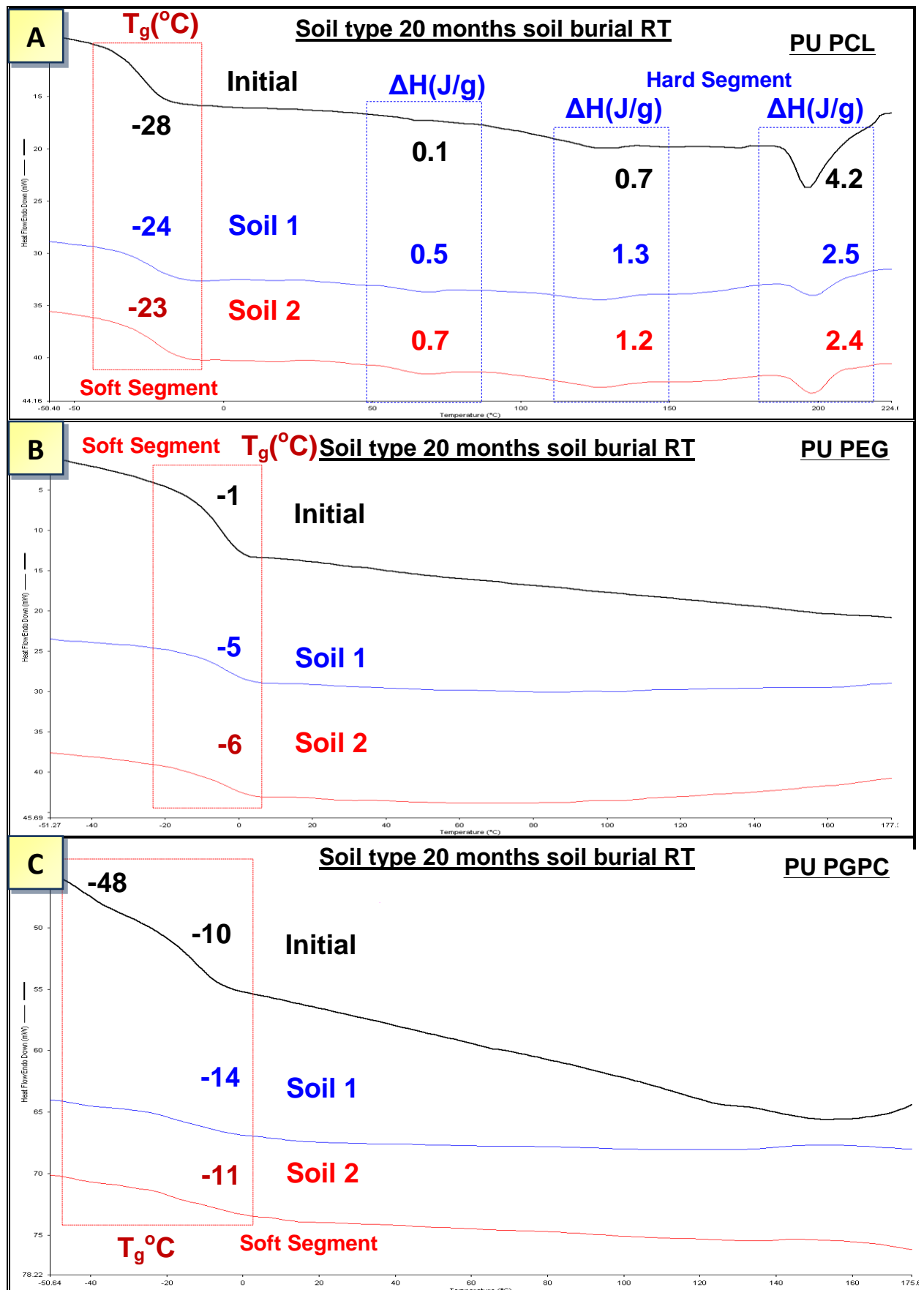


Figure 5.17 Effect of polyol on morphology changes during biodegradation in soil at RT and 50°C of PU PCL, PU PEG & PUPGPC.

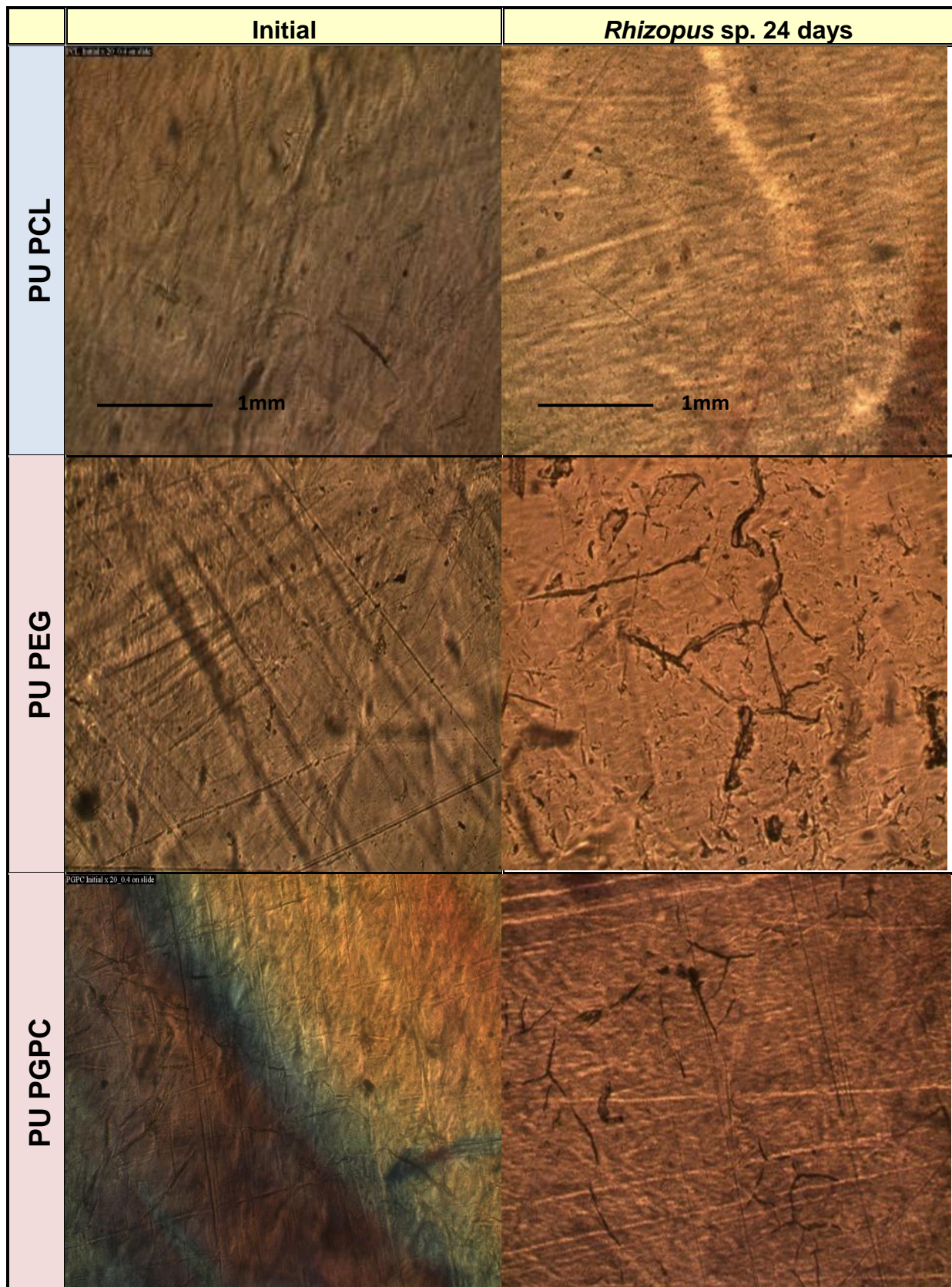


Figure 5.18 Effect of polyol on enzymatic degradation by lipase *Rhizopus* sp. PU PCL, PU PEG & PU PGPC by optical microscope images

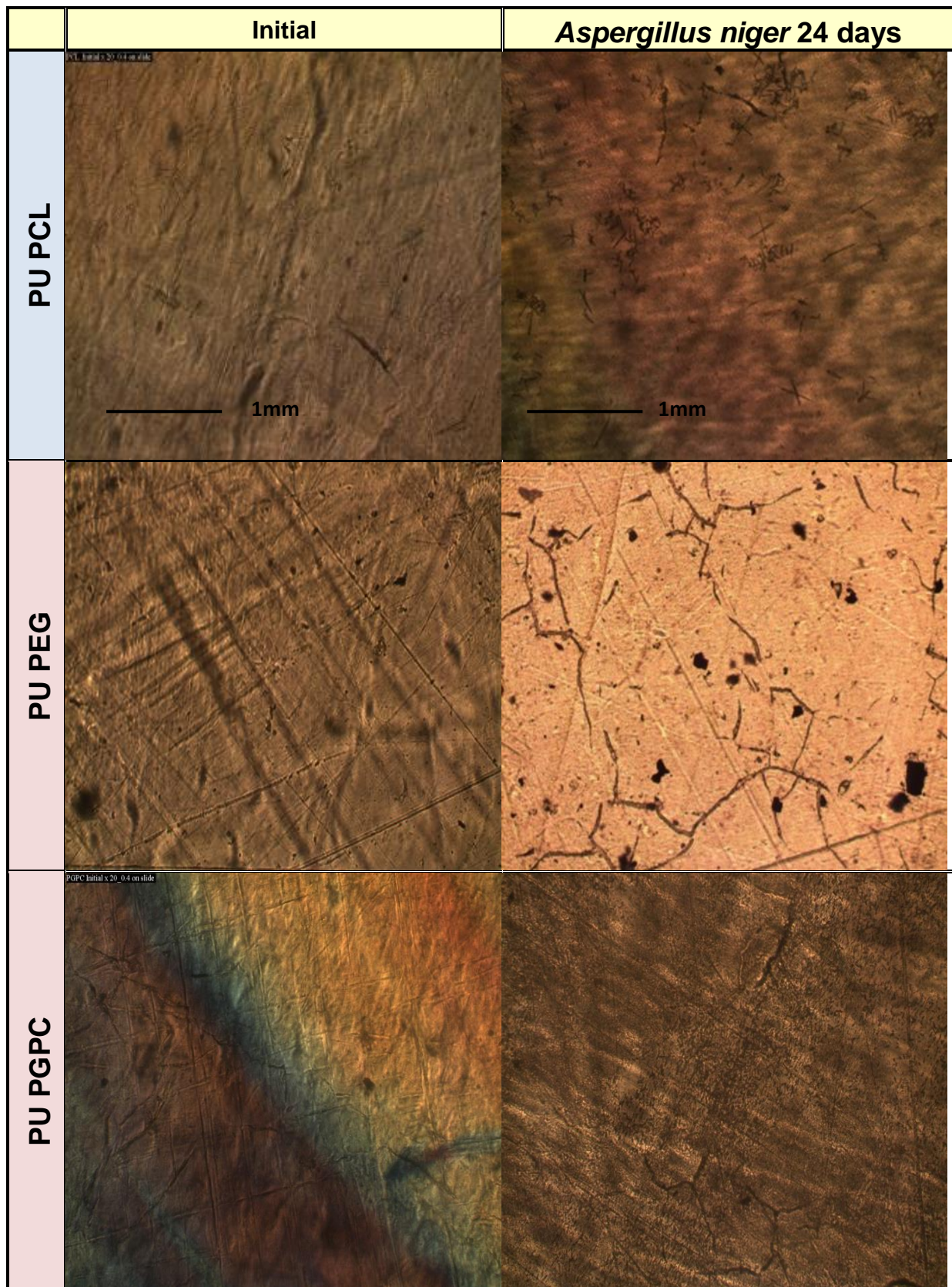


Figure 5.19 Effect of polyol on enzymatic degradation by lipase *Aspergillus niger*. PU PCL, PU PEG & PU PGPC by optical microscope images

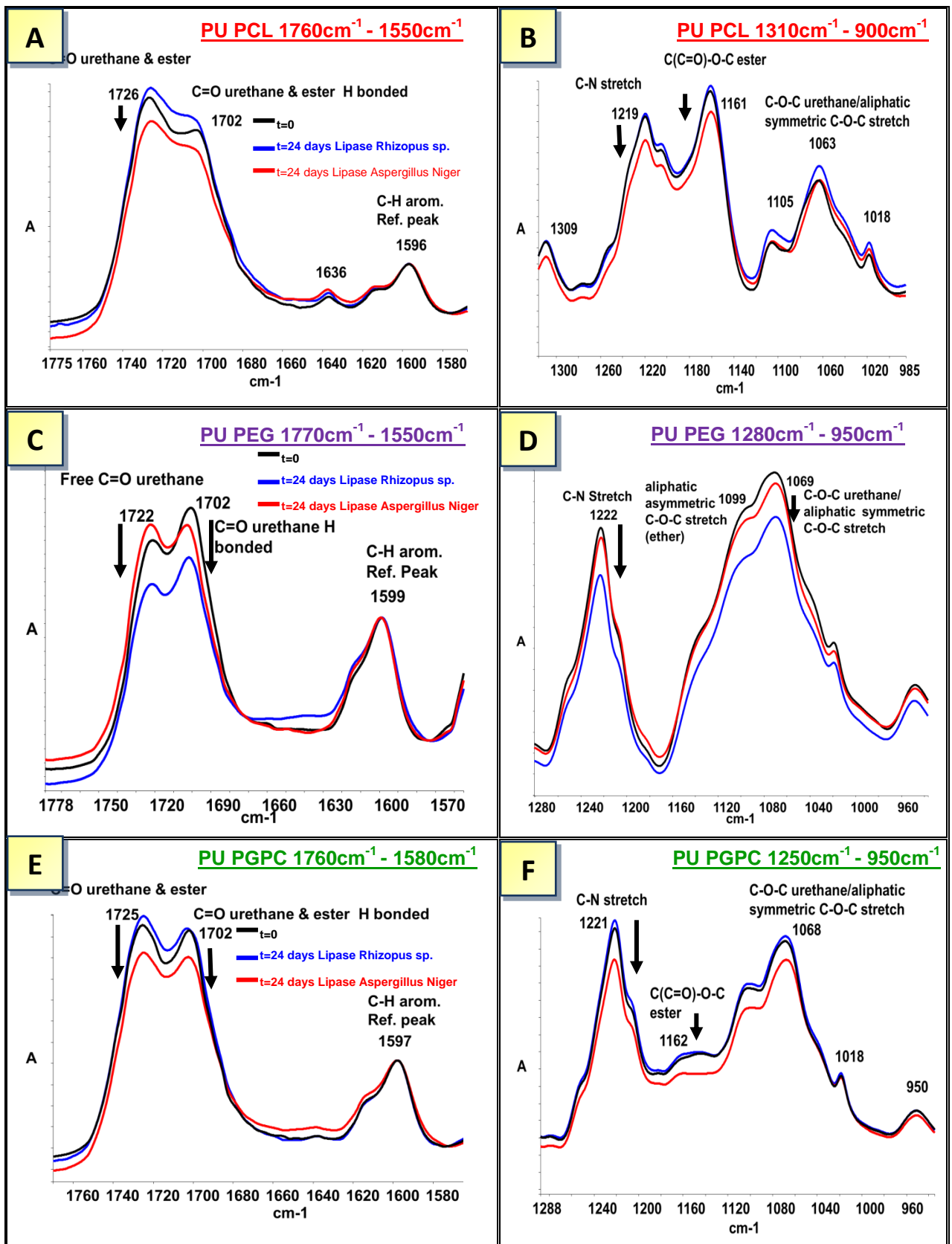


Figure 5.20 Effect of polyol on structural changes during enzymatic degradation by Lipase *Aspergillus niger* and *Rhizopus* sp. on PU PCL, PU PEG & PU PGPC determined by FTIR-ATR

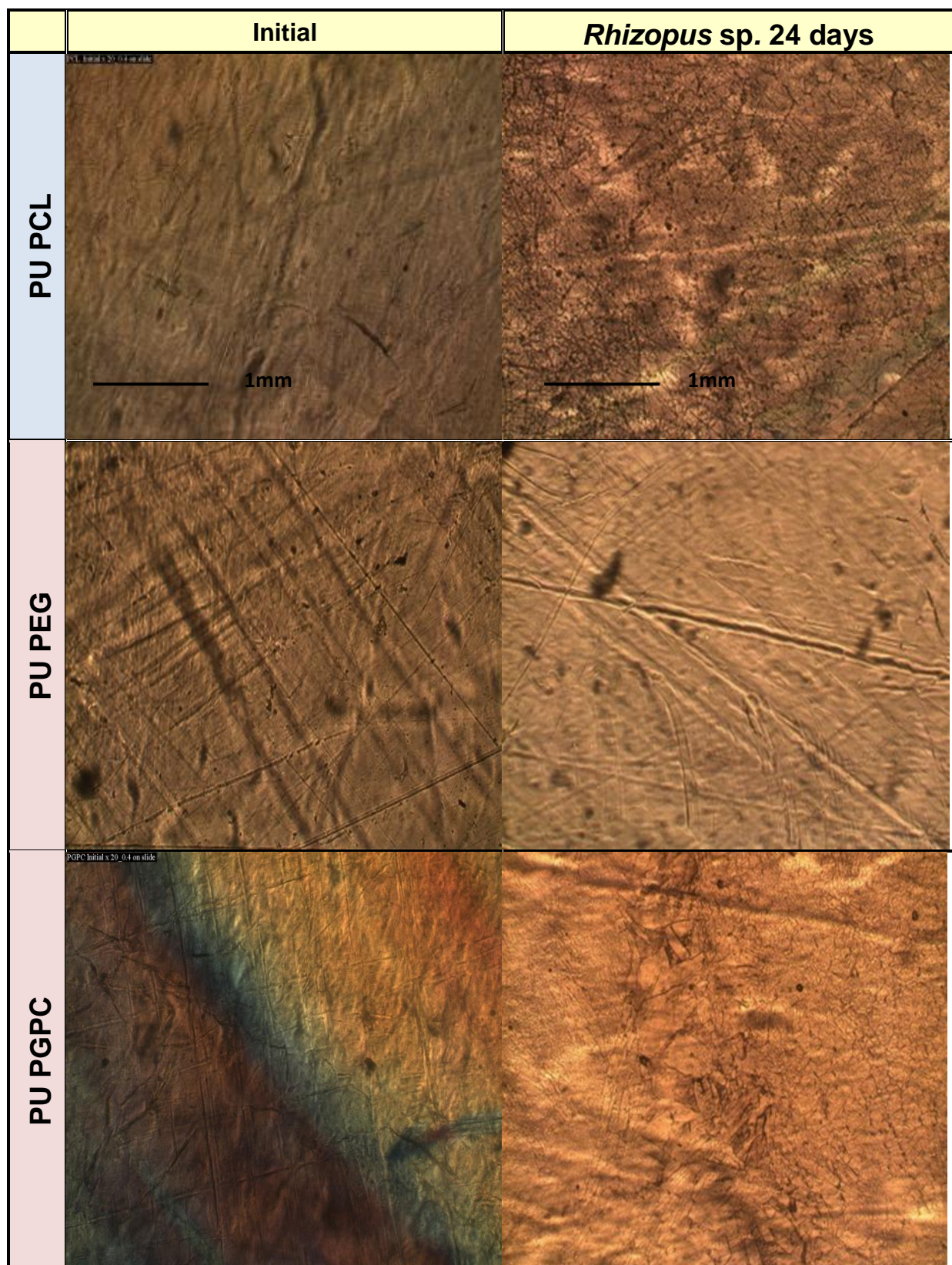


Figure 5.21 Effect of polyol on enzymatic degradation by protease *Rhizopus* sp. PU PCL, PU PEG & PU PGPC by optical microscope images

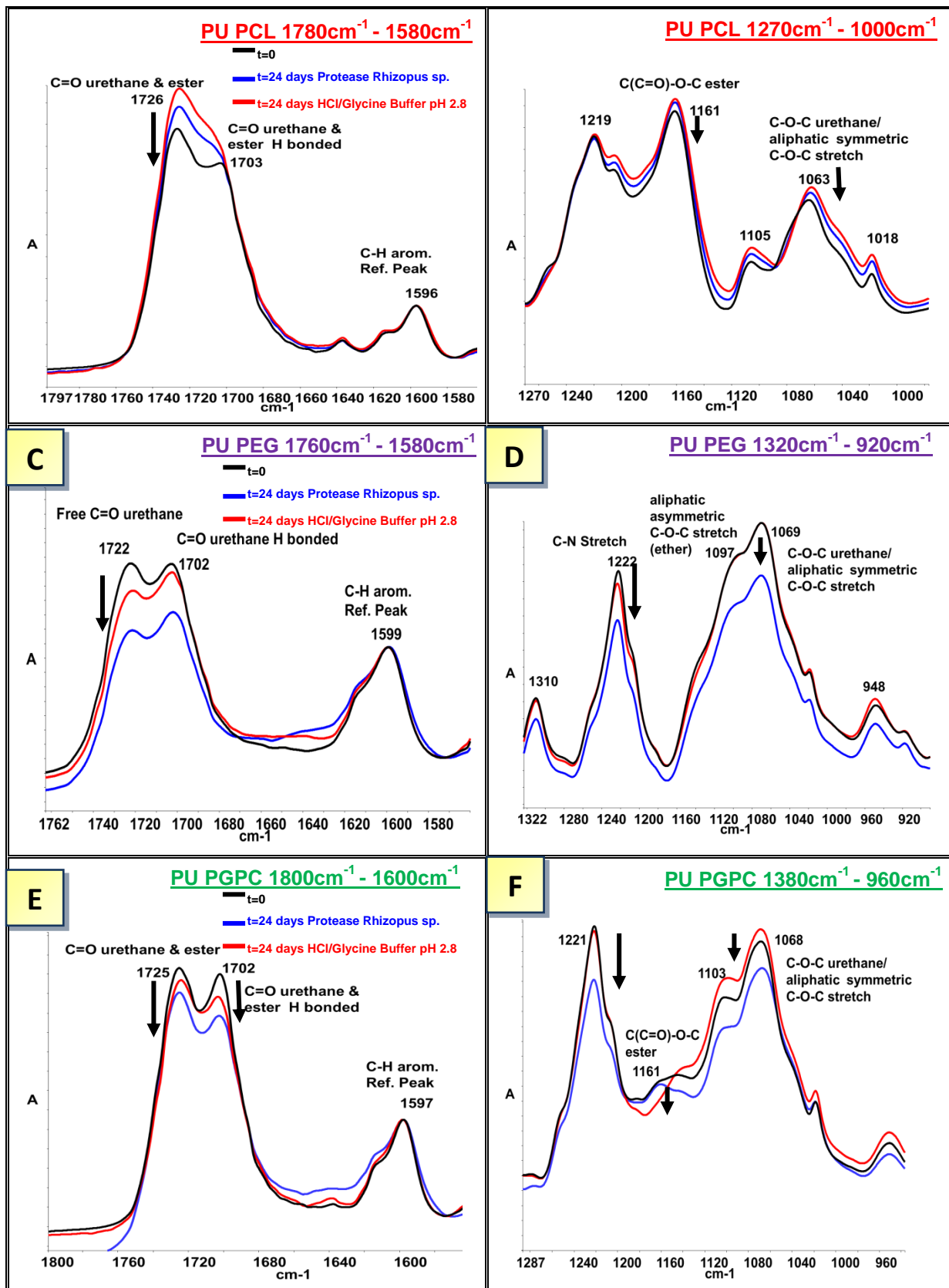


Figure 5.22 Effect of polyol on structural changes during enzymatic degradation by protease *Rhizopus* sp. on PU PCL, PU PEG & PU PGPC determined by FTIR-ATR

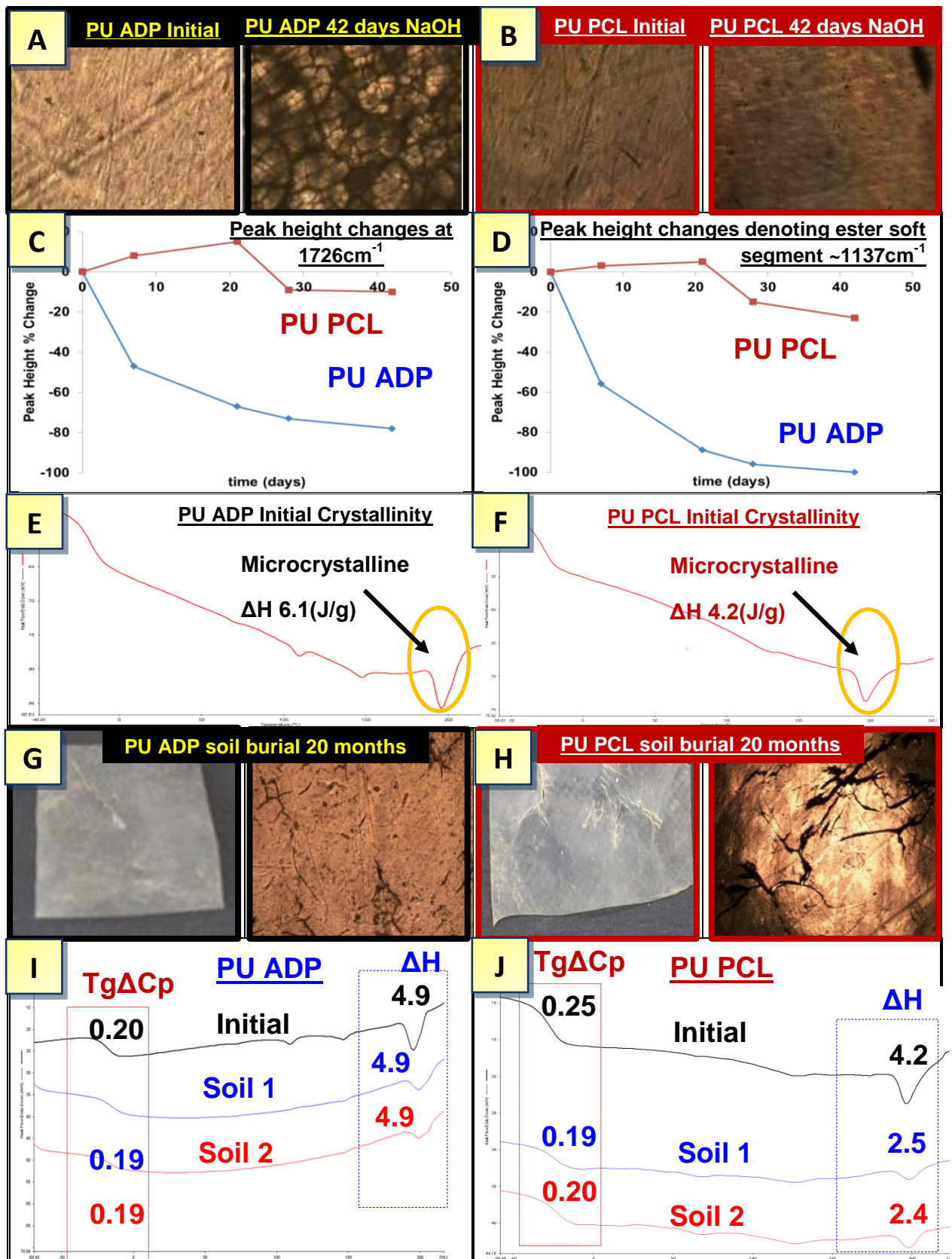


Figure 5.23 Showing the effect of altering the soft segment from ADP to PCL. **(A-B)** PU films after alkaline degradation, **(C-D)** FTIR-ATR peak heights at 1161cm^{-1} , **(E-F)** crystallinity of PU ADP and PU PCL, **(G-H)** PU films after 20 months soil burial at RT, **(I-J)** Changes in crystallinity and soft segment degradation after soil burial.

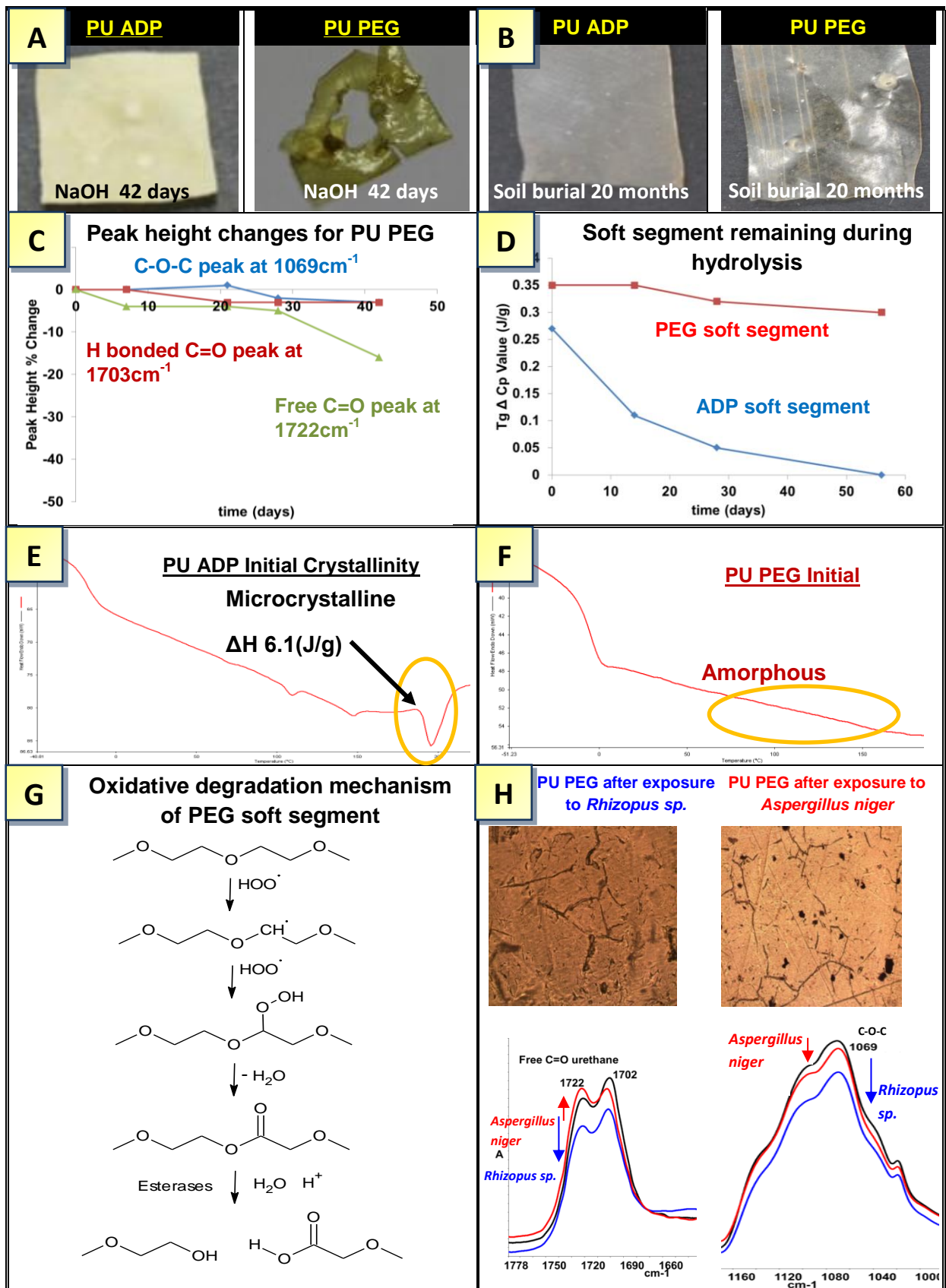


Figure 5.24 Showing the effect of altering the soft segment from ADP to PEG. **(A-B)** PU films after alkaline and soil burial degradation, **(C-D)** FTIR-ATR peak height changes and soft segment degradation, **(E-F)** crystallinity of PU ADP and PU PEG, **(G)** Oxidative degradation mechanism for polyethers, **(H)** enzymatic degradation

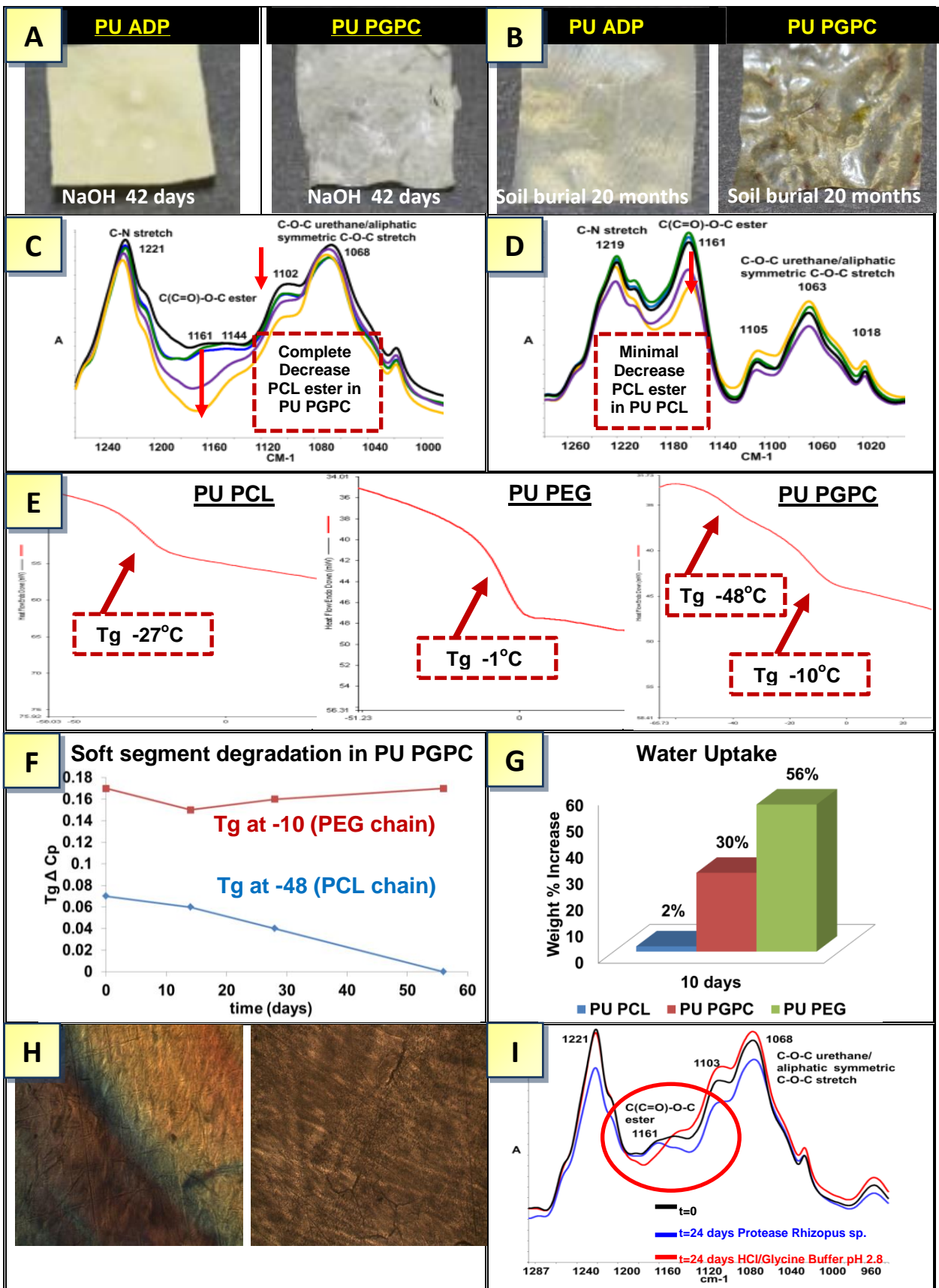


Figure 5.25 Effect of a PCL/PEG soft segment blend. **(A-B)** PU films after alkaline and soil burial degradation, **(C-D)** FTIR-ATR peak height changes at 1161cm^{-1} , **(E)** Effect of PCL/PEG blend on phase separation, **(G)** Effect of PCL/PEG blend on PU hydrophilicity, **(H-I)** Effect of PCL/PEG blend on enzymatic degradation

Chapter 6

The Role of Additives on the Degradation and Biodegradation of Polyurethanes

6.1 Objectives and methodology

Many mechanisms are involved in the degradation and biodegradation of PU and include but not limited to, chemical hydrolysis, enzymatic hydrolysis by microbes, and external environmental weathering conditions such as UV induced photo-oxidation. Results from previous chapters have highlighted that the degradation and biodegradation of PU is dependent on many factors, and include the method of synthesis, the type of isocyanate used and the type of polyol. All of these elements were seen to have a profound effect on the interactions between the hard and soft segments as well as the extent of crystallinity, which in turn have affected the rate of degradation and biodegradation to varying degrees.

As a progression of the systematic analysis of the components of PU and how they affect degradation and biodegradation, the work described in this chapter will examine how the addition of different additives used during the synthesis of PU affect the rate of degradation and biodegradation. One of the main uses of additives with respect to polymeric materials is to protect and prolong the life of the polymer during processing and exposure to external environments. However, additives are currently being used as a method to increase the rate of degradation and biodegradation [9, 72, 80, 161].

Iron stearate and microcrystalline cellulose (at 2% wt each) **Table 6.1a**, were added to the control sample **PU ADP** with the aim of inducing photo-oxidation (iron stearate) and consequently increasing the rate of hydrolysis of the polymer. The addition of cellulose was thought to increase hydroxyl content and hence water absorption. Cellulose is also a natural substrate which can be broken down by enzymes and, thus increasing enzymatic hydrolysis to which PU was shown to be relatively resistant, **Figs. 5.8-5.9, Fig. 4.13 & Fig. 3.20**.

A natural montmorillonite modified with a quarternary ammonium salt; Cloisite 30B was also examined, and added (12% wt), **Table 6.1b**, to three PUs synthesised by Eurothane Ltd; **PU PR, PU CE and PUI** (Group 5). This modified organoclay has been used in previous studies to improve the physical properties of polymers [127, 162, 163].

6.2 Results

6.2.1 Characterisation of PU CE and PUI (Effect of the additives cellulose and iron stearate)

Full characterisation of these samples was performed prior to any degradation and biodegradation experiments, in order to compare the degraded samples to the virgin samples, and thereby provide a full understanding of the changes taking place to the chemical structure and morphology of the PU samples during degradation. Chemical structure was characterised by FTIR-ATR, thermal stability by TGA and the morphological profile was obtained by DSC analysis. Samples were synthesised by Eurothane Ltd in granule form, therefore, prior to characterisation, samples were pressed to films (100-120 μm), see **Table 2.3**. Additives were incorporated into the PU in powder form and mixed into the PU during synthesis.

All samples in group 4 (**PU CE, PUI**) were found to be insoluble in acetone, acetonitrile, ethanol, water and hexane, as of that for PU samples in groups 1-3, see **Table 2.4**. The samples were partially soluble in dimethyl sulfoxide and soluble in tetrahydrofuran and dimethylformamide, and the use of these additives did not affect the solubility of the sample. Past studies [33, 55] and results from previous chapters have shown hydrophilicity to influence the rate of hydrolysis of PU, therefore the hydrophilicity of each sample was measured by water absorption prior to the experimental work, see **Section 2.2.2**. From the results shown in **Fig.6.1a**, it can be noted that the addition of the additives increased the extent of water absorption by almost 100% in comparison to the control sample **PU ADP**, (**PU CE 8.5%, PUI 8.2%, PU ADP 4.5%**).

Chemical structure was characterised by FTIR-ATR and the spectrum for each sample is given in **Fig.6.1**. It was noted that the absorbance spectra for these two samples was almost identical to that of the control sample **PU ADP**, **Chapter 3, Section 3.2., Fig. 3.2a, and Fig 6.1**.

Cellulose and iron stearate were also characterised by FTIR-ATR prior to addition into the PU, and these spectra are given in **Chapter 2, Fig. 2.4**. The most notable absorbances observed for the microcrystalline cellulose was the absorbance at 3327 cm^{-1} which corresponds to the O-H stretching vibration and the C-O stretching vibration at 1025 cm^{-1} . For iron stearate, the notable absorbances were the CH₂ stretching vibration at 2850 cm^{-1} and the C-O stretching vibration of the carboxylic acid group at 1444 cm^{-1} . It was surmised that some of these peaks relating specifically to the additives would be observed in the PU samples **PU**

CE and **PUI**, however this was not found to be the case, therefore, in order to determine whether the additives had been incorporated into the PU samples, microscope images were obtained, and are given in **Fig.6.2**. The microscopic image for **PU CE** shows an almost porous like structure in the PU film, so much so that it was difficult to determine whether the cellulose had been mixed successfully, therefore a polarised image was obtained, **Fig 6.2b**. It can be seen that although the FTIR-ATR spectra did not display absorbances relating to the additives in the two PU samples (**PU CE** and **PUI**), the microscopic images did in fact show that both the microcrystalline cellulose and iron stearate had been incorporated successfully.

The thermal stability of each sample was evaluated by TGA prior to degradation experiments as of that for PU groups 1-3, see **section 2.3.4**. The thermograms for each sample are given in **Fig.6.3**. It was found that the addition of cellulose to PU had a minimal effect on thermal stability. The greatest mass loss of the hard segment of **PU CE** occurred at 330°C (**PU ADP** 336°C), and that of the soft segment at 436°C (**PU ADP** 427°C). However, the addition of iron stearate to PU was seen to affect the thermal stability dramatically with greatest mass loss of the soft segment occurring at a 310°C for **PUI**, compared to the control **PU ADP** (336°C), and that of the hard segment at 383°C, (**PU ADP** 436°C), and from these findings it can be stated that the addition of iron stearate decreased the thermal stability of the PU.

The initial morphology of **PU CE** and **PUI** was examined by DSC and compared to the control sample **PU ADP**, **Fig 6.4**. One endotherm relating to the highly ordered microcrystalline region was observed at 202°C [107, 109] for **PU CE** and 197°C for **PUI** indicating that both of these PU films were highly crystalline in nature with ΔH values of 8.31 J/g (**PU CE**) and 7.16 J/g (**PUI**), more than the control sample **PU ADP** (ΔH 6.1 J/g). The T_g values were examined to provide an indication of microphase separation between the hard and soft segments in the PU samples [41, 54, 108]. It was found that there was little difference in the T_g values between **PU CE**, **PUI** and the control sample **PU ADP**, with T_g values of -15°C, -15°C and -18°C respectively. Therefore, adding either cellulose or iron stearate did not affect the phase separation significantly. However, it was thought that the increase in crystallinity may reduce the rate of degradation of the PU samples.

6.2.2 Characterisation of PU PR30, PU CE30 and PUI 30 (Effect of Cloisite 30B)

Full characterisation of the PU samples in group 5 containing Cloisite 30B (12% wt.); **PU PR30**, **PU CE30** and **PUI 30** was performed as of that for the group 4 samples (**see section 6.2.1**).

The solubility of all the samples in this group were similar to that of PU groups 1-4 in which samples were insoluble in acetone, acetonitrile, ethanol, water and hexane, partially soluble in dimethyl sulfoxide and soluble in tetrahydrofuran and dimethylformamide, therefore the addition of Cloisite 30B did not affect the solubility of the PU samples in this group

Sample films were prepared using the solvent casting method in which the appropriate amount of PU was dissolved in THF, and the of Cloisite 30B (12% wt), dispersed in THF and was added and sonicated for 3.5 hours. The solution was poured into 80mm glass petri dishes which were then left overnight until the THF had evaporated, (method is one which had been used previously) [110].

Hydrophilicity of **PU PR30**, **PU CE30** and **PUI 30** was obtained by the water uptake method, measured by submerging the sample in water and noting the weight increase until equilibrium was obtained, and the results are given in **Fig.6.5**. **Fig 6.5a** shows the % weight increase of PU samples containing Cloisite 30B and compared to **PU ADP**. Cloisite 30B containing PU was shown to be more hydrophobic than the control sample **PU ADP**, (**PU ADP 4.5%**, **PU PR30 2%**, **PUI 30 2%**, **PU CE30 3%**). **PU CE30** was compared to **PU CE**, **Fig 6.5b**, and a dramatic difference was noted, with **PU CE30** being more hydrophobic than **PU CE** (**PU CE 8.5%**, **PU CE30 3%**). The same was observed for both **PUI 30**, (**PUI 8.2%**, **PUI 30 2%**) and **PU PR30**, (**PU PR 3.6%**, **PU PR30 2%**), **Figs. 6.5c & d**. From these results it can be concluded that the addition of Cloisite 30B had significantly increased the hydrophobicity of the PU.

The chemical structure was characterised by FTIR-ATR, and the spectrum for each sample is given in **Fig.6.6**. The spectrum for **PU CE30** was similar to that of the spectrum for **PU CE**, (**see section 6.2.1**). However, there were some notable differences, specifically the peak at $\sim 1700\text{cm}^{-1}$ denoting the hydrogen bonded C=O ester/urethane linkages, which was seen to increase with the addition of Cloisite 30B. Also noted was an increase in the peak at 1078cm^{-1} which relates to the C-O-C linkages contained within the hard and soft segments, **Fig.6.6a**. The same was observed for **PUI 30** and **PU PR30**, with an increase in the peak at $\sim 1700\text{cm}^{-1}$ and a large increase in the peak at 1077cm^{-1} , **Figs. 6.6b & c**.

For all of the spectra in this group, a peak at 992cm^{-1} denoting the Si-O-Si linkages was expected to be observed due to the addition of the nanoclay additive, (**see section 2, Fig. 2.4c**) however this peak was not present, and this was thought to be due to the method of analysis used, with the FTIR-ATR technique only measuring the surface of the PU film. Therefore it was suspected that the nanoclay additive was dispersed within the bulk of the PU films and not present on the surface. To examine the dispersion of the nanoclay, TEM

analysis was performed and the results are given in **Fig.6.7**. From the images obtained it can be seen that the nanoclay was present and well dispersed within the PU films.

The addition of Cloisite 30B to the PU samples was found to increase the thermal stability. **Fig. 6.8** displays the TGA thermograms where it can be noted that thermal degradation of the hard segment for **PU CE30** occurred at 330°C, for **PU PR30**, was at 318°C and for **PUI 30** at 310°C. The soft segment of the PU samples on the other hand exhibited greater thermal stability after the addition of the organoclay; **PU CE30** soft segment degradation occurred at 439°C (**PU CE** 427°C), **PU PR30** soft segment degradation at 408°C (**PU PR** 390°C), and **PUI 30** soft segment degradation at 400°C (**PUI** 383°C).

Crystallinity and phase separation were determined using DSC, and results are given in **Fig. 6.9**. Phase separation was ascertained by examining the T_g value from the DSC thermographs and it was found that the addition of Cloisite 30B did not alter phase separation for **PU CE30**, **PUI 30** and **PU PR 30** with the T_g value for **PU CE30** at -15°C (**PU CE** -15°C) and **PUI 30** at -15°C (**PUI** -15°C), **Figs. 6.9 & 6.4**. **PU PR30** -16°C (**PU PR** -16°C) **Fig. 6.9 & Chapter 3 Fig.3.4**.

A decrease in crystallinity for all samples was noted compared to the original samples which did not contain Cloisite 30B. Two endotherms were observed for all of the samples in this group (group 5) at around 176°C and 200°C, indicating that the hard segment was of a highly ordered microcrystalline nature. The area under each peak was determined to quantify the microcrystalline domains and for **PUI 30** and **PU CE30** and it was found that these endotherms were of a smaller area than those of the control samples **PU CE** and **PUI** which contained only one large endotherm at around 196°C, **Figs. 6.9 & 6.4**. For **PU PR30** the endotherm at 196°C denoting highly crystalline regions was found to be less than that of **PU PR**, (**PU PR30** ΔH 0.6, **PU PR** ΔH 1.8), **Fig 6.9 & Chapter 3 Fig 3.4**, again indicating that the addition of Cloisite 30B decreased the concentration of highly crystalline regions.

Degradation and biodegradation of the group 4 and group 5 samples were then determined by subjecting the samples to alkaline hydrolysis, enzymatic hydrolysis and soil burial, and the results for alkaline hydrolysis are given below.

6.2.3 Effect of additives (**PU CE** and **PUI**) on the rate of alkaline hydrolysis

Samples were placed into a 10% NaOH solution for a period of 42 days and removed at weekly intervals to monitor degradation visually and by weight loss, with the aim of increasing the rate of degradation by alkaline hydrolysis in comparison to the control sample (**PU ADP**). Results obtained, **Fig 6.10**, showed that this was the case, whereas both **PUI** and

PU CE films completely broken up after 42 days. Both weight loss and visual images revealed **PUI** to degrade at a faster rate than **PU ADP** (control) and **PU CE**, with weight losses of **100% (PUI), 58% (PU CE) and 44% (PU ADP)**, with the **PUI** film completely broken up after 28 days, **Fig.6.11**. Microscopic images from **PU CE** and **PUI** obtained during hydrolysis also displayed extensive cracking after just 7 days in comparison to **PU ADP**, **Fig.6.12**. Also noteworthy was the microscopic image of **PU CE**, which clearly showed the PU film to be of a porous like nature, and may be one of the reasons for the increased rate of degradation of **PU CE**. FTIR-ATR was performed on the PU samples at weekly intervals to ascertain structural changes taking place during alkaline degradation.

6.2.3.1 Structural changes of PU CE and PUI during alkaline hydrolysis

Structural changes of the PU sample during hydrolysis were monitored by FTIR-ATR and compared to the initial spectra obtained prior to experimentation, see **section 6.2.1**.

i) Spectral changes Hard Segment structure PUI and PU CE

For **PUI**, the peaks relating to the hard segment structure were similar to that of **PU ADP** see **Section 3.1.1 & Fig. 6.13a & b**. From the spectrum obtained, **Fig.6.13c & d**, it can be seen that there were numerous changes during hydrolysis for the 42 days. The N-H peak at 3322cm^{-1} shifted to 3299cm^{-1} after 42 days and this peak was seen to increase after 28 days which indicates structural changes in the hard segment.

Some notable changes to the peaks relating the hard segment were observed for **PU CE**. After 35 days hydrolysis the N-H peak at 3323cm^{-1} shifted to 3303cm^{-1} and increased gradually indicating structural changes in the hard segment, **Fig.6.13e**. This can further be supported by changes in the peak at 1528cm^{-1} associated with the N-H + C-N (amide II) band which decreased and shifted to 1519cm^{-1} after 35 days, **Fig.6.13f**.

ii) Spectral changes Hard/Soft Segment Structure PUI and PU CE

Both **PUI** and **PU CE** displayed dramatic changes in the peaks relating to the hard/soft segment. The peak at 1726cm^{-1} representing the C=O free ester/urethane groups was seen to drop drastically after 14 days for both samples indicating that the non-hydrogen bonded ester/urethane groups had been hydrolysed, **Fig.6.14c & e**. The peak at 1703cm^{-1} associated with the hydrogen bonded ester/urethane group decreased over the 42 day period, and also shifted to 1695cm^{-1} . Also noteworthy was a substantial decrease of the peak at 1066cm^{-1} for both samples, denoting C-O-C linkages contained in the hard and soft segments, **Fig.6.14d & f**. The peak at 1381cm^{-1} relating to the CH₂ linkages were found to decrease substantially for both samples during alkaline hydrolysis, **Fig.6.13d & f**, and this

coupled with the increase in the peak at 1479cm^{-1} (CH group deformation absorbance) implied that some degradation of the both the hard and soft segment had occurred.

iii) Spectral changes Soft Segment Structure PUI and PU CE

For both **PUI** and **PU CE**, the soft segment can be characterized by the peak at 1137cm^{-1} shown in **Fig.6.14d & f**, which is associated with the C-(C=O)-O ester group. This peak was seen to decrease substantially (90% decrease in peak height) after just 7 days of exposure to 10% NaOH solution, indicating that soft segment had been hydrolysed.

6.2.4 Effect of modified nanoclay (Cloisite 30b) on the rate of alkaline hydrolysis, (PU PR30, PU CE30 and PUI 30)

PU PR30, **PU CE30** and **PUI 30** were subjected to accelerated alkaline hydrolysis, as of that for PU groups 1-4, **see Section 6.2.2**. Degradation was monitored both by weight loss and visually, and the results from these experiments are given in **Figs.6.15 & 6.16**. It can clearly be seen that the addition of Cloisite 30B increased the rate of alkaline hydrolysis significantly, **Fig.6.15** with all of the samples in this group becoming completely broken up after just 7 days, **Fig.6.16**. This was unexpected due to the hydrophobic nature of the samples (see section 6.2.2). To examine the changes taking place within the chemical structure during hydrolysis, FTIR-ATR analysis was undertaken.

6.2.4.1 Structural changes of PU PR30, PU CE30 and PUI 30 during alkaline hydrolysis

For all of the PU samples containing Cloisite 30B the most notable changes during alkaline hydrolysis were the peaks pertaining to the C=O ester and urethane linkages at 1728cm^{-1} , 1701cm^{-1} and 1138cm^{-1} . The trend was similar for all of the samples, with a dramatic decrease in the non-hydrogen bonded C=O ester/urethane peak at 1728cm^{-1} after only 7 days, **Fig.6.17**. The same was also observed for the peak at 1137cm^{-1} for all samples, with this peak disappearing after 7 days alkaline hydrolysis, **Fig.6.17**. Also noted was a substantial decrease in the peak at 1078cm^{-1} again for all samples, and this implies degradation of the C-O-C linkages contained within the hard segment and the hard/soft interfaces., **Fig.6.17**.

Changes to the hard segment structure are given in **Fig.6.18**, and display a similar trend for **PU PR30**, **PU CE30** and **PUI 30**. After 7 days of alkaline hydrolysis the peak at 3311cm^{-1} denoting the N-H group was seen to increase for all of the samples. A decrease in the peak at 1523cm^{-1} denoting the N-H urethane bend and C-N stretch was observed for **PU CE30** and **PUI 30**, and this indicated that some degradation of the urethane linkages had occurred.

The increase in the N-H stretch at 3311cm^{-1} was more than likely to be due to the formation of amine products during degradation.

A decrease was also observed in all of the peaks relating to the CH_2 moieties. **Fig. 6.18** displays these peaks for **PU PR30**, **PU CE30** and **PUI 30**, and it can be seen that the peaks at $\sim 2955\text{cm}^{-1}$, $\sim 1457\text{cm}^{-1}$ and 1381cm^{-1} all decreased after just 7 days of alkaline hydrolysis. This was observed for all of the PU samples in this group, and supports results from weight loss measurements and visual images in that substantial degradation of both the hard and soft segment had occurred.

6.2.4.2 Effect of Additives on Crystallinity during Alkaline Hydrolysis (PU PR30, PUI 30 and PU CE30)

Morphology of the PU samples was examined by DSC after exposure to alkaline hydrolysis for 7 days, and the results are given in **Fig.6.19**. Initial thermographs of **PU CE30**, **Fig 6.3** revealed a microcrystalline structure, with two endotherms observed at 195°C and 214°C . These peaks were seen to increase after 7 days indicating a more crystalline structure after degradation (ΔH initial 0.7 J/g & 1.15 J/g , after hydrolysis $\Delta H 18.78 \text{ J/g}$). The T_g value of **PU CE30** also indicated substantial structural changes to the PU sample with an initial value of -15°C , which then disappeared after 7 days, indicating that the soft segment had degraded.

Similar findings were also observed for **PUI 30**. The endotherms at 192°C and 208°C denoting highly crystalline hard segment domains increased from $\Delta H 0.9 \text{ J/g}$ to $\Delta H 23.7 \text{ J/g}$. after 7 days of exposure to the alkaline medium, **Fig. 6.19**. As of that for **PU CE30** the T_g for **PUI 30** was also seen to change dramatically after 7 days, which had an initial value of -15°C and then disappeared after 7 days, indicating that the soft segment had degraded.

PU PR30 also increased in crystallinity with the endotherms at 175°C and 196°C increasing from $\Delta H 1.3 \text{ J/g}$ and $\Delta H 0.6 \text{ J/g}$, respectively to $\Delta H 1.3 \text{ J/g}$ and $\Delta H 9.05 \text{ J/g}$ after 7 days hydrolysis, **Fig. 6.19**. As of that for **PUI 30** and **PU CE30**, a T_g value was not observed after 7 days alkaline hydrolysis, which indicated that the soft segment had degraded.

All of the samples in this group (group 5) and group 4 (PUI and PU CE) were placed in soil to monitor biodegradation, and the results are given below.

6.2.5 Susceptibility of polyurethane samples PUI and PU CE (Effect of Additives) towards biodegradation under soil burial conditions

PU samples were subjected to two different types of soil burial in order to assess their susceptibility towards microbial degradation in soil. The addition of additives was used to

determine whether iron stearate or cellulose would increase biodegradation under soil burial conditions. It would be assumed that the addition of iron stearate would increase the rate of biodegradation due to increased oxidative degradation occurring simultaneously with enzymatic/microbial degradation [9, 164]. The addition of cellulose would also be expected to increase the rate of biodegradation due to the fact that cellulose is a natural substrate which can be degraded by many microorganisms [77, 83, 85].

After 20 months of soil burial at RT there was limited weight loss in soil type 1, with the greatest weight loss occurring for **PUI** at 10% **Fig.6.20**. All of the PU film samples in group 4, in soil type 1 were still intact after 20 months and did not show any visible signs of cracking **Figs.6.21 & 6.22**. However, in soil type 2, **PU CE** was found to have degraded more than **PUI** and **PU ADP**, with a weight loss of 18%, **Fig.6.20**. After removal of the film from the soil, it was found that the film was not intact with part of film broken away from the sample. The remaining part of the film could not be recovered from the soil, and it was deduced that it had degraded.

The PU samples subjected to soil burial at 50°C after 5 months displayed a dramatic weight loss than those at RT **Fig.6.20**, with the greatest weight loss of 75% for **PUI**, although weight losses was also noted for **PU CE** at 62% and **PU ADP** 21%. After 5 months, the films **PUI** and **PU CE** were not intact and very fragile when removed from the soil **Fig.6.21**. In fact visible signs of cracking were observed after 3 months for **PU CE** **Fig.6.21**. In conclusion the PU films in this group were more susceptible to soil degradation with the addition of both of the additives iron stearate and cellulose at 50°C. Minimal degradation was observed for all samples in the soil at RT, however the addition of **PU CE** seemed to increase biodegradation in comparison to the other samples in this group.

6.2.5.1 Structural changes during soil burial at 50°C in PUI and PU CE monitored by FTIR-ATR.

Both **PU CE** and **PUI** displayed significant FTIR-ATR spectral changes during soil burial at 50°C, and these spectra are given in **Fig.6.23**. The peaks at 1726cm⁻¹ (1727cm⁻¹ **PUI**) and 1703cm⁻¹ denoting the free and hydrogen bonded C=O urethane and ester linkages respectively were seen to decrease after 5 months indicating that substantial degradation had occurred. This was deemed to be degradation of the soft segment, as the peak at 1138cm⁻¹ corresponding to the C-(C=O)-O-C ester linkages was also observed to decrease substantially after 5 months, with a new peak observed at 1038cm⁻¹ which was thought to correspond to the C-O stretch of an alcohol degradation product [105]. However, it was surmised that partial degradation of the hard segment had also occurred due to the small reduction in the peak at 1076cm⁻¹ and the new peak formed at 1659cm⁻¹, which is indicative

of amine degradation products [105]. However, whether the addition of cellulose and iron stearate to **PU ADP** increased biodegradation at 50°C is unclear, as **PU ADP** was also found to degrade after 5 months at this temperature.

6.2.5.2 Structural changes during soil burial at RT after 20 months in PUI and PU CE monitored by FTIR-ATR

Significant changes in the FTIR-ATR spectra were noted to both **PUI** and **PU CE** after 20 months soil burial and are given in **Fig.6.24**. A decrease was observed in the peaks relating to the C=O ester/urethane linkages at 1726cm⁻¹ and 1702cm⁻¹ for **PUI**, after burial in both soil type 1 and 2. However, the decrease in these peaks was more substantial for **PU CE**, indicating that this PU had degraded more than **PUI**. The same was observed for the peak at 1137cm⁻¹ denoting the O-C=O-C ester linkages, with this peak decreasing for both **PU CE** and **PUI** in both soil types.

Changes to the hard segment structure were also indicated, with the peak at 3317cm⁻¹ denoting the N-H urethane linkages increasing for **PU CE** after burial in soil type 1, **Fig. 6.24a**. This is more than likely due to the formation of amine degradation products. However, little change was noted with respect to the N-H bond after burial in soil type 2. The opposite was found for **PUI**, shown in **Fig.6.24b** with a large increase in the peak at 3318cm⁻¹ after burial in soil type 2, with the formation of a shoulder on this peak, indicating possible alcohol degradation products, however, this finding was not observed after burial in soil type 1.

6.2.6 Susceptibility of polyurethane samples PU PR30, PU CE30 and PUI 30 (Effect of Nanoclay, Cloisite 30b) towards biodegradation under soil burial conditions

The addition of Cloisite 30B to the PU samples **PU PR**, **PUI** and **PU CE** affected the rate of degradation under soil burial conditions at 50°C and RT. The results are given in **Fig 6.25**. After 5 months the **PU PR30** film was still intact with only minimal visual degradation observed. The weight loss also supported this finding with 72% weight remaining after the 5 months, **Fig.6.25a**. Greater degradation was observed for **PUI 30** and **PU CE30**, with 50% weight remaining for both of these PU films, **Fig.6.25a**. Visual images also supported this with the films fragile and brittle. Small sections of the films were also observed to have broken away from the original films indicating extensive degradation, **Fig.6.26**. Structural changes were monitored using FTIR-ATR. Conversely, the samples when subjected to soil

burial at RT displayed relatively little weight loss, **Fig 6.25b & c**. However, microscopic images did show some signs of degradation occurring for PU CE30 in soil type 2, **Fig. 6.27**.

6.2.6.1 Structural changes during soil burial at 50°C in PU PR30, PU CE30 and PUI 30 monitored by FTIR-ATR.

Noticeable differences were observed in the PU films after 5 months of soil burial at 50°C. Spectral changes for each of these samples are given in **Fig.6.28** and all of the samples in this group displayed similar changes. The peaks at ~1727cm⁻¹ denoting free C=O urethane and ester linkages were seen to decrease after the 5 months for all samples. The same was also observed for the peak at 1700cm⁻¹ denoting the hydrogen bonded C=O linkages. Degradation of the ester soft segment was also indicated for all of the samples with the peak at 1138cm⁻¹ decreasing dramatically after 5 months, **Fig.6.28**. A large peak at 1017cm⁻¹ was observed for **PU CE30** after 5 months soil burial, **Fig.6.28f**, which was not seen in the original sample, and this was thought to be due to the Si-O-Si linkage contained within the Cloisite 30B additive; as the PU film degraded the additive which was dispersed within the bulk of the sample was then exposed on the surface of the sample, thereby showing this peak on the spectrum of the degraded sample.

6.2.6.2 Structural changes during soil burial at RT after 20 months in PU PR30 and PU CE30 and PUI 30 monitored by FTIR-ATR

FTIR-ATR spectra obtained for **PUI 30** after 20 months soil burial revealed that minimal degradation had occurred for all samples, with almost no difference found between the initial spectra and after burial in soil 1, **Fig.6.29**. However, some minor differences were observed for the film buried in soil type 2, with decreases observed at 1726cm⁻¹, 1701cm⁻¹, 1529cm⁻¹ and 1222cm⁻¹, denoting the free and hydrogen bonded C=O ester/urethane linkages, C-N & N-H bend and C-N linkages respectively, **Fig.6.29**. No changes were observed relating to the soft segment ester groups given by the peaks at 1163cm⁻¹ and 1139cm⁻¹ for all samples. These results imply that the soft segment had remained intact with degradation occurring in the hard segment. However, as microscopic images for **PU CE30** displayed cracking within the film, degradation of this sample may have occurred in the bulk and not on the surface.

PU samples were then subjected to enzymatic hydrolysis.

6.2.7. Susceptibility of Polyurethane Samples PUI and PU CE (Effect of Additives) towards enzymatic degradation.

PU samples **PUI** and **PU CE** were exposed to fungal lipases from *Aspergillus niger* and *Rhizopus* sp. and a protease from *Rhizopus* sp. in order to ascertain rate of degradation by enzymatic hydrolysis.

Samples were immersed in a phosphate buffer solution containing the enzyme. After 24 days there was very little weight loss observed for any of the samples in this group (not shown), however, microscopic images did reveal signs of degradation dependant on the enzyme used, **Figs.6.30 & 6.31**. The PU samples in this group did not display any weight loss or visual degradation after exposure to the protease from *Rhizopus* sp. (not shown).

PU CE did seem susceptible to degradation by both *Rhizopus* sp. and *Aspergillus niger*, with cracking observed on both of these films, however the cracking was more extensive when **PU CE** was exposed to *Aspergillus niger*, **Figs.6.30 & 6.31**. Although the **PUI** film samples also displayed minor degradation after exposure to the lipases, the extent of degradation was not deemed to be as extensive as that of **PU CE**, **Figs. 6.30 & 6.31**. Results from FTIR-ATR analysis which are given in **Fig.6.32**, also supported these findings in that for both **PUI** and **PU CE** the peaks at 1702cm^{-1} (hydrogen bonded C=O) 1727cm^{-1} (non-bonded C=O) and 1137cm^{-1} (C=O ester) decreased after 24 days exposure, indicating that some degradation of the ester soft segment had occurred. There was also a small decrease in the peak at 1077cm^{-1} denoting C-O-C bonds **Fig. 6.32**, along with a small decrease at 1220cm^{-1} relating to the N-H and C-N group. Therefore it can be assumed that the hard segment was subjected to a limited amount of degradation. In comparison, **PU ADP** (control sample), displayed relatively minimal changes in the FTIR-ATR spectra after exposure to the lipases, with only small decreases observed at 1701cm^{-1} , 1727cm^{-1} and 1137cm^{-1} after exposure to *Aspergillus niger*, and no noticeable differences observed in the spectra after exposure to *Rhizopus* sp. This can further be supported by visual images in which minimal degradation was observed, **Figs. 6.30 & 6.31**, and one can conclude that the addition of both cellulose and iron stearate did increase susceptibility of PU towards enzymatic degradation, with the extent of degradation occurring in the order of **PU CE > PUI > PU ADP** for both *Aspergillus niger* and *Rhizopus* sp.

6.2.8. Susceptibility of Polyurethane Samples PU PR30, PU CE30 and PUI 30 (Effect of Modified Nanoclay cloisite 30b) towards enzymatic degradation

Samples were exposed to Lipases from *Aspergillus niger* and *Rhizopus* sp., and the results were disappointing in that no weight loss (not shown) or visual degradation, **Figs. 6.33-6.34** was observed after 24 days. Results from FTIR-ATR analysis also displayed relatively little structural changes to the PU films after exposure, **Fig 6.35**. A small decrease in the peak at 1726cm^{-1} was observed for all samples in this group, indicating degradation of the free ester/urethane C=O linkages, however, the peak denoting the ester linkages in the soft segment at 1137cm^{-1} was unchanged after exposure to the lipases for all samples, and can therefore conclude that partial degradation of the hard segment had occurred with little or no degradation occurring within the soft segment. This can be supported by a small decrease at 1220cm^{-1} denoting the C-N urethane linkages. Overall, these results were disappointing as none of the PU films in this group were susceptible towards enzymatic degradation by the enzymes used in this study.

6.3 Discussion

6.3.1 Effect of Cellulose and Iron Stearate as Additives on Polyurethane Degradation and Biodegradation

The cellulose and iron stearate were chosen as additives for **PU ADP**, due to their specific action that may contribute to degradation mechanisms of the polymer. Cellulose, which in itself is a natural polymer contains numerous hydroxyl groups, is was expected to increase the degradation and biodegradation by increasing the hydrophilicity of the PU result in an increase in the rate of hydrolysis. Iron stearate, on the other hand, was added to increase degradation by oxidative processes by acting as a pro-oxidant [9, 74, 164]

From the results obtained it was found that the addition of cellulose did increase the rate of hydrolysis under accelerated alkaline conditions, with a weight loss of 58% as opposed to the control sample **PU ADP** with a weight loss of 44%, **Fig.6.10**. However, the weight losses given do not highlight the significant differences in the rate of degradation between these samples, as visual images taken during the experiment revealed that **PU CE** had degraded significantly more than **PU ADP**, with the **PU ADP** film remaining intact and the **PU CE** becoming completely broken up after 42 days, **Fig.6.11**.

The morphology of **PU ADP** and **PU CE** were compared using DSC, and the thermographs for the un-degraded samples are given in **Fig.6.4**. It was found that the addition of cellulose altered the morphology of the PU dramatically with only one endotherm visible at $202\text{ }^{\circ}\text{C}$ (ΔH

8.31J/g), denoting highly structured crystalline regions contained within the hard segment. Conversely, **PU ADP** displayed three endotherms at 109 °C, 147 °C and 195 °C (ΔH 6.1 J/g), **Fig.6.4** indicating that although the hard segment contained a large proportion of highly structured crystalline domains, less ordered regions were also present. This was surprising in that previous studies have shown that an increase in crystallinity would decrease the rate of hydrolysis [59, 60, 100, 120]. Cellulose itself has been shown to be of a highly crystalline nature [83, 85], and has also been shown to increase crystallinity when incorporated into polymer systems [71, 81].

As the extent of hydrogen bonding in PUs has been shown to affect PU morphology, it was suspected that the addition of cellulose would increase hydrogen bonding interactions in **PU CE**, thereby increasing crystallinity. The extent of hydrogen bonding was determined by analysis of the FTIR-ATR spectra obtained on virgin samples using peak fitting software Origin, and measuring the area under each peak, this method has been used previously to determine the extent of hydrogen bonding in PUs [46, 143]. Results are given in **Table 6.2** and show that the extent of hydrogen bonding in **PU CE** decreased in comparison to **PU ADP**, therefore differences in phase separation were considered in order to provide an explanation as to the increased rate of hydrolysis.

Phase separation was determined by examination of the T_g value, which was found to increase slightly with the addition of the cellulose powder (**PU ADP** -18°C, **PU CE** -15°C), indicating that the hard and soft segments were less phase separated than the control sample **PU ADP**, **Fig.6.4**. Although previous studies have shown phase separation in PU to have an influence on the rate of degradation [54], this was not considered to be a major factor on the increased rate of hydrolysis of **PU CE** as the difference in the T_g values was minimal.

The addition of cellulose did increase the hydrophilic nature of the PU, which was found to be **4.5% (PU ADP) and 8.5% (PU CE)**. This increase was thought to be influential on the increased rate of hydrolytic degradation. Also noteworthy, was the ‘porous’ like film structure of PU CE which was observed using optical microscopy, **Fig.6.2A**. This was also suspected to have contributed to the increased rate of hydrolysis of **PU CE** in comparison to **PU ADP**. This ‘porosity’ has also been observed in other polymeric materials which have incorporated cellulose into the polymer bulk, and it has been speculated that the ‘porous’ structure increases the rate of degradation and biodegradation due to the higher interfacial area that this morphology confers [82], and therefore it was surmised that the porous morphology of **PU CE** resulted in more of the PU film samples being exposed to the NaOH solution, thereby increasing the rate of hydrolysis.

Similar findings were also observed after soil burial experiments, in which **PU CE** was placed into two different types of soil at RT for a period of 20 months. Minimal visual degradation was observed in respect of the control sample **PU ADP**, however, after burial in soil type 2 **PU CE** did display visual signs of degradation, with the film not intact upon removal, **Fig.6.21**. Limited degradation had occurred in soil type 1 though for either sample. Degradation of the urethane and ester linkages contained within **PU CE** had partially degraded, and the FTIR-ATR spectra denoting the urethane and ester linkages supported this, with decreases observed at 1726cm^{-1} and 1137cm^{-1} , **Fig 6.24c & e**. The degradation was not substantial, and this was thought to be due to the nature of the chemical components of this PU, which was synthesised with the same raw materials as that of the control sample **PU ADP** (MDI, BD, ADP), which had previously been found to be non-biodegradable. Therefore, although the addition of cellulose did not result in complete degradation of the PU sample under soil burial conditions, it did increase the biodegradability of a PU previously deemed to be non-biodegradable. This finding supports similar results in the literature in which the addition of cellulose fibres increased the biodegradability of polyethylene [82], and this has been thought to be due to not only the porous nature of the polymer matrix with the addition of cellulose, but also the fact that cellulose itself is a food source for microbes, which as they digest the cellulose, leaves indentations and cavities in the polymer surface which then facilitates increased biodegradation [82].

Previous studies have highlighted that hydrophobic interactions are involved in the enzymatic degradation of polymers [19, 57, 120], and it was thought that the increased hydrophilicity of **PU CE** would reduce the rate of enzymatic hydrolysis. However, enzymatic degradation of **PU CE** resulted in degradation occurring, which was found to be dependent on the choice of the enzyme, with the film samples being more susceptible towards enzymatic degradation by the lipase from *Aspergillus niger*, with extensive cracking observed microscopically, **Fig. 6.33**. This was supported by FTIR-ATR analysis with the peaks at 1702cm^{-1} (hydrogen bonded C=O) 1727cm^{-1} (non-bonded C=O) and 1137cm^{-1} (C=O ester) decreasing after 24 days exposure, **Fig. 6.32c & d**. The increased susceptibility towards enzymatic degradation by *Aspergillus niger* was thought to be due to the porous nature of the film, thereby exposing more surface area of the PU film to the enzyme.

Iron stearate has been added into polymeric materials in order to increase degradation by oxidative means [9, 74, 165], and therefore iron stearate was added as a means to possibly increase the degradation and biodegradation of the control **PU ADP**. The addition of iron stearate did increase the rate of hydrolysis of **PUI**, when samples were subjected to accelerated alkaline hydrolysis, and the samples were seen to degrade faster than both **PU ADP** and **PU CE**, with cracks appearing in the film after only 14 days, **Fig. 6.11**. Examination

of morphology by DSC, **Fig. 6.4**, revealed that as with **PU CE** the addition of iron stearate increased PU crystallinity, with the microcrystalline hard segment region increasing from ΔH 6.1 J/g for **PU ADP** to ΔH 7.2J/g for **PUI**, this was unexpected in that increased crystallinity has been associated with decreased degradation [30, 59] however, as the accelerated hydrolysis was performed at 45°C it was suspected that the addition of iron stearate made the PU more susceptible towards thermal degradation, by increasing the rate of hydrolysis, [34]. however, it was suspected that **PUI** would not induce an increase in degradation by soil burial at RT.

Results from soil burial experiments confirmed this suggestion. Soil burial at 50°C resulted in complete break up of **PUI** which was not observed to the same extent in **PU ADP** or **PU CE**, **Fig. 6.21**. However, soil burial at RT for 20 months did not reveal any signs of biodegradation visually for **PUI**, **Fig. 6.21**. This was confirmed by FTIR-ATR, which showed only minimal decreases in the peaks at 1725cm^{-1} and 1137cm^{-1} relating to the urethane and ester linkages, **Fig. 6.24**. These results confirmed that the increase in temperature to 50°C resulted in an increased rate of biodegradation of **PUI** under soil burial conditions compared to **PU ADP** and **PU CE**, again thought to be due to the thermal properties of **PUI**, however at RT no biodegradation of **PUI** was observed, **Fig. 6.21**.

Similar results were found when **PUI** was exposed to enzymatic degradation, with minimal degradation observed visually compared to **PU CE**, **Fig 6.30**. However, FTIR-ATR spectra did reveal degradation of the ester and urethane linkages, which were substantially greater than that of the control sample **PU ADP**, **Fig. 6.32**, indicating that the addition of iron stearate increased the rate of enzymatic degradation. This may be due to the structure of iron stearate, which in itself would probably be susceptible towards degradation by lipases, as the three stearate chains, which in themselves are esterified moieties of steric acid, are substrates for lipases, and therefore the hydrolysis of these ester groups may increase degradation within the PU matrix. However, this was not examined and therefore could possibly be investigated in the future.

6.3.2 Effect of the addition of Cloisite 30B on Polyurethane Degradation and Biodegradation

The addition of organoclays to alter polymer properties has been the focus of much research, and previous studies to increase biodegradation and degradation by the incorporation of such clays has resulted in conflicting results [73, 92-94], which seems to be dependent on the type of clays used, the concentration of clay and the type of polymer system, along with processing conditions and numerous other factors [161]. Cloisite 30B was added to the **PU CE30**, **PUI 30** and **PU PR30**, and compared to the control sample **PU ADP** and also the corresponding PUs without the clay; **PU CE**, **PUI** and **PU PR**, and the results obtained were interesting.

Accelerated hydrolysis of the samples proved to have a dramatic effect on all of the samples containing Cloisite 30B, with the all of the films completely broken up after only 7 days, and extensive cracking observed after 48 hours **Fig.6.16**, and results from FTIR-ATR spectra displayed significant decreases in the peaks pertaining to the C=O ester and urethane linkages at 1728cm^{-1} , 1701cm^{-1} and 1138cm^{-1} and a substantial decrease in the peak at 1078cm^{-1} . This was observed for all samples with little difference noted between them, therefore it could not be stated whether the addition of the organoclay with another additive (**PU CE30** and **PUI 30**) increased the rate of hydrolysis compared to **PU PR30** which contained only the clay. A decrease in the peak at 3311cm^{-1} denoting the N-H stretch of the urethane linkages was seen to increase for all of the samples, indicating the formation of amines, **Fig.6.18**.

This dramatic increase in the rate of alkaline hydrolysis, **Fig. 6.16**, was unexpected due to some of the physical properties, examined by DSC and TGA that these PU films displayed prior to the degradation experiments. Thermal stability was measured using TGA, and it was found that all of the samples in this group exhibited a greater thermal stability than the corresponding films without the addition of the organoclay, **Figs.6.3 & 6.8**. It was also noted that all of these films were somewhat crystalline in nature with an endotherm at $\sim 200^\circ\text{C}$, for **PU CE30 ΔH 1.15 J/g**, **PUI 30 0.9**, **PU PR30 ΔH 0.6 J/g**, **Fig.6.9**, denoting highly ordered microcrystalline domains, and as previous studies have shown, increased crystallinity gave rise to a decrease in the rate of degradation [121]. However, these crystalline domains were less in comparison to the control samples **PU CE (ΔH 8.3 J/g)**, **PUI (ΔH 7.2 J/g)** and **PU PR (ΔH 1.8 J/g)**.

Also surprising was the hydrophobicity that these films displayed after the addition of Cloisite 30B, (**PU PR30 2%**, **PU PR 3.6%**; **PUI 30 2%**, **PUI 8.2%**; **PU CE30 3%**, **PU CE 8.5%**) **Fig.6.5**. This phenomenon has previously been observed, and it was shown that Cloisite 30B

had a lower water affinity than unmodified montmorillonite due to the hydrophobicity of the modifier which contains long hydrophobic chains [86]. Previous studies, and results from earlier chapters found that increased hydrophobicity decreased the rate of hydrolysis, therefore it would be expected that this increase in hydrophobicity, would increase the crystallinity whereas thermal stability would decrease the rate of hydrolysis. However, the addition of Cloisite 30B was seen to dramatically increase the rate of hydrolysis, **Fig. 6.16**. Similar findings were observed by Jeong et al., [110] who incorporated Cloisite 30B in PU synthesised with PCL/MDI/BD. The addition of 7% clay increased weight loss after 12 days by over 30%, compared to the PU without clay, with a weight loss of <5% [110]. They explained the increase in hydrolysis by differences in phase separation, with the nanocomposites being more phase separated than the PCL/MDI/BD PU. However, this was not found to be the case here for **PU CE30**, **PUI 30** and **PU PR30**. Phase separation was examined using the Tg values obtained from virgin polymer samples containing Cloisite 30B and compared to the control samples which did not contain clays, and it was found that the addition of Cloisite 30B did not alter phase separation for any of the samples in this group (**PU CE Tg -15°C**, **PU CE30 Tg -15°C**), (**PUI Tg -15°C**, **PUI 30 Tg -15°C**), (**PU PR Tg -16°C**, **PU PR30 Tg -16°C**), **Figs. 6.4 & 6.9**, therefore this could not be offered as an explanation as to the increase in the rate of hydrolytic degradation. Subsequently, the extent of hydrogen bonding was examined using the Origin software by Lorenzian peak fitting program, to analyse the appropriate peak areas. It can be noted that the addition of the organoclay resulted in a small increase in hydrogen bonded C=O linkages denoted by the peak at 1701cm⁻¹, **Table 6.3**. This was found to be the case for all samples in this group, and was most notable for **PU CE30**, **Figs. 6.36-6.38**. However, this slight increase in hydrogen bonding would not explain the increased rate of hydrolytic degradation.

Addition of organoclays to increase degradation and biodegradation of PU has not been studied extensively, however some investigations have been reported [110, 166]. Addition of nanocomposites into PLA and PCL has been studied more extensively, and many of these studies found that the addition of organoclays increased the rate of hydrolysis dramatically [94, 167, 168]. Numerous explanations have been proposed as to the reason for this increase, and some of these theories include; decrease in crystallinity [169], higher water absorption properties [170] and chemical structure of organoclay [171]. From the results obtained, the only plausible explanation which could account for the increased rate of hydrolysis of **PU CE30**, **PUI 30** and **PU PR30** is the slight decrease in crystalline regions with the addition of the clay compared to the control samples **PU CE**, **PUI** and **PU PR** as addition of the clay in these samples resulted in a PU in which more hydrogen bonding occurring

between the hard and soft segments, **Table 6.3**, and were more hydrophobic than the control samples without the organoclay.

Soil burial and enzymatic degradation results proved disappointing. **PU PR30** and **PUI 30** did not display any signs of degradation either by weight loss or visually after soil burial at RT for 20 months, **Fig.6.27**. However, microscopic images of **PU CE30** did reveal signs of cracking of the PU film, similar to those found when films were exposed to alkaline hydrolysis, **Fig.6.27**. Weight loss measurements, **Fig. 6.20**, did not reveal any significant changes, and can therefore conclude that only minimal degradation had occurred. Structural changes in each of the PU samples were monitored by FTIR-ATR, in which only minor differences at 1726cm^{-1} , 1701cm^{-1} , 1529cm^{-1} and 1222cm^{-1} , were observed after burial in soil type 2, indicating minimal degradation of the hard segment or hard/soft segment interfaces, **Fig.6.29**. The soft segment ester groups had not degraded, with the peaks at 1163cm^{-1} and 1139cm^{-1} remaining unchanged after soil burial, **Fig.6.29 b,d & f**. which supported weight loss and visual findings. These results proved interesting in that these films completely degraded under alkaline conditions after 7 days, but proved to be relatively resistance to biodegradation. This is especially noteworthy in the case of **PU CE30**, which contained cellulose, and previous results for **PU CE** proved that the addition of cellulose into the PU matrix increased biodegradability however the addition of Cloisite 30B to this PU decreased the rate of biodegradation.

Exposure to lipases by *Aspergillus niger* and *Rhizopus* sp. revealed similar findings to that of soil burial with no weight loss or microscopic visual degradation observed for all samples, **Figs. 6.33 – 6.35**. The resistance towards biodegradation and enzymatic degradation of polymer nanocomposites has also been noted in previous studies [73, 92], and an explanation for this has been proposed by Bikiaris [161], who examined degradation of polyester nanocomposites, and suggested that reduced enzyme attack and growth occurs on polyester nanocomposites due to increased barrier properties and, reduction of the surface area available for enzymatic hydrolysis, due to the fact that nano additives cannot be degraded by enzymes, and their position on the surface of the polymer would reduce the rate of degradation [161]. This theory does make logical sense and could be applied to the samples examined in this chapter, specifically **PU CE30**, which when compared to the control sample **PU CE** exhibited a decreased rate in enzymatic degradation, **Figs. 6.33 & 6.30**.

6.3.3 Overall Summary of the effect of Additives on Polyurethane Degradation and Biodegradation

The work described in this chapter examined the effect of three additives on the hydrolytic, enzymatic and biodegradation of PUs.

Overall, comparison of the rate of degradation of **PU ADP**, **PU CE** and **PUI** was found to be dependent upon the method used to degrade the samples. Accelerated hydrolysis, **Fig.6.10**, revealed the rate of degradation to be in the order of **PU ADP< PU CE< PUI**. The addition of cellulose increased microcrystalline hard segment domains in the PU samples, **Fig. 6.4**, which was thought to decrease the rate of alkaline hydrolysis of **PU CE**, however this was not found to be the case, with **PU CE** degrading after 42 days while **PU ADP** the control sample remained intact, **Fig. 6.11**.

Biodegradation of the samples under soil burial conditions at 50°C was found to be in the order of **PU ADP < PU CE < PUI**, **Fig. 6.20**, however, at RT the order was **PU ADP < PUI < PU CE**, **Fig. 6.20**, and the difference was thought to be due to thermal degradation of PUI. Enzymatic degradation revealed that only **PU CE** had degraded significantly, therefore only **PU CE** was deemed to confer degradability on PU irrespective of the method of degradation, and this was thought to be due to the overriding effect of increased hydrophilicity, **Fig. 6.1a**, and porous like structure of the PU films, **Fig. 6.2a**, which increased the rate of alkaline hydrolysis, enzymatic hydrolysis and biodegradation.

Addition of the organoclay, Cloisite 30B into **PU PR**, **PU CE** and **PUI** resulted in mixed findings, and again was found to be dependent on the method used to degrade the samples. Results from alkaline hydrolysis revealed that addition of the clay accelerated hydrolysis dramatically with the films completely broken up after just 7 days, for **PU PR30**, **PU CE30** and **PUI 30**, **Fig 6.16**. All of the samples displayed greater thermal stability, **Figs. 6.3 & 6.8**, increased hydrophobicity, **Fig. 6.5**, and increased hydrogen bonding, **Table 6.3**, within the PU matrix than the control samples, all of which have previously been found to decrease the rate of hydrolysis. Therefore the most likely explanation as to this increase in hydrolytic degradation was the decrease in the microcrystalline domains, **Figs. 6.4 & 6.9**, with the addition of Cloisite 30B.

Biodegradation under soil burial conditions and enzymatic degradation produced opposite results to those of alkaline hydrolysis, in which the addition of the organoclay reduced degradation in the case of **PU CE30**, **Figs. 6.21 & 6.26**, and did not induce degradation of **PUI 30** or **PU PR30**. This was thought to be due to the inaccessibility of the microorganisms and enzymes to the PUs which displayed increased barrier properties.

Results

Table 6.1a Effect of Additives on PU Degradation

PU Code	Composition				M.w.t Ratio % polyol: isocyanate: chain extender	Method of synthesis (Table 3.1a)
	Soft segment polyol	Hard segment		Additive		
		Isocyanate	Chain Extender			
PU CE	Poly (ethylene adipate) (PEA)	Methylene diisocyanate (MDI)	Butane diol (BD)	Cellulose Powder (50µm) (2%)	1:3:2	OS-102
PUI	Poly (ethylene adipate) (PEA)	Methylene diisocyanate (MDI)	Butane diol (BD)	Iron Stearate (2%)	1:3:2	OS-102
PU PR	Poly(ethylene adipate) (PEA)	Methylene diisocyanate (MDI)	Butane diol (BD)	-	1:3:2	OS-102
PU Code	Chemical Structure					
PU PR PU CE & PUI						
	Additive PU CE - Cellulose 		Additive PUI - Iron Stearate 			

Table 6.1b Effect of Additive Cloisite 30B alone and in the Presence of other Additives on PU Degradation

PU Code	Composition				M.w.t Ratio polyol: isocyanate: chain extender	Method of synthesis (Table 3.1a)	
	Soft segment polyol	Hard segment		Additive			
		Isocyanate	Chain Extender				
PU PR30	Polyethylene adipate (PEA)	Methylene diisocyanate (MDI)	Butane diol (BD)	Cloisite 30B (12%)	1:3:2	PR - 102	
PU CE30	Polyethylene adipate (PEA)	Methylene diisocyanate (MDI)	Butane diol (BD)	Cellulose Powder (50µm) (2%) & Cloisite 30B (12%)	1:3:2	OS-102	
PUI 30	Polyethylene adipate (PEA)	Methylene diisocyanate (MDI)	Butane diol (BD)	Iron Stearate (2%) & Cloisite 30B (12%)	1:3:2	OS-102	
PU Code	Chemical Structure						
PU CE30 PU PR30 PUI 30							
PU PR30	No Additional Additive						
PU CE30	Additive Cellulose						
PUI 30	Additive Iron Stearate						

T is Tallow (65%,C₁₈; ~30%,C₁₆; ~5%,C₁₄)
Surfactant used in Cloisite 30B nanoclay

Table 6.2 Assignment of N-H and C=O bands, area of deconvoluted peaks

Sample Code	N-H Stretching Urethane		C=O Stretching Urethane/ester	
	Band I (area) Non- hydrogen Bonded $\nu \sim 3322\text{cm}^{-1}$	Band II (area) Hydrogen Bonded $\nu \sim 3332\text{cm}^{-1}$	Band I (area) Hydrogen Bonded $\nu \sim 1702\text{cm}^{-1}$	Band II (area) Non-hydrogen Bonded $\nu \sim 1727\text{cm}^{-1}$
PU ADP (Control)	2.3	2.6	14.7	16.2
PU PR	3.0	2.7	14.4	16.0
PU PR30	5.7	-	16.1	13.7
PUI	5.6	-	15.3	16.4
PUI 30	5.5	-	16.0	14.3
PU CE	5.0	-	14.7	17.5
PU CE30	6.3	-	18.0	15.5

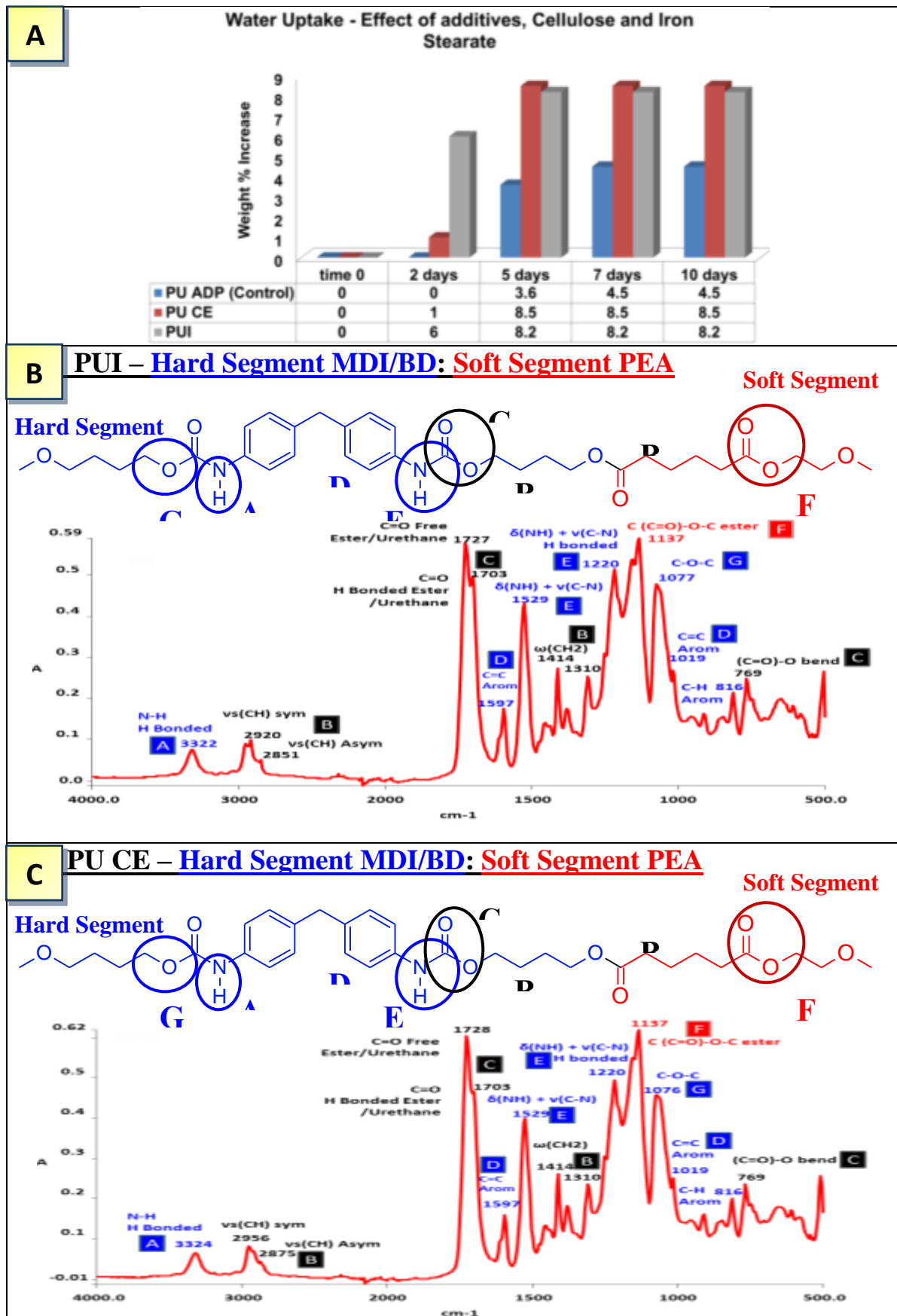


Figure 6.1 Hydrophilicity of PU samples (A) chemical structure characterisation of PU samples PUI (B), PU CE (C), by FTIR-ATR

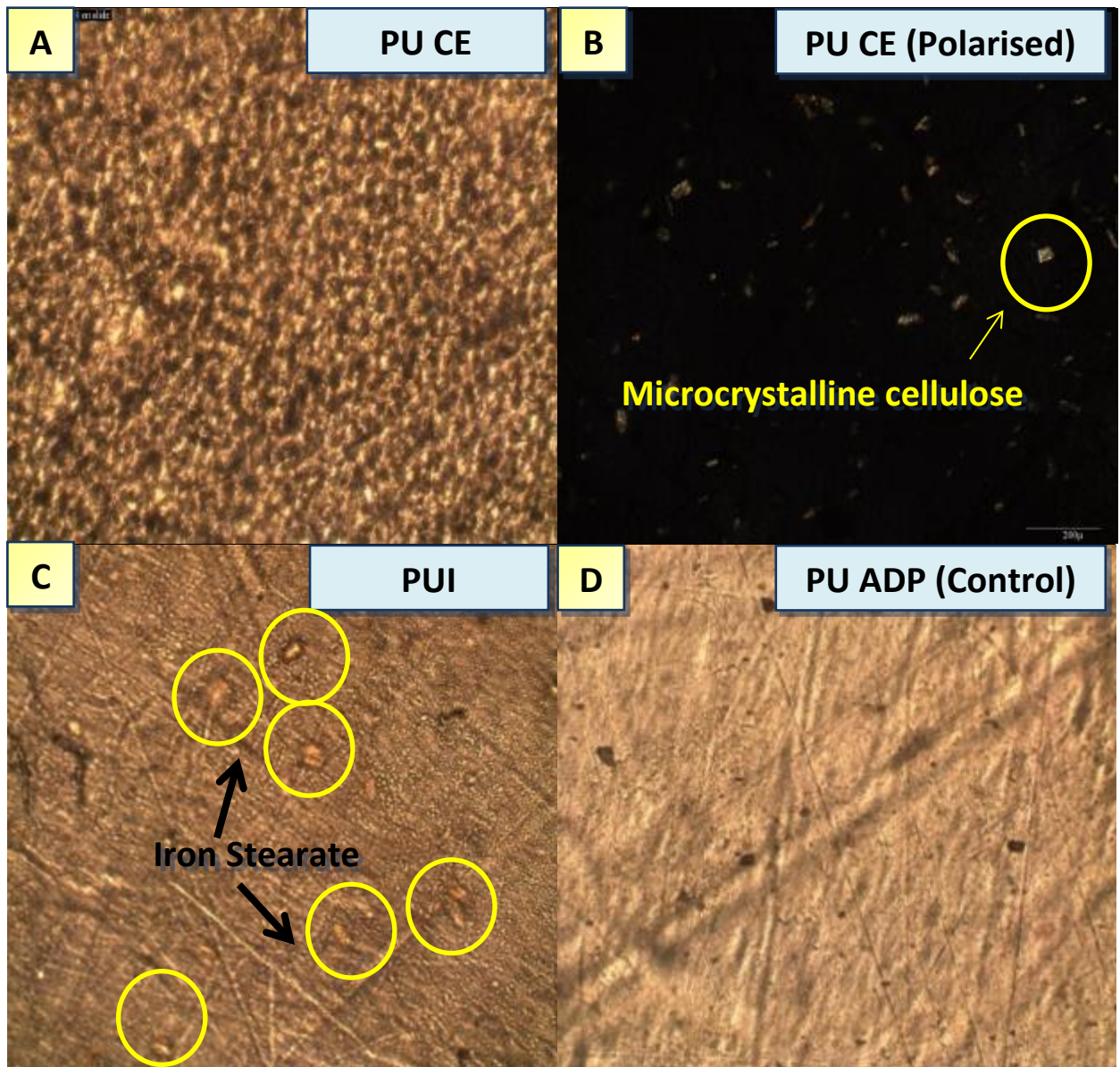


Figure 6.2 Microscopic images showing dispersal of cellulose in PU CE (**A-B**) and iron stearate in PUI (**C**) in comparison to the control sample PU ADP (**D**)

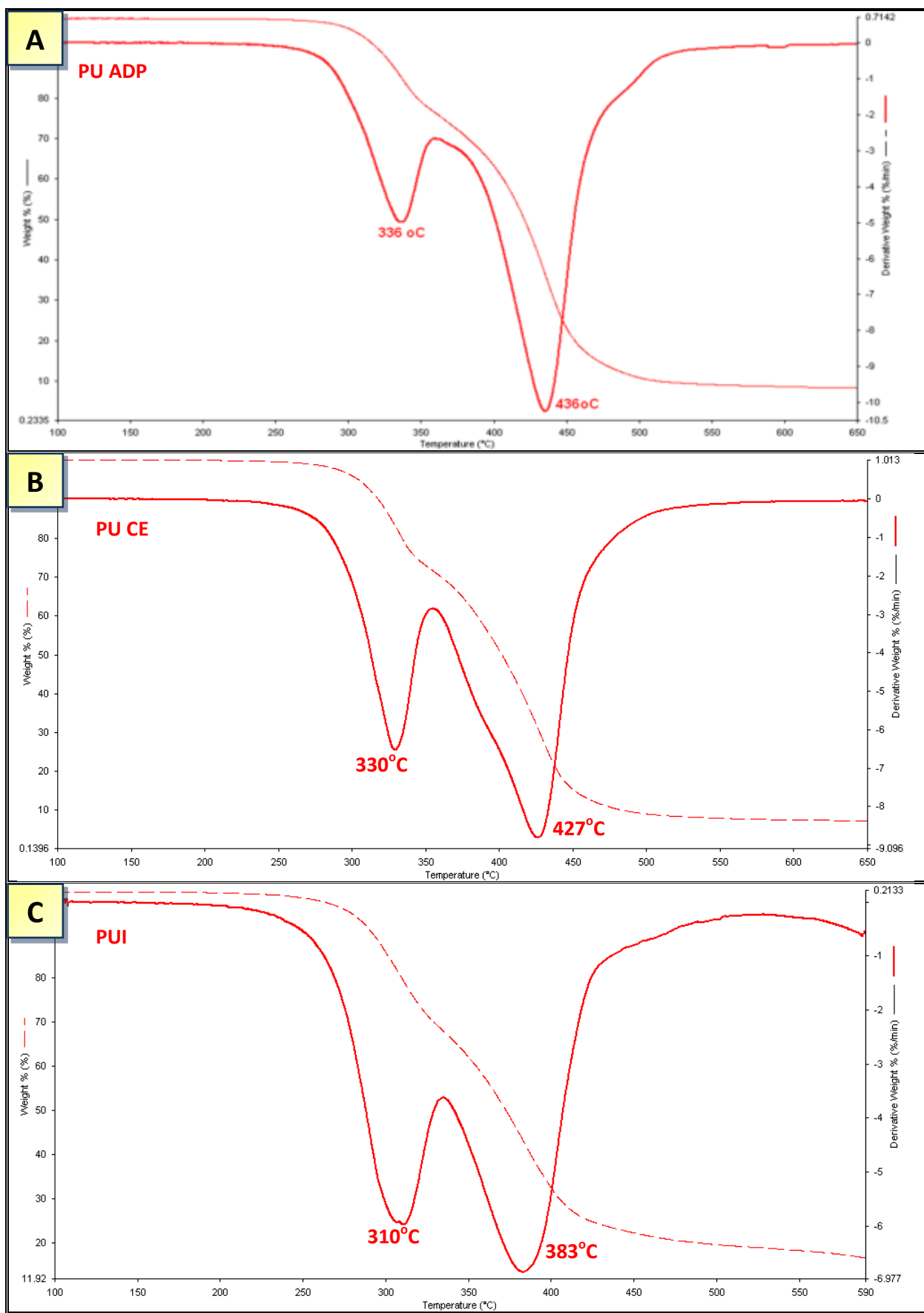


Figure 6.3 TGA thermal analysis characterisation of PU, PU ADP (A), PU CE (B), PUI (C)

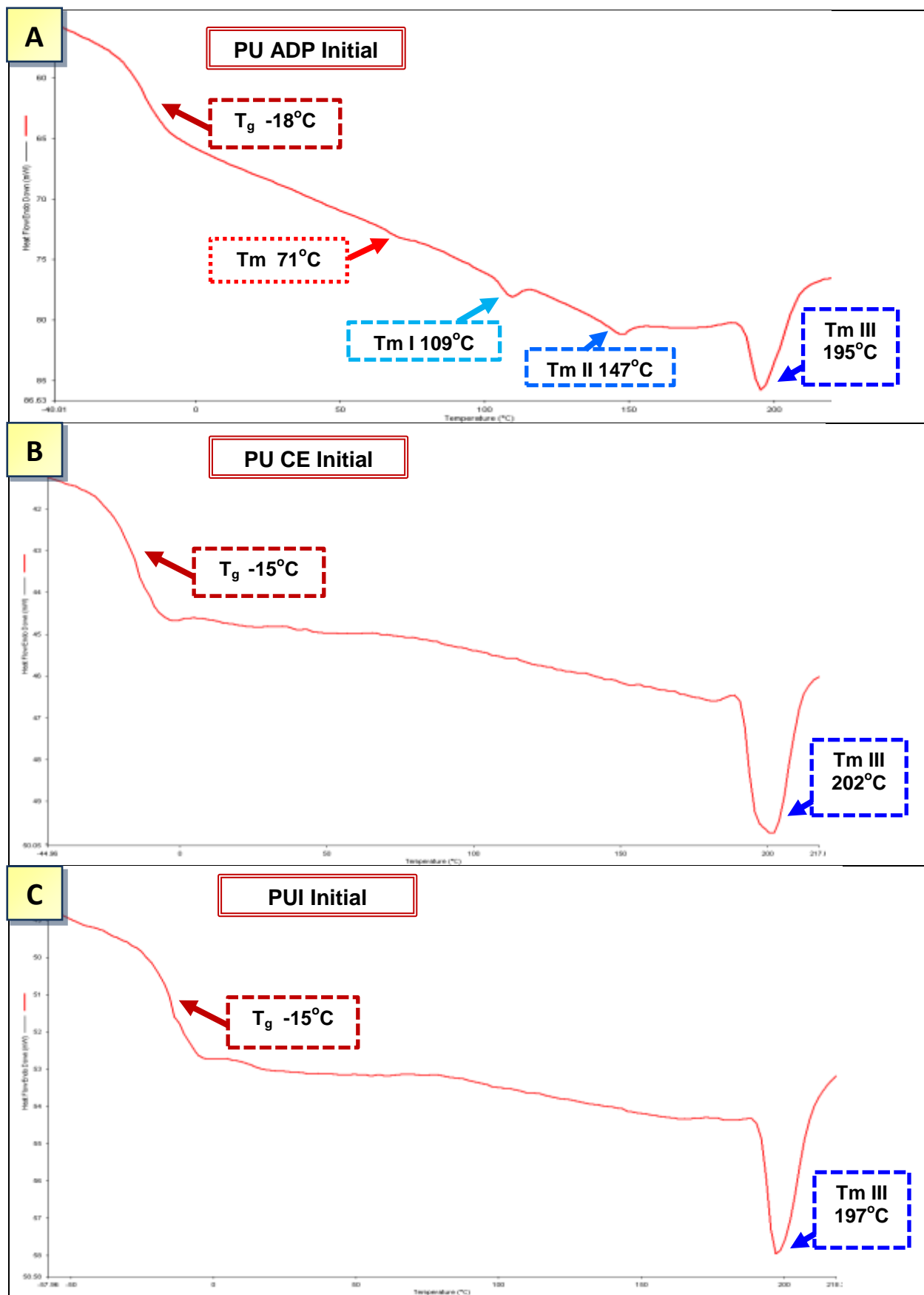


Figure 6.4 Morphology of PU using DSC; PU ADP (A), PU CE (B), PUI (C)

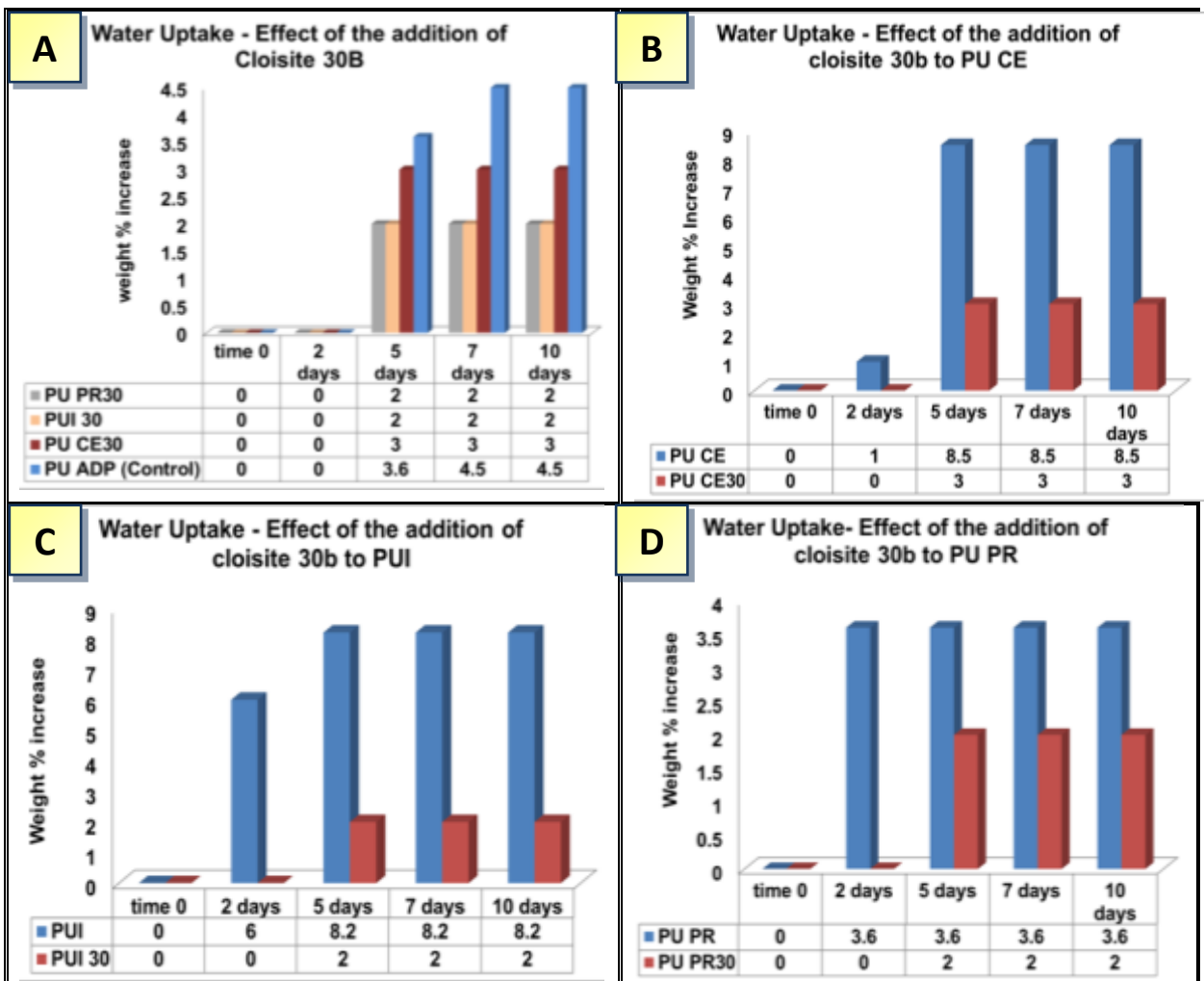


Figure 6.5 Hydrophilicity of PU samples determined by weight percentage increase of water uptake.

PU CE30, PU PR30, PUI 30 – Hard Segment MDI/BD: Soft Segment PEA

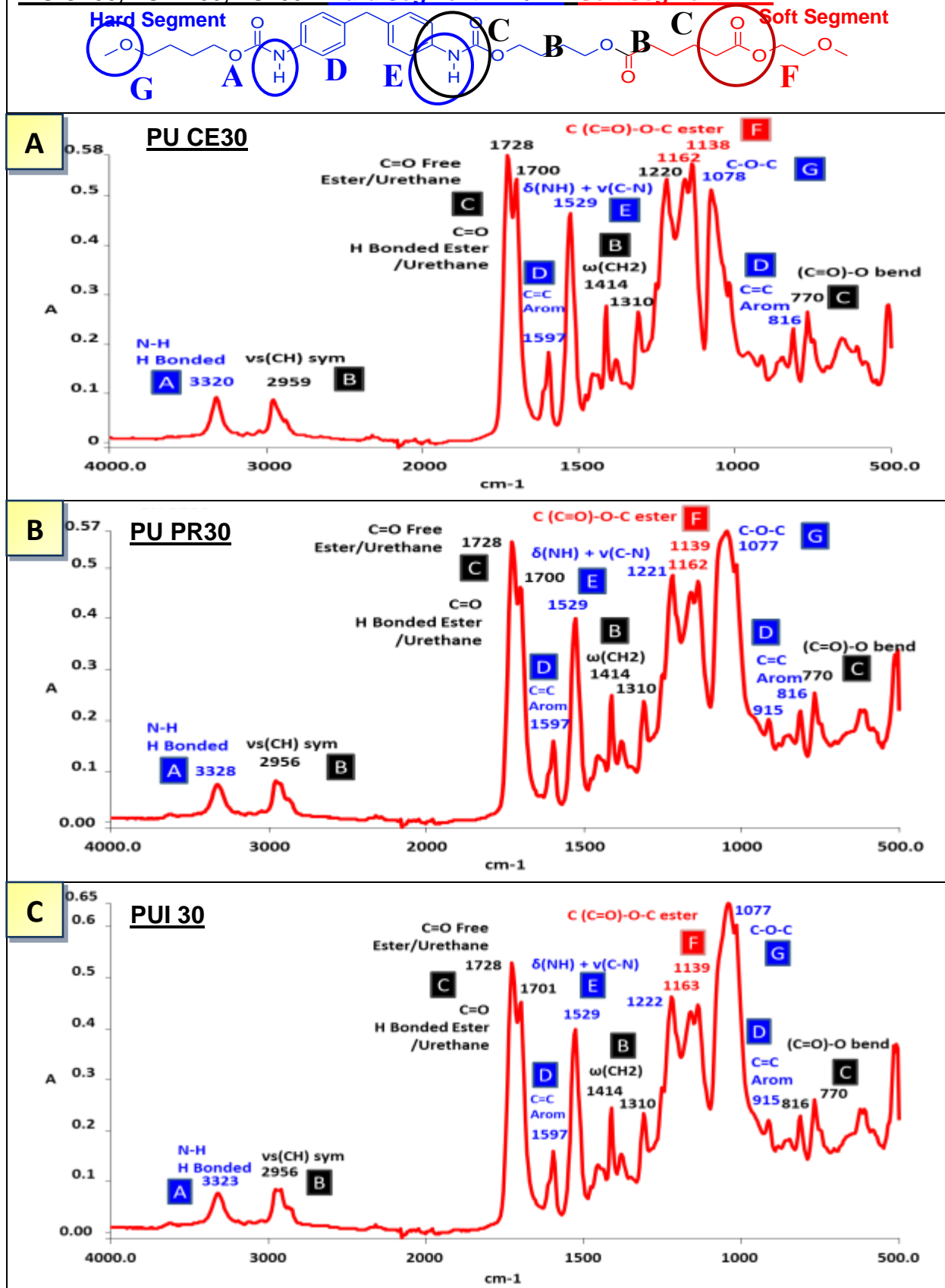


Figure 6.6 Chemical structure characterisation of PU samples PU CE30 (A), PU PR30 (B), PUI 30 (C) by FTIR-ATR

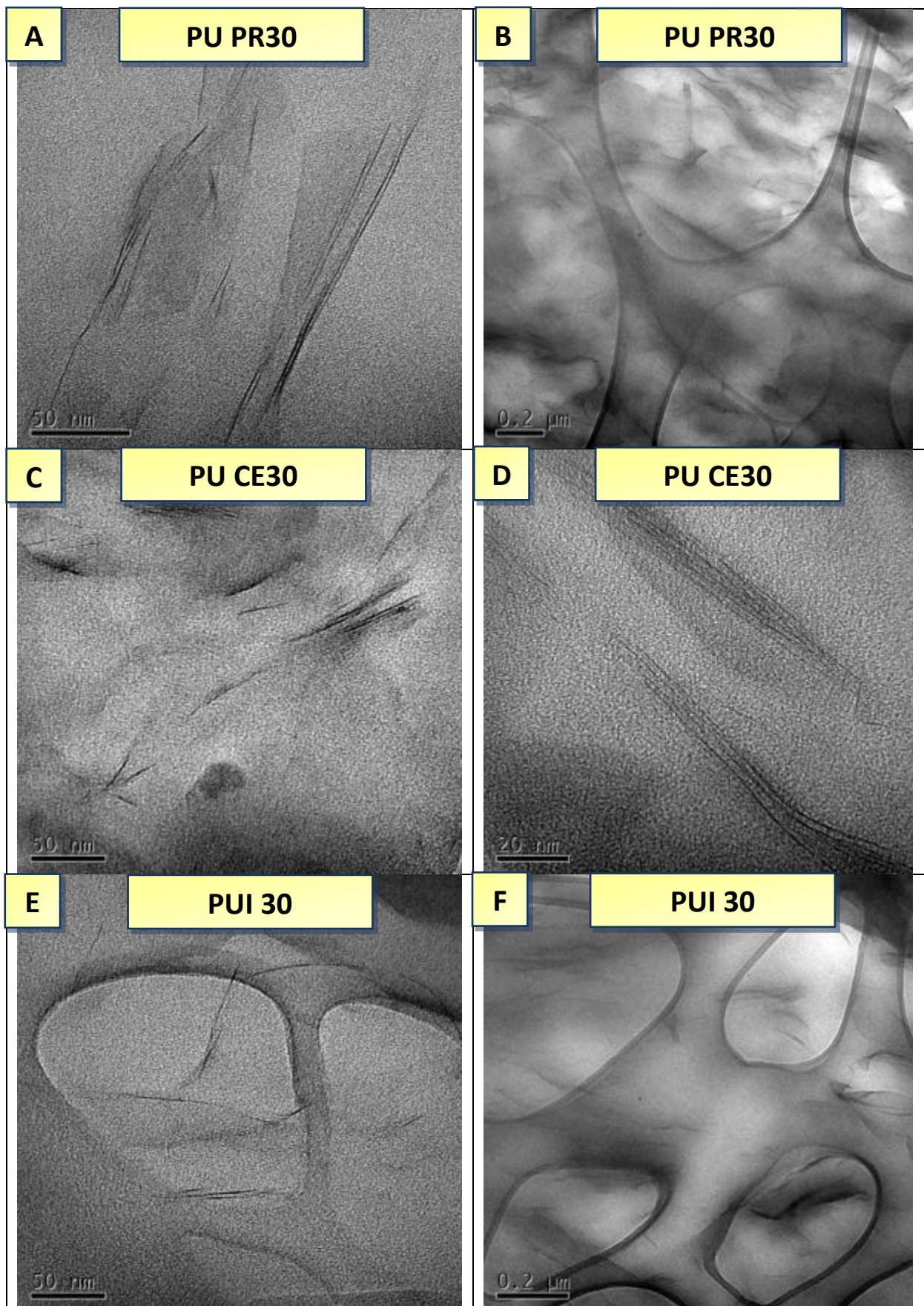


Figure 6.7 TEM images showing dispersal of cloisite 30b in PU PR30 (**A-B**), PU CE30 (**C-D**) and PUI 30 (**E-F**)

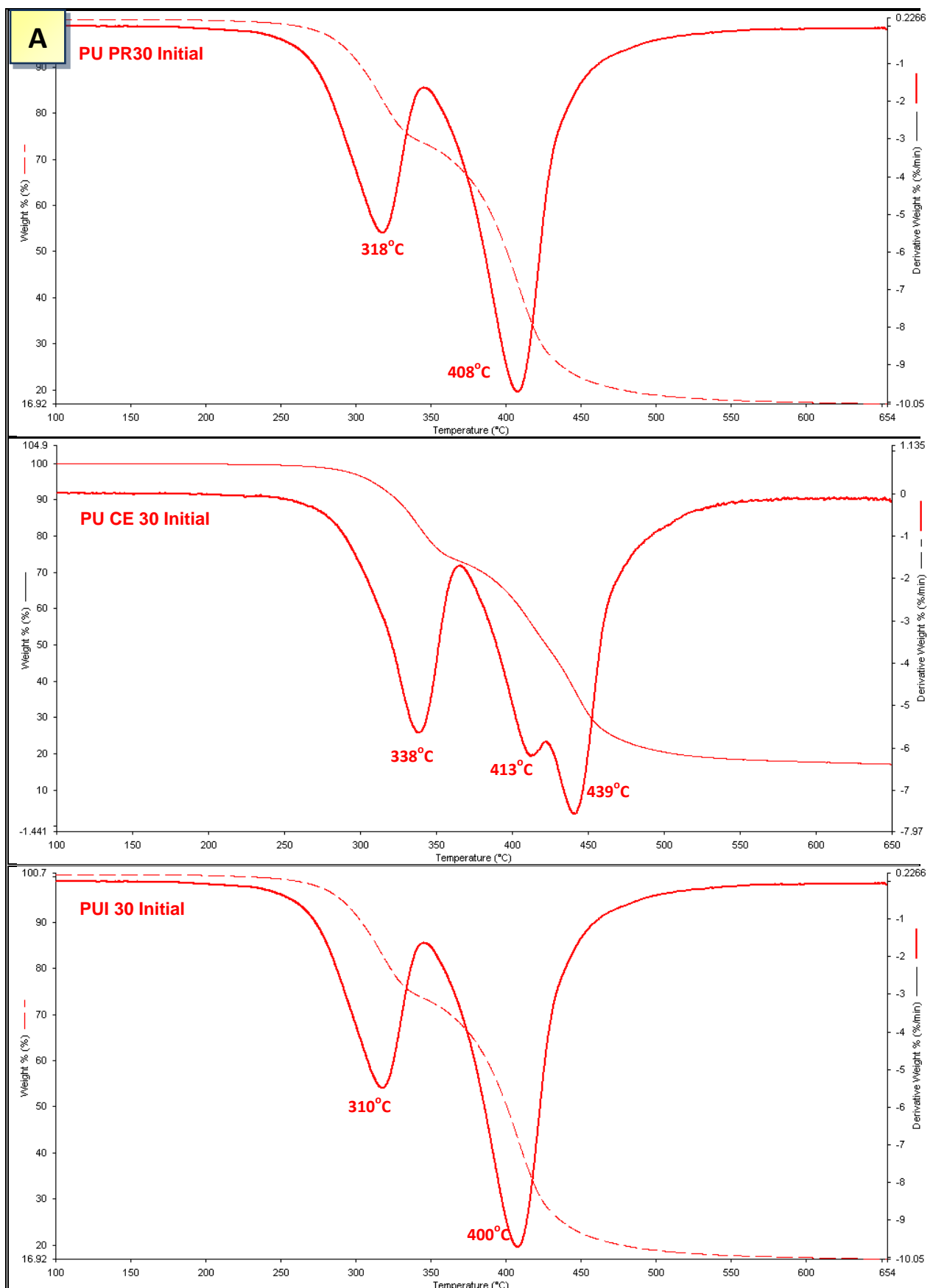


Figure 6.8 TGA thermal analysis characterisation of PU, PU PR30 (A), PU CE30 (B), PUI 30(C)

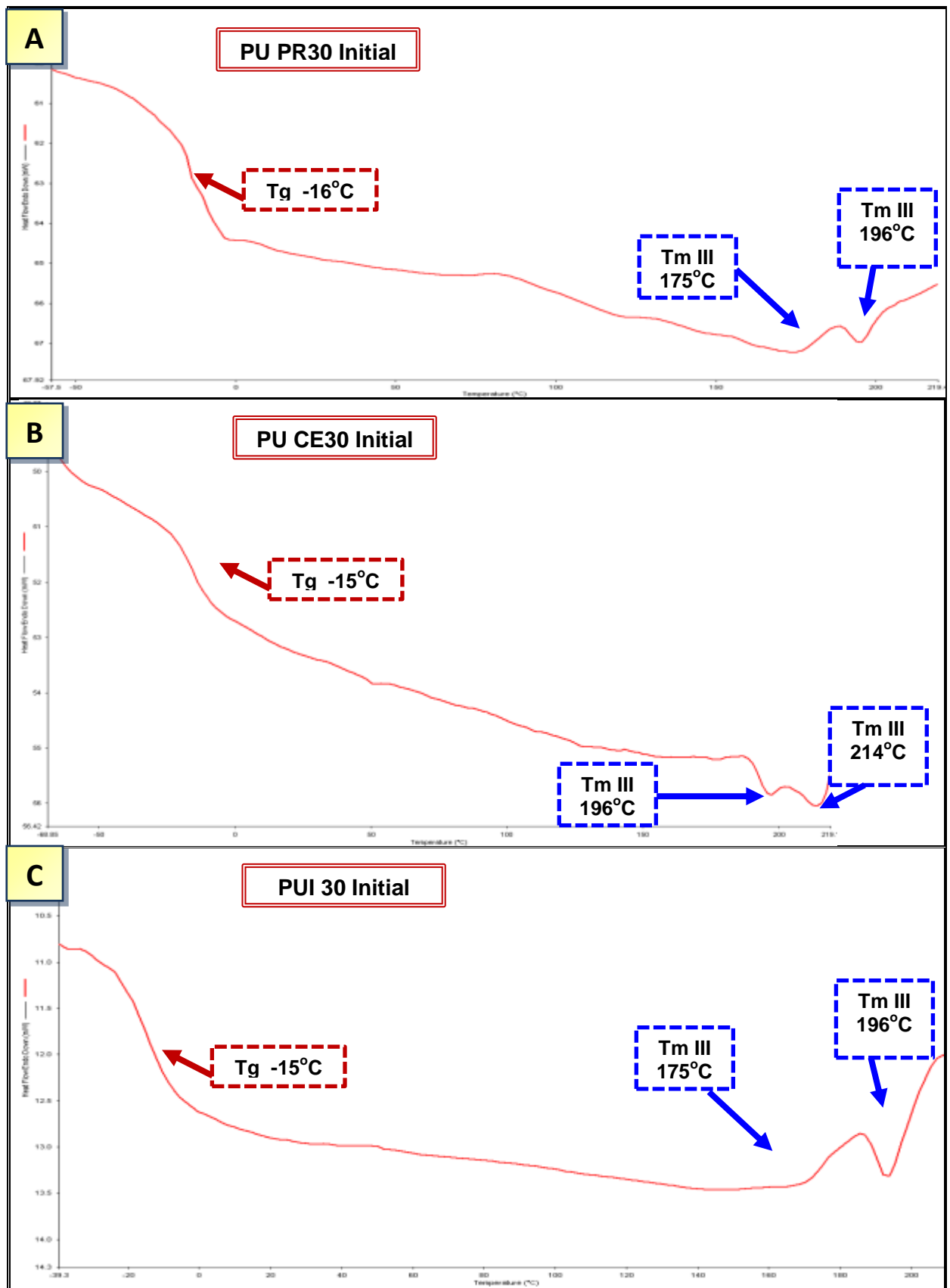
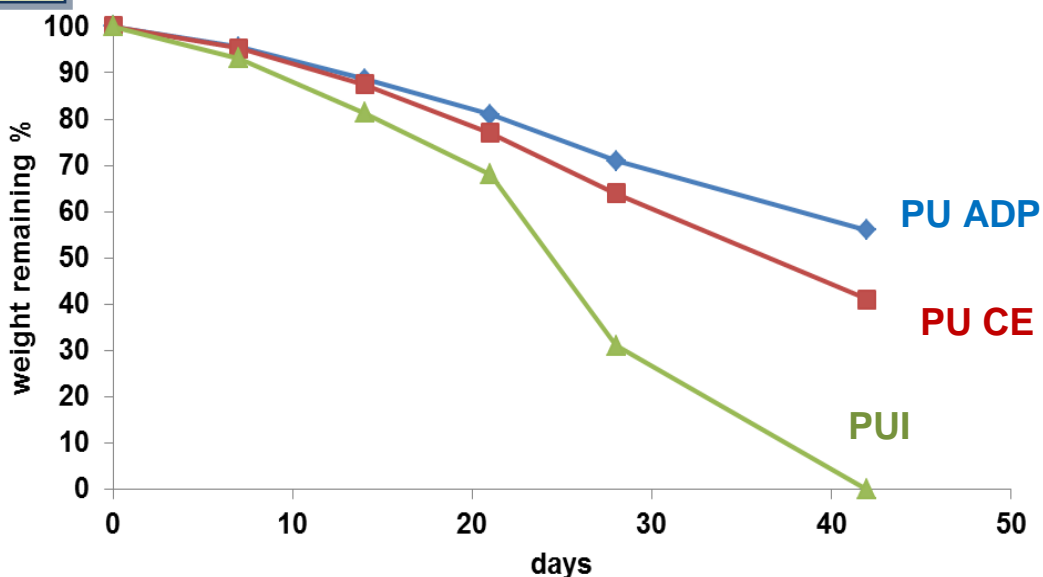


Figure 6.9 Morphology of PU using DSC; PU PR30 (A), PU CE30 (B), PUI 30(C)

A

Effect of additives on rate of hydrolytic degradation



Sample Code

Additive

Weight Remaining %

		0 days	7 days	14 days	21 days	28 days	42 days
PU ADP	No Additive	100	96	89	81	71	56
PU CE	Cellulose	100	95	87	78	67	42
PUI	Iron Stearate	100	92	82	69	32	0

B

Visual degradation during alkaline hydrolysis

Arbitrary scale of degradation stage

- min 0 no signs of cracking deformation
- 1 slight signs of limited surface degradation
- 2 deformation of sample (curling) & discolouration
- 3 visible cracks showing
- 4 Small pieces of sample broken away from film
- max 5 complete breaking of sample - small pieces

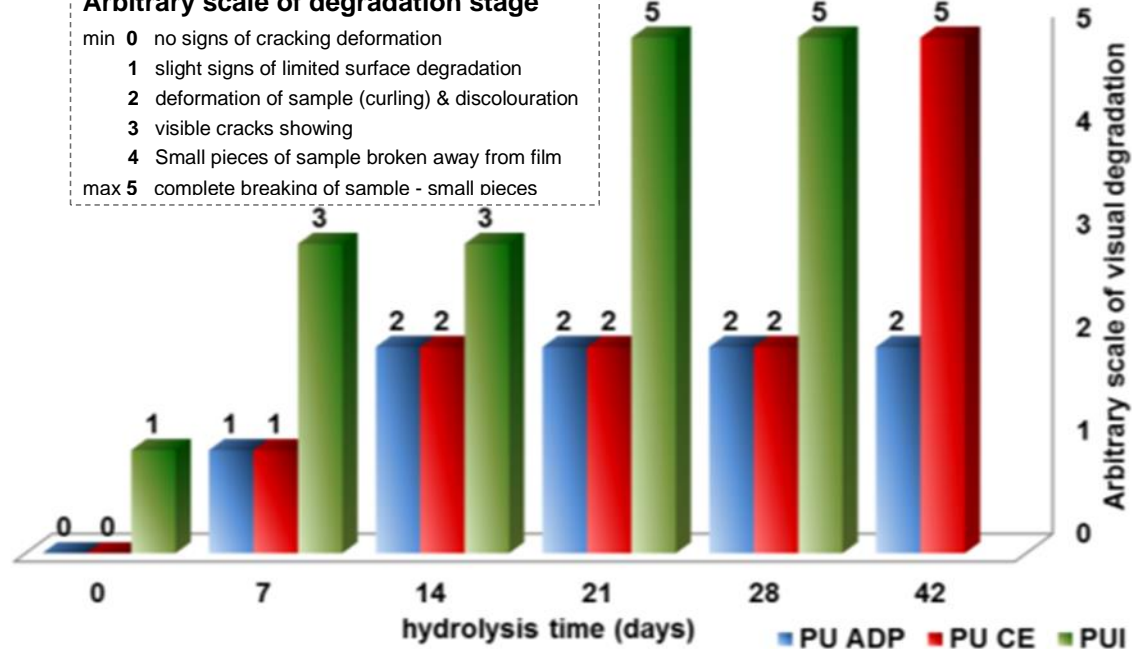


Figure 6.10 Effect of additives on the rate of hydrolytic degradation (A) with 10% NaOH (aq) (see table 2.1 & 2.2 pg. for acronyms). Visual surface cracking (B)

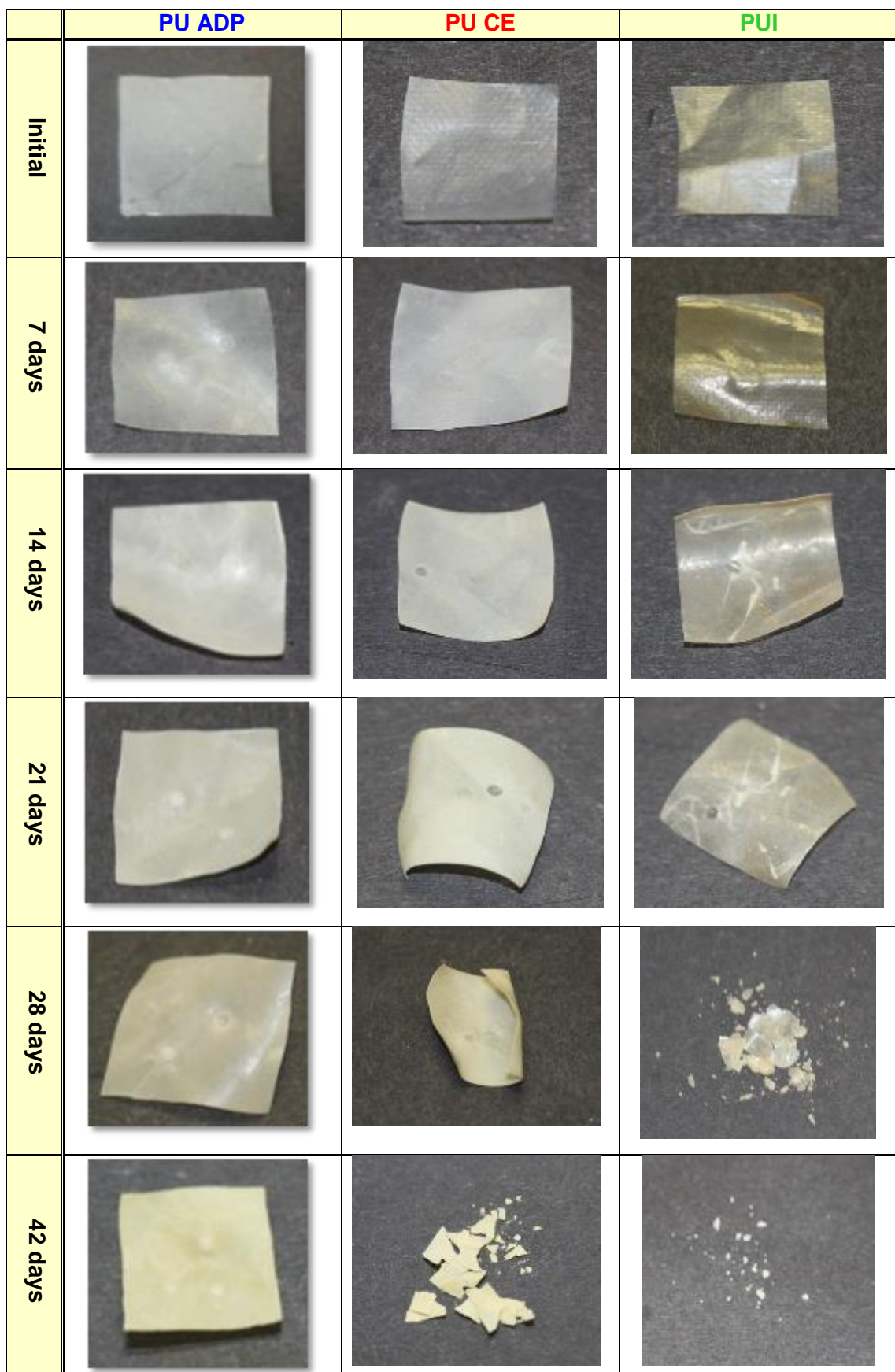


Figure 6.11 Photographic Images of PU ADP, PU CE & PUI during hydrolytic degradation with 10% NaOH (aq)

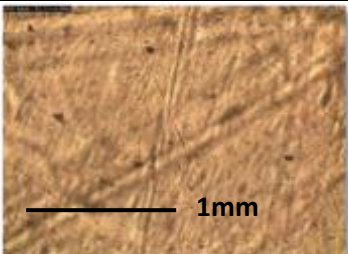
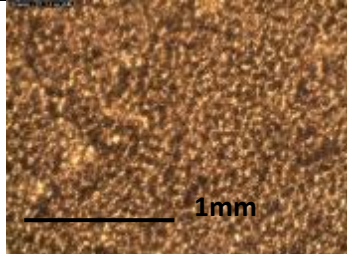
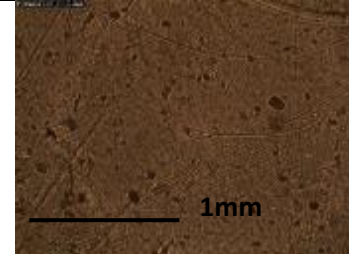
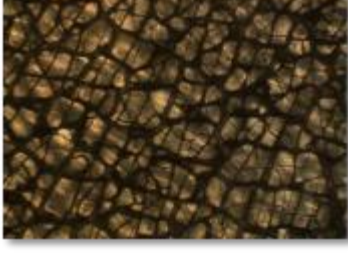
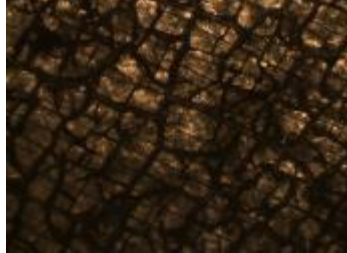
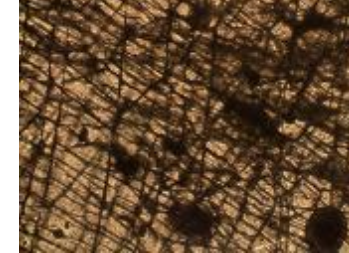
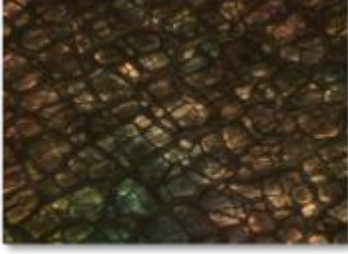
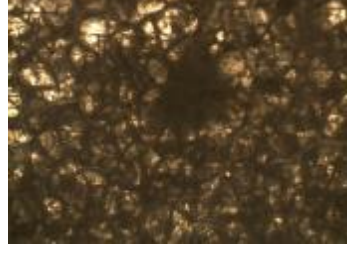
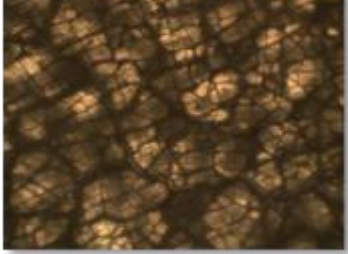
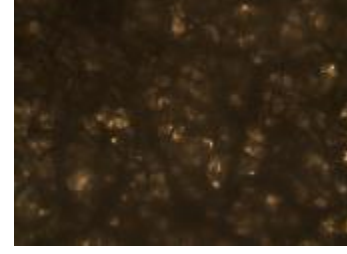
	PU ADP (one shot excess isocyanate)	PU CE (additive cellulose)	PUI (additive iron stearate)
Initial			
7 days			
14 days			
21 days			
28 days			
42 days			No Image PU PR degraded

Figure 6.12 Optical microscopic images of PU ADP, PU CE & PUI during alkaline hydrolysis

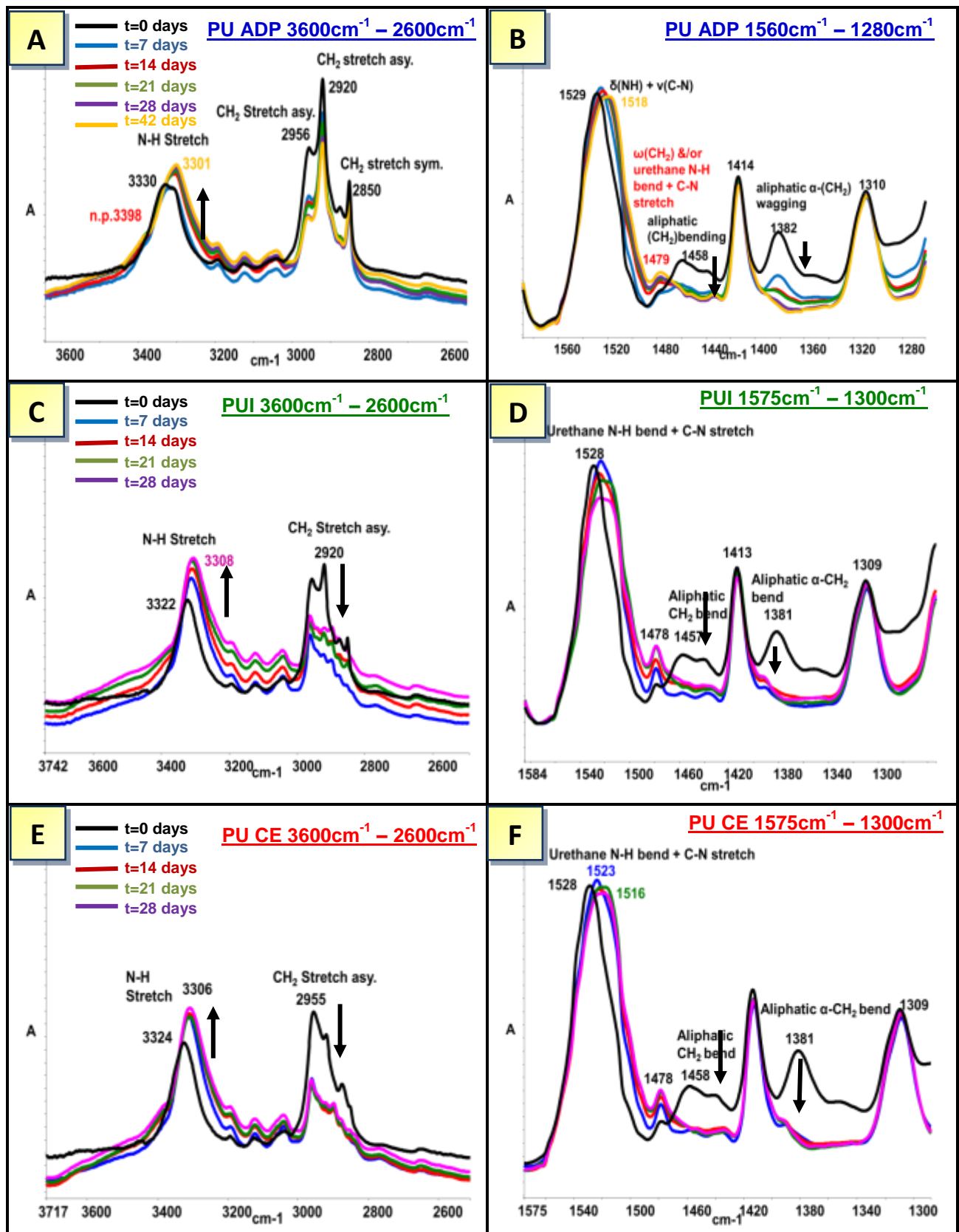


Figure 6.13 Structural changes of NH and CH₂ bonds during alkaline hydrolysis of PU ADP, PU CE & PUI by FTIR/ATR

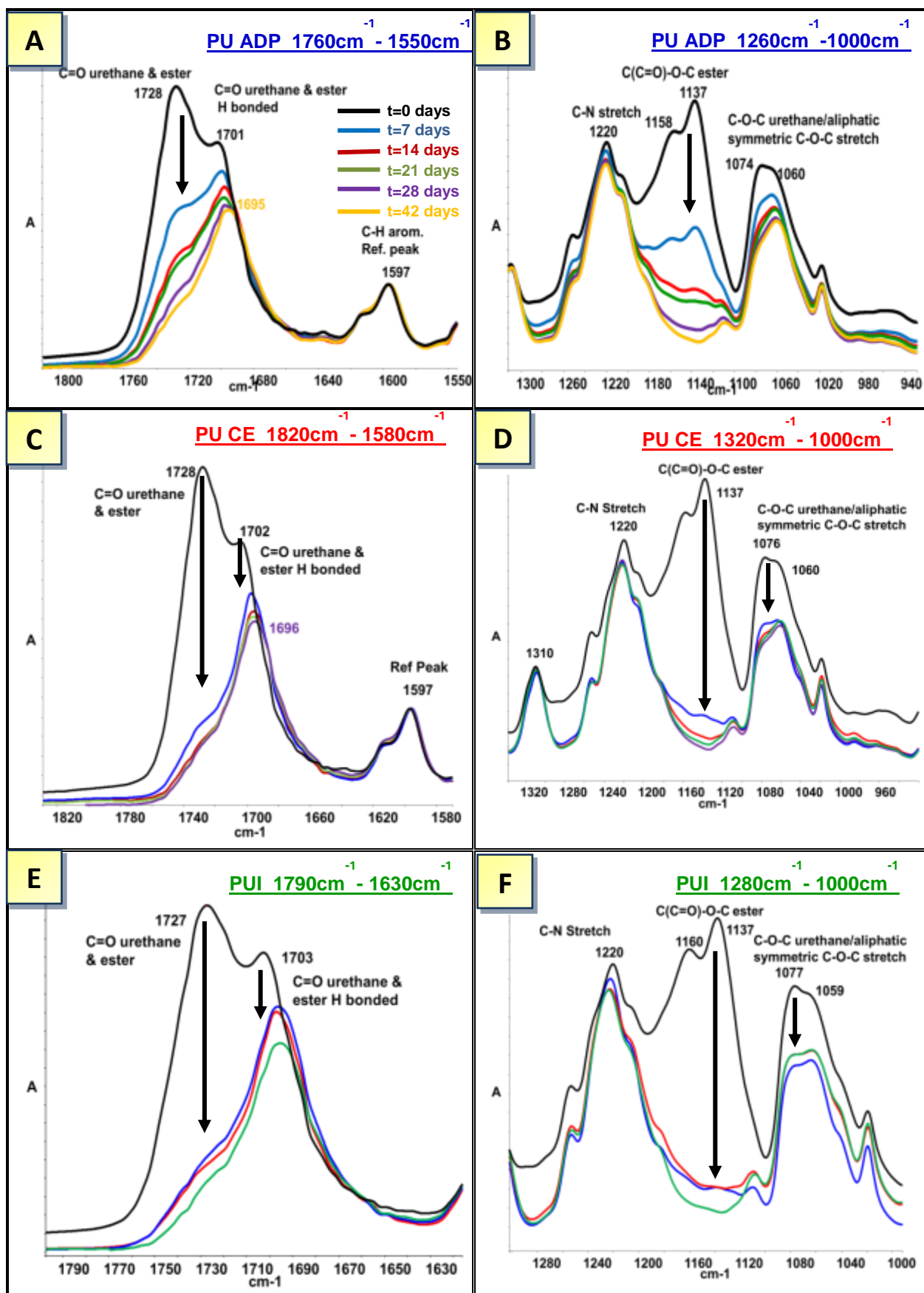


Figure 6.14 Structural changes of C=O and C-O-C urethane and ester linkages during alkaline hydrolysis of PU ADP, PU CE & PUI by FTIR/ATR

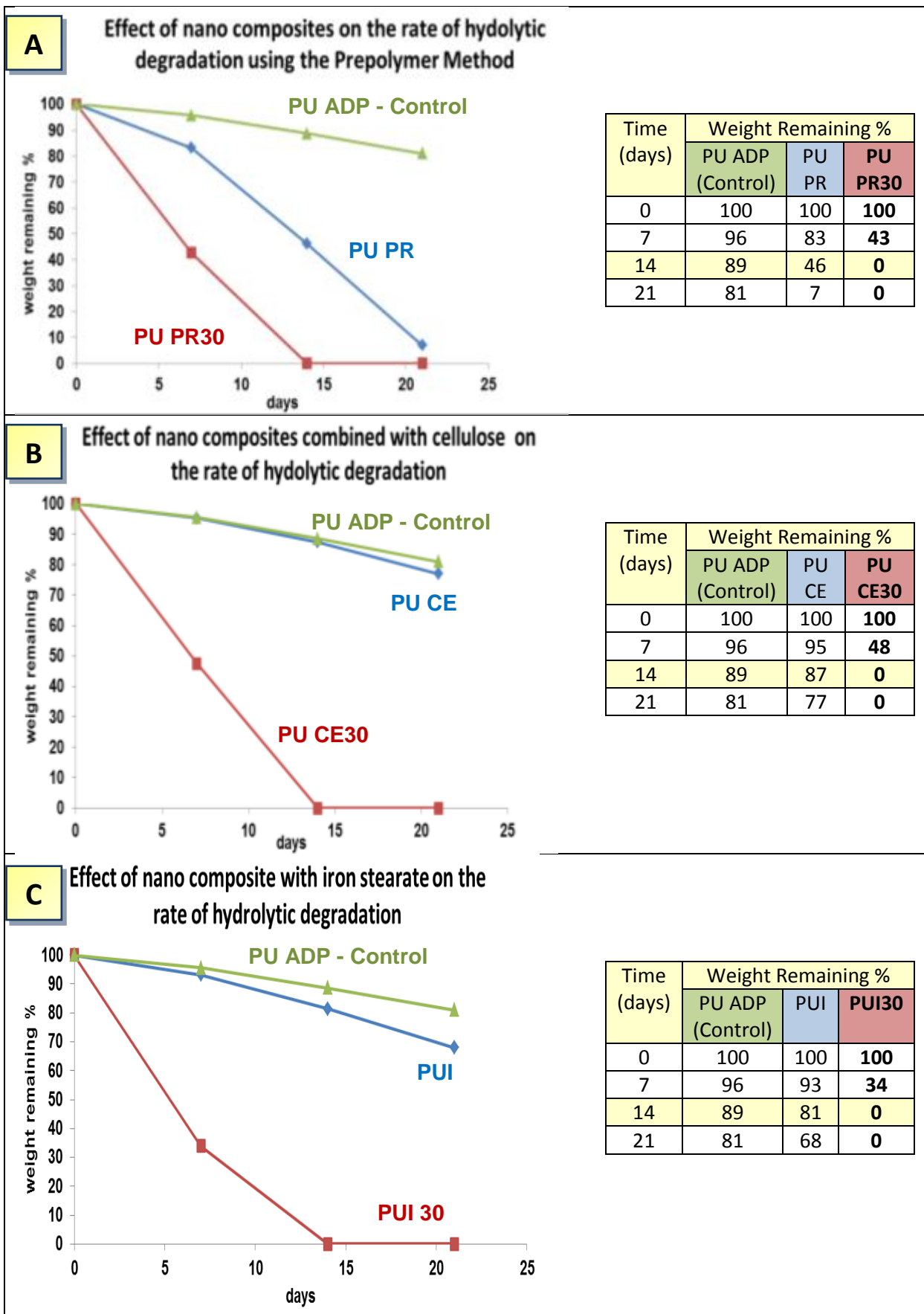


Figure 6.15 Effect of Cloisite 30B on the rate of hydrolytic degradation with 10% NaOH (aq)

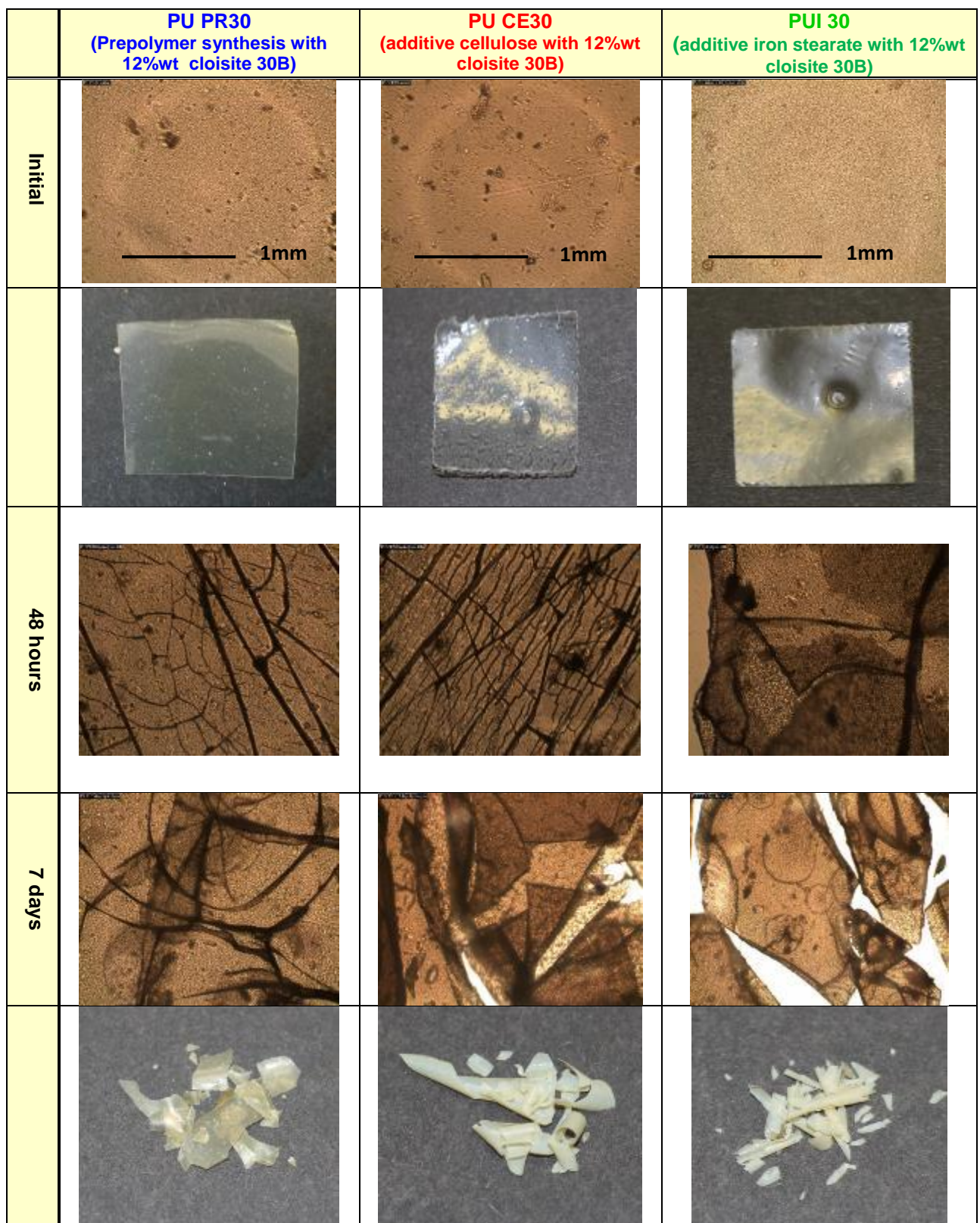


Figure 6.16 Photographic and microscopic Images of PU PR30, PU CE30 & PUI 30 during hydrolytic degradation with 10% NaOH (aq)

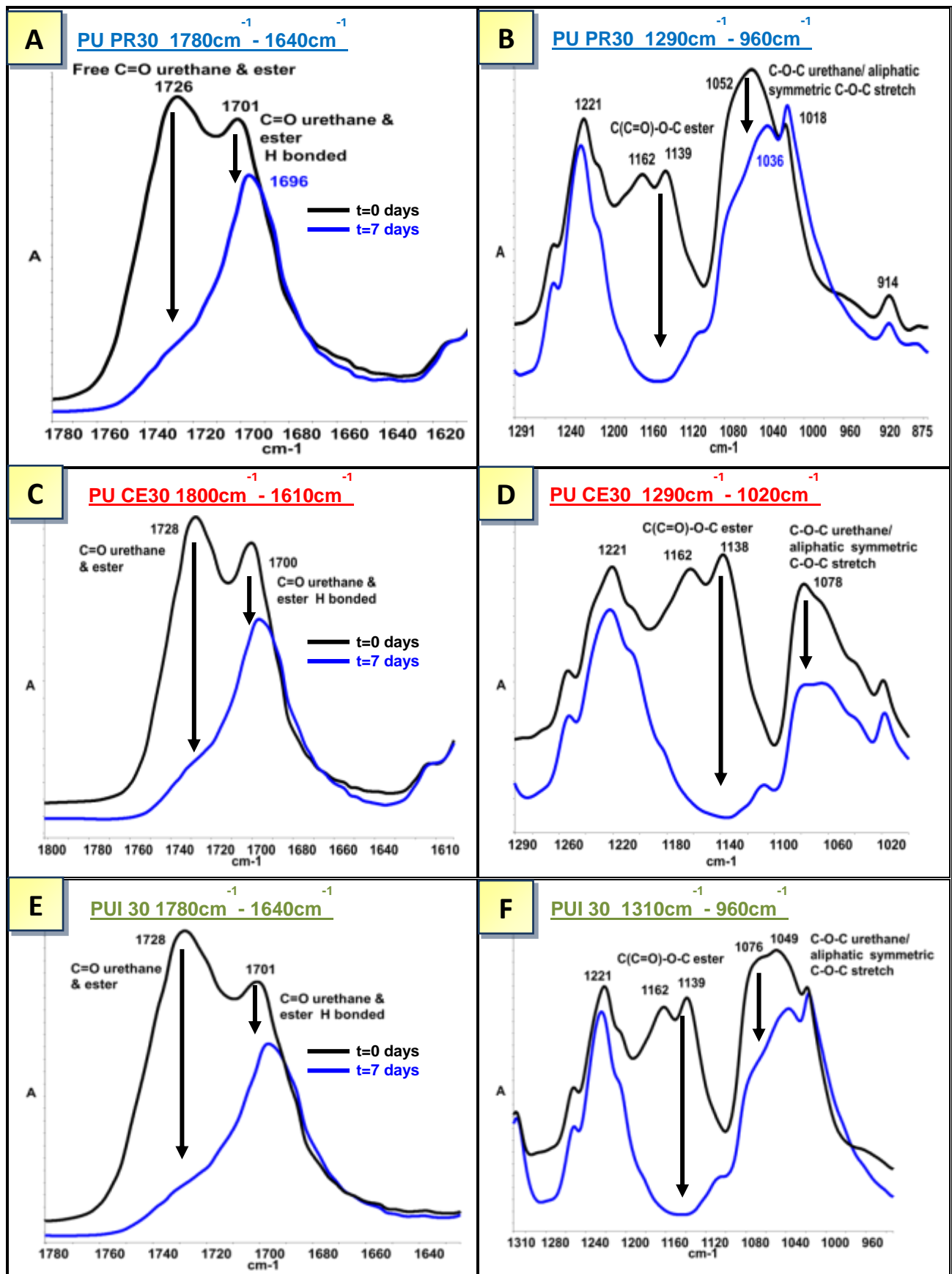


Figure 6.17 Structural changes of C=O and C-O-C urethane and ester linkages during alkaline hydrolysis of PU PR30, PU CE30 & PUI 30 by FTIR/ATR

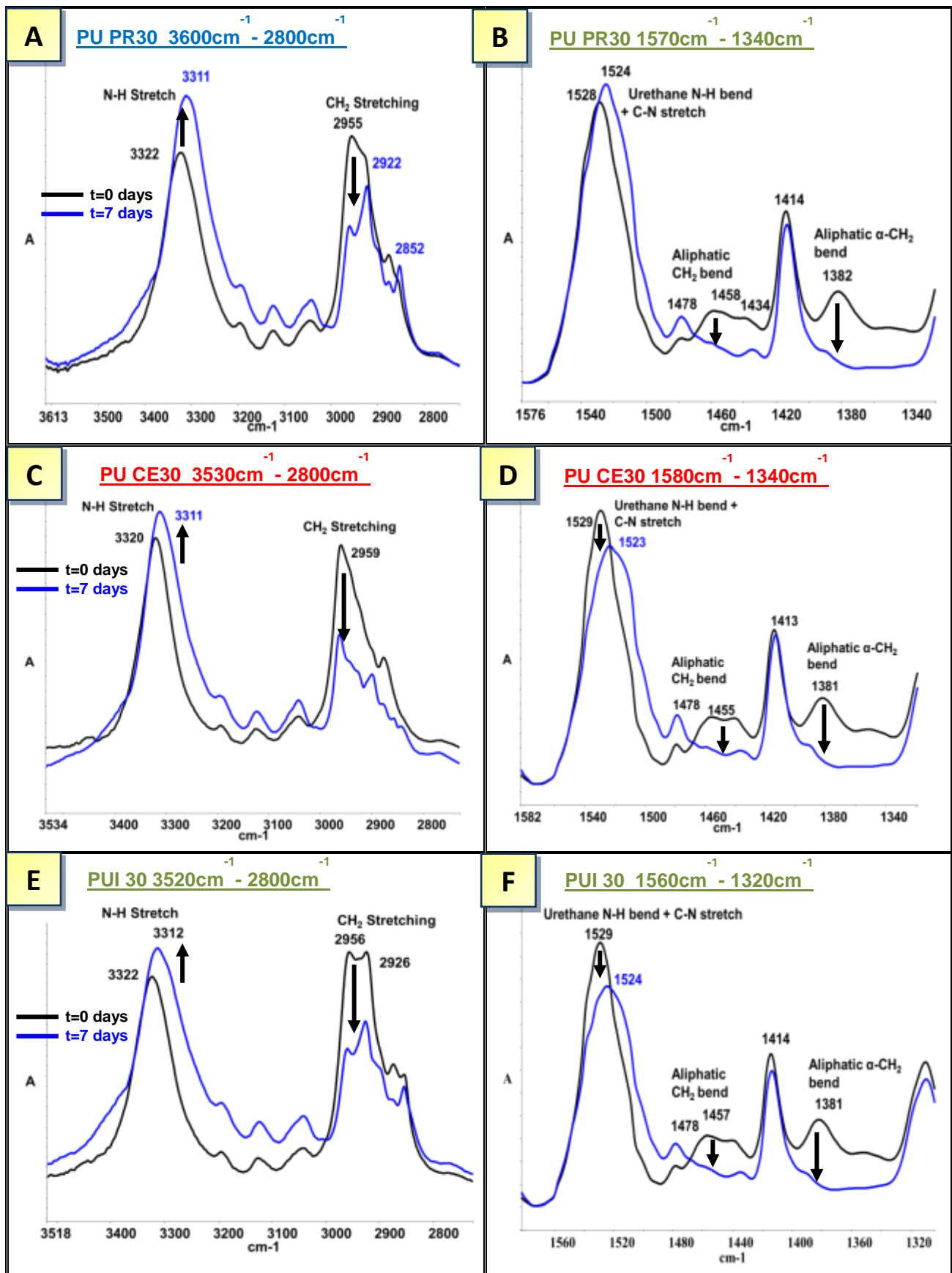


Figure 6.18 Structural changes of C=O and C-O-C urethane and ester linkages during alkaline hydrolysis of PU PR30, PU CE30 & PUI 30 by FTIR/ATR

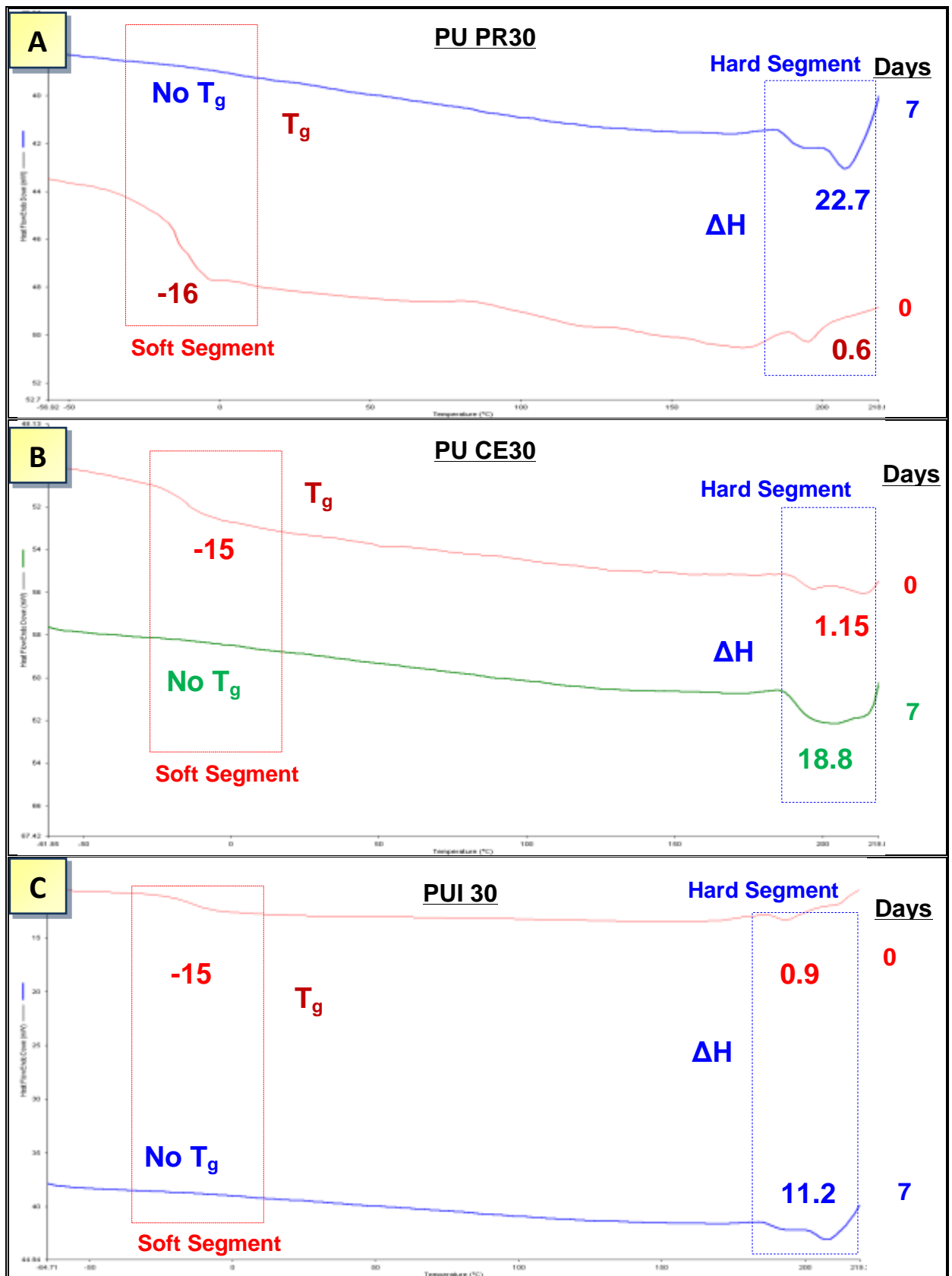


Figure 6.19 Morphology changes after alkaline hydrolysis of PU PR30, PU CE30 & PUI 30 by DSC

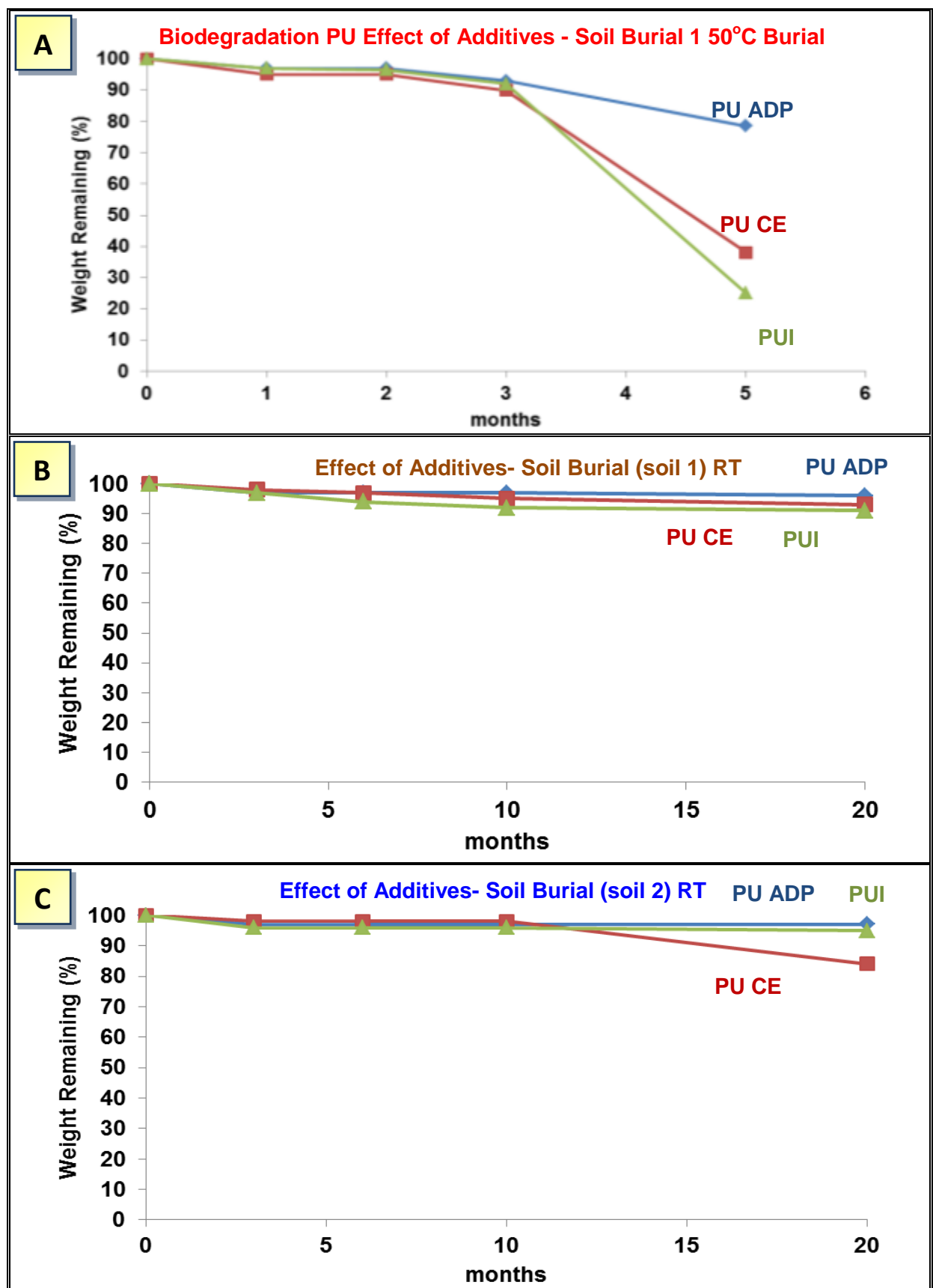


Figure 6.20 Effect of additives, cellulose and iron stearate on the rate of biodegradation under soil burial conditions, soil 1 50°C (A), soil 1 RT (B), soil 2 RT (C)

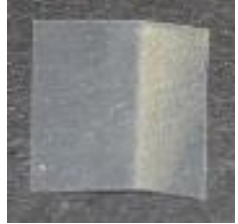
	PU ADP	PU CE	PUI
Initial			
3 months			
Soil 1 RT			
Soil 2 RT			
Soil 1 50°C			
5 months			
Soil 1 50°C			
20 months			
Soil 1 RT			
Soil 2 RT			

Figure 6.21 Photographic images of PU ADP, PU CE & PUI after soil burial

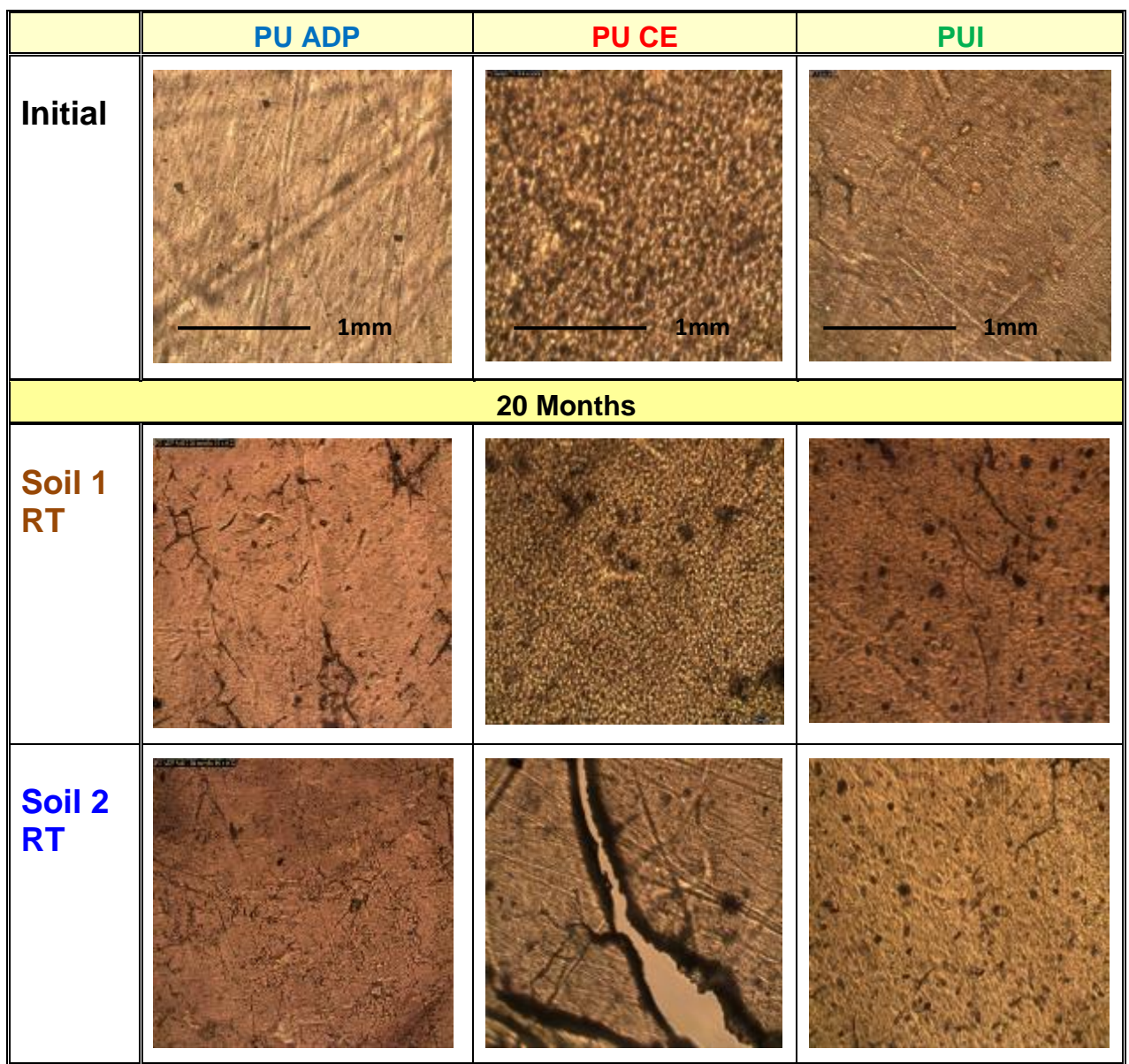


Figure 6.22 Optical microscopic images of PU ADP, PU CE & PUI during soil burial

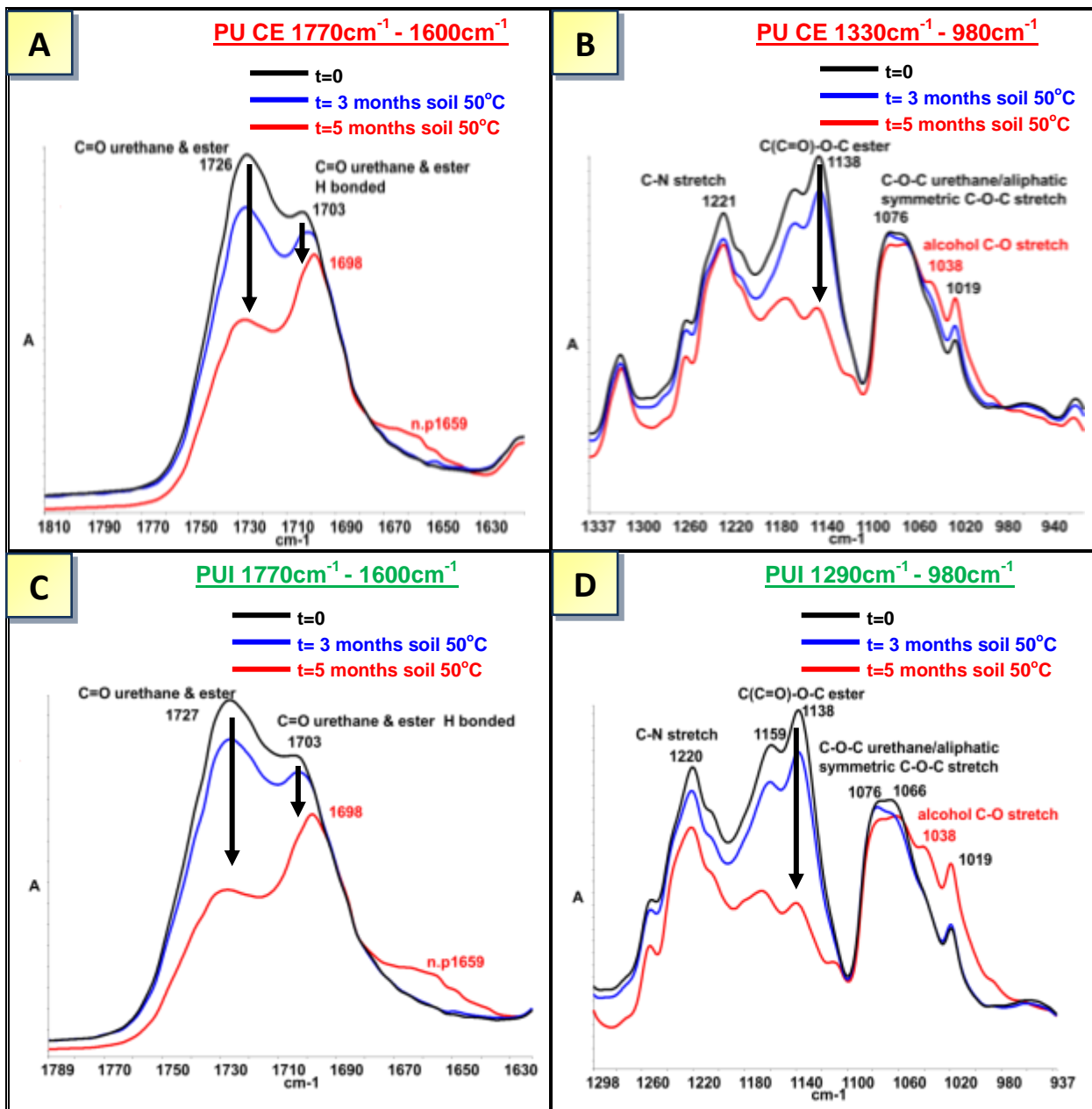


Figure 6.23 Effect of additives cellulose and iron stearate on C=O and C-O-C ester/urethane linkages during soil burial at 50°C of PU CE & PUI by FTIR/ATR

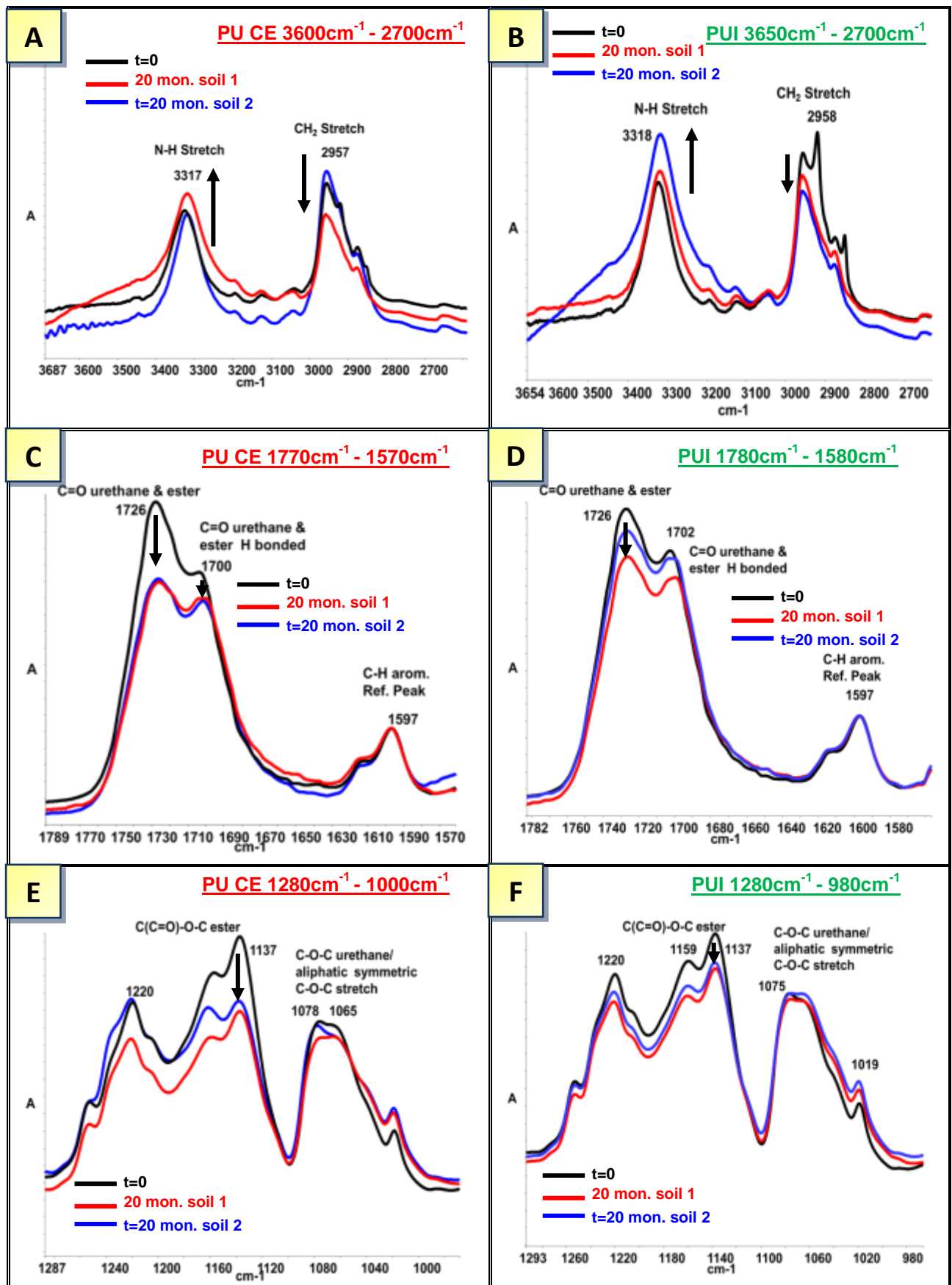


Figure 6.24 Structural changes of N-H, C=O and C-O-C urethane and ester linkages after soil burial at RT for 20 months of PU CE & PUI by FTIR/ATR

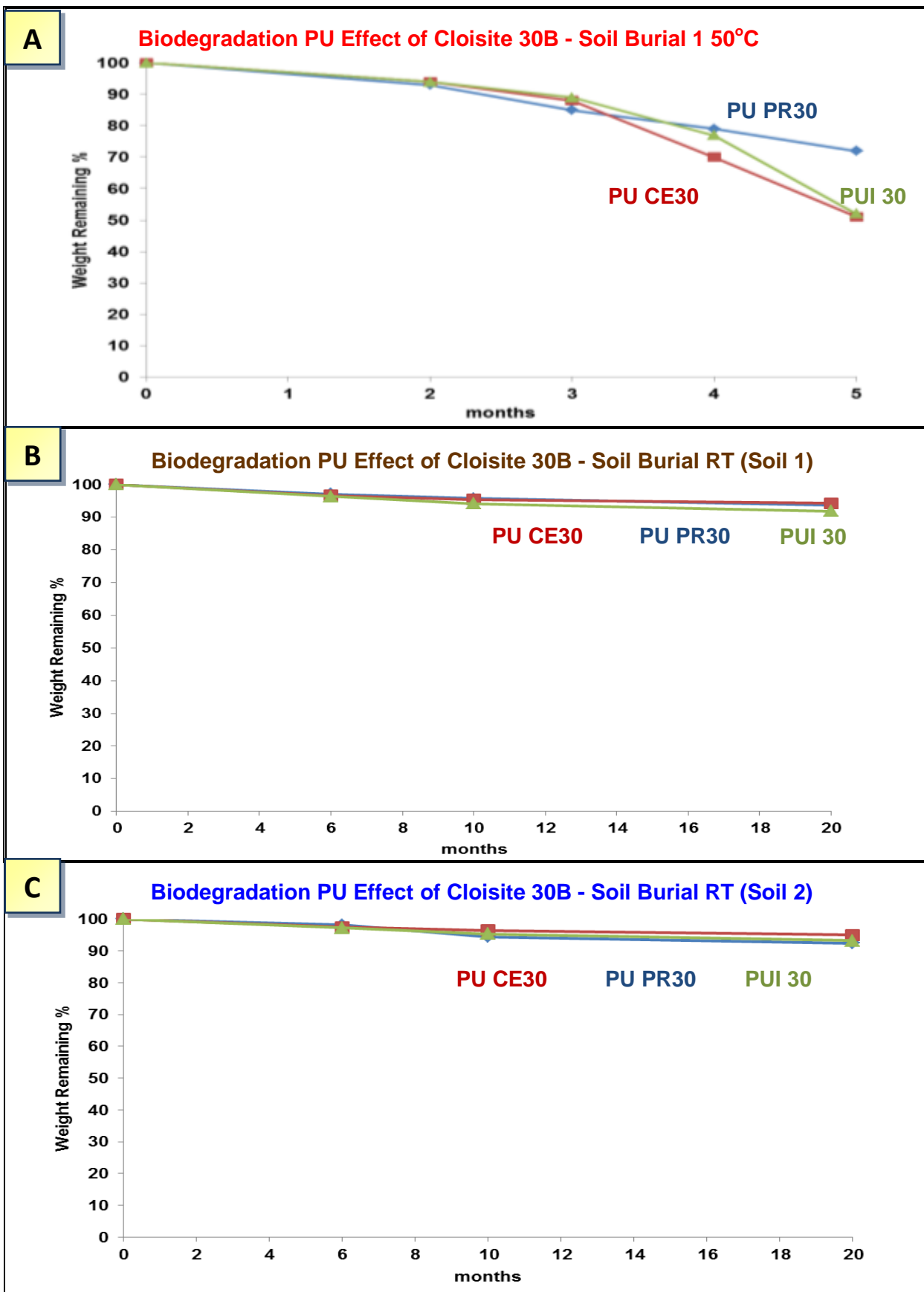


Figure 6.25 Effect of additive cloisite 30b on the rate of biodegradation under soil burial conditions, soil 1 50°C (A), soil 1 RT (B), soil 2 RT (C)

	PU PR30	PU CE30	PUI 30
Initial			
5 months			
Soil 1 50°C			
20 months			
Soil 1 RT			
Soil 2 RT			

Figure 6.26 Photographic images of PU PR30, PU CE30 & PUI 30 during soil burial

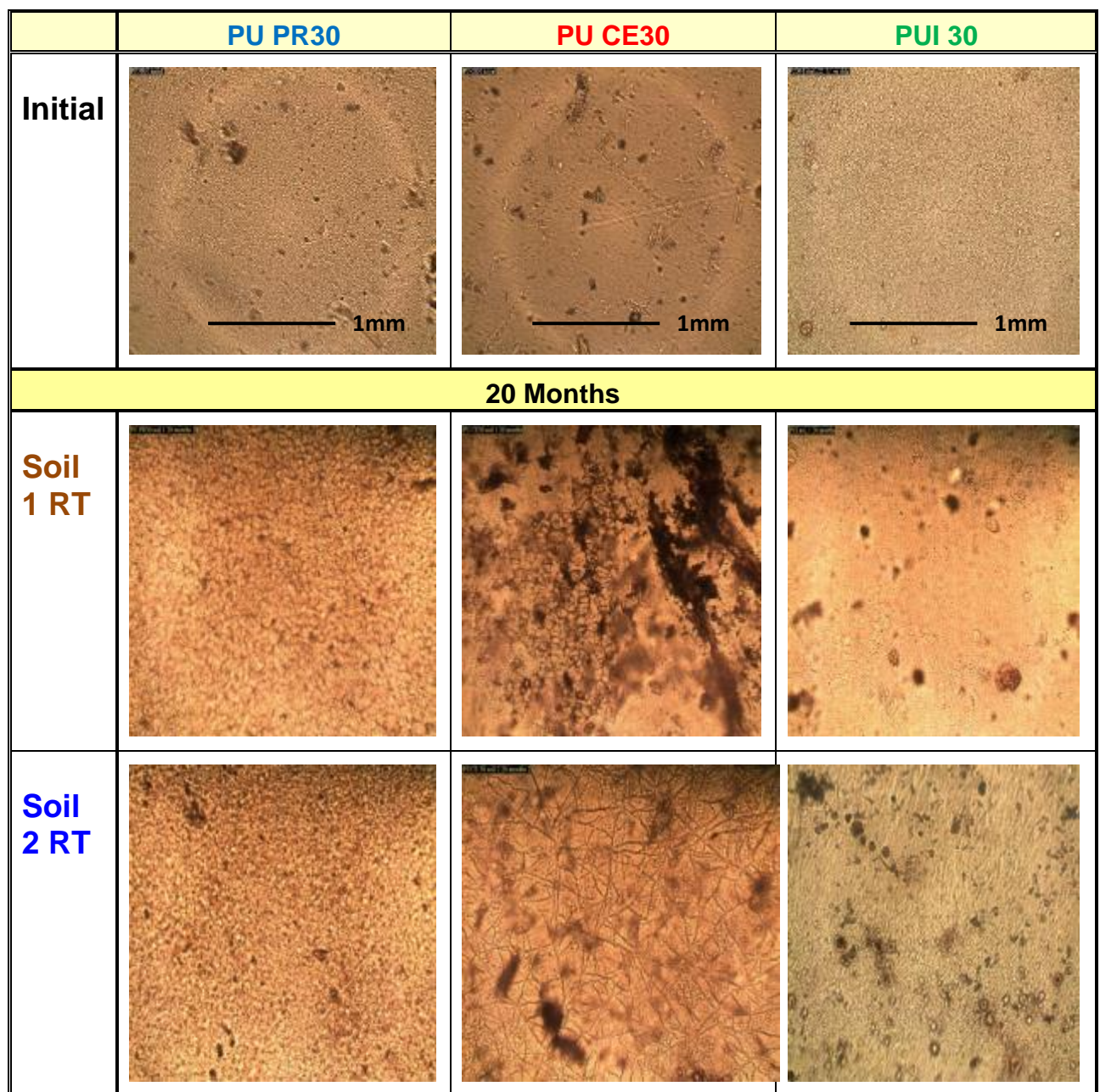


Figure 6.27 Optical microscopic images of PU PR30, PU CE30 & PUI 30 during soil burial

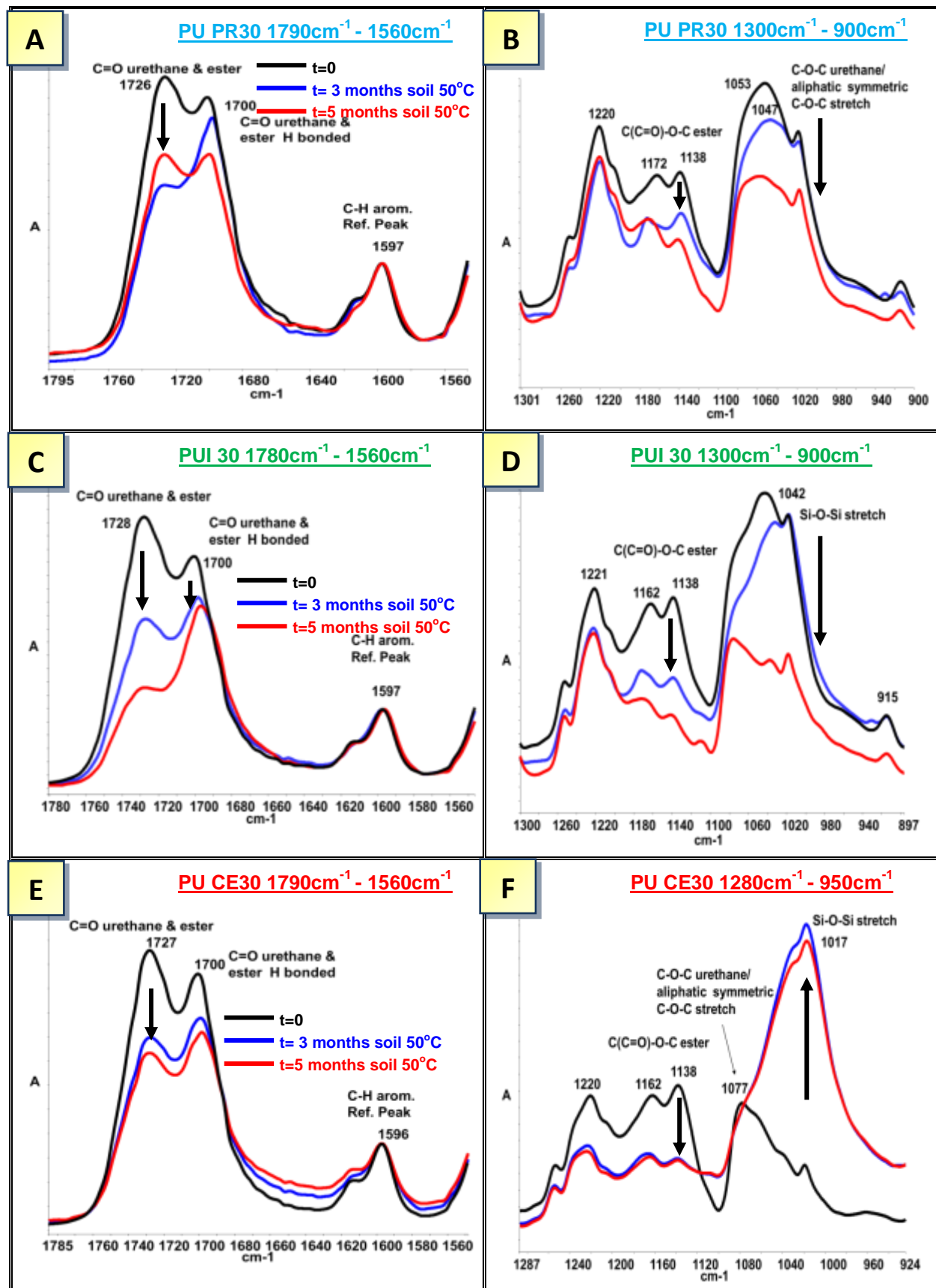


Figure 6.28 Structural changes of C=O and C-O-C urethane and ester linkages after soil burial at 50°C for 3 and 5 months of PU PR30, PU CE30 & PUI 30 by FTIR/ATR

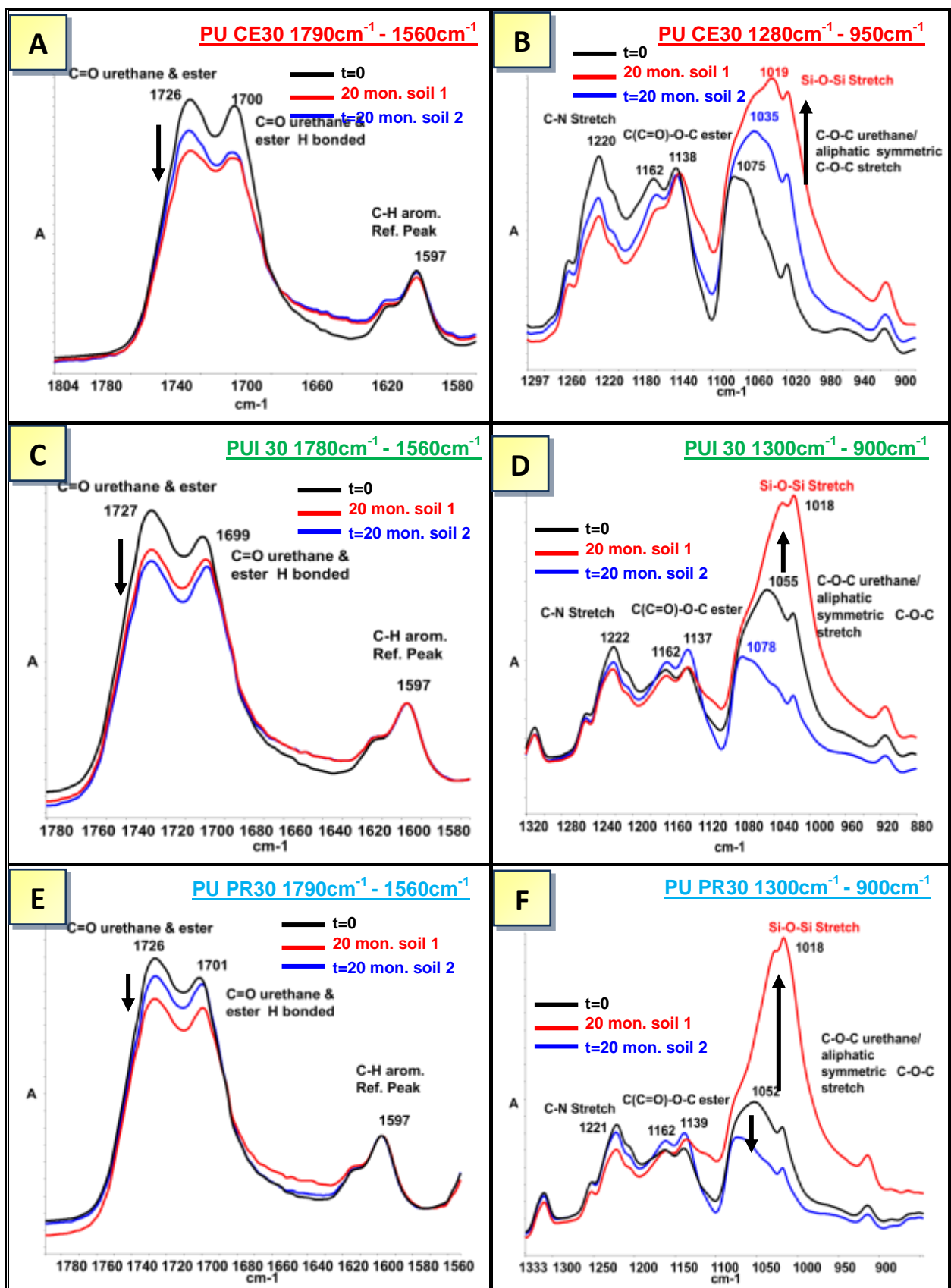


Figure 6.29 Structural changes of C=O and C-O-C urethane and ester linkages after soil burial after 20 months at RT of PU PR30, PU CE30 & PUI 30 by FTIR/ATR

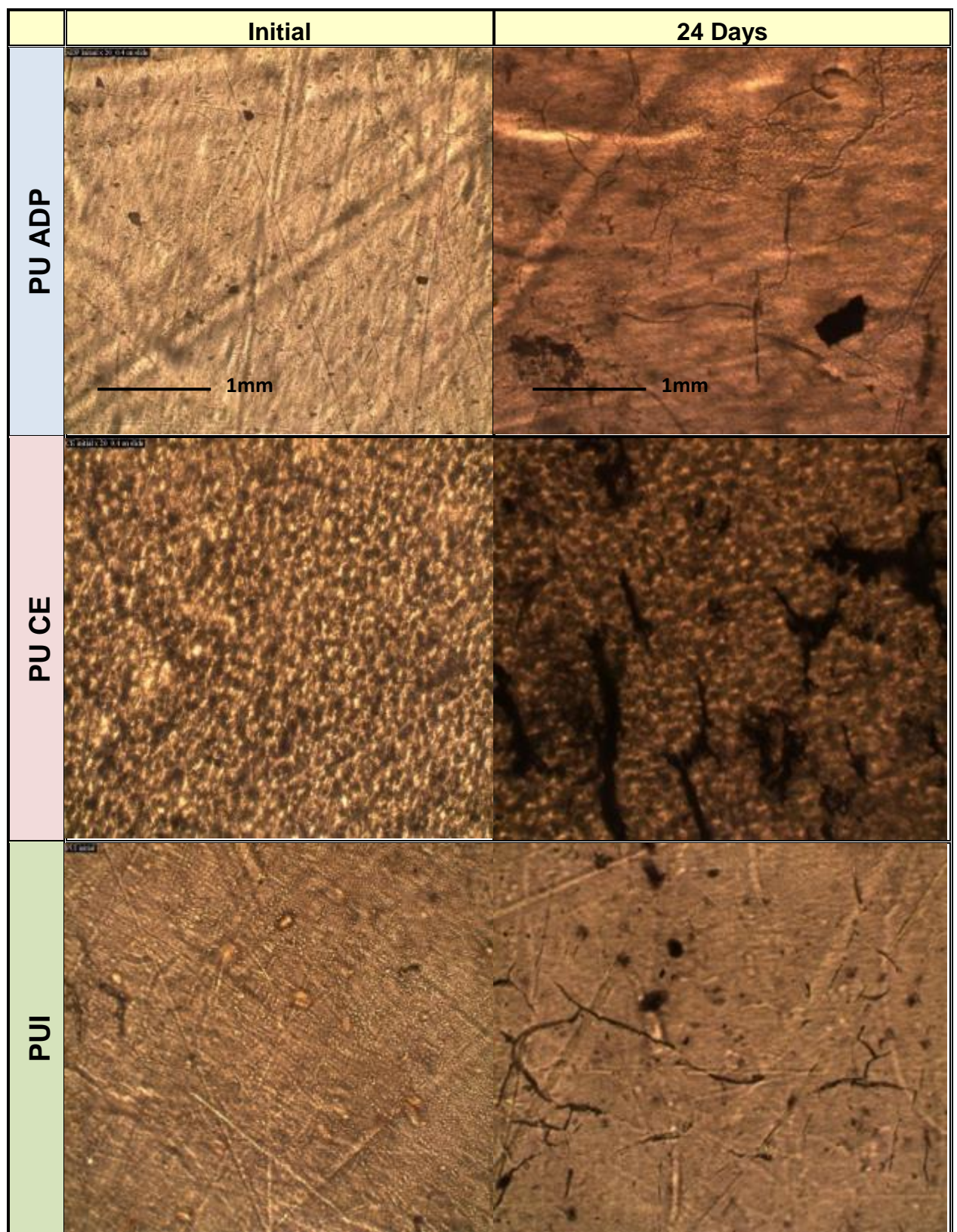


Figure 6.30 Effect of additives on enzymatic degradation by lipase *Aspergillus niger* PU ADP, PU CE & PUI by optical microscope images

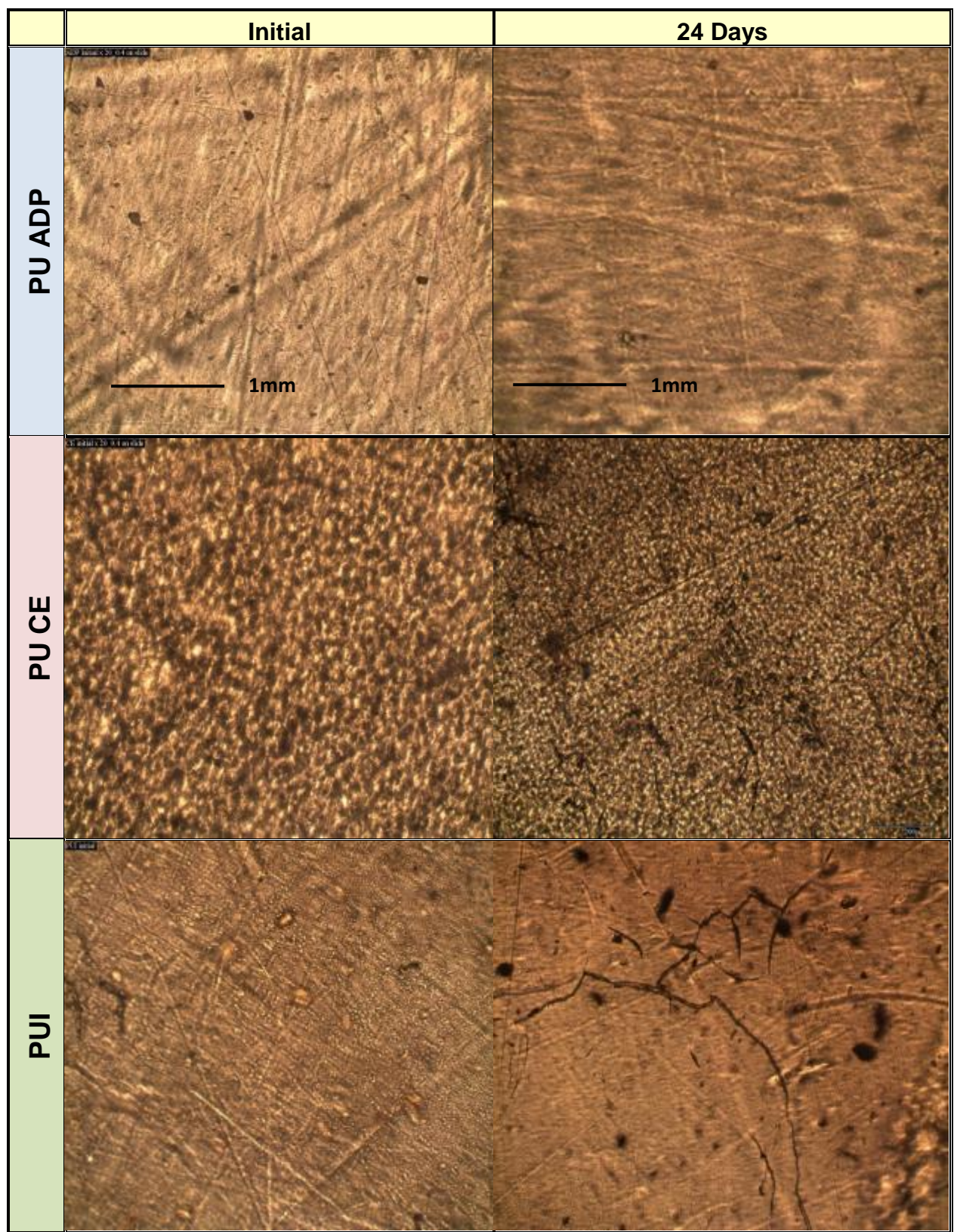


Figure 6.31 Effect of additives on enzymatic degradation by lipase *Rhizopus* sp. PU ADP, PU CE & PUI by optical microscope images

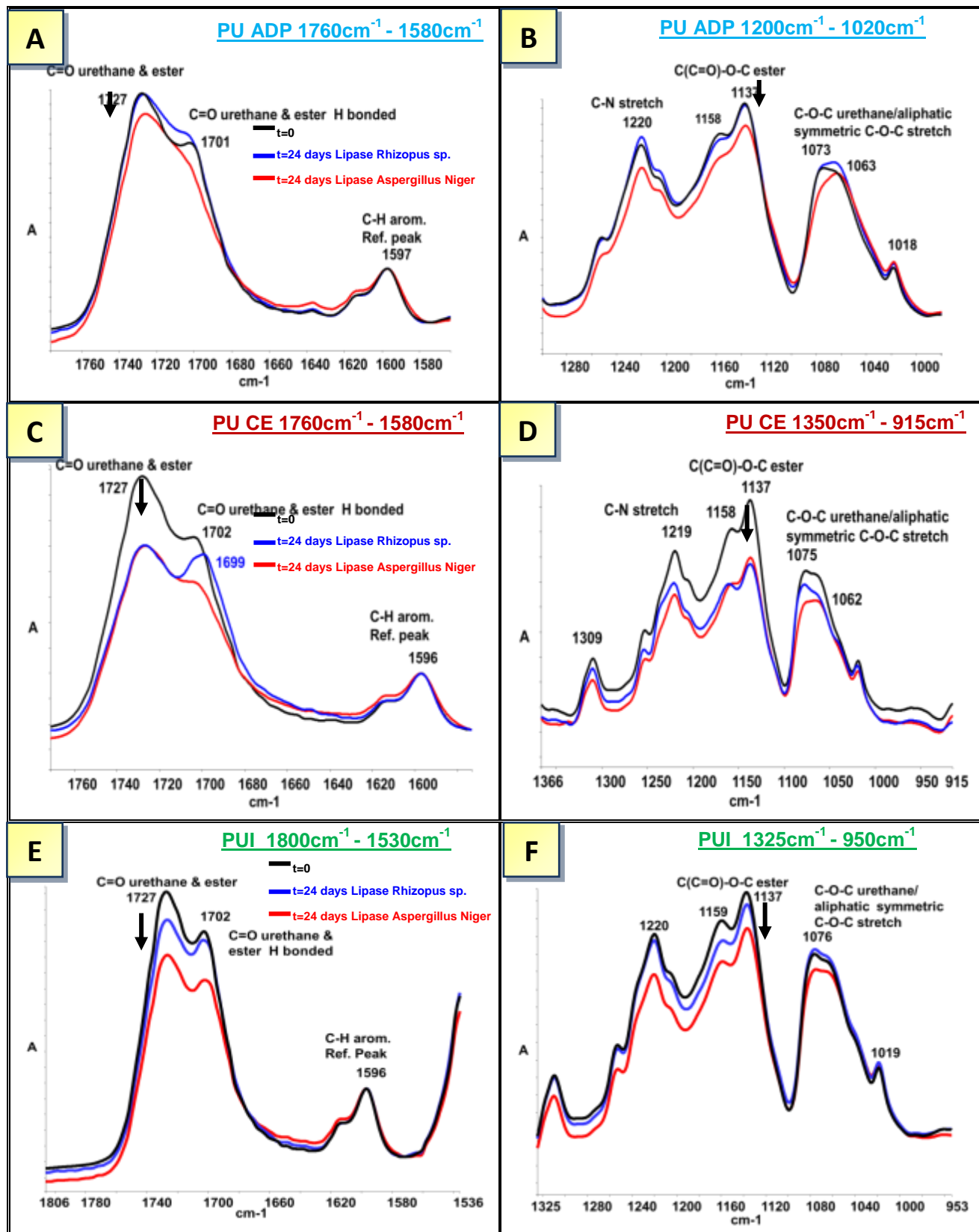


Figure 6.32 Effect of additives cellulose and iron stearate on structural changes during enzymatic degradation by lipase *Aspergillus niger* and *Rhizopus* sp. on PU ADP, PU CE & PUI determined by FTIR-ATR

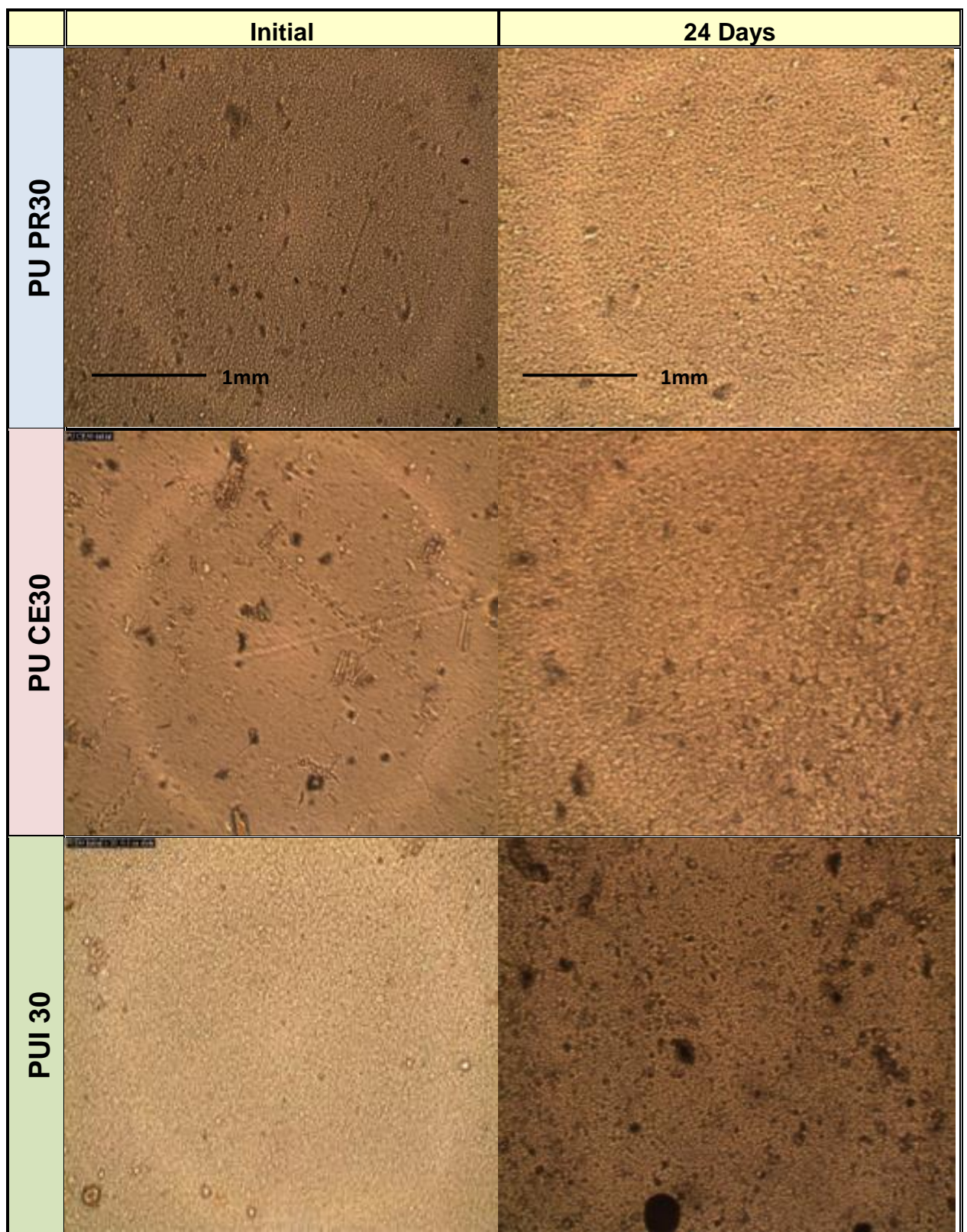


Figure 6.33 Effect of Cloisite 30B on enzymatic degradation by lipase *Aspergillus niger* PU PR30, PU CE30 & PUI 30 by optical microscope images

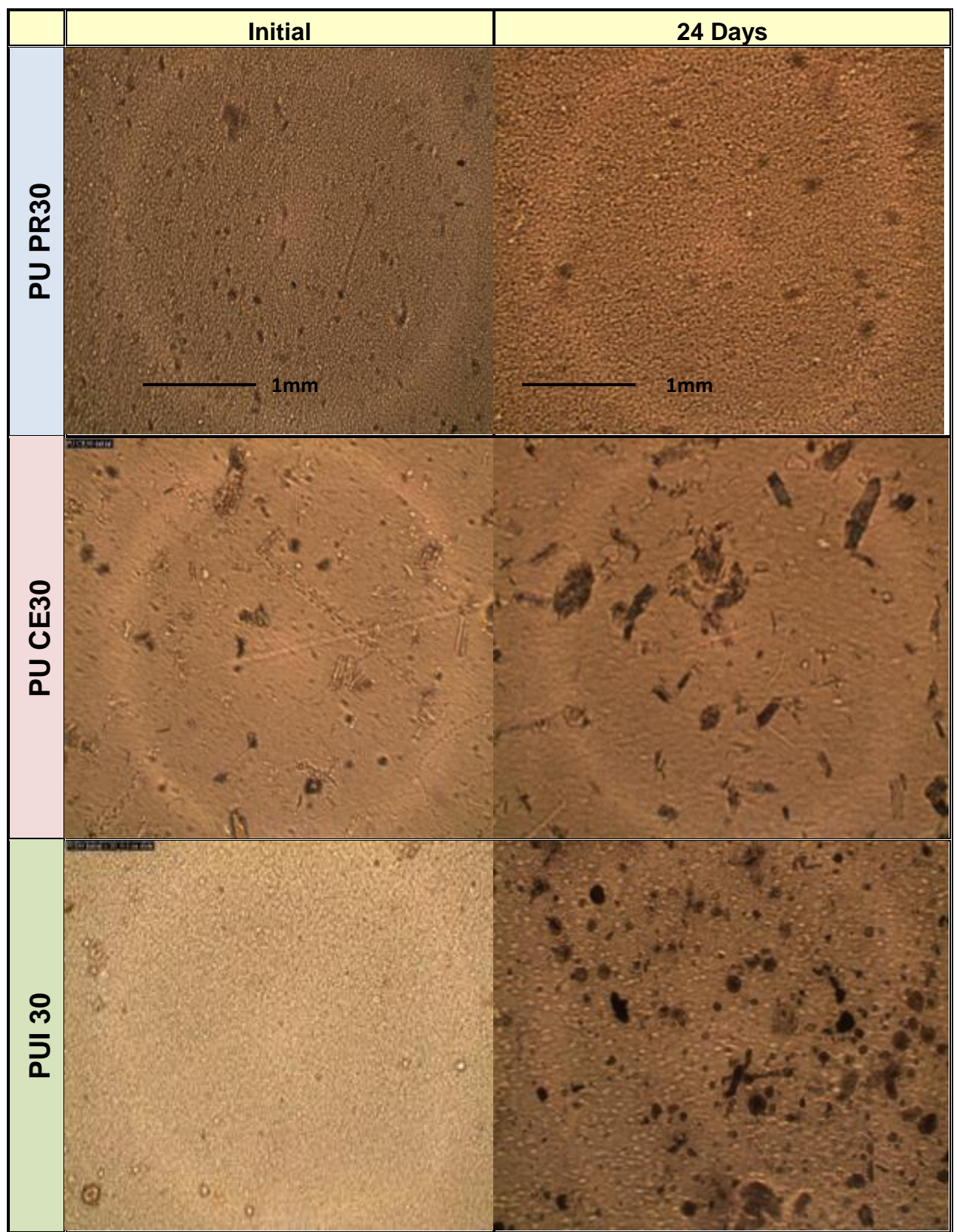


Figure 6.34 Effect of Cloisite 30B on enzymatic degradation by lipase *Rhizopus* sp. PU PR30, PU CE30 & PUI 30 by optical microscope images

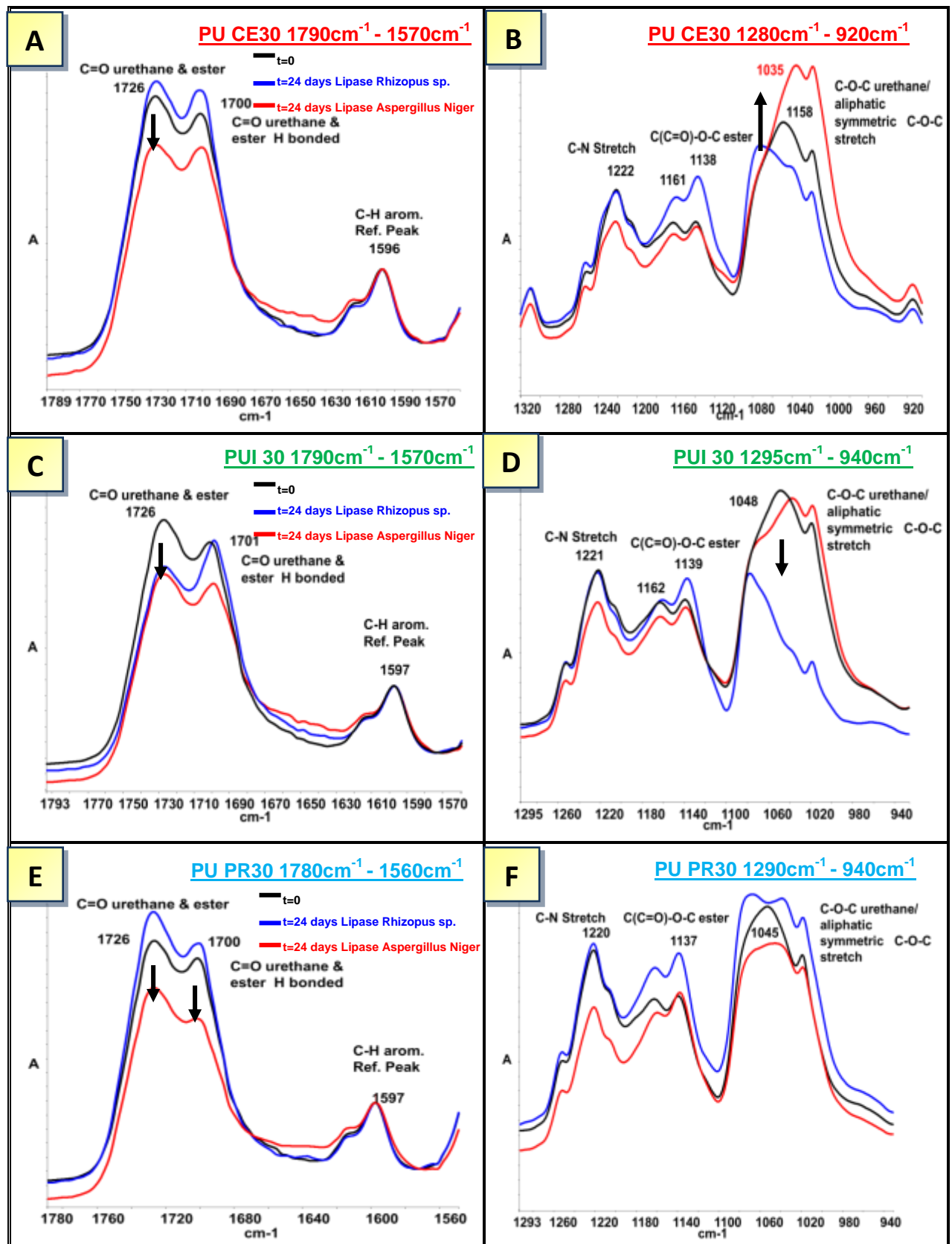


Figure 6.35 Effect of Cloisite 30B on structural changes during enzymatic degradation by lipase *Aspergillus niger* and *Rhizopus* sp. on PU CE30, PU PR30 & PUI 30 determined by FTIR-ATR

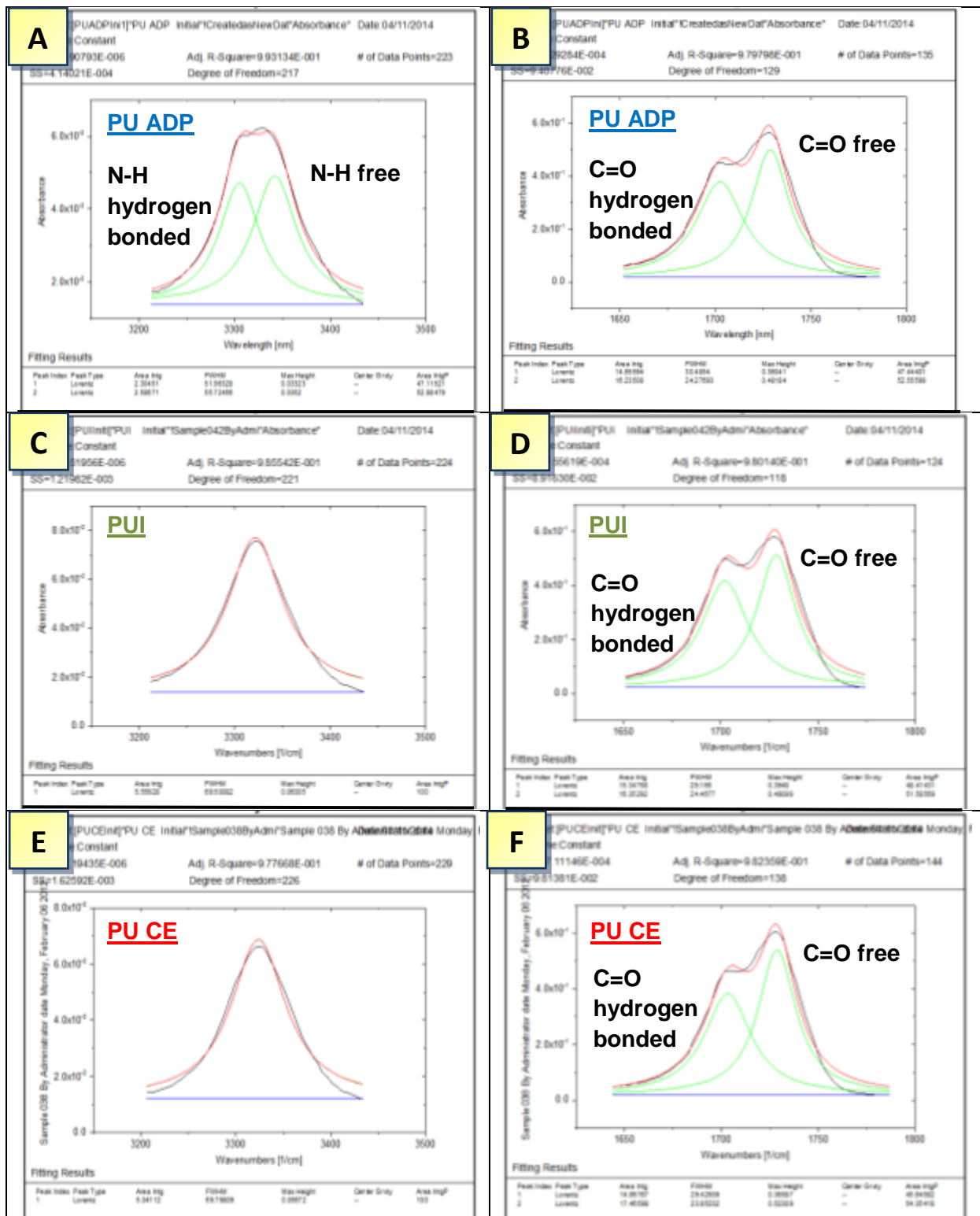


Figure 6.36 Effect of cellulose and iron stearate on hydrogen bonding in PUs

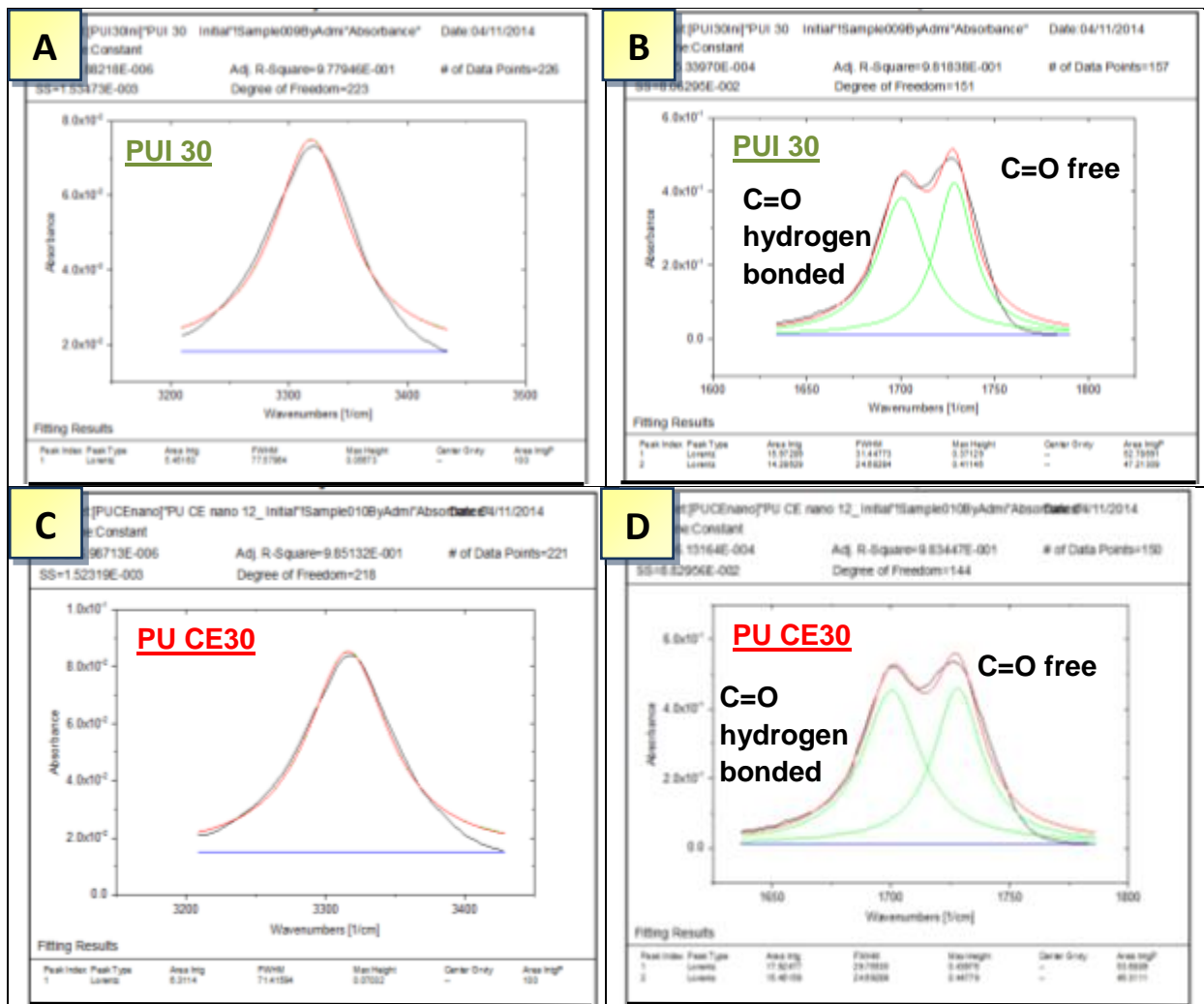


Figure 6.37 Effect of Cloisite 30B on hydrogen bonding in PUs

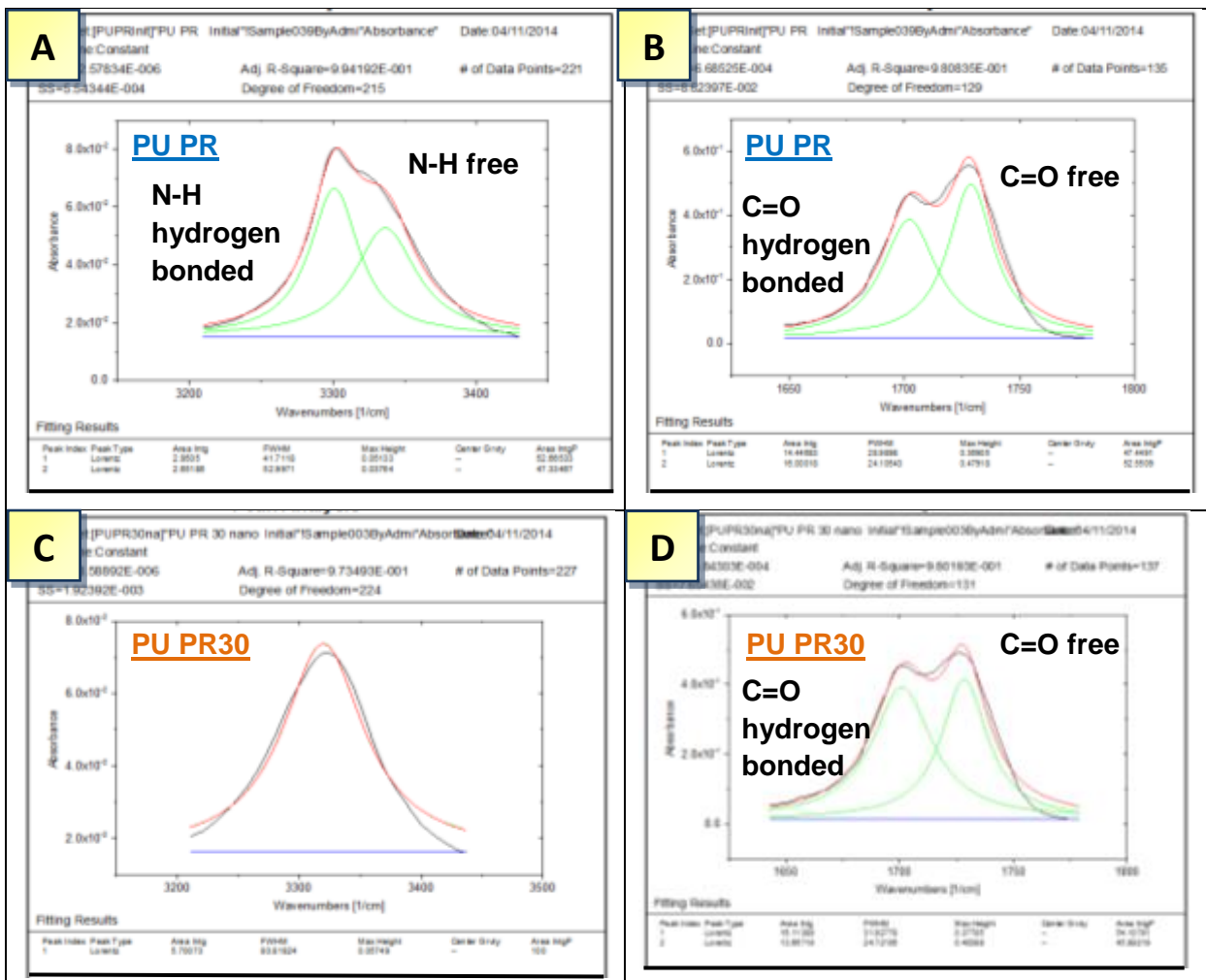


Figure 6.38 Effect of Cloisite 30B on hydrogen bonding in PUs

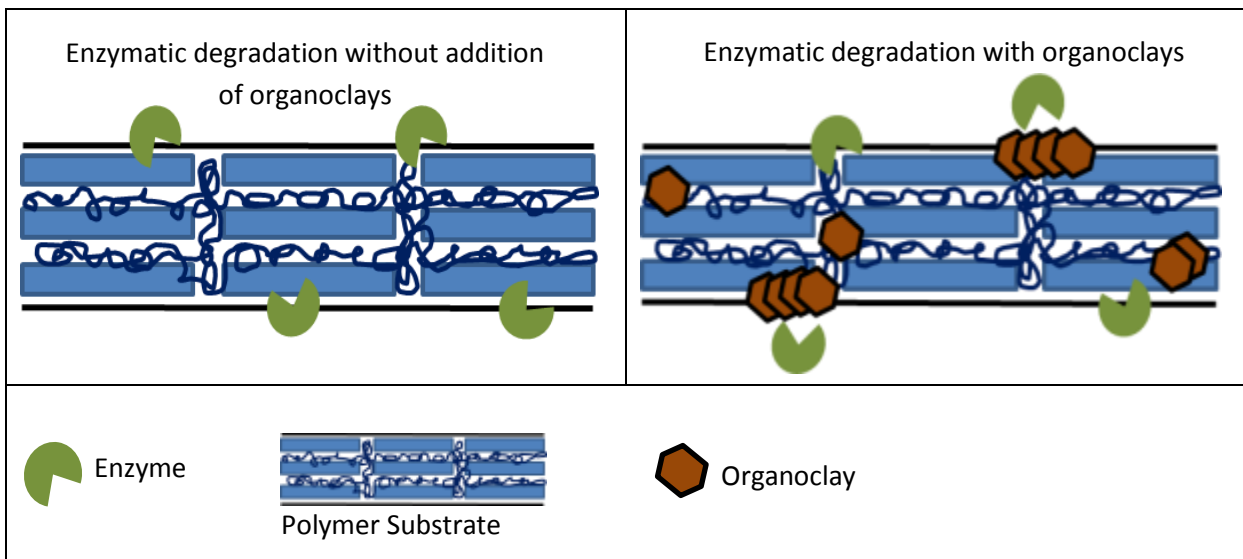


Figure 6.39 Effect of organoclays on the rate of enzymatic degradation

Chapter 7

Conclusions and Future Work

7.1 Conclusions

It can be concluded from the results discussed in **Chapters 3 to 6** that:

7.1.1 The method of synthesis was found to affect the rate of degradation and biodegradation of the TPU samples synthesised by Eurothane Ltd, with the PU sample synthesised by the pre-polymer method (**PU PR**) degrading faster than the PU synthesised by the one shot method (**PU ADP**), **Figs. 3.6 - 3.8**. Weight loss results during alkaline hydrolysis showed that **PU PR** (pre-polymer method), was more prone to degradation under alkaline conditions than **PU ADP** (one shot method), with a 7% weight remaining for **PU PR** after 21 days, (**PU ADP** 81% weight remaining) **Fig.3.6a**. This was supported by visual images in which the **PU PR** film became broken and fragile after 21 days while the **PU ADP** film remained intact even after 42 days, **Fig.3.8**. The reason for the increase in the rate of hydrolysis of **PU PR** is thought to be due to the morphology of the sample, and this was indeed found to be the case. Results from DSC analysis on the virgin films highlighted a difference in morphology dependent on the method of synthesis, with **PU ADP**, (synthesised by the one shot method) exhibiting a more crystalline structure than **PU PR** (synthesised by the pre-polymer method), **Fig. 3.4**. However, the T_g values were found to be similar for **PU ADP** (-18°C) and **PU PR** (-17°C), **Fig. 3.3**, indicating little difference in phase separation between the samples. An explanation as to the difference in crystallinity was thought to be due to the chain build up during synthesis. The pre-polymer method is more controlled and involves the rapid build-up of the molecular weight of the pre-polymer by the chain extender (BD), which then alters the morphology as the molecules become entangled and immobilized before order can be established. The one shot process in which all of the reactants are added at the same time resulted in highly crystalline mobile chain structures acting as crosslinks due to the lightly favoured reaction between BD and MDI, **Fig. 3.25**.

7.1.2 Neither **PU PR** nor **PU ADP** exhibited any significant degradation after exposure to the enzymes *Aspergillus niger*, *Aspergillus satoi* and *Rhizopus* sp., **Fig.3.20 & 3.22**. The same was observed after the samples had been buried in soil at RT for 20 months, with little biodegradation occurring in either **PU PR** or **PU ADP**, **Fig. 3.14**. It was concluded that the chemical components contained within the PU, had a greater influence than the method of synthesis with respect to enzymatic degradation, and the chemical components ADP, MDI and BD and the interactions between these components were not favourable substrates for enzymatic degradation. Overall, **PU PR** synthesised by the pre-polymer method was found to be less thermally stable, **Fig. 3.3**, less crystalline, **Fig. 3.4**, and more susceptible to hydrolysis, **Figs.3.6- 3.8**, than the PU synthesised by the one shot method (**PU ADP**). Therefore, in order to obtain PU's with limited shorter lifespans the pre-polymer method should be used, with a further possibility of increased biodegradation using alternative chemical constituents,

7.1.3 Altering the isocyanate was shown to have a profound effect on the morphology of the PU, with differences in phase separation, crystallinity and hydrogen bonding observed. **PUH ADP**, which contained the aliphatic isocyanate H₁₂MDI resulted in a TPU with increased phase separation, and increased hydrogen bonding, in comparison to the control sample **PU ADP** (aromatic isocyanate; MDI), **Figs. 4.2, 4.3 & 4.17**. It also resulted in a reduction of the amount of highly ordered crystalline structured regions, **Figs 4.2 & 4.3**. This change in morphology was shown to have a significant effect on the rate of degradation of the PU during alkaline hydrolysis, with the increased phase separation, and the reduction of crystalline regions in **PUH ADP** resulting in a faster rate of degradation, **Figs. 4.4 & 4.5**.

7.1.4 Alterating the isocyanate did not induce enzymatic degradation by the fungal enzymes *Aspergillus niger*, *Aspergillus satoi* and *Rhizopus* sp. nor did it increase the biodegradation under the soil burial conditions at RT, **Fig 4.11**, although **PUH ADP**, containing the aliphatic isocyanate did seem to confer a higher degree of enzymatic binding to the surface of the PU than the control sample **PU ADP** (aromatic isocyanate), **Fig. 4.14**, and this may have resulted in enzymatic degradation after a greater length of time. Although altering the isocyanate from MDI to H₁₂MDI did not influence the rate of biodegradation significantly, **Fig. 4.11**, it was considered to be more environmentally friendly to use PUs with aliphatic isocyanates for biodegradable PUs due to the possible toxic degradation/biodegradation products produced from PUs synthesised with an aromatic isocyanates.

- 7.1.5** The soft segment composition of the TPUs was shown to have a profound effect on the rate of degradation and biodegradation with a dramatic difference observed between **PU ADP** and **PU PCL** each of which contained a different polyester. **PU ADP** which contained an ADP soft segment was found to degrade at a faster rate under alkaline conditions than **PU PCL** which contained a PCL ester soft segment, **Fig 5.5**. The **PU PCL** film sample remained intact even after 56 days, with limited signs of degradation either visually or by weight loss **Figs 5.5 -5.7**. However, biodegradation under soil burial conditions produced results in contrast to accelerated alkaline hydrolysis. **PU ADP** (ADP ester) was not seen to degrade after soil burial for 20 months, however, **PU PCL** was found to be more biodegradable with visible cracks in the film noted, **Figs 5.12 & 5.13**. Previous studies, and results from Chapters 3 and 4 have shown that the extent of crystallinity affected the rate of degradation in PU, however this was not deemed to be the case in this instance, as the extent of crystallinity for **PU ADP** and **PU PCL** was found to be similar, **Fig 5.23**. Results from water absorption indicated that **PU PCL** was more hydrophobic than **PU ADP**, **Fig 5.1**, which supported previous literature in that the PCL ester soft segment in **PU PCL** is hydrophobic in nature, and this was believed to be the reason for the resistance towards accelerated alkaline hydrolysis, as water was not able to penetrate into the PCL soft segment. The increased rate of biodegradation under soil burial conditions for **PU PCL** was thought to be due to increased adhesion of microorganisms onto the surface of the PU which has previously been shown to occur through hydrophobic interactions between the microorganisms and the hydrophobic soft segment.
- 7.1.6** Altering the polyol from a polyester (ADP) to a polyether (PEG) was also found to influence the rate of degradation and biodegradation of the PU samples. Results from accelerated hydrolysis, enzymatic hydrolysis and soil burial revealed that the PU containing the polyether polyol (**PU PEG**) was found to degrade faster than **PU ADP**, which contained a polyester soft segment, **Fig 5.5**. The main reason for these findings was thought to be due to a combination of the amorphous nature of **PU PEG**, **Fig 5.24**, and also the increased hydrophilicity of **PU PEG**, **Fig 5.1**, which then resulted in an increase in the diffusion of water into the PU matrix and thereby accelerated its hydrolysis. The mechanism of degradation for **PU PEG** was speculated to depend upon the experimental conditions, with accelerated hydrolysis resulting in degradation of the hard segment by the hydrolysis of the urethane bonds, while the soft segment remained relatively unchanged, **Fig 5.24**. Exposure of **PU PEG** films to soil burial and enzymatic hydrolysis resulted in limited degradation of

both the hard and soft segments resulting from a combination of oxidative and microbial degradation mechanisms, **Fig 5.24**.

- 7.1.7 PU PGPC** containing a combination of PCL and PEG soft segment was found to degrade under both accelerated alkaline hydrolysis conditions **Figs 5.5 & 5.7**, and soil burial, **Figs 5.11-5.13**. The morphological profile of **PU PGPC** was found to be relatively amorphous in nature, and showed a greater degree of phase separation than its **PU PCL** and **PU PEG** counterparts, **Fig 5.4**. These two factors were considered to play a role in the rate of degradation and biodegradation of **PU PGPC**, however, the major factor regarding the rate of degradation of all of the samples in this group was deemed to be hydrophilicity of the PU sample, with a positive correlation observed between the rate of accelerated hydrolysis and hydrophilicity, **Figs 5.1 & 5.5**. The combination of a PEG and PCL soft segment resulted in a PU which contained hydrophilic domains from the PEG chains thereby enabling the diffusion of water into the PU, and also hydrophobic domains from the PCL chains conferring hydrophobic binding sites for degradation by microorganisms in the soil, therefore from the PUs examined in this study the soft segment containing a 50:50 PCL/PEG blend was considered to be the most conducive towards biodegradation and also exhibited substantial degradation during accelerated alkaline hydrolysis.
- 7.1.8** Determination of degradation in respect of alteration of the soft segment was found to be dependent on the method used. Accelerated alkaline hydrolysis measured by weight loss revealed that the rate of hydrolysis was in the order of **PU ADP > PU PEG > PU PGPC > PU PCL, Fig 5.5**. However, examination of the films visually revealed that the extent of degradation was in the order of **PU PEG > PU PGPC > PU ADP > PU PCL**, which was also the order of the hydrophilic nature of the PUs, **Figs. 5.1 & 5.7**. This difference between weight losses and visual images was mainly thought to be due to the hydrophilicity of **PU PEG** and **PU PGPC** which were thought to retain water in the bulk, even after drying, therefore distorting the weight loss measurements
- 7.1.9** The addition of microcrystalline cellulose and iron stearate affected the rate of degradation and biodegradation dependent on the method used to degrade the samples. Accelerated hydrolysis revealed the rate of degradation to be in the order of **PU ADP< PU CE< PUI, Fig. 6.10 - 6.12**. The increased rate of hydrolysis of **PUI** was deemed to be due to the reduced thermal stability of **PUI**, which was ascertained by TGA, **Fig. 6.3**. The addition of cellulose increased microcrystalline hard segment

domains in the PU samples **Fig 6.4**, however this did not reduce the rate of hydrolysis, with **PU CE** degrading after 42 days while **PU ADP** the control sample still remained intact, **Fig 6.11**. Biodegradation of the samples under soil burial conditions at 50°C was found to be in the order of **PU ADP < PU CE < PUI**, **Fig 6.20**, however, at RT the order was **PU ADP < PUI < PU CE**, **Figs 6.20 - 6.22**, and again the difference was thought to be due to the reduced thermal stability of **PUI** similar to its alkaline hydrolysis. Enzymatic degradation revealed that only **PU CE** had degraded significantly, **Figs 6.30 - 6.32**, therefore only **PU CE** was deemed to confer degradability on PU irrespective of the method of degradation, and this was thought to be due to the overriding effect of increased hydrophilicity and porous like structure of the PU film, **Fig. 6.2**, which increased the rate of alkaline hydrolysis, enzymatic hydrolysis and biodegradation by increasing the surface area exposed to the degradation media, **Fig. 6.2a**.

7.1.10 The effects of the addition of the organoclay, Cloisite 30B (12%) into PU was again found to be dependent on the method used to degrade the samples as of that for **PU CE** and **PUI**. Results from alkaline hydrolysis revealed that addition of the clay accelerated hydrolysis dramatically with the films completely broken up after just 7 days, for **PU PR30**, **PU CE30** and **PUI 30**, **Figs 6.15 - 6.16**. All of the samples displayed greater thermal stability, **Fig 6.8**, increased hydrophobicity, **Fig 6.5** and increased hydrogen bonding, **Figs 6.37 – 6.38**, within the PU matrix than the control samples **PU PR**, **PU CE** and **PUI**. However, the addition of Cloisite 30B also resulted in PUs with less microcrystalline domains, **Figs 6.4 & 6.9**. Therefore the most likely explanation as to this increase in hydrolytic degradation was due to this decrease in crystallinity. Biodegradation under soil burial conditions and enzymatic degradation produced opposite results to those of alkaline hydrolysis, in which the addition of the organoclay reduced degradation in the case of **PU CE30**, **Fig 6.22 & 6.26**, and did not induce degradation of **PUI 30** or **PU PR30**, **Fig 6.26**. This was thought to be due to the inaccessibility of the microorganisms and enzymes to the PUs which displayed increased hydrophobicity with the addition of the organoclay, **Fig 6.5**.

7.2 Recommendations for Further Work

7.2.1 This research and that by others have shown that degradation and biodegradation of TPU primarily occurs in their ‘soft segment’ (polyol), and although a variety of polyols were examined, it would be useful to examine other polyols which are deemed to be ‘biodegradable’ such as PLA, polyglycolic acid and polyhydroxyalkanoates.

7.2.2 A multitude of chemical constituents can be used in polyurethane synthesis as the ‘soft segment’ with the limiting factor being that the molecule contains at least either two hydroxyl or amine groups. It would be useful therefore to explore biological molecules which may be more prone to biodegradation as natural substrates, such as those from plant oils. Castor oil already contains a single hydroxyl group per fatty acid chain, and many other polyunsaturated fatty acids can be hydroxylated to make them potential candidates for biodegradable PUs.

7.2.3 This work showed that PUs synthesised by the pre-polymer method resulted in PUs which degraded faster under hydrolysis conditions and therefore, it would be useful to perform degradation and biodegradation experiments on PUs synthesised by the pre-polymer method which also contained chemical constituents and were found to be more degradable than the **PU PR** constituents, i.e. ADP, MDI and BD, such as; using a PCL/PEG soft segment and aliphatic isocyanate combination synthesised by the pre-polymer method.

7.2.4 During this work, the isocyanate and polyol were examined in respect of increasing biodegradability of TPUs. Future work could focus on alteration of the chain extender, not only by testing the effect of common chain extenders used commercially in TPU synthesis such as hexanediol, butanediol and diamines but also as described above in section 6.2.2, by exploring biological molecules to incorporate into TPUs as chain extenders.

7.2.5 This work highlighted the fact that the method of synthesis is an important factor on the rate of hydrolytic degradation. Therefore, further work should examine other synthesis

and processing conditions of TPUs; so as to determine the effect of process parameters such as reaction temperature, curing time and extrusion temperature etc on the rate of degradation and biodegradation.

7.2.6 The addition of Cloisite 30B was found to have a dramatic effect on the rate of degradation during alkaline hydrolysis but did not confer increased biodegradable properties on the PU. Further work could look at using other types of organoclays such as Bentonite and other modified montmorillonite clays. Also, more investigation into the interactions between the hard and soft segments and the organoclays in TPUs and the effect on degradation and biodegradation, better understood through the application of X-ray diffraction and small angle X-ray scattering techniques.

7.2.7 The incorporation of cellulose into TPU was found to increase hydrolytic and enzymatic degradation as well as biodegradation under soil burial conditions. As a follow up, it would be interesting to examine cellulosic derivatives known for their water absorbing capacity such as carboxymethylcellulose, as hydrophilicity was shown to increase degradation, as well examining the effect of the addition of other biopolymers into the PU matrix such as chitosan, starches, pectins and alginates.

References

- [1] R. Chandra and R. Rustgi, "Biodegradable polymers," *Progress in Polymer Science*, vol. 23, pp. 1273-1335, 1998.
- [2] A. A. Shah, F. Hasan, A. Hameed, and S. Ahmed, "Biological degradation of plastics: A comprehensive review," *Biotechnology Advances*, vol. 26, pp. 246-265, May-Jun 2008.
- [3] A. Hoshino and Y. Isono, "Degradation of aliphatic polyester films by commercially available lipases with special reference to rapid and complete degradation of poly(L-lactide) film by lipase PL derived from *Alcaligenes sp.*," *Biodegradation*, vol. 13, pp. 141-147, 2002.
- [4] R. L. Shogren, W. M. Doane, D. Garlotta, J. W. Lawton, and J. L. Willett, "Biodegradation of starch/polylactic acid/poly(hydroxyester-ether) composite bars in soil," *Polymer Degradation and Stability*, vol. 79, pp. 405-411, Mar 2003.
- [5] C. S. Wu and H. T. Liao, "Polycaprolactone-Based Green Renewable Ecocomposites Made from Rice Straw Fiber: Characterization and Assessment of Mechanical and Thermal Properties," *Industrial & Engineering Chemistry Research*, vol. 51, pp. 3329-3337, Feb 2012.
- [6] K. L. G. Ho, A. L. Pometto, A. Gadea-Rivas, J. A. Briceno, and A. Rojas, "Degradation of polylactic acid (PLA) plastic in Costa Rican soil and Iowa State University compost rows," *Journal of Environmental Polymer Degradation*, vol. 7, pp. 173-177, Oct 1999.
- [7] M. Harada, K. Iida, K. Okamoto, H. Hayashi, and K. Hirano, "Reactive compatibilization of biodegradable poly(lactic acid)/poly(epsilon-caprolactone) blends with reactive processing agents," *Polymer Engineering and Science*, vol. 48, pp. 1359-1368, Jul 2008.
- [8] W. Mizuno, M. Sano, C. J. Song, T. Nakatani, M. Yoshida, and S. Takeuchi, "Evaluation of biodegradability of several biodegradable plastics in natural environments," *Kobunshi Ronbunshu*, vol. 60, pp. 622-628, 2003.
- [9] C. Abrusci, J. L. Pablos, T. Corrales, J. Lopez-Marin, I. Marin, and E. Catalina, "Biodegradation of photo-degraded mulching films based on polyethylenes and stearates of calcium and iron as pro-oxidant additives," *International Biodeterioration & Biodegradation*, vol. 65, pp. 451-459, Jun 2011.
- [10] J. L. Pablos, C. Abrusci, I. Marin, J. Lopez-Marin, F. Catalina, E. Espi, et al., "Photodegradation of polyethylenes: Comparative effect of Fe and Ca-stearates as pro-oxidant additives," *Polymer Degradation and Stability*, vol. 95, pp. 2057-2064, Oct 2010.
- [11] J. P. Eubeler, M. Bernhard, and T. P. Knepper, "Environmental biodegradation of synthetic polymers II. Biodegradation of different polymer groups," *Trac-Trends in Analytical Chemistry*, vol. 29, pp. 84-100, Jan 2010.
- [12] C. Prisacariu, *Polyurethane Elastomers from Morphology to Mechanical Aspects*. New York: Springer, 2011.

- [13] C. Hepburn, *Polyurethane Elastomers*. New York: Elsevier science Publishing Co Inc, 1982.
- [14] M. a. Markets. (2011, 28/10/14). *Global MDI, TDI and Polyurethane Market by Type, Applications, Prices, Regulations, Trends and Forecasts 2011-2016*. Available: <http://www.marketsandmarkets.com/Market-Reports mdi-tdi-polyurethane-market-381.html>
- [15] I. Javni, W. Zhang, and Z. S. Petrovic, "Effect of different isocyanates on the properties of soy-based polyurethanes," *Journal of Applied Polymer Science*, vol. 88, pp. 2912-2916, Jun 24 2003.
- [16] W. Hettrich and R. Becker, "New isocyanates from amino acids," *Polymer*, vol. 38, pp. 2437-2445, May 1997.
- [17] M. K. Hassan, K. A. Mauritz, R. F. Storey, and J. S. Wiggins, "Biodegradable aliphatic thermoplastic polyurethane based on poly(epsilon-caprolactone) and L-lysine diisocyanate," *Journal of Polymer Science Part a-Polymer Chemistry*, vol. 44, pp. 2990-3000, May 2006.
- [18] M. Rogulska, A. Kultys, and S. Pikus, "Studies on thermoplastic polyurethanes based on new diphenylethane-derivative diols. III. The effect of molecular weight and structure of soft segment on some properties of segmented polyurethanes," *Journal of Applied Polymer Science*, vol. 110, pp. 1677-1689, Nov 2008.
- [19] T. Nakajima-Kambe, Y. Shigeno-Akutsu, N. Nomura, F. Onuma, and T. Nakahara, "Microbial degradation of polyurethane, polyester polyurethanes and polyether polyurethanes," *Applied Microbiology and Biotechnology*, vol. 51, pp. 134-140, Feb 1999.
- [20] M. Ionescu, *Chemistry and Technology of Polyols for Polyurethanes*. Shrewsbury: Smithers Rapra Technology, 2005.
- [21] S. R. Barratt, A. R. Ennos, M. Greenhalgh, G. D. Robson, and P. S. Handley, "Fungi are the predominant micro-organisms responsible for degradation of soil-buried polyester polyurethane over a range of soil water holding capacities," *Journal of Applied Microbiology*, vol. 95, pp. 78-85, 2003.
- [22] L. Cosgrove, P. L. McGeechan, G. D. Robson, and P. S. Handley, "Fungal communities associated with degradation of polyester polyurethane in soil," *Applied and Environmental Microbiology*, vol. 73, pp. 5817-5824, Sep 2007.
- [23] G. Mathur and R. Prasad, "Degradation of Polyurethane by Aspergillus flavus (ITCC 6051) Isolated from Soil," *Applied Biochemistry and Biotechnology*, vol. 167, pp. 1595-1602, Jul 2012.
- [24] J. R. Russell, J. Huang, P. Anand, K. Kucera, A. G. Sandoval, K. W. Dantzler, et al., "Biodegradation of Polyester Polyurethane by Endophytic Fungi," *Applied and Environmental Microbiology*, vol. 77, pp. 6076-6084, Sep 2011.
- [25] G. T. Howard, "Biodegradation of polyurethane: a review," *International Biodeterioration & Biodegradation*, vol. 49, pp. 245-252, 2002 2002.

- [26] S. Sarkar, P. Basak, and B. Adhikari, "Biodegradation of Polyethylene Glycol-Based Polyether Urethanes," *Polymer-Plastics Technology and Engineering*, vol. 50, pp. 80-88, 2011.
- [27] E. M. Christenson, J. M. Anderson, and A. Hittner, "Biodegradation mechanisms of polyurethane elastomers," *Corrosion Engineering Science and Technology*, vol. 42, pp. 312-323, Dec 2007.
- [28] A. Takahara, A. J. Coury, R. W. Hergenrother, and S. L. Cooper, "Effect of soft segment chemistry on the biostability of segmented polyurethanes 1 invitro oxidation," *Journal of Biomedical Materials Research*, vol. 25, pp. 341-356, Mar 1991.
- [29] J. D. Gu, "Microbiological deterioration and degradation of synthetic polymeric materials: recent research advances," *International Biodeterioration & Biodegradation*, vol. 52, pp. 69-91, 2003.
- [30] J. Kloss, F. S. M. de Souza, E. R. da Silva, J. A. Dionisio, L. Akcelrud, and S. F. Zawadzki, "Polyurethanes elastomers based on poly(epsilon-caprolactone) diol: Biodegradation evaluation," *Macromolecular Symposia*, vol. 245, pp. 651-656, 2006.
- [31] J. H. Hong, H. J. Jeon, J. H. Yoo, W. R. Yu, and J. H. Youk, "Synthesis and characterization of biodegradable poly(epsilon-caprolactone-co-beta-butyrolactone)-based polyurethane," *Polymer Degradation and Stability*, vol. 92, pp. 1186-1192, Jul 2007.
- [32] S. H. Chen, C. T. Tsao, H. C. Chou, C. H. Chang, C. T. Hsu, C. N. Chuang, et al., "Synthesis of poly(lactic acid)-based polyurethanes," *Polymer International*, vol. 62, pp. 1159-1168, Aug 2013.
- [33] H. Yeganeh, H. Jamshidi, and S. Jamshidi, "Synthesis and properties of novel biodegradable poly(epsilon-caprolactone)/poly(ethylene glycol)-based polyurethane elastomers," *Polymer International*, vol. 56, pp. 41-49, Jan 2007.
- [34] D. K. Chattopadhyay and D. C. Webster, "Thermal stability and flame retardancy of polyurethanes," *Progress in Polymer Science*, vol. 34, pp. 1068-1133, Oct 2009.
- [35] B. I. Dahiyat, E. M. Posadas, S. Hirosue, E. Hostin, and K. W. Leong, "Degradable biomaterials with elastomeric characteristics and drug carrier function," *Reactive Polymers*, vol. 25, pp. 101-109, Jun 1995.
- [36] G. A. Skarja and K. A. Woodhouse, "In vitro degradation and erosion of degradable, segmented polyurethanes containing an amino acid-based chain extender," *Journal of Biomaterials Science-Polymer Edition*, vol. 12, pp. 851-873, 2001.
- [37] J. N. Baumgartner, C. Z. Yang, and S. L. Cooper, "Physical property analysis and bacterial adhesion on a series of phosphonated polyurethanes," *Biomaterials*, vol. 18, pp. 831-837, Jun 1997.
- [38] P. Krol, "Synthesis methods, chemical structures and phase structures of linear polyurethanes. Properties and applications of linear polyurethanes in polyurethane elastomers, copolymers and ionomers," *Progress in Materials Science*, vol. 52, pp. 915-1015, Aug 2007.

- [39] A. Eceiza, M. D. Martin, K. de la Caba, G. Kortaberria, N. Gabilondo, M. A. Corcuera, *et al.*, "Thermoplastic polyurethane elastomers based on polycarbonate diols with different soft segment molecular weight and chemical structure: Mechanical and thermal properties," *Polymer Engineering and Science*, vol. 48, pp. 297-306, Feb 2008.
- [40] Y. J. Li, W. X. Kang, J. O. Stoffer, and B. Chu, "Effect of hard segment flexibility on phase separation of segmented polyurethanes," *Macromolecules*, vol. 27, pp. 612-614, Jan 1994.
- [41] Y. He, D. L. Xie, and X. Y. Zhang, "The structure, microphase-separated morphology, and property of polyurethanes and polyureas," *Journal of Materials Science*, vol. 49, pp. 7339-7352, Nov 2014.
- [42] M. M. Coleman, K. H. Lee, D. J. Skrovanek, and P. C. Painter, "Hydrogen bonding in polymers 4. infrared temperature studies of a simple polyurethane," *Macromolecules*, vol. 19, pp. 2149-2157, Aug 1986.
- [43] J. Mattia and P. Painter, "A comparison of hydrogen bonding and order in a polyurethane and poly(urethane-urea) and their blends with poly(ethylene glycol)," *Macromolecules*, vol. 40, pp. 1546-1554, Mar 2007.
- [44] I. Yilgor, E. Yilgor, I. G. Guler, T. C. Ward, and G. L. Wilkes, "FTIR investigation of the influence of diisocyanate symmetry on the morphology development in model segmented polyurethanes," *Polymer*, vol. 47, pp. 4105-4114, May 2006.
- [45] L. S. Zha, M. Y. Wu, and J. J. Yang, "Hydrogen bonding and morphological structure of segmented polyurethanes based on hydroquinone-bis(beta-hydroxyethyl)ether as a chain extender," *Journal of Applied Polymer Science*, vol. 73, pp. 2895-2902, Sep 1999.
- [46] B. F. D'Arlas, L. Rueda, K. De la Caba, I. Mondragon, and A. Eceiza, "Microdomain composition and properties differences of biodegradable polyurethanes based on MDI and HDI," *Polymer Engineering and Science*, vol. 48, pp. 519-529, Mar 2008.
- [47] T. L. Wang and T. H. Hsieh, "Effect of polyol structure and molecular weight on the thermal stability of segmented poly(urethaneureas)," *Polymer Degradation and Stability*, vol. 55, pp. 95-102, 1997.
- [48] T. O. Ahn, I. S. Choi, H. M. Jeong, and K. Cho, "Thermal and mechanical properties of thermoplastic polyurethane elastomers from different polymerization methods," *Polymer International*, vol. 31, pp. 329-333, 1993.
- [49] S. Yamasaki, D. Nishiguchi, K. Kojio, and M. Furukawa, "Effects of polymerization method on structure and properties of thermoplastic polyurethanes," *Journal of Polymer Science Part B-Polymer Physics*, vol. 45, pp. 800-814, Apr 2007.
- [50] P. Vermette, J. Griesser, G. Laroche, and R. Guidoin, *Biomedical Applications of Polyurethanes*. Texas USA: Eureka!Com, 2001.
- [51] S. Abouzahr and G. L. Wilkes, "Structure property studies of polyester based and polyether based MDI-BD segmented polyurethanes - effect of one stage vs 2 stage polymerisation conditions," *Journal of Applied Polymer Science*, vol. 29, pp. 2695-2711, 1984.

- [52] K. Dusek, M. Spirkova, and I. Havlicek, "Network formation of polyurethanes due to side reactions," *Macromolecules*, vol. 23, pp. 1774-1781, Mar 1990.
- [53] B. Singh and N. Sharma, "Mechanistic implications of plastic degradation," *Polymer Degradation and Stability*, vol. 93, pp. 561-584, Mar 2008.
- [54] Y. L. Luo, Y. Miao, and F. Xu, "Synthesis, phase behavior, and simulated in vitro degradation of novel HTPB-b-PEG polyurethane copolymers," *Macromolecular Research*, vol. 19, pp. 1233-1241, Dec 2011.
- [55] S. Vlad, I. Spiridon, C. V. Grigoras, M. Drobota, and A. Nistor, "Thermal, mechanical and wettability properties of some branched polyetherurethane elastomers," *E-Polymers*, p. 11, Jan 2009.
- [56] C. Y. Gong, S. Z. Fu, Y. C. Gu, C. B. Liu, B. Kan, H. X. Deng, et al., "Synthesis, Characterization, and Hydrolytic Degradation of Biodegradable Poly(ether ester)-Urethane Copolymers Based on epsilon-Caprolactone and Poly(ethylene glycol)," *Journal of Applied Polymer Science*, vol. 113, pp. 1111-1119, Jul 2009.
- [57] N. Lucas, C. Bienaime, C. Belloy, M. Queneudec, F. Silvestre, and J. E. Navas-Saucedo, "Polymer biodegradation: Mechanisms and estimation techniques," *Chemosphere*, vol. 73, pp. 429-442, Sep 2008.
- [58] N. Vasanthan and O. Ly, "Effect of microstructure on hydrolytic degradation studies of poly (L-lactic acid) by FTIR spectroscopy and differential scanning calorimetry," *Polymer Degradation and Stability*, vol. 94, pp. 1364-1372, Sep 2009.
- [59] L. H. Chan-Chan, R. Solis-Correa, R. F. Vargas-Coronado, J. M. Cervantes-Uc, J. V. Cauich-Rodriguez, P. Quintana, et al., "Degradation studies on segmented polyurethanes prepared with HMDI, PCL and different chain extenders," *Acta Biomaterialia*, vol. 6, pp. 2035-2044, Jun 2010.
- [60] Y. W. Tang, R. S. Labow, and J. P. Santerre, "Enzyme-induced biodegradation of polycarbonate polyurethanes: Dependence on hard-segment concentration," *Journal of Biomedical Materials Research*, vol. 56, pp. 516-528, Sep 15 2001.
- [61] A. A. Shah, F. Hasan, J. I. Akhter, A. Hameed, and S. Ahmed, "Degradation of polyurethane by novel bacterial consortium isolated from soil," *Annals of Microbiology*, vol. 58, pp. 381-386, 2008.
- [62] M. Cregut, M. Bedas, M. J. Durand, and G. Thouand, "New insights into polyurethane biodegradation and realistic prospects for the development of a sustainable waste recycling process," *Biotechnology Advances*, vol. 31, pp. 1634-1647, Dec 2013.
- [63] A. C. Groenhof, "Composting: Renaissance of an age-old technology," *Biologist*, vol. 45, pp. 164-167, 1998.
- [64] Y. D. Kim and S. C. Kim, "Effect of chemical structure on the biodegradation of polyurethanes under composting conditions," *Polymer Degradation and Stability*, vol. 62, pp. 343-352, 1998.
- [65] K. A. Whitehead, T. Deisenroth, A. Preuss, C. M. Liauw, and J. Verran, "The effect of surface properties on the strength of attachment of fungal spores using AFM perpendicular force measurements," *Colloids and Surfaces B-Biointerfaces*, vol. 82, pp. 483-489, Feb 1 2011.

- [66] A. Watanabe, Y. Takebayashi, T. Ohtsubo, and M. Furukawa, "Dependence of Biodegradation and Release Behavior on Physical Properties of Poly(caprolactone)-Based Polyurethanes," *Journal of Applied Polymer Science*, vol. 114, pp. 246-253, Oct 2009.
- [67] J. Bart, *Additives in Polymers, Industrial Analysis and Applications*. Chichester: John Wiley and Sons Ltd, 2005.
- [68] R. Pfaendner, "How will additives shape the future of plastics?," *Polymer Degradation and Stability*, vol. 91, pp. 2249-2256, Sep 2006.
- [69] G. Drobny, *Handbook of Thermoplastic Elastomers*: William Andrew Publishing/Plastics Designs Library, 2007.
- [70] S. C. Tjong, "Structural and mechanical properties of polymer nanocomposites," *Materials Science & Engineering R-Reports*, vol. 53, pp. 73-197, Aug 2006.
- [71] M. R. Calil, F. Gaboardi, M. A. G. Bardi, M. L. Rezende, and D. S. Rosa, "Enzymatic degradation of poly (epsilon-caprolactone) and cellulose acetate blends by lipase and alpha-amylase," *Polymer Testing*, vol. 26, pp. 257-261, Apr 2007.
- [72] J. W. Rhim, H. M. Park, and C. S. Ha, "Bio-nanocomposites for food packaging applications," *Progress in Polymer Science*, vol. 38, pp. 1629-1652, Oct-Nov 2013.
- [73] K. Fukushima, C. Abbate, D. Tabuani, M. Gennari, P. Rizzarelli, and G. Camino, "Biodegradation trend of poly(epsilon-caprolactone) and nanocomposites," *Materials Science & Engineering C-Materials for Biological Applications*, vol. 30, pp. 566-574, May 2010.
- [74] S. Al-Malaika, A. M. Marogi, and G. Scott, "Mechanisms of antioxidant action - time controlled photoantioxidants for polyethylene based on soluble iron compounds," *Journal of Applied Polymer Science*, vol. 31, pp. 685-698, Feb 5 1986.
- [75] S. Al-Malaika, A. Marogi, and G. Scott, "Mechanisms of antioxidant action - time controlled stabilization of polypropylene by transition metal dithiocarbamates," *Polymer Degradation and Stability*, vol. 18, pp. 89-98, 1987.
- [76] S. Al-Malaika, A. Marogi, and G. Scott, "Mechanisms of antioxidant action - transformations involved in the antioxidant function of metal dialkyl dithiocarbamates III," *Journal of Applied Polymer Science*, vol. 33, pp. 1455-1471, Apr 1987.
- [77] R. Sabo, L. W. Jin, N. Stark, and R. E. Ibach, "Effect of Environmental Conditions on the Mechanical Properties and Fungal Degradation of Polycaprolactone/Microcrystalline Cellulose/Wood Flour Composites," *Bioresources*, vol. 8, pp. 3322-3335, 2013.
- [78] K. M. Zia, M. Barikani, I. A. Bhatti, M. Zuber, and H. N. Bhatti, "Synthesis and characterization of novel, biodegradable, thermally stable chitin-based polyurethane Elastomers," *Journal of Applied Polymer Science*, vol. 110, pp. 769-776, Oct 15 2008.
- [79] T. Travinskaya, Y. Savelyev, and E. Mishchuk, "Waterborne polyurethane based starch containing materials: Preparation, properties and study of degradability," *Polymer Degradation and Stability*, vol. 101, pp. 102-108, May 2014.

- [80] M. P. Arrieta, E. Fortunati, F. Dominici, E. Rayon, J. Lopez, and J. M. Kenny, "PLA-PHB/cellulose based films: Mechanical, barrier and disintegration properties," *Polymer Degradation and Stability*, vol. 107, pp. 139-149, Sep 2014.
- [81] M. R. Calil, F. Gaboardi, C. G. F. Guedes, and D. S. Rosa, "Comparison of the biodegradation of poly(epsilon-caprolactone), cellulose acetate and their blends by the Sturm test and selected cultured fungi," *Polymer Testing*, vol. 25, pp. 597-604, Aug 2006.
- [82] D. Oldak, H. Kaczmarek, T. Buffeteau, and C. Sourisseau, "Photo- and bio-degradation processes in polyethylene, cellulose and their blends studied by ATR-FTIR and Raman spectroscopies," *Journal of Materials Science*, vol. 40, pp. 4189-4198, Aug 2005.
- [83] L. R. Lynd, P. J. Weimer, W. H. van Zyl, and I. S. Pretorius, "Microbial cellulose utilization: Fundamentals and biotechnology," *Microbiology and Molecular Biology Reviews*, vol. 66, pp. 506-+, Sep 2002.
- [84] C. Sanchez, "Lignocellulosic residues: Biodegradation and bioconversion by fungi," *Biotechnology Advances*, vol. 27, pp. 185-194, Mar-Apr 2009.
- [85] P. Beguin, "Molecular biology of cellulose degradation," *Annual Review of Microbiology*, vol. 44, pp. 219-248, 1990.
- [86] L. N. Luduena, A. Vazquez, and V. A. Alvarez, "Effect of the type of clay organo-modifier on the morphology, thermal/mechanical/impact/barrier properties and biodegradation in soil of polycaprolactone/clay nanocomposites," *Journal of Applied Polymer Science*, vol. 128, pp. 2648-2657, Jun 2013.
- [87] L. Bistricic, G. Baranovic, M. Leskovac, and E. G. Bajsic, "Hydrogen bonding and mechanical properties of thin films of polyether-based polyurethane-silica nanocomposites," *European Polymer Journal*, vol. 46, pp. 1975-1987, Oct 2010.
- [88] G. Gorrasi, M. Tortora, and V. Vittoria, "Synthesis and physical properties of layered silicates/polyurethane nanocomposites," *Journal of Polymer Science Part B-Polymer Physics*, vol. 43, pp. 2454-2467, Sep 2005.
- [89] F. Khan and Y. Dahman, "A Novel Approach for the Utilization of Biocellulose Nanofibres in Polyurethane Nanocomposites for Potential Applications in Bone Tissue Implants," *Designed Monomers and Polymers*, vol. 15, pp. 1-29, 2012 2012.
- [90] Y. I. Tien and K. H. Wei, "Thermal transitions of montmorillonite/polyurethane nanocomposites," *Journal of Polymer Research-Taiwan*, vol. 7, pp. 245-250, Dec 2000.
- [91] S. Pavlidou and C. D. Papaspyrides, "A review on polymer-layered silicate nanocomposites," *Progress in Polymer Science*, vol. 33, pp. 1119-1198, Dec 2008.
- [92] T. F. Wu, T. X. Xie, and G. S. Yang, "Preparation and characterization of poly(epsilon-caprolactone)/Na+-MMT nanocomposites," *Applied Clay Science*, vol. 45, pp. 105-110, Jul 2009.
- [93] S. Dutta, N. Karak, J. P. Saikia, and B. K. Konwar, "Biocompatible epoxy modified bio-based polyurethane nanocomposites: Mechanical property, cytotoxicity and biodegradation," *Bioresource Technology*, vol. 100, pp. 6391-6397, Dec 2009.

- [94] N. K. Singh, B. Das Purkayastha, J. K. Roy, R. M. Banik, M. Yashpal, G. Singh, *et al.*, "Nanoparticle-Induced Controlled Biodegradation and Its Mechanism in Poly(epsilon-caprolactone)," *Acs Applied Materials & Interfaces*, vol. 2, pp. 69-81, Jan 2010.
- [95] C. Bastioli, *Handbook of Biodegradable Polymers*. Shrewsbury: Rapra Technology Limited, 2005.
- [96] J. P. Eubeler, M. Bernhard, S. Zok, and T. P. Knepper, "Environmental biodegradation of synthetic polymers I. Test methodologies and procedures," *Trac-Trends in Analytical Chemistry*, vol. 28, pp. 1057-1072, Oct 2009.
- [97] K. L. E. Kaiser, "Review of biodegradability tests for the purpose of developing regulations," *Water Quality Research Journal of Canada*, vol. 33, pp. 185-211, 1998.
- [98] S. Oprea, "Dependence of fungal biodegradation of PEG/castor oil-based polyurethane elastomers on the hard-segment structure," *Polymer Degradation and Stability*, vol. 95, pp. 2396-2404, Dec 2010.
- [99] K. Krasowska, H. Janik, A. Gradys, and M. Rutkowska, "Degradation of polyurethanes in compost under natural conditions," *Journal of Applied Polymer Science*, vol. 125, pp. 4252-4260, Sep 2012.
- [100] L. Tatai, T. G. Moore, R. Adhikari, F. Malherbe, R. Jayasekara, I. Griffiths, *et al.*, "Thermoplastic biodegradable polyurethanes: The effect of chain extender structure on properties and in-vitro degradation," *Biomaterials*, vol. 28, pp. 5407-5417, Dec 2007.
- [101] M. Friedman, "Applications of the ninhydrin reaction for analysis of amino acids, peptides, and proteins to agricultural and biomedical sciences," *Journal of Agricultural and Food Chemistry*, vol. 52, pp. 385-406, Feb 2004.
- [102] S. S. Umare and A. S. Chandure, "Synthesis, characterization and biodegradation studies of poly(ester urethane)s," *Chemical Engineering Journal*, vol. 142, pp. 65-77, Aug 2008.
- [103] K. Hiltunen, J. Tuominen, and J. V. Seppala, "Hydrolysis of lactic acid based poly(ester-urethane)s," *Polymer International*, vol. 47, pp. 186-192, Oct 1998.
- [104] L. Rueda-Larraz, B. F. d'Arlas, A. Tercjak, A. Ribes, I. Mondragon, and A. Eceizaa, "Synthesis and microstructure-mechanical property relationships of segmented polyurethanes based on a PCL-PTHF-PCL block copolymer as soft segment," *European Polymer Journal*, vol. 45, pp. 2096-2109, Jul 2009.
- [105] S. J. McCarthy, G. F. Meijis, N. Mitchell, P. A. Gunatillake, G. Heath, A. Brandwood, *et al.*, "In-vivo degradation of polyurethanes: transmission-FTIR microscopic characterization of polyurethanes sectioned by cryomicrotomy," *Biomaterials*, vol. 18, pp. 1387-1409, Nov 1997.
- [106] S. Hsu and T. B. Huang, "The susceptibility of poly(ether)urethanes to enzymatic degradation after oxidative pretreatment," *Polymer Degradation and Stability*, vol. 67, pp. 171-178, 2000 2000.

- [107] T. R. Hesketh, J. W. C. Vanbogart, and S. L. Cooper, "Differential scanning calorimetry analysis of morphological changes in segmented elastomers," *Polymer Engineering and Science*, vol. 20, pp. 190-197, 1980 1980.
- [108] L. M. Leung and J. T. Koberstein, "DSC annealing study of microphase separation and multiple endothermic behaviour in polyether based polyurethane block copolymers," *Macromolecules*, vol. 19, pp. 706-713, Mar 1986.
- [109] E. G. Bajsic, V. Rek, A. Sendijarevic, V. Sendijarevic, and K. C. Frisch, "DSC study of morphological changes in segmented polyurethane elastomers," *Journal of Elastomers and Plastics*, vol. 32, pp. 162-182, Apr 2000.
- [110] E. H. Jeong, J. Yang, H. S. Lee, S. W. Seo, D. H. Baik, J. H. Kim, et al., "Effective preparation and characterization of montmorillonite/poly(epsilon-caprolactone)-based polyurethane nanocomposites," *Journal of Applied Polymer Science*, vol. 107, pp. 803-809, Jan 2008.
- [111] D. K. Dempsey, J. L. Robinson, A. V. Iyer, J. P. Parakka, R. S. Bezwada, and E. M. Cosgriff-Hernandez, "Characterization of a resorbable poly(ester urethane) with biodegradable hard segments," *Journal of Biomaterials Science-Polymer Edition*, vol. 25, pp. 535-554, Apr 13 2014.
- [112] H. Yeganeh and P. Hojati-Talemi, "Preparation and properties of novel biodegradable polyurethane networks based on castor oil and poly(ethylene glycol)," *Polymer Degradation and Stability*, vol. 92, pp. 480-489, Mar 2007.
- [113] L. J. Zhou, D. Liang, X. L. He, J. H. Li, H. Tan, J. S. Li, et al., "The degradation and biocompatibility of pH-sensitive biodegradable polyurethanes for intracellular multifunctional antitumor drug delivery," *Biomaterials*, vol. 33, pp. 2734-2745, Mar 2012.
- [114] J. R. Schoonover, D. G. Thompson, J. C. Osborn, E. B. Orler, D. A. Wroblewski, A. L. Marsh, et al., "Infrared linear dichroism study of a hydrolytically degraded poly(ester urethane)," *Polymer Degradation and Stability*, vol. 74, pp. 87-96, 2001 2001.
- [115] U. Zafar, A. Houlden, and G. D. Robson, "Fungal Communities Associated with the Biodegradation of Polyester Polyurethane Buried under Compost at Different Temperatures," *Applied and Environmental Microbiology*, vol. 79, pp. 7313-7324, Dec 2013.
- [116] S. Oprea and F. Doroftei, "Biodegradation of polyurethane acrylate with acrylated epoxidized soybean oil blend elastomers by Chaetomium globosum," *International Biodeterioration & Biodegradation*, vol. 65, pp. 533-538, Jun 2011.
- [117] Y. Wu, C. Sellitti, J. M. Anderson, A. Hiltner, G. A. Lodoen, and C. R. Payet, "An FTIR-ATR investigation of invitro poly(ether urethane) degradation," *Journal of Applied Polymer Science*, vol. 46, pp. 201-211, Sep 15 1992.
- [118] H. J. Qi and M. C. Boyce, "Stress-strain behavior of thermoplastic polyurethanes," *Mechanics of Materials*, vol. 37, pp. 817-839, Aug 2005.
- [119] Y. T. Shieh, H. T. Chen, K. H. Liu, and Y. K. Twu, "Thermal degradation of MDI-based segmented polyurethanes," *Journal of Polymer Science Part a-Polymer Chemistry*, vol. 37, pp. 4126-4134, Nov 1999.

- [120] J. P. Santerre, K. Woodhouse, G. Laroche, and R. S. Labow, "Understanding the biodegradation of polyurethanes: From classical implants to tissue engineering materials," *Biomaterials*, vol. 26, pp. 7457-7470, Dec 2005.
- [121] S. Mondal and D. Martin, "Hydrolytic degradation of segmented polyurethane copolymers for biomedical applications," *Polymer Degradation and Stability*, vol. 97, pp. 1553-1561, Aug 2012.
- [122] C. Wilhelm, A. Rivaton, and J. L. Gardette, "Infrared analysis of the photochemical behaviour of segmented polyurethanes - 3. Aromatic diisocyanate based polymers," *Polymer*, vol. 39, pp. 1223-1232, Mar 1998.
- [123] C. P. Christenson, M. A. Harthcock, M. D. Meadows, H. L. Spell, W. L. Howard, M. W. Creswick, *et al.*, "Model MDI butanediol polyurethanes - molecular structure morphology, physical and mechanical properties," *Journal of Polymer Science Part B-Polymer Physics*, vol. 24, pp. 1401-1439, Jul 1986.
- [124] L. Irusta and M. J. Fernandez-Berridi, "Aromatic poly(ester-urethanes): effect of the polyol molecular weight on the photochemical behaviour," *Polymer*, vol. 41, pp. 3297-3302, Apr 2000.
- [125] C. Wilhelm and J. L. Gardette, "Infrared analysis of the photochemical behaviour of segmented polyurethanes .1. Aliphatic poly(ester-urethane)," *Polymer*, vol. 38, pp. 4019-4031, Aug 1997.
- [126] Y. M. Song, W. C. Chen, T. L. Yu, K. Linliu, and Y. H. Tseng, "Effect of isocyanates on the crystallinity and thermal stability of polyurethanes," *Journal of Applied Polymer Science*, vol. 62, pp. 827-834, Oct 1996.
- [127] J. M. Cervantes-Uc, J. I. M. Espinosa, J. V. Cauch-Rodriguez, A. Avila-Ortega, H. Vazquez-Torres, A. Marcos-Fernandez, *et al.*, "TGA/FTIR studies of segmented aliphatic polyurethanes and their nanocomposites prepared with commercial montmorillonites," *Polymer Degradation and Stability*, vol. 94, pp. 1666-1677, 2009.
- [128] T. K. Chen, T. S. Shieh, and J. Y. Chui, "Studies on the first DSC endotherm of polyurethane hard segment based on 4,4'-diphenylmethane diisocyanate and 1,4-butanediol," *Macromolecules*, vol. 31, pp. 1312-1320, Feb 24 1998.
- [129] A. Loredo-Trevino, G. Gutierrez-Sanchez, R. Rodriguez-Herrera, and C. N. Aguilar, "Microbial Enzymes Involved in Polyurethane Biodegradation: A Review," *Journal of Polymers and the Environment*, vol. 20, pp. 258-265, Mar 2012.
- [130] S. H. Abd-Alrahman, Z. H. Zidan, M. I. Abdel-Megeed, M. M. Almaz, M. M. Salem-Bekhit, S. M. Yakout, *et al.*, "Bioremediation of Water Contaminated with Fenitrothion and Butachlor using Microorganisms Isolated from Soil," *Journal of Pure and Applied Microbiology*, vol. 7, pp. 1757-1762, Sep 2013.
- [131] A. Ceci, O. Maggi, F. Pinzari, and A. M. Persiani, "Growth responses to and accumulation of vanadium in agricultural soil fungi," *Applied Soil Ecology*, vol. 58, pp. 1-11, Jul 2012.
- [132] J. B. Kantak, A. V. Bagade, S. A. Mahajan, S. P. Pawar, Y. S. Shouche, and A. A. Prabhune, "Isolation, Identification and Optimization of a New Extracellular Lipase Producing Strain of Rhizopus sp," *Applied Biochemistry and Biotechnology*, vol. 164, pp. 969-978, Aug 2011.

- [133] Y. Kamimura and K. Hayano, "Properties of protease extracted from tea-field soil," *Biology and Fertility of Soils*, vol. 30, pp. 351-355, Jan 2000.
- [134] C. L. Barberis, G. Pena, C. Carranza, and C. E. Magnoli, "Effect of indigenous mycobiota on ochratoxin A production by *Aspergillus carbonarius* isolated from soil: ochratoxin in mixed cultures," *Mycotoxin research*, vol. 30, pp. 1-8, 2014 Feb (Epub 2013 Oct 2014).
- [135] C. S. Carranza, M. V. Bergesio, C. L. Barberis, S. M. Chiacchiera, and C. E. Magnoli, "Survey of *Aspergillus* section Flavi presence in agricultural soils and effect of glyphosate on nontoxicigenic *A.flavus* growth on soil-based medium," *Journal of applied microbiology*, vol. 116, pp. 1229-40, 2014 May (Epub 2014 Feb 2014).
- [136] T. Matsuzawa, G. M. C. Takaki, T. Yaguchi, K. Okada, T. Gono, and Y. Horie, "Two new species of *Aspergillus* section Fumigati isolated from caatinga soil in the State of Pernambuco, Brazil," *Mycoscience*, vol. 55, pp. 79-88, Mar 2014.
- [137] C. Prisacariu, E. Scortanu, and B. Agapie, "The effect of the hard sequence ordering on the mechanical behaviour of polyurethane elastomers," *International Journal of Polymer Analysis and Characterization*, vol. 17, pp. 312-320, 2012.
- [138] M. Karamanlioglu and G. D. Robson, "The influence of biotic and abiotic factors on the rate of degradation of poly(lactic) acid (PLA) coupons buried in compost and soil," *Polymer Degradation and Stability*, vol. 98, pp. 2063-2071, Oct 2013.
- [139] D. Rosu, L. Rosu, and C. N. Cascaval, "IR-change and yellowing of polyurethane as a result of UV irradiation," *Polymer Degradation and Stability*, vol. 94, pp. 591-596, Apr 2009.
- [140] L. Irusta and M. J. Fernandez-Berridi, "Photooxidative behaviour of segmented aliphatic polyurethanes," *Polymer Degradation and Stability*, vol. 63, pp. 113-119, 1999.
- [141] Y. W. Tang, R. S. Labow, and J. P. Santerre, "Enzyme-induced biodegradation of polycarbonate-polyurethanes: Dependence on hard-segment chemistry," *Journal of Biomedical Materials Research*, vol. 57, pp. 597-611, Dec 15 2001.
- [142] C. B. Liu, Y. C. Gu, Z. Y. Qian, L. Y. Fan, J. Li, G. T. Chao, et al., "Hydrolytic degradation behavior of biodegradable polyetheresteramide-based polyurethane copolymers," *Journal of Biomedical Materials Research Part A*, vol. 75A, pp. 465-471, Nov 1 2005.
- [143] Y. Shi, X. L. Zhan, Z. H. Luci, Q. H. Zhang, and F. Q. Chen, "Quantitative IR characterization of urea groups in waterborne polyurethanes," *Journal of Polymer Science Part a-Polymer Chemistry*, vol. 46, pp. 2433-2444, Apr 2008.
- [144] S. Desai, I. M. Thakore, B. D. Sarawade, and S. Devi, "Effect of polyols and diisocyanates on thermo-mechanical and morphological properties of polyurethanes," *European Polymer Journal*, vol. 36, pp. 711-725, Apr 2000.
- [145] F. K. Li, J. N. Hou, W. Zhu, X. Zhang, M. Xu, X. L. Luo, et al., "Crystallinity and morphology of segmented polyurethanes with different soft-segment length," *Journal of Applied Polymer Science*, vol. 62, pp. 631-638, Oct 1996.

- [146] T. Elzein, M. Nasser-Eddine, C. Delaite, S. Bistac, and P. Dumas, "FTIR study of polycaprolactone chain organization at interfaces," *Journal of Colloid and Interface Science*, vol. 273, pp. 381-387, May 2004.
- [147] M. Bouvier, A. S. Chawla, and I. Hinberg, "Invitro degradaiotn of a poly(ether urethane) by trypsin," *Journal of Biomedical Materials Research*, vol. 25, pp. 773-789, Jun 1991.
- [148] L. Irusta and M. J. Fernandez-Berridi, "Aromatic poly(ether-urethanes): effect of the polyol molecular weight on the photochemical behaviour," *Polymer*, vol. 40, pp. 4821-4831, Aug 1999.
- [149] W. S. Wang, P. Ping, H. J. Yu, X. S. Chen, and X. B. Jing, "Synthesis and characterization of a novel biodegradable, thermoplastic polyurethane elastomer," *Journal of Polymer Science Part a-Polymer Chemistry*, vol. 44, pp. 5505-5512, Oct 2006.
- [150] T. C. Wen, J. C. Fang, and A. Gopalan, "Morphology and conductivity changes in a thermoplastic polyurethane-based copolymer consisting of different soft segments," *Journal of Applied Polymer Science*, vol. 82, pp. 1462-1473, Nov 2001.
- [151] E. Marten, R. J. Muller, and W. D. Deckwer, "Studies on the enzymatic hydrolysis of polyesters. II. Aliphatic-aromatic copolyesters," *Polymer Degradation and Stability*, vol. 88, pp. 371-381, Jun 2005.
- [152] K. Krasowska, A. Heimowska, and M. Rutkowska, "Enzymatic and hydrolytic degradation of poly(epsilon-caprolactone) in natural environment," *Polimery*, vol. 51, pp. 21-26, 2006.
- [153] A. Hoglund, M. Hakkarainen, and A. C. Albertsson, "Degradation profile of poly(epsilon-caprolactone) - the influence of macroscopic and macromolecular biomaterial design," *Journal of Macromolecular Science Part a-Pure and Applied Chemistry*, vol. 44, pp. 1041-1046, Jul-Sep 2007.
- [154] C. X. F. Lam, S. H. Teoh, and D. W. Hutmacher, "Comparison of the degradation of polycaprolactone and polycaprolactone-(beta-tricalcium phosphate) scaffolds in alkaline medium," *Polymer International*, vol. 56, pp. 718-728, Jun 2007.
- [155] T. NakajimaKambe, F. Onuma, Y. Akutsu, and T. Nakahara, "Determination of the polyester polyurethane breakdown products and distribution of the polyurethane degrading enzyme of Comamonas acidovorans strain TB-35," *Journal of Fermentation and Bioengineering*, vol. 83, pp. 456-460, 1997 1997.
- [156] Q. Zhao, J. Tao, R. C. M. Yam, A. C. K. Mok, R. K. Y. Li, and C. J. Song, "Biodegradation behavior of polycaprolactone/rice husk ecocomposites in simulated soil medium," *Polymer Degradation and Stability*, vol. 93, pp. 1571-1576, Aug 2008.
- [157] M. A. Woodruff and D. W. Hutmacher, "The return of a forgotten polymer- Polycaprolactone in the 21st century," *Progress in Polymer Science*, vol. 35, pp. 1217-1256, Oct 2010.
- [158] L. A. Bosworth and S. Downes, "Physicochemical characterisation of degrading polycaprolactone scaffolds," *Polymer Degradation and Stability*, vol. 95, pp. 2269-2276, Dec 2010.

- [159] A. Zgola-Grzeskowiak, T. Grzeskowiak, J. Zembrzuska, and Z. Lukaszewski, "Comparison of biodegradation of poly(ethylene glycol)s and poly(propylene glycol)s," *Chemosphere*, vol. 64, pp. 803-809, Jul 2006.
- [160] M. A. Schubert, M. J. Wiggins, J. M. Anderson, and A. Hiltner, "Role of oxygen in biodegradation of poly(etherurethane urea) elastomers," *Journal of Biomedical Materials Research*, vol. 34, pp. 519-530, Mar 1997.
- [161] D. N. Bikaris, "Nanocomposites of aliphatic polyesters: An overview of the effect of different nanofillers on enzymatic hydrolysis and biodegradation of polyesters," *Polymer Degradation and Stability*, vol. 98, pp. 1908-1928, Sep 2013.
- [162] B. Finnigan, D. Martin, P. Halley, R. Truss, and K. Campbell, "Morphology and properties of thermoplastic polyurethane composites incorporating hydrophobic layered silicates," *Journal of Applied Polymer Science*, vol. 97, pp. 300-309, Jul 2005
- [163] M. Spirkova, J. Pavlicevic, A. Strachota, R. Poreba, O. Bera, L. Kapralkova, *et al.*, "Novel polycarbonate-based polyurethane elastomers: Composition-property relationship," *European Polymer Journal*, vol. 47, pp. 959-972, May 2011.
- [164] K. Rajakumar, V. Sarasvathy, A. T. Chelvan, R. Chitra, and C. T. Vijayakumar, "Effect of iron carboxylates on the photodegradability of polypropylene. II. Artificial weathering studies," *Journal of Applied Polymer Science*, vol. 123, pp. 2968-2976, Mar 2012.
- [165] R. Arnaud, P. Dabin, J. Lemaire, S. Almalaika, S. Chohan, M. Coker, *et al.*, "Photooxidation and biodegradation of commercial photodegradable polyethylenes," *Polymer Degradation and Stability*, vol. 46, pp. 211-224, 1994.
- [166] G. R. da Silva, A. da Silva-Cunha, F. Behar-Cohen, E. Ayres, and R. L. Orefice, "Biodegradation of polyurethanes and nanocomposites to non-cytotoxic degradation products," *Polymer Degradation and Stability*, vol. 95, pp. 491-499, Apr 2010.
- [167] H. Pan and Z. B. Qiu, "Biodegradable Poly(L-lactide)/Polyhedral Oligomeric Silsesquioxanes Nanocomposites: Enhanced Crystallization, Mechanical Properties, and Hydrolytic Degradation," *Macromolecules*, vol. 43, pp. 1499-1506, Feb 2010.
- [168] J. Raghunath, G. Georgiou, D. Armitage, S. N. Nazhat, K. M. Sales, P. E. Butler, *et al.*, "Degradation studies on biodegradable nanocomposite based on polycaprolactone/polycarbonate (80:20%) polyhedral oligomeric silsesquioxane," *Journal of Biomedical Materials Research Part A*, vol. 91A, pp. 834-844, Dec 1 2009.
- [169] Y. H. Lee, J. H. Lee, I. G. An, C. Kim, D. S. Lee, Y. K. Lee, *et al.*, "Electrospun dual-porosity structure and biodegradation morphology of Montmorillonite reinforced PLLA nanocomposite scaffolds," *Biomaterials*, vol. 26, pp. 3165-3172, Jun 2005.
- [170] Q. Li, J.-S. Yoon, and G.-X. Chen, "Thermal and Biodegradable Properties of Poly(L-lactide)/Poly(epsilon-Caprolactone) Compounded with Functionalized Organoclay," *Journal of Polymers and the Environment*, vol. 19, pp. 59-68, Mar 2011.
- [171] S. S. Ray, K. Yamada, M. Okamoto, and K. Ueda, "Control of biodegradability of polylactide via nanocomposite technology," *Macromolecular Materials and Engineering*, vol. 288, pp. 203-208, Mar 20 2003.